



**Novel Therapies for Cancer
Treatment: Designing High Affinity
Selective Ligands Against SIRT1
Enzyme**

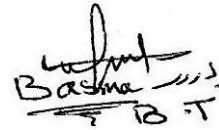
Basma Talib Al-Sudani

Biomedical Research Centre
School of Environment and Life Sciences
College of Science & Technology
University of Salford

Submitted in Partial Fulfilment of the Requirements for the
Degree of Doctor of Philosophy, June 2017

DECLARATION

I certify that this thesis, which I submit to the University of Salford a partial fulfilment of the requirements for a Degree of Doctor of Philosophy, is a presentation of my own research work. Wherever contributions of others are involved, every effort is made to indicate this clearly with due reference to the literature and acknowledgement of collaborative research and discussions. The content of this thesis has not been submitted for a higher degree at this or any other University.



Handwritten signature of Basma Talib Al-Sudani, including the name 'Basma' and the initials 'B.T.'.

Basma Talib Al-Sudani

TABLE OF CONTENTS

DECLARATION	I
TABLE OF CONTENTS	II
LIST OF FIGURES	VII
LIST OF TABLES	XIII
ACKNOWLEDGEMENTS.....	XIV
ABBREVIATIONS	XVI
ABSTRACT	XXI
1 INTRODUCTION.....	1
1.1 Cancer: a Historical Perspective.....	1
1.1.1 Carcinogenesis	1
1.1.2 Tumour Promotion and Tumour Suppression.....	4
1.2 Histone Deacetylases	6
1.2.1 Classification and Function of Histone Deacetylases	7
1.2.1.1 SIRT1	23
1.2.1.2 SIRT2	25
1.2.1.3 SIRT3	26
1.2.1.4 SIRT4.....	27
1.2.1.5 SIRT5	27
1.2.1.6 SIRT6.....	27
1.2.1.7 SIRT7	28
1.3 Functions of Mammalian Sirtuins	28
1.3.1 Gene Expression.....	29
1.3.2 Apoptosis and Cell Survival	31
1.3.3 Stress Resistance and Cell Survival	32
1.3.4 Cellular Senescence.....	33
1.3.5 DNA Repair	34
1.3.6 Inflammation.....	36
1.3.7 Development	37
1.3.8 Metabolism	37
1.4 Role of SIRT1 in Regulating Mammalian Aging.....	39
1.5 SIRT1 Activators.....	40
1.6 SIRT1 Inhibitors	45
1.7 SIRT1 and Cancer.....	46

1.8 ROS and DNA Damage	51
1.8.1 SIRT1 and ROS.....	52
1.9 Investigating SIRT1 as a Target for Cancer Therapeutic	54
1.10 Aptamers	57
1.10.1 Generation of Aptamers.....	58
1.10.1.1 SELEX	59
1.10.1.2 General Principles	59
1.10.1.3 Target Molecules	62
1.10.1.4 Random DNA Library.....	64
1.10.1.5 Selection	66
1.10.1.6 Amplification.....	71
1.10.1.7 Cloning and Characterisation	71
1.10.2 Aptamers and Antibodies.....	73
1.10.3 Application of Aptamers.....	73
1.10.4 Aptamers as Therapeutics	73
1.10.5 Why is an Aptamer Validated to be a Good Therapeutic?	75
1.10.6 <i>In Vivo</i> Stability of Nucleic Acid in Therapeutics	77
1.10.7 Circular Aptamers	79
1.11 Aim of the Study.....	81
2 MATERIALS & METHODS	82
2.1 Materials.....	82
2.2 Methods.....	87
2.2.1 Introduction.....	87
2.2.2 DNA Technology	88
2.2.2.1 Library Preparation	88
2.2.2.2 Denaturing Urea–Polyacrylamide Gel Electrophoresis (PAGE).....	89
2.2.2.3 Determination of Nucleic Acids on Gels by Gel Red Staining	90
2.2.2.4 Extraction of Nucleic Acids from Polyacrylamide Gels.....	90
2.2.2.5 Ethanol Precipitation.....	90
2.2.2.6 Phosphorylation of Linear BAS	91
2.2.2.7 Ligation of BAS by T4 DNA Ligation	91
2.2.2.8 Confirmation of circularity of the BAS Library	92
2.2.2.9 Removing the Linear ssDNA Template and Adenylated Intermediat	92
2.2.3 Protein Technology	92
2.2.3.1 SIRT1 Enzyme	92

2.2.3.2	Cleavage of GST-tag using PreScission Protease (PSP).....	92
2.2.3.3	Sodium Dodecyl Sulfate Polyacrylamide Gel Electrophoresis (SDS–.....	94
2.2.4	SELEX Methodology	94
2.2.4.1	Affinity Chromatography <i>In vitro</i> Selection Method	94
2.2.4.1.1	Immobilisation of SIRT1	94
2.2.4.1.2	<i>In Vitro</i> Selection of Circular Aptamers Against SIRT1 Enzyme	95
2.2.4.1.3	Conventional Polymerase Chain Reaction (PCR).....	97
2.2.4.1.4	<i>In Vitro</i> Selection of Linear Aptamers Against SIRT1 Enzyme	98
2.2.4.2	DNA Cloning.....	98
2.2.4.2.1	DNA Ligation.....	99
2.2.4.2.2	Transformation	99
2.2.4.2.3	Isolation of Plasmid DNA.....	99
2.2.4.2.4	Confirmation of Ligation	100
2.2.4.2.5	DNA Sequencing.....	100
2.2.5	Aptamer Characterisation	100
2.2.5.1	<i>In vitro</i> Characterisation of Activators and Inhibitors of SIRT1	101
2.2.5.2	SIRT1 Kinetics as a Function of the Concentrations of Fluor de Lys	102
2.2.5.3	Characterisation of the SIRT1 Enzyme Interaction with Selected	103
2.2.6	Cell Culture.....	103
2.2.6.1	Cell Maintenance	104
2.2.6.2	Storage and Resuscitation of Cell Lines	104
2.2.6.3	Cell Viability by MTT Assay	105
2.2.6.4	Measurement of Reactive Oxygen Species ROS Production.....	107
2.2.6.5	<i>In Vitro</i> Evaluation the Activity of SIRT1 Enzyme in Cells by Fluor.....	109
2.2.6.6	The Half Maximal Inhibitory Concentration (IC ₅₀) Value.....	109
2.2.6.7	Immunofluorescence Microscopy.....	110
2.2.7	<i>In vitro</i> Plasma Stability Assay of C3 Aptamer.....	110
2.2.7.1	Plasma Stability Assay of C3 Aptamer by Urea PAGE.....	110
2.2.7.2	Plasma Stability Assay of C3 Aptamer by HPLC-UV	111
2.3	Data Analysis	111
3	<i>IN VITRO</i> SELECTION AND IDENTIFICATION OF CIRCULAR AND LINEAR ssDNA APTAMERS AGAINST SIRTUIN1 ENZYME BY SELEX METHODOLOGY.	112
3.1	Introduction	112
3.2	Methods.....	113
3.3	Results.....	113

3.3.1 Circularisation of BAS Library	113
3.3.2 Cleavage of GST-tag from SIRT1 Enzyme using PreScission Protease.....	116
3.3.3 <i>In Vitro</i> Selection Circular BAS Aptamer Against SIRT1 Enzyme	116
3.3.4 <i>In Vitro</i> Selection Linear BAS Aptamer Against SIRT1 Enzyme	122
3.3.5 DNA Cloning and Sequencing.....	124
3.4 Discussion	125
4 CHARACTERISATION, KINETICS AND STABILITY OF APTAMERS	128
4.1 Introduction	128
4.2 Methods.....	133
4.3 Results.....	133
4.3.1 <i>In vitro</i> Characterisation Study of Activators and Inhibitors of the.....	133
4.3.2 SIRT1 kinetics as a Function of the Concentrations of Aptamers	142
4.3.3 Determination of Equilibrium Binding Characterisation of Circular3,.....	152
4.3.4 Plasma Stability Assay of C3 Aptamer by Urea PAGE and HPLC.....	156
4.4 Discussion	160
5 APTAMERS AS THERAPEUTICS.....	165
5.1 Introduction	165
5.1.1 Background to the Cell Lines and Expression of SIRT1.....	167
5.2 Methods.....	171
5.3 Results.....	171
5.3.1 Effect of Linear3, Linear4, Circular3 and Circular4 Aptamers on 8	172
5.3.1.1 Human Adenocarcinoma of Alveolar Basal Epithelial Cells (A549).....	172
5.3.1.2 Children Liver Hepatocellular Carcinoma Cells (HepG2).....	176
5.3.1.3 Breast Cancer (MCF7) Cells (oestrogen positive).....	180
5.3.1.4 Breast Cancer (MDA-MB-468) Cells (oestrogen negative)	184
5.3.1.5 Children Human Bone Osteosarcoma cells (U2OS).....	188
5.3.1.6 Colorectal Adenocarcinoma cells (Caco-2)	192
5.3.1.7 Aneuploid Immortal Keratinocyte (HaCaT) Cells.....	196
5.3.1.8 Normal Human Bronchial Epithelial Cells (Beas-2b)	200
5.3.2 Effect of Linear3, Linear4, Circular3 and Circular4 aptamers on Intracellular ROS Production in 8 Cell Lines	204
5.3.3 <i>In vitro</i> Study the Activity of SIRT1 Enzyme by C3 in Cells by Fluor de	209
5.3.4 Effect of C3 Aptamer on Ratio of Intracellular ROS Production and.....	214
5.3.5 Determination the Half Maximal Inhibitory Concentration (IC ₅₀)	219
5.3.6 Determine the Location of C3 Aptamer by Fluorescence Microscopy	223

5.4 Discussion	233
6 GENERAL DISCUSSION AND FUTURE PERSPECTIVES.....	237
6.1 Discussion	237
6.2 Future perspectives	245
7 REFERENCES	246

LIST OF FIGURES

Figure 1.1: Characteristics of Cancer.....	2
Figure 1.2: Basic steps of carcinogenesis: initiation, promotion and progression.	4
Figure 1.3: Cell cycle..	5
Figure 1.4: Histone modification: acetylation.	7
Figure 1.5: Classification of HDAC Class I, II, III and IV.	9
Figure 1.6: HDAC inhibition targets cell cycle progression..	12
Figure 1.7: The schematic diagram depicts the HDAC1 regulation in normal in vitro.....	13
Figure 1.8: Schematic representation of the class III HDACs (Sirtuins).....	18
Figure 1.9: The Sirtuins family of histone deacetylases.	22
Figure 1.10: Structure of SIRT1.	24
Figure 1.11: Interacting partners, substrates, and downstream effectors of SIRT1.....	29
Figure 1.12: Molecular interconnections between SIRT1.....	31
Figure 1.13: SIRT1 and cell survival..	32
Figure 1.14: Nuclear Sirtuins regulate genomic stability.....	35
Figure 1.15: Function of SIRT1 in tissues relevant to organismal energy homeostasis	38
Figure 1.16: Small molecule activators of SIRT1.	41
Figure 1.17: Activation of SIRT 1 by the natural antioxidant resveratrol).	42
Figure 1.18: Mechanism of SIRT1 activation by resveratrol.	44
Figure 1.19: Small-molecule inhibitors of SIRT1	46
Figure 1.20: SIRT1 as a tumour suppressor or/and tumour promoter.	47
Figure 1.21: Activation and inhibition of many cellular processes by SIRT1	49
Figure 1.22: Model for SIRT1 apparent duality in cancer..	51
Figure 1.23: Relationship between ROS and SIRT1.	53
Figure 1.24: SIRT1's anticancer activity.	56
Figure 1.25: Diagram of aptamer binding to SIRT1 protein.	57
Figure 1.26: Molecular recognition of targets by aptamers	58
Figure 1.27: The principles of SELEX. <i>In vitro</i> selection of target-specific aptamers.....	61
Figure 1.28: Quadruplex structure of the thrombin binding aptamer	63
Figure 1.29: Triple-stranded complexes.....	64
Figure 1.30: The SELEX process..	69
Figure 1.31: Guanine-rich (G-rich) sequence that folds into a G-quadruplex structure	72

Figure 1.32: The molecular models (quadruplex) for the AS1411 aptamer.	74
Figure 1.33: Chemical structure of 2' fluorinated pyrimidine and 2' methoxy purine.	76
Figure 1.34: Circular aptamer synthesis.	79
Figure 1.35: Circularisation of aptamer by ligation.	80
Figure 2.1: GSTrap FF connect with syringe by adapter supplied.	93
Figure 2.2: Scheme of selection of circular aptamer against SIRT1.	96
Figure 2.3: Scheme of selection of linear aptamer against SIRT1.	98
Figure 2.4: 96-well plate template for MTT assay.	106
Figure 2.5: 96-well plate template for ROS assay.	108
Figure 3.1: Circularisation of BAS library.	114
Figure 3.2: Circularisation of BAS library.	115
Figure 3.3: Circularisation of BAS Ligase converts linear BAS into closed circular ssDNA	115
Figure 3.4: SDS-PAGE analysis of cleavage GST tag from SIRT1 enzyme.	116
Figure 3.5: 10% acrylamide gel analysis of aptamer selection against SIRT1 enzyme after 1 st round.	117
Figure 3.6: 10% acrylamide gel analysis of aptamer selection against SIRT1 enzyme after 2 nd round.	118
Figure 3.7: 10% acrylamide gel analysis of aptamer selection against SIRT1 enzyme after 3 rd round.	119
Figure 3.8: 10% acrylamide gel analysis of aptamer selection against SIRT1 enzyme after 4 th round.	119
Figure 3.9: 10% acrylamide gel analysis of aptamer selection against SIRT1 enzyme after 5 th round.	120
Figure 3.10: 10% acrylamide gel analysis of aptamer selection against SIRT1 enzyme after 6 th round.	120
Figure 3.11: 10% acrylamide gel analysis of aptamer selection against SIRT1 enzyme after 7 th round.	121
Figure 3.12: 10% acrylamide gel analysis of aptamer selection against SIRT1 enzyme after 8 th round.	121
Figure 3.13: 10% acrylamide gel analysis of PCR products during 8 th rounds of <i>in vitro</i> selection.	122
Figure 3.14: 10% acrylamide gel analysis of linear elution aptamer of <i>in vitro</i> selection.	123
Figure 3.15: 10% acrylamide gel analysis of PCR products aptamers <i>in vitro</i> selection.	123

Figure 4.1: Reaction Scheme of the SIRT1 Fluorescent Activity Assay.	129
Figure 4.2: Substrate concentration versus enzyme reaction velocity	130
Figure 4.3: Lineweaver-Burke Plots.	132
Figure 4.4: Measurement of SIRT1 activity with Fluor de Lys assay (activators).....	135
Figure 4.5: Measurement of SIRT1 activity with Fluor de Lys assay (inhibitors).....	135
Figure 4.6: The best fit of the data yielded a Kdissociation constant of circular1 aptamer ..	137
Figure 4.7: The best fit of the data yielded a Kdissociation constant of circular2 aptamer ..	137
Figure 4.8: The best fit of the data yielded a Kdissociation constant of circular3 aptamer ..	138
Figure 4.9: The best fit of the data yielded a Kdissociation constant of circular4 aptamer ..	138
Figure 4.10: The best fit of the data yielded a Kdissociation constant of circular5 aptamer	139
Figure 4.11: The best fit of the data yielded a Kdissociation constant of circular6 aptamer	139
Figure 4.12: The best fit of the data yielded a Kdissociation constant of linear1 aptamer ...	140
Figure 4.13: The best fit of the data yielded a Kdissociation constant of linear2 aptamer ...	140
Figure 4.14: The best fit of the data yielded a Kdissociation constant of linear3 aptamer ...	141
Figure 4.15: The best fit of the data yielded a Kdissociation constant of linear4 aptamer ...	141
Figure 4.16: A plot of the reaction velocity (V_0) versus circular3 aptamer	142
Figure 4.17: A double-reciprocal plot of SIRT1 kinetics for circular3 aptamer	143
Figure 4.18: The amount of product formed at different concentrations of circular3 aptamers	144
Figure 4.19: A plot of the reaction velocity (V_0) versus circular4 aptamer	145
Figure 4.20: A double-reciprocal plot of SIRT1 kinetics for circular4 aptamer	145
Figure 4.21: The amount of product formed at different concentrations of circular4 aptamers	146
Figure 4.22: A plot of the reaction velocity (V_0) versus linear3 aptamer	147
Figure 4.23: A double-reciprocal plot of SIRT1 kinetics for linear3 aptamer	148
Figure 4.24: The amount of product formed at different concentrations of linear3 aptamers	149
Figure 4.25: A plot of the reaction velocity (V_0) versus linear4 aptamer	150
Figure 4.26: A double-reciprocal plot of SIRT1 kinetics for linear4 aptamer	150
Figure 4.27: The amount of product formed at different concentrations of linear4 aptamer.	151
Figure 4.28: An idealised sensorgram showing the baseline, association, and dissociation phases.	153
Figure 4.29: Determination of the affinities of C3 aptamers for SIRT1	154
Figure 4.30: Determination of the affinities of C4 aptamers for SIRT1	154

Figure 4.31: Determination of the affinities of L3 aptamers for SIRT1	155
Figure 4.32: Determination of the affinities of L4 aptamers for SIRT1	155
Figure 4.33: Stability of the circular3 aptamer in human plasma by 10% urea PAGE	156
Figure 4.34: Stability of the circular3 aptamer in human plasma by HPLC-UV method.....	157
Figure 4.35: Stability of the circular3 aptamer with endonuclease digestion by HPLC-UV	158
Figure 4.36: Stability of the circular3 aptamer with endonuclease digestiona by urea PAGE	159
Figure 5.1: Models illustrating possible functions of SIRT1 in tumour suppression.	166
Figure 5.2: <i>In vitro</i> cell viability of (A549) cells was detected by MTT assay.	172
Figure 5.3: <i>In vitro</i> cell viability of (A549) cells was detected by MTT assay.	173
Figure 5.4: <i>In vitro</i> cell viability of (A549) cells was detected by MTT assay	173
Figure 5.5: <i>In vitro</i> cell viability of (A549) cells was detected by MTT assay	174
Figure 5.6: <i>In vitro</i> cell viability of (A549) cells was detected by MTT assay	174
Figure 5.7: <i>In vitro</i> cell death percentage of (A549) cells.....	175
Figure 5.8: <i>In vitro</i> cell viability of (HepG2) cells was detected by MTT assay	176
Figure 5.9: <i>In vitro</i> cell viability of (HepG2) cells was detected by MTT assay	177
Figure 5.10: <i>In vitro</i> cell viability of (HepG2) cells was detected by MTT assay	177
Figure 5.11: <i>In vitro</i> cell viability of (HepG2) cells was detected by MTT assay.	178
Figure 5.12: <i>In vitro</i> cell viability of (HepG2) cells was detected by MTT assay	178
Figure 5.13: <i>In vitro</i> cell death percentage of (HepG2)	179
Figure 5.14: <i>In vitro</i> cell viability of (MCF-7) cells was detected by MTT assay	180
Figure 5.15: <i>In vitro</i> cell viability of t (MCF-7) cells was detected by MTT assay.	181
Figure 5.16: <i>In vitro</i> cell viability of (MCF-7) cells was detected by MTT assay	181
Figure 5.17: <i>In vitro</i> cell viability of (MCF-7) cells was detected by MTT assay	182
Figure 5.18: <i>In vitro</i> cell viability of (MCF-7) cells was detected by MTT assay	182
Figure 5.19: <i>In vitro</i> cell death percentage of (MCF-7) cells.....	183
Figure 5.20: <i>In vitro</i> cell viability of (MDA-MB-468) cells was detected by MTT assay ...	184
Figure 5.21: <i>In vitro</i> cell viability of (MDA-MB-468) cells was detected by MTT assay ...	185
Figure 5.22: <i>In vitro</i> cell viability of (MDA-MB-468) cells was detected by MTT assay. ..	185
Figure 5.23: <i>In vitro</i> cell viability of (MDA-MB-468) cells was detected by MTT assay. ..	186
Figure 5.24: <i>In vitro</i> cell viability of (MDA-MB-468) cells was detected by MTT assay. ..	186
Figure 5.25: <i>In vitro</i> cell death percentage of (MDA-MB-468) cells.....	187
Figure 5.26: <i>In vitro</i> cell viability of (U2OS) cells was detected by MTT assay.....	188
Figure 5.27: <i>In vitro</i> cell viability of (U2OS) cells was detected by MTT assay.....	189

Figure 5.28: <i>In vitro</i> cell viability of (U2OS) cells was detected by MTT assay	189
Figure 5.29: <i>In vitro</i> cell viability of (U2OS) cells was detected by MTT assay	190
Figure 5.30: <i>In vitro</i> cell viability of (U2OS) cells was detected by MTT assay	190
Figure 5.31: <i>In vitro</i> cell death percentage of (U2OS) cells.....	191
Figure 5.32: <i>In vitro</i> cell viability of (Caco-2) cells was detected by MTT assay.	192
Figure 5.33: <i>In vitro</i> cell viability of (Caco-2) cells was detected by MTT assay	193
Figure 5.34: <i>In vitro</i> cell viability of (Caco-2) cells was detected by MTT assay	193
Figure 5.35: <i>In vitro</i> cell viability of (Caco-2) cells was detected by MTT assay	194
Figure 5.36: <i>In vitro</i> cell viability of (Caco-2) cells was detected by MTT assay	194
Figure 5.37: <i>In vitro</i> cell death percentage of (Caco-2) cells	195
Figure 5.38: <i>In vitro</i> cell viability of (HaCaT) cells was detected by MTT assay	196
Figure 5.39: <i>In vitro</i> cell viability of (HaCaT) cells was detected by MTT assay	197
Figure 5.40: <i>In vitro</i> cell viability of (HaCaT) cells was detected by MTT assay	197
Figure 5.41: <i>In vitro</i> cell viability of (HaCaT) cells was detected by MTT assay	198
Figure 5.42: <i>In vitro</i> cell viability of (HaCaT) cells was detected by MTT assay	198
Figure 5.43: <i>In vitro</i> cell death percentage of (HaCaT) cells	199
Figure 5.44: <i>In vitro</i> cell viability of (Beas-2b) cells was detected by MTT assay.....	200
Figure 5.45: <i>In vitro</i> cell viability of (Beas-2b) cells was detected by MTT assay.....	201
Figure 5.46: <i>In vitro</i> cell viability of (Beas-2b) cells was detected by MTT assay.....	201
Figure 5.47: <i>In vitro</i> cell viability of (Beas-2b) cells was detected by MTT assay.....	202
Figure 5.48: <i>In vitro</i> cell viability of (Beas-2b) cells was detected by MTT assay.....	202
Figure 5.49: <i>In vitro</i> cell viability of (Beas-2b) was detected by MTT assay.....	203
Figure 5.50: Effects of L3, L4, C3 and C4 aptamers on ROS production in A549 cells.....	205
Figure 5.51: Effects of L3, L4, C3 and C4 aptamers on ROS production in MCF-7 cells ...	205
Figure 5.52: Effects of L3, L4, C3 and C4 aptamers on ROS production in MDA-MB-468	206
Figure 5.53: Effects of L3, L4, C3 and C4 aptamers on ROS production in U2OS cells.....	206
Figure 5.54: Effects of L3, L4, C3 and C4 aptamers on ROS production in Caco-2 cells ...	207
Figure 5.55: Effects of L3, L4, C3 and C4 aptamers on ROS production in HepG2 cells ...	208
Figure 5.56: Effects of L3, L4, C3 and C4 aptamers on ROS production in HepG2 cells ...	208
Figure 5.57: Effects of L3, L4, C3 and C4 aptamers on ROS production in Beas-2b cells..	209
Figure 5.58: SIRT1 activity in A549 cells.....	210
Figure 5.59: SIRT1 activity in HepG2 cells.....	211
Figure 5.60: SIRT1 activity in MCF-7 cells.....	211
Figure 5.61: SIRT1 activity in MDA-MB-468 cells	212

Figure 5.62: SIRT1 activity in U2OS cells	212
Figure 5.63: SIRT1 activity in Caco-2 cells	213
Figure 5.64: SIRT1 activity in HaCaT cells	213
Figure 5.65: SIRT1 activity in Beas-2b cells	214
Figure 5.66: Dose-response curves of IC ₅₀ for C3 aptamer in A549 cells	220
Figure 5.67: Dose-response curves of IC ₅₀ for C3 aptamer in HepG2 cells	220
Figure 5.68: Dose-response curves of IC ₅₀ for C3 aptamer in MCF-7 cells	221
Figure 5.69: Dose-response curves of IC ₅₀ for C3 aptamer in MDA-MB-468 cells	221
Figure 5.70: Dose-response curves of IC ₅₀ for C3 aptamer in U2OS cells	222
Figure 5.71: Dose-response curves of IC ₅₀ for C3 aptamer in Caco-2 cells	222
Figure 5.72: Dose-response curves of IC ₅₀ for C3 aptamer in HaCaT cells	223
Figure 5.73: Fluorescence microscopy analysis of C3 aptamer in A549	225
Figure 5.74: Fluorescence microscopy analysis of C3 aptamer in HepG2	226
Figure 5.75: Fluorescence microscopy analysis of C3 aptamer in HepG2	227
Figure 5.76: Fluorescence microscopy analysis of C3 aptamer in MCF-7	228
Figure 5.77: Fluorescence microscopy analysis of C3 aptamer in MDA-MB-468	229
Figure 5.78: Fluorescence microscopy analysis of C3 aptamer in U2OS	230
Figure 5.79: Fluorescence microscopy analysis of C3 aptamer in HaCaT	231
Figure 5.80: Fluorescence microscopy analysis of C3 aptamer in Beas-2b	232

LIST OF TABLES

Table 1.1: Classification of histone deacetylases depending on sequence homology	8
Table 1.2: Classification of HDAC depending on members	10
Table 1.3: The mammalian Sirtuins	19
Table 2.1: Sequence of BAS library and primers that used in SELEX.....	88
Table 2.2: Sequences of 10 aptamers	102
Table 3.1: Nucleotide sequences of basic-SELEX linear and circular aptamers	124
Table 3.2: Nucleotide sequences of 10 aptamers with and without primers.	125
Table 4.1: k_d and k_a constants \pm SEM for all selected aptamers.	136
Table 4.2: V_{max} and K_m for C3 aptamer \pm standard error.....	143
Table 4.3: V_{max} and K_m for C4 aptamer \pm standard error.	146
Table 4.4: V_{max} and K_m for L3 aptamer \pm standard error.....	148
Table 4.5: V_{max} and K_m for L4 aptamer \pm standard error.	151
Table 4.6: Association binding parameters resulting.....	155
Table 5.1: The percentage of ROS normalised to control of A549.	216
Table 5.2: The percentage of ROS normalised to control of HepG2.....	216
Table 5.3: The percentage of ROS normalised to control of MCF-7	217
Table 5.4: The percentage of ROS normalised to control of U2OS	217
Table 5.5: The percentage of ROS normalised to control of MDA-MB-468	218
Table 5.6: The percentage of ROS normalised to control of Caco-2.....	218
Table 5.7: The percentage of ROS normalised to control of HaCaT.....	219

ACKNOWLEDGEMENTS

This thesis represents the great effort of four years of hard work at cancer research biomedical laboratory. This is including my work on the aptamers and delivering the data of my important findings in more than 8 national and international conferences related to the aptamers and molecular biochemistry. Since my first day in my PhD I felt the importance of this project and felt I have been given a unique opportunity to do my PhD in this unique research. As much as I liked the work on discovery, I wished my findings in this work can help cancers patients and I hope this can be progressed quickly to put efficient end to the pain of patients. In this opportunity, I would like to thank the people who have played a major role in the success of this project and encouraged me from the first moment of my arrival in the United Kingdom and so far.

First and foremost, I would like to express my highest gratitude to Dr. Patricia Ragazzon who was abundantly helpful and offered invaluable assistance, support and guidance during the last years and for giving me the opportunity to perform the research for my doctoral project in her laboratory. She has been supportive since I began working on the aptamer. Ever since Patricia has supported me not only by providing a research assistantship over almost four years but also academically and emotionally through the rough road to finish this thesis. She helped me come up with the thesis topic and guided me over almost a two year of development. And during the most difficult times when writing this thesis, she gave me the support to move on.

My great gratitude to the most valued people in my life, who gave me an infinite love, support, encouragement and understood all my needs during my study time, my solely love my husband Ahmed and my lovely kids Mina and Mohammed, a great thank to your patience and continuous encouragement which I would never be able to continue without them, you always pushed me forward during the difficult times. Thank you to my family in Iraq who did not forget me in their prayers, especially my mum who bore the pain of being far from her in order to my dreams to be achieved and see my success in the end of this long journey. My deep love and grateful to my brother Ali to all the support he did and to surrounding me with his love and encouragement, and to my sole sister Farah who always prayed to me to have the success in my PhD.

I also would like to express about my grateful to the Iraqi ministry of higher education to sponsoring my research, and a special thank to Dr. Ali Al-Adeeb, the previous minister, who let me achieve the dream of my life in studying the PhD in the UK and getting this scholarship.

My special thanks extend to my wonderful friends Basma, Muna and Israa, they were a true friend ever since we began to share a lab in 2014. Basma is an amazing person in too many ways.

I would also like to thank all the members of the Biomedical Research Centre in Salford University for all the support and a good working atmosphere.

I feel deeply grateful to all the people who gave me any kinds of help wherever in Salford University.

Finally, I would like to acknowledge Salford Postgraduate Research Fund in the University of Salford for the numerous awards to attend the international conferences.

Basma Al-Sudani

ABBREVIATIONS

°C	Temperature in degrees Celsius
3D	3 dimension
ADP	Adenosine diphosphate ribose
ADPR	ADP-ribose peptide-imidate intermediate Alpha
APC	Adenomatous Polyposis Coli
APS	Ammonium persulfate
AR	Androgen receptor
ART	Mono-ADP-Ribosyl Transferase
ATP	Adenosine 5'-triphosphate
BAS	Library of ssDNA
BAX	Bcl-2-like protein 4
BCLIIA	Mamalian protein
bp	Base pair(s)
BSA	Bovine serum albumin
C	Cytoplasm
C1	Circular1 aptamer
C18	Octadecyl carbon chain
C2	Circular2 aptamer
C3	Circular3 aptamer
C4	Circular4 aptamer
C5	Circular5 aptamer
C6	Circular6 aptamer
CAMK1	Calcium/calmodulin-dependent protein kinase type 1
CDK	Cyclin-dependent kinases
cDNA	Complementary DNA
CH₃	Methyl group
CobB	Bacterial protein that belongs to the sirtuin family
CoREST	REST corepressor 1
COX II	Cytochrome c oxidase subunits II
COX IV	Cytochrome c oxidase subunits (complex IV)

CREB	cAMP response element binding protein
CtBP	C-terminal-binding protein 1
CTIP2	Chicken protein
DAC	NAD ⁺ Dependent Deacetylase,
DBC1	Deleted in breast cancer-1
DHT	Dihydrotestosterone
DNA	Deoxyribonucleic acid
DNMT1	DNA (cytosine-5)-methyltransferase 1
dNTP	Deoxyribonucleotide triphosphate
E	Enzyme
E2F1	Protein Transcription factor
EDTA	Ethylenediaminetetraacetic Acid
Em	Emissions
ES	Enzyme-substrate
Ex	Excitation
F	Florid
FOXO	Forkhead box protein O1
g	Gram
G	Guanosine
GDP	Guanosine diphosphate
G-rich	Guanosine-rich
GSH	Glutathione
GST	Glutathione-S-transferase
GTP	Guanosine-5'-triphosphate
GTPase	A large family of hydrolase enzymes
h	Hour(s)
HDAC	Histone deacetylase
HDRP	Histone deacetylase-related protein
HPLC	High-performance liquid chromatography
Hsp90	Heat shock protein 90
IMAC	Immobilised metal affinity column
IPTG	Isopropyl β -D-1-thiogalactopyranoside

JIP1	A member of the JNK-interacting protein group of scaffold proteins
K₋₁	Rate constant for association of E + S
K_{cat}	Number of substrate molecule each enzyme site converts to product per unit time
K_d	Dissociation constant
KDa	Kilo Dalton
Ku70	Protein in human
L.B	Lauding buffer
L1	Linear1 aptamer
L2	Linear2 aptamer
L3	Linear3 aptamer
L4	Linear4 aptamer
LB	Luria broth, is a nutrient-rich media
LDH	Lactate dehydrogenase.
LOH	Loss of Heterozygosity
M	Molar (mol/l)
MAPK	Mitogen activated protein kinase
MEF	Mouse embryonic fibroblasts
MEF2	Myocyte enhancer factor 2
MgCL₂	Magnesium chloride
min	Minute(s)
MITR	HDAC-related protein
ml	Milliliter
mM	Millimolar
MREs	Molecular recognition elements
MYC	A regulator gene that codes for a transcription factor
N	Nuclease
Na	Sodium
NAD⁺	Nicotinamide adenine dinucleotide oxidized
NADPH	Reduced form of nicotinamide adenine dinucleotide phosphate
NCoR	Nuclear receptor co-repressor 1
NES	Nuclear export signal

NF-κB	Nuclear factor kappa-light-chain-enhancer of activated B cells
nM	Nanomolar
nm	Nano-meter
nt	Nucleotide(s)
NTP	Nucleotide triphosphate
O	Oxygen
OAADPr	2' -O-acetyl-ADP-ribose
p¹⁹(ARF)	Distinct tumour suppressors
P21	Cyclin-dependent kinase inhibitor 1 or CDK-interacting protein 1
P27	Kinase inhibitory protein 1 (Kip1)
p53	Tumour suppresser protein p53
PAGE	Polyacrylamide gel electrophoresis
PARP	Poly ADP ribose polymerase
PCR	Polymerase chain reaction
pg	Picogram is equal to one trillionth of a gram (10^{-12} g)
PGC-1α	Peroxisome proliferator-activated receptor gamma coactivator 1- α
PML	Promyelocytic leukemia protein
pmol	Picomole is equal to 10^{-12} moles
PP1	Protein phosphatase 1
PreScission	Human rhinovirus 3C protease
RAS	Proto-oncogenes
RB	Retinoblastoma
rDNA	Ribosomal DNA
RNA	Ribonucleic acid
RPD3	Histone deacetylase (HDAC) complexes RPD3C(L) and RPD3C(S)
rpm	Rotations per minute
RT	Room temperature
RT-PCR	Real time- polymerase chain reaction
RUNX2	Run- related transcription factor2
s	Second(s)
S	Substrate
SDS	Sodium dodecyl sulfate

SDS-PAGE	Sodium dodecyl sulfate-Polyacrylamide gel electrophoresis
SE14	Lysine-specific demethylase
SELEX	Systematic Evolution of Ligands by EXponential enrichment
Sir	Silent information regulator
Sir2	Silent Information Regulator 2
siRNA	Small interference RNA
SMRT	Silencing mediator for retinoid or thyroid-hormone receptors
SRC	Proto-oncogene tyrosine-protein kinase
SRP	Surface Plasmon Resonance
ss	Single-stranded
SUMO-1	Small ubiquitin-related modifier 1
SUV39H1	Histone-lysine N-methyltransferase
T	Thymine
TBE	3.3', 5.5'-tetramethylbenzidine
TEMED	N,N,N',N'-Tetramethylethylenediamine
TNF	Tumour necrosis factor
tp53	Tumour suppressor protein
Tris	Tris-(Hydroxymethyl)-Aminomethane
TSGs	Tumour suppressor genes
U	Unit
U	Unite
UV	Ultraviolet
V	Volt (s)
WAF1/CIP1	Cyclin-dependent kinase inhibitor 1
X-Gal	BCIG for 5-bromo-4-chloro-3-indolyl- β -D-galactopyranoside
YY1	Yin Yang 1 is a transcriptional repressor protein
Zn⁺²	Zinc
α	Alpha
γ	Gama
μg	Micro gram
μL	Micro liter
μM	Micromole

ABSTRACT

The word ‘Sirtuin’ or Sir2 proteins are a class of proteins that possess either mono-ADP-ribosyltransferase, or deacylase activity, including deacetylase. SIRT1 is the most studied mammalian Sirtuins and predominantly localised in the nucleus and cytoplasm. Many Sirtuins targets are involved in cancer and in many types of cancers, SIRT1 is found to be overexpressed. Recent observations support SIRT1 being both an oncogene and a tumour suppressor, depending on the cancer etiology and type of tissue. To answer the question “How can SIRT1 behave as a tumour suppressor?”, highly selective ligands (aptamers) were developed against SIRT1 enzyme as the first step towards the development of an alternative chemotherapy for cancer diseases. The objectives of current study are to: (i) produce by *in vitro* SELEX procedures, SIRT1 binding single-stranded DNA (ssDNA) aptamers; (ii) characterise the interactions between selected aptamers and SIRT1 *in vitro* and determine their equilibrium dissociation constant (KD) values and; (iii) investigate the effects of selected aptamers on cancer cell lines. To achieve these objectives, ssDNA aptamers capable of binding SIRT1 enzyme were generated *in vitro* using a sequential approach known as SELEX. A total of eight novel SIRT1 aptamers (circular and linear), four circular aptamers from 8 rounds of circularisation-SELEX procedure, and the other four linear aptamers from 12 rounds of a basic-SELEX procedure were generated.

The initial screening using the Fluor de Lys-SIRT1 assay for SIRT1 enzymatic activity *in vitro* indicated that an activator SIRT1 enzyme (circular3, circular4, linear3 and linear4) were obtained, these aptamers showed acceptable values of K_m and V_{max} to SIRT1 enzyme in kinetic characterisation studies. After equilibrium binding characterisation study of both linear and circular aptamers by SPR, it was show that circular3 and linear3 aptamers are good binder to SIRT1 enzyme, with the low KD constant (27.07 ± 0.959 nM and 48.3 ± 0.986 nM) respectively with highly exhibited stability for circular3 in human plasma.

To investigate the effects of aptamers in cancer cell lines, it has been found that the lung cancer epithelial model A549, the colorectal adenocarcinoma model Caco-2, the liver hepatic model HepG2 were very sensitive with an IC_{50} (0.32, 0.67, 0.2 μ M) respectively. Both breast cancer models (MCF-7 and MDA-MB-468) were highly sensitive with an IC_{50} (0.14 and 0.13 μ M), the very difficult to treat MCF-7 and the extremely challenging oestrogen negative MDA-MB-468 proved to be substantially sensitive with the longer exposure. A special mention should be the osteosarcoma model U2OS, this cancer is very prevalent as bone cancer in children and adults over 60 years of age, with prognosis being related to the cancer stage and

ABSTRACT

current treatment leaving extremely non-desirable side effects, the aptamer was very effective on this cell line with $IC_{50} = 0.06 \mu\text{M}$. Notably, pre-treatment of adult human keratinocyte HaCaT cells with aptamers resulted in markedly decreased cell viability and the $IC_{50} = 0.123 \mu\text{M}$. The most interesting point was that the aptamer was very safe on normal cell line Beas-2b, which indicated that it is safe to non-cancerous tissue.

In conclusion, a pharmacological activation of SIRT1 enhanced cell death suggesting a tumour suppressive function of SIRT1 and the high-affinity SIRT1- aptamers identified in this study may be used in the future for cancer treatment.

1 INTRODUCTION

1.1 Cancer: a Historical Perspective

The earliest known descriptions of cancer appear in several papyri from Ancient Egypt (American Cancer Society, 2009). The Edwin Smith Papyrus was written around 1600 B.C and contains a description of cancer, as well as a procedure to remove breast tumours by cauterisation. It wryly observed that the disease had no cure. The great Greek physician, Hippocrates, recognised as the Father of Medicine, described cancer using the terms *karkinos* “*carcinus*” and “*carcinoma*”. Even though this suggests physicians were aware of cancer, it wasn’t until the 17th century when the origin and progression of cancer become clear. Developments in science and technology have enabled the understanding of a portion of the molecular mechanisms that regulate cancer initiation and progression, which in turn has facilitated developing several therapies for its management and treatment (Kabra, 2010). However, treatment options remain side effects off target effects and deaths attributed to cancer are still a major cause of mortality throughout the world.

Cancer is the second leading cause of death in economically developed countries (following heart diseases). 1 in 3 men in the United Kingdom while 1 in 4 women are at risk for cancer throughout their life time, according to data collected by the National Cancer Research Institutes (NCRI, 2013). To fully combat cancer, continued research into the molecular causes and novel therapies must be completed. Undertaken this task which seems to become more tangible with each passing day as new technologies for this research becomes available.

1.1.1 Carcinogenesis

Carcinogenesis is the formation of a cancer, whereby normal cells are transformed into cancer cells (Hanahan and Weinberg, 2000). While cells in a body undergo a tightly regulated cycle of generation, division and death, cancer cells typically evade cell death and are capable of constant multiplication and expansion (Barrett *et al.*, 1999; Rabindra *et al.*, 2012). Independence in growth signals and insensitivity to growth-inhibitory signals, evasion of apoptosis, sustained replicative ability and angiogenesis, tissue invasion and metastasis are the prominent features of cancerous cells that separate them from normal cells as shown in figure 1.1 (Hanahan and Weinberg, 2000).

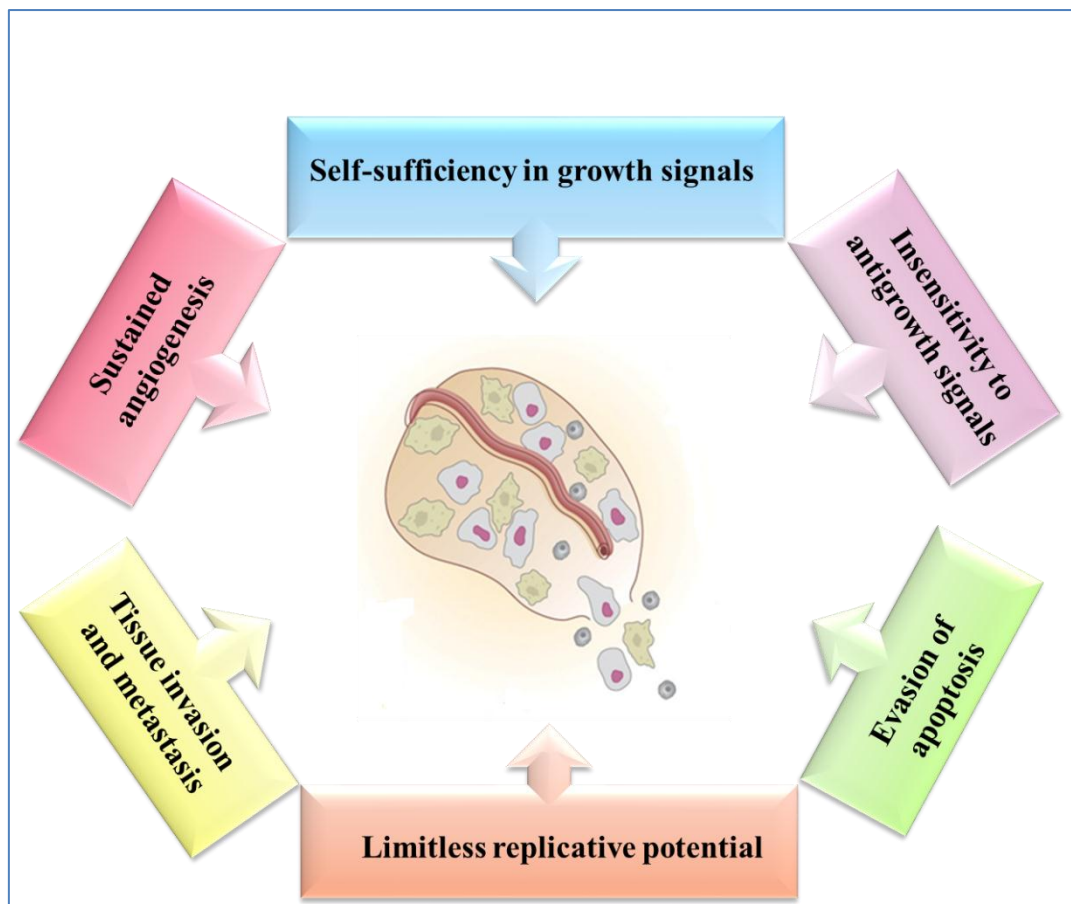


Figure 1.1: Characteristics of Cancer, (Adapted from Hanahan and Weinberg 2000).

Evidence suggests that a single unregulated and genetically unstable cell can cause cancer by multiplying indefinitely and forming clones (Kabra, 2010). After formation of clones, they expand and accumulate genetic mutations, facilitating Darwinian Selection programmed for neoplastic progression of cancer cells in the micro-environment, where they are present (Barrett *et al.*, 1999).

In most cases, cellular transformation is a result of activation of oncogenes or suppression of tumour suppressor genes (Vineis *et al.*, 2010). Cellular oncogenes, also called proto-oncogenes, are normal genes required for important functions in the cell. These genes, however, can be transformed into oncogenes by retroviruses resulting in abnormal cellular proliferation (Lodish *et al.*, 2000). On the other hand, tumour suppressor genes limit cellular transformation. These genes encode proteins that inhibit cell cycle progression, promote DNA damage repair and bring about cell death in the event of mutations or stress (Sherr, 2004). Knudson, (1971) presented the ‘two-hit hypothesis’ according to which carcinogenesis is carried out in a bi-step mutational event, and is valid for a majority of tumour suppressor genes.

According to Maroni *et al.*, (2013) in order for cancer to progress, it needs to lose, mutate or inactivate both alleles of tumour suppressor genes.

Siddiqui *et al.*, (2015) established that initiation, promotion and progression are the three basic steps of carcinogenesis as shown in figure 1.2. During initiation, irreversible changes in the cell which are generally an insult to the DNA of the cell. The most common carcinogens that promote initiation of cancer include aromatic hydrocarbons, radiation (ionising and ultraviolet), retrovirus and other biological substances. These carcinogens can cause multiple mutations in the DNA of the cells such that the DNA repair machinery is impaired. As a result, cell cycle checkpoints are deregulated and the cell divides and proliferates despite the mutations. Tumour promotion involves the proliferation and expansion of the mutant and genetically unstable cell and accumulation of further mutations with each round of cell division such that the resulting population of cells is capable of surviving in normally unsuitable cellular environments (Loftus and Finlay, 2017). The progression step comprises of tumour cells that have attained malignant properties, invasiveness and metastatic capabilities. Mutations that occur during the process of carcinogenesis do not just involve the genetic alteration (deletion, translocation, point mutation, duplication or amplification) of oncogenes or tumour suppressor genes, but can also be epigenetic changes such as modifications of gene promoters by acetylation/deacetylation or methylation/demethylation (Feinberg *et al.*, 2002; Feinberg and Tycko, 2004). Considering the complexity of cancer, it is of utmost importance to investigate the genes that are involved in its manifestation and the molecular mechanisms which explain their deregulation in order to find a cure to the disease.

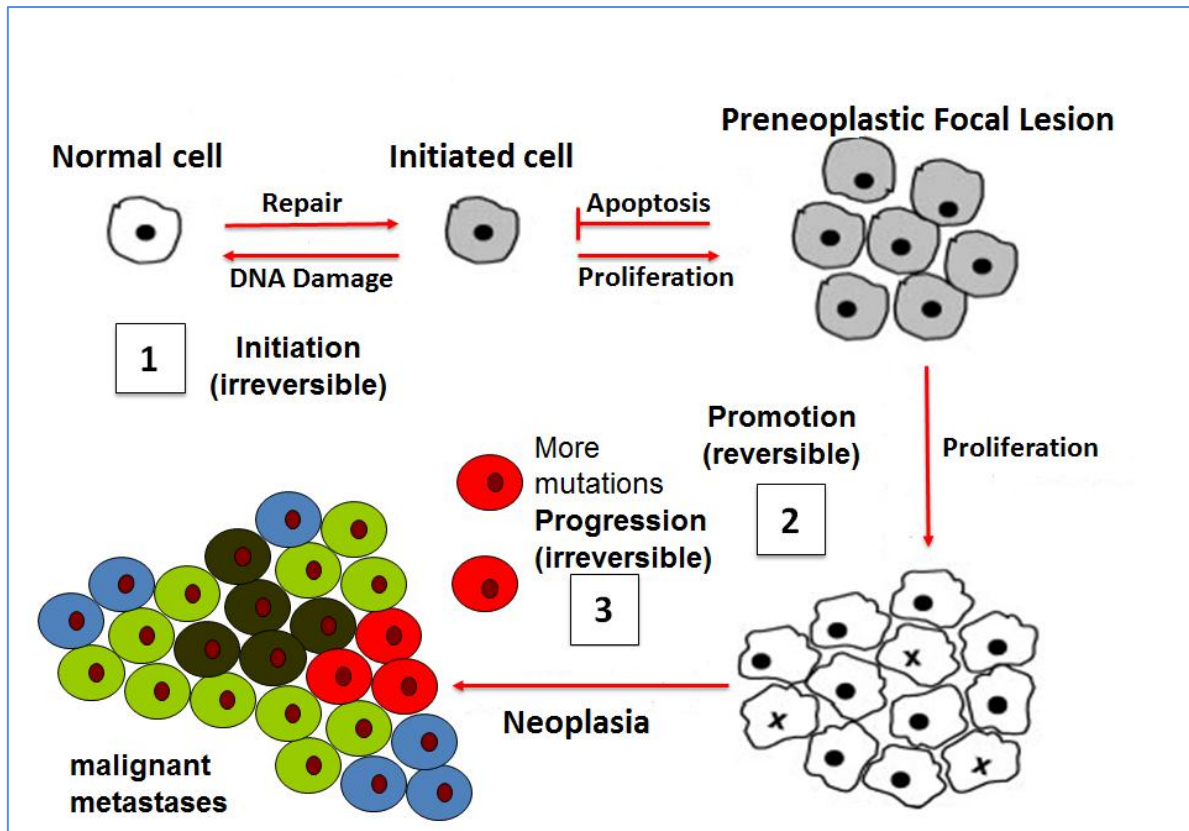


Figure 1.2: Basic steps of carcinogenesis: initiation, promotion and progression. (1) Initiation involves the alteration, change, or mutation of genes arising spontaneously or induced by exposure to a carcinogenic agent. Genetic alterations can result in dysregulation of biochemical signalling pathways associated with cellular proliferation, survival, and differentiation, which can be influenced by a number of factors, including the rate and type of carcinogenic metabolism and the response of the DNA repair function. (2) The promotion stage is a relatively lengthy and reversible process in which actively proliferating paraneoplastic cells accumulate. Progression is the phase between a premalignant lesion and the development of invasive cancer. (3) Progression is the final stage of neoplastic transformation, where genetic and phenotypic changes and cell proliferation occur. This involves a fast increase in the tumour size, where the cells may undergo further mutations with invasive and metastatic potential. Metastasis involves the spread of cancer cells from the primary site to other parts of the body through the bloodstream or the lymph system, (Adapted from Siddiqui *et al.*, 2015).

1.1.2 Tumour Promotion and Tumour Suppression

Tumour genesis is highly influenced by the role of oncogenes and tumour suppressor genes (Avalos *et al.*, 2014). Cells contain many normal genes that are involved in regulating cell proliferation. Some of these genes can be mutated to forms that promote uncontrolled cell proliferation. The normal forms of these genes are called proto-oncogenes, while the mutated, cancer-causing forms are called oncogenes. Oncogenes actively promote proliferation (analogous to the gas pedal of cell cycle). Mutations that convert proto-oncogenes to oncogenes typically increase the activity of the encoded protein or increase the expression of the normal gene. Such mutations are dominant or gain-of-function mutations. Therefore, only one copy of the gene needs to be mutated in order to promote cancer. Posttranslational modifications of the

protein such as phosphorylation can contribute to its stability and constitutive expression which may lead to enhanced cell cycle progression and proliferation. (Seth, 2006), figure 1.3 demonstrates the cell cycle.

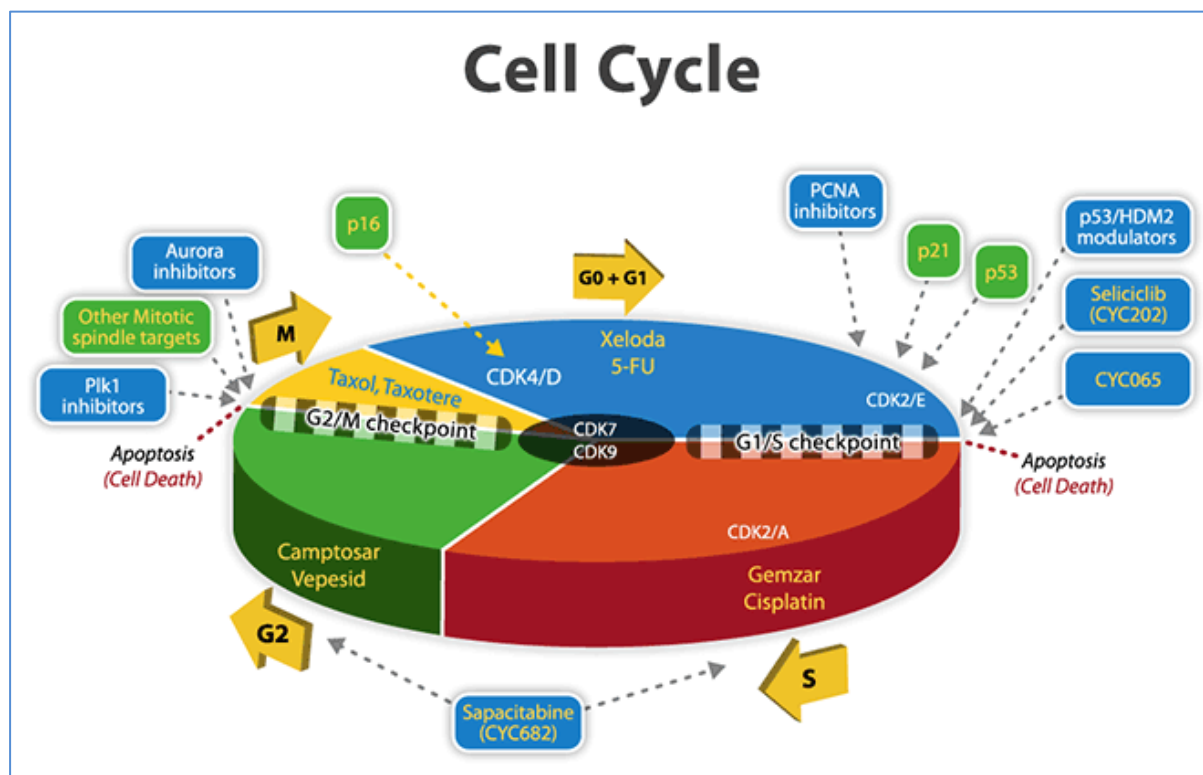


Figure 1.3: Cell cycle. The cell cycle is composed of four phases: G1 phase (Gap 1), in which the cell grows and prepares to synthesize DNA; S phase (DNA Synthesis), in which the cell synthesizes DNA; G2 or second gap (Gap 2), in which the cell prepares to divide and; M phase (Mitosis), in which cell division occurs, (adapted from Murray, 2004).

Alterations in tissue specific expression profiles can also cause the gene to behave as an oncogene. Some examples of oncogenic protein products include RAS, SRC, MYC. Milburn *et al.*, (1990) established RAS is a small GTPase switch, which is activated only when bound to the GTP and remains inactive while bound to GDP (Lu *et al.*, 2016). The mitogen activated protein kinase (MAPK) pathway is one of the most important pathways whose signal transduction is regulated by the RAS. The MAPK is involved in cellular processes such as proliferation, migration, adhesion and apoptosis. When a constitutively active mutant RAS is overexpressed the signal transduction pathways are deregulated consequently promoting invasion and metastasis. Thus, activating RAS mutations are found in several types of cancers (Prior, 2012).

The action of the tumour suppressor genes is found to be anti-oncogenic (Milburn *et al.*, 1990). Tumour suppressor genes have a repressive role towards the cell cycle progression and cell division. Their role is to repair the damaged DNA; however, in case of extensive damage they may also initiate apoptosis. Two of the well-known and important tumour suppressors are retinoblastoma susceptibility gene (RB) and p53, they commonly exhibit inactivating mutations and loss of heterozygosity (LOH, is a common genetic event in cancer development) in the manifestation of most cancers (Knudson, 1971). TP53 gene encodes p53 as a transcription factor (Lane, 1992). p53 is found in cells in low quantities, however, upon DNA damage or stress, it is secreted in large quantities and activated to transcriptionally induce various genes that take part in cell cycle check-points or cell death e.g. WAF1/CIP1 and BAX (Giono and Manfredi, 2006). RB is a cell cycle inhibiting protein, which undergoes alterations after translation for regulation of its activation. RB would efficiently bind to E2F1/DP1 inhibiting their transcriptional function in its hypophosphorylated state (between M and G1); hence, is considered in such a state (Neganova and Lako, 2008). The cyclins and CDK proteins hyperphosphorylate RB during cell transition from G1 to S phase, the RB is inactivated and dissociates from the E2F1/DP1 complex. Consequently, transcription of genes having functional roles in cell cycle progression and division starts. Throughout S, G2 and M phases RB is hyperphosphorylated (Fattaey *et al.*, 1993; Henley and Dick, 2012). Histone deacetylases (HDACs) is recruited by Rb-E2F1 complex as promoters of E2F1 target genes for silencing their transcription (Lai *et al.*, 1999).

There is a need for continued research in tumour promotion and suppression, as its causes are still unclear. Progress in biological research has helped discover and analyse new genes for role in tumourigenesis.

1.2 Histone Deacetylases

Enzymes which can remove the acetyl group from the ϵ -amino group of lysine residues on histones are known as histone deacetylases (HDACs) (EC 3.5.1.98) (Glawson, 2016). They act as antagonists to histone acetyltransferases (HATs) (EC 2.3.1.48), which are responsible for transferring an acetyl group to the lysine residues (Hannah Wapenaar and Dekker, 2016). DNA condensation and supercoiling is promoted by the histones, which are positively charged proteins and act by tightly binding to the negatively charged DNA. When lysine residues are acetylated the positively charged histones are neutralised talking in terms of charge relaxing

the DNA-histone interaction as shown in figure 1.4. An actively transcribing region, where transcription factors and other proteins can bind to the DNA, is marked by this relaxation. HDACs increase the positivity of the histones by removal of acetyl groups, which makes their bond with DNA strong and consequently transcription is stopped. The ‘Histone Code’ is a combination of histone modifications like methylation, phosphorylation, ubiquitination and acetylation, the histone code greatly impacts Histone-DNA and Histone-protein interactions (Strahl and Allis, 2000; Jenuwein and Allis, 2001).

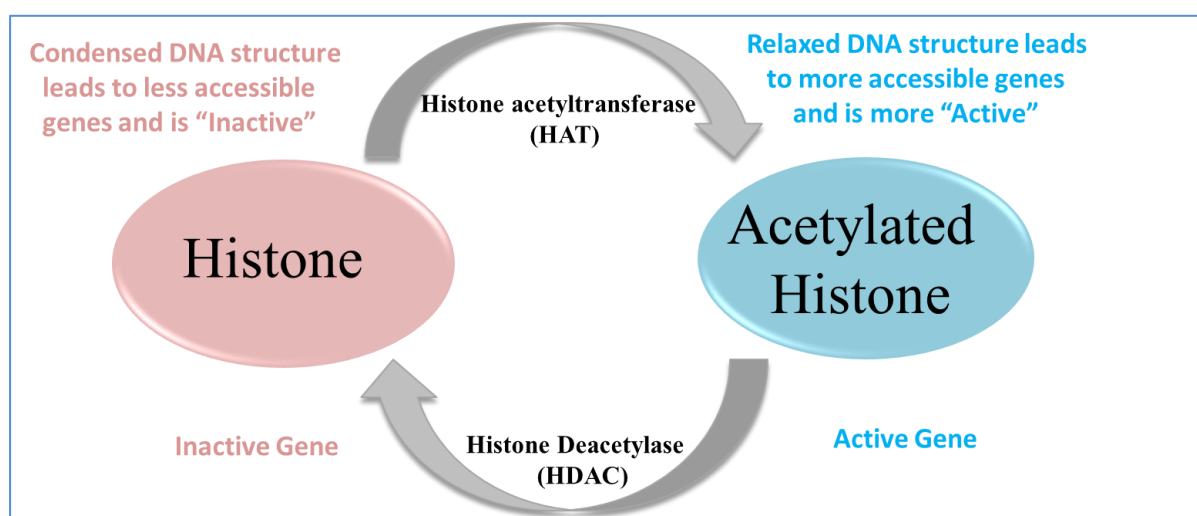


Figure 1.4: Histone modification: acetylation, (adapted from Mau and Yung, 2014).

All the acetylated Lys9 on histone H3; acetylated Lys16 on histone H4 and methylated lys4 on histone H4 are closely related to the transcriptionally active DNA. Gu and Roeder, (1997) discovered that some non-histone proteins were also acetylated by HATs, proposing that the HATs and HDACs are not restricted to modifications of histones. Numerous transcription factors having an important role in cancer are found to be regulated by HDACs and HATs.

1.2.1 Classification and Function of Histone Deacetylases

Human histone deacetylases are classified into four classes: Class I, Class II, Class III and Class IV, depending on sequence homology to the yeast original enzymes and domain organisation (Dokmanovic *et al.*, 2007) as demonstrated in table 1.1. Class I, II and IV are considered "classical" HDACs whose activities are inhibited by trichostatin A (TSA) and have a zinc dependent active site, whereas Class III enzymes are a family of NAD⁺-dependent proteins known as Sirtuins and are not affected by TSA (Imai *et al.*, 2000). Homologues to

these three groups are found in yeast having the names: reduced potassium dependency 3 (Rpd3), which corresponds to Class I; histone deacetylase 1 (hda1), corresponding to Class II; and silent information regulator 2 (Sir2), corresponding to Class III. Class IV contains just one isoform (HDAC11), which is not highly homologous with either Rpd3 or hda1 yeast enzymes (Yang and Seto, 2008), and therefore HDAC11 is assigned to its own class. The Class III enzymes are considered a separate type of enzyme and have a different mechanism of action; these enzymes are NAD⁺-dependent, whereas HDACs in other classes require Zn²⁺ as a cofactor (Barneda-Zahonero and Parra, 2012).

Table 1.1: Classification of histone deacetylases depending on sequence homology to the yeast original enzymes. y = yeast, h = human, m = mouse, d = drosophila, c = C. elegans, ch = chicken, ma = maize. (adopted from Marmorstein, 2001).

Class	Members	Properties
I. yRdp3-like	y, ma RPD3; y, h, m, d, c, ch HDAC1	-TSA-sensitive
	y, h, m, d, c, ch HDAC2;	-Tightly associated with regulatory proteins
	y, h, m, d, c, ch HDAC3; yHOS3	-N-terminal deacetylase domain
II. yHda1-like	yHDA1; hHDAC4; hHDAC5;	-TSA-sensitive
	hHDAC6 h, ch HDAC7;	-Tightly associated with regulatory proteins
	h, ch HDAC8; mHDA1;	-C-terminal deacetylase domain
	m, d HDA2; yHOS1; yHOS2	-Shuttles between nucleus and cytoplasm
III. ySir2-like	Ia - ySIR2, hSIRT1, yHST1	-NAD ⁺ -dependant
	Ib - yHST2, hSIRT2, hSIRT3	-Different members are nuclear or cytoplasmic
	Ic - yHST3, yHST4	
	II - hSIRT4	
	III - hSIRT5	
	IV - hSIRT6, hSIRT7	

“Sirtuin” is an alternate name for Class III and consists of SIRT1, 2, 3, 4, 5, 6, 7, which pose close resemblance to yeast Sir2 gene. Class IV consists of HDAC11, which is similar to Class I and Class II (Gregoretta *et al.*, 2004; Glozak and Seto, 2007). Class I and II share sequence similarity and are called the classical HDAC enzymes. Zn²⁺ is required for the catalytic activity of these enzymes. Sirtuins do not share any sequence similarity with the classical HDACs and require NAD⁺ to carry out the enzymatic reaction (Blander and Guarente, 2004). Figure 1.5 illustrates the classification of all classes of HDAC clarifying the catalytic domain for each class. While table 1.2 demonstrates the classification of HDAC depending on members, catalytic sites, subcellular localisation, tissue distribution, substrates, binding partners and knockout phenotype.

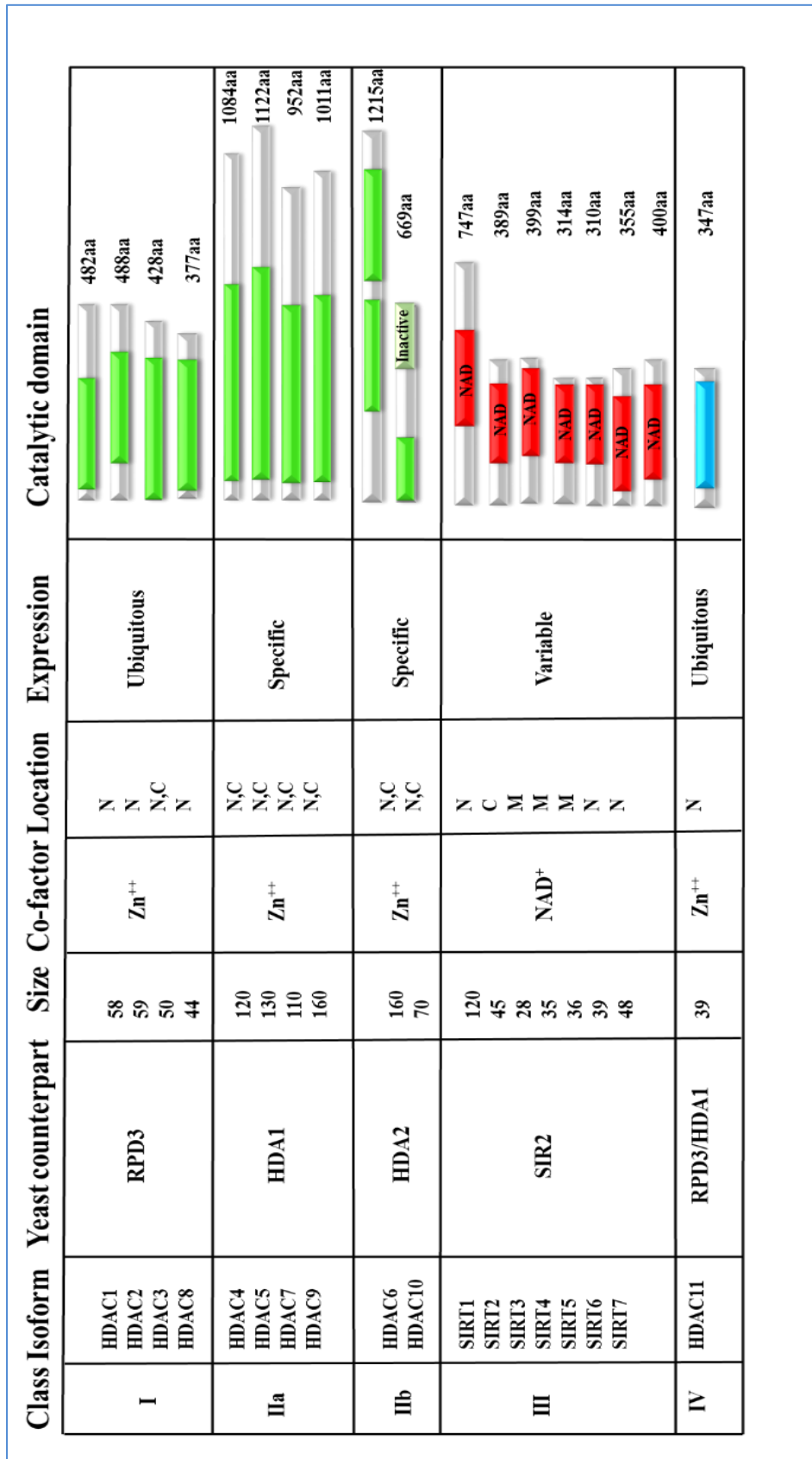


Figure 1.5: Classification of HDAC Class I, II, III and IV, The Bars depict the length of the protein. The catalytic domain is shown in green for class I and II, red in class III and blue in class IV. (adapted from Shiratawa *et al.*, 2013).

Table 1.2: Classification of HDAC depending on members, catalytic sites, subcellular localisation, tissue distribution, substrates, binding partners and knockout phenotype, (adopted from Dokmanovic *et al.*, 2007).

Class	Members	Catalytic sites	Subcellular localisation	Tissue distribution	Substrates	Binding partners	Knockout phenotype
I	HDAC1	1	Nucleus	Ubiquitous	Androgen receptor, SHP, p53, MyoD, E2F1, STAT3	–	embryonic lethal, increased histone acetylation, increase in p21 and p27
	HDAC2	1	Nucleus	Ubiquitous	Glucocorticoid receptor, YY1, BCL6, STAT3	–	Cardiac defect
	HDAC3	1	Nucleus	Ubiquitous	SHP, YY1, GATA1, RELA, STAT3, MEF2D	–	–
	HDAC8	1	Nucleus/cytoplasm	Ubiquitous?	–	EST1B	–
IIA	HDAC4	1	Nucleus / cytoplasm	heart, skeletal muscle, brain	GCMA, GATA1, HP1	RFXANK	Defects in chondrocyte differentiation
	HDAC5	1	Nucleus / cytoplasm	heart, skeletal muscle, brain	GCMA, SMAD7, HP1	REA, Oestrogen receptor	Cardiac defect
	HDAC7	1	Nucleus / cytoplasm / mitochondria	heart, skeletal muscle, pancreas, placenta	PLAG1, PLAG2	HIF1A, BCL6, endothelin receptor, ACTN1, ACTN4, androgen receptor, Tip60	Maintenance of vascular integrity, increase in MMP10
	HDAC9	1	Nucleus / cytoplasm	brain, skeletal muscle	–	FOXP3	Cardiac defect
IIB	HDAC6	2	Mostly cytoplasm	heart, liver, kidney, placenta	α -Tubulin, HSP90, SHP, SMAD7	RUNX2	–
	HDAC10	1	Mostly cytoplasm	liver, spleen, kidney	–	–	–
III	Sirtuins in mammals (SIRT1, SIRT2, SIRT3, SIRT4, SIRT5, SIRT6, SIRT7)	Details in table 1.3 page19	Details in table 1.3 page19	Details in table 1.3 page19	Details in table 1.3 page19	Details in table 1.3 page19	–
	Sir2 in the yeast <i>S. cerevisiae</i>	–	–	–	–	–	–
IV	HDAC11	2	Nucleus / cytoplasm	brain, heart, skeletal muscle, kidney	–	–	–

Class I Histone Deacetylases HDAC 1, 2, 3 and 8 are the members of Class I of histone deacetylase having an N-terminal deacetylase domain and a C-terminal tail. The first histone deacetylase that was identified and then characterised is HDAC1 having an N-terminal deacetylase domain and a C-terminal tail which contains tandem CK-2 phosphorylation sites along with a sumoylation motif (Taunton *et al.*, 1996; Sengupta and Seto, 2004). The function of HDAC1 is improved by its phosphorylation, the mutation of the phosphorylation sites prevents the enzymatic activity and disables the protein to form complexes with other corepressors (Pflum *et al.*, 2001). HDAC1 and 2 are usually a part of protein complexes that are recruited to the DNA by DNA binding proteins and these protein complexes enhance the enzymatic activity of HDACs. Three such complexes have been identified, namely, Sin3 (is an evolutionarily conserved corepressor that exists in different complexes with the histone deacetylases HDAC1 and HDAC2) (Grzenda *et al.*, 2009), NuRD (Nucleosome remodeling deacetylase complex, is a group of associated proteins with both ATP-dependent chromatin remodeling and histone deacetylase activities) (Denslow and Wade, 2007) and CoREST (is encoded protein binds to the C-terminal domain of REST (repressor element-1 silencing transcription factor)) (Grozinger and Schreiber, 2002; You *et al.*, 2001) which mediate chromatin modification and transcription repression by deacetylation and methylation and hence play a significant role in maintaining cell cycle progression, genomic stability and homeostasis. Retinoblastoma protein (RB) is another protein to which HDAC1 would associate and inhibit the cell cycle (Luo *et al.*, 1998). Another example of proteins associated with HDAC1 includes DNA methyltransferase1 (DNMT1), a complex is formed by RB and E2F1 (a key transcription factor necessary for cell growth, DNA repair, and differentiation) to repress the transcription from E2F1 target genes (Robertson *et al.*, 2000). However, disruption of both HDAC1 alleles results in embryonic lethality due to proliferation defects. Cyclin-dependent kinase inhibitors p21 and p27 are upregulated in HDAC1-deficient embryos resulting in reduced cellular proliferation and histones H3 and H4 are hyperacetylated thereby causing changes in other histone modifications (Lagger *et al.*, 2002) as shown in figure 1.6.

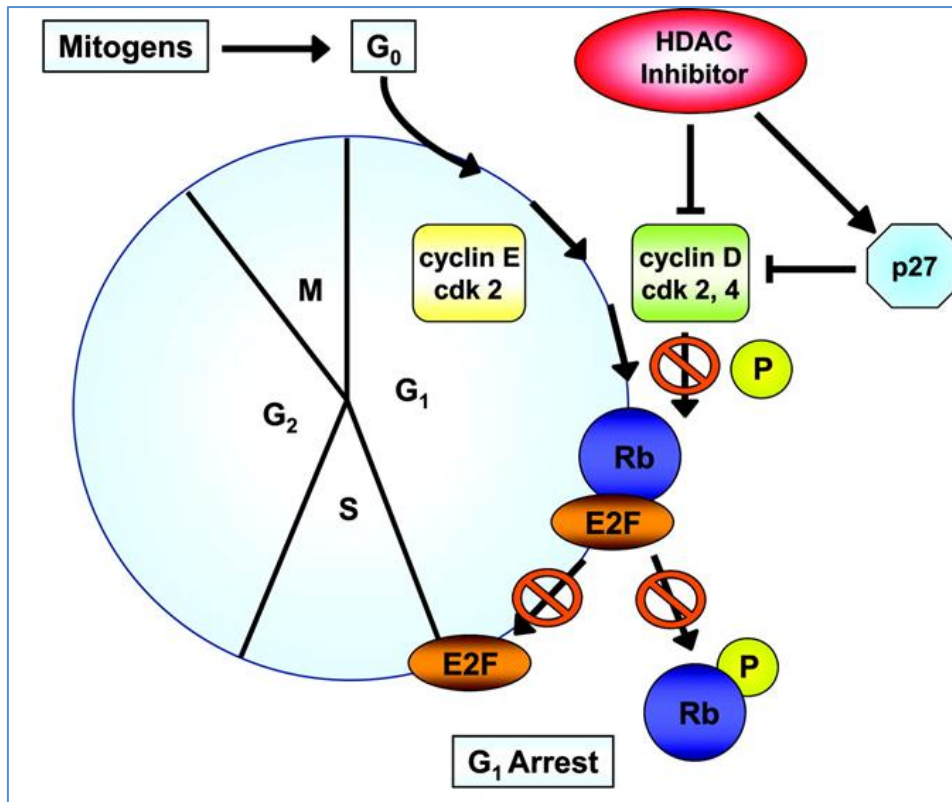


Figure 1.6: HDAC inhibition targets cell cycle progression. Cell cycle progression is dependent on the orchestrated expression, activation and holoenzyme formation of cyclins and CDK. HDAC inhibition blocks cell cycle progression through repression of cyclin D1. Impaired activation of cyclin-CDK complexes inhibits mitogen-induced Rb phosphorylation and downstream activation of E2F-regulated genes, resulting in G₁ arrest. (Findeisen *et al.*, 2011).

Halkidou *et al.*, (2004) identified evidence of HDAC1 upregulation in prostate cancer and relatively a decrease in p21 levels, which promote cellular proliferation. Posttranslational modifications such as sumoylation by SUMO-1 may be used to regulate HDAC1, which would increase the transcriptional repression function of this enzyme (David *et al.*, 2002). Figure 1.7 illustrates the comparison of HDAC1 regulation in normal cells and tumour cells.

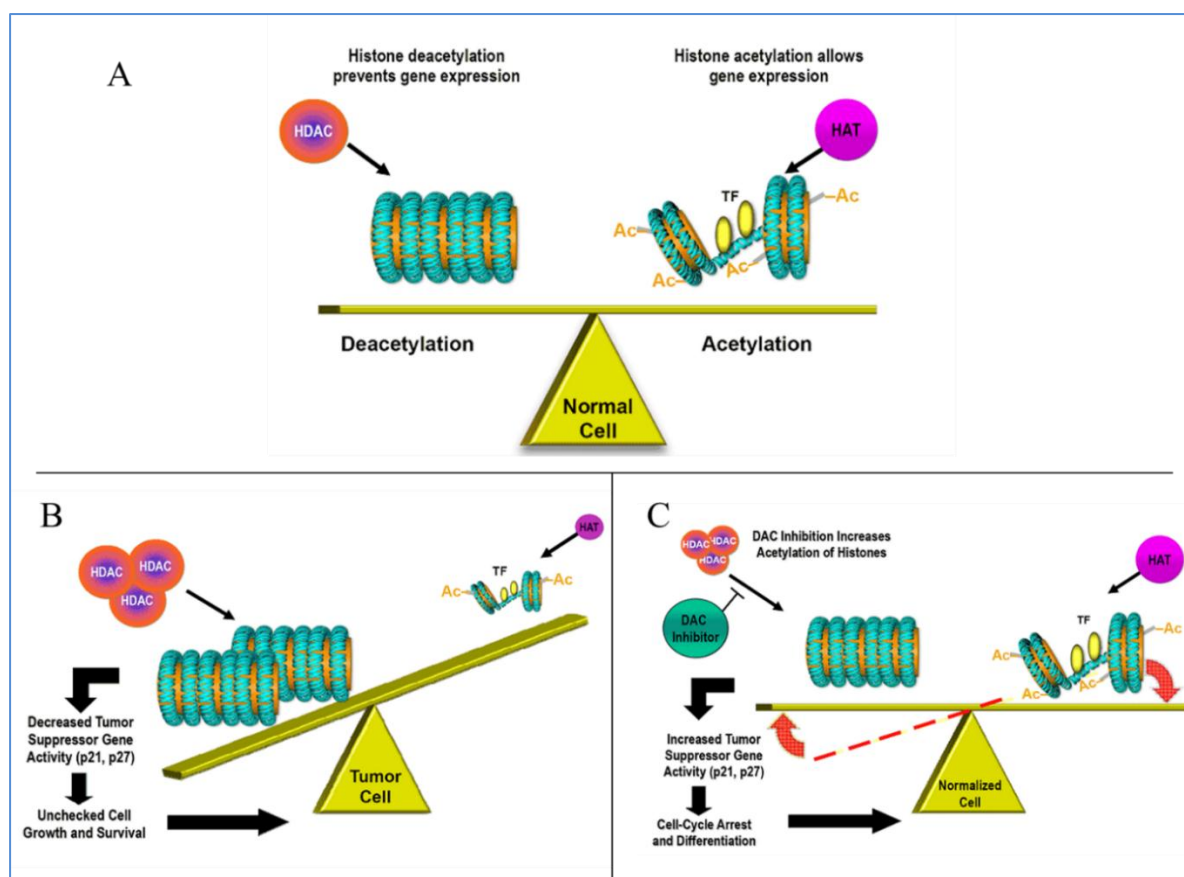


Figure 1.7: The schematic diagram depicts the HDAC1 regulation in normal in vitro. (A) Normal cells, (B) Tumour cells and (C) Normalised cells. AC: Acetyl group, TF: Transcription factors, (Adapted from Alzoubi, 2013).

The sequence of HDAC2 is substantially similar to that of the HDAC1. The HDAC2 can be found in combination with HDAC1 in several protein complexes. It promotes transcriptional repression by interaction with YY1 (Yang *et al.*, 1996). It also carries out transcriptional repression by interactions with DNA methyltransferase DNMT1 (Rountree *et al.*, 2000). The transcriptional function of NF- κ B via association with HDAC1 can be down regulated by HDAC2 (Ashburner *et al.*, 2001). HDAC2 is overexpressed in polyp stage of colorectal carcinoma (Huang *et al.*, 2005). This overexpression is stimulated by loss of the Adenomatous Polyposis Coli (APC) gene (Zhu *et al.*, 2004). The HDAC2 is similar to the HDAC1 in yet another area as its decreased levels are also associated with increased p21 levels and apoptosis (Huang *et al.*, 2005).

The identification and cloning of the HDAC3 was carried out based on its similarity with HDAC8, the fourth member of Class I HDACs, was cloned and characterised based on DAC1 and 2 (Seto1 and Yoshida, 2014). It also binds to YY1 and acts as a transcriptional repressor, similar to HDAC2. The characteristic that differentiates the HDAC3 contains both nuclear

import and export sequences which enable its presence both in the nucleus and in the cytoplasm; whereas both HDAC1 and 2 are only present inside the nucleus (Takami and Nakayama, 2000; Yang *et al.*, 2002). HDAC3 has also been shown to form a stable complex with nuclear hormone receptor corepressor, NCoR (nuclear receptor co-repressor 1, is a transcriptional coregulatory protein which contains several nuclear receptors interacting domains): this interaction improves the repressive activity of the NCoR and the deacetylase activity of HDAC3 by confirming the NCoR (Wen *et al.*, 2000).

HDAC8, the fourth member of Class I HDACs, was cloned and characterised based on sequence similarity to the other Class I histone deacetylases. It is localised within the nucleus like HDAC1 and 2 and its gene encoding is located on the X-chromosome (Buggy *et al.*, 2000; Hu *et al.*, 2000; Van den Wyngaert *et al.*, 2000). Protein kinase A is involved in the phosphorylation, which inhibits the deacetylase activity of HDAC8 and consequently the hyperacetylated histones H3 and H4 are formed (Lee *et al.*, 2004; Yang and Seto, 2008). Its phosphorylation also activates CREB (cyclic AMP-response element-binding protein), which is an important activator of genes for metabolism and survival (Japasia *et al.*, 2009). HDAC8 has the ability to form a complex with CREB and PP1, (a dephosphatase enzyme) to inactivate the CREB transcriptional function. The role of HDAC in transcription regulation is proved to be rather significant (Gao *et al.*, 2009). The cancerous activity in lung, colon and cervix is inhibited by reducing HDAC8 with the help of the siRNA, indicating the role of this enzyme in tumour cell proliferation (Vannini *et al.*, 2004).

Class II Histone Deacetylases are homologous to yeast HDA1 or Histone deacetylase1 and are further classified into two groups: Class IIa and Class IIb which include HDAC 4, 5, 7 and 9 and HDAC6 and 10 respectively. There are extended N-terminus present on the HDACs of Class IIa which contains sites for 14-3-3 and myocyte enhancer factor2 (MEF2, is important regulators of cellular differentiation and consequently play a critical role in embryonic development) binding. The MEF2 binding motif is conserved from *C. elegans* to mammals (Yang and Gregoire, 2005).

The first histone deacetylase to be identified and characterised from this group is the HDAC4. The HDAC4 has the ability to move between the nucleus and cytoplasm by means of active nuclear export. In the nucleus, HDAC4 can associate with MEF2A and repress its transcriptional activation thereby repressing skeletal myogenesis (Miska *et al.*, 1999). The deacetylase activity of the HDAC4 may be regulated by manipulation of its differential

localisation. This enzyme consists of an N-terminal nuclear import sequence and C-terminal nuclear export motif and binds to 14-3-3 facilitating its cytoplasmic localisation (Wang *et al.*, 2000; Wang and Yang, 2001). This histone has a role in the MAPK (mitogen-activated protein kinase, is a type of protein kinase that is specific to the amino acids serine, threonine, and tyrosine) pathway; it is phosphorylated after forming a complex with ERK1/2 (extracellular signal-regulated kinase 2) (Zhou *et al.*, 2000b). Increased levels of nuclear HDAC4 and decreased MEF2-mediated transcription leads to expression of oncogenic RAS.

The HDAC5 is a histone deacetylase that takes part in chromatin modelling during cell differentiation (Verdel and Khochbin, 1999). HDAC5 is also able to move between the nucleus and the cytoplasm like HDAC4. Its cytoplasmic localisation is facilitated by the interaction of enzyme with 14-3-3, which also regulates the enzymatic effect of HDAC5 (Grozing and Schreiber, 2000). It can inhibit the transcriptional function of MEF2 by interacting with it (Lemercier *et al.*, 2000). However, the deacetylase activity of HDAC5 does not directly influence the interaction with MEF2 and the consequent repression, which is facilitated by N-terminal non-deacetylase domain of the HDAC even though a fully functional deacetylase domain is also present. The recruitment of other HDACs (HDAC3 and 4) may be responsible for the repressive function of HDAC5 on MEF2 (Kabra, 2010).

The sequence similarities with the HDAC4 and 5 led to the identification and characterisation of HDAC7 (Fischle *et al.*, 2001). In half of the protein there is a deacetylase domain in the C-terminal while the other half contains NLS (nuclear localisation signal) sequence in the N-terminal. HDAC7 becomes enzymatically active upon interaction with the HDAC3. The interaction is facilitated by the co-repressors SMRT (silencing mediator for retinoid and thyroid receptors) and NCoR as both the HDACs cannot bind directly (Fischle *et al.*, 2001). This enzyme is also able to shuttle between nucleus and cytoplasm; however, the evidence of enzymatic activity is only associated with the nuclear HDAC7 (Fischle *et al.*, 2001). It is phosphorylated by calmodulin kinase I (CAMK I). The cytoplasmic localisation and stabilisation is facilitated by the interaction of the phosphorylated HDAC7 with 14-3-3 (Li *et al.*, 2004).

The sequence similarity with HDAC4 other Class IIa histone deacetylases forms the basis of cloning and characterisation of HDAC9 (Zhou *et al.*, 2001). This enzyme has splice variants 9a, 9b and 9c also known as Histone deacetylase-related protein, HDRP. There is no nuclear localisation sequence in HDAC 9a and 9b but have deacetylase domain in the N-terminal half

of the protein whereas there is no deacetylase domain at all in the 9c or HDRP (also called MITR, is MEF2-interacting transcription repressor) only the NLS sequence (de Ruijter *et al.*, 2003). In order to make up the deficiency of its deacetylase domain HDRP can form a complex with HDAC1 and HDAC3 (Zhou *et al.*, 2000a). In order to repress the MEF2 activity it can form complexes with co-repressor CtBP (COOH-terminal-binding protein) and the other HDACs (Zhang *et al.*, 2001). However, it is interesting to note that there are sites present for binding of MEF2, and it has been discovered that HDAC9 can be transcriptionally activated by MEF2 at the event of muscle cell differentiation. Thus, a negative feedback loop can be speculated between HDAC9 and MEF2 (Haberland *et al.*, 2007).

The HDAC6 and 10 make up the Class IIb. These histones deacetylases are similar to one another but quite different from that of Class IIa. Two tandem catalytic domains are a unique character of HDAC6 (Verdel *et al.*, 2000). HDAC6 is the first histone of the Class to be identified; it is readily available in cytoplasm but may also be found in the nucleus (Verdel *et al.*, 2000). The lack of nuclear localisation is the strong nuclear export signal located N-terminal to the first catalytic domain. There exists a tetra deca peptide repeat domain C-terminal to the second catalytic domain of this HDAC. SE14 (photoperiod-sensitivity gene) is a set of eight repeats, demonstrates the capability of the HDAC to target acetyl microtubule and shows the unique structure which is required for leptomycin-B –resistant cytoplasmic localisation of HDAC6 (Bertos *et al.*, 2004).

The cytoplasmic anchorage of HDAC6 is facilitated by the NES (a nuclear export signal) and SE14. Another unique domain of HDAC6 includes C-terminal to the SE14 repeats, which is a cysteine and histidine-rich domain named ZnF-UBP (zinc-finger ubiquitin binding domain), mostly found in different ubiquitin-specific proteases. Due to this domain HDAC6 can bind with mono- and poly-ubiquitin chains (Seigneurin Berny *et al.*, 2001; Boyault *et al.*, 2006). The proteasomal degradation of the ubiquitinated proteins is highly effected by strong bond between HDAC6 and ubiquitin. For the continuation of processing of ubiquitinated proteins, p97/VCP (valosin-containing protein) can bind to HDAC6 and break its bond from the ubiquitin complex (Boyault *et al.*, 2006). HDAC6 has not been found to deacetylate any histones *in vivo* but there are other substrates of HDAC6, which are non-histone in nature. The α -tubulin in assembled microtubules can be deacetylated by HDAC6 (Hubbert *et al.*, 2002; Matsuyama *et al.*, 2002). Acetylated alpha-tubulin are required by proteins like kinesin-1 for transport of proteins such as JIP1 (a member of the JNK-interacting protein group of scaffold proteins that selectively mediates JNK signaling by aggregating specific components of the

MAPK cascade), the deacetylation of alpha-tubulin proteins disrupts this transport (Reed *et al.*, 2006). The molecular chaperone Hsp90 (heat shock protein 90) is also deacetylated by HDAC6, which mediates the assembly of protein complexes involved in cell signalling (Kovacs *et al.*, 2005). Lack of HDAC6 would cause hyperacetylation of Hsp90, which would cause it to detach from its co-chaperone and loses its ability to form the chaperone complex.

In some cases, there is evidence that the HDAC6 can also be localised in the nucleus deacetylation nuclear targets but mostly it is only present in cytoplasm. The runt-related transcription factor 2 (RUNX2) from the cytoplasm recruits it for promotion of WAF1/CIP1 (cyclin-dependent kinase inhibitor p21) to encode p21 protein in differentiating osteoblasts (Westendorf *et al.*, 2002), establishing that it regulates tissue-specific gene expression.

The sequence similarity with HDAC6 led to the identification of HDAC10 (Fischer *et al.*, 2002; Guardiola and Yao, 2002). Similar to HDAC6 it has two catalytic domains; however, C-terminal catalytic domain is functionally inactive, it is localised both within the nucleus and in the cytoplasm and contains alternatively spliced variants (Fischer *et al.*, 2002; Guardiola and Yao, 2002; Kao *et al.*, 2002). There is evidence of its role in transcriptional repression as it is able to interact with HDAC2 and SMRT complexes (Fischer *et al.*, 2002).

The structure, enzymatic activity, localisation and function of the Class I and II histones differentiate them from Sirtuins, which are homologous to the proteins encoded by the yeast SIR genes as shown in figure 1.8 and table 1.3.

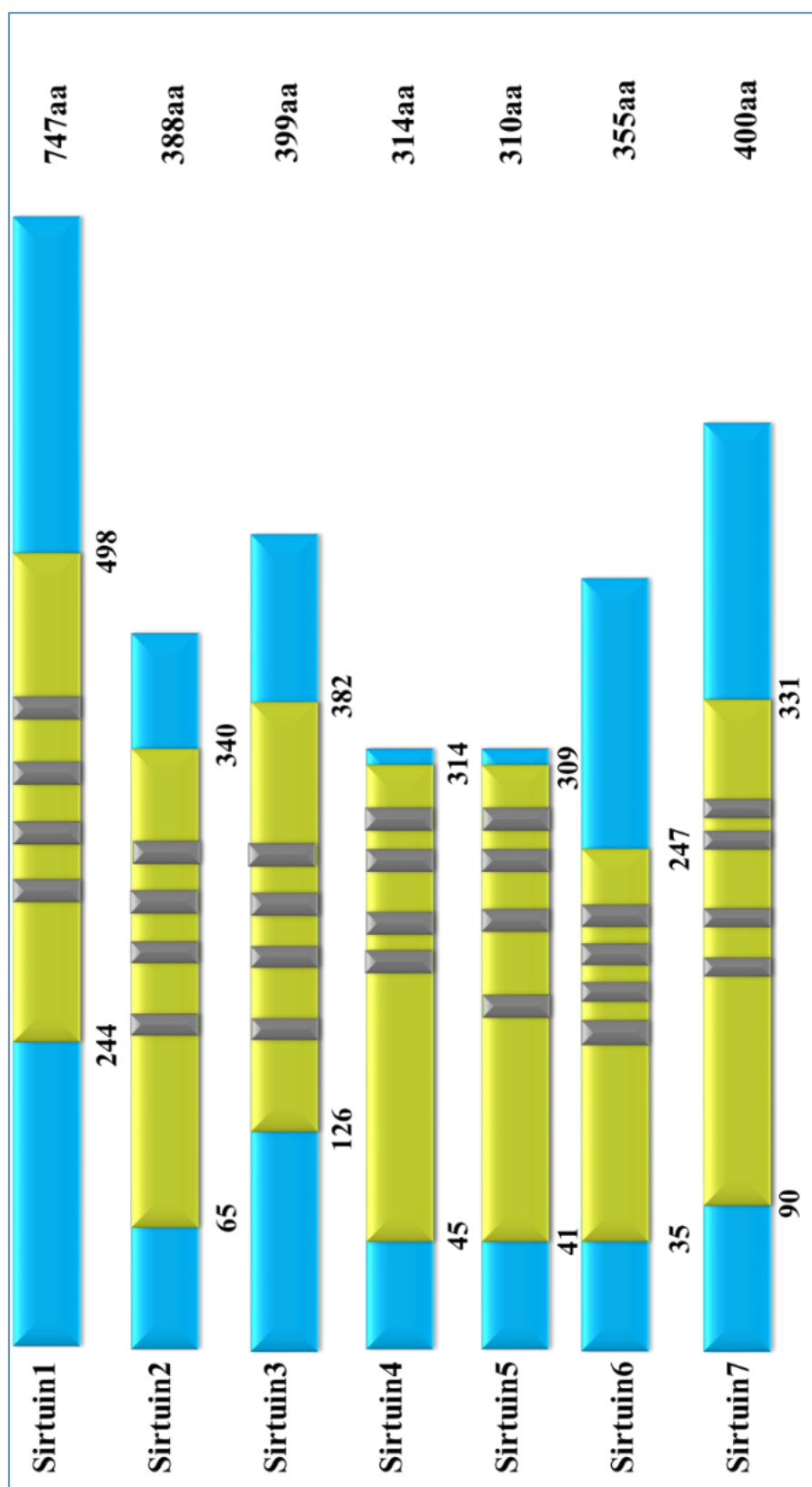


Figure 1.8: Schematic representation of the class III HDACs (Sirtuins). The Sirtuins are highly conserved nicotinamide adenine dinucleotide (NAD⁺) dependent protein deacetylases (DAC) or ADP-ribosyltransferases (ART) which can be subdivided into four classes based on their phylogenetic lineage. The subcellular localisation, DAC or ART binding domains (green) and zinc binding domains (dark grey) are depicted. “aa” is amino acid (adapted from Michan and Sinclair, 2007).

Table 1.3: The mammalian Sirtuins (McGuinness *et al.*, 2011).

	Enzymatic activity	Localisation	Substrates/targets	Function
SIRT1	Deacetylase	Nuclear/cytoplasmic	p53, FOXO, NF κ B, MyoD, Ku70, LXR, PPAR γ , p300, Tat, PCAF, ER α , AR, SMAD7, PCAF, p73, Sox9, HES1, PGC1 α , HEY2, NcoR/SMRT, E2F1, RelA/p65	Glucose metabolism, fatty-acid and cholesterol metabolism, differentiation, insulin secretion, and neuroprotection
SIRT2	Deacetylase	Nuclear/cytoplasmic	α -tubulin, FOXO	Cell-cycle control, tubulin deacetylation
SIRT3	Deacetylase	Mitochondrial	AceCS2, GDH complex1	ATP production, regulation of mitochondrial proteins deacetylation, and fatty-acid oxidation
SIRT4	ADP-ribosyltransferase	Mitochondrial	GDH, IDE, ANT	Insulin secretion
SIRT5	Deacetylase	Mitochondrial	CPS1	Urea cycle
SIRT6	Deacetylase ADP-ribosyltransferase	Nuclear	NF κ B, Hif1 α , helicase, DNA polymerase β	Telomeres and telomeric functions, DNA repair
SIRT7	Deacetylase	Nuclear	RNA polymerase type I, E1A, SMAD6	RNA polymerase I transcription

Kobayashi *et al.*, (2004) stated the function of the yeast Sir2 gene was to suppress the recombination between copies of tandem repeated rDNA. Aparicio *et al.*, (1991) added that Sir2 was also responsible for silencing genes near the telomeres in *S. cerevisiae*. Later, it was elucidated that the hypoacetylation of the histones at the ϵ -amino group of N-terminal lysine residues caused the silencing of the mating-type loci and telomeres; however, the histone deacetylation *in vivo* is a consequence of overexpression of Sir2 (Meijsing and Ehrenhofer-Murray, 2001). Sir2 and its homologs are found in various organisms, from bacteria to humans, which indicate its relation to an evolutionarily conserved family of genes.

Research on bacterial homolog CobB (bacterial protein that belongs to the sirtuin family) suggested that Sir2 may carry out NAD⁺ -dependent mono-ADP-ribosyltransferase activity (Tsang and Escalante-Semerena, 1998). Up to five human cDNAs that shared close resemblance to yeast Sir2 were discovered by 1999, which enable the scientists to furnish that NAD⁺ can be metabolised by the Sirtuins and they function via mono-ADP-ribosylation of proteins (Frye, 1999). Tanner *et al.*, (2000) demonstrated nicotinamide, deacetylated lysine and 1-O-acetyl-ADP-ribose as the end products as products of Sir2 catalysed the deacetylation reaction of an acetylated lysine residue in presence of NAD⁺.

Hence, it can be said that Sir2 is linked with 2 enzyme mechanisms i.e. deacetylation and NAD⁺ metabolism. This is basis of differentiation between the members of Sir2 family, Sirtuins, and the other two classes of HDACs. First two classes of HDACs require Zn²⁺ for their catalytic function while Sirtuins require NAD⁺.

Sirtuins have been linked with aging in different studies (Sack *et al.*, 2012; Watroba and Szukiewicz, 2016). Poole *et al.*, (2012) found that presence of ERCs (Extra-chromosomal Circles) in yeast cells accelerates aging. The recombination of rDNA repeats leads to the formation of ERCs. Sinclair and Guarente, (1997) concluded that the replication machinery from genomic DNA is balanced down by amplification of ERCs, shortening the life-span of the yeast cells. Fritze *et al.*, (1997) found that transcriptional silencing at the rDNA locus can be induced by Sir2. The life-span of a yeast cell can be increased up to 30% by introducing an extra copy of Sir2, which is done by suppression of rDNA recombination (Kaeberlein *et al.*, 1999). Other scientists also reported increase in life-span of different species by introduction of Sir2, for example *C. elegans* (Tissenbaum and Guarente, 2001) and *Drosophila* (Rogina and Helfand, 2004). Increased life-span upon calorie restriction (CR) has been demonstrated in a variety of organisms from yeast to mammals. (Rogina and Helfand, 2004). Sir2 was found to

play a role in increasing life-span upon CR in yeast. In Sir2 deleted genotypes, CR did not increase life-span in yeast or *Drosophila* suggesting the importance of Sir2 in CR-mediated longevity (Lin *et al.*, 2000; Rogina and Helfand, 2004). Previous studies suggested that CR promoted respiration instead of fermentation which increased the NAD⁺/NADH ratio by decreasing NADH levels thereby stimulating the activity of Sir2 (Lin *et al.*, 2002). However, Riesen and Morgan, (2009) demonstrated that the CR alone can increase the life-span of the yeast cell by reducing the extent and frequency of rDNA recombination without requiring rDNA silencing done by Sir2. Research is being carried out on human Sirtuins-mediated-CR-induced longevity of life-span (Lin *et al.*, 2002).

There are seven members of the mammalian sirtuin family i.e. SIRT 1-7. Each sirtuin is unique with its conserved 275 amino acid catalytic core domain and, particular N and C-terminal sequences and unique cellular localisations, SIRT1, 6 and 7 are predominantly located in nucleus, while Sirtuin3, 4 and 5 are found in mitochondria (Huang *et al.*, 2010). SIRT1 and 2 are also found in cytoplasm (North and Verdin, 2007; Tanno *et al.*, 2007) as illustrated in figure 1.9. Qihuang Jin *et al.*, (2007) were found that SIRT1 was able to partially localise in cytoplasm in certain cell lines and this investigation showed that localisation of SIRT1 in cytoplasm led to increased cell sensitivity to apoptosis. SIRT1 contains two nuclear localisation signals as well as two nuclear exportation signals (Tanno *et al.*, 2007). The balanced functionality of these signals determines the presence of SIRT1 in either the nuclear or the cytoplasmic compartment and explains why SIRT1 location may differ depending on the cell type or tissue evaluated (Canto´ and Auwerx, 2012). For instance, while SIRT1 is mainly found in the nuclear compartment in COS-7 cells (McBurney *et al.*, 2003; Sakamoto *et al.*, 2004), it is abundantly found in the cytosol of rodent β -cells, myotubes and cardiomyocytes (Moynihan *et al.*, 2005; Tanno *et al.*, 2007). While the implications and regulation of SIRT1 shuttling are still largely unknown, some experiments indicate that SIRT1 shuttles from the nuclei to the cytosol upon inhibition of insulin signalling (Tanno *et al.*, 2007). The latter observations suggested a link between SIRT1 activity and the sensing of the metabolic status of the cell (Canto´ and Auwerx, 2012). Research is still being carried on the function of these Sirtuins and this field is still being explored.

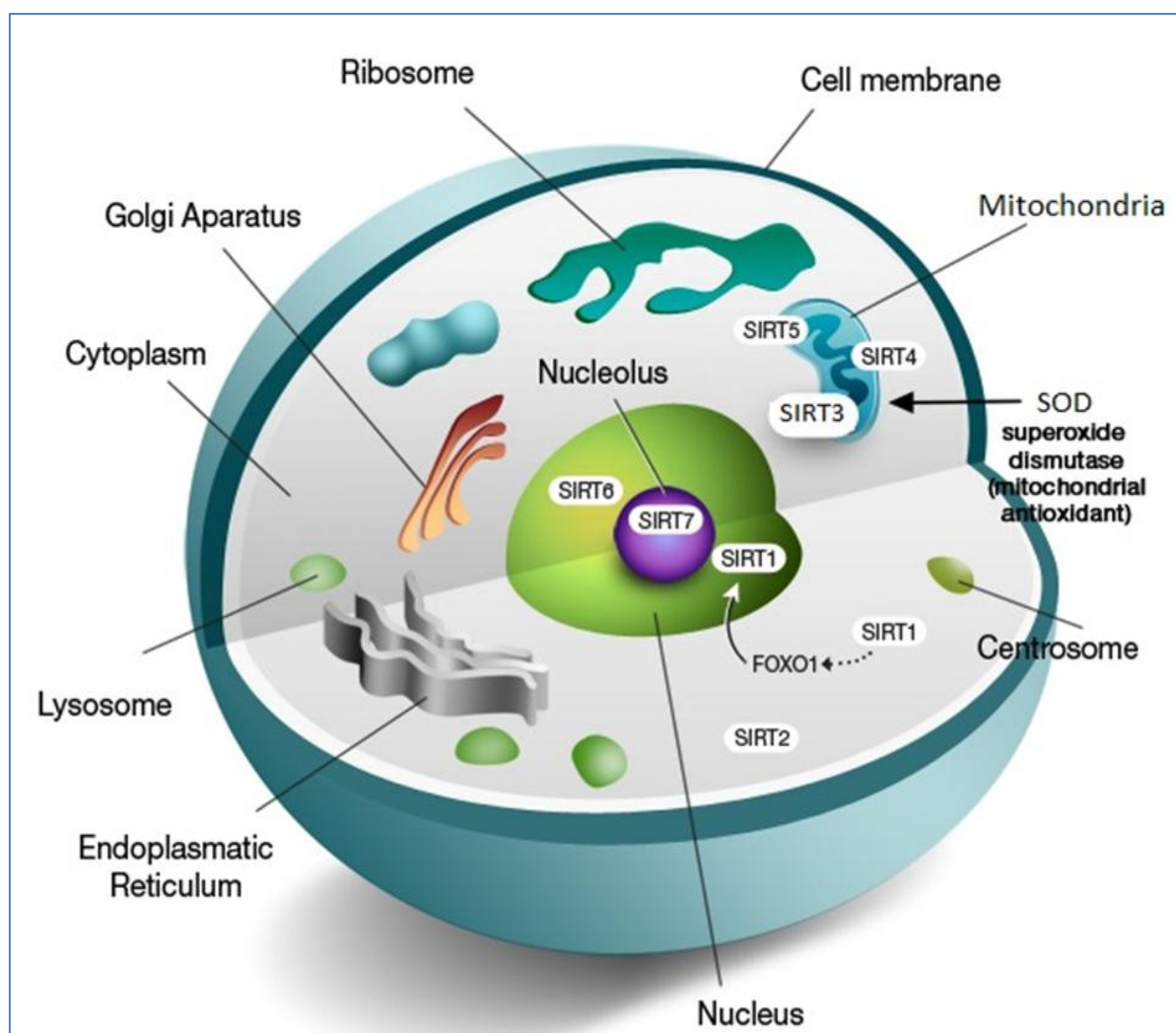


Figure 1.9: The Sirtuins family of histone deacetylases is a family of 7 proteins that all of them except SIRT 4 have been shown to have deacetylase activity (adapted from David, 2013).

HDAC11 belongs to the Class IV Histone Deacetylases that was unravelled when similarities were seen in both class I and II HDACs in the core catalytic domain (Gao *et al.*, 2002). It is also located within the nucleus and is only seen in some tissues that suggested that have tissue-specific functions. It is also found to be overexpressed in various cancer cells lines and because of that studies on its role in tumourigenesis are being performed. It is normally located in protein complexes that possess HDAC6 (Gao *et al.*, 2002). HDAC11 is linked to CDT1 (DNA replication factor) that is a rereplication licensing factor. HDAC11 deacetylates CDT1 located at lysine residues assisting with ubiquitinylation and degradation. It also maintains the stability of CDT1 (Glozak and Seto, 2009). It is also responsible for immune activation and is linked with Antigen Presenting Cells (APCs) and functions to inhibit the expression of IL-10 while inducing inflammatory APCs which can prime naïve T cells and re-

establishes responsiveness of tolerant T cells (Villagra *et al.*, 2009). As HDAC11 histone deacetylase has been discovered recently, its functions are still unclear.

1.2.1.1 SIRT1

SIRT1 is the first classified member of human Sirtuin family. Frye, (2000) declared it to be the closest homolog of yeast Sir2 gene, researchers have been focusing on this particular Sirtuin. It is localised in Nucleus and cytoplasm, which then works as a protein deacetylase and acts as an NAD⁺ -dependent histone. 747 amino acids combine to form human SIRT1 which can be split into four chief portions (figure 1.10). Amino acids 1-182 constitute the N-terminal domain, amino acids 183-243 constitute the allosteric site, amino acids 244-498 constitute the catalytic core and amino acids 499-747 constitute the C-terminal domain (Autiero *et al.*, 2009). A single amino acid in SIRT1, Glu²³⁰, located in a structured N-terminal domain, was critical for activation by all previously reported of Sirtuin Activating Compounds STAC scaffolds and a new class of chemically distinct activators (Hubbard *et al.*, 2013). The amino and carboxyl terminal domains have non- α , non- β structure and these disorganised regions of the protein work as flexible linkers with its substrate proteins. It has been determined through anchor analysis that 14 disorganised binding regions for specific substrates are present in SIRT1 (Hubbard *et al.*, 2013).

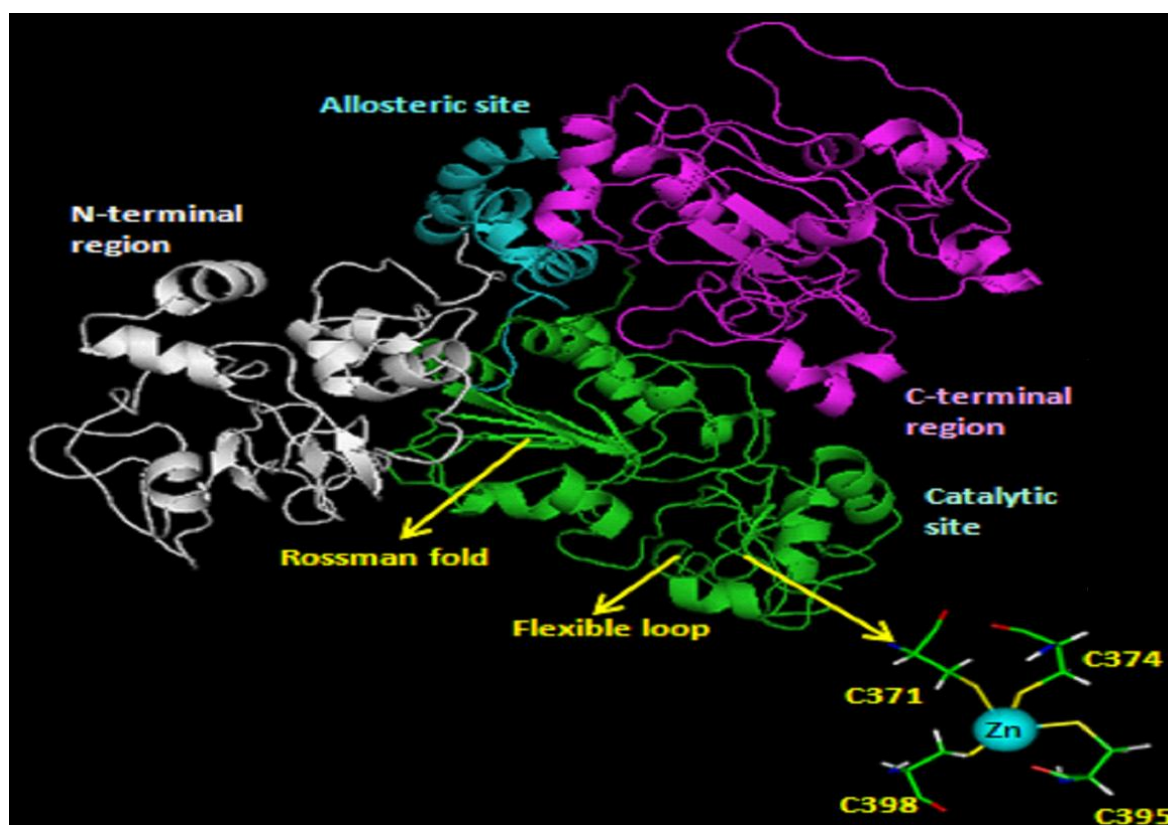


Figure 1.10: Structure of SIRT1 (Autiero *et al.*, 2009).

Knockout experiments in mice have shown that SIRT1 is important for embryonic development (McBurney *et al.*, 2003). It was found that the severity of the phenotype of SIRT1 null mice depended on the genetic background of the mice but in most cases, the loss of SIRT1 was embryonic lethal. However, a very small proportion of SIRT1 null mice were born viable but failed to survive more than a few months beyond birth (Cheng *et al.*, 2003; McBurney *et al.*, 2003). These viable mice had obvious phenotypic abnormalities including smaller size, sterility and eye and heart development defects.

SIRT1 represses transcription by deacetylate histone H3 lys9, histone H4 lys16 and histone H1 lys26, which in their deacetylates form facilitate the condensation and compaction of chromatin (Vaquero *et al.*, 2004). Some of the earliest studies on SIRT1 were carried out on p53, the results showed the deacetylating ability of SIRT1, which led to inhibition of the transcriptional function of p53 (Luo *et al.*, 2001; Vaziri *et al.*, 2001; Langley *et al.*, 2002). Repressing the transcription of p53 gives way to a tumour growth. Recent research, however, has shown that while SIRT1 deacetylates p53, there is no biological outcome of this deacetylation (Kamel *et al.*, 2006; Solomon *et al.*, 2006). SIRT1 is found to regulate and deacetylate other transcription factors such as (i) forkhead family (FOXO) are a family of

transcription factors that play important roles in regulating the expression of genes involved in cell growth, proliferation, differentiation, and longevity (Motta *et al.*, 2004), (ii) Ku70 is a protein that, in humans, is encoded by the XRCC6 gene (Cohen *et al.*, 2004), (iii) Nuclear factor kappa-light-chain-enhancer of activated B cells (NFκB) is a protein complex that controls transcription of DNA (Yeung *et al.*, 2004), cytokine production and cell survival, (iv) E2F1 a key transcription factor necessary for cell growth, DNA repair, and differentiation (Wang *et al.*, 2006) and, (v) Nibrin (NBS1) is a protein which in humans is encoded by the NBN gene (Yuan and Seto, 2007). SIRT1 regulates some major proteins like Peroxisome Proliferator Activated Receptor γ (PPAR γ) and Peroxisome Proliferator-Activated Receptor Gamma co-activator 1-alpha (PGC-1 α) and hence has a crucial role in the metabolic pathways (Picard *et al.*, 2004; Nemoto *et al.*, 2005). Mitochondrial biogenesis and metabolism depend upon SIRT1 in case of calorie restriction. Evidence has shown that SIRT1 levels also influence the insulin signalling pathway (Kloting and Bluher, 2005). In the insulin, resistant cells, low levels of SIRT1 were found, whereas the insulin sensitivity is improved in the cells where SIRT1 is overexpressed, which shows that these genes can be employed in management of Type 2 diabetes (Sun *et al.*, 2007).

1.2.1.2 SIRT2

The molecular mechanism behind SIRT2 cell cycle is poorly understood. A recent study suggested that SIRT2 possesses the ability to localise to the nuclei when the cell is in G2/M phase of mitosis and can deacetylate histone H4 lys16 (Vaquero *et al.*, 2006). It is proposed that it assists with the chromatin condensation before the process of cell division takes place (Inoue *et al.*, 2007). It was also suggested just like SIRT1, SIRT2 also has regulatory capabilities and is known for the regulation of FOXO3 by the process of deacetylation when in stress or when there is calorie restriction (CR). Because of deacylation caused by SIRT2, it promotes FOXO to bind to the DNA which later causes transcription of FOXO target genes to express proteins like manganese superoxide dismutase, p27kip1 and pro-apoptotic BIM. SIRT2 also reduces the production of reactive oxygen species (ROS) in the cell and increases the process of apoptosis when the cell is in stress (Wang *et al.*, 2007). SIRT2 is also cytosolic and has the tendency of preserving deacetylase activity to control various cellular metabolic functions occurring within the body.

SIRT2 lies within the cytoplasm (Perrod *et al.*, 2001). It has both NAD⁺ dependent deacetylase and mono-ADP-ribosyl transferase activity. It causes α -tubulin deacetylation leading to a decrease in the assigned microtubular function within the cell. SIRT2 either works alone or in conjugation with HDAC6 by forming a complex to perform this function (North *et al.*, 2003). Not only that, it is also responsible for providing microtubular stability and producing cell movements. SIRT2 also influences homeobox transcription factor HOXA10 suggesting its effect on mammalian growth by the functions by acting on its proteins by mechanisms that are unknown till now (Bae *et al.*, 2004). SIRT2 overexpression also lengthens the mitotic phase of the cell cycle and a reduction in SIRT2 protein levels helps limiting the period of mitotic cell cycle (Dryden *et al.*, 2003).

1.2.1.3 SIRT3

SIRT3 possesses both NAD⁺ dependent deacetylase as well as ADP-ribosyl transferase activity. It stays within the mitochondria because of N-terminal mitochondrial localisation sequence (Onyango *et al.*, 2002). It was seen that SIRT3 is present within the inner mitochondrial membrane and its levels peak in brown adipose tissues as compared to the white adipose tissues. The levels of SIRT3 mRNA were seen to be increased because of environmental temperature stress and CR within the brown adipose tissues of rodents establishing a role in adaptive thermogenesis (Shi *et al.*, 2005). SIRT3 promotes the expression of the master metabolic regulator PGC-1 α , ATP synthetase and uncoupling protein UCP1 within the inner membrane of the mitochondria leading to activation of mitochondrial genes, oxygen consumption and respiration (Shi *et al.*, 2005). New studies performed established that SIRT3 is both mitochondrial and nuclear Sirtuin. Usually it resides in the nucleus where deacetylation of histone H3 lys9 and histone H4 lys16 take place because it causes inhibition of gene transcription but remains within the mitochondria when stress signals such as UV or etoposides are generated. It is thought that under stress, the nuclear exit of SIRT3 is necessary for rapid activation of nuclear genes that react when in stress (Scher *et al.*, 2007). A study demonstrated functional polymorphism of SIRT3 which is linked to a longer life-span in humans, thus making this the only Sirtuin directly associated to human longevity (Bellizzi *et al.*, 2005).

1.2.1.4 SIRT4

SIRT4 is also located within the mitochondria (Michishita *et al.*, 2005). It acts as an ADP-ribosyl transferase instead of a histone deacetylase (Ahuja *et al.*, 2007). Its expression in pancreas is greatly linked to insulin secretion (Haigis *et al.*, 2006). ADP ribosylation of glutamate dehydrogenase (GDH) occurs when NAD^+ is utilised by SIRT4 for converting glutamate to α -ketoglutarate within the mitochondria of pancreatic β -cells. ADP ribosylation decreases the enzymatic activity of GDH leading to inhibition of glutamate metabolism utilised to produce ATP (Haigis *et al.*, 2006). Since ATP promotes insulin secretion, SIRT4 represses the secretion of insulin from pancreatic β -cells in response to glutamate.

1.2.1.5 SIRT5

SIRT5 is also a mitochondrial deacetylase (Michishita *et al.*, 2005) that is expressed in various tissues (Frye, 1999). SIRT5 has the tendency to deacetylate locally acetylated cytochrome C lying within the mitochondrial inter-membrane space which influences the process of respiration or formation of the apoptosomes (Schlicker *et al.*, 2008). The incomplete knowledge of SIRT5 functions also suggests the deacetylation of CPS1 (carbamoyl phosphate synthases 1) that is an important enzyme in the urea cycle for detoxification of ammonia (Nakagawa *et al.*, 2009). CPS1 (Carbamoyl Phosphate Synthetase I) is regulated by SIRT5. This is seen in cells in fasting conditions when elevated NAD^+ levels increase the breakdown of amino acids leading to increased blood ammonia levels. SIRT5 is thus responsible for ammonia detoxification.

1.2.1.6 SIRT6

SIRT6, exhibits ADP-ribosyl transferase activity as it is a nuclear enzyme (Liszt *et al.*, 2005). It is greatly linked to heterochromatic regions of the nucleus (Michishita *et al.*, 2005). SIRT6 influences base excision repair (BER) and loss of this gene results in age-associated degenerative processes (Mostoslavsky *et al.*, 2006). Latest studies put forward the idea that SIRT6 levels get elevated when the cell gets deprived of nutrients which is because of stabilisation of the proteins. The gene p53 increases the levels of SIRT6 in normal conditions as compared to the stress conditions where it is inhibited (Kanfi *et al.*, 2008). SIRT6 also deacetylates histone H3 lys9 located on telomeric regions of the gene leading to a stabilised

chromatin state in an area where telomeres are located. Mutation of SIRT6 leads to premature senescence and telomeric fusion (Michishita *et al.*, 2008). Furthermore, SIRT6 works in association with the RelA subunit of NFκB and deacetylate histone H3 lys9 located at the NFκB target gene promoters leading to silencing of transcription genes that regulate cellular senescence and apoptosis (Kawahara *et al.*, 2009). Various studies are being carried out on SIRT6 because it is seen to be an important regulator of cellular processes.

1.2.1.7 SIRT7

SIRT7 also is localised within the nucleolus (Michishita *et al.*, 2005). It is a recently discovered Sirtuin, the functions of which have not yet been known. SIRT7 is thought to be a part of the RNA polymerase I transcriptional machinery that causes Pol I transcription. The substrate that acts on the transcriptional machinery is however unknown. Deacetylase activity of SIRT7 and ADP-ribosyl transferase action is also unknown. NAD⁺ is thus required by the cell to activate Pol I machinery by an unknown mechanism (Ford *et al.*, 2006).

1.3 Functions of Mammalian Sirtuins

SIRT1, the best characterised among of mammalian Sirtuins, is a nuclear deacetylase whose substrates include proteins primarily but not exclusively involved in transcriptional regulation, thus influencing diverse aspects of organismal physiology such as differentiation, cell survival, and metabolism (figure 1.11).

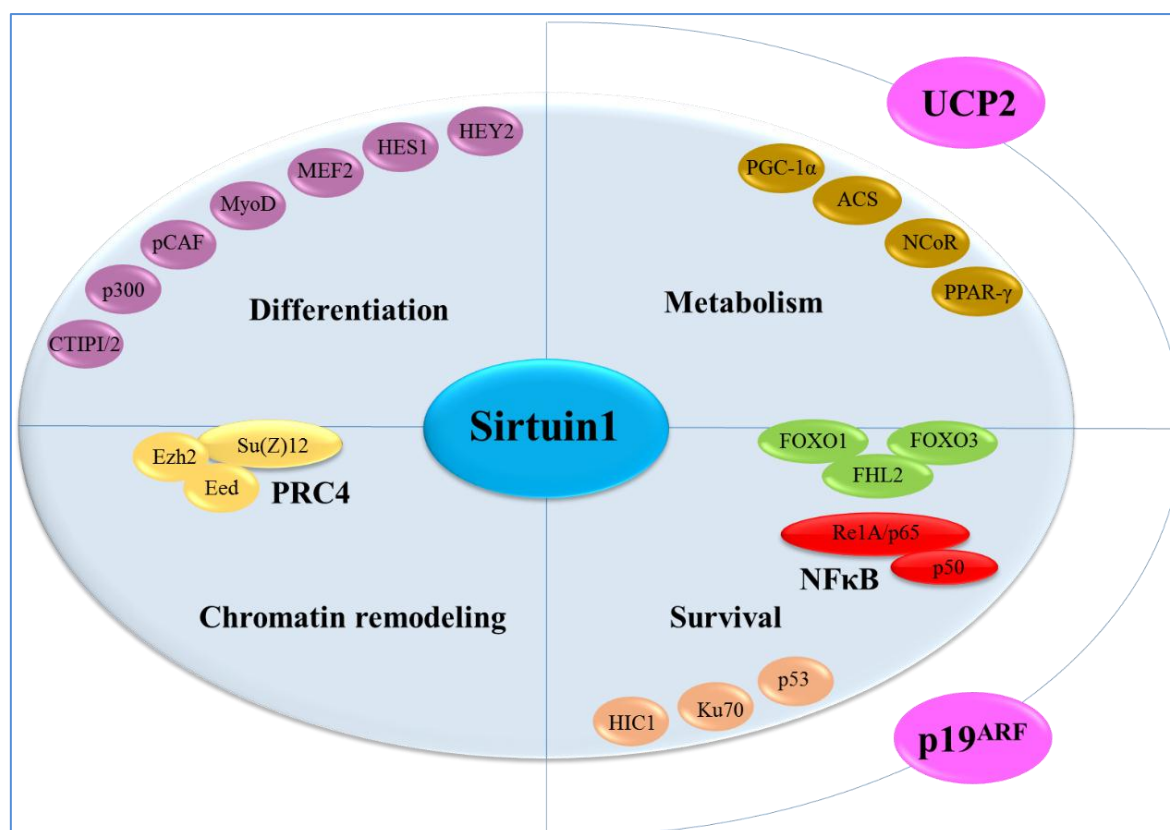


Figure 1.11: Interacting partners, substrates, and downstream effectors of SIRT1 (adapted from Dimitrios and Wilhelm, 2006).

1.3.1 Gene Expression

Histone hypo-acetylation leads to the repression of gene expression (Gallinari *et al.*, 2007). Histone hypo-acetylation by the action of SIRT1, leads to formation of heterochromatin (chromatin but relatively tightly packaged). The deacetylation locations for different proteins are histone protein H1 at the lysine residues 9 and 26, H3 at 14 and H4 at 16. SIRT1 is also responsible for gene expression by targeting transcription factors. TAFI68 [TBP (TATA-box binding protein) associated factor I 68], p300, PACF [p300/cAMP-response-element-binding protein-associated factor], GCN5, MyoD, MEF2 (MADS box transcription factor enhancer factor 2), p19ARF, p53, HIC1, NF- κ B, PGC-1 α , PPAR, aP2, FOXO1, 3a and 4, E2F1, p73, BCA3, Hes1 and Hey2, BCL11A, CTIP2, NCoR, SMRT, UCP2, HIV-Tat (Luo *et al.*, 2001; Muth *et al.*, 2001; Vaziri *et al.*, 2001; Takata *et al.*, 2003; Cheng *et al.*, 2003; Senawong *et al.*, 2003; Fulco *et al.*, 2003; van der Horst *et al.*, 2004; Motta *et al.*, 2004; Cohen *et al.*, 2004; Brunet *et al.*, 2004; Vaquero *et al.*, 2004; Picard *et al.*, 2004; Bae *et al.*, 2004; Yeung *et al.*, 2004; Zhao *et al.*, 2005; Bouras *et al.*, 2005; Chen *et al.*, 2005; Pagans *et al.*, 2005; Senawong *et al.*, 2005; Kobayashi *et al.*, 2005; Chua *et al.*, 2005; Ford *et al.*, 2006; Bordone *et al.*, 2006;

Gao *et al.*, 2006; Nakae *et al.*, 2006; Solomon *et al.*, 2006; Wang *et al.*, 2006; Dai *et al.*, 2007; Gerhart-Hines *et al.*, 2007) are some of the non-histone targets of the SIRT1. The TBP containing complex has constituent component known as TAF168. Transcription done by RNA polymerase I is regulated by a TIF (transcription initiation factor)-IB/SL. RNA Pol I-mediated transcription *in vitro* is repressed when SIRT1 deacetylates the TAF168 decreasing its ability to bind to the DNA (Muth *et al.*, 2001). Acetyltransferase p300 is also inhibited when SIRT1 binds and deacetylates it at lysine 1020 and 1024. Cell differentiation and metabolism are influenced by inhibition of p300, which acts as a limiting transcription cofactor (Wang *et al.*, 2006).

SIRT1 has been associated with epigenetic gene regulation in cancer cells (Liu and McCall, 2013). The polycomb repressive complex 4 (PRC4) carries the SET domain (a protein domain) histone methyltransferase Ezh2 (Enhancer of zeste homolog 2) (Kuzmichev *et al.*, 2005), SIRT1 has been found to be a part of the PRC4 and hence regulates the expression of its target genes as shown in (figure 1.12). There is some evidence that cancer specific epigenetic variations may be caused by PRC4-mediated histone modifications. The histone H1-K26 is also deacetylated by SIRT1, H1-K26 facilitates in spreading hypo-methylated histone H3-K79 and in heterochromatin formation. This shows the importance of SIRT1 in epigenetic modifications of DNA (Vaquero *et al.*, 2004). The cell having low levels of SIRT1 in mammals have reduced levels of H3 tri-MeK9, H4-MeK20 and H4-K16 hyperacetylation (Imai *et al.*, 2000). Reduced levels of H4-K16 acetylation and H4-K20 trimethylation indicate the epigenetic a modification in cancer cells and tumour-derived cell lines (Fraga *et al.*, 2005). Notably, SIRT1 localises specifically to the promoters of tumour suppressor genes whose DNA is hypermethylated and silenced in many cancers (Ghosh, 2000).

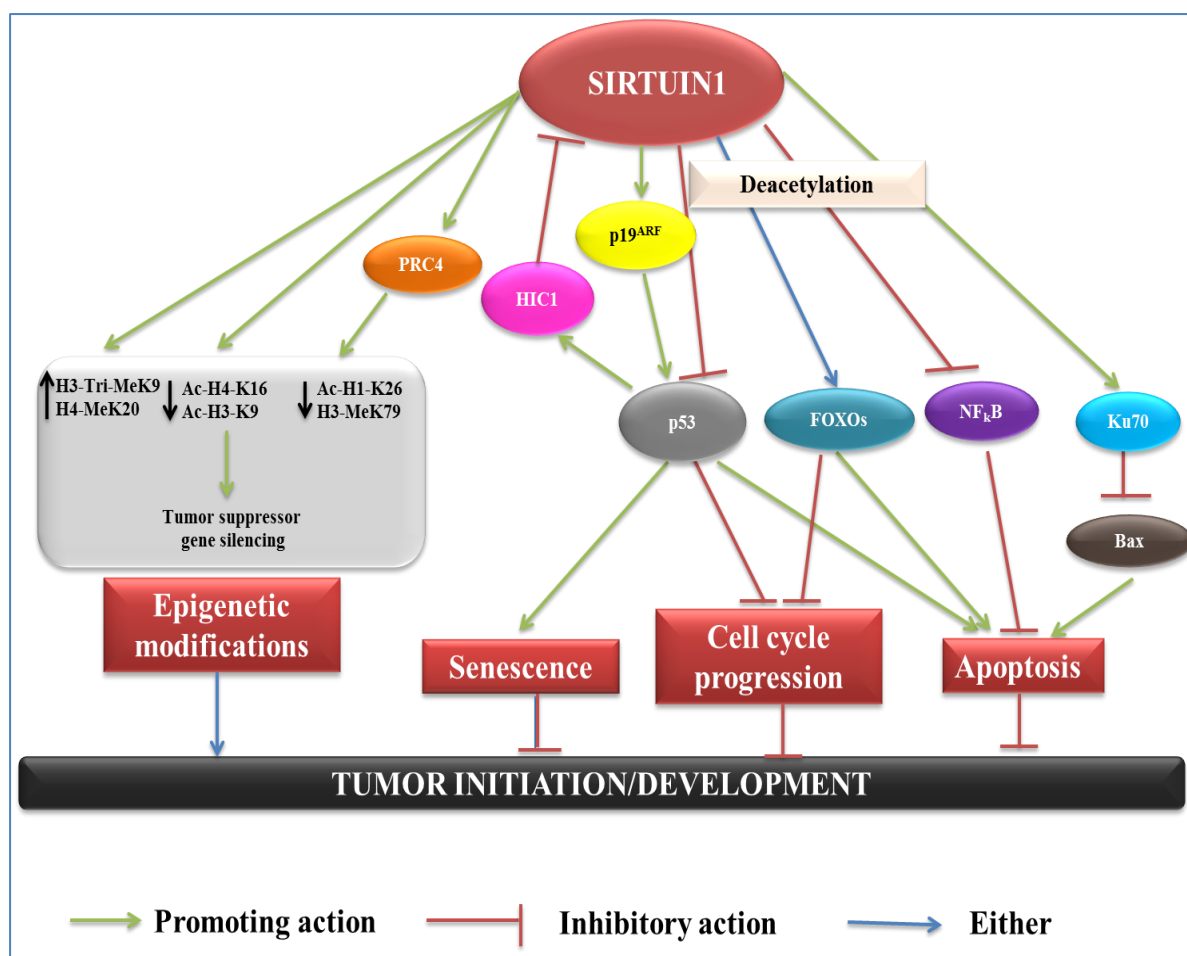


Figure 1.12: Molecular interconnections between SIRT1 and pathways involved in tumour initiation/progression (adapted from Dimitrios and Wilhelm, 2006).

1.3.2 Apoptosis and Cell Survival

SIRT1 plays a role in apoptosis by targeting multiple proteins such as p53, p73, E2F, HIC1 and Ku70. SIRT1 binds the tumour suppressor p53 and deacetylates it at multiple lysine residues, thereby inhibiting p53 transactivation and suppressing apoptosis in response to oxidative stress and DNA damage (figure1.13) (Luo *et al.*, 2001; Vaziri *et al.*, 2001). SIRT1 also binds HIC1 (hypermethylated in cancer 1) transcriptional repressor and mediates the bypass of apoptosis, potentially by promoting cell survival and tumourigenesis via p53. Since HIC1 can repress SIRT1 expression and p53 can trans activate HIC1 transcription, SIRT1, HIC1 and p53 are believed to act in a complex loop where HIC1 represses SIRT1, promoting p53 activity and apoptosis under stress. However, under conditions, where cells are to be recovered from DNA damage, p53 down-regulates HIC1, which induces SIRT1 transcription and promotes cell survival (Ghosh, 2000).

Another mechanism by which SIRT1 regulates apoptosis is by binding and deacetylating the DNA repair factor Ku70. Ku70 acts as an inhibitor of Bax mediated apoptosis. Deacetylated Ku70 complexes with the proapoptotic factor Bax, sequestering it away from mitochondria, thereby blocking it from triggering apoptosis in human embryonic kidney (HEK) 293 cells in response to stress (Cohen *et al.*, 2004). SIRT1 also binds the cell proliferation and cell-cycle regulator, E2F1, and inhibits the apoptotic function of E2F1. On the other hand, E2F1 binds directly to the SIRT1 promoter and induces its transactivation, forming a negative feedback loop between SIRT1 and E2F1 functions. This mutual regulation of SIRT1 and E2F1 protects against DNA damage (Wang *et al.*, 2006). SIRT1 also targets p73, which is a protein involved in apoptosis. The mechanism of binds SIRT1 on p73 is similar to that on p53, as it inhibits p73 mediated apoptosis in (HEK) 293 cells by binding to it and deacetylating it (Dai *et al.*, 2007).

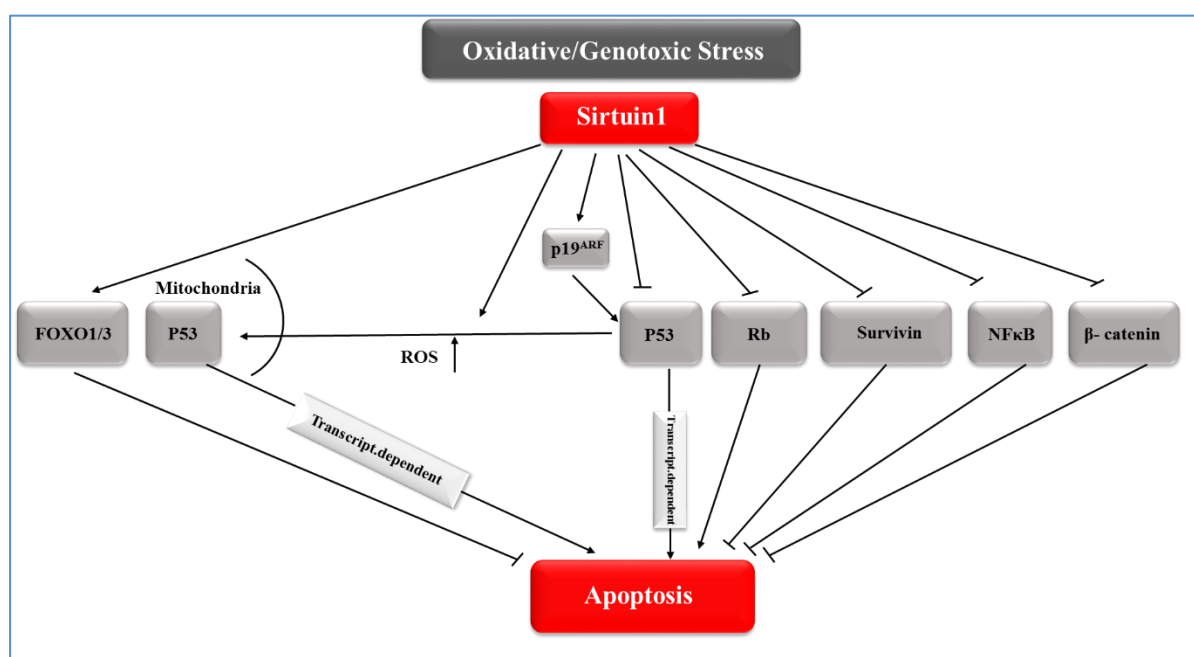


Figure 1.13: SIRT1 and cell survival. Under different forms of stress, Sirtuins control cell fate through, among other mechanisms, modulation of apoptosis. The decision process before a situation is based as a result on a complex net of interactions and targets established by different Sirtuins. The main described mediators and pathways of this Sirtuin-dependent signalling are indicated (adapted from Bosh-Preseque and Vaquero, 2011).

1.3.3 Stress Resistance and Cell Survival

Regulation of Forkhead transcription factors (FOXOs) by SIRT1 signifies its role in cell survival. FOXO1, FOXO3a and FOXO4 are the transcription factors of the forkhead family that can be deacetylated by SIRT1. The expression of DNA repair and cell cycle checkpoint genes is increased and stress induced apoptosis is reduced when FOXO3a in neurons and

fibroblasts is affected by SIRT1 (Brunet *et al.*, 2004; Motta *et al.*, 2004). SIRT1 also deacetylates FOXO4 and rescues its repression under oxidative stress, thereby increasing expression of growth arrest and DNA-damage-inducible 45 (GADD45) (van der Horst *et al.*, 2004; Kobayashi *et al.*, 2005). GADD45 proteins serve as tumour suppressors in response to diverse stimuli, connecting multiple cell signaling modules. Defects in the GADD45 pathway can be related to the initiation and progression of malignancies. Moreover, induction of GADD45 expression is an essential step for mediating anti-cancer activity of multiple chemotherapeutic drugs and the absence of GADD45 might abrogate their effects in cancer cells (Tamura *et al.*, 2012). In transformed cells deacetylation of FOXO4 through SIRT1 suppresses the pro-apoptotic proteases caspase-3 and 7. SIRT1 is localised from nucleus to cytoplasm, by its regulation through caspase-9 and Bcl-xL (Ohsawa *et al.*, 2006).

Action of SIRT1 on FOXO1 provides a defence mechanism for pancreatic β -cells against cytotoxicity induced by glucose (Kitamura *et al.*, 2005). In diabetic patients, chronically high plasma glucose causes cytotoxicity leading to β -cell degeneration. This is believed to be caused by increased mitochondrial oxidation rates, due to higher glucose levels, leading to increased ROS production. In order to prevent apoptosis under these conditions, SIRT1 must sustain FOXO1-mediated transcription of MafA and NeuroD for regulated expression of insulin gene2 (Ghosh, 2007).

1.3.4 Cellular Senescence

Cellular senescence refers to the essentially irreversible arrest of cell proliferation (growth) that occurs when cells experience potentially oncogenic stress (Campisi, 2013). However, there is no clear stance on the role of SIRT1 in cellular senescence. Some studies suggest that in certain cases SIRT1 is found in vicinity of PML (promyelocytic leukemia) inside nuclear bodies. PML proteins act as co-activator or co-repressor for many of the apoptotic transcription factors. Inhibition of the pro-apoptotic factor p53 by SIRT1 facilitates in saving primary mouse embryonic fibroblasts from PML-mediated premature cellular senescence (Langley *et al.*, 2002). On the other hand, evidence of SIRT1 promoting cellular senescence is also present, in SIRT1 null MEFs (mouse embryonic fibroblasts) extended replicative potential and increased proliferation during chronic stress specifically under sub-lethal stress is quite evident (Chua *et al.*, 2005). The level of SIRT1 are seen to decrease in dividing tissue of older mice, such as testis and thymus or other serially passaged cells, however in immortalised cells or post-mitotic

organs no such thing could be observed (Sasaki *et al.*, 2006). Thus, although SIRT1's regulatory role in senescence is conflicting, SIRT1 mediated regulation of senescence may play a significant role regarding tumourigenesis in the elderly and aging.

1.3.5 DNA Repair

The cells are constantly exposed to genomic insults caused by normal cellular processes or genotoxic agents such as ultra-violet (UV) and ionizing radiation (IR). To fight against genomic instability, eukaryotic cells have developed four major DNA damage response (DDR) pathways, including base-excision repair (BER), nucleotide-excision repair (NER), homologous recombination (HR) and non-homologous end joining (NHEJ) (Hoeijmakers, 2001). BER and NER are two repair pathways preferentially for single-strand breaks (SSB) and repair the nucleotides by using the template sister strand. In contrast, for double-strand breaks (DSB), cells are prone to choose either HR or NHEJ. In HR a homologous DNA region from a sister chromatid is used as a template to reconstitute the damaged area (Thompson and Schild, 2001) while NHEJ modifies and ligates the broken DNA ends with little homology (Lieber, 2008). Sirtuins have regulated multiple DNA repair pathways and efficiently maintained genomic stability as shown in figure 1.14 (Zhen *et al.*, 2016).

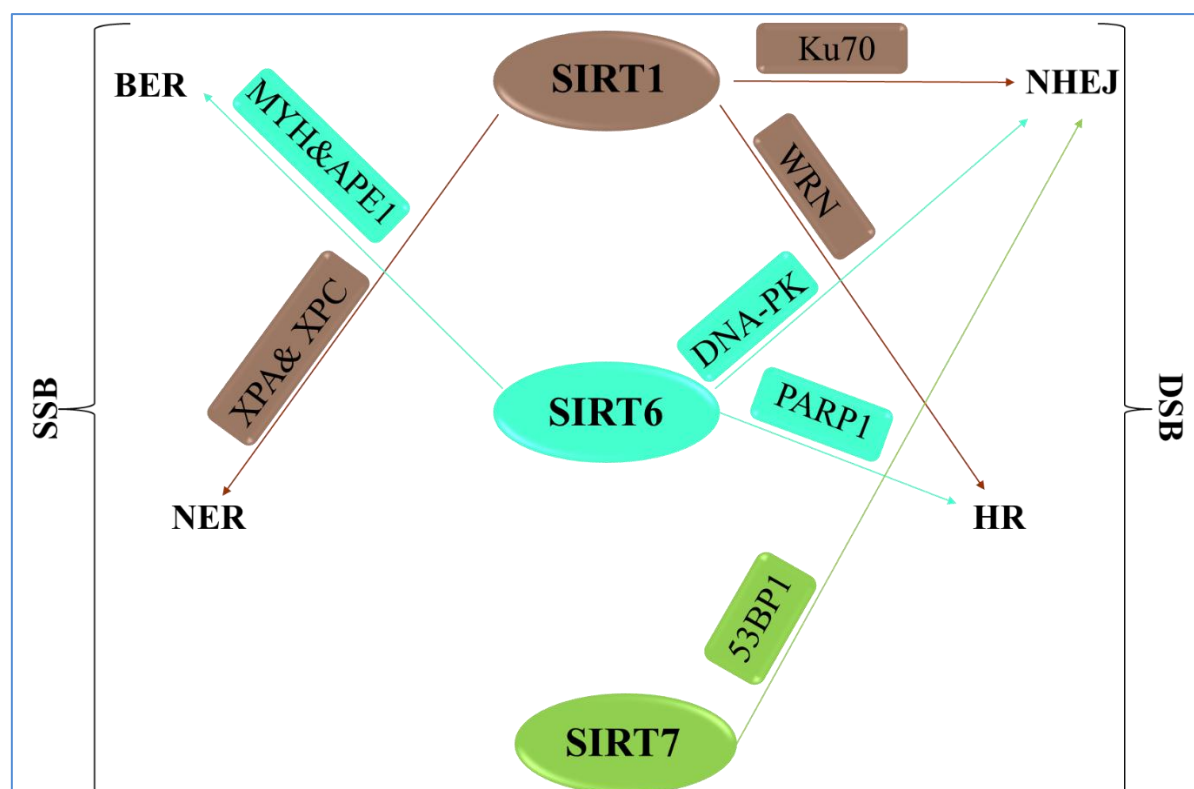


Figure 1.14: Nuclear Sirtuins regulate genomic stability and their roles in the DDR (DNA damage response) are summarised. SIRT1 is implicated in diverse DNA repair pathways. SIRT1 promotes HR (homologous recombination) DNA repair by deacetylating WRN (is a multi-functional protein involving DNA replication, recombination and repair), a DNA helicase. It also regulates NHEJ (non-homologous end joining) and NER (nucleotide-excision repair) through Ku70 and XPA and XPC (xeroderma pigmentosum A and C) after genotoxic stimuli. Like SIRT1, SIRT6 modulates DNA repair pathways at multiple layers. SIRT6 affects BER in a PARP1-dependent manner and recruit's DNA-PK (DNA-dependent protein kinase) to promote NHEJ. It interacts with two major BER enzymes (base excision repair) MYH (MutY homologue, is a DNA glycosylase) and APE1 (Apurinic/aprimidinic endonuclease 1) as well. Most recent study uncovered SIRT7 induce NHEJ by recruiting repair factor 53BP1. (adapted from Zhen *et al.*, 2016).

Recent studies have highlighted a unique feature of SIRT1 in regulating DNA damage repair as well as its role in maintaining telomere length and genomic stability (Rajendran *et al.*, 2011; Zhang *et al.*, 2014; Yamashita *et al.*, 2014). Upon genotoxic stress, SIRT1 moves from silent promoters to sites of DNA damage, deacetylating histones H1 (Lys26) and H4 (Lys16) and contributing to the recruitment of DNA damage factors (Vaquero *et al.*, 2004; Oberdoerffer *et al.*, 2008; Dobbin *et al.*, 2013). SIRT1 is recruited to DSBs (DNA double strand breaks) in an ATM (Ataxia Telangiectasia Mutated) kinase-dependent manner (Jeong and Haigis, 2015). This recruitment is important for histone variant (γ -H2AX) foci formation and accumulation of the DNA damage response DDR-related proteins such as Rad51 (is a eukaryote gene), NBS1 (Nibrin is a protein associated with the repair of double strand breaks (DSBs) which pose serious damage to a genome) and BRCA1 (breast cancer 1) at the breaks.

Important role for SIRT1 in DNA damage repair includes DSB (DNA double strand breaks) repair by HR (homologous recombination) (Oberdoerffer *et al.*, 2008; Uhl *et al.*, 2010). SIRT1 promotes HR by deacetylating WRN, a member of the RecQ DNA helicase family (In prokaryotes RecQ is necessary for plasmid recombination and DNA repair) with functions in maintenance of genomic stability. Another study has reported that SIRT1 interacts with telomere *in vivo* and SIRT1 overexpressed mice display increased HR DNA repair throughout the entire genome (Jeong and Haigis, 2015). Moreover, SIRT1 is also involved in non-homologous end joining (NHEJ) DNA repair. Deacetylation of Ku70 by SIRT1 enhances Ku70-dependent DNA repair and inhibits mitochondrial apoptosis after genotoxic stimuli. SIRT1-dependent KAP1 deacetylation also positively regulates NHEJ (Lin *et al.*, 2015). Results establish the functional significance of KAP1 (KRAB-associated protein-1, is a protein that in humans is encoded by the TRIM28 gene) deacetylation in the DDR, highlighting a potential SIRT1-KAP1 regulatory mechanism for DSB repair that is independent from modulating the infrastructure of the chromatin. Finally, SIRT1 can regulate NER (nucleotide-excision repair) by deacetylating and activating xeroderma pigmentosum A and C proteins (XPA and XPC) upon UV damage. Deacetylated XPA and XPC recognise DNA SSBs and recruit other NER factors at the breaks for DNA repair (Jeong and Haigis, 2015).

1.3.6 Inflammation

By regulation of NF- κ B, SIRT1 also plays a role in inflammation. NF- κ B (nuclear factor kappa-light-chain-enhancer of activated B cells) is a protein complex that controls transcription of DNA, cytokine production and cell survival. The activity of NF- κ B is regulated by SIRT1 by more than one mechanism (Yeung *et al.*, 2004). The transactivation potential of NF- κ B is inhibited by SIRT1 by deacetylation of its subunit RelA/p65 (Yeung *et al.*, 2004). The pro-inflammatory responses mediated by NF- κ B may be increased by cigarette smoke extracts, it is done by decreasing the interaction between SIRT1 and RelA/p65 and subsequent increase in acetylation and activation of NF- κ B (Yang *et al.*, 2007). High levels of SIRT1 have been expressed in calorie restricted rodents, showing decreased inflammatory responses. Anti-inflammatory properties like reduction of the pro-inflammatory cytokine ‘tumour necrosis factor (TNF) has been noticed in SIRT1 activating compounds via a high-throughput screen (Napper *et al.*, 2005).

1.3.7 Development

SIRT1 has been found to have a role in development. McBurney *et al.*, (2003) used a Sir2 knockout transgenic mice model to demonstrate the significance of SIRT1 in embryogenesis and gametogenesis. Under this experiment only 50% of the expected number of off springs were born, out of which only 20% survived to adolescence. Phenotypic defects such as small size, slow development defects in eye morphogenesis and cardiac septation were prevalent in the mice that survived, they were sterile both male and female demonstrating low sperm count and inability to ovulate respectively, which is thought to be caused by hormonal imbalance (McBurney *et al.*, 2003). SIRT1's regulation of the transcriptional repressors Hes1 and Hey2 can help us understand the developmental defects in SIRT1 knockout mice, Hes1 and Hey2 are rather important in development (Takata *et al.*, 2003). Additionally, SIRT1 is found to have a regulatory effect on BCL11A (mammalian protein), which is responsible for the haematopoietic cell development and malignancies (Senawong *et al.*, 2005). The role of SIRT1 in development is confirmed by a report showing markedly high levels of SIRT1 expression in the heart, brain, spinal cord and dorsal root ganglia of embryos (Sakamoto *et al.*, 2004). There is evidence of involvement of other Sirtuins in development as SIRT2 interacts with the homeobox transcription factor, important for embryogenesis, HOXA10 (Bae *et al.*, 2004).

1.3.8 Metabolism

Induction of SIRT1 in fasting tissues such as the brain, fat, kidney, muscle and liver, led to the speculation of a role of SIRT1 played in metabolism (Cohen *et al.*, 2004). SIRT1, SIRT3 and SIRT4 are the three mammalian Sirtuins involved in regulation of metabolism (Nogueiras *et al.*, 2012). SIRT1 plays a role in the regulation of hepatic gluconeogenesis by potentiating FOXO1 activity in hepatocytes to direct glucose metabolism towards gluconeogenesis (Frescas *et al.*, 2005). Deacetylation of PGC-1 α (Peroxisome proliferator-activated receptor gamma coactivator 1-alpha) by SIRT1 leads to repression of glycolysis and promotion of gluconeogenic gene expression (figure 1.15). Up-regulation of PGC-1 α is caused by high levels of NAD⁺ and pyruvate (Rodgers *et al.*, 2005). Mitochondrial function and metabolic homeostasis are regulated by PGC-1 α through SIRT1, increasing the oxygen consumption in muscle fibres and induces oxidative phosphorylation and consequently mitochondrial biogenesis (Rodgers *et al.*, 2005; Lagouge *et al.*, 2006). The mitochondrial membrane potential

is decreased by increase in cellular respiration and production of reactive oxygen species caused by SIRT3 (Shi *et al.*, 2005). The mitochondrial genes such as PGC-1 α , UCP2 (Mitochondrial uncoupling protein 2) and COX (Cyclooxygenase) II and IV and ATP synthetises are also induced by SIRT3. AceCS1 (Acetyl-CoA synthetise) in the cytoplasm and AceCS2 in the mitochondria, convert acetate to acetyl CoA in mammalian cells (Hallows *et al.*, 2006). Acetyl CoA is a micro molecule, which is essential in synthesis of fatty acids and amino acids. SIRT1 deacetylates and activates AceCS1 while SIRT3 is found responsible for deacetylating and activating AceCs2 (Hallows *et al.*, 2006 and Schwer *et al.*, 2006). In the pancreatic cells, amino-acid stimulated insulin secretion is regulated by SIRT4 (Haigis *et al.*, 2006). This Sirtuin is also involved in regulation of glutamate dehydrogenase (GDH) by mono-ADP-ribosylation, which inhibits GDH and decelerates the conversion of ketoglutarate from glutamate.

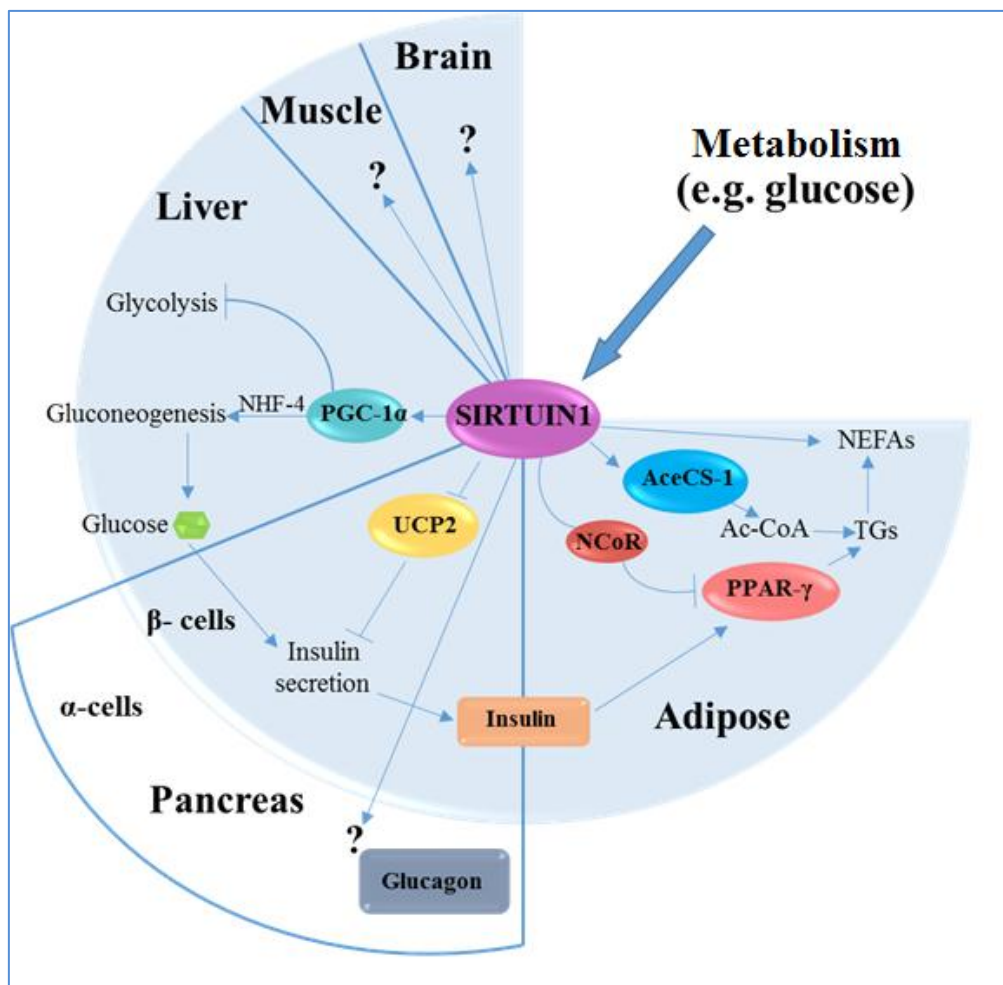


Figure 1.15: Function of SIRT1 in tissues relevant to organismal energy homeostasis (adapted from Dimitrios and Wilhelm, 2006).

In fasting condition, up-regulation of SIRT1 in white adipose tissue (WAT) indicates the potential role of SIRT1 in synthesis and release of fat. The interaction of SIRT1 with PPAR- γ proved its role in fat metabolism by regulating adipogenesis and fat storage (Picard *et al.*, 2004). Moreover, SIRT1 also regulates the levels of the adipocyte derived hormone adiponectin by acting through FOXO1 (Qiao *et al.*, 2006).

1.4 Role of SIRT1 in Regulating Mammalian Aging

The regulation of human longevity by Sirtuins has not been yet elucidated although SIRT1 orthologs in lower organisms have been revealed to play a direct role in it. A positive role of SIRT1 in maintaining mammalian aging has been revealed by the cellular model for aging, which evaluates cellular senescence as a demonstration of aging (Vaziri *et al.*, 2001). A central role in cellular senescence signifying a constructive role of SIRT1 in slowing down cellular senescence is played by p53, which is inactivated and deacetylated by SIRT1 (Luo *et al.*, 2001; Vaziri *et al.*, 2001). P53 acetylation and early senescence induced by promyelocytic leukemia protein (PML) oncogene is repressed by over-expression of SIRT1 in mouse embryonic fibroblasts (MEFs) (Langley *et al.*, 2002). Also, SIRT1 inhibitor, Sirtinol has been shown to trigger senescence in human breast cancer MCF-7 cells and non-small lung cancer H1299 cells (Ota *et al.*, 2006).

Paradoxically, SIRT1 has also been shown to induce replicative senescence as shown in SIRT1 deleted MEFs that show extended replicative lifespan due to failure to upregulate p19^(ARF) and p53 in response to chronic oxidative stress (Chua *et al.*, 2005). These observations suggest that SIRT1 may regulate senescence differently depending on stress conditions and inducing agents. Recently, SIRT1 has been shown to protect against stress-induced senescence-like phenotype in human endothelial cells by acting through p53 (Ota *et al.*, 2007). Moreover, down-regulation of SIRT1 was shown to accelerate an aging-like phenotype in mouse (Sommer *et al.*, 2006). The other positive role of SIRT1 in promoting longevity in the cellular model for aging has been shown to be through the Forkhead proteins. SIRT1 physically binds and deacetylates the FOXO proteins thereby regulating their activity. It has been shown that SIRT1's regulation is required for FOXO mediated cellular stress response to protect cells from oxidative insults.

1.5 SIRT1 Activators

The apparent role of SIRT1 and its orthologs in extending longevity has prompted searching for compounds that can activate SIRT1 since such compounds can potentially extend lifespan in absence of CR or genetic alteration. Resveratrol, the first ever such molecule, a compound synthesised in plants as response to stress was discovered around 1999 (Howitz *et al.*, 2003). Resveratrol, Butein, Quercetin, Piceatannol, and Myrcetin are some of the polyphenol activators of SIRT1 that have been discovered and called the Sirtuin Activating Compounds or STACs (Wood *et al.*, 2004). Subsequently, much more potent and efficacious SIRT1 activators were reported as potential therapeutics for the treatment of diabetes (e.g. SRIT1720, SRT2183, and SRIT1460) (figure 1.16) (Milne *et al.*, 2007; Venkatasubramanian *et al.*, 2016).

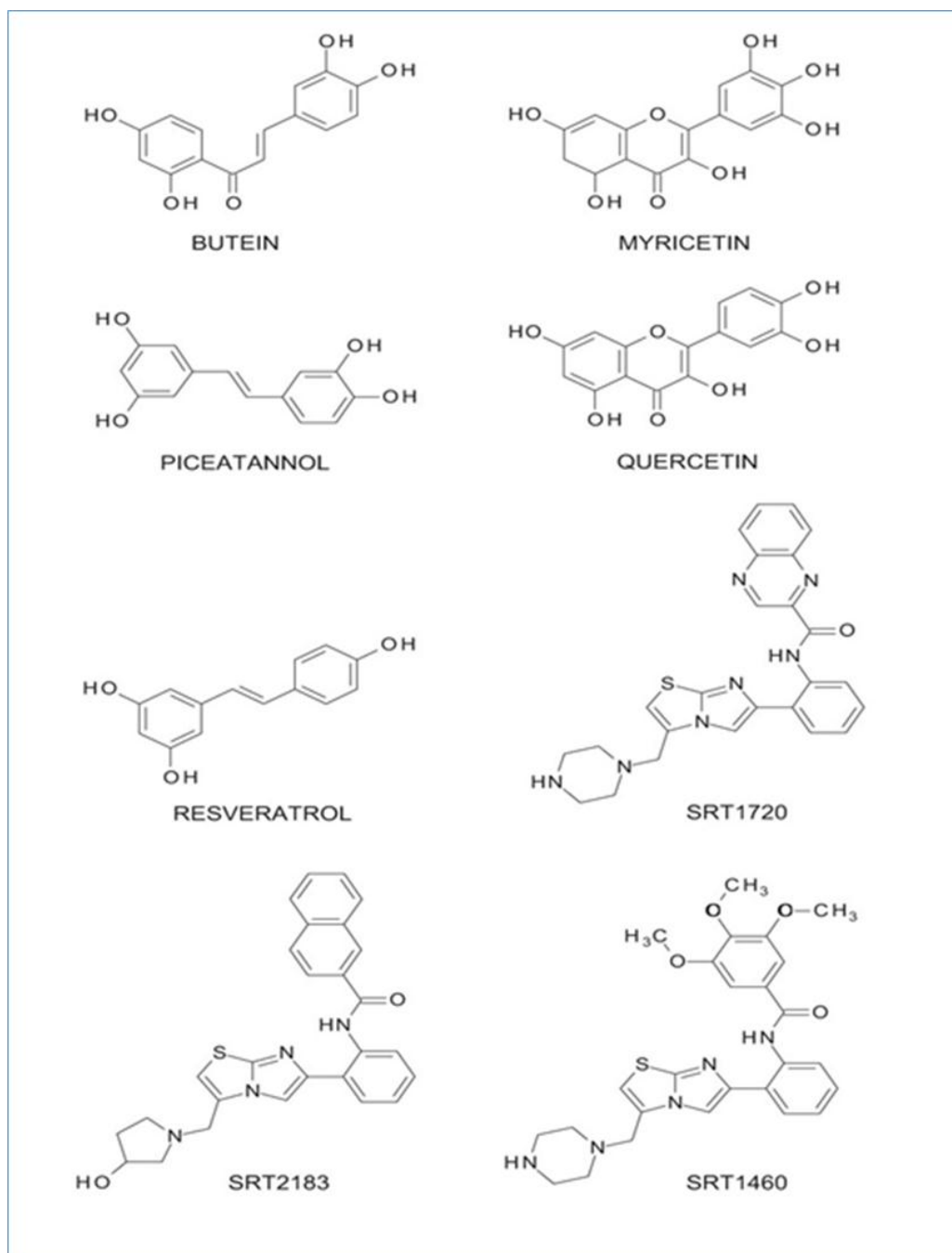


Figure 1.16: Small molecule activators of SIRT1, (adapted from Stünkel and Campbe, 2011).

The catalytic activity of SIRT1 *in vitro* increased upon addition of resveratrol, a polyphenolic compound present in grape skin, and a diversity of plants products like fruits and nuts. Afterwards, imitation of the calorie restriction and extended lifetime in fruit flies, yeast, worms and fish was seen by it (Wood *et al.*, 2004). The mechanism by which resveratrol functions is not yet clear. However, in *S.cerevisiae*, *C. elegans* and *D. melanogaster*, the effect of resveratrol is SIRT1 dependent and is not further extended by CR, indicating that it may act through CR pathway (figure 1.17).

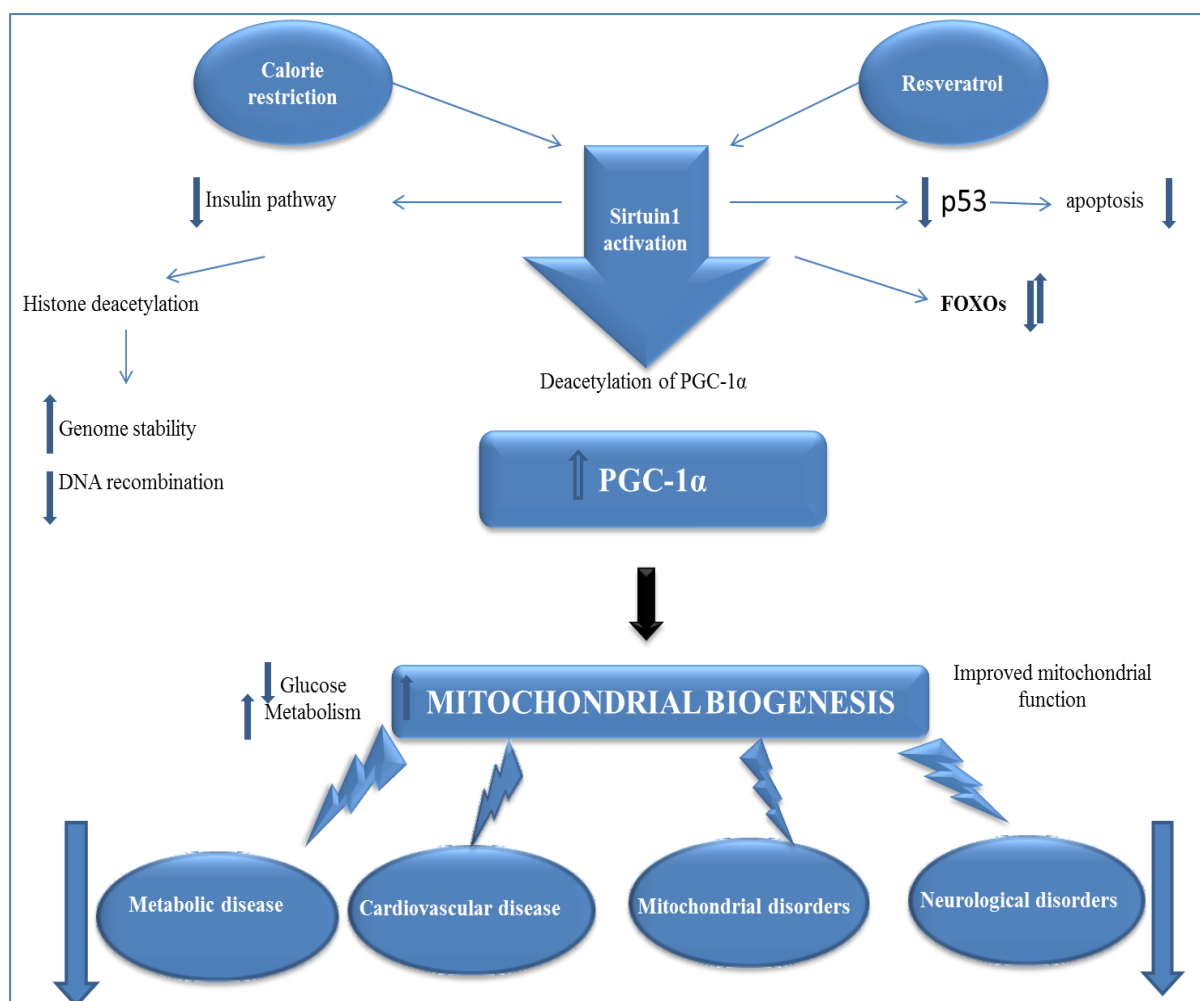


Figure 1.17: Activation of SIRT 1 by the natural antioxidant resveratrol, (Markus and Morris, 2008).

A range of progressions in mammals including neuroprotection, differentiation, tumour suppression and inflammation are modulated by resveratrol (Anekonda, 2006; Baur *et al.*, 2006; Labinsky *et al.*, 2006). Consistently, cancer, heart diseases, brain damage, hearing loss, anorexia and damage to tissues are some of the diseases that are affected by resveratrol in mammals (Baur and Sinclair, 2006). Similar to lower organism, it also elicits CR mimicking physiological changes in mammals, for example it improves tissue pathology and endurance, increases mitochondrial biogenesis, insulin sensitivity and decreases fat accumulation, blood insulin and insulin-like growth factor 1 (IGF-1) (Baur *et al.*, 2006; Lagouge *et al.*, 2006). Lately, resveratrol has been shown to increase the survival of high calorie fed mice by shifting its physiology towards standard diet mice with increased mitochondria, lower blood glucose and insulin and a hepatic gene expression profile matching the lean mice. This is consistent with the fact that increased SIRT1 activity can increase PGC-1 α activity. Also, mice fed with resveratrol show highly deacetylated PGC-1 α in multiple tissue, indicating a role of SIRT1 activity (Lagouge *et al.*, 2006).

It has been observed that SIRT1 mediated deacetylation of PGC-1 α controls the resveratrol stimulated activation of mitochondrial function. Endorsing cell endurance by decetylation of p53, stopping adipocyte segregation by repressing peroxisome proliferator-activated receptor gamma (PPAR- γ), liberating cells polyglutamine toxicity and sensitising cells to tumour necrosis factor alpha (TNF- α) induced apoptosis by triggering nuclear factor kappa-light-chain-enhancer of activated B cells (NF- κ B) deacetylation are some of the other effects mimicking SIRT1 activation, brought about by resveratrol (Howitz *et al.*, 2003; Picard *et al.*, 2004; Yeung *et al.*, 2004; Parker *et al.*, 2005). Modulation of some pathways by resveratrol independent of SIRT1. On the other hand, a couple of recent reports have shown that resveratrol inhibits insulin response by disrupting insulin-induced (insulin receptor substrate1 IRS) protein complex and this action is independent of SIRT1. In another report resveratrol was shown to stimulate AMPK activity in neurons independent of SIRT1 and dependent on liver kinase B1 (LKB1) (Zhang, 2006; Dasgupta *et al.*, 2007). New evidence supports that the indirect activation of SIRT1 by resveratrol is mediated by the activation of AMPK. AMPK acts as a primary initial sensor that increases NAD⁺ levels, thus inducing a higher deacetylation of SIRT1 targets, PGC-1 α and FOXO1, due to concomitant increases of SIRT1 activity (Canto *et al.*, 2009; Canto *et al.*, 2010). One study has demonstrated that metabolic effects of resveratrol can be accounted by elevation of cAMP levels both in skeletal muscle and white adipose tissue by inhibiting phosphodiesterase, because resveratrol competes with cAMP in its binding site. The elevation of cytosolic cAMP activates the cAMP effector protein Epac1 (Guanine nucleotide exchange factor), which increases levels of cytosolic Ca⁺², thus inducing AMPK phosphorylation via calcium/calmodulin-dependent protein kinase II. The activation of AMPK increases NAD⁺ levels, thus leading to SIRT1 activation (Park *et al.*, 2012). A diagram of this mechanism is shown in figure 1.18.

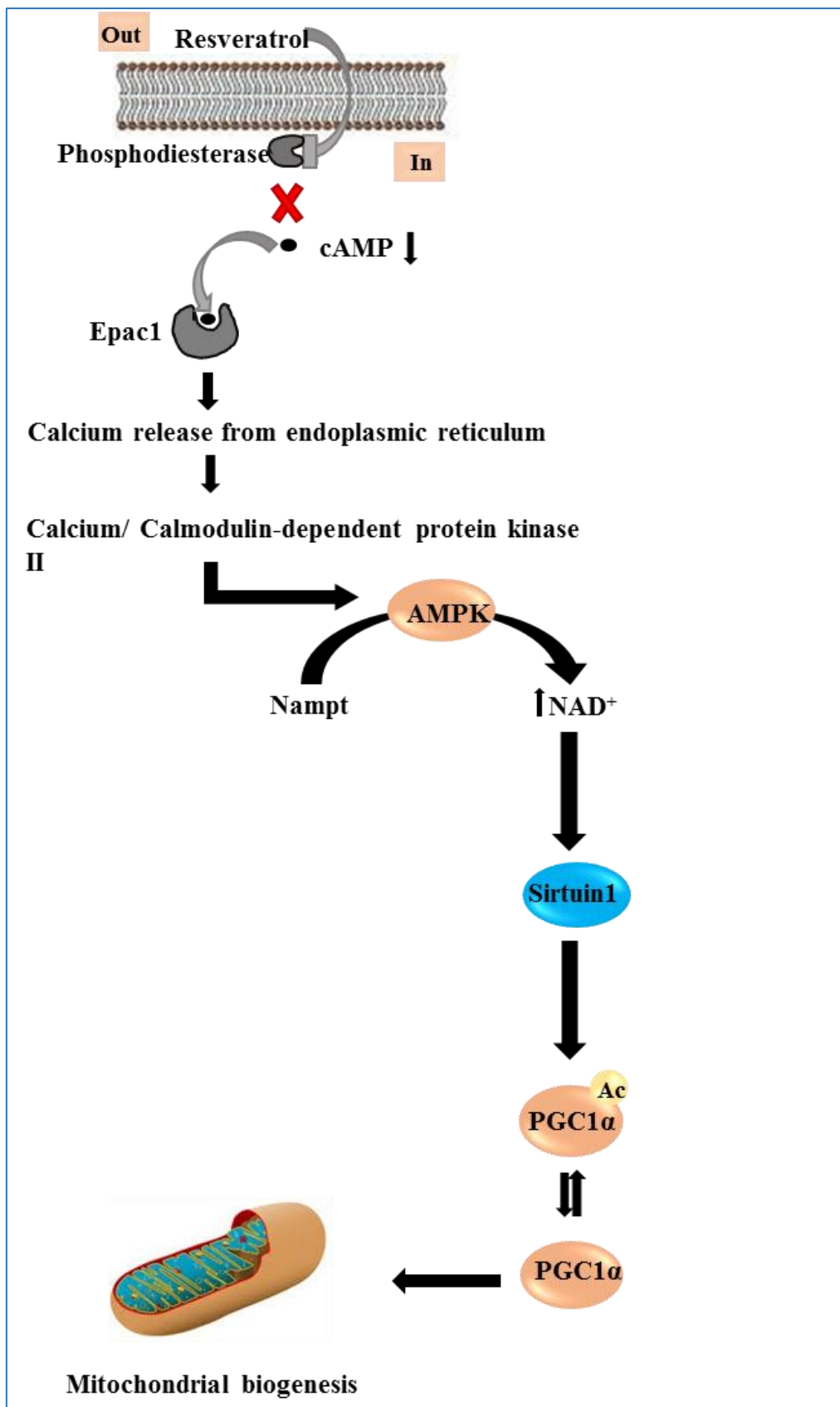


Figure 1.18: Mechanism of SIRT1 activation by resveratrol. The metabolic effects of resveratrol can be accounted for competitive inhibition of cAMP-degrading phosphodiesterase and the elevation of cytosolic calcium via the cAMP effector protein Epac1. This pathway activates the calcium/calmodulin-dependent protein kinase II which phosphorylates AMPK, which in turn increases of NAD⁺ levels, thus leading ultimately to SIRT1 activation (adapted from Jose and Francisco, 2012).

1.6 SIRT1 Inhibitors

The biological functions of SIRT1 have triggered interest in the development of SIRT1 activators and inhibitors. As mentioned earlier, SIRT1 required NAD⁺ for its enzymatic activity and deacetylate the substrate along with metabolism of NAD⁺ to release nicotinamide, O-acetyl ADP-ribose and the deacetylated substrate. The deacetylation reaction involves an enzyme-ADP-ribose intermediate (Landry *et al.*, 2000). Physiological amounts of nicotinamide noncompetitively inhibit SIRT1 *in vitro*, as it was then revealed. In addition, the level of inhibition by nicotinamide (IC₅₀ < 50µM) was found to be the same or more than the most effective known synthetic inhibitors of the same protein class. It was suggested that attaching to a preserved pocket neighbouring NAD⁺, nicotinamide inhibits deacetylation and NAD⁺ hydrolysis is blocked (Bitterman *et al.*, 2002). It was confirmed in recent times that nicotinamide inhibition is the result of nicotinamide intercepting an ADP-ribosyl-enzyme-acetyl peptide intermediate with regeneration of NAD⁺ (transglycosidation) (Jackson *et al.*, 2003). A number of chemical inhibitors of SIRT1 are also often employed. SIRT1 is repressed successfully by treatment with Sirtinol, Splitomicin, Suramin, NF023 and NF279 (figure 1.19) at a low micro molar scale level. A comparatively powerful inhibitor, being about 1000-fold more effective than nicotinamide, was in recently described, EX527 (Napper *et al.*, 2005; Porcu and Chiarugi, 2005).

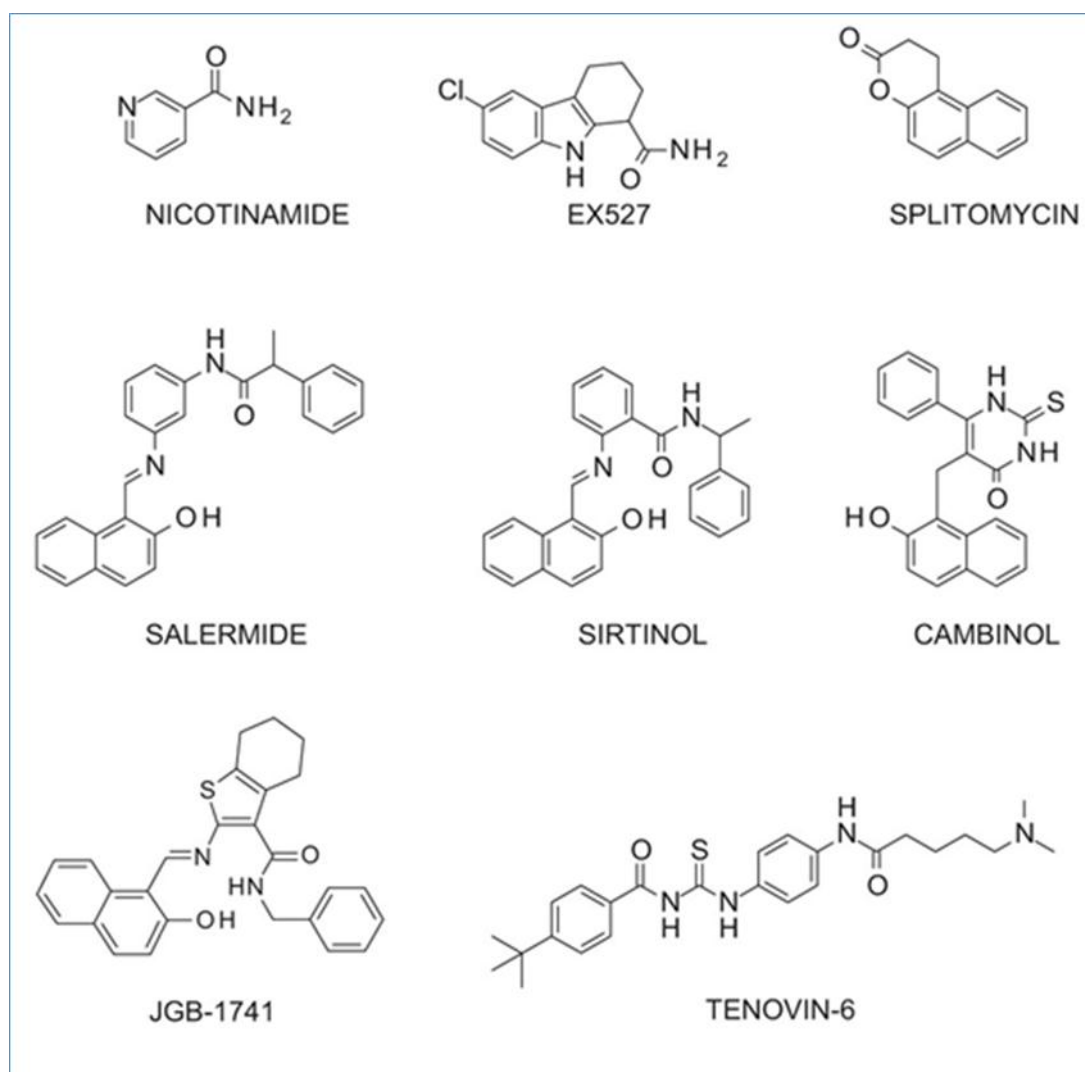


Figure 1.19: Small-molecule inhibitors of SIRT1, (adapted from Stunkel and Campbe, 2011).

1.7 SIRT1 and Cancer

SIRT1 and its association with cancers have been the point of interest in the past. The controversial theories regarding cancer and Sirtuins are being tested for being tumour promoter or either tumour suppressor focusing on the cellular context and its targets in specific signaling pathways or related to specific cancers that are illustrated in figure 1.20. SIRT1 is a tumour suppressor gene that suggested by role it plays in maintaining stability of the genome via chromatin regulation and DNA repair (Saunders and Verdin, 2007; Stunkel *et al.*, 2007; Fan and Luo 2010). Herranz *et al.*, (2010) created a metabolic syndrome-associated liver cancer model in which (SIRT1- transgenic mice) were at a lower risk to establishing liver cancer and show an enhanced protection of hepatocytes from both DNA damage and metabolic damage as seen in wild type (WT) mice. These results support SIRT1 tumour suppression activity in

aging- and metabolic syndrome-associated cancer. Interestingly, a couple studies found that SIRT1 had a suppressive activity in tumour cell growth by suppressing NF- κ B (Bosh-Preseque and Vaquero, 2011), whereas a transcription factor playing a central role in the regulation of the innate and adaptive immune responses and carcinogenesis, the dysregulation of which leads to the onset of tumourigenesis and tumour malignancy (Kiernan *et al.*, 2003).

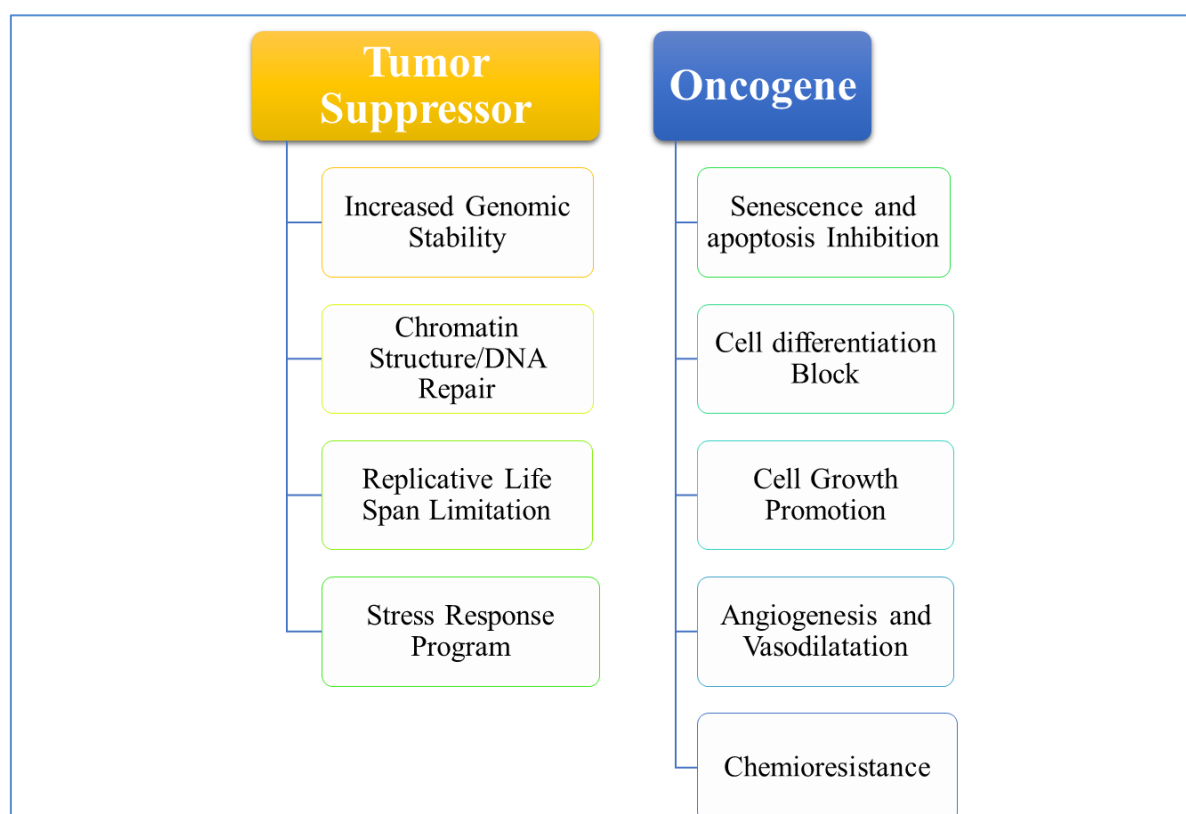


Figure 1.20: SIRT1 as a tumour suppressor or/and tumour promoter. The evidence reported supports both an oncogenic and a tumour suppressor role for SIRT1. Here, we indicate the different functions described for SIRT1 that support one role or the other (adapted from Bosh-Preseque and Vaquero, 2011).

SIRT1 also has a role in tumour suppression that was put forward by Firestein *et al.*, (2008). It was seen that a higher rate of expression of SIRT1 in the $APC^{min/+}$ mice caused a decrease in development of colon cancer. The decrease was because of SIRT1 as it was thought to have caused deacetylation of β -catenin along with promotion of cytoplasmic restriction of oncogenic forms of β -catenin which is limited to the nucleus (Firestein *et al.*, 2008). Other research performed by Yuan *et al.*, (2007) established that SIRT1 behaves as a tumour suppressor. This action is because of involvement of c-Myc-SIRT1 feedback loop that causes cellular transformation and c-Myc activity. When c-Myc attaches to the promoter of SIRT1, it causes the expression of SIRT1. SIRT1 the results in deacetylation of c-Myc which decreases its stability that is established from figure 1.21. Thus, transformational activity of c-Myc is

vulnerable in presence of SIRT1 (Yuan *et al.*, 2009). The association of SIRT1 as a tumour suppressor is confirmed from earlier studies. Thus, the risk of developing cancer has been decreased suggesting a lengthened lifespan causing a progressive improvement of SIRT1 function in metabolic conditions (Deng, 2009).

On the other hand, SIRT1 also causes tumour initiation and progression by blocking apoptosis and senescence. SIRT1 overexpression can inhibit stress-induced apoptosis by chromatin structure modulation and by deacetylation of non-histone proteins, like p53, Rb, BCL6, Ku70, FOXO, E2F1 (Luo *et al.*, 2001; Heltweg *et al.*, 2006; Wang *et al.*, 2006). SIRT1 expression is greatly elevated in various cancers (Bradbury *et al.*, 2005; Lim, 2006; Stunkel *et al.*, 2007; Hida *et al.*, 2007; Huffman *et al.*, 2007). The activity and the expression of SIRT1 are kept in place by a range of key factors in cancer. If deregulation results in SIRT1 overexpression or activation, it is suggesting that increased levels of SIRT1 could be an outcome rather than a cause, of cancer (Bosh-Preseque and Vaquero, 2011). The reason behind this is because of the role of SIRT1 in preventing apoptosis and senescence as various tumours get dependant on SIRT1 overexpression, establishing its role in tumour development. The association was seen in neuroblastomas, chemoresistant leukaemia ovarian and some breast cancer cells and in osteosarcomas. It was seen in biopsies taken from cancer patients who were previously treated with chemotherapeutic agents showed higher SIRT1 levels as compared to untreated samples (Chu *et al.*, 2005). It was also seen that ectopic SIRT1 overexpression enhanced P-glycoprotein expression by deacetylating FOXO1 and causing chemotherapeutic drug resistance for drugs like doxorubicin in cancer cells while depletion of SIRT1 by siRNA prevents the occurrence of drug-resistant phenotype (Chu *et al.*, 2005). Research as suggested that SIRT1 activator resveratrol possesses chemopreventive activity against various cancers, like leukaemia, skin cancer, DMBA-induced mammary tumours (in rats), and prostate cancer (Aziz *et al.*, 2005; Whitsett *et al.*, 2006; Harper *et al.*, 2007; Li *et al.*, 2007).

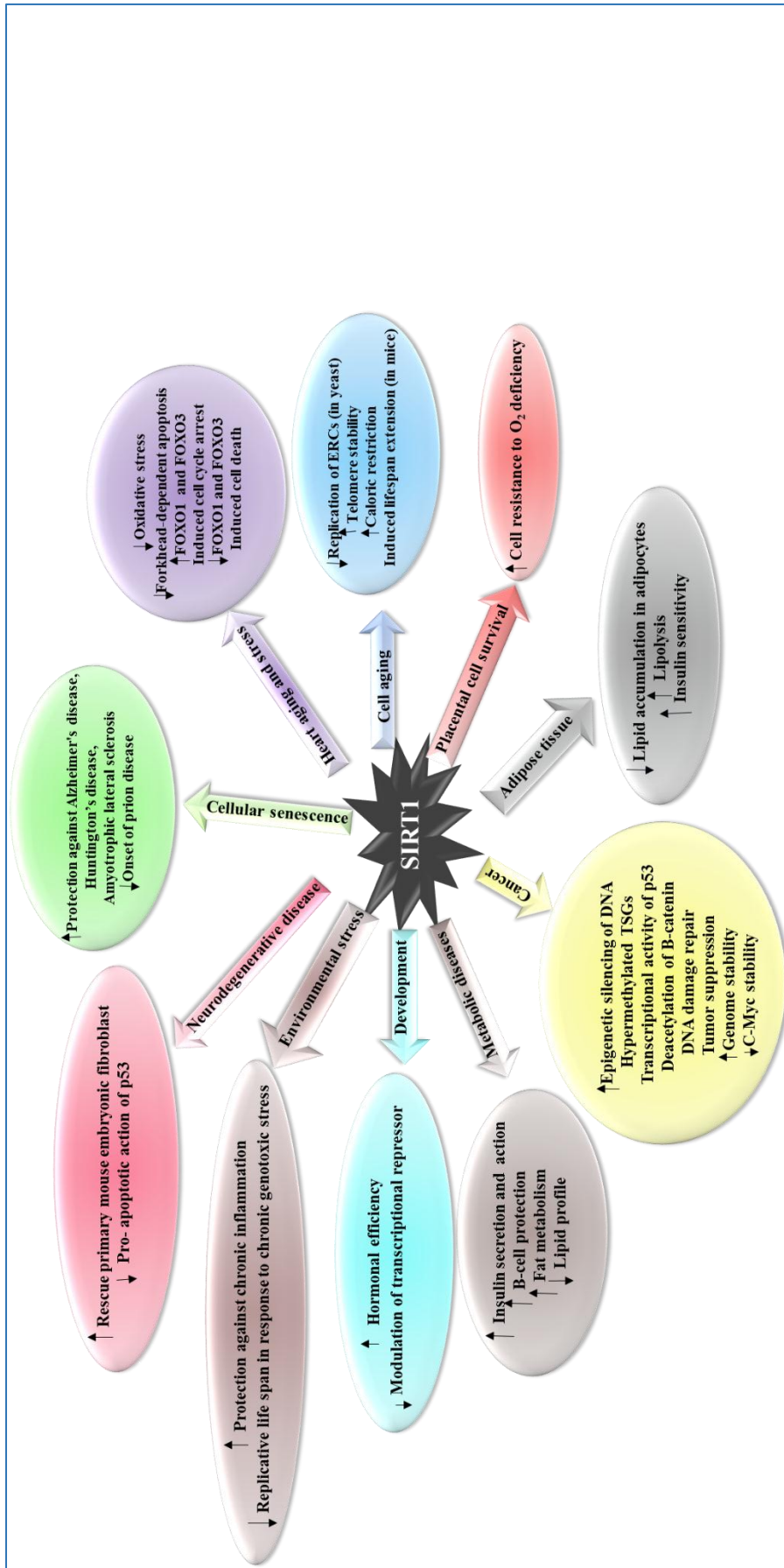


Figure 1.21: Activation and inhibition of many cellular processes by SIRT1 (adapted from Rahman and Islam, 2011).

SIRT1 is also associated with tumour promotion because it causes angiogenesis (Bosh-Preseque and Vaquero, 2011). As SIRT1-mediated deacetylation decreases the functions of various tumour suppressors including p73, p53, and HIC1, it has been suggested that SIRT1 causes tumour growth and development (Vaziri *et al.*, 2001; Chen *et al.*, 2005). Potente *et al.*, (2007) saw an abnormal postnatal neovascularisation because of endothelial-restricted SIRT1 mutation in mice who lack the deacetylase domain of SIRT1 gene. SIRT1-deficient zebrafish also displayed vascular patterning defects and haemorrhages because of dysregulated endothelial sprouting, associated with regulation of the expression of various genes linked to vascular endothelial homeostasis and remodelling (Potente *et al.*, 2007). Much remains to be established on how SIRT1 exerts its multiple functions in cancer and on how these functions affect tumorigenesis. Current knowledge suggests as shown in figure 1.22, that under normal conditions, in response to stress or to DNA damage, SIRT1 might promote cell survival via cell cycle arrest, DNA repair, or inhibition of apoptosis. If the stress signal becomes chronic or the levels of damage cross a certain threshold, then SIRT1 could induce cell senescence (Bosh-Preseque and Vaquero, 2011). However, following chronic stress or DNA damage, the loss of a tumour suppressor or of any other checkpoint-related factor could cause an imbalance in these regulatory processes and induce SIRT1 overexpression beyond a critical limit (Kim *et al.*, 2008; Zhao *et al.*, 2008). This in turn would agree with the drastic reduction in the very high levels of SIRT1 protein in undifferentiated cells as differentiation progresses. As cancer development is involved in dedifferentiation of cells, it could imply restoration of SIRT1 protein to predifferentiation levels (Bosh-Preseque and Vaquero, 2011). These results give powerful proof that SIRT1 may be an important regulator of cancer development, whether SIRT1 functions as an oncogene or as a tumour suppress remains to be determined.

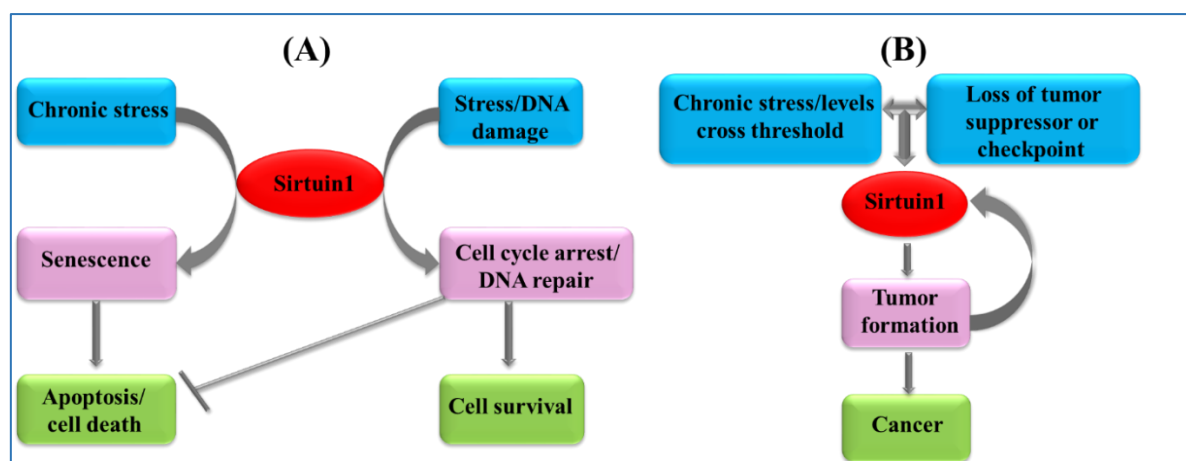


Figure 1.22: Model for SIRT1 apparent duality in cancer. (A) Under stress conditions, SIRT1 promotes cell cycle arrest, DNA repair, and, ultimately, cell survival. In chronic stress conditions or under certain massive levels of DNA damage, SIRT1 induces senescence and apoptosis. (B) Under chronic stress and loss of tumour suppressors or checkpoints, SIRT1 promotes tumour formation and cancer. A feedback between tumour progression and SIRT1 levels is established, resulting in reinforced dedifferentiation, cell growth, and cell survival, (adapted from Bosh-Preseque and Vaquero, 2011).

1.8 ROS and DNA Damage

ROS can be defined as chemically reactive molecules containing oxygen that cause conformational changes in cellular and genetic structures. Peroxides, superoxide, hydroxyl radical, and singlet oxygen are some common examples of ROS. ROS are natural by-products of the normal biological metabolism of oxygen and play a significant role in cell signalling pathways and maintaining homeostasis. The ROS levels in cancer cells are usually higher in comparison to the normal cells, however, ROS scavenging system of cancer cells is also stronger than the normal cells for the maintenance of homeostasis. This particular biochemical property of cancer cells i.e. high ROS concentration can be used a potential therapeutic target because ROS are crucial to the development and progression of cancer, because they can induce mutations in DNA and hence cause genomic instability and release tumourigenic signals (Storz, 2005). ROS are very dangerous to the DNA as they can cause DNA strand breakage, which is followed by alterations in purine and pyrimidine bases and sister chromatid exchanges which is very harmful as it can lead to the inactivation of tumour suppressor genes or even the activation of oncogenes, thus the malignant potential of the tumour becomes higher (Storz, 2005). Nonetheless, these high levels of ROS may also be channelled to cause death of cancer cells (Dong *et al.*, 2016). Many chemotherapeutic agents employ this mechanism of action i.e. cause cancer cell death or cell growth inhibition by up-regulation of ROS production (Kotamraju *et al.*, 2002; Conklin, 2004). Oxygen radicals are cytotoxic and many anticancer

therapies like the chemotherapeutic agent doxorubicin, etoposide and cisplatin or radiotherapy and photodynamic therapy work on this principal and generate high concentrations of superoxide and oxygen radicals within carcinoma cells (Yokomizo *et al.*, 1995; Brown and Bicknell, 2001). However, long term oxidative stress within carcinomas can also lead to resistance to these drugs by upregulation of defence systems against antioxidant rendering the therapy useless. The use of these agents as a monotherapy could cause harm rather than good, depending on the concentration in which they are administered, as ROS may induce tumour progression or even cell death.

1.8.1 SIRT1 and ROS

The role of SIRT1 in mediating an oxidative stress response by directly deacetylating several transcription factors responsible for regulation of antioxidant genes has been established on the basis of evidence. It is noteworthy that many members of the FOXO family of transcription factors are activated by SIRT1. These factors promote the expression of stress response genes including Superoxide Dismutase 2, mitochondrial SOD2 (Brunet *et al.*, 2004; Motta *et al.*, 2004; van der Horst *et al.*, 2004; Merksamer *et al.*, 2013). SIRT1 functions regulates itself with the help of early growth response protein ERG1 (a member of the erythroblast transformation-specific family of transcription factors) for the regulation of SOD2 for protection of contracting muscle cells from oxidative stress (Pardo and Boriek *et al.*, 2012; Pardo *et al.*, 2011). SIRT1 is also responsible for promotion of mitochondrial biogenesis through the activation of peroxisome proliferator-activated receptor coactivator-1 α (PGC-1 α) (Rodgers *et al.*, 2005). PGC-1 α is involved in increasing the mitochondrial mass and upregulating the expression of oxidative stress genes such as glutathione peroxidase (GPx1), catalase, and manganese SOD (MnSOD) (St-Pierre *et al.*, 2006). Additionally, the p65 subunit of NF- κ B through direct deacetylation is also inactivated by SIRT1. NF- κ B inhibits the suppression of the inducible nitric oxide synthase (iNOS) and nitrous oxide production and be held responsible for lower the cellular ROS load (Lee *et al.*, 2009; Merksamer *et al.*, 2013) as shown in figure 1.23.

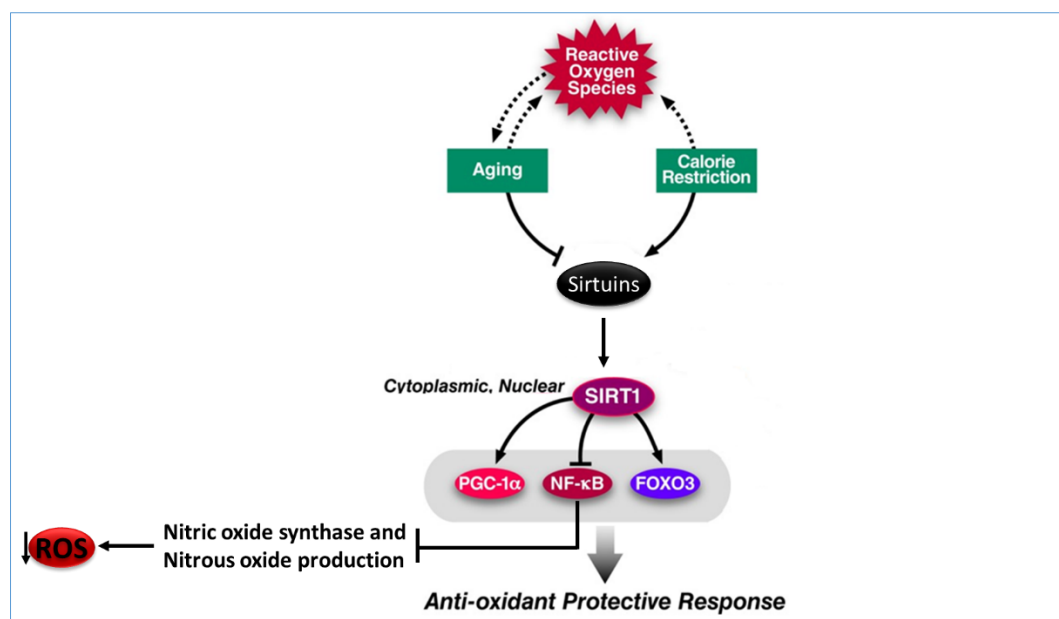


Figure 1.23: Relationship between ROS and SIRT1 (adapted by St-Pierre *et al.*, 2006).

Resveratrol has been tested as a prophylactic anti-cancer agent. The results showed that axonal protection and other cellular processes that are SIRT1-dependent (Araki *et al.*, 2004), like fat mobilisation (Yeung *et al.*, 2004) and inhibition of NF- κ B-dependent transcription (Picard *et al.*, 2004) were enhanced by resveratrol. It also activates SIRT1 which is responsible for increasing DNA stability (Howitz *et al.*, 2003; Wood *et al.*, 2004). It also reduces the proliferation rate of different types of human malignant cell lines. Resveratrol shows preventive action against tissue-type plasminogen activator TPA-mediated mouse skin tumour formation. Resveratrol regulates apoptosis and it also induces delay in the cell cycle or accumulation of cells in S (synthesis) and G2 (Gap2) phase (Stivala *et al.*, 2001; Bhat and Kosmeder, 2001; Bhat and Pezzuto, 2002). Resveratrol-mediated regulation of apoptosis occurs most likely by the suppression of NF- κ B (Manna *et al.*, 2000). NF- κ B is implicated in development of cancer by increasing survival of cells. One mechanism by which resveratrol inhibits NF- κ B includes the decreased phosphorylation of I κ B α (nuclear factor of kappa light polypeptide gene enhancer in B-cells inhibitor, alpha) by the IKK complex (an enzyme complex that is involved in propagating the cellular response to inflammation). Resveratrol is known for suppression of the activated signalling kinases such as protein kinase C (PKC) and protein kinase D (PKD) (Stewart *et al.*, 2000; Haworth and Avkiran, 2001; Storz *et al.*, 2004). These enzymes are activated by oxidative stress and phorbol ester-and are related with cancer development and NF- κ B activation (Stewart *et al.*, 2000; Haworth and Avkiran, 2001; Stewart and O` Brian, 2004). It has also been shown that resveratrol suppresses the transcriptional activation of cytochrome P450 1A1 and that it is responsible for inhibition of activities of cyclooxygenase1

(COX-1) and cyclooxygenase 2 (COX-2) which are responsible for enzymatic inflammatory response (Subbaramaiah *et al.*, 1998). Altogether, resveratrol is a natural antioxidant which is a potential chemopreventive agent and can be used to treat cancer the only limitation is side effect to normal cells because resveratrol is cytotoxic for the normal cells as well.

As ROS plays a dual role in cancer development, it has an application as pro-oxidant- and antioxidant- agent cancer prevention and therapy (Magda *et al.*, 2001; Fruehauf and Meyskens, 2007; Wang and Yi, 2008; Trachootham *et al.*, 2009). Pro-oxidant-based anticancer agents increase the ROS production along with weakening the antioxidant defence system of cancer cells. The antioxidant-based agents perform by scavenging intracellular ROS, improving the ROS-scavenging enzyme activities, and inhibiting NOX (NADPH oxidases) activity. Both of these approaches in the right proportion make the perfect combination for treatment of cancer (Gupta *et al.*, 2012).

1.9 Investigating SIRT1 as a Target for Cancer Therapeutic

SIRT1 has emerged as a drug development target for treating age-dependent diseases such as cancer (Kim *et al.*, 2008). An excessive amount of SIRT1 is expressed by primary cells, and these levels usually fall during cellular aging so that replicative senescence is avoided and one is secured from tumourigenesis (Chua *et al.*, 2005). Replicative senescence is a kind of tumour suppression. SIRT1 is crucial for restricting replicative lifespan which suggests that SIRT1 works as a tumour suppressor. Mouse embryonic fibroblasts (MEFs) derived from SIRT1-null mice are prone to spontaneous immortalisation, suggesting that SIRT1 behaves as a growth-suppressive gene in culture (Chua *et al.*, 2005). Furthermore, hematopoietic stem cells from SIRT1-null mice have increased proliferation potential, and shRNA knockdown of SIRT1 in human fibroblasts accelerates cell proliferation (Blethrow *et al.*, 2007; Narala *et al.*, 2008). SIRT1 has also been shown to inhibit androgen receptor-dependent cell proliferation in prostate tumour cells (Fu *et al.*, 2006). Recent publications also showed that transgenic overexpression of SIRT1 in the intestine inhibited polyp formation in the *Apc^{Min}* mice, as mentioned earlier (Firestein *et al.*, 2008), whereas SIRT1 deficiency led to increased tumour formation in p53-null mice (Wang *et al.*, 2008). These observations suggest that SIRT1 may suppress tumour growth under certain conditions, and that SIRT1 activators could be used for cancer treatment or prevention (Saunders and Verdin, 2007).

The SIRT1 activator may work as a beneficial chemopreventative agent in case SIRT1 behaves as a tumour suppressor (Athar *et al.*, 2007). Activation of SIRT1 will: (i) increase expression of PGC-1 α with reduction of reactive oxygen species (ROS), (ii) interaction with FOXO3 for antioxidants effect and arrest of cell cycle, (iii) interaction with NF- κ B and Ku70 reducing inflammation and leading to apoptosis, (iv) epigenetic modifications by modifying the expression of H3-TriMeK9, H4-MeK20, Ac-H4-K16, Ac-H3-K9, Ac-H1-K26, H3-MeK79 and (vii) in neurogenesis increasing the expression of deacetylation RAR β , reducing the β -amyloid plaques and increasing deacetylation of tau protein (T protein that stabilise microtubules), reducing the tangles. In addition, a recently identified endogenous activator of SIRT1 designated active regulator of SIRT1 (AROS) binds to the N-terminus of SIRT1 and potentiates its deacetylase activity toward p53 in the damage response (Kim *et al.*, 2007) as shown in figure 1.24.

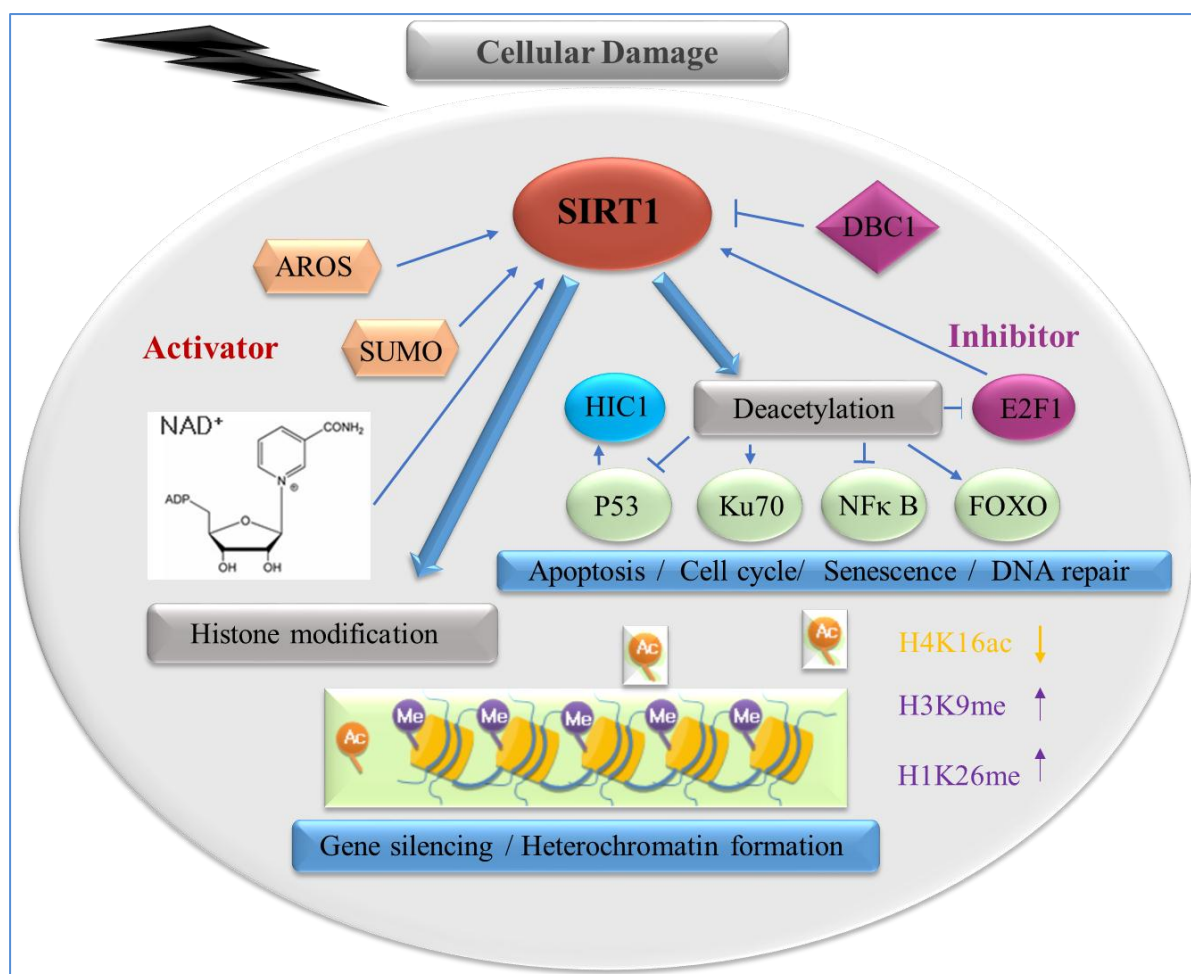


Figure 1.24: SIRT1's anticancer activity (adapted from Kim and Um, 2008).

Studies have shown that the SIRT1 activator resveratrol, a polyphenol found in wines and thought to harbor major health benefits, induces apoptosis in response to Tumour Necrosis Factor ($\text{TNF}\alpha$) via NF- κ B inhibition, and has chemopreventive activity against various cancers, including leukemia, skin cancer, and prostate cancer (Yeung *et al.*, 2004; Aziz *et al.*, 2005; Suzuki *et al.*, 2013). Resveratrol also induces autophagy, and it has been shown that this occurs in a SIRT1-dependent manner (Morselli *et al.*, 2011). On the other hand, in a cell-culture model of rotenone-induced cell death, resveratrol was reported to protect against rotenone-induced apoptosis and enhance degradation of α -synucleins (a protein that is abundant in the human brain), which was shown to occur by induction of autophagy (Wu *et al.*, 2011). The resveratrol derivative Longevinex (a product that activates 9 times more genes than plain resveratrol) has the curious effect of increasing autophagy after prolonged administration, and this correlates with increased SIRT1 levels, as well as FOXO nuclear translocation (Mukherjee *et al.*, 2010; Kozako, *et al.*, 2014).

Subsequent studies in this field are going to make evident the exact function of SIRT1 at the cancer site and it is hoped that new chemotherapeutic functions of SIRT1 activators are going to be determined. In accordance with this, it is suggested that very selective ligands such as aptamers, should be created and investigated in various cancer cell lines for the regulated activity of SIRT1 as shown in figure 1.25. The purpose of which would be to find out the manner in which SIRT1 acts as a tumour suppressor.

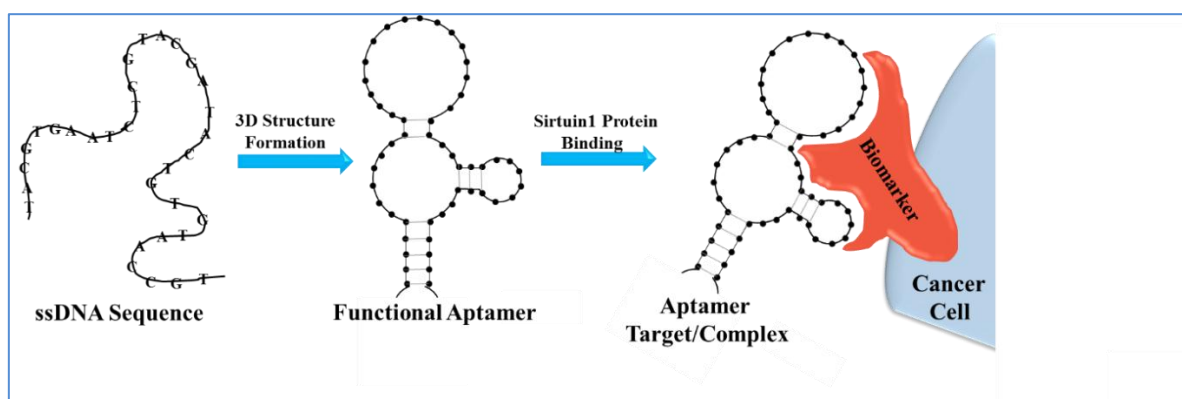


Figure 1.25: Diagram of aptamer binding to SIRT1 protein (adapted from Sun *et al.*, 2014).

1.10 Aptamers

The encyclopaedia of Analytical Chemistry (Aragonés *et al.*, 2012) has defined aptamers as “Artificial nucleic acid ligands that can be generated against amino acids, drugs, proteins and any molecules. They are isolated from complex libraries of synthetic nucleic acid by an iterative process of adsorption, recovery and re-amplification”. Single-stranded DNA or RNA (ssDNA or ssRNA) molecules that can bind to pre-selected targets including proteins and peptides with high affinity and specificity are termed as Aptamers (Ellington and Conrad, 1995; Gold *et al.*, 2002). Their 3D structure enables them to bind with a specific target molecule with considerable high specificity and affinity (Stoltenburg *et al.*, 2005). The 3-D conformations of oligonucleotides, rather than the nucleotide sequence are the responsible for binding potential of aptamers (Sampson, 2003). The overall 3-D structure can be made up of quadruplexes, triplexes, pseudoknots, hairpins, bulges, loops and stems made by single strand of nucleic acids. Aptamers are capable of binding through a good fit with several different targets ranging from one single molecule to molecules in single organism. Formation of hydrogen bonds, van der Waals and electrostatic interactions, stacking of aromatic rings, compatibility of structures or combination of these contribute to this good fit (Hermann, 2000) as shown in figure 1.26.

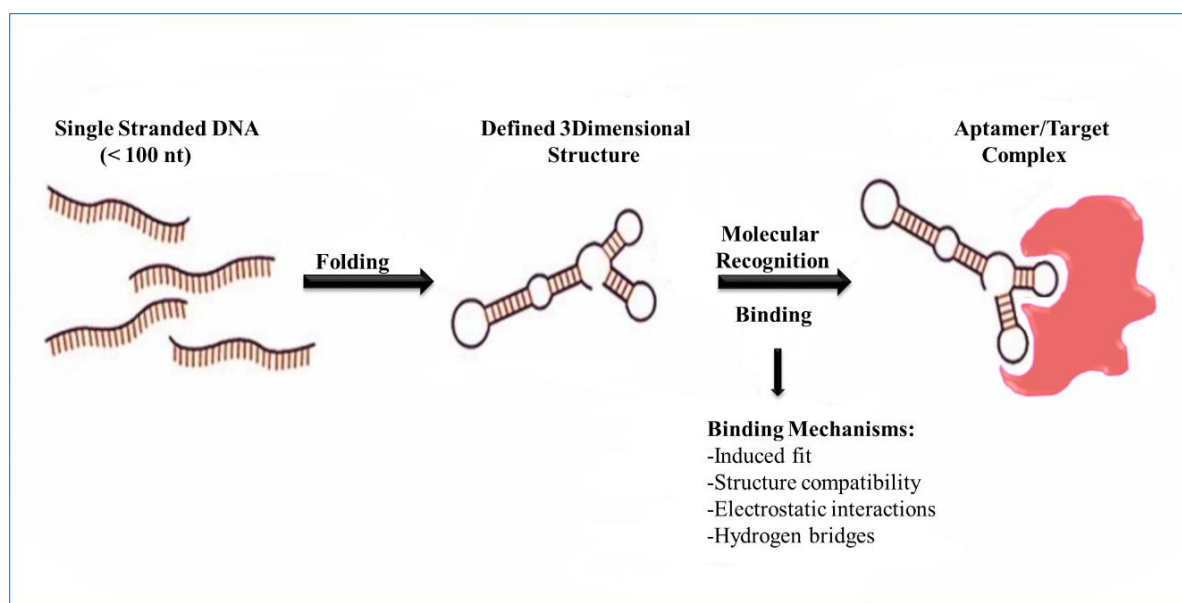


Figure 1.26: Molecular recognition of targets by aptamers with defined three dimensional structures (adapted from Stoltenburg *et al.*, 2007).

1.10.1 Generation of Aptamers

Ligands which are capable of binding to target entities with high specificity and good affinity can be designed in two major ways i.e. through either combinatorial chemistry or rational design (Marimuthu *et al.*, 2012). The approach of designing ligands through rational design is based on identification of molecules able to bind with the target using chemical wisdom and intuition. To some extent, the approach also relies on luck for identifying the desired molecule (Bowser, 2005). Combinatorial chemistry, on the other hand, involves the synthesis of a huge number of molecules giving rise to libraries followed by evaluation of molecules to determine the potential ligand molecules.

The approach of combinatorial chemistry is used to generate and select aptamers. During 1990, a revolutionary technique of combinatorial chemistry namely *in vitro* selection (Ellington and Szostak, 1990), *in vitro* evolution (Joyce, 1989) or Systematic Evolution of Ligands by EXponential enrichment (SELEX) (Tuerk and Gold, 1990) was developed for the generation of aptamers.

1.10.1.1 SELEX

The technique of Systematic Evolution of Ligands by EXponential enrichment (SELEX) was developed in 1990. This technique has been extensively applied to evolve aptamers.

1.10.1.2 General Principles

In 1990, two different research groups used the technique of SELEX for the first time to produce aptamers (Tuerk and Gold, 1990). A combinatorial nucleic acid library was used by Tuerk and Gold to identify aptamers, particularly RNA oligonucleotides, which can bind to non-nucleic acid entities with strong affinity and high selectivity (Stoltenburg *et al.*, 2007). The researchers explored the binding of bacteriophage T4 DNA polymerase (gp43) to the ribosome binding site in the messenger RNA. Sequences of gp43 involved in this binding were selected using an RNA pool randomised at certain sites. This method of selection was named as SELEX (Tuerk and Gold, 1990). Ellington and Szostak also employed the same method to identify the RNA molecules which can form a 3D structure allowing it to bind with certain small ligands like Cibacron Blue and other organic dyes (Ellington and Szostak, 1992). SELEX has turned into an extensively used procedure in medical, pharmaceutical and molecular biological research.

The SELEX technique is represented in figure 1.27. The procedure begins with a random DNA library containing various sequence motifs ranging from 10^{13} to 10^{15} in number. These are developed chemically (James, 2000). The DNA library must be transformed into RNA library. However, if the procedure is aimed at evolution of DNA aptamers, the library does not need to be treated and is utilised directly. The sequence motifs are incubated with substrate for suitable time to allow binding. Following incubation, the oligonucleotides strongly bound with the substrate are separated from weakly bound or unbound ones. Next step is elution and amplification of substrate bound oligonucleotides. Amplification of DNA aptamers is executed through PCR and that of RNA aptamers is done through RT-PCR. In the case of evolution of DNA aptamers, the next step is conversion of newly synthesised double stranded DNA into single stranded DNA and after enrichment; this pool is utilised in the subsequent SELEX cycle. In this way, the starting random set undergoes successive rounds of selection and amplification to generate few sequences having strong affinity for binding with substrate (Stoltenburg *et al.*, 2007).

Usually, SELEX is performed with some modifications and some additional steps aimed at achieving highly specific aptamers. The additional steps mostly used include negative selection or subtraction. Through these steps, oligonucleotides capable of binding with the substrates with high specificity are isolated in an exceedingly selective way. In addition to this, extent of selection as well as target concentration can be altered to obtain efficient aptamers (Stoltenburg *et al.*, 2007). The procedure completes after sufficient enrichment of the selected oligonucleotides. Usually the PCR products are added to vector molecules which are then used for transforming competent bacterial strains resulting in development of aptamer clones. Next step is the extraction of clones followed by sequence analysis to locate the aptamer sequences. However, since innovative sequencing techniques are now available, steps of cloning can be escaped and oligonucleotides can be sequenced directly with the help of primers (Bayrac *et al.*, 2011).

In the final step, the selected pool of aptamers is processed through certain post-SELEX modifications which are meant for various purposes like improving stability, reporting ability and for immobilisation. Even though different modifications are made in this technique for different purposes, some basic steps continue to be the part of the procedure (Stoltenburg *et al.*, 2007).). These steps include:

- 1- Binding
- 2- Partition
- 3- Elution
- 4- Amplification
- 5- Conditioning

The methods of this technique are dependent on library, type substrate, selection, amplification and conditioning. Subsequent sections contain detailed description of the libraries, substrates and steps involved in the technique.

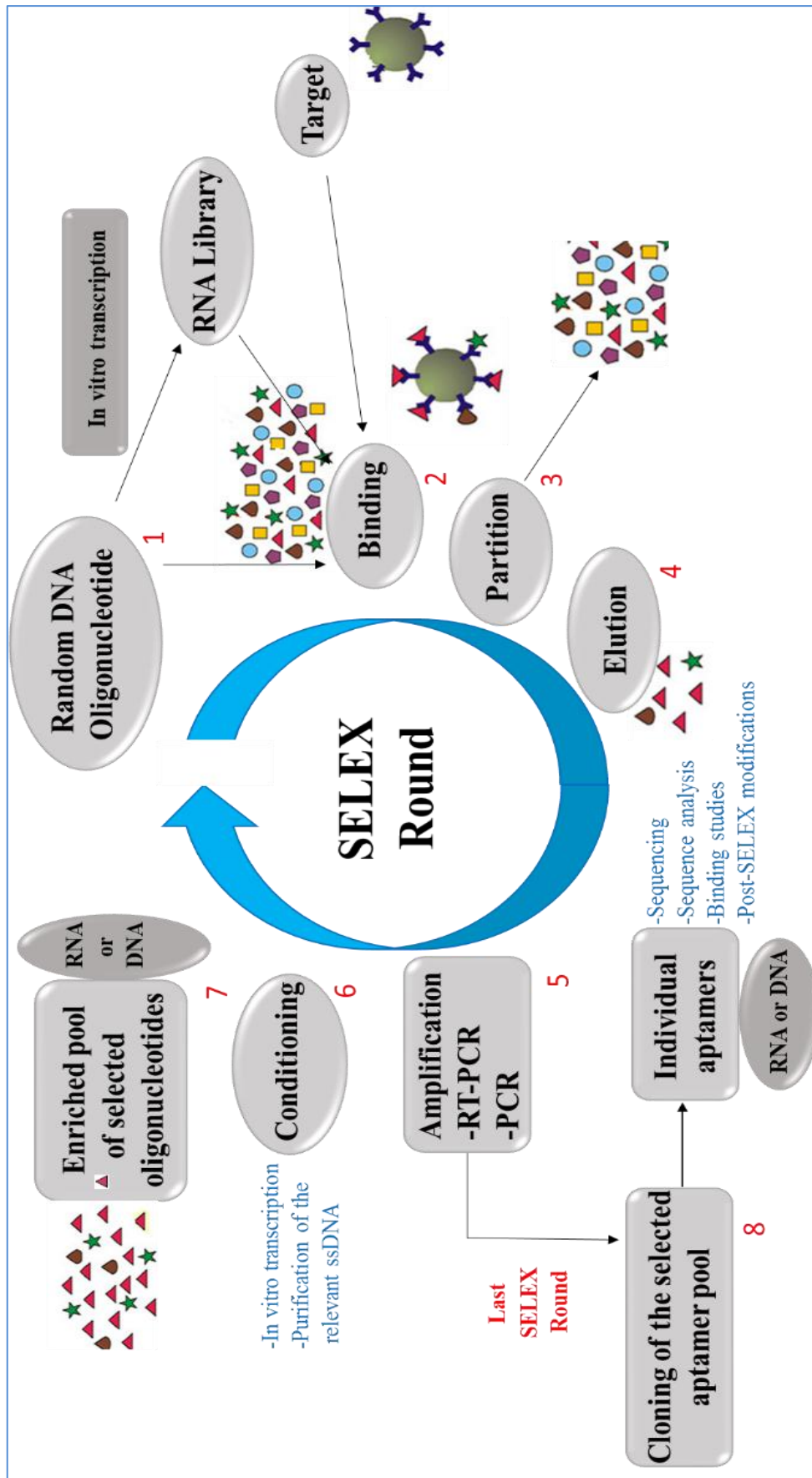


Figure 1.27: The principles of SELEX. *In vitro* selection of target-specific aptamers using SELEX technology (adapted from Stoltenburg *et al.*, 2007).

1.10.1.3 Target Molecules

Researchers have carried out SELEX for various substrates since 1990 when it was first described (Ellington and Szostak, 1990). Substrates used for aptamer binding include simple inorganic molecules, small organic molecules, peptides, proteins, carbohydrates, antibiotics as well as complex substrates like whole cells, viruses and bacteria (Famulok, 1999; Wilson and Szostak, 1999; Göringer *et al.*, 2003; Klussmann, 2006). Aptamers can be developed for substrates which possess innate ability to interact with nucleotides, nucleic acids, cofactors and nucleic acid binding proteins such as enzymes or regulatory proteins, but also for molecules by nature not associated with nucleic acids like growth factors (Jellinek *et al.*, 1994; Green *et al.*, 1996). Ciesiolka *et al.*, (1995) and Hofmann *et al.*, (1997) described the selection of RNA aptamers with affinities for Zn^{2+} and Ni^{2+} , respectively. In both cases an affinity matrix charged with those metal ions was used for the isolation of selective binding RNA molecules from a randomised RNA library, adopting a method for the purification of proteins with an extension of histidine. In few examples the SELEX technology was also applied to select aptamers targeting nucleic acid structures (Stoltenburg *et al.*, 2007). Tertiary RNA structures play an important role in several biological processes, e.g. as regulatory domains of gene expression. Aptamers could help to understand such structures. By interfering biological processes mediated by tertiary RNA structures, e.g. in pathogens, these aptamers could also function as therapeutic oligonucleotides (Duconge and Toulme, 1999; Toulme *et al.*, 2003). According to the ratio among the publications concerning aptamers, most of the aptamers were selected for proteins or for peptides as special epitopes of a protein of interest. Proteins exhibit very large, multifunctional surfaces, which make them excellent aptamer targets (Bock *et al.*, 1992). Thrombin was the first protein target used for an aptamer selection that normally does not interact with nucleic acids (Bock *et al.*, 1992). The anti-thrombin DNA aptamer folds into a G-quartet structure (figure 1.28) and can inhibit thrombin function (Ulrich *et al.*, 2002).

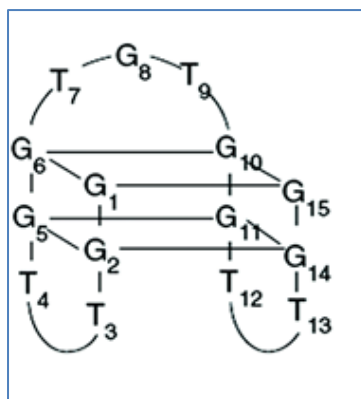


Figure 1.28: Quadruplex structure of the thrombin binding aptamer, (Adapted from Cai *et al.*, 2014).

This aptamer is one of the best studied aptamers and is widely used as model system for aptamer applications (Stoltenburg *et al.*, 2007). In addition to defined single target molecules the SELEX technology can also be applied to complex target mixtures, whole cells, tissues, and organisms. In this case the final aptamer pool can be more complex dependent on the number and abundance of potential target molecules, but also on the affinity of the aptamers (Ulrich *et al.*, 2002; Wang *et al.*, 2003). In most of these SELEX experiments directed towards complex mixtures the selected aptamers are targeting cell surface molecules, often proteins. Aptamer selection can be for example directed at alterations in the cell surface structures caused by changes of the environmental conditions or by diseases (Blank *et al.*, 2001; Ulrich *et al.*, 2002; Wang *et al.*, 2003; Göringer *et al.*, 2003). The multitude of different targets used in SELEX experiments implicates that the selection of aptamers is possible for virtually any target. However, there are some general prerequisites for a potential target to successfully select aptamers with high affinity and specificity (Stoltenburg *et al.*, 2007). Defined single target molecules should be present in sufficient amount and with high purity. This helps to minimise the enrichment of unspecifically binding oligonucleotides and to increase the specificity of the selection (Stoltenburg *et al.*, 2007). Some target features that facilitate an aptamer selection are positively charged groups (e.g. primary amino groups), the presence of hydrogen bond donors and acceptors and planarity (aromatic compounds) (Wilson and Szostak, 1999; Rimmele, 2003). The aptamer selection is more difficult for targets with largely hydrophobic character and for negatively charged molecules (e.g. containing phosphate groups). These target requirements are caused by the basic principles of the intermolecular interactions in an aptamer-target complex. The aptamers bind to their targets by a combination of complementarity in shape, stacking interactions between aromatic compounds and the nucleobases of the aptamers, electrostatic interactions between charged groups or hydrogen

bonding (Patel *et al.*, 1997; Hermann and Patel, 2000). In presence of the target, and on formation of the binding complex, the aptamers undergo adaptive conformational changes. The folding into defined 3-D structures permits the aptamers to completely encapsulate small target molecules by generating a specific binding pocket. In higher molecular weight targets like proteins, different substructures on the molecule surfaces are involved in aptamer binding (Stoltenburg *et al.*, 2007). For example, side chains of basic amino acids (lysine, arginine) are often responsible for intermolecular hydrogen bonding. The binding complexes of aptamers targeting nucleic acids are mostly characterised by loop-loop interactions (kissing complexes) between two hairpin structures or involving internal loops and bulges. Triple-stranded complexes can also be generated by binding of a single-stranded domain or oligonucleotide to a double-stranded nucleic acid (Klussmann, 2006) as shown in figure 1.29.



Figure 1.29: Triple-stranded complexes (Bacolla and Vasquez, 2014).

1.10.1.4 Random DNA Library

The library to be used for SELEX is one of the most crucial aspects of the method (Marshall and Ellington, 2000). The SELEX begins with a random DNA library developed chemically. A standard DNA synthesiser is used to develop this oligonucleotide library. During this development, a central random sequence of 20-80 nucleotides with flanking regions of 18-21 nucleotides that form the binding site for primers during PCR. As single strands of DNA are synthesised in the library, they can be used directly as they are for the SELEX experiment. However, in some cases, this oligonucleotide library is amplified on huge scale prior to next step of the technique i.e. selection. This is done for damaged DNA whose processing by PCR is useless (Marshall and Ellington, 2000). For RNA aptamers, the chemically synthesised DNA

library is converted into RNA library so that first step of the RNA SELEX technique can be performed. In contrast to the DNA library, sense primers are added with T7 promoter sequence in the RNA libraries (Stoltenburg *et al.*, 2007).

For RNA aptamer SELEX, start with the single-stranded DNA as a template, double-stranded DNA is formed using the PCR. Next step is transcription of DNA library into RNA library with the help of T7 RNA polymerase (Stoltenburg *et al.*, 2007). This RNA library is now ready to be used for RNA SELEX as the starting library. It is worth mentioning that for every cycle of SELEX, reverse transcription and amplification of selected RNA pool is carried out through RT-PCR with the help of same primers. Moreover, new RNA pool for subsequent cycle is synthesised again via *in vitro* transcription using the same procedure discussed above. It appears that primer binding sites are involved in steps of PCR only; however, these regions are there in all sequences and play role in determining the overall shape of the oligonucleotides. Another crucial aspect of the procedure is the design of primer binding regions (Urak *et al.*, 2016). The primers to be used in the procedure should have appropriate annealing temperatures. It is also important to prevent formation of heterodimers and self-dimers. It can be stated that primer design, oligonucleotide library and efficiency of amplification through the PCR are crucial for successful execution of subsequent steps of the SELEX. For that reason, a library demonstrating significant interaction between constant regions should not be used (Sefah *et al.*, 2010).

Besides the above mentioned aspects of the library to be used in the SELEX, size of randomised region must also be taken into consideration (Usually, oligonucleotides comprising 20-80 nucleotides are employed for performing SELEX). The number of types of DNA in the library rises with the size of random regions thereby elevating the chances of identifying good binders. It has been reported that functionality of certain variants of aptamers are 20-30 mer only (Davis & Szostak 2002; Nutiu & Li. 2005). It implies that small randomised regions can suitably be used for the SELEX. Still, pools having large randomised regions demonstrate greater structural complexity and for that reason they have proved to be good for complex targets and substrates which do not bind with nucleic acids naturally.

1.10.1.5 Selection

Selection is an important step of the SELEX technology and involves incubation of the oligonucleotides with the substrates, separation of unbound and weakly bound sequences from strongly bound sequences and finally elution of the bound sequences so that they can be used in subsequent stages. As there are different kinds of sequences in the random library demonstrating varying specificities and affinities. An accurate approach for selection is to make sure that sequences with high affinities and specificities are sustained through subsequent cycles and sequences with low affinities are discarded (Bianchini *et al.* 2001).

Separation of oligonucleotides serves to be a critical step of the selection phase. Efficiency of the technique largely relies on the separation strategy for evolving good aptamers with suitable designs. In most of the employed protocols of SELEX, targets are immobilised (columns, tubes, etc.) to carry out separation of unbound and bound oligonucleotides (Liu and Stormo, 2005). Utilisation of affinity columns serve to be the most common technique for separation of oligonucleotides. In this procedure, the target is attached on a packed column (Stoltenburg *et al.*, 2007). The oligonucleotide pool is then passed through the column. Sequences which are capable of binding with the substrate bind to them and hence remain attached with the column while other sequences which cannot bind with substrate pass straight through the column as well as elute. In this way, binding sequences get separated from others. Different kinds of affinity columns can be used for separation of oligonucleotides such as immobilised metals, polyhistidine tagging, glutathione S-transferase (GST) and biotin-streptavidin type columns (Takagaki and Manley, 1997; Waybrant *et al.*, 2012).

Initially, biotin-streptavidin affinity columns were used for SELEX protocols for separation (Low *et al.*, 2009). Streptavidin demonstrates high specificity for biotin and value of affinity constant for biotin-streptavidin has found to be around 10^{-14} picomolar. First the substrate is tagged with biotin followed by incubation with streptavidin Agarose beads contained in a column. They offer some added advantages of easy handling, low cost and availability. In addition to these, polyhistidine tags have also been utilised by numerous researchers because of their convenient handling. They have good binding affinity for cobalt or nickel and for that reason an immobilised metal affinity column (IMAC) can be used for immobilisation of the substrate (Feng *et al.*, 2011). Immobilised metals have been employed by researchers as substrates for selection of certain aptamers like arsenic aptamers (Kim *et al.*, 2009).

The glutathione S-transferase (GST) has also been increasingly used for SELEX procedures. In this case, substrate is tagged at amino terminal end of the GST fusion protein. This permits immobilisation onto a fixed support by attaching to its substrate i.e. Glutathione (GSH) (Weiss *et al.*, 1997; Dobbelstein *et al.*, 1995; Kim *et al.*, 2002). In addition to affinity columns, the separation can be executed through other affinity surfaces. Furthermore, agarose beads and magnetic beads can serve as a good support for immobilisation of substrate proteins and may help in heterogeneous selection methods (Stoltenburg *et al.*, 2005; Cox and Ellington, 2001). The same strategy is used in immobilisation of substrates on beads as that of affinity columns. Selection is aided by beads when a solution containing substrate molecule is incubated with them. The selected binding sequences can be eluted easily after the incubation with the help of magnet or spin column. Aptamers having binding affinity for influenza virus and oncostatin M (is a pleiotropic cytokine that belongs to the interleukin 6 group of cytokines) have been selected using microtitre plate, another affinity surface (Gopinath *et al.*, 2006).

Several different microtitre plates are available which use the same rule for immobilisation as used by affinity columns. In case of microtitre plates, the substrate is first allowed to adhere with the surface of plate with the help of tags (Hall *et al.*, 2001). After this, unbound sites are covered through a blocking agent like bovine serum albumin (BSA). Mixture of oligonucleotides is then introduced in the plate followed by incubation. After incubation, oligonucleotide mixture is washed off to remove the unbound oligonucleotide thereby selecting the oligonucleotides which can bind with the substrate (Ogasawara *et al.*, 2007). An easy and rapid method of separation involves utilisation of nitrocellulose membrane filters (Hall *et al.*, 2001). These membrane filters allow selection of aptamers which bind specifically with peptides and extremely small molecules. Nevertheless, a considerable limitation of using nitrocellulose filters is its poor efficiency i.e. more than ten selection rounds are usually needed. Filtration method for separation using nitrocellulose membrane was used for the first time by Gold and Tuerck while selecting aptamers for organic dyes. Later, it has been used by researchers for selection of aptamers against proteins like protein kinase, human IgE and mouse prion protein (Conrad *et al.*, 1994; Wiegand *et al.*, 1996; Ogasawara *et al.*, 2007).

Innovative methods for separation as well as modified versions of earlier methods have been developed. Geiger *et al.*, described the method of negative selection in 1996 (figure 1.30) for removal of non-specific binding sequences (Geiger *et al.*, 1996). In this method, the substrate is not immobilised but non-specific binding sequences remain attached to the fixed support or membrane and non-binding sequences are permitted to pass through.

Later Jensen *et al.*, introduced counter SELEX in 1994 which involves evolving aptamers which are capable of distinguishing among closely related proteins (Jensen *et al.*, 1995). The researchers altered the substrate of aptamers during subsequent rounds of SELEX. In this way, they selected aptamers which were unable to bind with the substrate. Increasing interest of researchers is in SELEX techniques through which it is possible to evolve aptamers capable of differentiating substrates contained in complex mixtures (Jiehua *et al.*, 2012). For instance, Deconvolution-SELEX is a technique capable of selecting aptamers which can bind to its substrate in a complex environment (Morris *et al.*, 1998). In this case, the selection procedure can be performed using the native form of the substrate and simple medium with no problems of validation (Morris *et al.*, 1998). It also allows employment of aptamers at large scale. These days, researchers are interested in designing selection techniques which do not involve immobilisation of substrate.

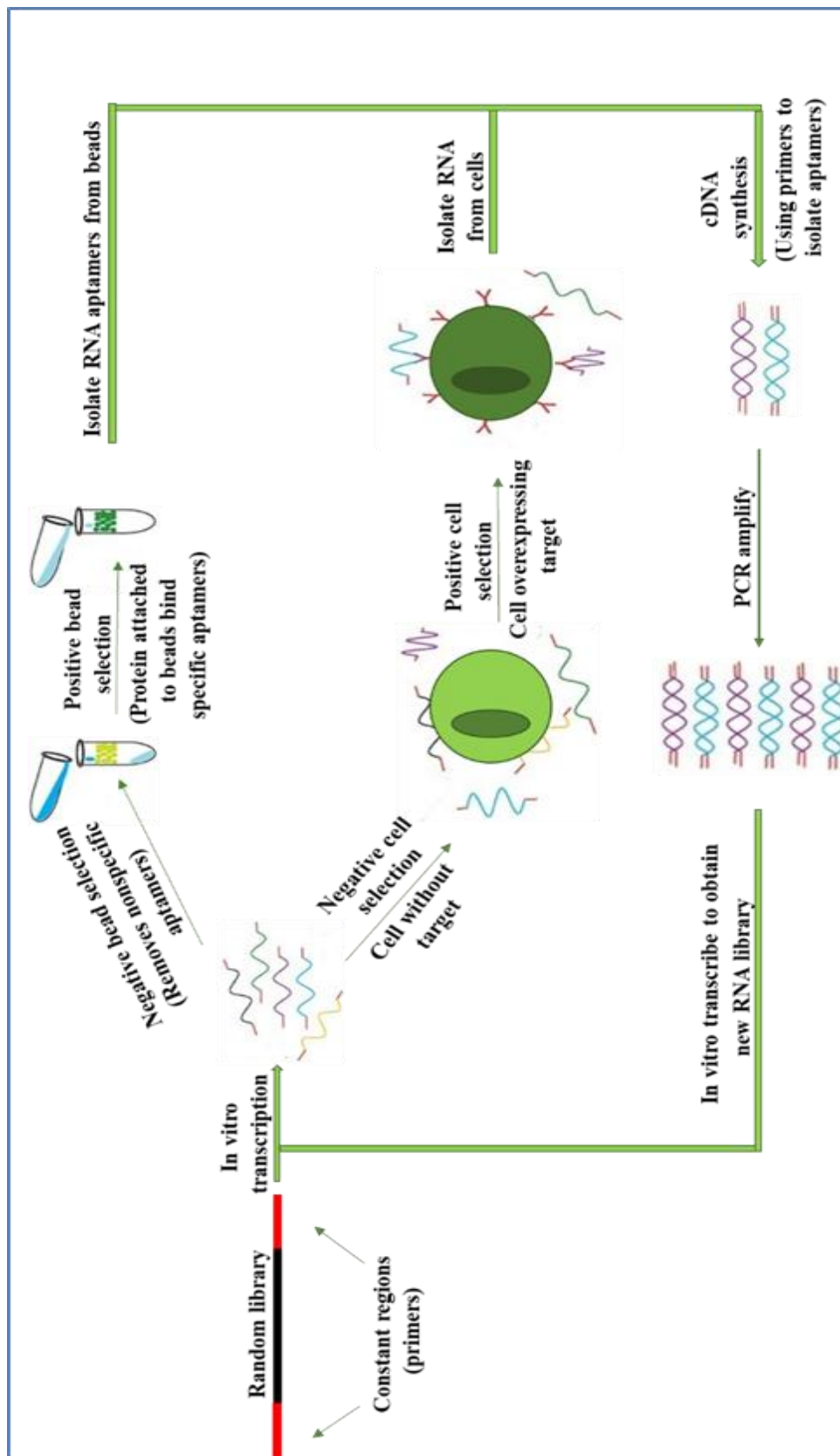


Figure 1.30: The SELEX process. An initial DNA library is transcribed into RNA and the aptamers that bind to cells or beads with no target protein are eliminated. The remaining aptamers are applied to cells or beads with target protein and the bound aptamers are retrieved, amplified, and the SELEX process repeats (adapted from Jiehua *et al.*, 2012).

After immobilising the targets, unbound targets and oligonucleotides can be washed off conveniently. Initially, affinity chromatography with immobilisation of substrates on column made up of sepharose or agarose was employed (Liu and Stormo, 2005; Tombelli *et al.*, 2005). Besides these, micro magnetic beads have also been used extensively since their surface to size ratio are high and they can be handled conveniently with low substrate concentration (Lupold *et al.*, 2002; Kikuchi *et al.*, 2003; Murphy *et al.*, 2003; Stoltenburg *et al.*, 2005). Besides immobilisation of substrates, some other methods are also available for separation of oligonucleotides. Ultra-filtration with nitrocellulose filters is one of the most extensively used methods in this regard (Schneider *et al.*, 1993; Bianchini *et al.*, 2001). Even though this method is easy to perform, a number of downsides of filtration have also been reported like non-specific interaction of the membrane with oligonucleotides. These undesired interactions of sequences can lead to non-specific enrichment of certain sequences during the SELEX.

Apart from immobilisation and ultrafiltration, several other techniques including capillary electrophoresis (Mendonsa and Bowser, 2004; Mosing *et al.*, 2005; Tang *et al.*, 2006), flow cytometry (Davis *et al.*, 1996; Yang *et al.*, 2003), electrophoretic mobility shift assay (Tsai and Reed, 1998), surface plasmon resonance (Misono and Kumar, 2005), and centrifugation (Homann and Goring, 1999; Rhie *et al.*, 2003) have also been used for separation. Quantification of bound and/or unbound sequences is also required for proceeding to subsequent steps of the SELEX. Radioactive nucleotides are usually utilised to determine the quantity of bound sequences. This tool is of high sensitivity since it is capable of detecting nucleic acids in small concentrations (Ellington and Szostak, 1990; Beinoraviciute-Kellner *et al.*, 2000 and Shi *et al.*, 2002). However, fluorescence labelling is now being employed to quantify nucleic acids since use of radioactive material has several limitations such as health risks and requirement of an isotope library (Davis *et al.*, 1996; Rhie *et al.*, 2003; Stoltenburg *et al.*, 2005). Following removal of unbound sequences, elution of bound sequences is executed usually through denaturation. Treatment with heat or chemicals like EDTA, SDS or urea denatures the bound sequences. Still, competitive binding or affinity elution can also be used for elution (Stoltenburg *et al.*, 2007).

1.10.1.6 Amplification

There is a direct correlation between number of selected sequences and number of substrates and population of sequence in the library during each cycle of the SELEX. With the help of PCR, enrichment of the selected binding sequence is done. As the library, which was used in the beginning contained a large number of different sequences with every sequence being rare in the library, PCR serves to be a useful tool for amplification of the selected sequences. Through the PCR, an exponential increment in the amount of eluted sequences is achieved. Apart from amplification, PCR proves to be helpful in other aspects as well. For instance, additional groups can be added to the sequences with no difficulty with the help of altered nucleic acids or attachment to primers. These additional groups can work for immobilisation or detection of desired sequences. Primers attached with fluorescent substance or biotin is widely used for this purpose. Fluorescent substance is used for quantification of binding sequences thereby allowing estimation of SELEX's progress. On the other hand, biotin is used for immobilising the binding sequences on streptavidin beads allowing their elution (Stoltenburg *et al.*, 2007).

1.10.1.7 Cloning and Characterisation

Cloning and characterisation of aptamers serve to be the concluding phase of the SELEX technology. The process of selection is usually terminated after six to twenty rounds of selection, depending upon the efficiency of the procedure. Oligonucleotide pool of the final round is cloned and analysed to determine suitable aptamers with strong affinities (Conrad *et al.*, 1995). Sequence analysis of over fifty clones is usually done. To identify similar and most common sequences, sequence alignment programs are employed. In general, most common sequences mostly prove to be the sequences with best affinity; however, other sequences must also be analysed in terms of specificity and affinity. Besides sequence analysis, determination of secondary structure provides useful data regarding binding domains of the sequences. Secondary conformations are usually determined through mfold (Zuker, 2003). This program calculates the possible configuration of single-stranded nucleic acids by energy minimising method considering stems, loops and bulges. The determined consensus motifs often are located in stem-loop structures (Jiang *et al.*, 1997; Horn *et al.*, 2004; Nishikawa *et al.*, 2004; Lee *et al.*, 2005), but they are even found in different secondary or tertiary structures. For

example, several authors describe conspicuous G-rich binding motifs which form G-quadruplexes as shown in figure 1.31 (Macaya *et al.*, 1993; Wilson and Szostak, 1998; Andreola *et al.*, 2001). Others found pseudoknot formations that are responsible for target binding (Burke *et al.*, 1996; Nix *et al.*, 2000; Chaloin *et al.*, 2002).

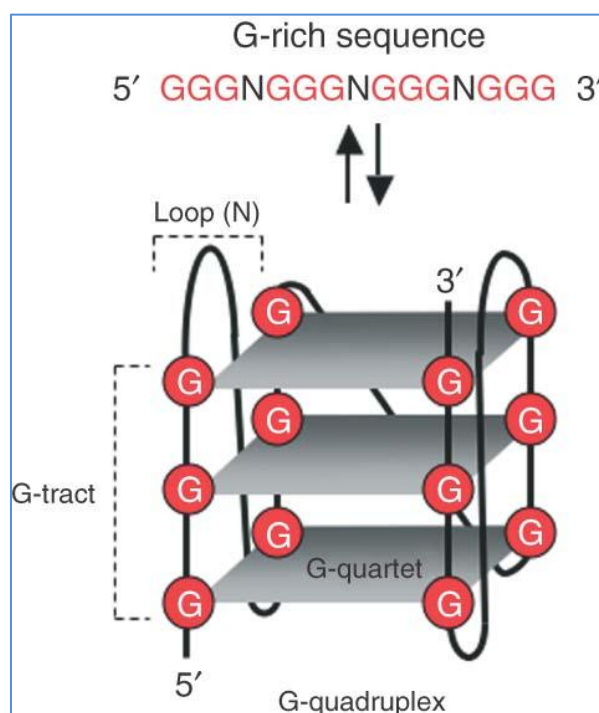


Figure 1.31: Guanine-rich (G-rich) sequence that folds into a G-quadruplex structure (Millevoi *et al.*, 2012).

These days, the above mentioned steps of cloning can be avoided while performing SELEX. This is because innovative technologies are being developed in where sequencing of oligonucleotide pools can be done without cloning. These technologies include SOLiD, Illumina GAIIx and 454 (Stoltenburg *et al.*, 2007). A pool which needs to be sequenced is first amplified with the help of primers having 454 flanks. In this case, it is possible to read up to 10,000 sequences and the associated cost is only 1000\$ approximately. It also ensures sequencing of all the selected oligonucleotides and provides statistical information for selection as well. When potential candidates for aptamers are identified through sequencing, aptamers having highest specificity and affinity is identified. Binding of these candidates with targets is tested for this purpose. An efficient measure of binding efficiency of aptamers is affinity constant (K_d). High affinities for substrate is indicated by small value of K_d . Researchers have identified aptamers with K_d in the range of picomolar to micro molar (Waybrant *et al.*, 2012).

Specificity is also taken into consideration, besides binding while identifying the best aptamer. Specificity is determined by evaluating the binding affinities of an aptamer for similar

target molecules. An aptamer demonstrates superior folding structure having negative value for Gibbs free energy, high specificity and high binding affinity.

1.10.2 Aptamers and Antibodies

A number of properties make aptamers typically dominant over antibodies and powerfully attractive therapeutic agents (Rusconi *et al.*, 2002). Three-dimensional (3D) identification is used by aptamers to attach to their targets, just like antibodies. In the low picomolar to low nanomolar range, aptamers distinguished by their high specificity and elevated affinity to their targets respect to antibodies. Displaying minor to no immunogenicity, as compared to antibodies, aptamers are more stable, particularly DNA aptamer (Eyetechnology Study Group, 2003). Yet, aptamer research is novel but capable and its development is quicker in comparison with the antibody technology.

1.10.3 Application of Aptamers

During the past twenty years, aptamers have been produced by different biotech companies and research groups for different applications. Aptamers have applications in environmental field, pharmaceutical industry and analytical chemistry. Researchers and industrialists are getting more and more interested in applications of aptamers such as: aptamers as detection reagents, use of Aptamers in affinity chromatography, aptamers for target validation, use of aptamers in diagnostics and aptamers as therapeutics (Klug *et al.*, 1999; Hermann and Patel, 2000; Thiel, 2004).

1.10.4 Aptamers as Therapeutics

The functional blockage of the cell surface nucleolin represents a potential target for the development of anti-cancer therapeutics. AS1411 is a G-rich 26-nucleotide that contains only guanines and thymine (5'-GGTGGTGGTGGTTGTGGTGGTGGTGG-3') and exists in solution as a guanine-quartet-mediated dimer as shown in figure 1.32; it is thought to elicit its therapeutic effects through its interaction with nucleolin (Bates *et al.*, 2009). AS1411 was discovered as part of a screen of antisense oligonucleotides for antiproliferative activity (Bates *et al.*, 1999). In common with other therapeutics discovered by cell-based screening (as

opposed to screening or selection against individual protein targets) it is less certain what its exact mechanism of action is. AS1411 inhibits the proliferation of cells in a wide range of cancer cell lines. The suggested mechanism of action for the antiproliferative activity of AS1411 includes binding to, and subsequent internalisation by, cell-surface nucleolin followed by binding to cytoplasmic nucleolin (Bates *et al.*, 2009).

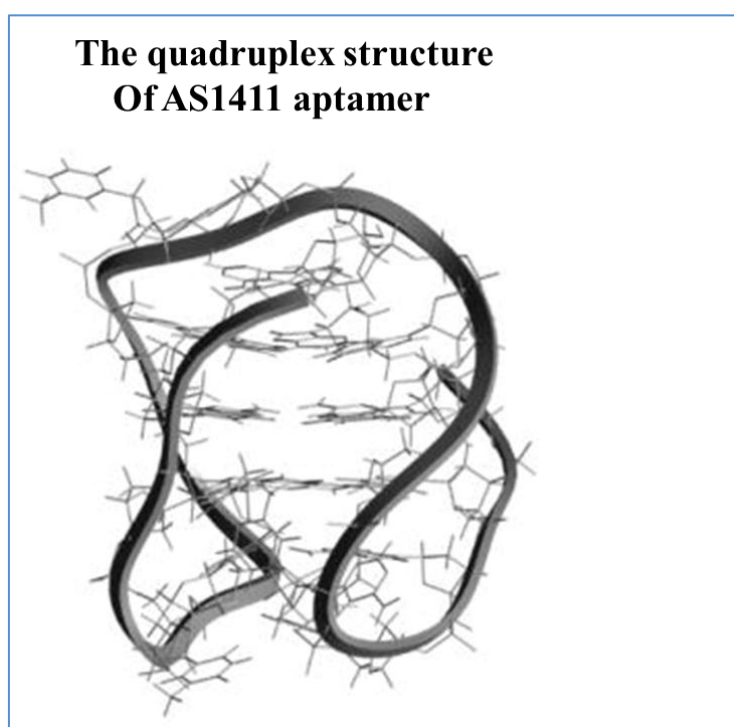


Figure 1.32: The molecular models (quadruplex) for the AS1411 aptamer. The quadruplex structure is believed to allow DNA aptamers to act as ligands at cell surface receptors in an interaction which is analogous to antigen-antibody binding. (Adapted from Bates *et al.*, 2009).

AS1411 is currently in phase II clinical trials for acute myeloid leukaemia with Phase I trials completed in 2008 (Shi *et al.*, 1999; Bock *et al.*, 1992). A number of features make them suitable candidates for application in therapeutics. In contrast to antibodies, aptamers demonstrate high stability and regain their native structure after being affected by extreme conditions, for that reason, they have long shelf life. Another beneficial aspect, for instance, they can be added with certain groups facilitating their transport (Keefe *et al.*, 2010). Similarly, conjugation with polyethylene glycol or cholesterol improves bioavailability of aptamers (Bock *et al.*, 1992; Wu *et al.*, 2007). Modifications of their 3' or 5' ends result in improvement in their *in vivo* stability (Rusconi *et al.*, 2004). Several other modifications have also been reported in the literature for different therapeutic purposes. Still therapeutic aptamers are challenged by few limitations. They can only be administered directly through injections at the target site or introduced to the

blood circulation (Burmeister *et al.*, 2005; Sheehan and Lan, 1998). Owing to their size, aptamers demonstrate limited potential for passing through biological barriers in order to bind with intracellular substrates (Bock *et al.*, 1992; Opalinska and Gewirtz, 2002). It has recently been reported that development of nanoparticles (Rong *et al.*, 2010; Yang *et al.*, 2011; Savla *et al.*, 2011; Kurosaki *et al.*, 2012) can help with an additional advantage of very extensive utilisation in aptamer therapeutics but they are toxic. Circular aptamers could be used in application of therapeutics and in the following sections we will explain it.

1.10.5 Why is an Aptamer Validated to be a Good Therapeutic?

A wide range of applications is covered by aptamers including, employment of SELEX can recognise aptamers adjacent to therapeutically significant proteins for example thrombin, HIV and reverse transcriptase, aptamers show powerful inhibitory features in opposition to their protein targets. The reason why they are considered to be very effective is that they act against small molecules and monoclonal antibodies is their chemical nature because of their 3D arrangement for molecular identification are particularised by the nucleic acid sequence of aptamers (Bunka and Stockley, 2006). They squeeze into various small gaps situated on the surface (active site where enzymes act to produce an effect) of various proteins to cause an inhibitory action against various blockbuster drugs like Gleevec (Novartis), Viagra (Pfizer) and Tamiflu (Roche) (Bunka and Stockley, 2006). Aptamers also creates fissures that attach to various parts of the protein molecule (Nimjee *et al.*, 2005). Aptamers can adhere firmly because of increased surface area of its targets leading to disruption in protein bonds (Bunka and Stockley, 2006). For example, of an anti-HIV reverse transcriptase (RT) aptamer which has the tendency of enveloping ~2600 Å of the RT surface causing a decrease in production of resistant strains produced against the drug (Tuerk *et al.*, 1992; Bunka and Stockley, 2006). Expensive robots and well-equipped libraries are helpful as they provide small molecule high-throughput screening leading to the synthesis of aptamers against the same target very easily. Aptamers are to be selected wholly from a test tube maintaining accuracy and attraction that should strongly be limited and should be specific against immunogenic or toxic targets (Nimjee *et al.*, 2005). When such drugs are administered at an elevated dose (beyond the therapeutic range) in humans, aptamers then lack their immunogenicity and toxicity (Nimjee *et al.*, 2005). Along with that, aptamer antibodies against complementary base-pairing or anionic polymer, the strength of the aptamer can be reversed (Oney *et al.*, 2009; Rusconi *et al.*, 2004).

A fine-tuning of aptamers which would not be accessible to an antibody-based therapy can be acquired by these approaches. Also, synthetic derivation, chemical stability, temperature antibodies and little molecules (Jayasena, 1999; Nimjee *et al.*, 2005). Nucleases degrade natural phosphodiester oligonucleotides and hence for employment in cell studies, they would be inapt. Aptamers are frequently capped at their 5' and 3' end, and the phosphate backbone and nucleobases are frequently customised to make aptamers defiant to nuclease degradation (Mayer, 2009a; Nimjee *et al.*, 2005). For therapeutic usefulness, 2' fluorinated pyrimidine and 2' methoxy purine are general alterations (figure 1.33) (Keefe and Cload, 2008; Famulok, 2009).

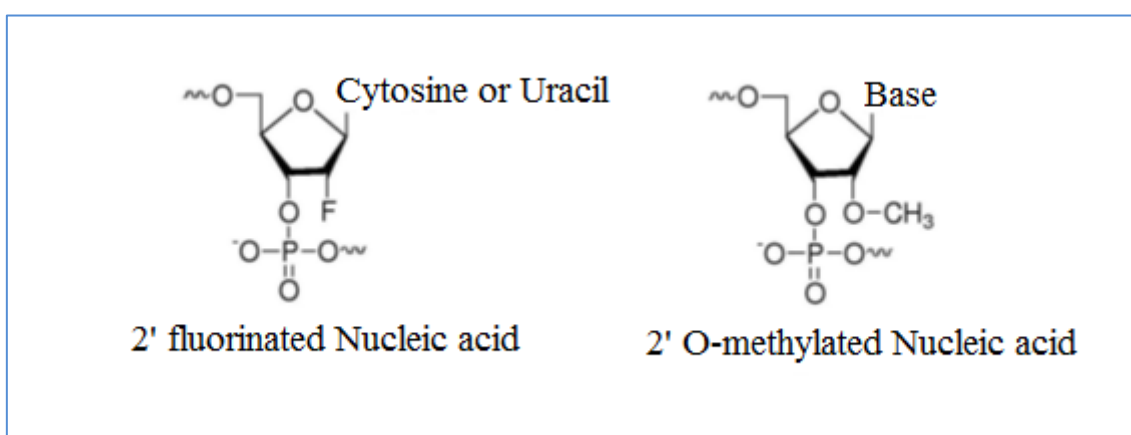


Figure 1.33: Chemical structure of 2' fluorinated pyrimidine and 2' methoxy purine.

For the cure of inflammatory diseases and haematological complications, Noxxon Pharma is a biotech company with their centre of attention being the study and development of spiegelmers (L-aptamers). In phase 1 clinical pipeline is a spiegelmer aptamer, NOX-E36, employed to treat diabetic nephropathy (www.noxxon.com). At present, several aptamers have stepped into various levels of the drug development pipeline, or the method to bring to the market, a novel drug from the lab-bench (Bunka *et al.*, 2010; Keefe *et al.*, 2010). Vascular entry is a feasible approach to access these targets, without having to enter the aptamers to the cells. The therapeutic potential of cell surface targets such as membrane antigen, viral surface proteins is comparatively high. In addition to the therapeutic effect these aptamers are also useful otherwise (Keefe *et al.*, 2010).

To sum up very concisely, aptamers are validated to be excellent therapeutics for three major reasons:

- 1-Aptamers are easily selected by SELEX against any molecular therapeutic targets including toxins.
- 2-Aptamers possess properties equivalent or even superior to antibodies and small molecules in aspects such as affinity, specificity and ease of synthesis.
- 3-Aptamers are chemical in nature and can be modified.
- 4-Because they compose the nucleic acid which are nontoxic, this helps significantly shorten the time in preclinical stage in the drug development process.

1.10.6 *In Vivo* Stability of Nucleic Acid in Therapeutics

In vivo stability of nucleic acids is an important issue in investigations involving nucleic acids. It is quite established that nucleic acids, especially ribonucleic acids are prone to activity of nucleases found in the cell. Hence the issue of stability of nucleic acids *in vivo* must be given attention for efficient application of aptamers as entities capable of penetrating cells. *In vivo* stability of nucleic acids can be enhanced through different chemical modifications in the technique (Gu, 2011). To date, huge number of studies have been carried out on stabilisation of RNA molecules via modifying its 2' end like 2'-O-CH₃ and 2'-F, 2'-NH₂ modifications. These approaches proved to be quite effective in improving RNA stability in media supplied with serum (Ulrich *et al.*, 2006). In addition to this, locked nucleic acids also improve interactions between base pairs and make them resistant to nuclease activity (Veedu and Wengel, 2009). The approach of improving stability of nucleic acids through modifications is however challenged by the chances of adverse effects on the secondary structure which are responsible for functionality of aptamers (Gu, 2011). Yet, this problem can be avoided by adding chemical groups or making any other modification in the functional form of aptamer so that the functional properties are not affected by the modification. Another approach is to select aptamers which are inherently resistant to the nuclease activity. A number of different aptamers adopt G-quadruplex structure (Dapic *et al.*, 2002; Choi *et al.*, 2009). Stability of aptamers taken from G-rich libraries has recently been explored by a research group and it was determined that aptamers stability in serum and their penetration in cells is improved by development of G-quadruplex structures (Dapic *et al.*, 2002; Choi *et al.*, 2010) which are extensively studied, highly stable secondary structures of DNA (Hardin *et al.*, 2000). Moreover, these structures identify and replace cancerous cells on preferential basis (Choi *et al.*, 2010). According to a proposition, G-quadruplex structures at AS1411 are naturally capable of binding with the

predominant nucleolin protein present on cancerous cells. This protein aids uptake of the aptamer by the cell (Teng *et al.*, 2007).

In addition to these, circular nucleic acids have also proved to be stable since they have no 3' or 5' ends exposed to be acted upon by exonuclease digestion (Gu, 2011). SELEX technology can make use of combination of the above mentioned methods for evolving aptamers which demonstrate good stability and internalisation potential.

To date, numerous aptamer constructs have been described that are able to modulate the immune response against cancer (Gilboa *et al.*, 2013). They provide a similar or even superior activity to that of the corresponding monoclonal Ab, and their superior targeted delivery capacity confers on them less off-target side effects (Gilboa *et al.*, 2015). Thanks to their plasticity, aptamers are a very promising tool as immune-modulatory ligands, since they can be engineered to either activate or block an immune-modulatory receptor (Pastor *et al.*, 2013; Gilboa *et al.*, 2013; Soldevilla *et al.*, 2015). They can be customised to target this immunomodulation to the tumour site and can be engineered for delivering almost any kind of cargo as well (Keefe *et al.*, 2010). In 2003 the development of first immune-checkpoint-blockade RNA aptamer that binds CTLA-4 was published by Gilboa's group (Santulli-Marotto *et al.*, 2003). The selection of these anti-CTLA-4 aptamers was the first being used with immunotherapeutic intentions and opened the door to a new platform in cancer immunotherapy. Furthermore, several aptamers have been described in an immunotherapy context towards some cytokine blockade. An aptamer known as R5A1 that binds to IL-10R has been selected and optimised to block the interaction between IL-10 and its receptor on the surface of immune-system cells. IL-10 is known to be secreted by tumour cells and promote immune-modulatory responses that favor tumour establishment and growth (Berezhnoy *et al.*, 2012). The aptamer bound to IL-10 receptor on the cell surface and blocked IL-10 function *in vitro*. Moreover, the aptamer sequence and therefore the structure were optimised by truncation, discarding putative steric domains increasing aptamer affinity (soldevilla *et al.*, 2016).

1.10.7 Circular Aptamers

Of most relevance for potential therapeutic applications, some common nucleic acid stabilisation strategies have encountered problems associated with toxic degradation products (Levin, 1999). In addition, modification performed post-selection can alter the subtle binding interactions of the selected natural aptamer (Boiziau *et al.*, 1999; Blank *et al.*, 2001). Circularisation of natural aptamers is an attractive alternative to chemical modification for improving aptamer stability. With the majority of nucleic acid degradation activity arising from plasma exonucleases (Shaw *et al.*, 1991), modification of exposed termini often achieves a sufficient improvement in stability for use *in vivo* (Kurreck, 2003), and circular constructs eliminate this primary source of degradation entirely. Moreover, circularisation permits the use of natural nucleotides, which should avoid potential toxicity associated with chemical modification. In principle, circular aptamer constructs can be produced by either intra- or intermolecular ligation followed by exonucleolysis of unreacted products, a straightforward and efficient approach to their preparation (figure 1.34). With selected aptamers often forming a stem-loop structure, closing the stem into a duplex with a hairpin loop should not appreciably alter the binding loop structure and may confer added stability. Furthering this concept, two stem-loop aptamers with complementary overhangs can in principle be ligated to form a double-headed dumbbell aptamer linked by a duplex region. The key point in this regard that circularisation process should perform before and after SELEX in each round as shown in figure 1.35. The benefits of circular aptamers may lie in the development of aptamer therapeutics for diseases that require simultaneous binding of two or more targets, such as intravascular coagulopathy (Norman *et al.*, 2003) and cancer (Zacharski, 2002).

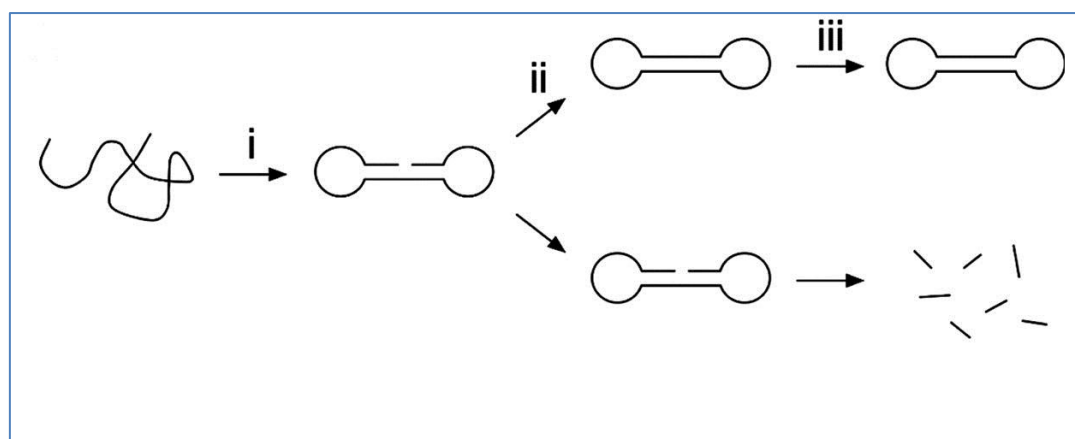


Figure 1.34: Circular aptamer synthesis. Oligonucleotide is (i) heated and slow cooled to form aptamer heads and duplex region, followed by (ii) ligation, and (iii) exonucleolysis to degrade any uncircularised oligonucleotide, leaving only intact circular aptamer (adapted from Daniel *et al.*, 2006).

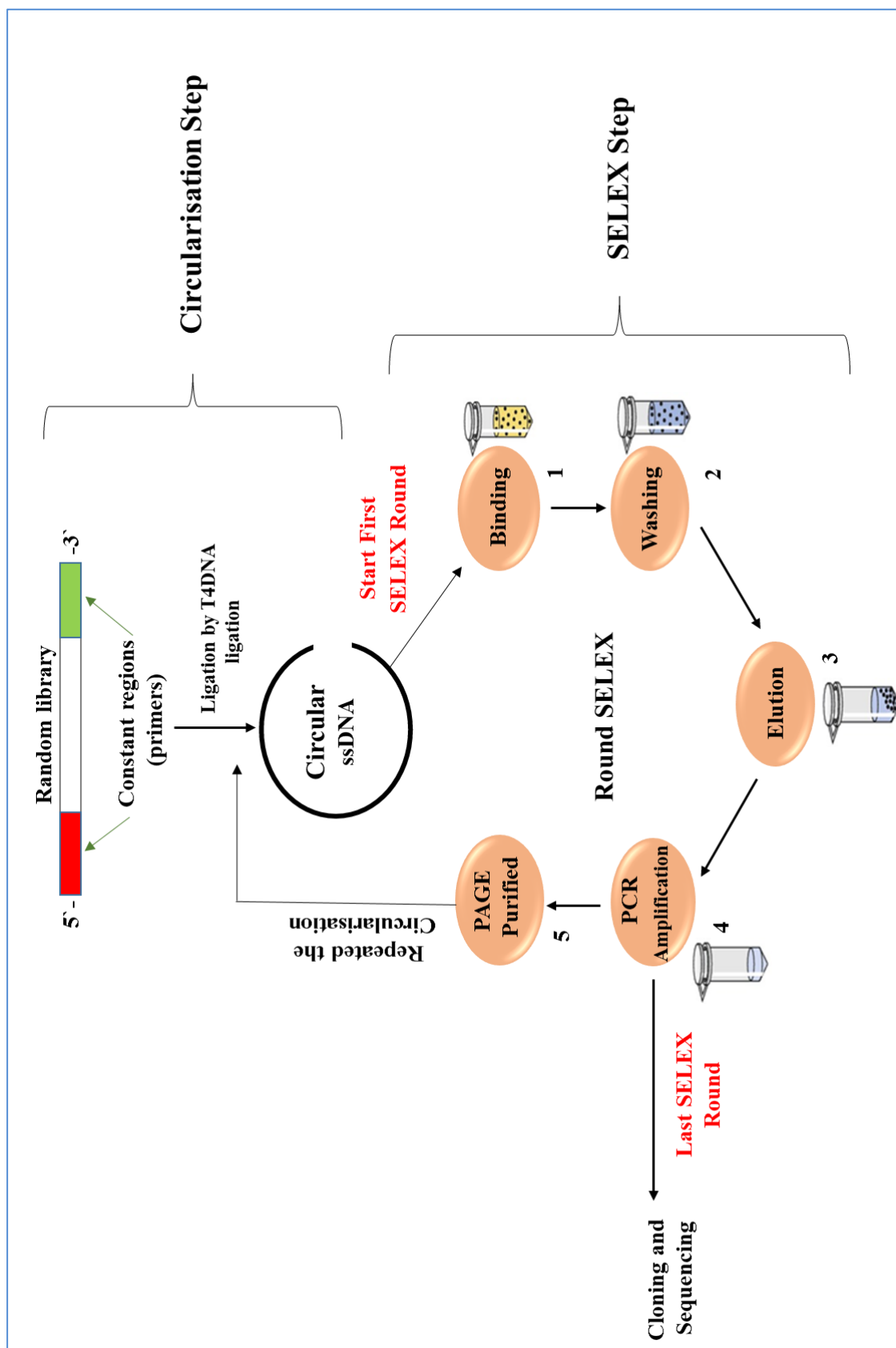


Figure 1.35: Circularisation of aptamer by ligation then start the first-round SELEX, after finishing the first round the circularisation was repeated to start the next round.

1.11 Aim of the Study

Many Sirtuins targets are involved in cancer and in many types of cancers, SIRT1 is found to be overexpressed. In more recent literature, it has been found that SIRT1 functions as an oncogene as well as a tumour suppressor, depending on the kind of tissue and cancer etiology. Although the SIRT1 deacetylase activity of SIRT1 toward p53 may firmly assign to the protein a specific function in tumour promotion, several studies including (i) expression studies in tumours, (ii) manipulation of SIRT1 levels in animals, and (iii) pharmacological approaches have challenged this hypothesis leading to the opposite view that SIRT1 may function as a tumour suppressor. This study aims to find answers to the question, “How can SIRT1 behave as a tumour suppressor?” In this regard, we propose to:

- 1- Develop highly selective ligands (circular and linear aptamers) against SIRT1 enzyme as a therapy for cancer.
- 2- Study the interactions between selected aptamers and SIRT1 enzyme *in vitro*.
- 3- Study the interactions between selected aptamers and SIRT1 enzyme in a range of cancer cell lines as the first step towards the development of an alternative chemotherapy for cancer diseases.

2 MATERIALS & METHODS

2.1 Materials

1- DNA Oligonucleotide:

DNA oligoes	Sequence (5`-3`)	Supplier
-BAS Library	TTCGGAAGAGATGGCGAC-N40- CGAGCTGATCCTGATGGAA	TriLink BioTechnologies
-BAS P1 Primer	TTCGGAAGAGATGGCGAC	TriLink BioTechnologies
-BAS P3 Primer	ATGTCGTGCGTGCTA-SP18- TTCCATCAGGATCAGCTCG	TriLink BioTechnologies
-BAS P3-notail Primer	TTCCATCAGGATCAGCTCG	TriLink BioTechnologies
-BAS ligation splint	TCTCTTCCGAATTCCATCAGGA	TriLink BioTechnologies

2- Molecular biology:

Materials	Supplier
- <i>E. coli</i> DH5 α , Cat no. BIO-85027	Bioline, UK
-EcoRI digestion, Cat no. ER0275	Thermo Scientific, USA
-Exonuclease I, Cat no. EN0581	Thermo Scientific, USA
-Gel Red Nucleic Acid Gel Stain, Cat no. BT41002	Biotium, UK
-HyperLadder™ 25bp, Cat no. Bio-33057	BioLabs, UK
-ISOLATE II PCR and Gel kit, Cat no. BIO-52059	Bioline, UK
-Maxima Hot Start PCR Master Mix (2X), Cat no. K1052	Thermo Scientific, USA
-Molecular biology reagents, water, nuclease-free, Cat no. R0581	Thermo Scientific, USA
-Nucleospin® Extract II kit	Qiagen, Valencia
-PreScission Protease, Cat no. 27-0843-01	GE HealthCare, USA
-QIAEX II Gel Extraction Kit (150), Cat.no.20021	Qiagen, UK
-QIAprep Spin Miniprep Kit, Cat no. 27104	Qiagen, Valencia
-SIRT1, GST-tagged, Cat no. SIRT1-462H	Creative BioMart, USA
-T4 DNA ligase, Cat no. 2011A	Takara, Japan
-T4 polynucleotide kinase (PNK), Cat no. EK00312	Thermo Scientific, USA

-TA-cloning kit, Cat no. K1213	Thermo Scientific, USA
-VENT DNA polymerase	Biolabs, Ipswich, UK
-X-Gal, Cat no. R0941	Thermo Scientific, USA

3- Chemicals:

Materials	Supplier
-10x TBE solution (Tris- borate, EDTA buffer)	Severn Biotech Ltd. UK
-2', 7'-dichlorofluorescein diacetate (DCFDA), Cat no. ab113851	Abcam, UK
-Acrylamide: Bis-Acrylamide 29:1 solution 30% DNase and RNase free, electrophoresis tested	Fisher BioReagents Ltd. UK
-Acrylamide: Bis-Acrylamide 29:1 solution 40% DNase and RNase free, electrophoresis tested	Fisher BioReagents Ltd. UK
-Ammonium persulfate (APS)	Fisher Ltd. USA
-DAPI	Thermo Fisher Scientific, USA
-Dimethyl sulfoxide (DMSO)	Fisher Scientific, USA
-Dodecyl sulfate, sodium salt, 99%	Sigma-Aldrich Ltd. USA
-EDTA	Sigma-Aldrich Ltd. USA
-Ethanol	Fisher Ltd. USA
-Fetal bovine serum FBS	Fisher Scientific, USA
-Formalin 4%	Sigma-Aldrich, USA
-MTT (3-(4,5-dimethylthiazol-2-yl)-2,5-diphenyltetrazolium bromide)	Fisher Scientific, USA
-PBS	Gibco, UK
-Roswell Park Memorial Institute-1640 (RPMI-1640) medium	Gibco, Merelbeke, Belgium
-SIRT1 fluorometric drug discovery kit, Cat no. AK-555	Enzo Life Science, UK
-Sodium acetate, 99+%, a.c.s. reagent	Sigma-Aldrich Ltd. USA
-Sodium chloride NaCl	Sigma-Aldrich Ltd. USA
-TBHP (Tert-Butyl Hydrogen Peroxide)	Abcam, UK
-TEMED	Fisher Ltd. USA

-Tris-Cl	Sigma-Aldrich Ltd. USA
-TritonX-100	Sigma-Aldrich, USA
-Urea	Sigma-Aldrich Ltd. USA

4- Laboratory Equipment

Equipment	Company
-A ProteOn™ GLM Sensor Chip	Bio-Rad GLM, USA
-Acrylamide gel chamber EPS-300X	C.B.S Scientific, Taiwan
-Autoclave ST19T	Dixons, UK
-Concentrator plus	Eppendorf, UK
-Cool Centrifuge	Hermle, Germany
-Cytation™ 3 Cell Imaging Multi-Mode Reader	BioTek, USA
-Dry bath	Labnet, USA
-Eppendorf Centrifuge MiniSpin® plus	OrtoAlresa, SPANISH
-Freezer –20°C	Biocold, UK
-Freezer –80°C	Premium U410
-Fridge 4°C	Biocold, UK
-Gel Doc system	Bio-Rad, USA
-HPLC-UV	Agilent tech, USA
-Incubator shaker	Innova 40, USA
-Luminometer Microplate Readers	BMG Lab tech, Germany
-Microwave	Samsung, Korea
-Nano drop	Thermo Scientific, USA
-PCR Apparatus	Stratagene, USA
-pH–Meter HI2211	HANNA, USA
-Pipettes P2, P20, P200, P1000	Rainin Instrument, USA
-Platform shaker STR6	STUART Scientific, UK
-ProteOn™ XPR36	Bio-Rad, USA
-UV Scan	GiBox Syngene, USA
-Vortex	SciQuip, UK
-Water Bath	GFL, Germany

5- Buffers**1. Laemmli–Loading Buffer (2×)**

0.5 M Tris–HCl (pH 6.8)

2% (w/v) SDS

20% (v/v) glycerol

2% (v/v) 2–mercaptoethanol

2% (v/v) bromophenolblue

2. SDS–PAGE Running Buffer (5×)

192 mM Tris–HCl

1.9 M Glycin

0.5% SDS

3. Elution buffer (for extract the ssDNA)

5 M NaCl

1 M Tris-HCl (pH 7.5)

0.5 M EDTA (pH 8.0)

In 200 ml ddH₂O**4. Binding buffer (for cleavage GST) pH 7.3**

140 mM NaCl

2.7 mM KCl

10 mM Na₂ HPO₄1.8 mM KH₂PO₄**5. PreScission cleavage buffer pH 7.5**

50 mM Tris-HCl

150 mM NaCl

1 mM EDTA

1 mM dithiothreitol DTT

6. Coupling buffer pH 8.3 (Immobilisation of protein)0.2 M NaHCO₃

0.5 M NaCl

7. Binding buffer TBS pH 7.5 (Immobilisation of protein)

50 mM Tris-Base

150 mM NaCl

8. Equilibration buffer (Immobilisation of protein)

1 mM HCl (ice cold)

9. Aqueous buffer pH 7.0 (Immobilisation of protein)1.2 g NaH₂PO₄0.885 g Na₂HPO₄1 L ddH₂O**10. Binding buffer for SELEX pH 7.4**

100 mM NaCl

5 mM MgCl₂**11. Washing buffer 1 for SELEX pH 7.4**

150 mM NaCl

5 mM MgCl₂**12. Washing buffer 2 for SELEX pH 7.4**

300 mM NaCl

5 mM MgCl₂**13. Washing buffer 3 for SELEX pH 7.4**

600 mM NaCl

5 mM MgCl₂

14. Washing buffer 4 for SELEX pH 7.4

900 mM NaCl

5 mM MgCl₂**15. Elution buffer for SELEX pH 7.4**

1500 mM NaCl

5 mM MgCl₂**2.2 Methods****2.2.1 Introduction**

The methodology described here the generation of aptamers for SIRT1 enzyme using SELEX strategy including: affinity matrix preparation, isolation, identification and characterisation of SIRT1 enzyme and selected aptamers sequences. The latter includes studies using FLUOR DE LYS® fluorescent assay for SIRT1 aptamers characterisation and kinetics, Surface Plasmon Resonance (SPR) binding assay to determine the KD values. To investigate the effects of aptamers on viability of cancer cell lines and the cellular redox state *in vitro*; MTT, ROS and fluorescent imaging assays were used with several cancer cell lines such as: A549 (human adenocarcinoma of alveolar basal epithelial cells), MCF7 (breast cancer cell lines, oestrogen positive and model for majority of breast cancers), MDA-MB-468 (breast cancer oestrogen negative), CaCo-2 (colorectal adenocarcinoma), HepG2 (children liver hepatocellular carcinoma) and U2OS (children human bone osteosarcoma), as a normal model Beas2b (normal human bronchial epithelial cells) and HaCaT (human keratinocyte cell line) were used. The susceptibility of natural nucleic acids to nucleolytic degradation is a serious hurdle for their applications. Plasma stability assays by HPLC-UV and gel electrophoresis were performed to evaluate the stability of the C3 aptamer in human plasma.

2.2.2 DNA Technology

2.2.2.1 Library Preparation

The library used for selection was made up of a 40nt randomised region flanked by 18nt and 19nt fixed primer sites with a total sequence length of 77nt. The library was referred as the BAS single stranded DNA library with the nucleotide sequence of 5'-TTCGGAAGAGATGGCGAC-N40-CGAGCTGATCCTGATGGAA-3'. The library was desalted and lyophilised by the manufacture (TriLink, San Diego, USA). For the amplification of library BAS, the following two primers were used: BAS P1, 5'-TTCGGAAGAGATGGCGAC-3', and BAS P3, 5'-ATGTCGTGCGTGCTA-SP18-TTCCATCAGGATCAGCTCG-3'. BAS ligation splint 5'-TCTCTTCCGAATTCCATCAGGA-3' was used as a linker sequence to facilitate circularisation of the BAS library. BAS P3-notail primer 5'-TTCCATCAGGATCAGCTCG-3' was used in a TA-cloning kit. BAS library was further purified using poly acrylamide gel electrophoresis (PAGE) on a 10% denaturing gel (8 M urea). Table 2.1 demonstrates the ssDNA library with primers.

Table 2.1: Sequence of BAS library and primers that used in SELEX.

Oligonucleotide	Sequence (5'-3')
BAS Library	TTCGGAAGAGATGGCGAC-N40-CGAGCTGATCCTGATGGAA
BAS P1 Primer	TTCGGAAGAGATGGCGAC
BAS P3 Primer	ATGTCGTGCGTGCTA-SP18-TTCCATCAGGATCAGCTCG
BAS P3-untailed Primer	TTCCATCAGGATCAGCTCG
BAS Ligation Splint	TCTCTTCCGAATTCCATCAGGA

2.2.2.2 Denaturing Urea–Polyacrylamide Gel Electrophoresis (PAGE)

Denaturing secondary DNA structures is carried out by urea PAGE or denaturing urea polyacrylamide gel electrophoresis employing 6-8 M urea according to Summur *et al.*, (2009). This method is utilised for the separation of polyacrylamide gel matrix fragments between 2 to 500 bases. These fragments have extremely minute difference in lengths. The type of acrylamide solution decides the movement of the sample; a higher concentration helps in breaking up of the lower molecular weight fragments. The unstructured DNA molecules can also be separated by combining urea at a temperature of 45-55° C. The method helps to evaluate single stranded DNA fragments.

For BAS library, gels including 10% acrylamide, and 8M Urea were prepared with 77 nt. These gels were then run in 1xTBE buffer at 15 V/cm.

Content for one gel:

Materials	ml
Acrylamide concentration	10%
-UREA	4.8 g
-30% Acryl (29:1)	2.5
-10x TBE	1.0
-Deionized water	6.58

The solution was heated for 20s in the microwave and mixed, then added these materials:

Materials	µl
-TEMED	4.0
-30% APS	33

The bands were visualised by UV transilluminators.

2.2.2.3 Determination of Nucleic Acids on Gels by Gel Red Staining

Gel Red is a sensitive, stable and environmentally safe fluorescent nucleic acid dye, which interacts with the bases of nucleic acids. It is an intercalating agent commonly used as a nucleic acid stain on polyacrylamide gels. The gels were stained by Gel Red solution (added 15 μ l of Gel Red 10,000X stock reagent and 5 ml of 1 M NaCl to 45 ml H₂O) for 30 min and visualised on an ultraviolet transilluminator at 302 nm. Bands of desired length were extracted from a polyacrylamide gel.

2.2.2.4 Extraction of Nucleic Acids from Polyacrylamide Gels

To extract the ssDNA from a polyacrylamide gel, the gel was visualised on an UV transilluminator at 302 nm, and the desired band was cut out precisely from the gel. The gel was then chopped into small pieces and put into a 1.5 ml eppendorf tube. About two volumes of elution buffer (8 ml of 5 M NaCl, 2 ml of 1 M Tris-Cl, pH 7.5, 0.4 ml of 0.5 M EDTA, pH 8.0; were added to 200 ml ddH₂O) were added to the tube and incubated at RT with shaking for overnight. The sample was then centrifuged and the supernatant was recovered carefully. The purified nucleic acids could be obtained by ethanol precipitation.

2.2.2.5 Ethanol Precipitation

Ethanol precipitation is a commonly used technique for concentrating and purify DNA preparations in aqueous solution. It was carried out according to Zeugin &Hartley (1985). The mechanism is that nucleic acids are polar and soluble in water, which is polar too, while insoluble in the ethanol. Before precipitation, the salt concentration of the sample was adjusted to 0.3 M by adding 1/10 volume of 3 M sodium acetate. Two volumes of cold 100% ethanol were added to the sample, and then placed at -20° C at overnight. The sample was spun at 11,000g in a microcentrifugation for 30 min to harvest the precipitated DNA. The supernatant was decanted carefully. The pellet was washed by adding 1 ml of 70% ethanol and spinning for 5s. The supernatant was then decanted carefully. A working stock of BAS library was obtained by resuspending the purified pellet in 50 μ l Milli-Q ddH₂O and quantification by UV spectroscopy. The BAS library was prepared for circularisation by phosphorylation using T4 polynucleotide kinase (PNK).

2.2.2.6 Phosphorylation of Linear BAS

Prepared the following reaction mixture:

Material	μl
-Linear BAS stock (1660 pmol)	2.0
-Reaction buffer A for T4 Polynucleotide Kinase (10X)	66.4
-ATP (10 mM)	66.4
-T4 Polynucleotide Kinase (332 U)	33.2
-Water, nuclease-free	496.3

The total volume of 664 μl mixture reaction were mixed, spun briefly then incubated at 37° C for 1h. After incubation, heated at 75° C for 10 min. After this, phosphorylation reaction was directly used for ligation by T4 DNA ligase.

2.2.2.7 Ligation of BAS by T4 DNA Ligation

Prepared the following reaction mixture:

Material	μl
-Linker BAS (1660 pmol)	2.0
-Phosphorylation reaction (500 nM)	664
-T4 DNA Ligase Buffer (10X)	400
-Water nuclease free	2920

The reaction mixture was heated at 90° C for 1 min then cooled at room temperature for 10 min. The 14 μl of 4900 U T4 DNA ligase were added then mixed thoroughly and incubated at 16° C overnight. Ligation reactions were ethanol precipitation and PAGE purification by using poly acrylamide gel electrophoresis (PAGE) on a 10% denaturing gel (8 M urea).

Circular bands were identified by UV transilluminators as the closest band with a decreased mobility versus a linear marker. Circular stock was purified and quantitated by the previously mentioned protocol. The circularised ssDNA product migrates slower (above) the linear ssDNA band; the adenylated-oligo intermediate can be seen as a band just above the linear ssDNA.

2.2.2.8 Confirmation of circularity of the BAS Library

Circularity of the BAS library was confirmed using EcoRI digestion by manufacturer recommended protocol and extending incubation time to overnight at 37° C.

2.2.2.9 Removing the Linear ssDNA Template and Adenylated Intermediate from the Reaction

The circularisation reaction was terminated by ethanol precipitation, the remaining linear ssDNA substrate and linear single-stranded adenylated intermediate removed by treatment with Exonuclease I which digests linear ssDNA (Kuhn and Frank-Kamenetskii, 2005). The circular ssDNA is resistant to these exonucleases, while the linear ssDNA and adenylated intermediate are digested. The linear ssDNA and adenylated intermediate were eliminated by addition of 20 U of Exonuclease I, followed by incubation at 37° C for 45 min.

2.2.3 Protein Technology

2.2.3.1 SIRT1 Enzyme

In this research study, recombinant human SIRT1, GST-tagged (SIRT1-462H) was used as an enzyme that binds with circular and linear aptamer. Before beginning the selection of circular and linear aptamer against SIRT1 enzyme, the GST tag was cleaved from the enzyme by PreScission Protease on-column GSTrap FF (GE HealthCare).

2.2.3.2 Cleavage of GST-tag using PreScission Protease (PSP)

Pre-Scission protease used to remove the GST affinity tag from SIRT1 enzyme. The GST and human rhinovirus 3C protease are available in the PreScission Protease, which is a naturally obtained fusion protein. This protease cleaves GST fusion proteins generated from the pGEX-6P vectors pGEX-6P-1, pGEX-6P-2, and pGEX-6P-3 and through protease control at the same time. The Gly and Gln remain of the recognition sequence of LeuGluValLeuPheGln/GlyPro were split through the PreScission Protease. A syringe was filled with binding buffer and connect the GSTrap FF column (1 ml) to the syringe using the adapter supplied as shown in figure 2.1.

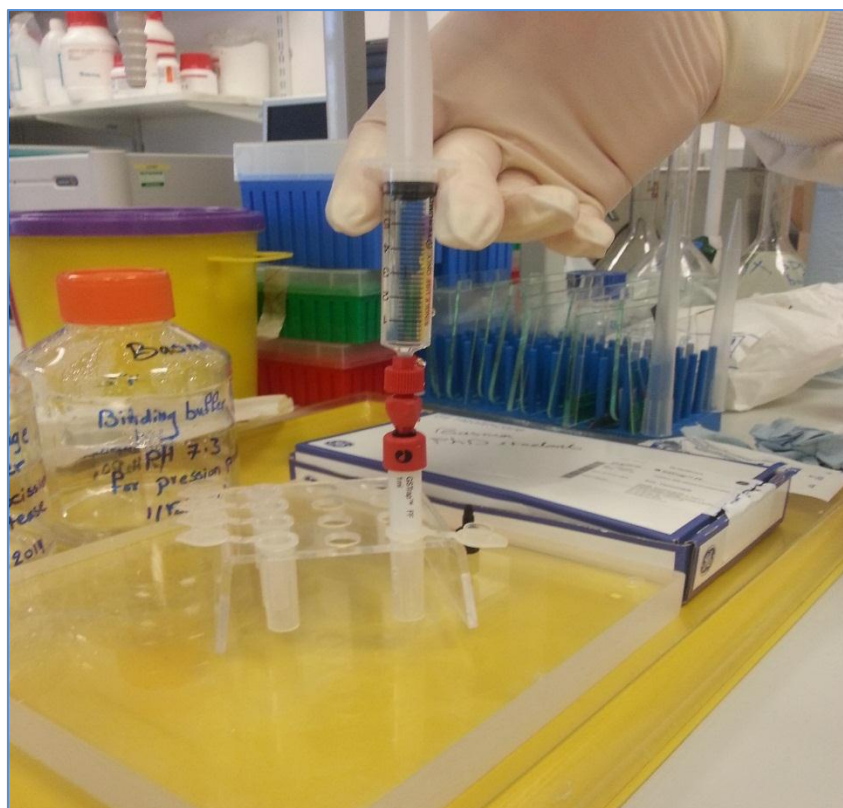


Figure 2.1: GSTrap FF connect with syringe by adapter supplied.

Equilibrated the column with five column volumes (5 ml) of binding buffer then washed the column with 10 (1 ml) column volumes of PreScission cleavage buffer. The following components were assembled in separate 1.5 mL tube:

Material	μ l
-PreScission protease (2 U)	1.5
-SIRT1 enzyme (0.09 mg/ml)	150 μ g
-Cleavage buffer (1X)	298.35
-Total volume	200

The PreScission Protease mixture was loaded onto the column using a syringe; incubated the column at 4° C overnight. In the next day 3 ml of PreScission cleavage buffer were loaded into the column and collected the elution (0.5–1 ml/tube). The elution solution was contained the SIRT1 enzyme, while the GST moiety of the fusion protein and the PreScission Protease were remained bound to GSTrap FF. The extent of cleavage of SIRT1 enzyme was determined by SDS- PAGE.

2.2.3.3 Sodium Dodecyl Sulfate Polyacrylamide Gel Electrophoresis (SDS–PAGE)

Sodium dodecyl sulfate polyacrylamide gel electrophoresis (SDS–PAGE) is a technique to separate proteins according to their electrophoretic mobility (Win and Craig, 1994). SDS, an anionic detergent, which denatures secondary and non–disulfide–linked tertiary structures, applies a negative charge to each protein in proportion to its mass. So SDS–protein complexes can migrate through the gel in accordance to the size of protein. A discontinuous buffer system with stacking gel and separating gel is used to increase the resolution of protein separation during SDS–PAGE. The stacking gel contains chloride ions, which migrate faster through the gel than the protein sample, while the electrophoresis buffer contains glycine ions, which migrate slower. The protein molecules are trapped in a band between these ions. As the protein enters the separating gel, which has a smaller pore size, a higher pH and a higher salt concentration, the glycine is ionised, the voltage gradient is dissipated and the protein is separated based on size. Gels were prepared in an Expedeon mini–gel set (Expedeon Ltd, UK) with 20% separating gel and 4% stacking gel. The samples were mixed with 2X Laemmli–loading buffer and boiled at 95° C for 5min. The gels were run in SDS–PAGE running buffer at 8 V/cm. Proteins were visualised using Instant Blue stain.

2.2.4 SELEX Methodology

2.2.4.1 Affinity Chromatography *In vitro* Selection Method

An affinity chromatography based method was used for the *in vitro* selection of aptamers against the SIRT1 enzyme.

2.2.4.1.1 Immobilisation of SIRT1

The method was based on the immobilisation of the SIRT1 enzyme to an NHS-HP SpinTrap column (1 ml) (GE HealthCare) with the functionality of the column dependent on the manufacturer’s recommendations.

First step, prepare the media by adding 200 μ l of 50% gel solution into the column, then removing the storage solution by centrifugation for 1 min at 150 g. 400 μ l of ice-cold 1 mM HCL was added to the column and rotated in the container for a minute, at 150 g to stabilise the solution. The entire process was repeated thrice.

On reaching the equilibrium stage, 200 μ l of protein solution, (0.5 to 1.0 mg/ml in coupling buffer) were added with the solution so form and suspend manually for incubation by slow mixing for around 30 min and centrifuged for 1 min at 150 g to remove excessive enzyme. Any remaining active groups were blocked with washing by alternating between high pH buffer and low pH buffer. Equilibration for the binding was achieved by adding 400 μ l binding buffer, and stirring thrice for 1 min at 150 g.

2.2.4.1.2 *In Vitro* Selection of Circular Aptamers Against SIRT1 Enzyme

For the initial round of selection, 100 pmol of circularised BAS library were added to 200 μ l of binding buffer in column containing SIRT1 and incubated for 2h at 37° C as shown in figure 2.2. A stringent system of buffers was designed to provide a highly specific ssDNA aptamers. The binding buffer was composed of 100 mM NaCl, and 5 mM MgCl₂ at a pH of 7.4 and selection were carried out at 37° C to obtain aptamers for use in physiological situations. Wash and elution buffers were formulated with the same 5 mM MgCl₂ compositions, but differing in concentrations of NaCl from 0.15 M-1.5 M respectively. A wash step with 5 columns (1 ml) volumes of binding buffer to allow for the washing out of weak binders due to increased stress on the interaction caused by the high volume and salt concentration of wash preceded an elution step of 1.5 column volumes. The DNA precipitated from the supernatant with 500 μ l of 100% cold ethanol and was spun at 21,000 g at 4° C for 30 min.

The pellet was washed once with 70% ethanol and repeated the centrifugation step then dried and re-suspended in 20 μ l water and set up PCR in 100 μ l volumes.

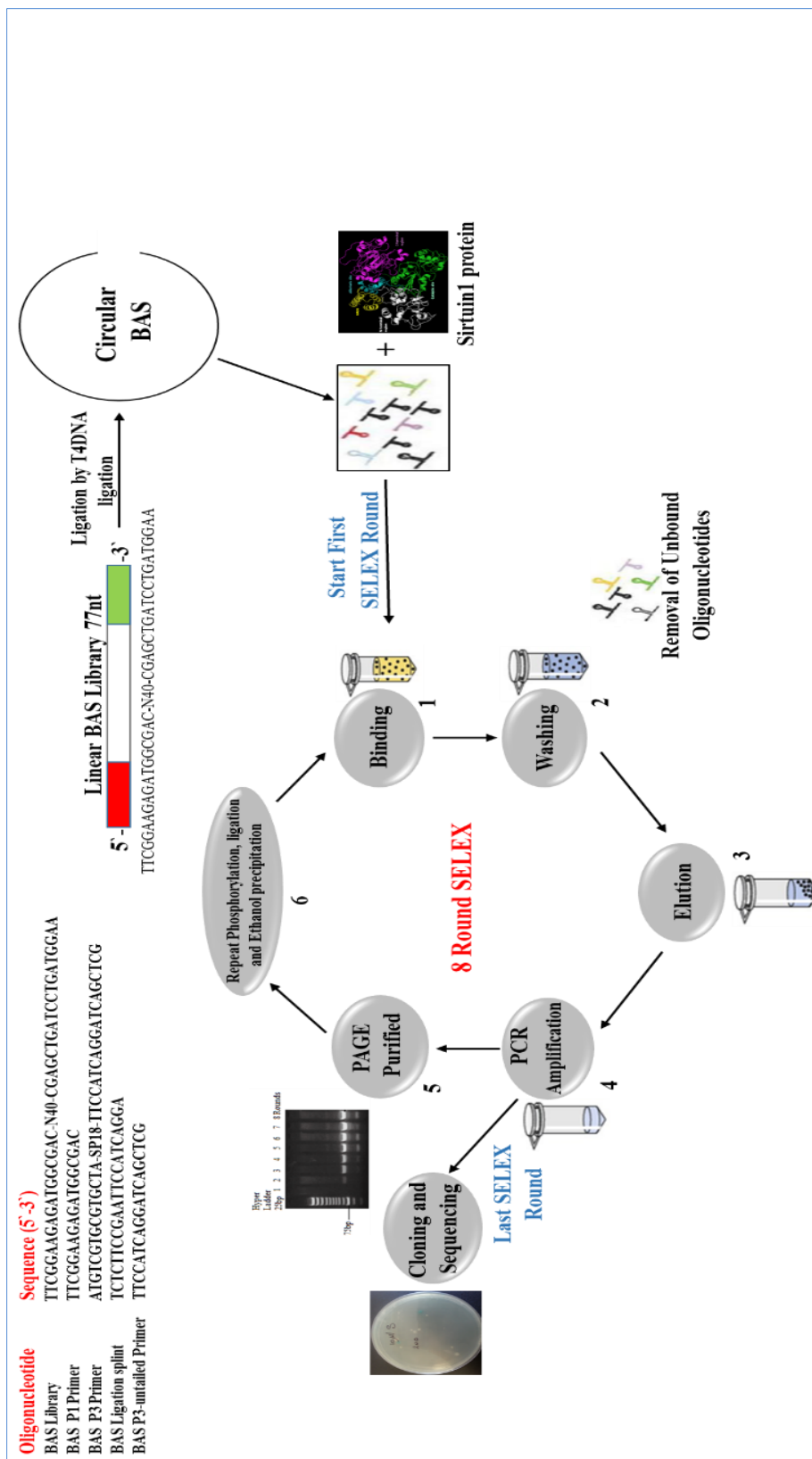


Figure 2.2: Scheme of selection of circular aptamer against SIRT1.

2.2.4.1.3 Conventional Polymerase Chain Reaction (PCR)

A primer mediated enzymatic amplification of precisely cloned or genomic DNA sequences is known as Polymerase Chain Reaction (PCR). The PCR process aims to amplify a template DNA through use of thermostable DNA polymerase enzyme which then catalyses the reaction where excess of an oligonucleotide primer pair and four deoxynucleoside triphosphates (dNTPs) are utilised for formation of millions of copies of the target sequence. It is automated for routine functions in the laboratories all over the world. A repetitive set of three significant steps that describe one PCR cycle is required for the PCR process. A denaturing process for the DNA at 94° C is the first step. Second step involves annealing of two oligonucleotide primers towards the single-stranded template. The enzymatic extension of the primers to generate copies that could be used as templates in ensuing cycles is the final step. In this experiment, Maximam Hot Start PCR Master Mix (2X) was utilised. All the PCR reactions were conducted at a volume of 100µl as presented below.

1 µM of BAS P1 and BAS P3 primers plus 20 µl of BAS purified from the first selection round were used for the of PCR amplification process. There are 18 atom hexaethyleneglycol spacer in the antisense primer BAS P3 (Integrated DNA Technologies) which connects the complementary primer region to a 15nt random sequence. This helps with strand separation of the PCR products by PAGE. There was a 95° C-30 second denaturation step, a 50° C-45 second annealing step and a 72° C-10 second extension step run on a Robo Cycler Gradient 96 included in the 20 cycle PCR program. Urea PAGE was used in order to purify the reaction and band visualisation through UV transilluminators. DNA band was eluted by ISOLATE II PCR and Gel kit. The technique mentioned for formation of the initial library was used to phosphorylate and circularise the pooled PCR products. Around 8 rounds were repeated for all the steps of selection circular aptamers as against SIRT1 enzyme. To clone through the PCR protocol, the final population from the selection experiment was kept ready for the process. For this an un-tailed variant, BAS P3-notail was used instead of BAS P3 primer. This led to double stranded DNA that is appropriate for utilisation in a TA-cloning kit.

2.2.4.1.4 *In Vitro* Selection of Linear Aptamers Against SIRT1 Enzyme

According to the protocol of linear aptamer, it is the same protocol of the circular aptamer but without circularisation of BAS library and the initial round of selection, added 2.5 μ l of 1000 pmol BAS library as shown in figure 2.3.

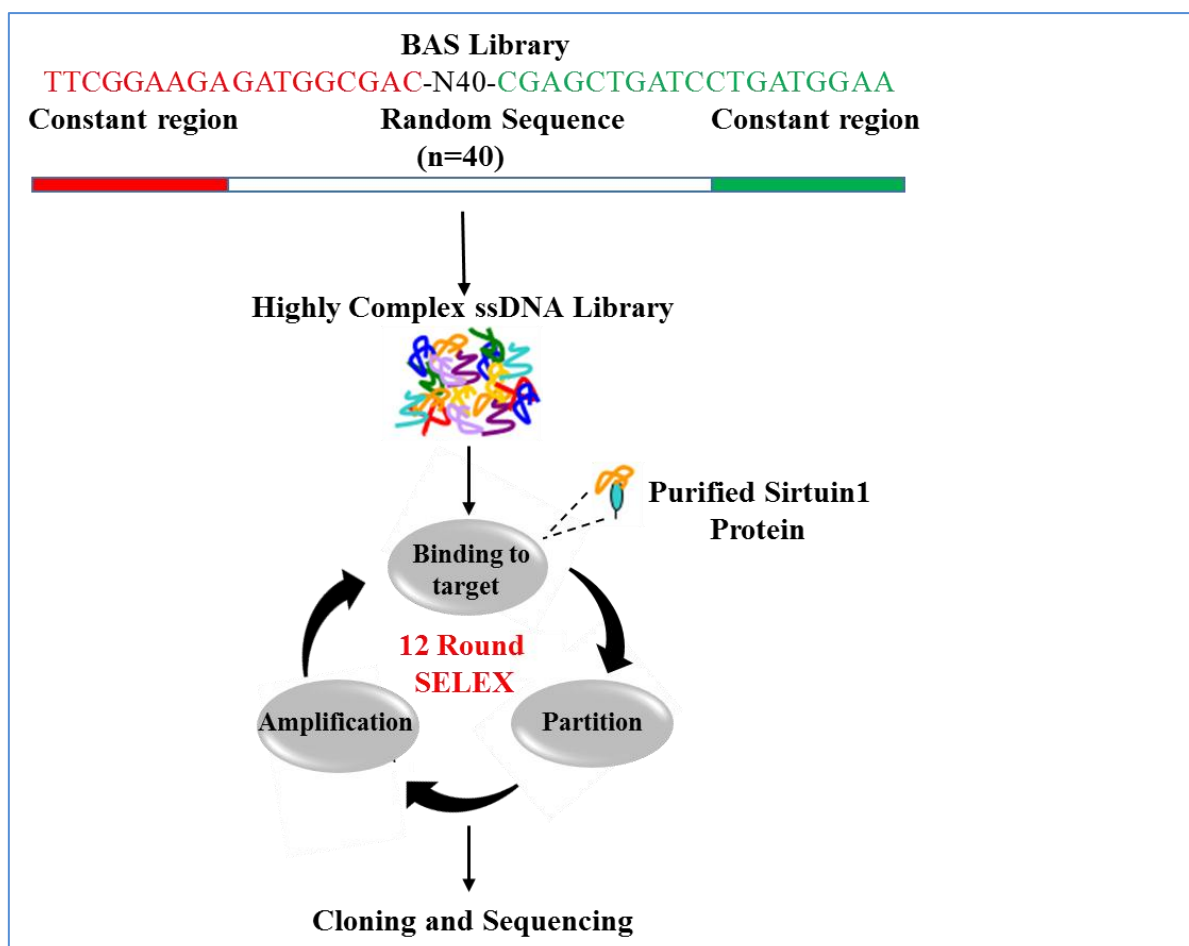


Figure 2.3: Scheme of selection of linear aptamer against SIRT1.

2.2.4.2 DNA Cloning

The final population of the selection experiment was prepared for cloning by the secondary PCR protocol. Secondary PCR was used with 2 μ l of purified primary PCR product as template. Additional reaction components consist of 200 μ M dNTP, 1 μ M each of BAS P1 and BAS P3 primers, buffer and VENT DNA polymerase. PCR products of the 8th rounds of circular aptamer and 12th rounds of linear aptamer were purified for the cloning using the Nucleospin® Extract II kit, which removed unincorporated nucleotides, primers and polymerase. BAS P3

primer is replaced with an un-tailed variant, BAS P3-notail, resulting in double stranded DNA suitable for use in a TA-cloning kit.

2.2.4.2.1 DNA Ligation

The ligation reactions were mixed by pipetting 2 µl of each purified PCR product (0.52 pmol) and added to 6 µl of 5X ligation buffer with the addition of 3 µl of Vector Ptz57R/T (0.17 pmol ends) and 1 µl of 3 U T4 DNA ligase in a final reaction volume of 30 µl. Thereafter, the reaction mixture was stirred for 5 min and then kept on 4° C overnight.

2.2.4.2.2 Transformation

E. coli DH5α high efficiency competent cells were used for transformation. The tube of frozen cells, removed from -70° C, and placed in an ice bath until it thawed. The cells were mixed by gently flicking the tube. For each transformation reaction, 50 µl of 10 pg/µl cells were mixed with 2.5 µl (100 pg) ligation products. The tubes were gently mixed and then placed on ice for 20 min. Then incubated the tubes for 1.5h at 37° C with shaking (~ 150 rpm). For each transformation, 100 µl cell cultures were plated onto duplicate LB/100 µg/ml ampicillin 50 µg/ml/IPTG/X-Gal plates. Each colony containing solution was incubated overnight at 37° C with gentle shaking.

2.2.4.2.3 Isolation of Plasmid DNA

Many of colonies were picked and inoculated into LB media supplemented with 50 µg/ml ampicillin and incubated overnight at 37° C with shaking. The preparation of the plasmid conducted using QIAprep Spin Miniprep Kit. Briefly, 2 ml cell culture were centrifuged for 30s at 11,000 g to pellet the bacteria. Buffer A1 (resuspension buffer), A2 (a lysis buffer solution) and A3 (neutralisation buffer) were added to the pellet in turn to lyse the cell. The tube was centrifuged for 5 to 10 min at 11,000 g to clear the lysate. The supernatant, loaded onto a NucleoSpin® Plasmid column and centrifuged for 1 min at 11,000 g bound the plasmid DNA to the silica membrane. The membrane was washed with 600 µl buffer A4 (a washing buffer) and centrifuged for 5s. The plasmid DNA from each column was eluted using 50 µL of AE buffer (10 mM Tris-Cl, 1 mM EDTA, pH 8.0) which was added carefully onto the column filter and incubated at RT for 1 min before centrifugation at 13,000 g for 1 min. Following

centrifugation, the columns were discarded and the eluted plasmid DNA from each column was quantified by measuring absorption spectra at 260 nm using a WPA Biowave II UV-visible Spectrophotometer. The purified plasmid DNA from each column was stored at -20° C until further use.

2.2.4.2.4 Confirmation of Ligation

Before sequencing, successful insertion of the selected aptamers was confirmed by restriction enzyme digestion of the inserted-plasmid DNA. The digested products were separated by urea acrylamide gel electrophoresis, and visualised using the Gel Doc system. Briefly, 10 µl of each purified plasmid DNA was added individually into micro centrifuge tubes. This was followed by the addition of 1.5 µl of restriction digest buffer and 3.5 µl of EcoRI restriction enzyme (containing 10 U) into each tube. Thereafter, all tubes were incubated at 37° C for 30 mins. The digestion reaction was stopped by heating each tube to 65° C for 5 mins to denature the restriction enzyme. Following denaturation, the digested DNA from each tube was stained using 2X gel loading and subsequently separated by electrophoresis using a 10% urea gel. The 77 bp DNA bands containing the desired aptamer sequences were confirmed by comparison with a low range DNA ladder when visualised using the Gel Doc system.

2.2.4.2.5 DNA Sequencing

For each clone, 0.6 µg purified plasmid DNA was mixed with 20 pmol forward primers in a 100 µl PCR tube. All aptamer samples were outsourced (Source Bio Science, UK). The Data of sequencing were analysed by DNAMAN 5.29 software (Lynnon corp., Quebec, QC, Canada).

2.2.5 Aptamer Characterisation

SIRT1 aptamers identified from the SELEX procedure were characterised with respect to their [i] *in vitro* characterisation of activators and inhibitors of the SIRT1 enzyme, [ii] SIRT1 kinetics as a function of the concentrations of Fluor de Lys®-SIRT1 Substrate and NAD⁺, and [iii] KD values using SPR. All aptamers utilised in the characterisation studies were commercially synthesised by Integrated DNA Technologies (California, USA) at a 100 nmol

scale at the 5'- and -3' end of each oligonucleotide sequence and circular aptamer followed previous protocol of circularisation.

2.2.5.1 *In vitro* Characterisation of Activators and Inhibitors of SIRT1

Enzyme

SIRT1 fluorometric drug discovery kit (AK-555, Enzo Life Science, UK) was used to study the activity of SIRT1 activators and inhibitors with 10 aptamers (linear1, linear2, linear3, linear4, circular1, circular2, circular3, circular4, circular5 and circular6) as in table 2.2. The assay was done according to the manufacturer's instructions using a fluorescent emission at 460 nm with excitation at 360 nm. Briefly, 10 µl of (0.8 µM, 0.4 µM, 0.2 µM and 0.1 µM from linear1, linear2, linear3, linear4, circular1, circular3 and circular5 aptamers), (0.3 µM, 0.15 µM, 0.075 µM and 0.0375 µM from circular2, circular4 and circular6 aptamers), 200 µM resveratrol, 200 µM suramin and 200 µM nicotinamid were incubated with 5 µl of 0.2 U/µl SIRT1 enzyme per well at 37° C prior to substrate addition. The reaction was initiated by adding 25 µl of 2X Substrates in assay buffer (40% Assay Buffer, 60% 3.33X Substrates), then stopped by adding 50 µl of 1X Developer II/2 mM nicotinamide. At this time 25 µl of 2X Substrate solution was added to "Time Zero" samples. Incubated plate at room temperature for at least 45 min, then samples were read using Luminometer Microplate Readers fluorescence measurement system with an excitation wavelength of 350-380 nm and detection of emitted light in the range 450-480 nm. SIRT1 enzyme activity was calculated after subtracting the background. The experiment included suramin, an inhibitor of SIRT1 activity and resveratrol, an activator of SIRT1 activity.

Table 0.2: Sequences of 10 aptamers, sequences of C2, C4, C6, L2, L4 the same sequences of C1, C3, C5, L1, L3 respectively, but with primers.

Aptamers	Sequences (5`-3`)
Circular 1(C1)	TTGCGGCATTTTGCCTTCCTGTTTTGCTCACCCAGAAAC
Circular 2(C2)	TTCGGAAGAGATGGCGAC TTGCGGCATTTTGCCTTCCTGTTTTGCTCACCCAGAAAC CGAGCTGATCCTGATGGAA
Circular 3(C3)	CGAGTGGGTTACATCGAAACTGGATCTCAACAGCGGTAAC
Circular 4(C4)	TTCGGAAGAGATGGCGAC CGAGTGGGTTACATCGAAACTGGATCTCAACAGCGGTAAC CGAGCTGATCCTGATGGAA
Circular 5(C5)	CACTCCCTCTGCGTGCGAATTTTGCCTATGGCGCATATTC
Circular 6(C6)	TTCGGAAGAGATGGCGAC CACTCCCTCTGCGTGCGAATTTTGCCTATGGCGCATATTC CGAGCTGATCCTGATGGAA
Linear 1 (L1)	CGGACTGCAACCTATGCTATCGTTGATGTCTGTCCAAGCA
Linear 2 (L2)	TTCGGAAGAGATGGCGAC CGGACTGCAACCTATGCTATCGTTGATGTCTGTCCAAGCA CGAGCTGATCCTGATGGAA
Linear 3 (L3)	CACTTTTCGGGGAAATGTGCGCGGAACCCCTATTTGTTTA
Linear 4 (L4)	TTCGGAAGAGATGGCGAC CACTTTTCGGGGAAATGTGCGCGGAACCCCTATTTGTTTA CGAGCTGATCCTGATGGAA

2.2.5.2 SIRT1 Kinetics as a Function of the Concentrations of Fluor de Lys-SIRT1 Substrate and NAD⁺

SIRT1 kinetics was validated using a SIRT1 Fluorimetric Drug Discovery kit. 2 μ M, 1 μ M, 0.5 μ M and 0.1 μ M of linear3, linear4, circular3 and circular4 aptamers were added to SIRT1 (2 U/well) and incubated (37° C) with the indicated concentrations of peptide substrate and 100 μ M NAD⁺. Reactions were stopped at indicated times (5 min,15 min,30 min and 45 min) with Fluor de Lys® Developer II/2 mM nicotinamide and fluorescence measured at a wavelength in the range, Ex. 360 nm and Em. 460 nm.

2.2.5.3 Characterisation of the SIRT1 Enzyme Interaction with Selected Aptamers using Surface Plasmon Resonance (SPR)

The affinity of the selected aptamers (linear3, linear4, circular3 and circular4) for their SIRT1 enzyme target was determined using ProteOn™ XPR36 protein interaction array system. The principle is based on the optical phenomenon of SPR. The system was operated at 25° C in running buffer consisting of 100 mM NaCl, 5 mM MgCl₂, pH 7.4, depending on the selection conditions. A ProteOn™ GLM Sensor Chip was conditioned using 1 M NaCl and 50 mM NaOH for 1 min three times, according to the manufacturer's instructions. A range of protein concentrations from 12.5, 25, 50, 100, 200, 400 and 800 nM were tested under different injection times and the optimum conditions used were 100 µl of 800 nM SIRT1 enzyme in running buffer perfused over each individual channel at the rate of 25 µl/min for 60s pulse. The ligands (aptamers) were prepared in their selection buffers (phosphate buffer containing 100 mM NaCl, 5 mM MgCl₂, pH 7.4) at 10 µM and were injected at a medium pace over the surface at 25 µl/min. After the injection was complete, the complex was washed for an additional 30s with 1X binding buffer. The chip surfaces were regenerated down to protein level by application 1.5 M NaCl, 5 mM MgCl₂, pH 7.4 in 30s pulses. Determination of association (K_a) and dissociation constants (K_d) of the aptamer-SIRT1 complexes were evaluated using a ProteOn Manager™ software supplied by the manufacturer (ProteOn™ XPR36).

2.2.6 Cell Culture

Human adenocarcinoma of alveolar basal epithelial cells (A549), breast cancer cell lines oestrogen positive (MCF7), breast cancer oestrogen negative (MDA-MB-468) and children human bone osteosarcoma (U2OS) were originally obtained from Sigma Aldrich and stored in the Cell Bank of the Biomedical Research Centre at the University of Salford. Colorectal adenocarcinoma (Caco-2) and children liver hepatocellular carcinoma (HepG2) were purchased from American Type Culture Collection ATCC (Middlesex, UK). A549, MCF-7, MDA-MB-468, U2OS, Caco-2 and HepG2 cell lines were used as model cancer cells for this study. Human keratinocyte cell line (HaCaT) was purchased from CLS Cell Lines Service (GmbH, Germany). Normal human bronchial epithelial cells (Beas2b) were also obtained from American Type Culture Collection ATCC (Middlesex, UK), Beas-2b cell line was used as normal model cell line.

2.2.6.1 Cell Maintenance

A549, HepG2 and MDA-MB-468 cells were maintained in Roswell Park Memorial Institute-1640 (RPMI-1640) medium (Gibco, Merelbeke, Belgium) supplemented with 0.5% fetal bovine serum FBS (Fisher Scientific, USA) and 1% L-Glutamine (Lonza, UK) as well as to 1% Penicillin-Streptomycin-Amphotericin B 100X (Lonza, UK) as antiseptic. MCF-7, U2OS and CaCo-2 cells were maintained in DMEM medium (Lonza, UK) supplemented with 0.5% fetal bovine serum FBS and 1% L-Glutamine (Lonza, UK) as well as to 1% Penicillin-Streptomycin-Amphotericin B 100X (Lonza, UK) as antiseptic. Beas2b cells were maintained in BEGM medium containing all the recommended supplements (Lonza, UK). Cells were cultured in 75 cm² flasks and incubated in 5% CO₂/ 95% humidified air at 37° C. Once the cells reached 90% confluency, flasks containing A549, HepG2, MDA-MB-468, MCF-7, U2OS, CaCo-2 or Beas2b cells were passaged under sterile conditions. The cells were washed with 5 ml of phosphate buffered saline solution (PBS) and then incubated for 2 min in trypsin solution at 37° C to allow cells to detach from the bottom of the flask. An equal volume of complete growth media was added and the cell suspension was transferred into a 50 ml conical tube. Cells were then centrifuged at 1200 rpm for 3min. The supernatant was discarded and the cell pellet resuspended in fresh supplemented growth media. Cells were then counted under the microscope on a haemocytometer and used as required.

2.2.6.2 Storage and Resuscitation of Cell Lines

Following trypsinisation of a confluent 75 cm² flask, the cell suspension was centrifuged at 1200 rpm for 3 min. The cell pellet was then resuspended in 4ml freezing medium (Life Technologies) and 1ml aliquots were added to cryovials (Thermo Fisher Scientific, Loughborough, UK). The cells were stored at -80° C for 24h and were stored under liquid nitrogen for long-term storage. Cells stored under liquid nitrogen were quickly thawed at 37° C and added to 10 ml fresh growth media. The cells were harvested by centrifugation and resuspended in 25 ml of fresh medium and transferred to a 75 cm² flask and grown.

2.2.6.3 Cell Viability by MTT Assay

The MTT assay was used to assess the effects of aptamers (linear3, linear4, circular3 and circular4) on cancer cell viability. A 100 μ l from all cells suspensions (A549, MCF7, MDA-MB-468, CaCo-2, HepG2, U2OS, HaCaT and Beas2b) were dispensed into 96-well flat-bottom tissue culture plates (Falcon, USA) at concentrations of 5×10^3 cells per well and incubated 24h under standard conditions; 4×10^3 cells/well for 48h incubation, and 3×10^3 cells/well for 72h incubation. After 24h, the cells were treated with 2.5 μ M aptamers (linear3, linear4, circular3 and circular4) then cells were exposed to 50 μ M TBHP (Tert-Butyl Hydrogen Peroxide) before and after 4h from adding the aptamers as shown in figure 2.4. After a recovery period 24h, 48h and 72h, the cell culture medium was removed and cultures were incubated with medium containing 30 μ l of MTT solution (3 mg/ml MTT in PBS) (3-(4,5-Dimethylthiazol-2-yl)-2,5-Diphenyltetrazolium Bromide) for 4h at 37° C. After 4h this medium was removed by gentle inversion and tapping onto paper. Control wells received only 100 μ l growth media. 100 μ l of dimethyl sulfoxide (DMSO) was added to each well, the plates were then kept at room temperature in the dark for about 15-20 min. The absorbance of each well was measured by multiscan reader at a wavelength of 540 nm and correcting for background absorbance using a wavelength of 650 nm.

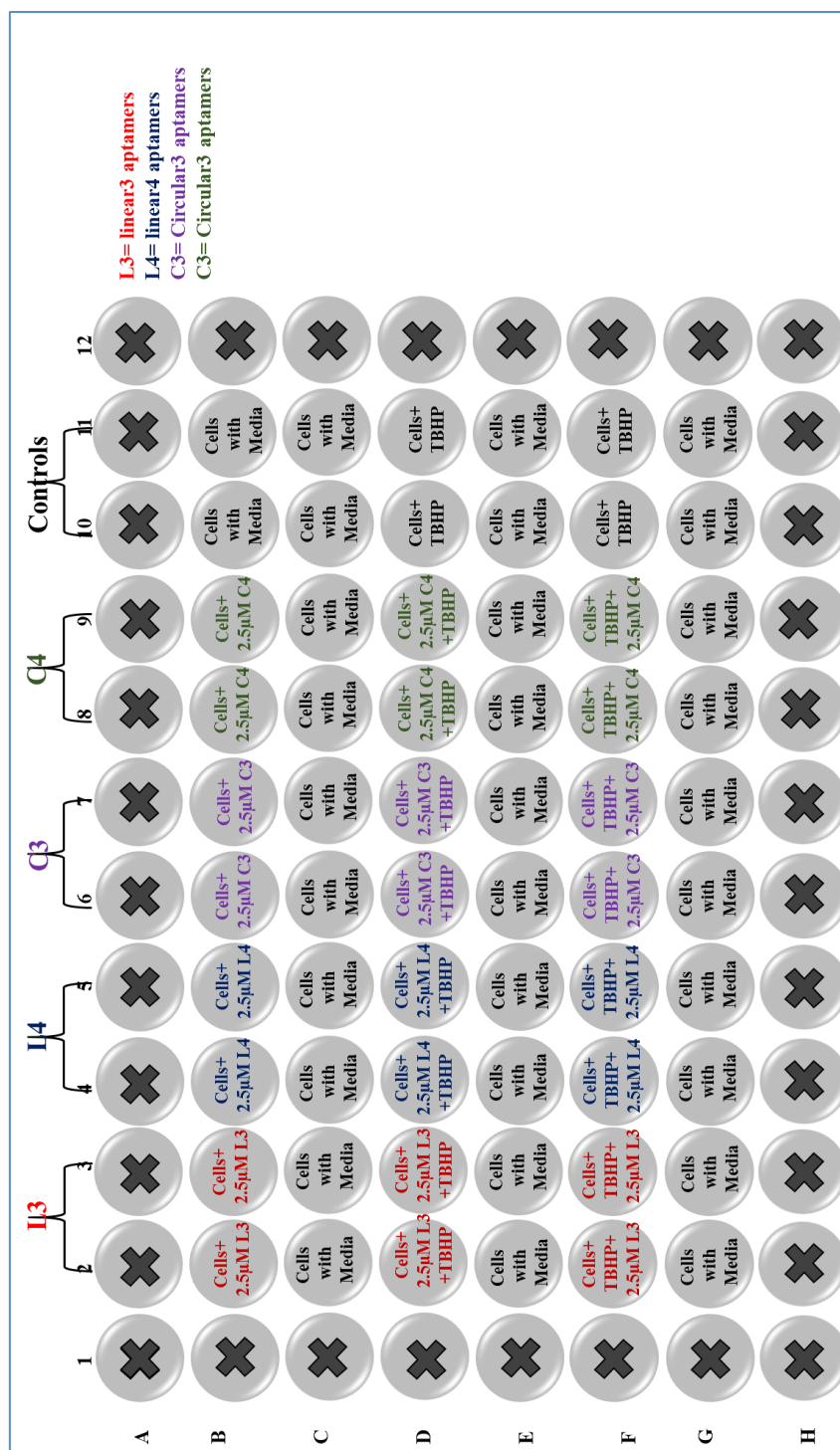


Figure 2.4: 96-well plate template for MTT assay. Column 2 and 3 are duplicate of linear3 aptamers, whereas line 2B and 3B contains cells and 2.5 µM L3 aptamer; line 2D and 3D contains cells and 2.5 µM L3 aptamer then after 4h added 50 µM TBHP; line 2F and 3F contains cells and 50 µM TBHP then after 4h added 2.5 µM L3 aptamer. Column 4 and 5 are duplicate of linear4 aptamers, whereas line 4B and 5B contains cells and 2.5 µM L4 aptamer; line 4D and 5D contains cells and 2.5 µM L4 aptamer then after 4h added 50 µM TBHP; line 4F and 5F contains cells and 50 µM TBHP then after 4h added 2.5 µM L4 aptamer. Column 6 and 7 are duplicate of circular3 aptamers, whereas line 6B and 7B contains cells and 50 µM C3 aptamer; line 6D and 7D contains cells and 2.5 µM C3 aptamer then after 4h added 50 µM TBHP; line 6F and 7F contains cells and 50 µM TBHP then after 4h added 2.5 µM C3 aptamer. Column 8 and 9 are duplicate of circular4 aptamers, whereas line 8B and 9B contains cells and 2.5 µM C4 aptamer; line 8D and 9D contains cells and 2.5 µM C4 aptamer then after 4h added 50 µM TBHP; line 8F and 9F contains cells and 50 µM TBHP then after 4h added 2.5 µM C4 aptamer. Column 10 and 11 are duplicate of controls, whereas line 11B, 12B, 1-12C1-12E and 1-12G contains cells with media; line 10D, 11D, 10F and 11F contains cells with TBHP.

2.2.6.4 Measurement of Reactive Oxygen Species ROS Production

Intracellular reactive oxygen species (ROS) production was measured in aptamers-treated and in control cells using 2',7'-dichlorofluorescein diacetate (DCFDA). A 100 μ l from all cells suspensions (A549, MCF7, MDA-MB-468, CaCo-2, HepG2, U2OS and Beas2b) were dispensed into 96-well flat clear-bottom dark sided tissue culture plates (Falcon, USA) at concentrations of 25,000 cells per well and incubated 24h under standard conditions. After 24h, the cells were treated with 2.5 μ M aptamers (linear3, linear4, circular3 and circular4) then cells were exposed to 50 μ M TBHP (Tert-Butyl Hydrogen Peroxide) before and after 4h from adding the aptamers as shown in figure 2.5. After a recovery period 6h, the cell culture medium was removed and washed the cells in 100 μ l/well 1x buffer, then 1x buffer was removed and cells stained by adding 100 μ l/well of the DCFDA solution (10 μ l of 20 Mm DCFDA solution with 10 ml 1X buffer). The culture was incubated with the DCFDA solution for about 45 min at 37° C. After that, DCFDA solution was removed and 100 μ l/well 1X buffer were added. Fluorescent units were measured in each well using luminometer microplate readers fluorescence measurement system with an excitation wavelength of 485 nm and an emission wavelength of 535 nm.

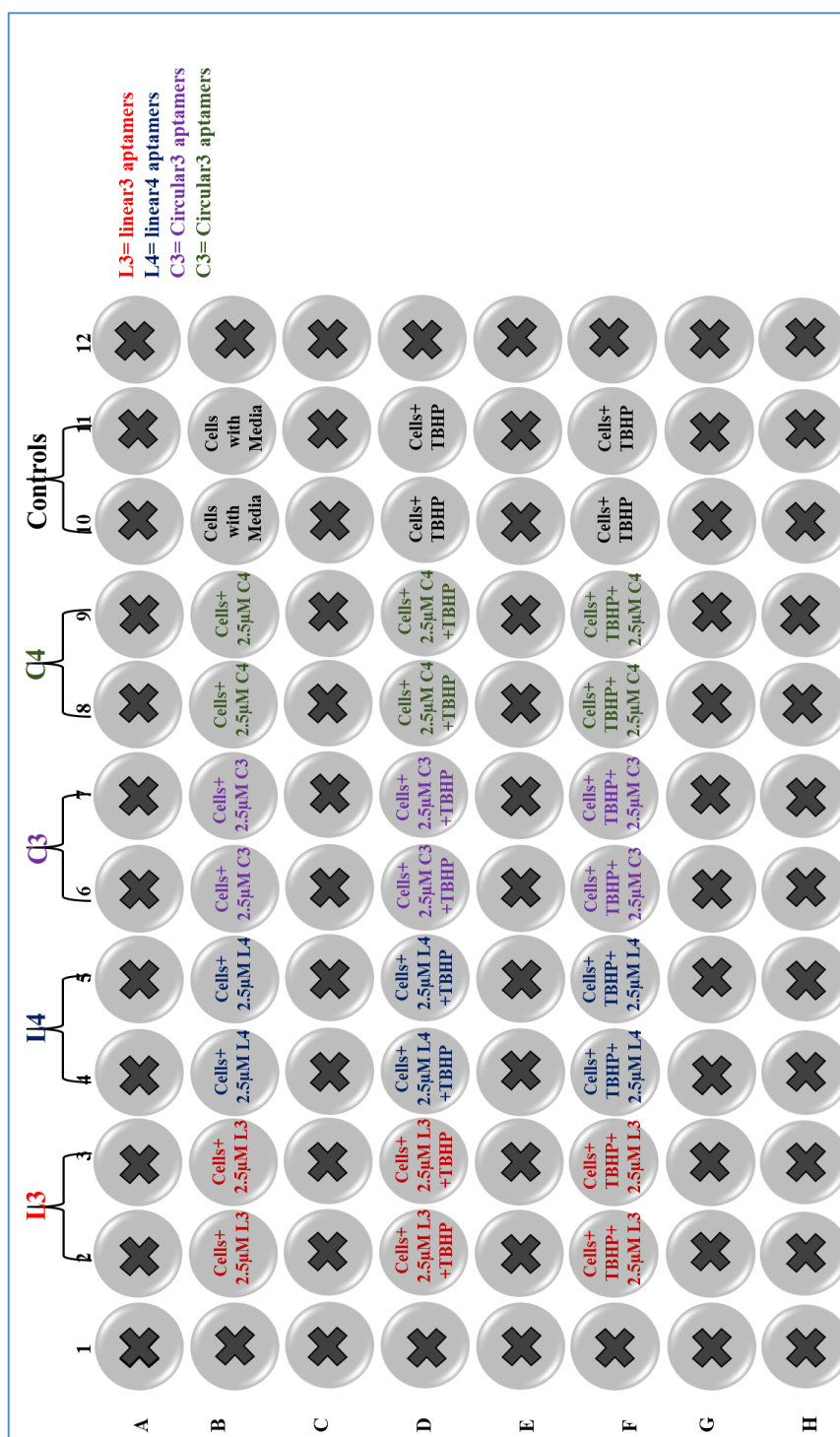


Figure 2.5: 96-well plate template for ROS assay. Column 2 and 3 are duplicate of linear3 aptamers, whereas line 2B and 3B contains cells and 2.5 µM L3 aptamer; line 2D and 3D contains cells and 2.5 µM L3 aptamer then after 4h added 50 µM TBHP; line 2F and 3F contains cells and 50 µM TBHP then after 4h added 2.5 µM L3 aptamer. Column 4 and 5 are duplicate of linear4 aptamers, whereas line 4B and 5B contains cells and 2.5 µM L4 aptamer; line 4D and 5D contains cells and 2.5 µM L4 aptamer then after 4h added 50 µM TBHP; line 4F and 5F contains cells and 50 µM TBHP then after 4h added 2.5 µM L4 aptamer. Column 6 and 7 are duplicate of circular3 aptamers, whereas line 6B and 7B contains cells and 2.5 µM C3 aptamer; line 6D and 7D contains cells and 2.5 µM C3 aptamer then after 4h added 50 µM TBHP; line 6F and 7F contains cells and 50 µM TBHP then after 4h added 2.5 µM C3 aptamer. Column 8 and 9 are duplicate of circular4 aptamers, whereas line 8B and 9B contains cells and 2.5 µM C4 aptamer; line 8D and 9D contains cells and 2.5 µM C4 aptamer then after 4h added 50 µM TBHP; line 8F and 9F contains cells and 50 µM TBHP then after 4h added 2.5 µM C4 aptamer. Column 10 and 11 are duplicate of controls, whereas line 11B and 12B contains cells with media; line 10D, 11D, 10F and 11F contains cells with TBHP.

2.2.6.5 *In Vitro* Evaluation the Activity of SIRT1 Enzyme in Cells by Fluor de Lys Deacetylase

Deacetylase activity of SIRT1 was measured using the Fluor de Lys Deacetylase kit (BML-AK500, Enzo Life Science, UK) according to the manufacturer's instructions. Briefly, 4×10^4 cells were plated in 100 μ l of appropriate media in the presence of 2 μ M of TSA in 0.1% (v/v) ethanol (to inhibit class I and II HDACs and all remaining activity can be attributed to SIRT1), after 24h the media were removed and 50 μ l of medium containing 10 μ l of (0.25, 0.5 and 1 μ M from C3 aptamer), 100 and 200 μ M resveratrol, 100 μ M suramin and 100 μ M nicotinamide were incubated for 3h at 37° C prior to substrate addition. The reaction was initiated by adding 25 μ l of 2X Fluor de Lys substrate; the plate was incubated for 5h at 37° C, followed by addition of 50 μ l of 1X Developer II/2 mM nicotinamide. After further incubation for 45 min at 37° C, the fluorescence was measured using microplate-reading fluorimeter capable of excitation at a wavelength in the range 350-380 nm and detection of emitted light in the range 450-480 nm. SIRT1 enzyme activity was calculated by subtracting the background in the presence of suramin, an inhibitor of SIRT1 activity and resveratrol, an activator of SIRT1 activity.

2.2.6.6 The Half Maximal Inhibitory Concentration (IC₅₀) Value Determination

The IC₅₀ of the drug can be determined by constructing a dose-response curve and examining the effect of different concentrations of the antagonist on reversing agonist activity. IC₅₀ values can be calculated for a given antagonist by determining the concentration needed to inhibit half of the maximum biological response of the agonist. IC₅₀ values are very dependent on conditions under which they are measured. In general, the higher concentration of inhibitor, the more agonist activity will be lowered. IC₅₀ value increases as agonist concentration increases. Furthermore, depending on the type of inhibition other factors may influence IC₅₀ value. According to the *in vitro* MTT assay, the IC₅₀ represents the concentration of the tested C3 aptamer that is required for 50% inhibition of the cell viability. Based on the obtained data using the *in vitro* MTT assay, the IC₅₀ values for C3 aptamer at 72h after the cells

exposure to C3 aptamer. To determine the IC₅₀ values, the concentration range used of C3 aptamer was 0.0078 - 1.00 µM.

2.2.6.7 Immunofluorescence Microscopy

Cells were seeded at approximately 10,000 cells per well in 96-well clear bottom imaging tissue culture plates. Eighteen hours later, cells were either treated with 1 µM C3 aptamer and incubated in 5% CO₂/ 95% humidified air at 37° C overnight, after that the cells were washed 3 times in PBS, fixed for 5 min at room temperature with Formalin 4%, washed 2 times in PBS, then permeabilised by 0.5% Triton X-100 for 5 mins, washed 3 times with PBS; nonspecific binding was blocked with 3% FBS for 1h at room temperature, then the blocking solution were removed, 100 µl/well of Anti-SIRT1 antibody (Abcam, ab104833) were added to cells and incubated overnight at 4° C in a wet tray. In the next day, cells washed 3 times in PBS, and incubated for 2h in dark at room temperature with 1:2000 Alexa Fluor 546 goat anti-mouse IgG (AF546) (Life Technologies-USA)/1% FBS in PBS, then cells washed 3 times in PBS. At the end, the preparations were treated with 10 µl mounting medium containing DAPI to stain cell nuclei left for 1hr before the microscopic examination using Cytation™ 3 Cell Imaging Multi-Mode Reader.

2.2.7 In vitro Plasma Stability Assay of C3 Aptamer

2.2.7.1 Plasma Stability Assay of C3 Aptamer by Urea PAGE

The susceptibility of natural nucleic acids to nucleolytic degradation is a serious hurdle for their therapeutic applications. Plasma stability assays were performed to evaluate the stability of the aptamer in human plasma (Sigma, UK). Assessment of stability was performed as described (Klussmann *et al.*, 1996). 10 µl of C3 aptamer in 90% human plasma in 10X PBS, pH 7.2 was incubated at simulated body temperature for a series of times (0, 15, 30, 60, 120, 240 min and 24h) at a concentration of 1 µM. To maintain conditions of constant pH and sample concentration, lengthy incubations were performed in an incubator at 37° C, 94.5% humidity and 5% carbon dioxide. Aliquots were mixed with equal volumes of stop solution (8 M urea, 50 mM EDTA) and frozen at -20° C. The samples (1 µM C3 aptamers each) were separated on 10% denaturing (8.3 M urea) polyacrylamide gels. The gels were stained in Gel Red staining, and visualised at 254 nm.

2.2.7.2 Plasma Stability Assay of C3 Aptamer by HPLC-UV

HPLC method carried out according to Shaw *et al.*, (1995). 300 µl of C3 aptamer in 90% human plasma buffered in 10X PBS, pH 7.2 was incubated at simulated body temperature for a series of times (0, 15, 30, 60, 120, 240 min and 24h) at a concentration of 1 µM. C3 aptamer samples was purified using C18 RP column. 100 µl of C3 aptamer in water was incubated at Zero time and after 24h as a control. The HPLC-UV system used was G1329B. The mobile phases used were: A: HPLC grade water, B: Acetonitrile (HPLC grade, Fisher). The flow rate was 1.4 ml/min and the C18 RP column temperature was maintained at 37° C by a column oven. The gradient profile was linear to 100% B in 10min and held at 100% B for 2 min. The detection wavelength was 256 nm and the injection volume was 50 µl. Total cycle time between injections was 20 min. Data were acquired and stored by a Peak Pro data acquisition system (Agilent Chemstation software).

2.3 Data Analysis

All statistical analysis of SIRT1 aptamers characterisation, kinetic and IC₅₀ data were performed using the nonlinear curve fitting software Origin 9.1 software. Comparison between all groups within the same plate of MTT and ROS assay were evaluated by one-way ANOVA with Tukey (Origin 9.1 software), comparison between the same group within the same plate of MTT and ROS assay were evaluated by paired t-test using (IBM SPSS Statistics 20) statistical software. Values of $p < 0.05$ were considered statistically significant.

3 *IN VITRO* SELECTION AND IDENTIFICATION OF CIRCULAR AND LINEAR ssDNA APTAMERS AGAINST SIRTUIN1 ENZYME BY SELEX METHODOLOGY.

3.1 Introduction

Nucleic acids due to their ability to create Watson-Crick base pairing, have long been exploited as molecular recognition elements (MREs). This use has been to form detection tools for DNA and has developed from the classical Southern blotting approach (Southern, 1975) to the advanced microarray platforms (Schena *et al.*, 1995). As a sensing material, the utilisation of nucleic acids has increased from nucleic acid detection to the recognition of non-nucleic acid targets. This comprises of proteins, small molecules, viruses, mammalian cells, bacteria, and parasites (Bunka *et al.*, 2006). This has been improved through the formation of the process of *in vitro* selection or also referred as SELEX (Ellington and Szostak, 1990; Tuerk and Gold, 1990). The identification of extremely selective functional nucleic acid sequences referred to as aptamers is the concluding outcome of the SELEX process. Aptamers are single stranded DNA, RNA, and modified nucleic acid molecules having the capability to develop distinct tertiary structures and keep a particular target for the purpose of binding. In this chapter, a detailed approach for isolation of linear and circular ssDNA aptamers for a SIRT1 enzyme target taken from a random-sequence DNA library by using an affinity column-based SELEX procedure is explained. The work presented here outlines the results of experiments using a NHS-HP SpinTrap column-based SELEX strategy including affinity matrix preparation, isolation, identification of SIRT1 enzyme and selected aptamers sequences. These investigations included: [i] preparation of SIRT1 target-immobilised affinity chromatography; [ii] performing conventional PCR amplifications to enrich selected sequences; [iii] and cloning the sequences of aptamers. The reasons behind investigating each of the aforementioned methods are explained as followed.

Affinity columns play an important role in generating aptamers binding to protein, and there have been a reports (Ferreira *et al.*, 2006) utilising affinity columns for producing aptamers against target. Ferreira *et al.* (2006) reported the isolation of a 25-base-long variable region for their ability to bind to the unglycosylated form of the MUC1 protein using a based SELEX methodology. This aptamer had KD value of 47nM. Based on this report, it was reasoned that

a similar strategy might be successfully applied for selecting SIRT1 specific aptamers. In the basic SELEX procedure, conventional PCR was chosen and the aptamer-bound elution from each cycle of selection were used as the template for PCR amplification.

In summary, the aim of this chapter was to establish a practical laboratory procedure for generating ssDNA aptamers capable of binding to SIRT1 enzyme with the objectives of development of a novel designing high affinity and selectivity ligands.

3.2 Methods

All methods for selection aptamers were described in chapter 2 section 2.2.2.2–2.2.2.9 for circular aptamers and section 2.2.2.2–2.2.2.5 for linear aptamers.

3.3 Results

3.3.1 Circularisation of BAS Library

Linear BAS of 77 bases was circularised by phosphorylation of linear BAS stock using T4 polynucleotide kinase then directly used this reaction for ligation by T4 DNA ligase. The efficiency of circularisation reaction can be readily assessed by gel electrophoresis. When ligating oligos, approximately 3 μ l of the 100 pmol circularisation reaction was loaded into the gel lane of a 10% acrylamide 8 M urea denaturing gel. The circularised BAS product migrated slower (above) than the linear BAS band (figure 3.1).

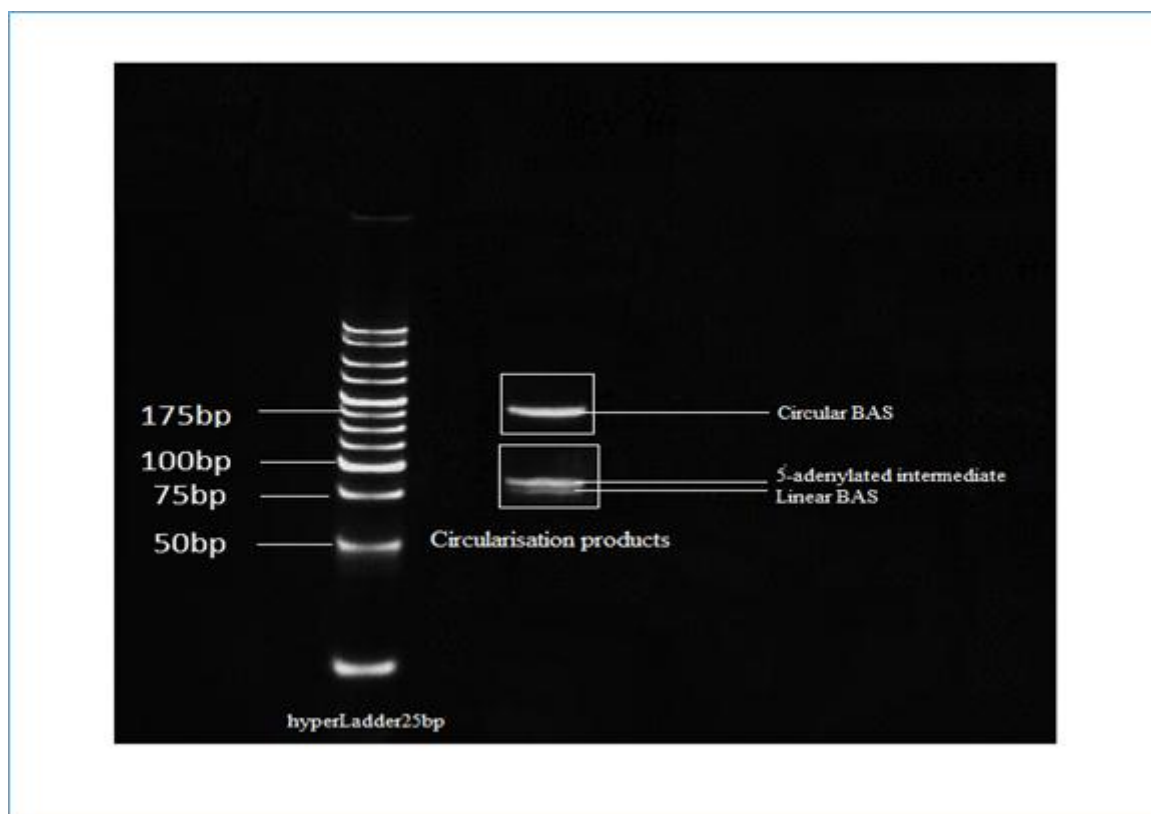


Figure 3.1: Circularisation of BAS library. 77-nucleotide BAS oligo was converted to a circular BAS. Lane 1, DNA markers 25bp; lane 2, circularisation proceeds through an adenylated intermediate.

In the figure 3.1 an adenylated-oligo intermediate can be seen as a band just above the linear BAS. This 5'-adenylated intermediate consists in initial part of ligation, the remaining linear BAS and linear single-stranded adenylated intermediate were removed by treatment with ExonucleaseI (which digests linear ssDNA). The circular BAS is resistant to these exonucleases, while the linear BAS and adenylated intermediate are digested as shown in figure 3.2. Figure 3.3 demonstrated the all steps of circularisation BAS Library.

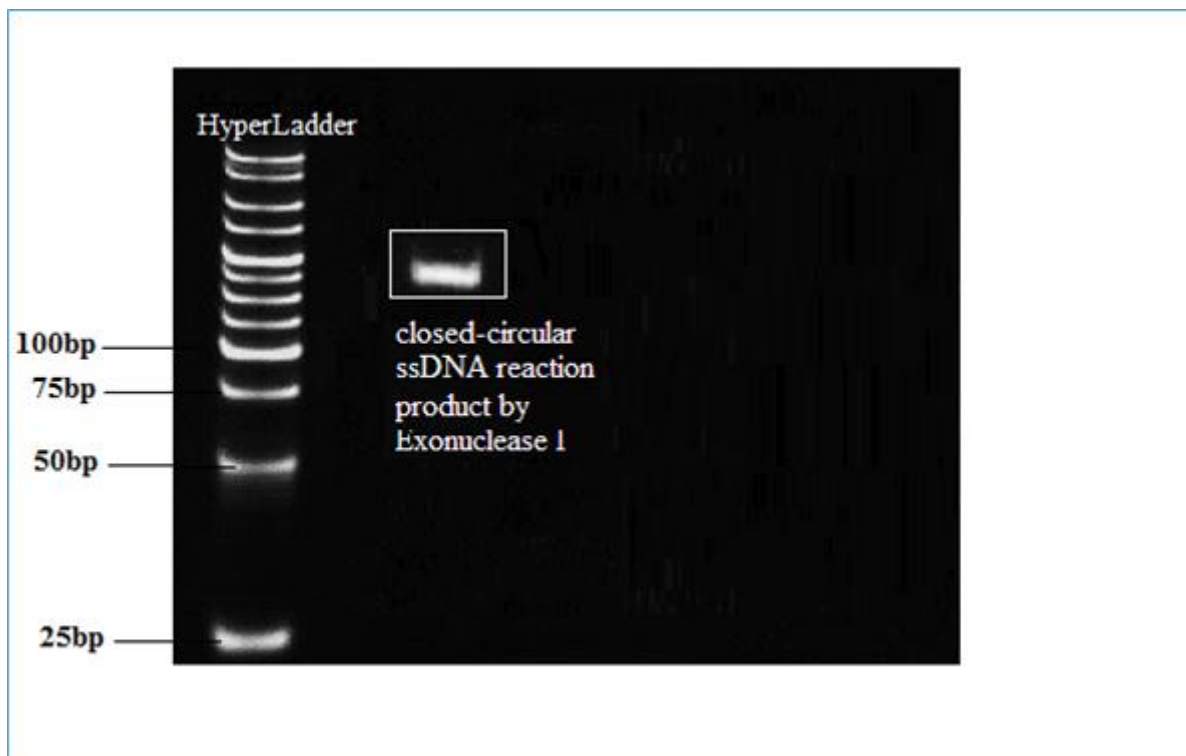


Figure 0.2: Circularisation of BAS library. 77-nucleotide BAS oligo was converted to a circular BAS. Lane 1, DNA markers; lane 2, closed-circular BAS reaction product.

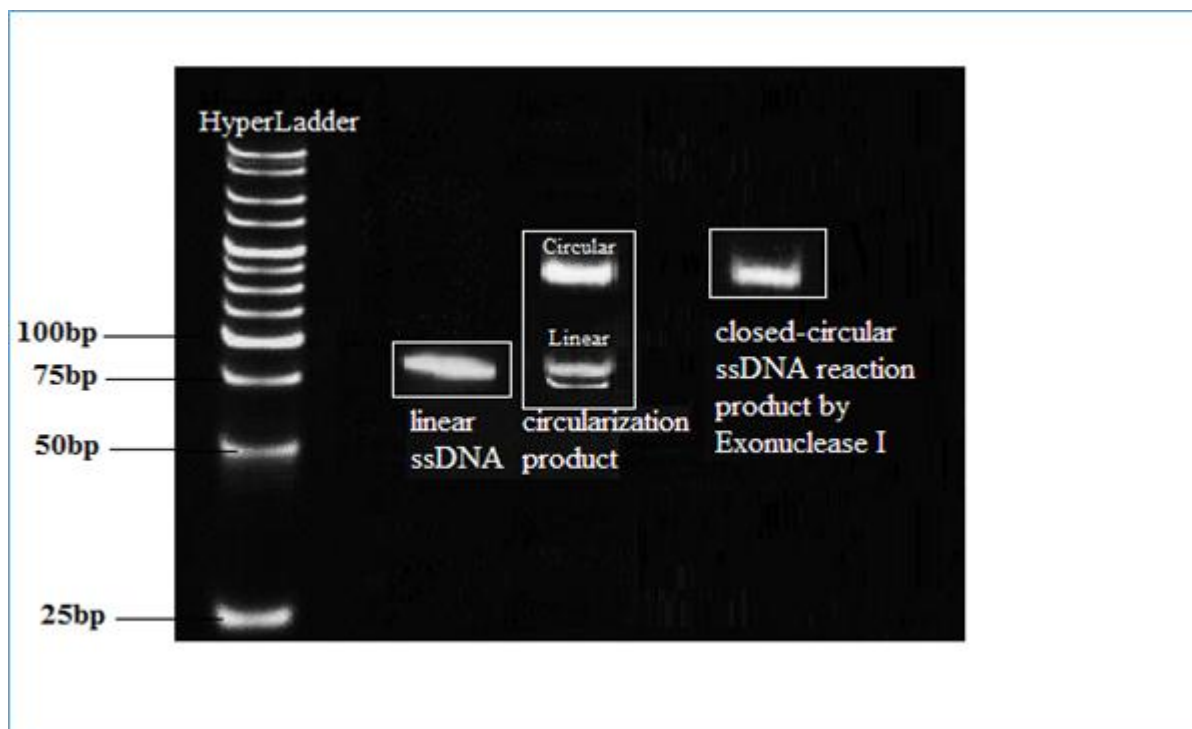


Figure 0.3: Circularisation of BAS Ligase converts linear BAS into closed circular ssDNA. A 77-nucleotide BAS oligo was converted to a circular ssDNA. Lane 1, DNA markers 25bp; lane 2, 77-nucleotide linear BAS oligo; lane 3, circularisation proceeds through an adenylated intermediate; lane 4, closed-circular BAS reaction product.

3.3.2 Cleavage of GST-tag from SIRT1 Enzyme using PreScission Protease (PSP)

SIRT1 enzyme has the GST-tag. GSTrap FF column was used to cleavage the GST tag using preScission protease enzyme. The purification stages and chromatographic profiles were evaluated by SDS-PAGE using 4–20% stacking polyacrylamide gel and stained with Instant Blue stain. Figure 3.4 demonstrated the SDS-PAGE analysis of cleavage GST tag from SIRT1 enzyme, lane 4 shows the native SIRT1 enzyme after treated with preScission protease on GSTrap FF column.

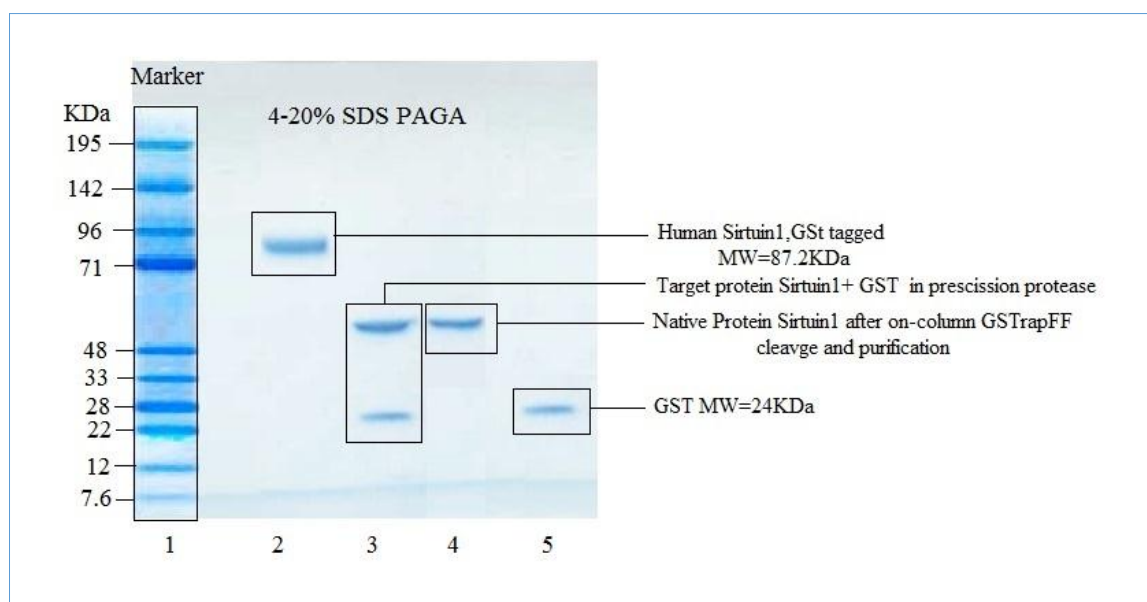


Figure 3.4: SDS-PAGE analysis of cleavage GST tag from SIRT1 enzyme. Lane1 marker protein; Lane2 recombinant SIRT1, GST tagged Purity> 80%; Lane3 target enzyme in PreScission protease; Lane4 Native enzyme after cleavage GST; Lane5 Eluted GST from column.

3.3.3 *In Vitro* Selection Circular BAS Aptamer Against SIRT1 Enzyme

In order to obtain circular ssDNA aptamers with specificity toward target SIRT1 enzyme, modification of the original SELEX protocol was required in order to increase selection pressure on the aptamer library. BAS library with a random sequence of 40 nt was used as precursor pool for the selection of aptamers for SIRT1 enzyme. The random region was flanked by primer binding sites of 18nt and 19nt to facilitate PCR amplification.

For the first round of selection SIRT1 enzyme was immobilised on NHS HP SpinTrap column, 100 pmol circular BAS with 200 μ L binding buffer was incubated with the target enzyme. The binding buffer used for the selection was (100 mM NaCl, 5 mM MgCl₂, pH 7.4). This buffer solution was chosen for *in vitro* selection experiment, because osmolality and ion concentrations usually match those of the human body (Eric *et al.*, 2008).

N40 stands for a randomised sequence of 40 nucleotides, a region where the enzyme will bind and trigger a conformational change to elute DNA aptamers from the NHS HP SpinTrap column and unbound oligonucleotides were washed away. For each fraction a 100 second time interval was provided, giving a total elution time of 5 min. This time interval seems to be sufficient in that it did allow a fair quantity of aptamers to elute from the column, after a period of time the aptamers will eventually dissociate from the column. In this case, the main focus is to evolve and optimise specificity of DNA aptamers binding to a target enzyme and the concentration of the target enzyme. Thus, each round requires analysis of PCR products and repeated the original SELEX protocol mentioned previously.

The SELEX cycle was iterated 8 rounds, the analysis of washed unbound BAS and eluted of bound BAS of each round are shown in figures (3.5-3.12). In round one of SELEX, lower amount of DNA aptamers eluted from the column. The analysis of the washed and eluted BAS products after 1st round demonstrates in figure 3.5.

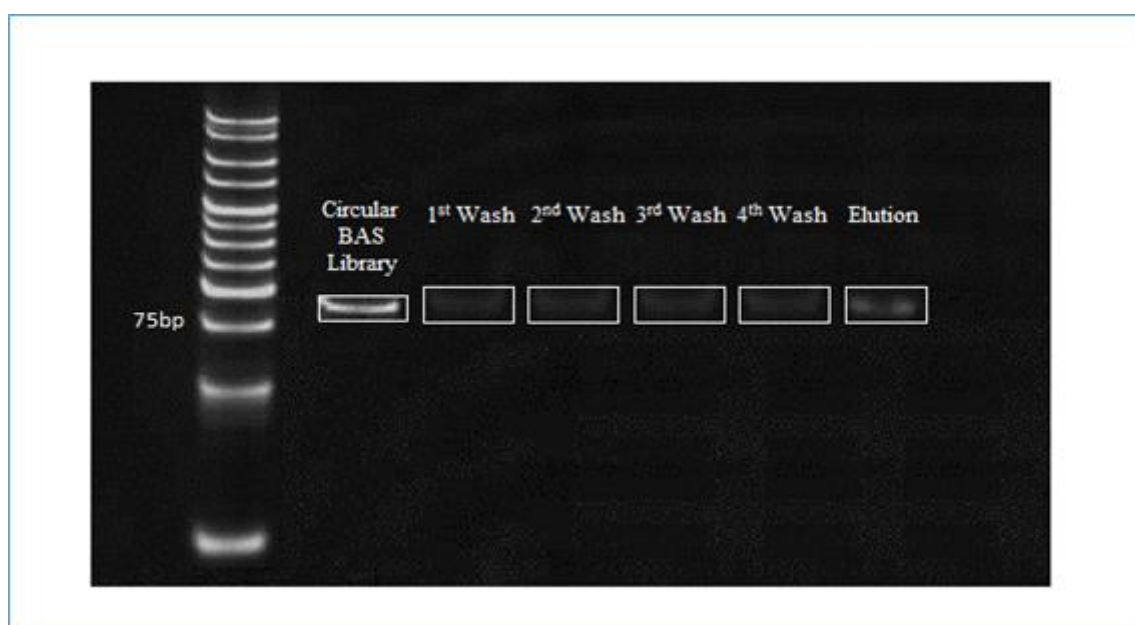


Figure 3.5: 10% acrylamide gel analysis of aptamer selection against SIRT1 enzyme after 1st round. Lane1, HyperLadder 25bp; Lane2, the initial amount of circular BAS library; Lane3, the unbound BAS from the 1st washed; Lane4, the unbound BAS from the 2nd Washed; Lane5, the unbound BAS from the 3rd washed; Lane6, the unbound BAS from the 4th washed; Lane7, the elution of bound BAS after 1st round.

As figure 3.6 suggests, the amount of aptamers that have eluted after 2nd round increased as compared with the eluted aptamer after the 1st round.

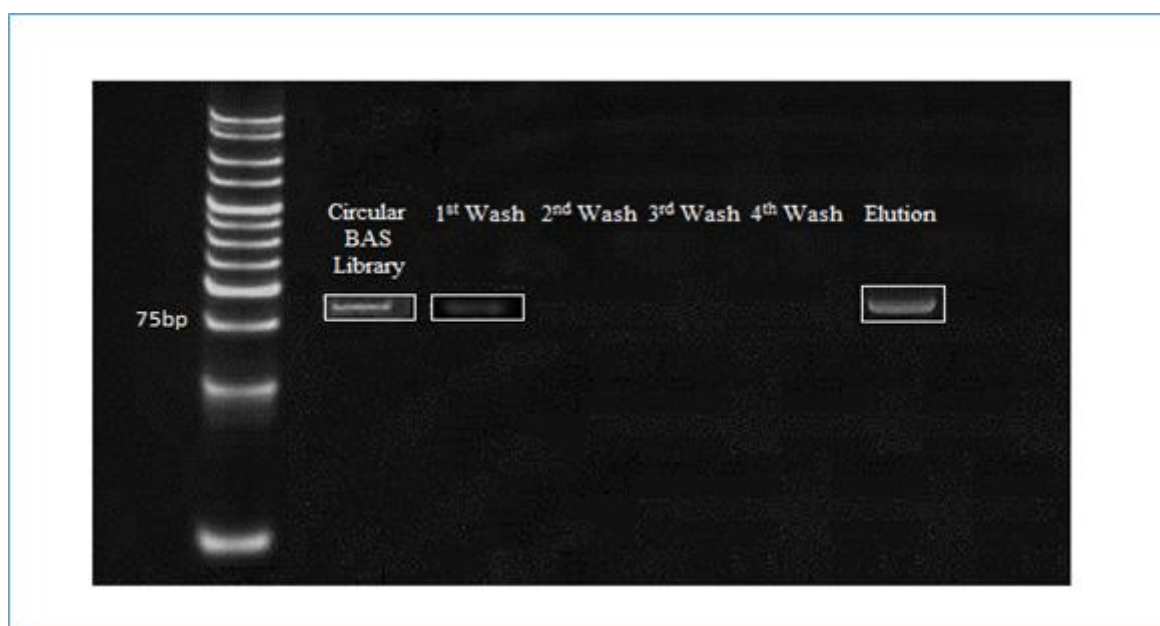


Figure 0.6: 10% acrylamide gel analysis of aptamer selection against SIRT1 enzyme after 2nd round. Lane1, HyperLadder 25bp; Lane2, the circular BAS library from the PCR product of the 1st round; Lane3, the unbound BAS from the 1st washed; Lane4, the unbound BAS from the 2nd Washed; Lane5, the unbound BAS from the 3rd washed; Lane6, the unbound BAS from the 4th washed; Lane7, the elution of bound BAS after 2nd round.

As can be seen in figures (3.7-3.12), rounds (3rd to 8th) of SELEX selection reveals clearly visible elution product bands as compared to the previous round. This is indicated that the ssDNA aptamers have been well developed, in that the aptamers with higher specificity are eluting from the column and being amplified again thus increasing the concentration of DNA aptamers that elute from the column in response to the enzyme each round.

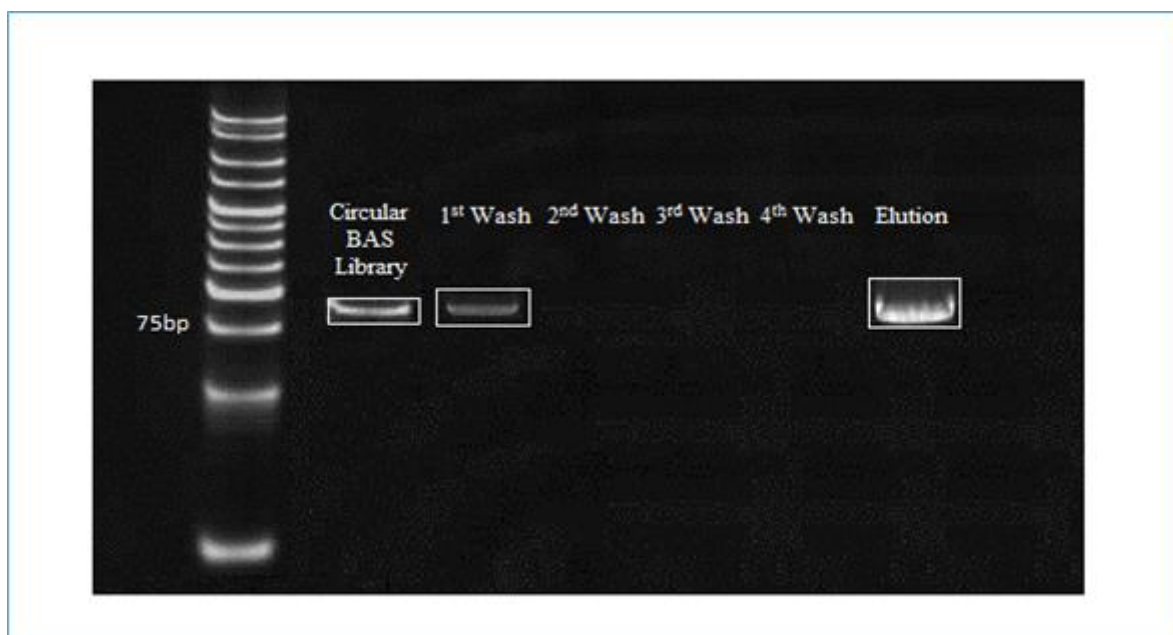


Figure 0.7: 10% acrylamide gel analysis of aptamer selection against SIRT1 enzyme after 3rd round. Lane1, HyperLadder 25bp; Lane2, the circular BAS library from the PCR product of the 2nd round; Lane3, the unbound BAS from the 1st washed; Lane4, the unbound BAS from the 2nd Washed; Lane5, the unbound BAS from the 3rd washed; Lane6, the unbound BAS from the 4th washed; Lane7, the elution of bound BAS after 3rd round.

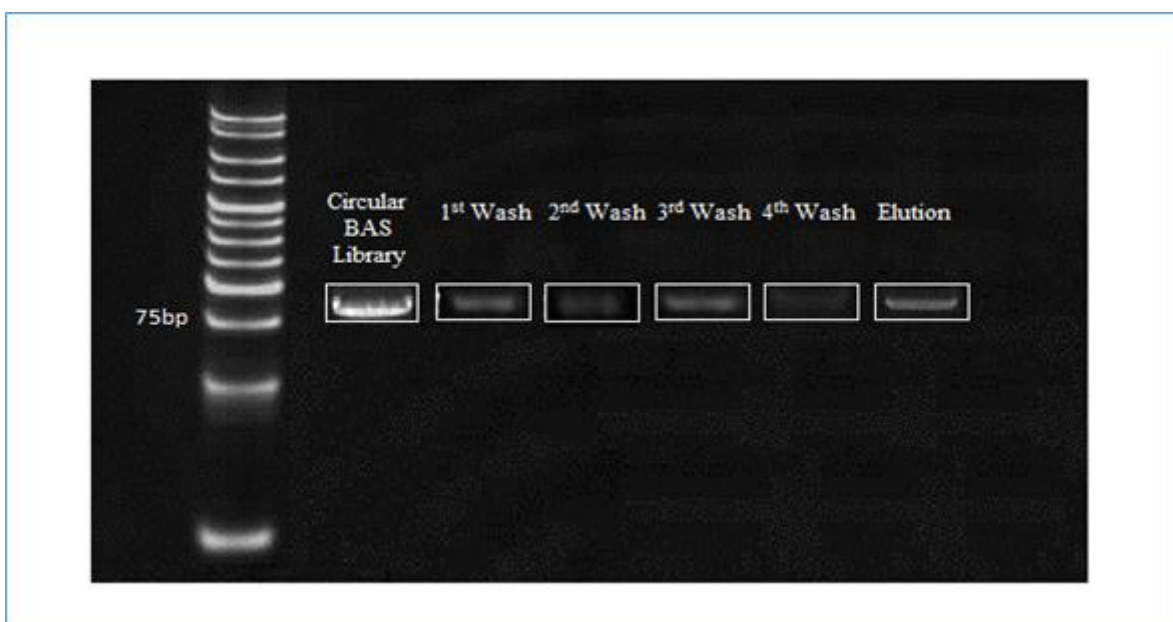


Figure 0.8: 10% acrylamide gel analysis of aptamer selection against SIRT1 enzyme after 4th round. Lane1, HyperLadder 25bp; Lane2, the circular BAS library from the PCR product of the 3rd round; Lane3, the unbound BAS from the 1st washed; Lane4, the unbound BAS from the 2nd Washed; Lane5, the unbound BAS from the 3rd washed; Lane6, the unbound BAS from the 4th washed; Lane7, the elution of bound BAS after 4th round.

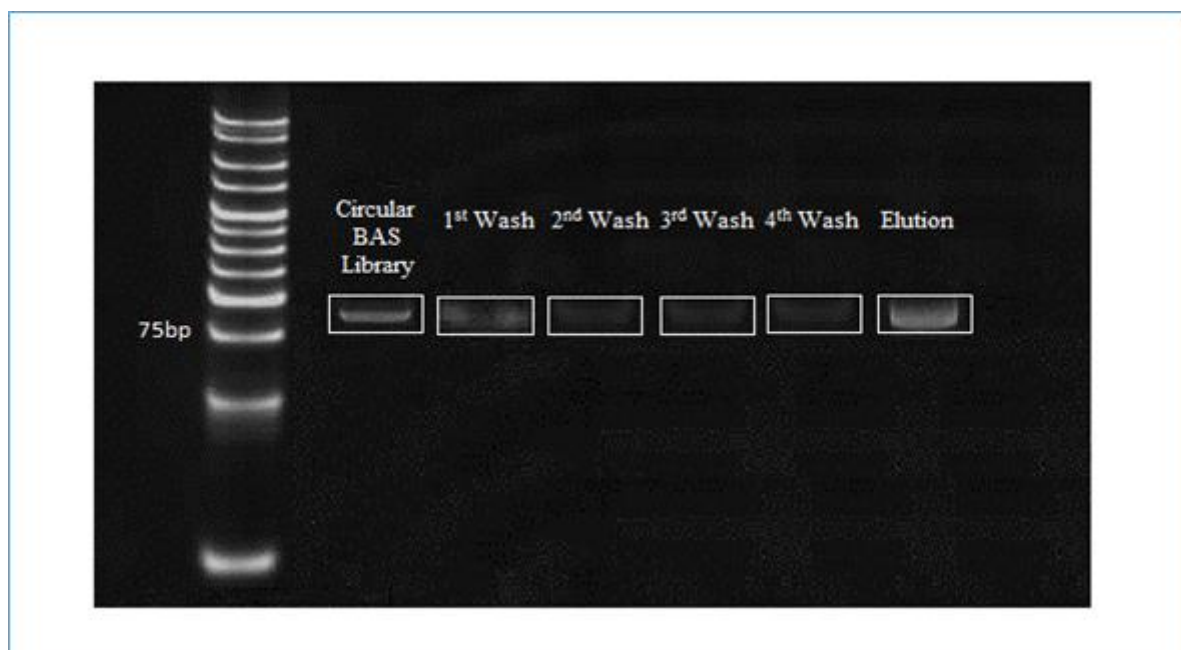


Figure 3.9: 10% acrylamide gel analysis of aptamer selection against SIRT1 enzyme after 5th round. Lane1, HyperLadder 25bp; Lane2, the circular BAS library from the PCR product of the 4th round; Lane3, the unbound BAS from the 1st washed; Lane4, the unbound BAS from the 2nd Washed; Lane5, the unbound BAS from the 3rd washed; Lane6, the unbound BAS from the 4th washed; Lane7, the elution of bound BAS after 5th round.

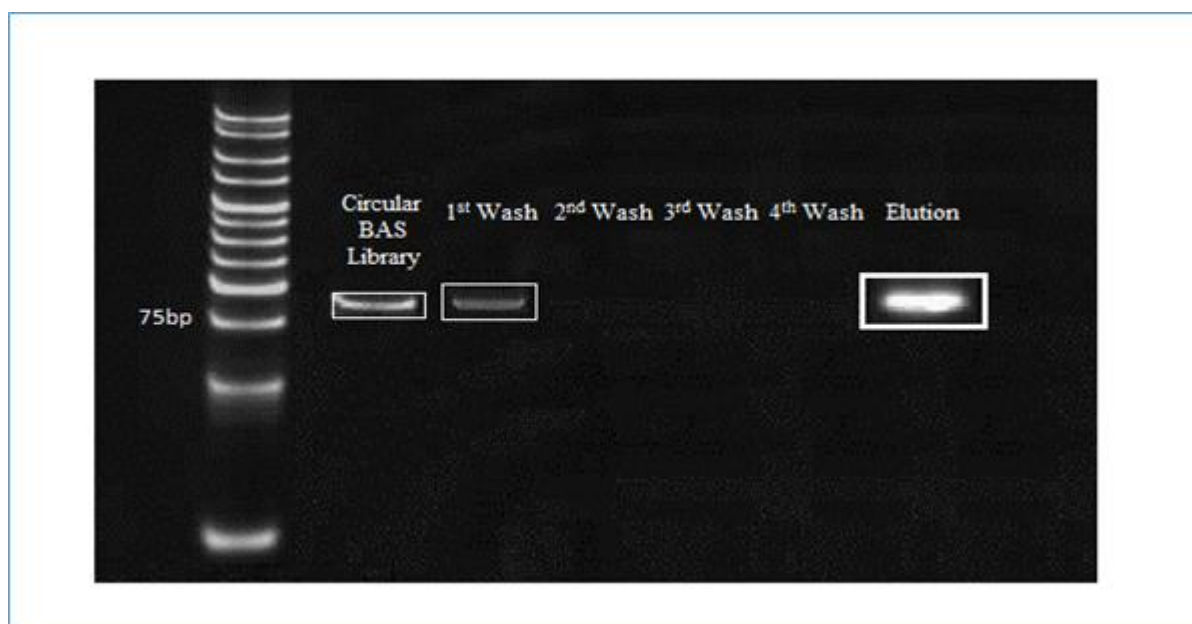


Figure 0.10: 10% acrylamide gel analysis of aptamer selection against SIRT1 enzyme after 6th round. Lane1, HyperLadder 25bp; Lane2, the circular BAS library from the PCR product of the 5th round; Lane3, the unbound BAS from the 1st washed; Lane4, the unbound BAS from the 2nd Washed; Lane5, the unbound BAS from the 3rd washed; Lane6, the unbound BAS from the 4th washed; Lane7, the elution of bound BAS after 6th round.

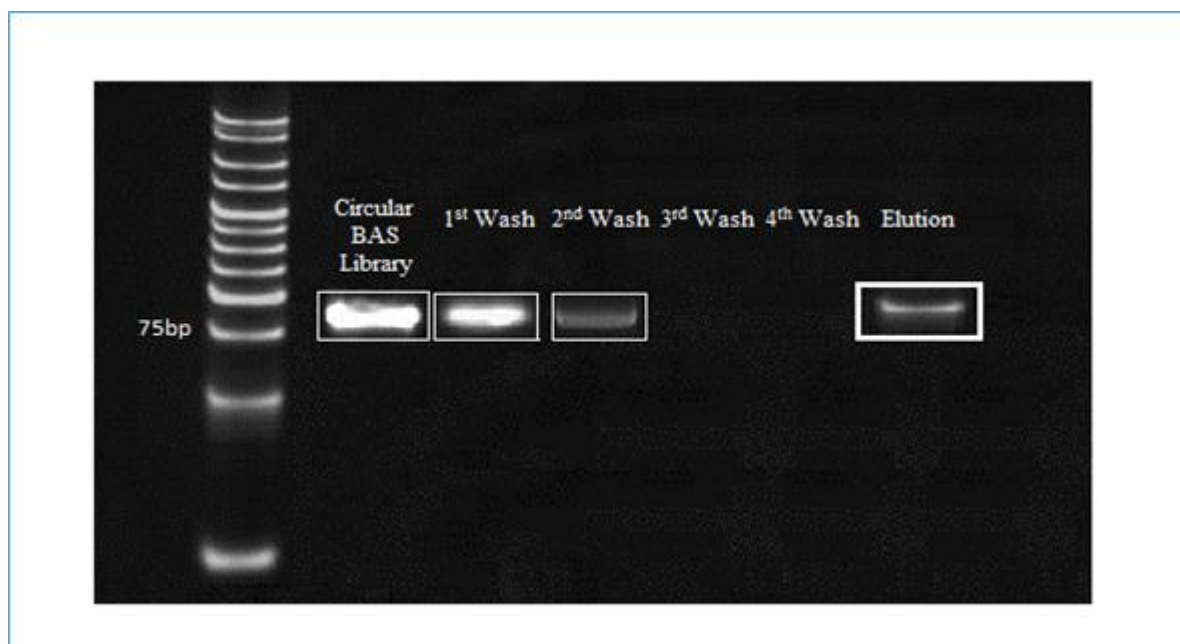


Figure 0.11: 10% acrylamide gel analysis of aptamer selection against SIRT1 enzyme after 7th round. Lane1, HyperLadder 25bp; Lane2, the circular BAS library from the PCR product of the 6th round; Lane3, the unbound BAS from the 1st washed; Lane4, the unbound BAS from the 2nd Washed; Lane5, the unbound BAS from the 3rd washed; Lane6, the unbound BAS from the 4th washed; Lane7, the elution of bound BAS after 7th round.

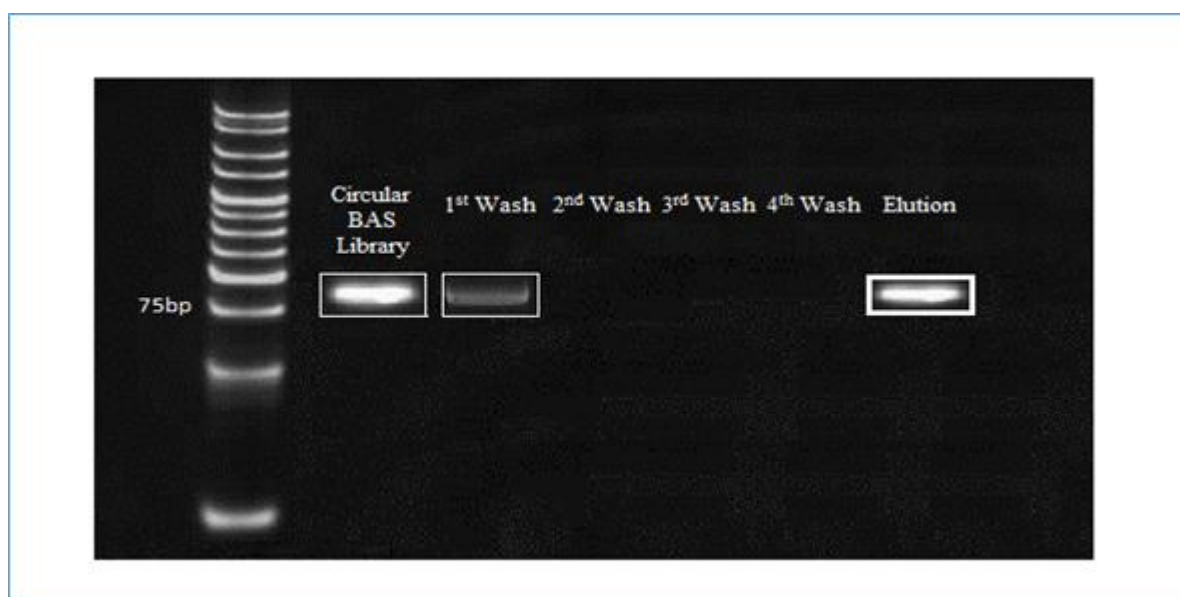


Figure 0.12: 10% acrylamide gel analysis of aptamer selection against SIRT1 enzyme after 8th round. Lane1, HyperLadder 25bp; Lane2, the circular BAS library from the PCR product of the 7th round; Lane3, the unbound BAS from the 1st washed; Lane4, the unbound BAS from the 2nd Washed; Lane5, the unbound BAS from the 3rd washed; Lane6, the unbound BAS from the 4th washed; Lane7, the elution of bound BAS after 8th round.

Figure 3.13 demonstrates the analysis of the 20 cycle PCR products after the 8th rounds of *in vitro* selection aptamer. The initial products from the first round may not show significant amplification, while the analysis of the PCR products after 20 cycles PCR for the 3rd round to 8th round demonstrates increased amount of DNA recovery.

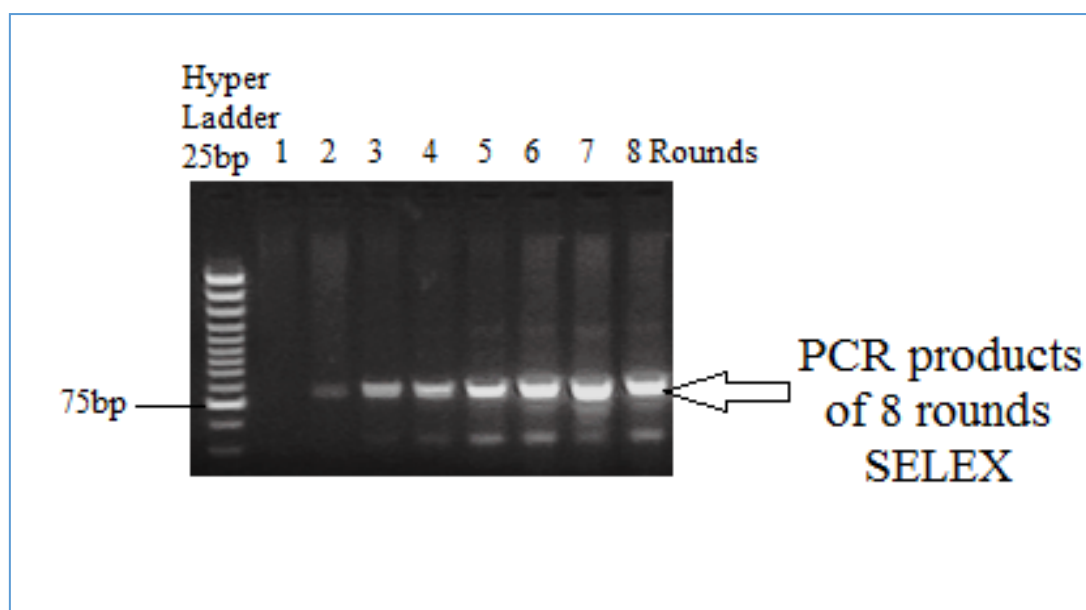


Figure 0.13: 10% acrylamide gel analysis of PCR products during 8th rounds of *in vitro* selection. Lane1, HyperLadder 25bp; Lane2, the PCR product of the 1st round; Lane3, the PCR product of the 2nd round; Lane4, the PCR product of the 3rd round; Lane5, the PCR product of the 4th round; Lane6, the PCR product of the 5th round; Lane7, the PCR product of the 6th round; Lane8, the PCR product of the 7th round; Lane9, the PCR product of the 8th round SELEX.

In summary, after 8th round SELEX, The results had been strongly suggested that we got a circular aptamer that can bind with SIRT1 enzyme.

3.3.4 *In Vitro* Selection Linear BAS Aptamer Against SIRT1 Enzyme

To isolate linear aptamers that specifically bind to SIRT1 enzyme, we utilised SIRT1 enzyme as a selection target. The random BAS library was used to screen ligands that bind to SIRT1 enzyme. Different pools of aptamers that bind to SIRT1 with high affinity and specificity were successfully obtained after 12th rounds of selection by SELEX. Each pool of aptamers was examined before and after PCR amplification on 10% urea gels. The aptamer pools migrated near the 77-bp bands of the HyperLadder, and their PCR products up to 80-bp bands of the HyperLadder as shown in figures 3.14 and 3.15.

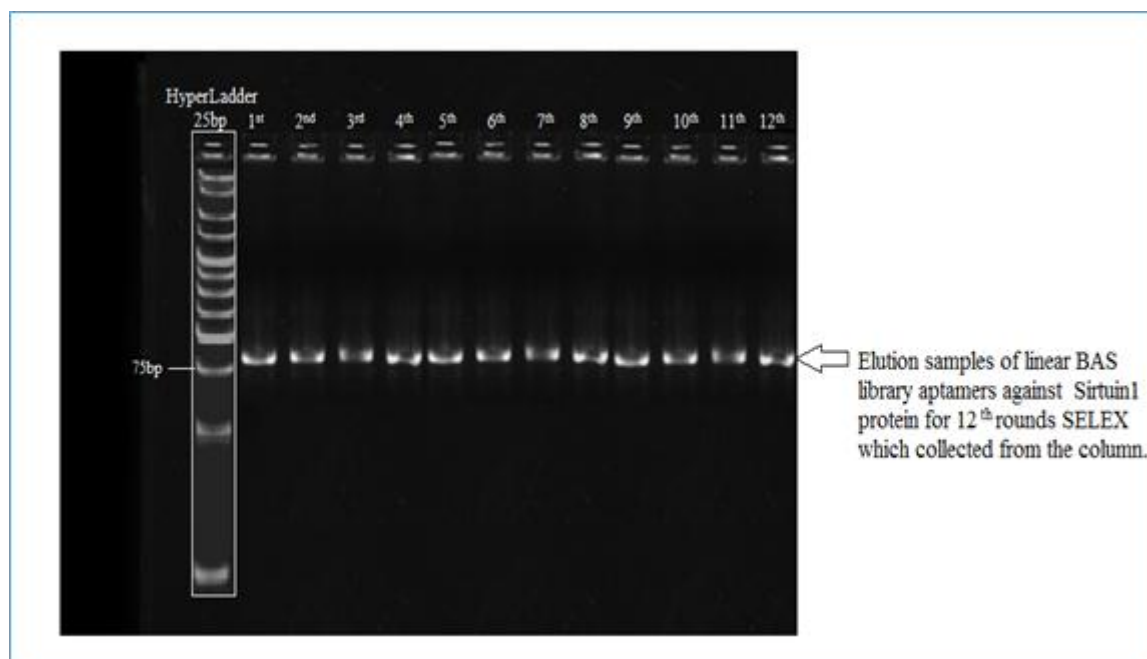


Figure 0.14: 10% acrylamide gel analysis of linear elution aptamer of *in vitro* selection against SIRT1 enzyme for 12th rounds SELEX before PCR. Lane1, HyperLadder 25bp; Lane2, the elution of bound BAS library after 1st washed; Lane3, the elution of bound BAS library after 2^{ed} washed; Lane4, the elution of bound BAS library after 3rd washed; Lane5, the elution of bound BAS library after 4th washed; Lane6, the elution of bound BAS library after 5th washed; Lane7, the elution of bound BAS library after 6th washed; Lane8, the elution of bound BAS library after 7th washed; Lane9, the elution of bound BAS library after 8th washed; Lane10, the elution of bound BAS library after 9th washed; Lane11, the elution of bound BAS library after 10th washed; Lane12, the elution of bound BAS library after 11th washed; Lane13, the elution of bound BAS library after 12th washed.

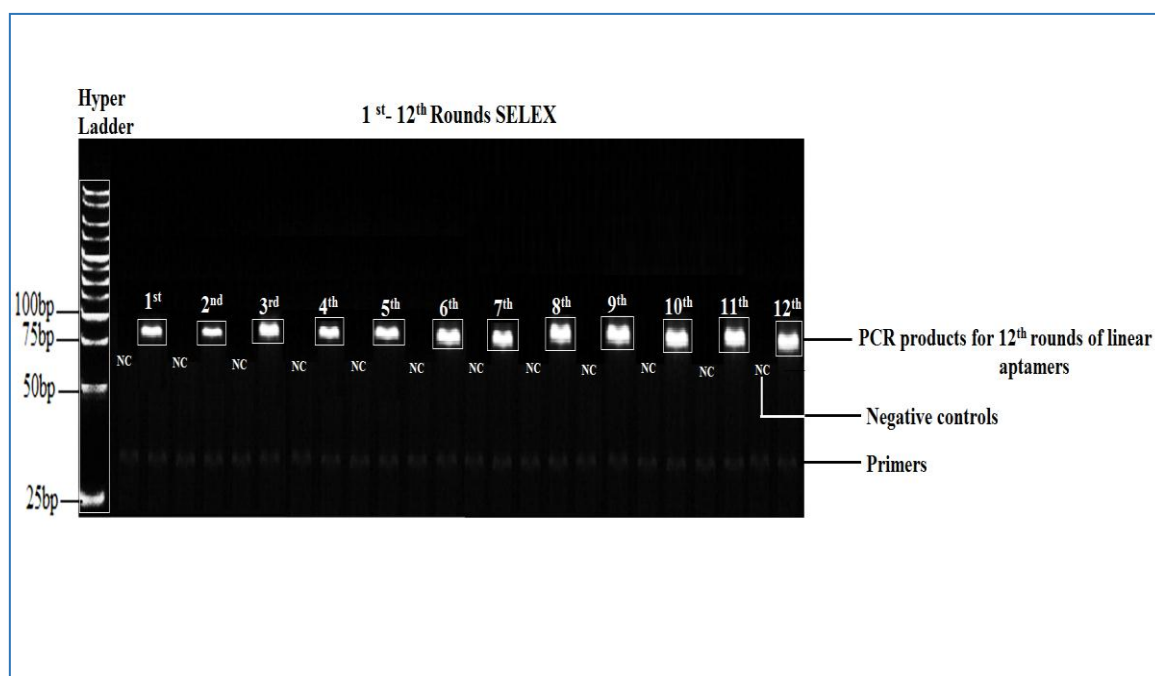


Figure 3.15: 10% acrylamide gel analysis of PCR products aptamers *in vitro* selection against SIRT1 enzyme for 12th rounds SELEX. Lane1, HyperLadder 25bp; Lane 2, 4, 6, 8, 10, 12, 14, 16, 18, 20, 22 and 24 are negative controls (NC). Lane 3, 5, 7, 9, 11, 13, 15, 17, 19, 21, 23, 25 are the PCR products of the 1st, 2^{ed}, 3rd, 4th, 5th, 6th, 7th, 8th, 9th, 10th, 11th and 12th round SELEX.

To sum up, after 12th round SELEX, The results in figures 3.14-3.15 showed that we got a linear aptamer that can bind with SIRT1 enzyme.

3.3.5 DNA Cloning and Sequencing

A total of 144 clones (for 72 circular and 72 linear) were sent for sequencing resulting in 100 (50 for circular and 50 for linear) complete sequences used in class analysis. The 100 sequences were sorted into 8 classes (linear1, linear2, linear3, linear4, circular1, circular2, circular3, and circular4) with sizes ranging from 6-19 frequency (Table 3.1). L3 and L4, represented by linear aptamers, composed the largest classes of linear aptamers representing 38% and 30% respectively of total 50 linear sequences. C2, C3 and C4 represented by circular aptamers, composed the largest classes of circular aptamers representing 24%, 28% and 36% respectively of total 50 circular sequences. Then 10 aptamers were synthesised {(linear3= L1 and L2), (linear4= L3 and L4), (circular2= C1 and C2), (circular3= C3 and C4) and (circular4= C5 and C6)}, 5 aptamers with primer (L2, L4, C2, C4 and C6) and 5 aptamers the primer regions were removed (L1, L3, C1, C3 and C5) as shown in table 3.2. L3, L4, C3 and C4 were selected for further study covering the most populous classes and a moderately populated class. While the goal of selection was to generate aptamers, the circular and linear sequences described herein have to be confirmed to function via a binding mechanism consistent with aptamers.

Table 0.1: Nucleotide sequences of basic-SELEX round 12 linear aptamers (Clones L1- L4) and round 8 circular aptamers (Clones C1-C4) in the N40 random region within each aptamer.

	Length(nt)	10	20	30	40	50	60	70	Frequency %		
		5`.....3`									
Linear		library TCGGAAGAGATGGCGAC.....N40.....CGAGCTGATCCTGATGGAA									
L1		ACAAGAGTCCACTATTAAGAACGTGGACTCCAACGTGCC								40nt	9
L2		CCAATAGGCCGAAATCGGCAAATCCCTTATAAATCCTGC								40nt	7
L3		CGGACTGCAACCTATGCTATCGTTGATGTCTGTCCAAGCA								40nt	19
L4		CACTTTTCGGGGAAATGTGCGCGGAACCCCTATTGTTTA								40nt	15
Circular											
C1		CAAGTGTAGCGGTACAGCTGCGCGTAACCACCACACCCGC								40nt	6
C2		TTGCGGCATTTGCCTTCTGTTTTGCTCACCCAGAAAC								40nt	12
C3		CGAGTGGGTTACATCGAACTGGATCTCAACAGCGGTAAC								40nt	14
C4		CACTCCCTCTGCGTGCGAATTTGCCTATGGCGCATATTC								40nt	18

Table 0.2: Nucleotide sequences of 10 aptamers with and without primers.

Aptamers	Sequences
Circular 1	TTGCGGCATTTTGCCTTCTGTTTTGGCTCACCCAGAAAC
Circular 2	TTCGGAAGAGATGGCGAC TTGCGGCATTTTGCCTTCTGTTTTGGCTCACCCAGAAAC CGAGCTGATCCTGATGGAA
Circular 3	CGAGTGGGTTACATCGAAACTGGATCTCAACAGCGGTAAC
Circular 4	TTCGGAAGAGATGGCGAC CGAGTGGGTTACATCGAAACTGGATCTCAACAGCGGTAAC CGAGCTGATCCTGATGGAA
Circular 5	CACTCCCTCTGCGTGCGAATTTTGCCTATGGCGCATATTC
Circular 6	TTCGGAAGAGATGGCGAC CACTCCCTCTGCGTGCGAATTTTGCCTATGGCGCATATTC CGAGCTGATCCTGATGGAA
Linear 1	CGGACTGCAACCTATGCTATCGTTGATGTCTGTCCAAGCA
Linear 2	TTCGGAAGAGATGGCGAC CGGACTGCAACCTATGCTATCGTTGATGTCTGTCCAAGCA CGAGCTGATCCTGATGGAA
Linear 3	CACTTTTCGGGGAAATGTGCGCGGAACCCCTATTTGTTTA
Linear 4	TTCGGAAGAGATGGCGAC CACTTTTCGGGGAAATGTGCGCGGAACCCCTATTTGTTTA CGAGCTGATCCTGATGGAA

3.4 Discussion

“Sirtuin” (SIR) signifies Silent Information Regulator. One of the most commonly studied mammalian Sirtuin is SIRT1 which is mainly limited to nucleus and cytoplasm (Tanno *et al.*, 2007; North and Verdin, 2007). There is a significant role of SIRT1 in regulating key signalling pathways (Picard *et al.*, 2004; Nemoto *et al.*, 2005). SIRT1 is basically an NAD⁺-dependent deacetylase, with its activators having possible therapeutic applications in age-related diseases like cancer. For this reason, one essential area of investigation is the function of SIRT1 in handling the proteins that are part of these pathways (Kim *et al.*, 2008). In the cancer disease, the role of SIRT1, either as a tumour promoter or suppressor is dependent on cellular context or the impact on a particular signaling pathway (Anastasiou *et al.*, 2006). In order to prevent aging and cancer, it is important that SIRT1 activity is controlled. The basis for development of anti-aging drugs is provided through SIRT1 activators like small chemical activators (SRT2183, resveratrol, and SRT1460), and small ubiquitin-like modifier (SUMO) (Kim *et al.*, 2008). Moreover, the rate of cell viability in culture decreases due to the pharmacological activation of SIRT1. These results indicate that SIRT1 performs as a context-dependent tumour suppressor, whereas it could also lead towards cell death once treatment is given with

chemotherapeutic agents likely because of the increased sensitivity of the cells that are rapidly dividing to DNA damaging agents (Kabra, 2010).

Modification of SIRT1 activity protein could lead to a new platform opportunity for drug discovery. In this regard, we are developing highly selective ligands (linear and circular aptamers) in order to study the modulated activity of SIRT1 within the series of cancer cell lines. Aptamers have been indicated to be activator for different targets *in vitro* and *in vivo*. Aptamers can identify the marker on the tumour cells surface and, if adequately labelled provide exact doses of cancer treatment by killing of the tumour cells only. The unfavorable side effects through damage to the rest of the body would be avoided (Ferreira *et al.*, 2008).

Ever since isolation of aptamers two decades ago, no significant studies have been conducted to analysis the circular or linear aptamers to bind SIRT1 enzyme as a target by SELEX methodology. No standard SELEX protocol has yet been development which is applicable to all targets. Length of the central random region is among the major elements for oligonucleotide library design. 30 nucleotides are required to construct simple single-stranded oligo-nucleotide motifs (Gold *et al.*, 1995) which includes hairpins, protuberances within helices, pseudoknots, and G-quartets. Larger the length of the random region, greater will be structure complexity of library, which facilitates the unknown or unattached targets and thus better selection of aptamers (Marshall and Ellington, 2000). Nonetheless, various SELEX experiments have indicated reduced effectivity of aptamer selection in the presence a region longer than 70 nt (Legiewicz *et al.*, 2005). In the light of this, an BAS library comprising of a 40nt central block of random sequence was employed for the *in vitro* selection of aptamers against SIRT1 enzyme. This length of the random region provides adequate level of structural complexity, economical chemical synthesis, and easily managed being used in the library. ssDNA aptamers tend to remain stable in much broader range of conditions including biological fluids such as serum and plasma. This enhances their suitability for clinical applications. In this study, for the circular and linear selection the SIRT1 enzyme was immobilised by using an NHS HP Spin Trap, blocked by using “blocking buffer: 50 mM Tris-HCL+ 1 M NaCl, pH 8.0” and then a chemically manufactured BAS library was included in addition to binding buffer.

Some researchers tend to employ a largely amplified random library before initiating the selection process. They do so to extract out the damaged DNA synthesis products, which cannot be augmented through by PCR (Marshall and Ellington, 2000). Hence, some of the

target-binding sequences are likely to be lost in the original library which consumes more time and material in the large-scale PCR process. In the original library, a large number of the oligonucleotides exhibited stable lengths on the denaturing gel. Owing to this, after finishing each step of PCR amplification process, an BAS library was employed to circularise a library with about 77 nt sequences by ligation. Exonucleases is used to eliminate any unligated aptamer before collecting the final product. An effective circular aptamer production depends upon the ligation efficiency of the PCR process. In the regular SELEX process, the production circular ssDNA preparation tends to consume most of the time, taking 7 days completing one round of circular aptamer selection, after optimisation of procedure.

Eight rounds of SELEX were completed to obtain circular ssDNA which specifically bind to SIRT1 enzyme (figures 3.5-3.13). The selection scheme was designed so that the ssDNA will bind to SIRT1 enzyme in solution high salt buffer. After eight rounds of selection, 72 clones of the ssDNA molecules in the library were obtained for consensus sequence family analysis. Three sequences were chosen based on their inclusion in consensus sequence families (table 3.1). Those sequences, C2, C3, and C4 with and without primer were assayed for their binding affinity to SIRT1 enzyme.

For linear aptamer, the SIRT1 enzyme was immobilised by NHS HP SpinTrap, blocked by “blocking buffer: 50 mM Tris-HCL+1 M NaCl, pH 8.0” and the BAS library was included along with binding buffer. Then, the bound BAS containing the aptamers were extracted. In the next step of selection, an asymmetric PCR was employed to enhance the bound BSA. The process was repeated several times until the adequate level of affinity for bound BAS was achieved.

Twelve rounds of SELEX were completed to obtain linear ssDNA which specifically bind to SIRT1 enzyme (figures 3.14-3.15). The selection scheme was designed the same of circular aptamers so that the ssDNA will bind to SIRT1 enzyme in solution high salt buffer. After twelve rounds of selection, 72 clones of the ssDNA molecules in the library were obtained for consensus sequence family analysis. Two sequences were chosen based on their inclusion in consensus sequence families (table 3.1). Those sequences, L3 and L4 with and without primer were assayed for their binding affinity to SIRT1 enzyme.

In conclusion, a stringent SELEX methodology is demonstrated to isolate circular and linear ssDNA aptamers with high affinity and specificity for the SIRT1 enzyme. The results validate our SELEX process with identifying new aptamers against SIRT1 enzyme.

4 CHARACTERISATION, KINETICS AND STABILITY OF APTAMERS

4.1 Introduction

A critical analysis of current knowledge and recent discoveries clearly indicates that activation or inhibition of SIRT1 modulation is beneficial against several diseases including neurodegeneration, cancer, inflammatory/ autoimmune, and metabolic disease (Carafa *et al.*, 2016; Vachharajani *et al.*, 2016). The chemistry and biomedical characterisation of SIRT1 activators are at a much earlier stage of development than SIRT1 inhibitors, thus suggesting that new alternatives may arise soon. Based on that, the potential selective modulation of SIRT1 will represent a promising area if new stable selective molecules can be designed as an activator for SIRT1.

In our study, Fluor de lys fluorescent assay system, was used successfully for study the characterising of SIRT1 enzyme activity with 10 aptamers (L1, L2, L3, L4, C1, C2, C3, C4, C5 and C6). The SIRT1 fluorescent activity assay/ drug discovery designed to measure the lysyl deacetylase activity of the recombinant human SIRT1. This system is ideal screening inhibitors, activators or kinetic assay of the enzyme under varying conditions. The FLUOR DE LYS SIRT1 assay is based on the FLUOR DE LYS SIRT1 substrate and FLUOR DE LYS Developer II combination. The assay procedure has two steps. First, the FLUOR DE LYS SIRT1 Substrate, which contains a peptide comprising amino acids 379-382 of human p53 (Arg-His-Lys-Lys(Ac)). Deacetylation of the substrate sensitises the substrate so that, in the second step, treatment with the FLUOR DE LYS Developer II produces a fluorophore as shown in figure 4.1.

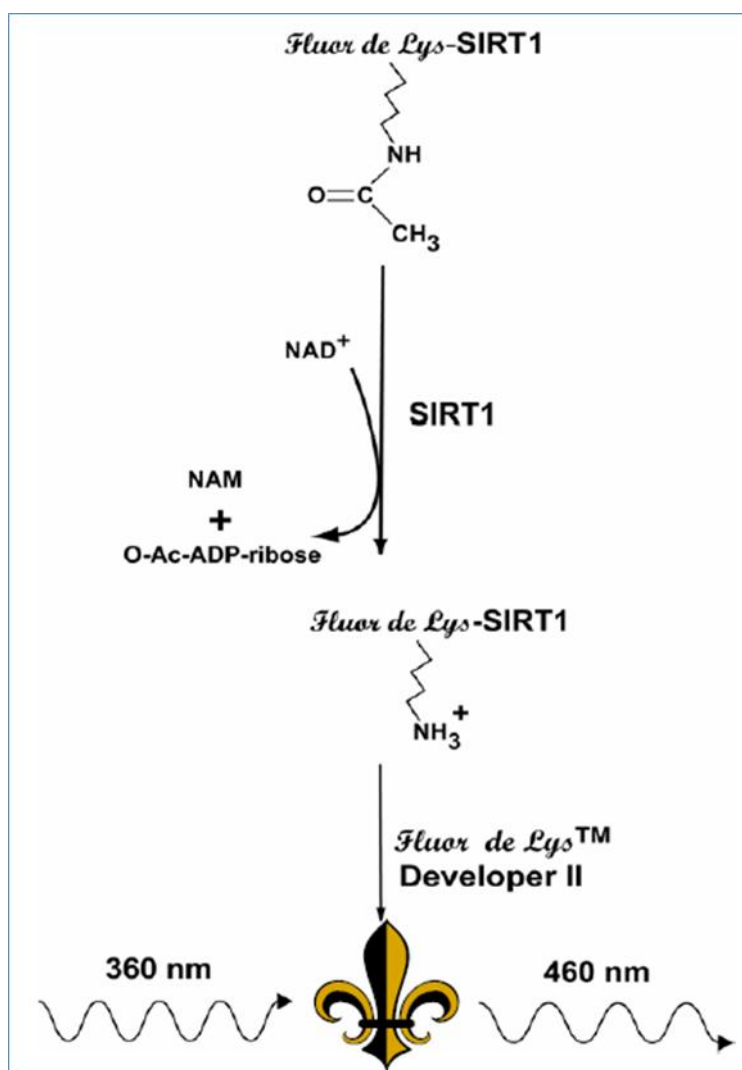
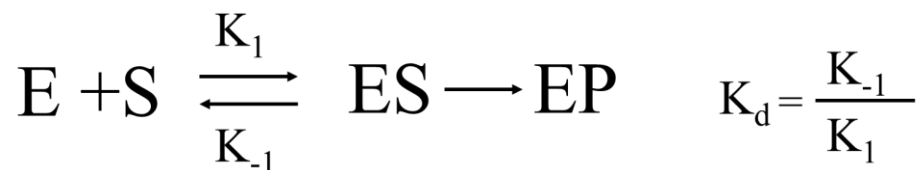


Figure 0.1: Reaction Scheme of the SIRT1 Fluorescent Activity Assay. NAD^+ -dependent deacetylation of the substrate by recombinant human SIRT1 sensitises it to Developer II, which then generates a fluorophore (symbol). The fluorophore is excited with 360 nm light and the emitted light (460 nm) is detected on a fluorometric plate reader. NAD^+ is consumed in the reaction to produce nicotinamide (NAM) and O-acetyl-ADP-ribose. http://www.blossombio.com/pdf/products/UG_BML-AK500.pdf

To address the kinetic mechanism of activation of the human SIRT1 enzyme with aptamers, we determined the effect of aptamers on the V_{\max} (velocity of enzyme-catalysed reaction) and the K_m (Michaelis-Menten constant) of SIRT1 for its aptamers.

To understand how SIRT1 enzymes function, we need a kinetic description of their activity. In general, an enzyme reaction is used to be processed in two-steps: substrate (S) and enzyme (E) binding for formation of an enzyme-substrate (ES) complex, following irreversible enzyme-substrate decomposition to free enzyme and product (P):



In an enzyme and substrate reaction, reaction velocity is directly proportional to the amount of substrate following first-order reaction. Once the enzyme is saturated with the substrate, rate of reaction is independent to the substrate concentration (figure 4.2) (Berg *et al.*, 2002).

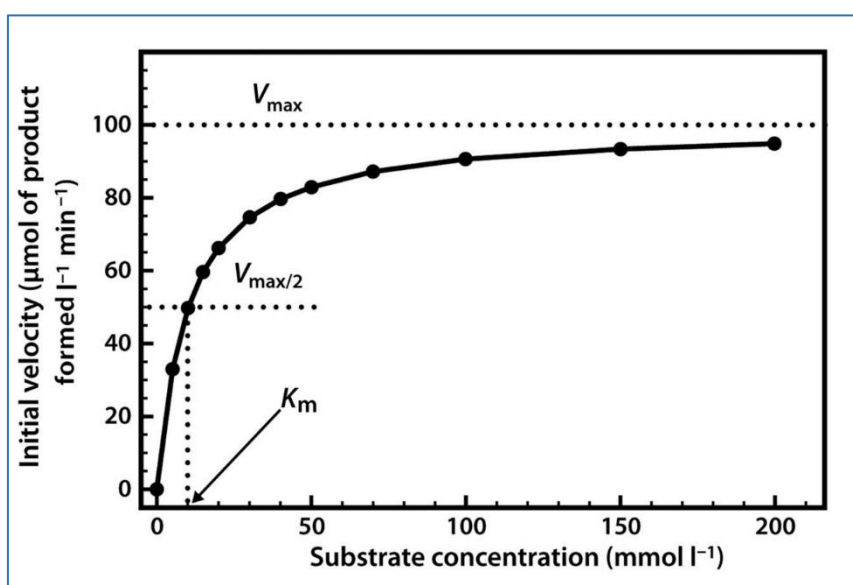


Figure 4.2: Substrate concentration versus enzyme reaction velocity, (Berg *et al.*, 2002).

There are three enzymes kinetic analysis: elucidating enzyme mechanism and comparing between enzymes, predicting enzyme activity under various conditions and developing enzyme inhibitors (or activators) as therapeutic agents. In the steady-state model assumption, the concentration of enzyme-substrate complex (ES) remains constant in time. From this assumption, Michaelis-Menten equation is derived as:

$$V = \frac{V_{\max} * [S]}{K_m + [S]}$$

Michaelis-Menten constant (K_m) is equivalent to the dissociation constant of the ES complex when $k_{cat} \ll k_{-1}$:

$$K_m = \frac{K_{-1} + K_{cat}}{K_1}$$

The K_m corresponds to substrate concentration at $V_{max}/2$. Since the K_m is almost same as the k_d , except for the presence of the k_{cat} term, it is related to the affinity or strength of binding of a substrate to the enzyme (Keener and Sneyd, 2008).

$$V_{max} = K_{cat} [E_T], [E_T] = [E] + [ES]$$

Maximum velocity (V_{max}) is achieved at high substrate levels ($[S] \gg K_m$). Thus, the entire enzyme is in the $[ES]$ form. Turn over number or catalytic efficiency is derived by V_{max} and the total amount of the enzyme when the enzyme is fully saturated with the substrate. k_{cat} indicates that the moles of products are produced by a single enzyme molecule in a certain period time (Yang, 2011).

$$K_{cat} = V_{max} / [E_T]$$

To calculate the important enzyme kinetic constants, a graphical analysis of the experimental data is necessary. Since the accurate determination of V_{max} on the graph, velocity versus $[S]$, is difficult, double reciprocal plots have been widely used via Lineweaver-Burke Plots (Yang, 2011) (Figure 4.3).

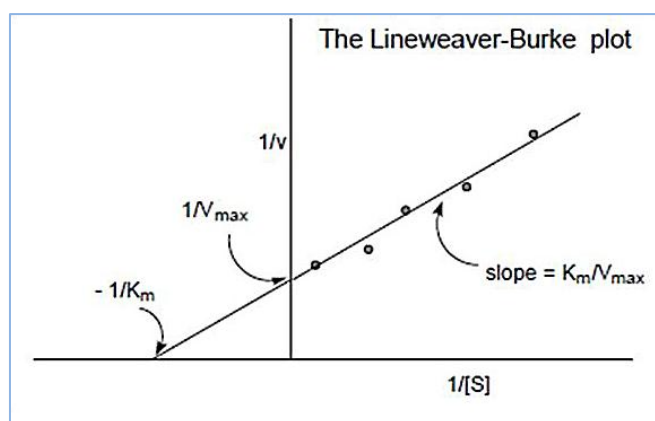


Figure 4.3: Lineweaver-Burke Plots, (Yang, 2011).

$$\frac{1}{V} = \frac{K_m}{[S]} \frac{1}{V_{\max}} + \frac{1}{V_{\max}}$$

$$y = 1/v, x = 1/[S]$$

$$y\text{-intercept} = 1/V_{\max}$$

$$\text{Slope} = K_m/V_{\max}$$

Experimentally, from the various concentration of the substrate versus recording the initial velocity, one could get Lineweaver-Burke Linear Plots. k_{cat}/K_m indicates the second order reaction of free enzyme (E) and free substrate (S). This is a significant term for describing the specificity/selectivity of the enzyme for a given substrate. In this study, SIRT1 kinetics for (L3, L4, C3 and C4) aptamers has been examined by comparing to SIRT1's kinetics for activator SIRT1 (resveratrol).

The final step for studying the mechanism of SIRT1 aptamer is estimation of the dissociation constant value (KD) of aptamers (L3, L4, C3 and C4) to determine how good aptamers bind and modulate to the SIRT1 enzyme. The lower KD, the more tightly bound the aptamer is to the target, this might/might not relate directly to the activity.

In our study, the binding affinity of the selected aptamers for SIRT1 enzyme target was determined by surface plasmon resonance (SPR) assay. Surface plasmon resonance (SPR) is fast becoming the method of choice for the determination of binding affinity (Di Primo *et al.*,

2014; Patching, 2014; Nguyen *et al.*, 2015; Puiu and Bala, 2016). This is due to the fact that it allows for real time determination of kinetic parameters such as K_D , k_{off} and k_{on} of protein-aptamer interactions. It is also a sensitive method allowing for the measurement of K_D down to 10^{-12} M (Tsuji *et al.*, 2009). The proteOn XPR36 biosensor, which uses SPR detection and permits real-time kinetic analysis of interacting molecules, was used to measure the molecular-binding kinetics of the selected aptamers.

Lastly, the most important point and a prerequisite for a potential therapeutic use of the aptamers is a reasonable stability in mammalian serum or plasma. Different from RNA, which is very easily degraded in biological fluids, DNA is much more stable, which suggests an advantage of DNA aptamers for clinical applications.

To sum up, the objectives of this chapter were to: [i] investigate aptamers whether activator or inhibitor to the SIRT1 by studying SIRT1 activity with Fluor de Lys assay; [ii] to gain an understanding of the mechanism by which aptamers accelerate SIRT1-catalysed deacetylation; [iii] determining the K_D values for the selected SIRT1 aptamers and [iv] determine the degradation rate for the best selected aptamer in plasma.

4.2 Methods

All methods were described in chapter 2, measurement of SIRT1 activity in section 2.2.5.1, SIRT1 kinetics as a function of the concentrations of aptamers in section 2.2.5.2, K_D values for the selected SIRT1 aptamers in section 2.2.5.3 as well as the stability of aptamer in plasma in section 2.2.7.

4.3 Results

4.3.1 *In vitro* Characterisation Study of Activators and Inhibitors of the SIRT1 Enzyme by Selected Aptamers

To measure SIRT1 activity with 10 aptamers (C1, C2, C3, C4, C5, C6, L1, L2, L3 and L4), we needed an assay able to detect specifically SIRT1 activity. Studies have demonstrated that SIRT1 binds to and regulates the activity of several transcription factors among which is p53 (Langley *et al.*, 2002). SIRT1 can interact with and deacetylate p53 on Lys382 inhibiting its

function (Solomon *et al.*, 2006). Indeed, Fluor de Lys assay (BML-AK555) was used to measure the SIRT1 activity in order to investigate if the aptamers activate or inhibit the SIRT1.

The results from Fluor de Lys assay are summarised in figures 4.4 and 4.5. These figures are demonstrating the SIRT1 enzyme activity, axis Y representing fluorescence data of SIRT1 activity for all aptamers divided by fluorescence data of SIRT1 activity at zero time) with axis X representing logarithm concentrations of 100 nM, 200 nM, 400 nM and 800 nM from linear1, linear2, linear3, linear4, circular1, circular3 and circular5 aptamers and 37.5 nM, 75 nM, 150 nM and 300 nM from circular2, circular4 and circular6 aptamers as compared with the activity of 200000 nM resveratrol (SIRT1 activator as a positive control) and 200000 nM suramin and nicotinamide (SIRT1 inhibitors as a negative control). The results of this experiment as shown in figure 4.4 suggests that the level of SIRT1 activity with 800 nM C3 aptamer is significantly higher than the activity of SIRT1 with activator control (200000 nM resveratrol), $p < 0.0001$. The activity of SIRT1 with 800 nM L3, 800 nM L4, 400 nM C3 and 300 nM C4 aptamers are increased nearly the level of SIRT1 with resveratrol at a concentration 200000 nM, $p < 0.05$ and the rest of aptamers (C1, C2, C6, L1 and L2) were non-active the SIRT1 enzyme ($p > 0.05$). Surprisingly, C5 aptamer decreased the activity of SIRT1 at 800, 400 and 200 nM concentrations as shown in figure 4.5, this is mean that C5 acted as inhibitor to SIRT1 enzyme approximately similar to inhibitor controls (200000 nM suramin and nicotinamide), $p < 0.05$.

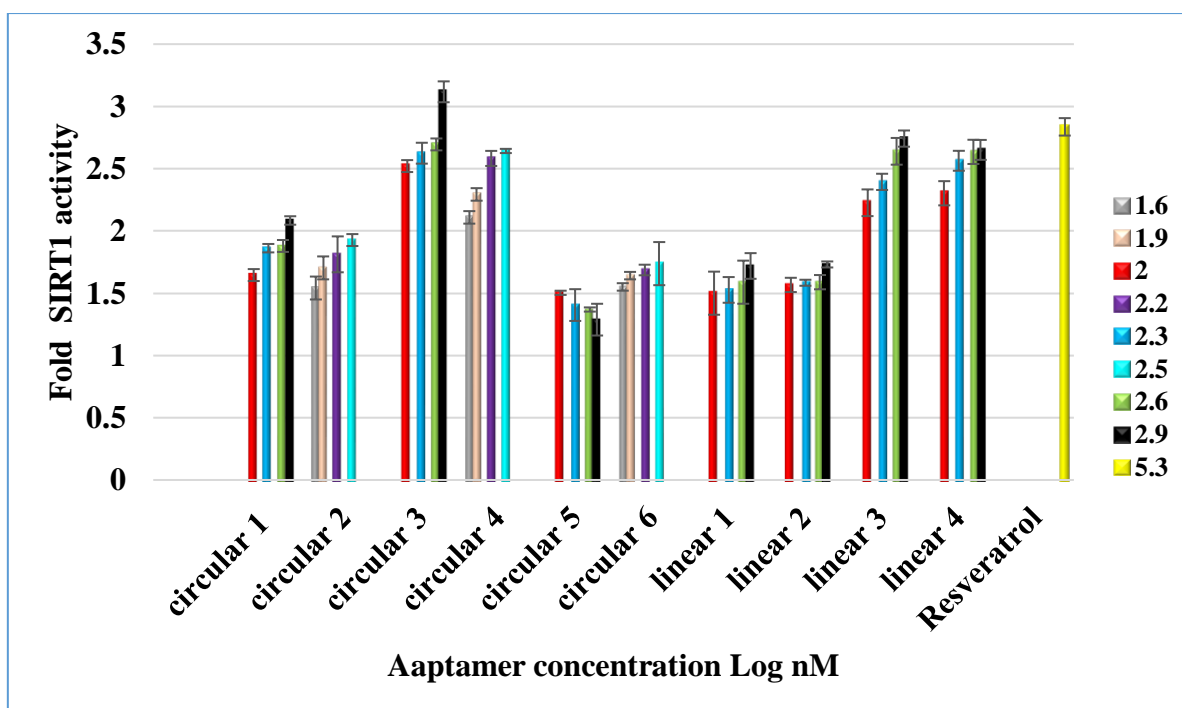


Figure 0.4: Measurement of SIRT1 activity with Fluor de Lys assay. SIRT1 activity was increased significantly with 800 nM C3 as compared with the activity of 200000 nM resveratrol (activator control). The activity of SIRT1 with 800 nM L3, 800 nM L4, 400 nM C3 and 300 nM C4 were convergent the activity of 200000 nM resveratrol. The significance was calculated by the ANOVA one-way test; lines = mean \pm standard error of the mean (SEM). $p < 0.0001$ of C3 compared with resveratrol and < 0.05 of C4, L3 and L4 compared with resveratrol.

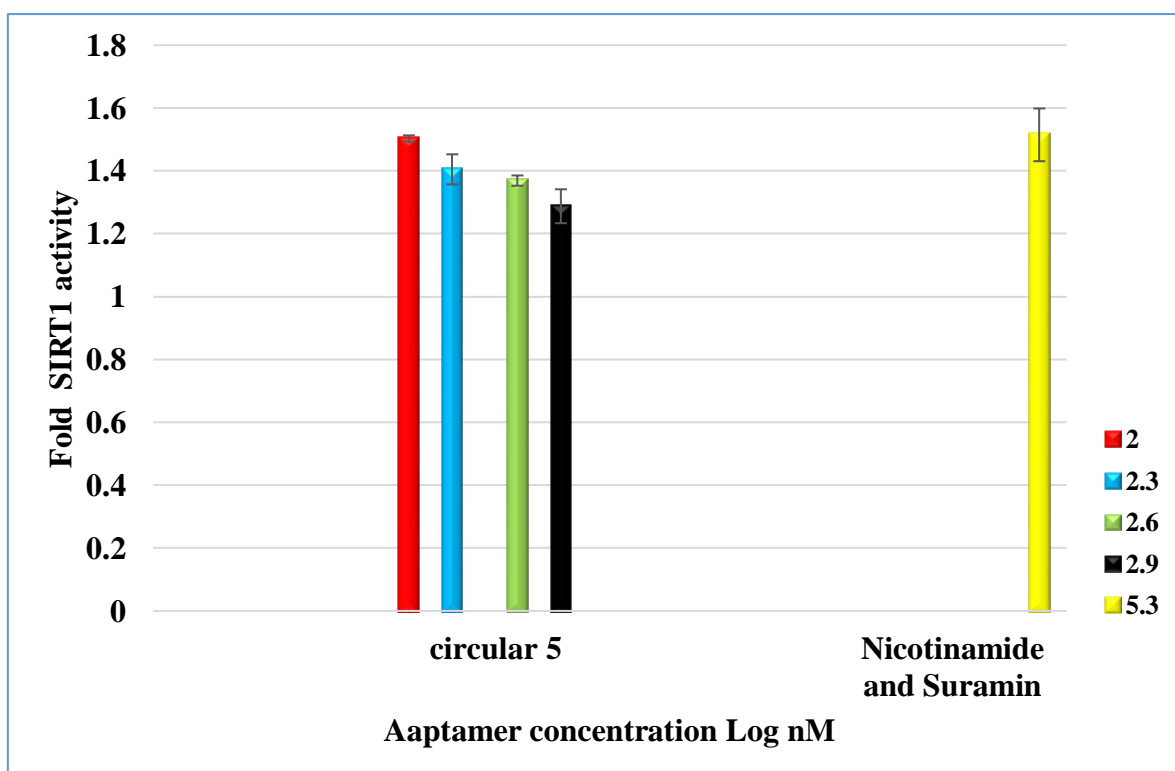


Figure 0.5: Measurement of SIRT1 activity with Fluor de Lys assay. SIRT1 activity with 800, 400, 200 and 100 nM C5 aptamer were nearly equal the activity of 200000 nM suramin and nicotinamide (inhibitor control). The significance was calculated by the ANOVA one-way test; lines = mean \pm standard error of the mean (SEM). $p < 0.05$ compared with suramin and nicotinamide.

Subsequently, the data of characterisation of SIRT1 enzyme activators and inhibitors were fitted on mathematical equation:

$$1 + \frac{K}{X - \sqrt{A + X + K - (A + X + k)^2 - 4 * A * X}}$$

using Origin 9.1 software (figures 4.6-4.15) to determine the k_d and k_a constants using nonlinear regression analysis to choose the best aptamers to complete the study of kinetics and binding affinity of these aptamers, see table 4.1.

Table 0.1: k_d and k_a constants \pm SEM for all selected aptamers.

	K_d (nM)	K_a (nM)
Circular 1	32 ± 3.5	0.03 ± 0.01
Circular 2	8.3 ± 1.3	0.12 ± 0.026
Circular 3	22.6 ± 4.9	0.04 ± 0.0134
Circular 4	7.1 ± 1.9	0.14 ± 0.07
Circular 5	-14.9 ± 3.5	-
Circular 6	3.8 ± 0.46	0.26 ± 0.045
Linear 1	26 ± 7.01	0.04 ± 0.016
Linear 2	18.6 ± 6.8	0.05 ± 0.019
Linear3	20.9 ± 3.7	0.05 ± 0.01
Linear4	3.5 ± 1.11	0.28 ± 0.09

Figure 4.8, 4.9, 4.14 and 4.15 demonstrate the K_d values of the C3, C4, L3 and L4 aptamers respectively. The K_d values for these aptamers (C3, C4, L3 and L4) were better than the rest of aptamers, C1, C2, C4, L1 and L3, as shown in figures 4.6, 4.7, 4.11, 4.12 and 4.13 because the low values of K_d and the Adj.R-Square is accepted as it is nearly 0.998. For C5 aptamer, the results revealed that it is inhibiting the SIRT1 and the K_d value is not accepted (-14.89 nM) as shown in figure 4.10. According to these results, C3, C4, L3 and L4 has been chose to study the kinetics and binding affinity with SIRT1.

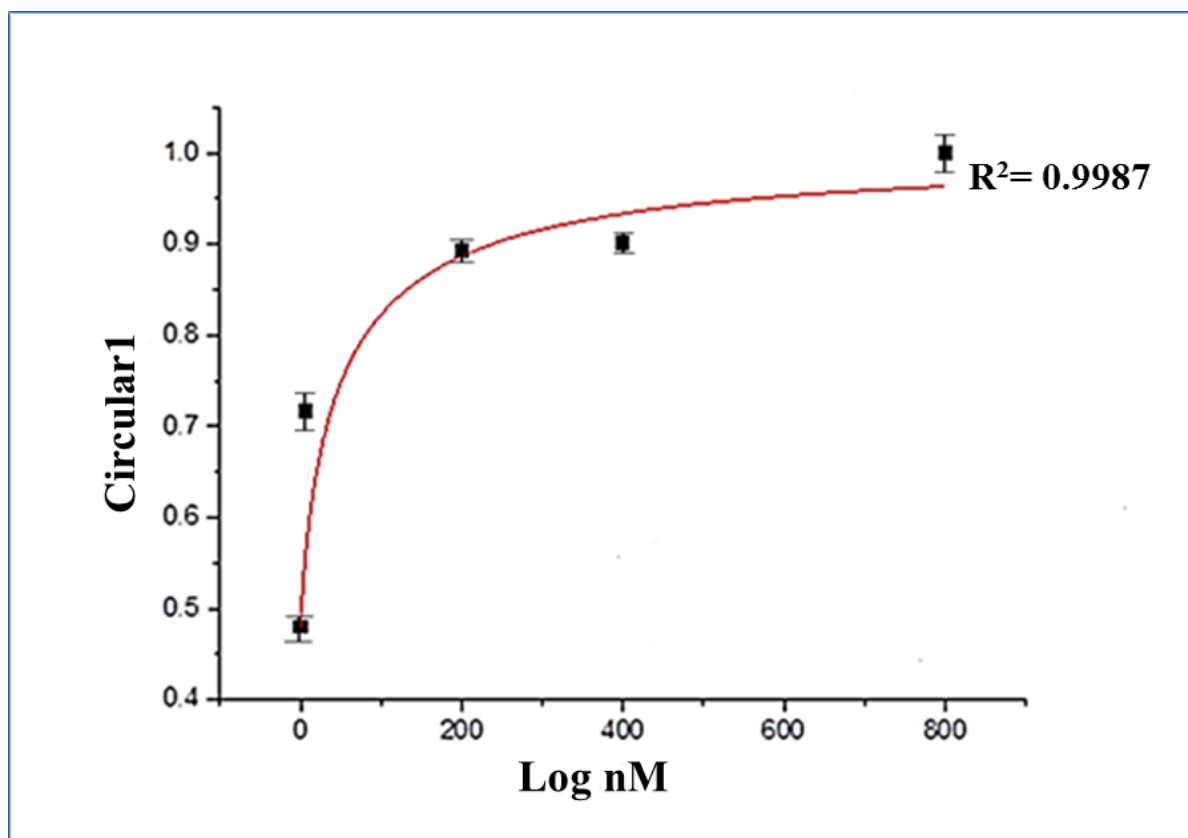


Figure 0.6: The best fit of the data yielded a K_d dissociation constant of circular1 aptamer with $SIRT1 = 32.7 \text{ nM}$. The error in K_d is calculated from the root mean square deviation of data points from the fit.

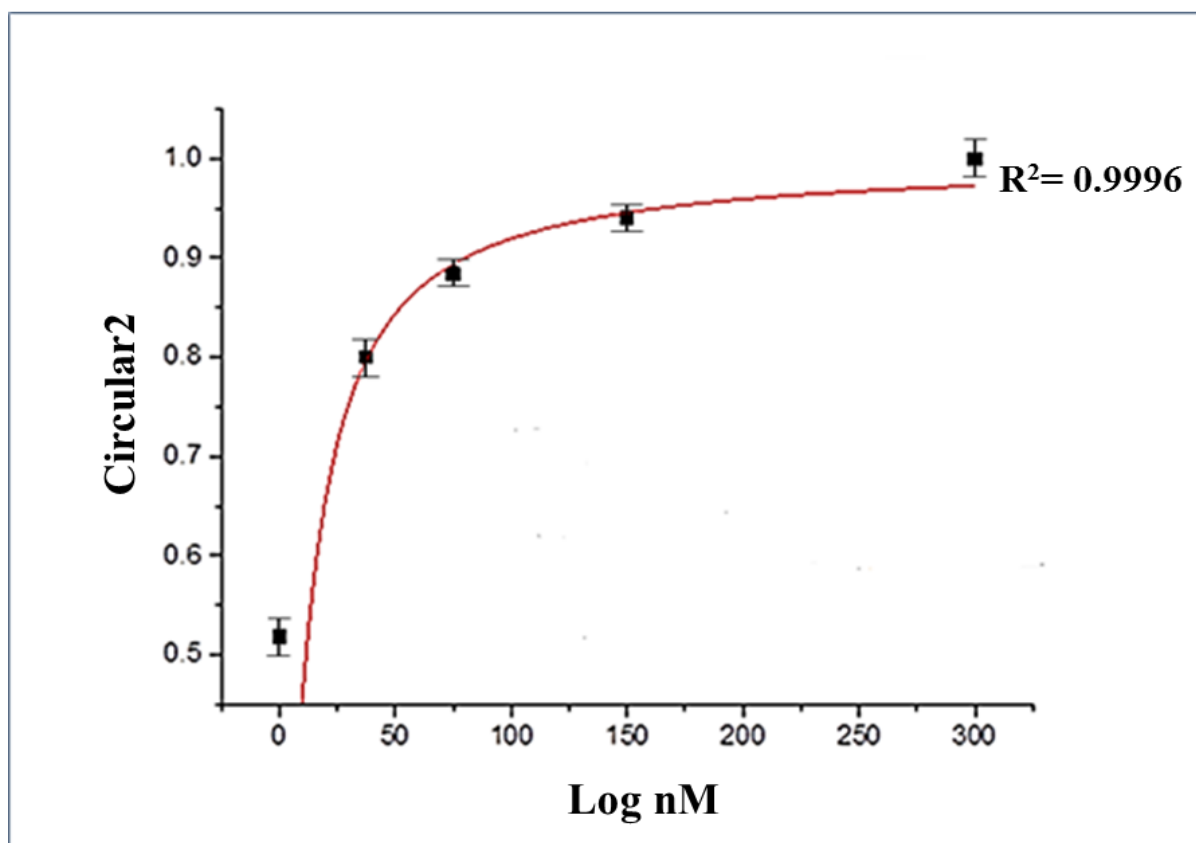


Figure 4.7: The best fit of the data yielded a K_d dissociation constant of circular2 aptamer with $SIRT1 = 8.3 \text{ nM}$. The error in K_d is calculated from the root mean square deviation of data points from the fit.

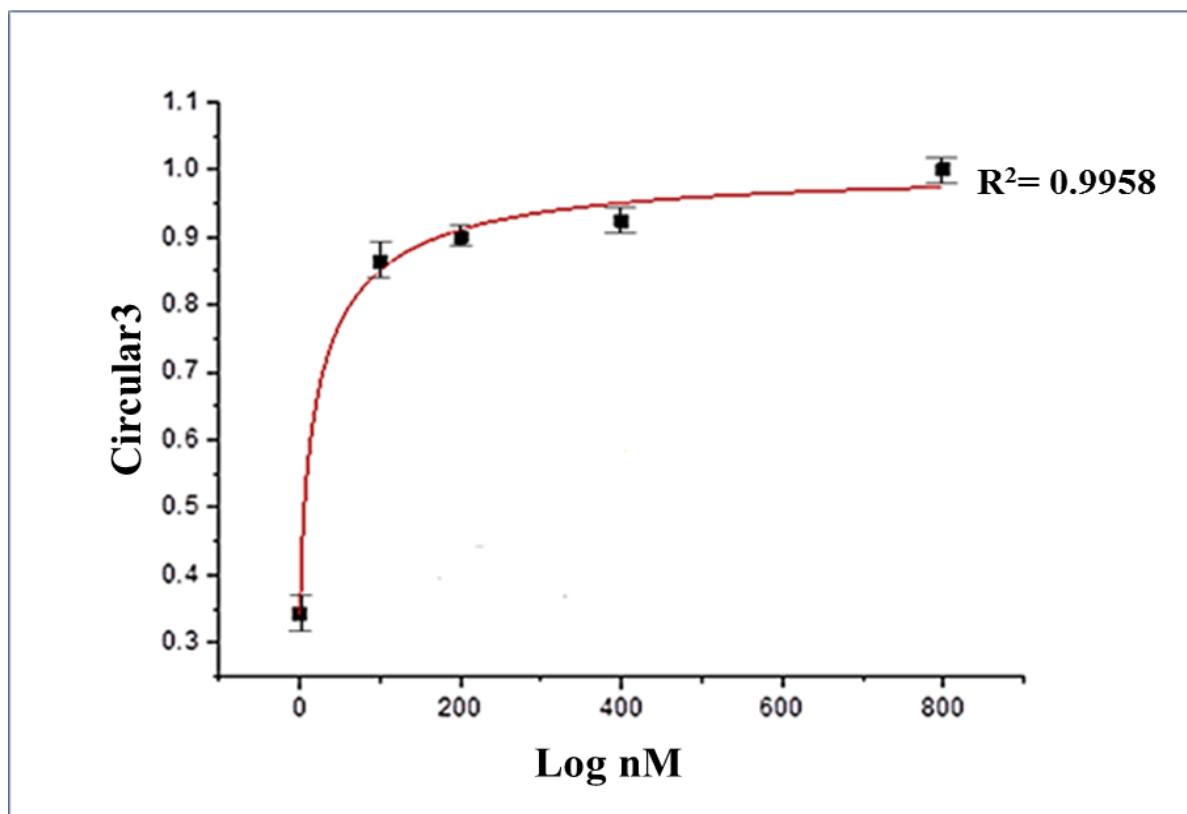


Figure 4.8: The best fit of the data yielded a K_d dissociation constant of circular3 aptamer with SIRT1 = **22.6 nM**. The error in K_d is calculated from the root mean square deviation of data points from the fit.

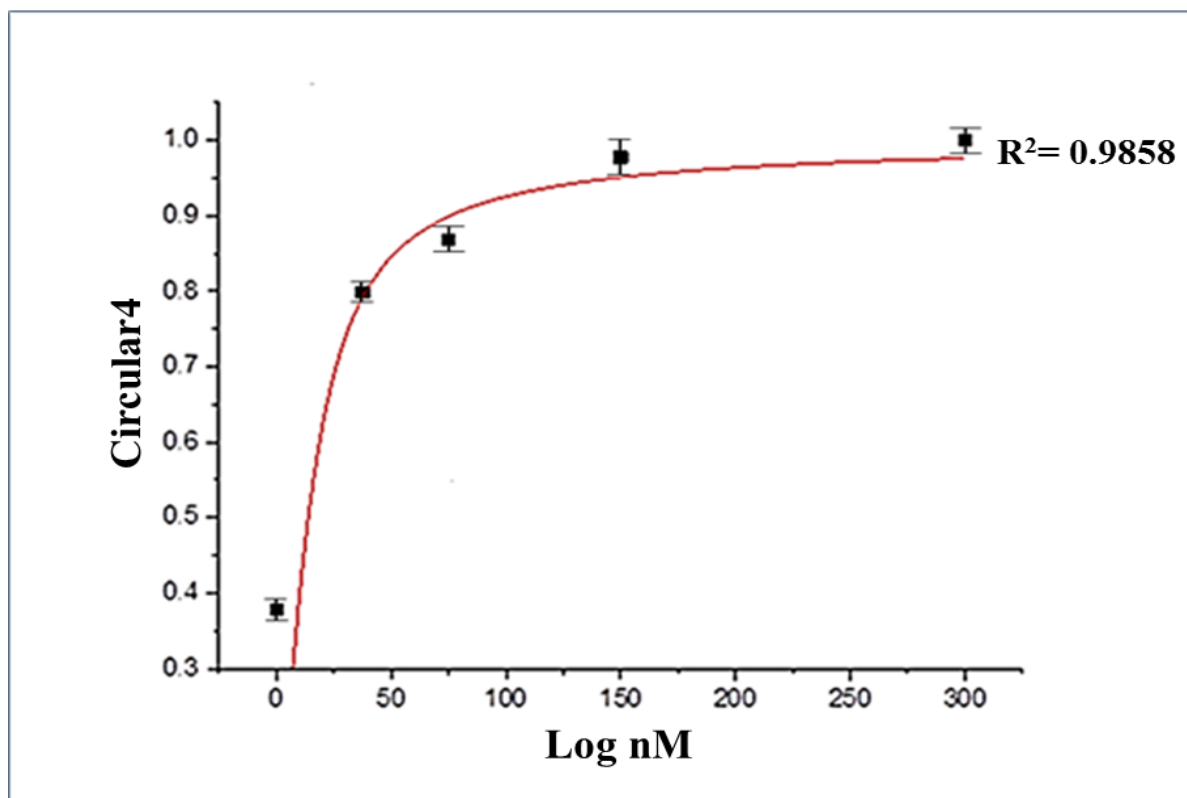


Figure 4.9: The best fit of the data yielded a K_d dissociation constant of circular4 aptamer with SIRT1 = **7.1 nM**. The error in K_d is calculated from the root mean square deviation of data points from the fit.

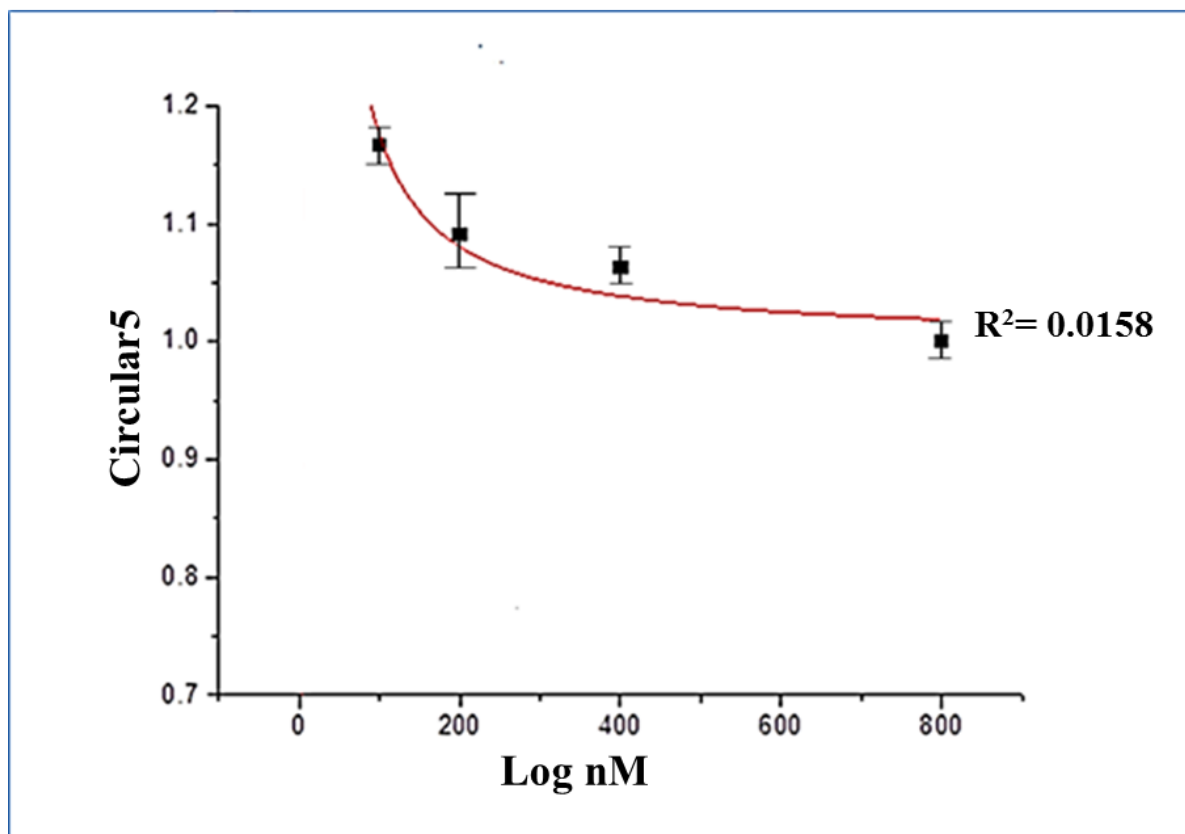


Figure 4.10: The best fit of the data yielded a K_d dissociation constant of circular5 aptamer with $SIRT1 = -14.8$ nM. The error in K_d is calculated from the root mean square deviation of data points from the fit.

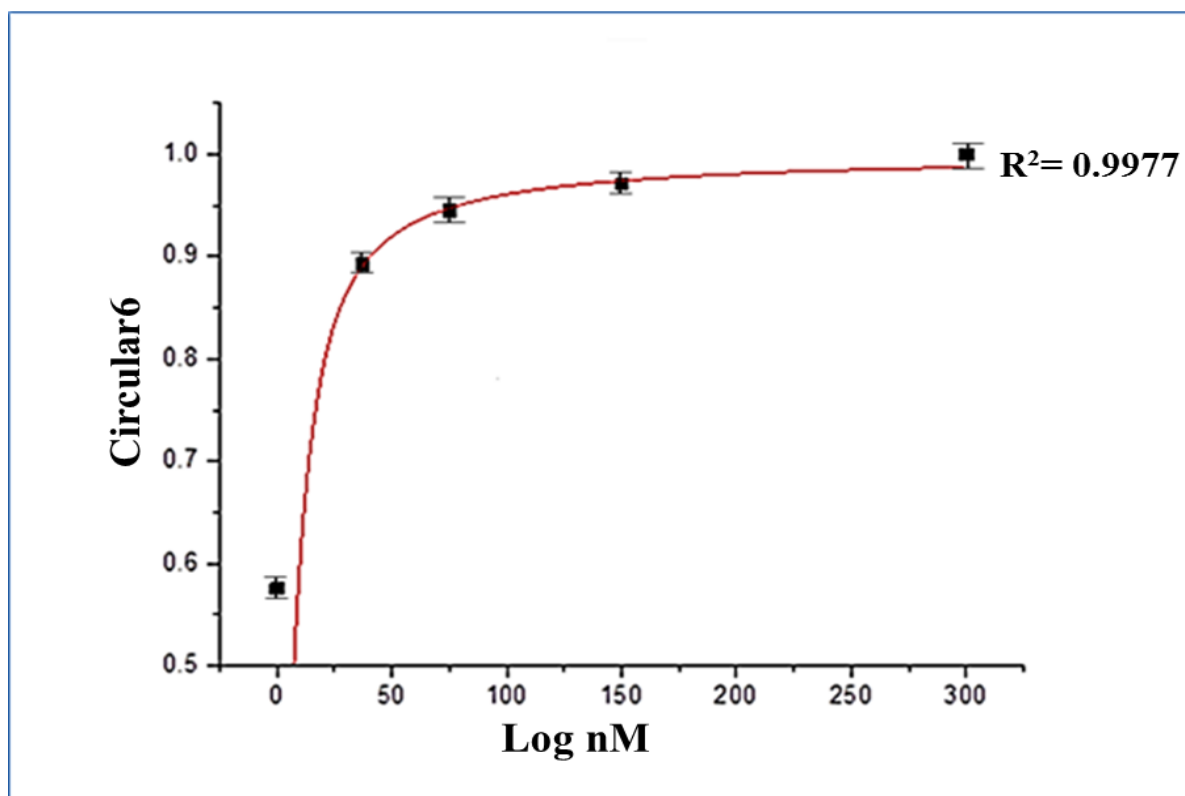


Figure 4.11: The best fit of the data yielded a K_d dissociation constant of circular6 aptamer with $SIRT1 = 3.8$ nM. The error in K_d is calculated from the root mean square deviation of data points from the fit.

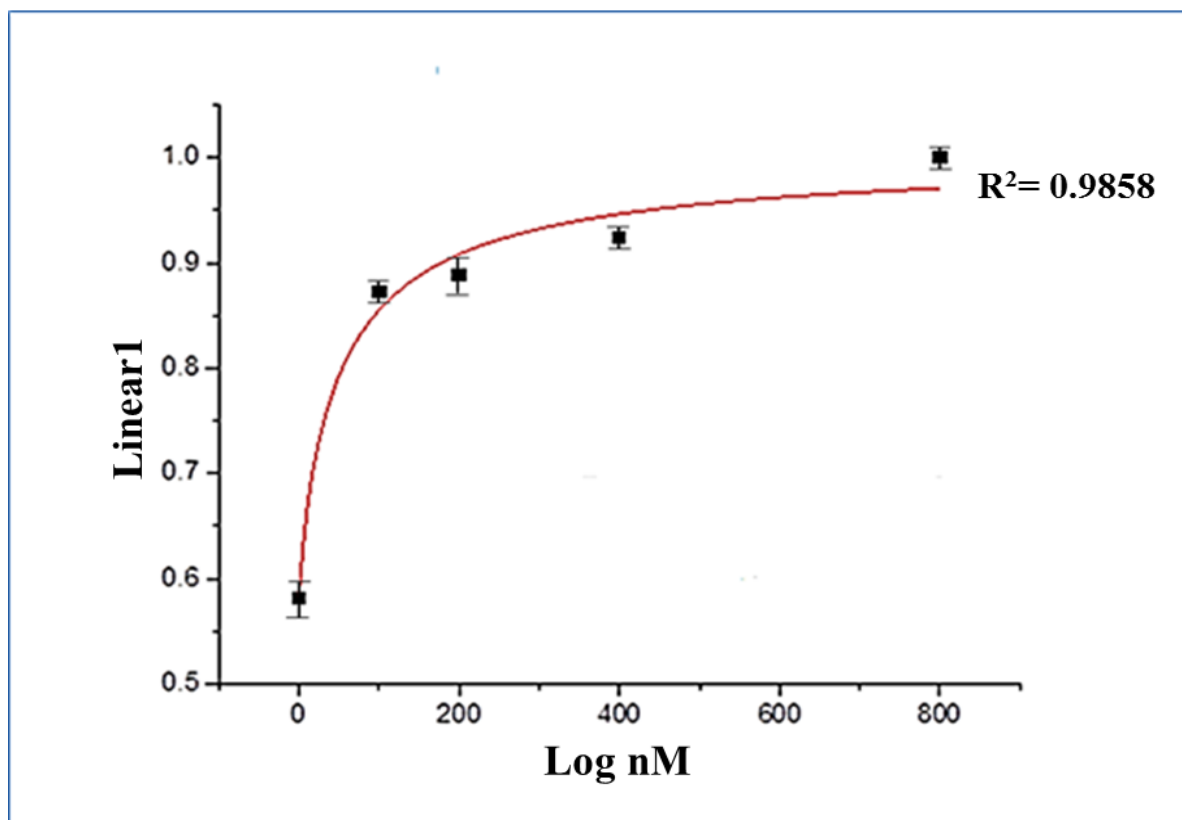


Figure 0.12: The best fit of the data yielded a K_d dissociation constant of linear1 aptamer with $SIRT1 = 26 \text{ nM}$. The error in K_d is calculated from the root mean square deviation of data points from the fit.

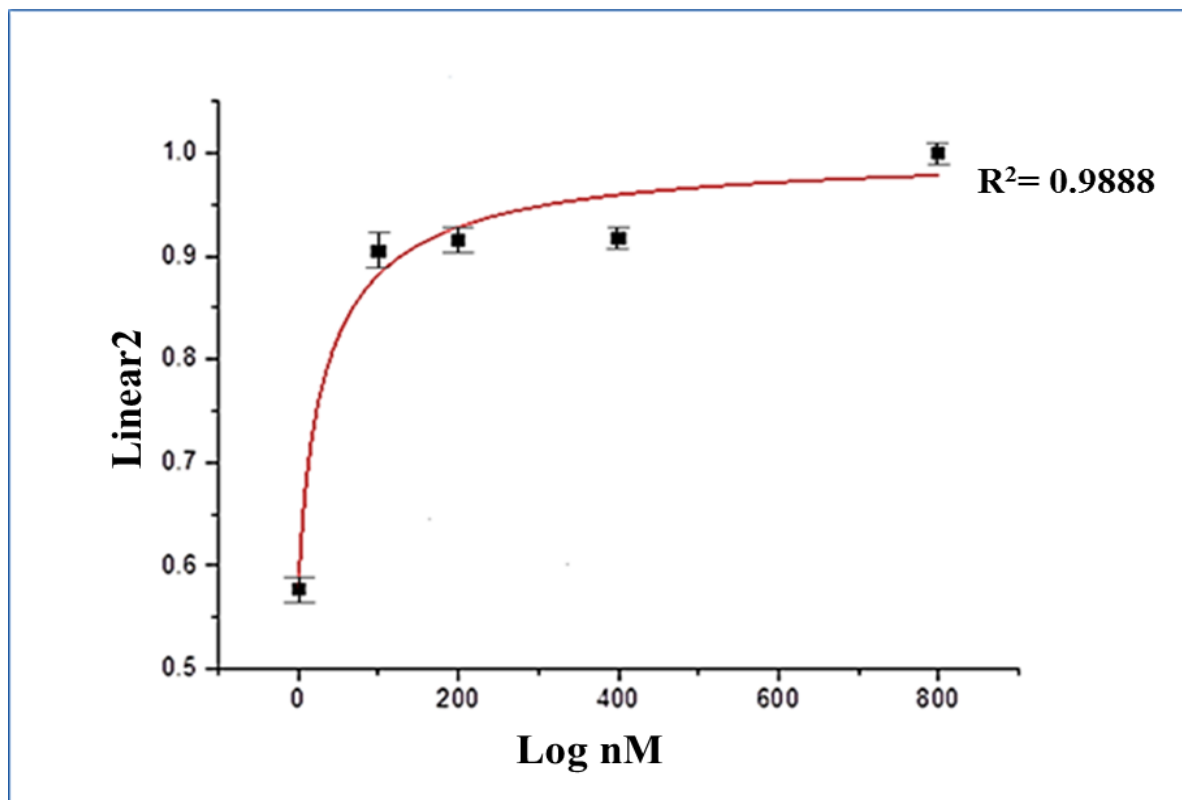


Figure 0.13: The best fit of the data yielded a K_d dissociation constant of linear2 aptamer with $SIRT1 = 18.6 \text{ nM}$. The error in K_d is calculated from the root mean square deviation of data points from the fit.

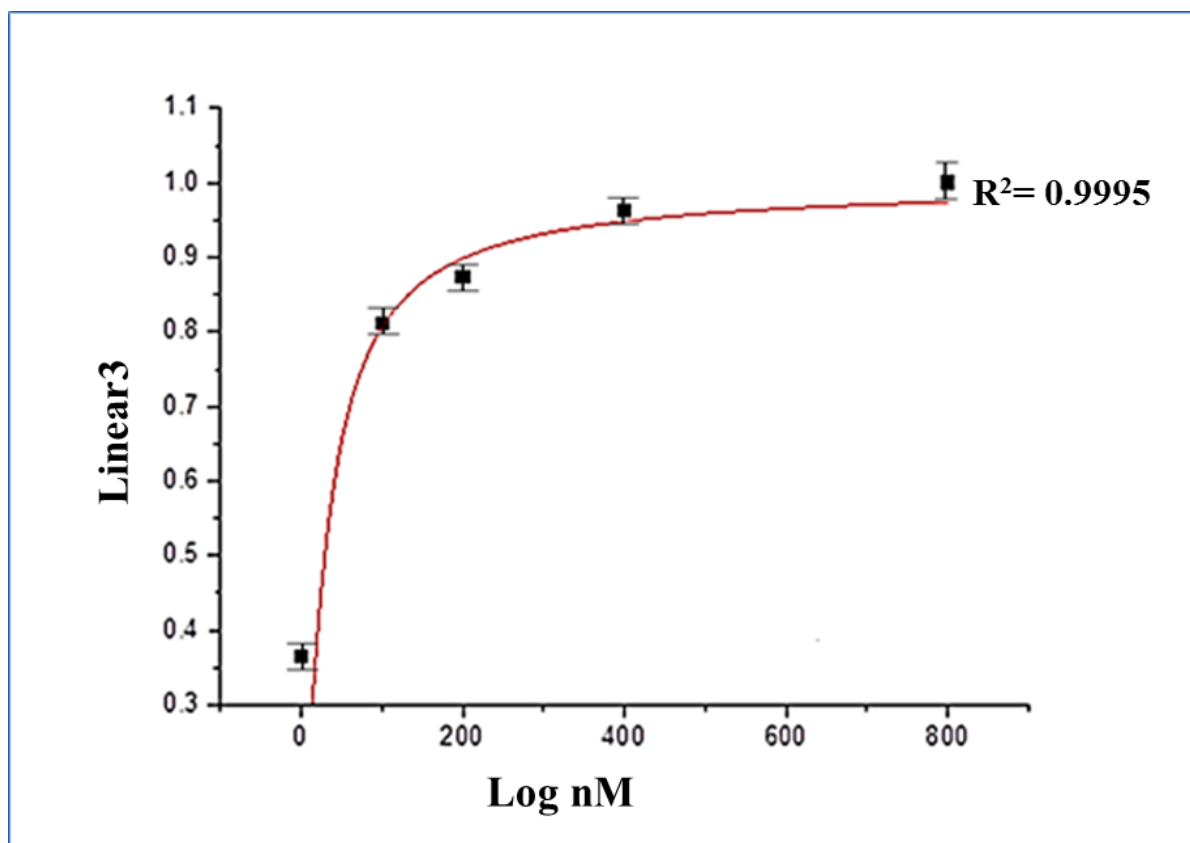


Figure 0.14: The best fit of the data yielded a $K_{dissociation}$ constant of linear3 aptamer with $SIRT1 = 20.9 \text{ nM}$. The error in K_d is calculated from the root mean square deviation of data points from the fit.

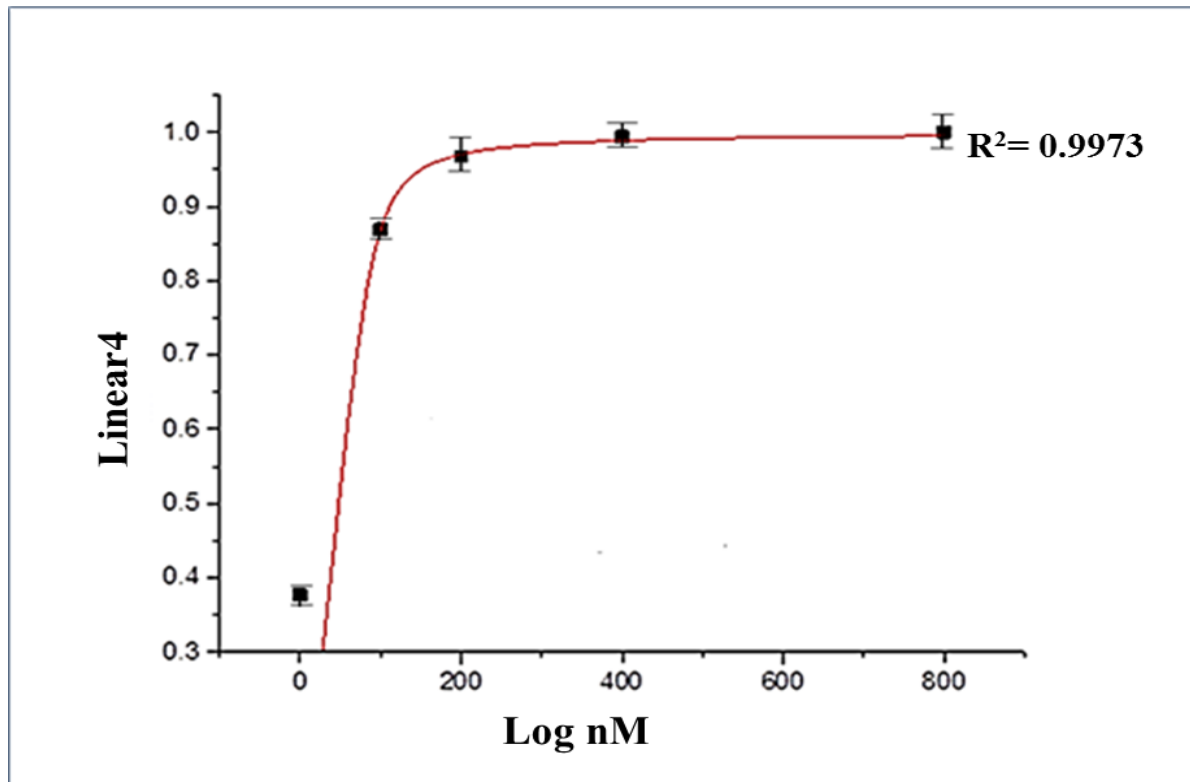


Figure 0.15: The best fit of the data yielded a $K_{dissociation}$ constant of linear4 aptamer with $SIRT1 = 3.4 \text{ nM}$. The error in K_d is calculated from the root mean square deviation of data points from the fit.

4.3.2 SIRT1 kinetics as a Function of the Concentrations of Aptamers

To calculate Michaelis constant (K_m) and Velocity maximum (V_{max}) values, a velocity versus substrate concentration [S] graph is required. SIRT1 was assessed for 5, 15, 30 and 45 min, and then an initial velocity was measured through the slope of these four points. Since the accurate determination of V_{max} on the graph, velocity versus substrate [S], is difficult, double reciprocal plots were used via Lineweaver-Burk Plots to determine the V_{max} and K_m . From our previous results, we decided to further studies on L3, L4, C3 and C4 as they showed the highest activities as well as K_d .

Figure 4.16 illustrates the C3 aptamer progress curve analysis at different concentrations (0.0001, 0.0005, 0.001 and 0.002 mM) and showed that V_{max} for the SIRT1 reaction is attained within 45 min at 37° C. The rate of catalysis rises linearly as C3 aptamer concentration increases and then begins to level off and approach a maximum at 0.002 mM C3 aptamer concentrations.

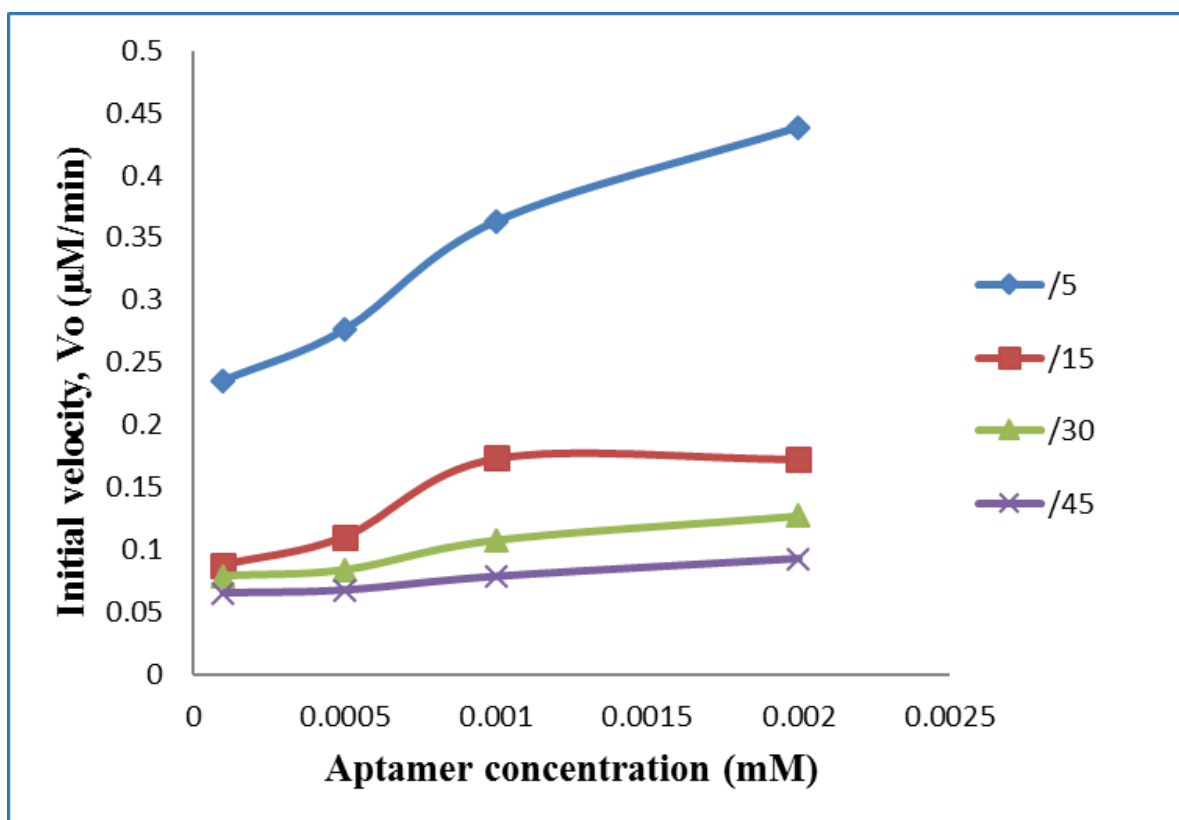


Figure 0.16: A plot of the reaction velocity (V_0) versus circular3 aptamer concentration (mM) for SIRT1 enzyme that obeys Michaelis-Menten kinetics shows that the maximal velocity (V_{max}) is approached asymptotically. The initial velocity (V_0) for each aptamer concentration is determined from the slope of the curve at the beginning of a reaction, when the reverse reaction is insignificant. The Michaelis constant (K_m) is the C3 concentration yielding a velocity of $V_{max}/2$.

The Lineweaver-Burk plot in figure 4.17 and table 4.3 summarises the data of K_m value and V_{max} of C3 aptamer. The plot of initial velocity and C3 aptamer concentration was a hyperbolic curve at each time investigated and all Lineweaver-Burk plots were linear. Lowering of K_m value as shown in table 4.2 confirmed that kinetic mechanism of C3 aptamer activation is by enhanced binding of aptamer with the SIRT1 enzyme. The obtained maximum velocity V_{max} and Michaelis constant K_m of the reaction catalysed by C3 aptamers at concentrations (0.0001, 0.0005, 0.001 and 0.002 mM) were less than the V_{max} and K_m of 0.2 mM resveratrol (control) as shown in table 4.2.

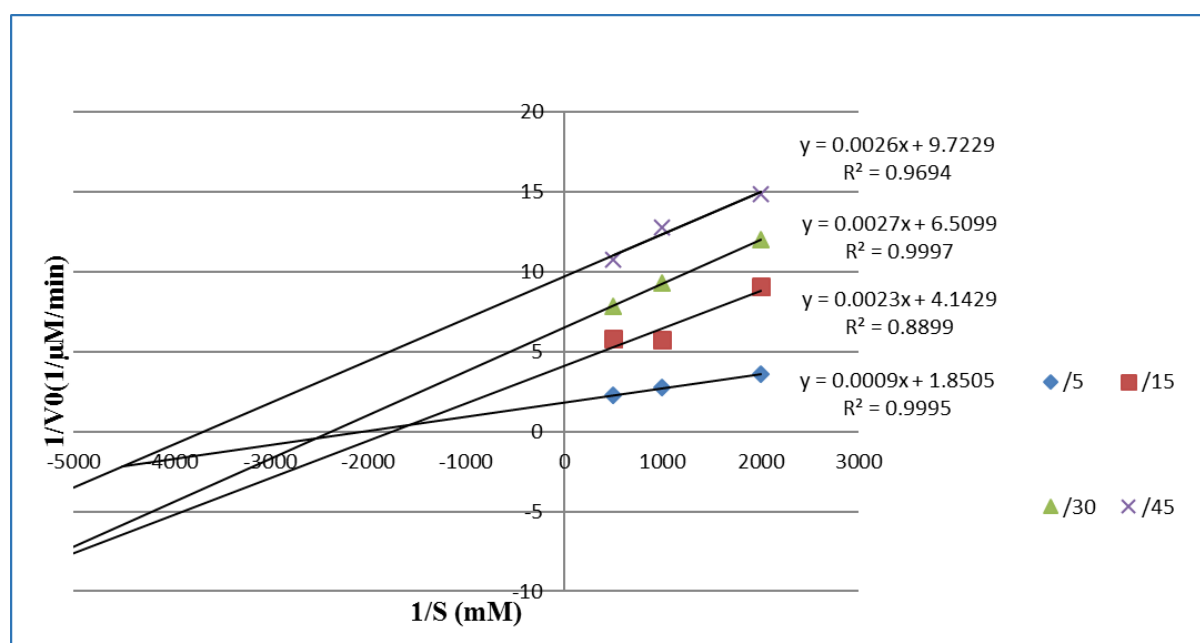


Figure 0.17: A double-reciprocal plot of SIRT1 kinetics for circular3 aptamer is generated by plotting $1/V_0$ as a function $1/[S]$. The slope is the K_m/V_{max} , the intercept on the vertical axis is $1/V_{max}$, and the intercept on the horizontal axis is $-1/K_m$.

Table 0.2: V_{max} and K_m for C3 aptamer \pm standard error.

	5min		15min		30min		45min	
	V_{max}	K_m	V_{max}	K_m	V_{max}	K_m	V_{max}	K_m
Circular 3 at 0.0001, 0.0005, 0.001 and 0.002 mM	0.54 μ M ± 0.098	0.000486 μ M ± 0.00031	0.24 μ M ± 0.1	0.000437 μ M ± 0.00019	0.154 μ M ± 0.023	0.00041 μ M ± 0.00033	0.102 μ M ± 0.008	0.000267 μ M ± 0.00031
Resveratrol at 0.2 mM	0.25 μ M ± 0.15	0.002 μ M ± 0.0014	0.13 μ M ± 0.09	0.002 μ M ± 0.0014	0.069 μ M ± 0.104	0.002 μ M ± 0.0014	0.056 μ M ± 0.043	0.002 μ M ± 0.0014

The extent of SIRT1 enzyme activity formation is determined as a function of time for a series of C3 aptamer concentrations (figure 4.18). As expected, in each case, the activity of SIRT1 formed increases with time, although eventually a time is reached when there is no net change in the concentration of C3 aptamer. The most important point in this figure is all the concentrations of C3 aptamers were significantly increased the activity of SIRT1 as compared with 200 μ M resveratrol activator, $p < 0.001$.

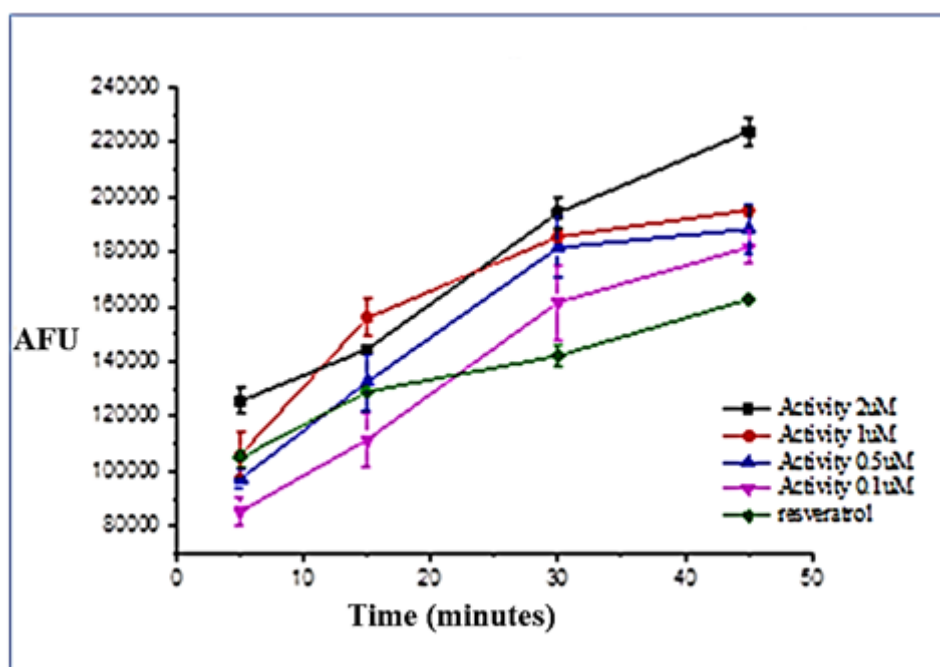


Figure 0.18: The amount of product formed at different concentrations (circular3 aptamers at 0.1, 0.5, 1 and 2 μ M and 200 μ M resveratrol) are plotted as a function of time, $p < 0.001$.

In the same context, kinetic examination of SIRT1 enzyme activity with circular4 aptamer showed in figures 4.19 and 4.20. At a fixed concentration of SIRT1 enzyme, V_0 is almost linearly proportional to C4 aptamer concentration when C4 aptamer concentration is 0.0001, 0.0005 and 0.001 mM but is nearly independent of C4 aptamer concentration when C4 aptamer concentration is 0.002 mM. The K_m value and V_{max} of SIRT1 enzyme with C4 aptamer at series time (5, 15, 30 and 45min) demonstrated in table 4.3.

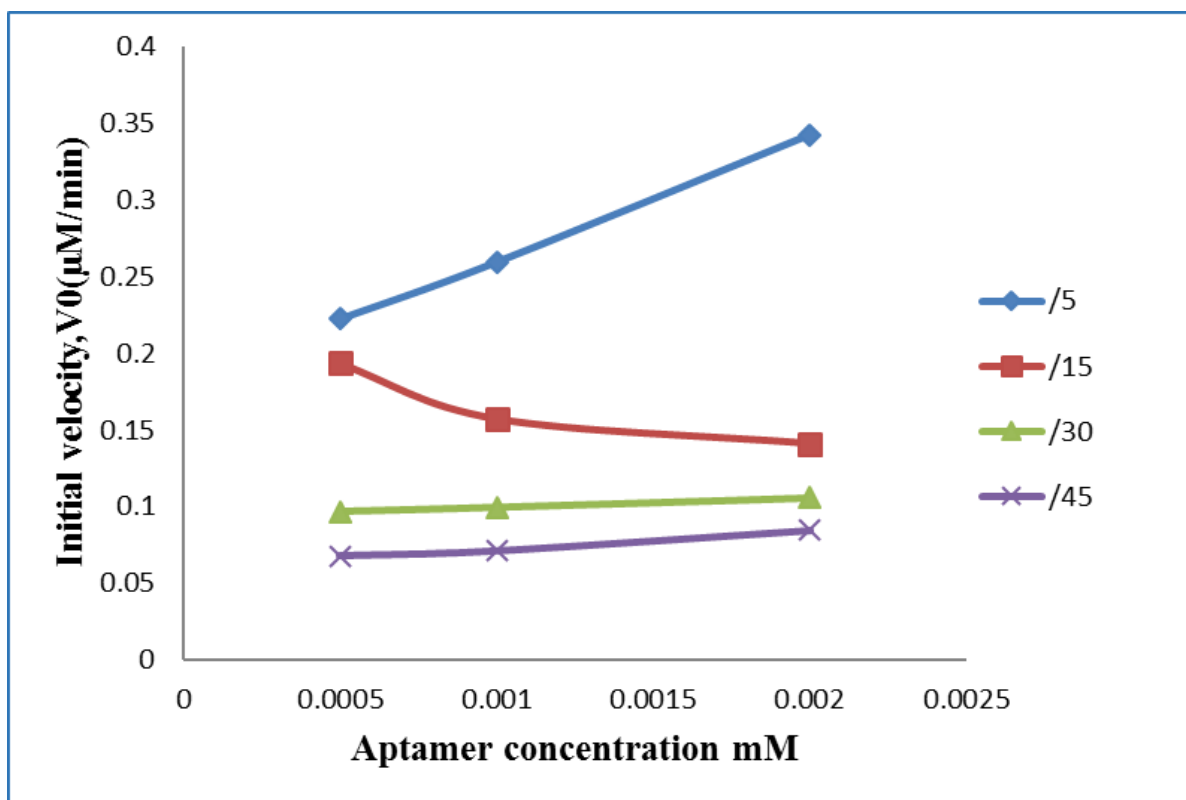


Figure 0.19: A plot of the reaction velocity (V_0) versus circular4 aptamer concentration (mM) for SIRT1 enzyme that obeys Michaelis-Menten kinetics shows that the maximal velocity (V_{max}) is approached asymptotically. The initial velocity (V_0) for each aptamer concentration is determined from the slope of the curve at the beginning of a reaction, when the reverse reaction is insignificant. The Michaelis constant (K_m) is the C4 concentration yielding a velocity of $V_{max}/2$.

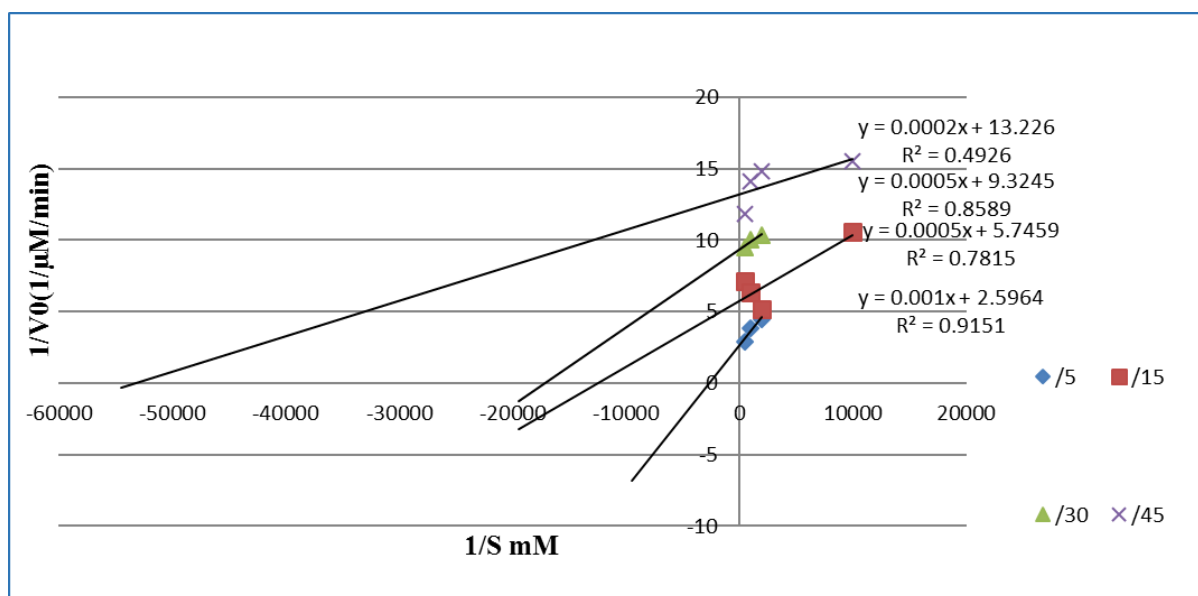


Figure 4.20: A double-reciprocal plot of SIRT1 kinetics for circular4 aptamer is generated by plotting $1/V_0$ as a function $1/[S]$. The slope is the K_m/V_{max} , the intercept on the vertical axis is $1/V_{max}$, and the intercept on the horizontal axis is $-1/K_m$.

Table 0.3: V_{max} and K_m for C4 aptamer \pm standard error.

	5min		15min		30min		45min	
	V_{max}	K_m	V_{max}	K_m	V_{max}	K_m	V_{max}	K_m
Circular 4 at 0.0001, 0.0005, 0.001 and 0.002 mM	0.3 μ M \pm 0.042	0.00007 μ M \pm 0.0000606	0.174 μ M \pm 0.027	0.000059 μ M \pm 0.000064	0.12 μ M \pm 0.002	0.000026 μ M \pm 0.0000563	0.076 μ M \pm 0.0056	0.000015 μ M \pm 0.0000102
Resveratrol at 0.2 mM	0.25 μ M \pm 0.15	0.002 μ M \pm 0.0014	0.13 μ M \pm 0.09	0.002 μ M \pm 0.0014	0.069 μ M \pm 0.104	0.002 μ M \pm 0.0014	0.056 μ M \pm 0.043	0.002 μ M \pm 0.0014

To examine this activation of in more detail, we determined the dependence of C4 aptamer concentration on SIRT1 activity at different time (5, 15, 30, 45min). In figure 4.21, C4 aptamer is seen to activate the SIRT1 in time course at different concentration as well as resveratrol. These results demonstrate, for the first time, that C4 aptamer can accelerate the reaction at 2 μ M more than the other C4 aptamer concentration. Likewise, all the concentration of C4 aptamers increased the activity of SIRT1 as compared with 200 μ M resveratrol activator, $p < 0.05$.

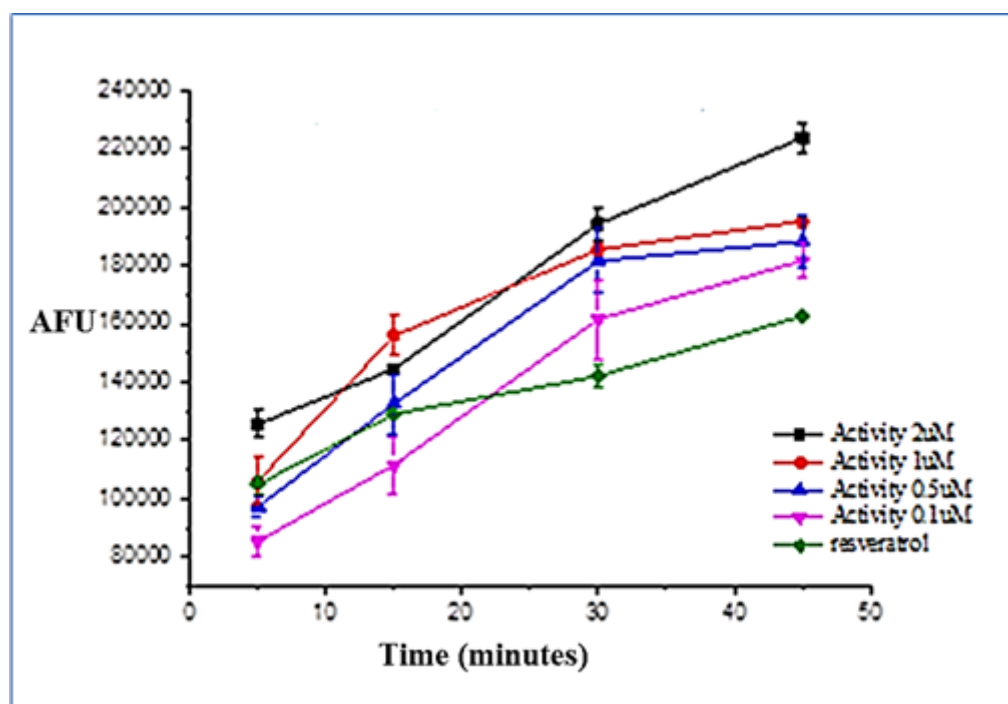
**Figure 4.21:** The amount of product formed at different concentrations (circular4 aptamers at 0.1, 0.5, 1 and 2 μ M and 200 μ M resveratrol) are plotted as a function of time, $p < 0.05$.

Figure 4.22 illustrates the relationship between initial velocity and linear3 aptamer concentration at different times. The relationship between rate of reaction and concentration of L3 aptamer depends on the affinity of the SIRT1 enzyme for its aptamer. This is usually expressed as the K_m of the SIRT1 enzyme, an inverse measure of affinity. Low concentration of L3 aptamer at 5 min, there is a steep increase in the rate of reaction with increasing L3 aptamer concentration. The catalytic site of the SIRT1 enzyme is empty, waiting for L3 aptamer to bind, for much of the time, and the rate at which product can be formed is limited by the concentration of L3 aptamer which is available. As the concentration of L3 aptamer increases, the SIRT1 enzyme becomes saturated with L3 aptamer. As soon as the catalytic site is empty, more L3 aptamer is available to bind and undergo reaction. The rate of formation of product now depends on the activity of the SIRT1 enzyme itself, and adding more L3 aptamer will not affect the rate of the reaction to any significant effect.

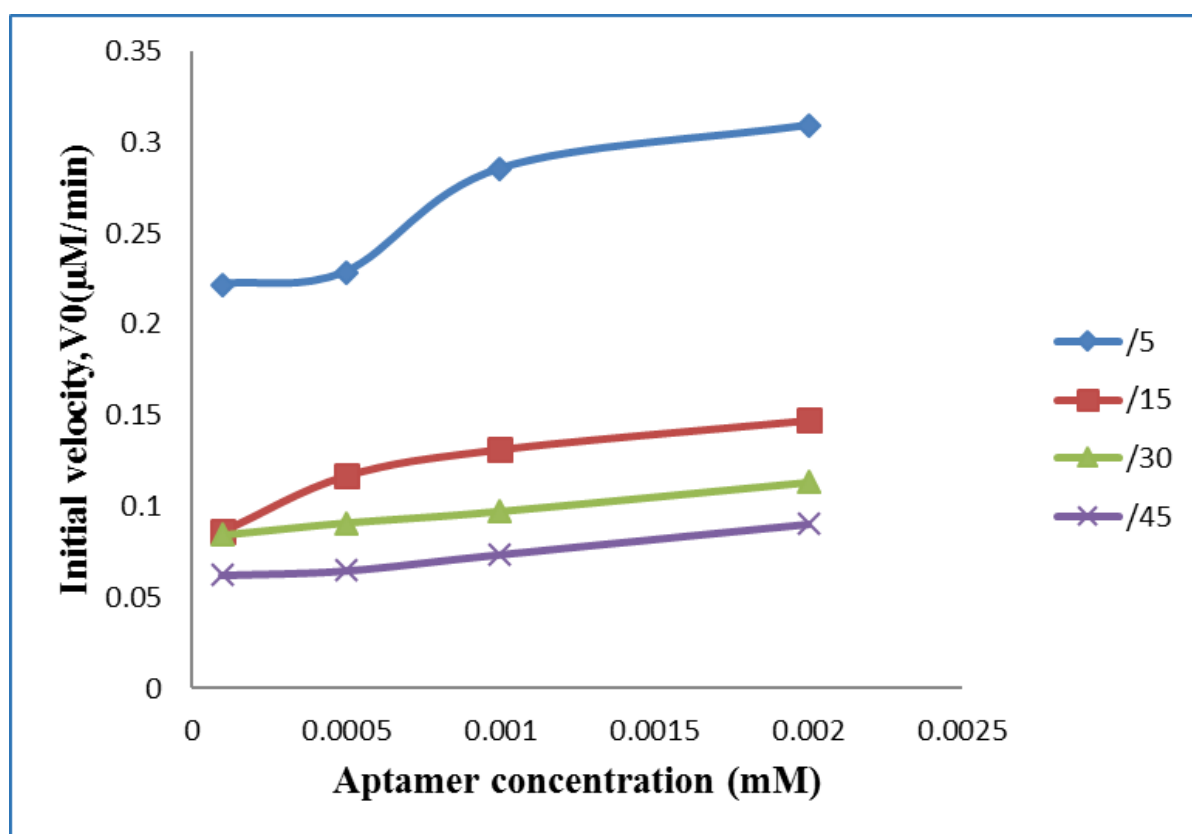


Figure 4.22: A plot of the reaction velocity (V_0) versus linear3 aptamer concentration (mM) for SIRT1 enzyme that obeys Michaelis-Menten kinetics shows that the maximal velocity (V_{max}) is approached asymptotically. The initial velocity (V_0) for each aptamer concentration is determined from the slope of the curve at the beginning of a reaction, when the reverse reaction is insignificant. The Michaelis constant (K_m) is the L3 concentration yielding a velocity of $V_{max}/2$.

K_m and V_{max} value for SIRT1 enzyme with L3 aptamer were determined by used double reciprocal plots via Lineweaver-Burk Plots as shown in figure 4.23 and the values is demonstrated in table 4.4.

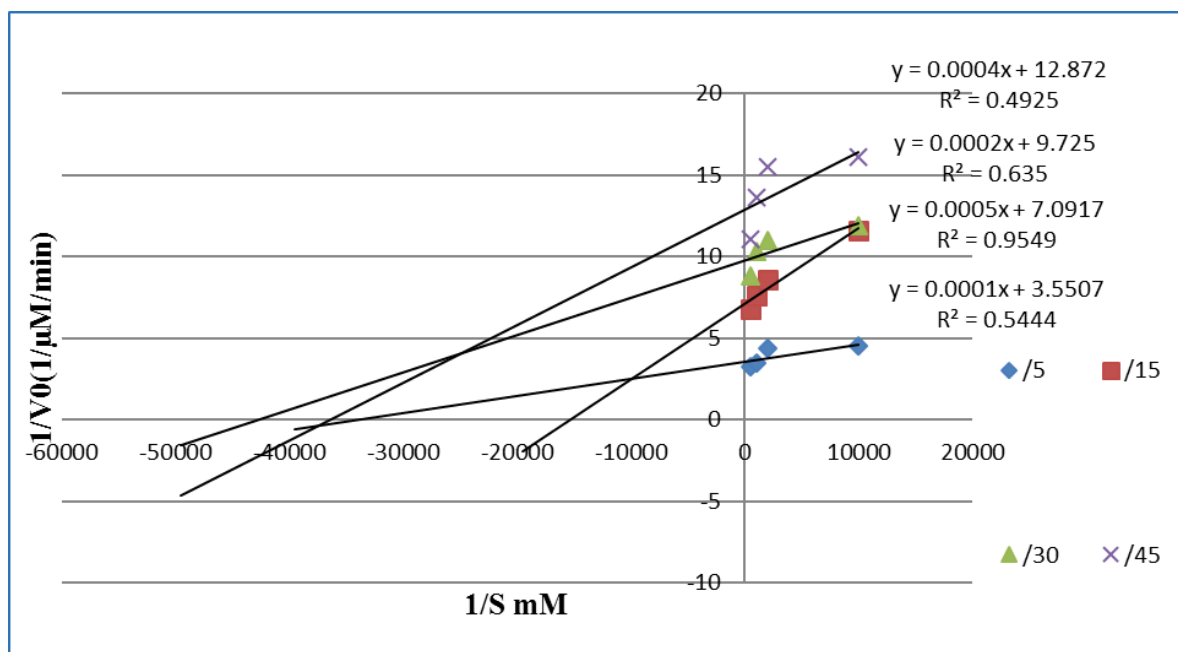


Figure 0.23: A double-reciprocal plot of SIRT1 kinetics for linear3 aptamer is generated by plotting $1/V_0$ as a function $1/[S]$. The slope is the K_m/V_{max} , the intercept on the vertical axis is $1/V_{max}$, and the intercept on the horizontal axis is $-1/K_m$.

Table 0.4: V_{max} and K_m for L3 aptamer \pm standard error.

	5min		15min		30min		45min	
	V_{max}	K_m	V_{max}	K_m	V_{max}	K_m	V_{max}	K_m
Linear 3 at 0.0001, 0.0005, 0.001 and 0.002 mM	0.282 μ M ± 0.0258	0.000364 μ M ± 0.000028	0.144 μ M ± 0.0075	0.000074 μ M ± 0.000024	0.104 μ M ± 0.00702	0.00003 μ M ± 0.000019	0.0776 μ M ± 0.0065	0.000031 μ M ± 0.000021
Resveratrol at 0.2 mM	0.25 μ M ± 0.15	0.002 μ M ± 0.0014	0.13 μ M ± 0.09	0.002 μ M ± 0.0014	0.069 μ M ± 0.104	0.002 μ M ± 0.0014	0.056 μ M ± 0.043	0.002 μ M ± 0.0014

The activity of SIRT1 enzyme was increased markedly at 0.1, 0.5, 1 and 2 μ M concentration of L3 aptamer as compared with the activator control (200 μ M resveratrol) ($p < 0.01$) as indicated in figure 4.24.

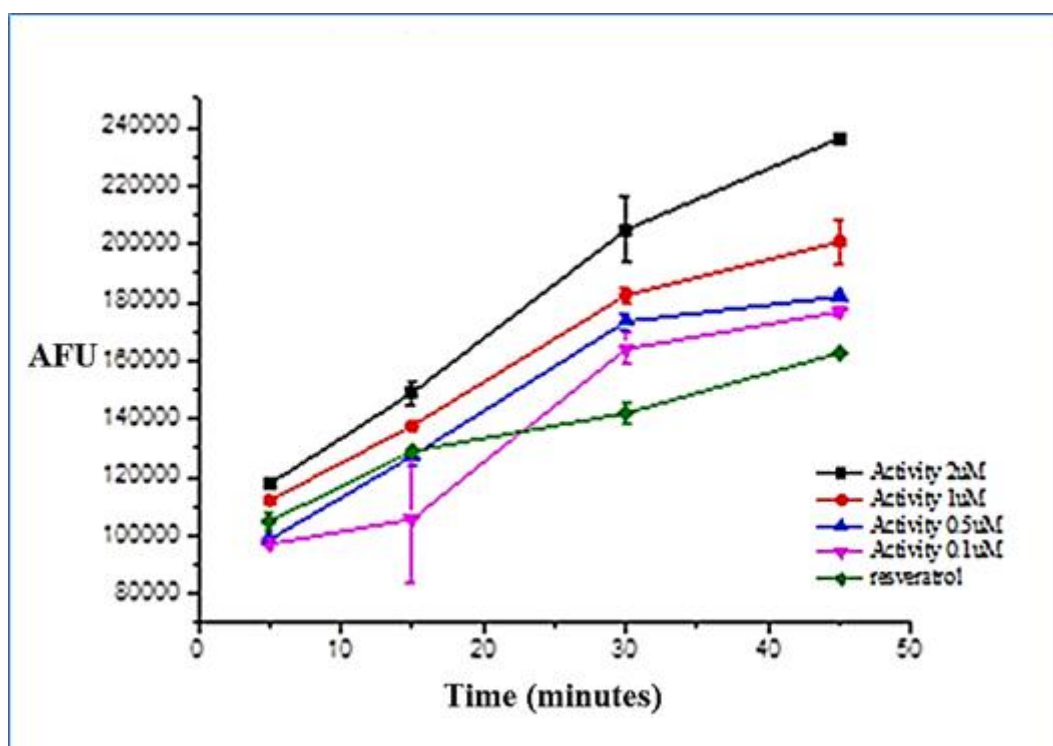


Figure 4.24: The amount of product formed at different concentrations (linear3 aptamers at 0.1, 0.5, 1 and 2 μM and 200 μM resveratrol) are plotted as a function of time, $p < 0.01$.

The K_m and V_{max} of Linear4 aptamer were also estimated as in the previously described method of C3, C4 and L3 aptamers as demonstrated in figures 4.25 and 4.26. The values of these kinetics constants of SIRT1 enzyme with L4 aptamer as compared with resveratrol control shown in table 4.5.

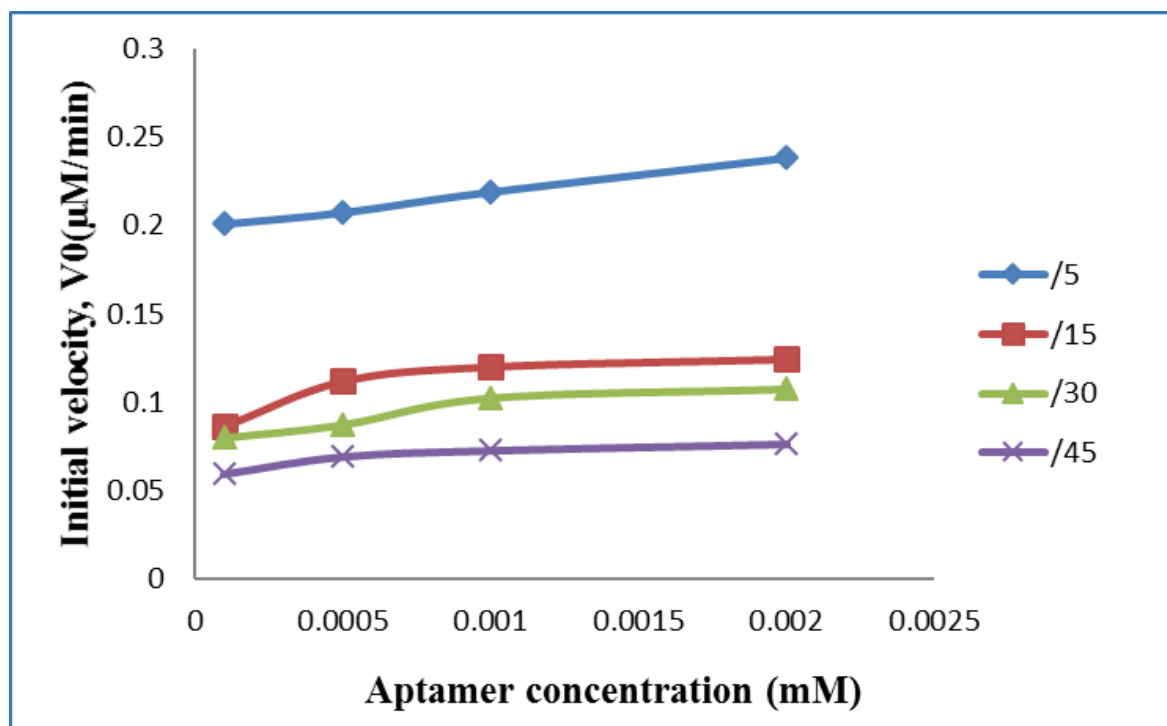


Figure 0.25: A plot of the reaction velocity (V_0) versus linear4 aptamer concentration (mM) for SIRT1 enzyme that obeys Michaelis-Menten kinetics shows that the maximal velocity (V_{max}) is approached asymptotically. The initial velocity (V_0) for each aptamer concentration is determined from the slope of the curve at the beginning of a reaction, when the reverse reaction is insignificant. The Michaelis constant (K_m) is the L4 concentration yielding a velocity of $V_{max}/2$.

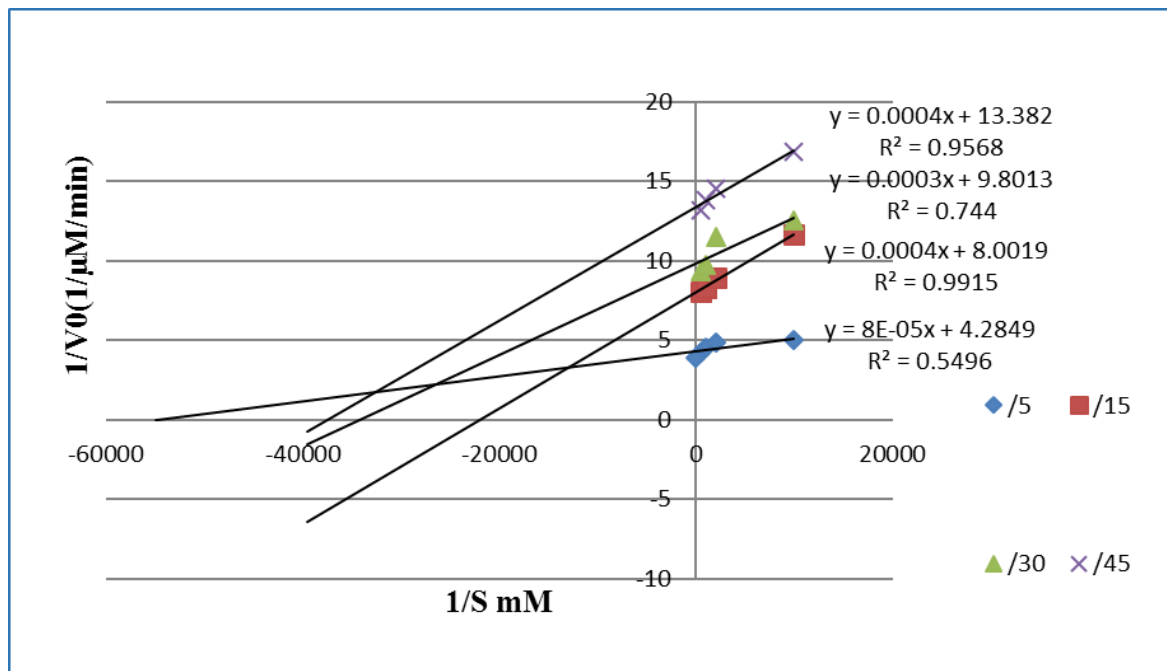
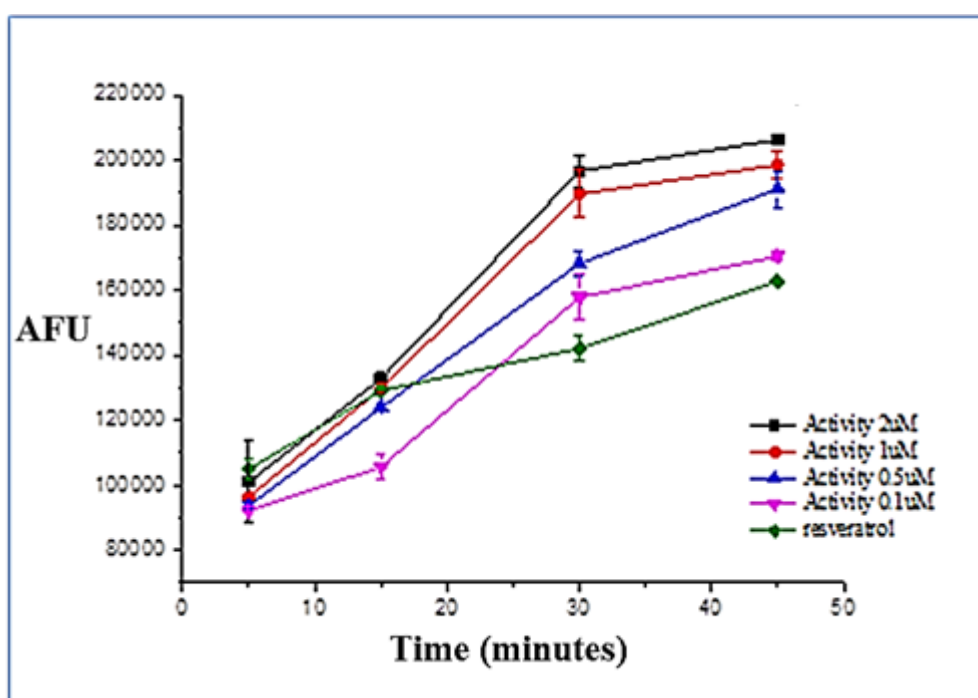


Figure 4.26: A double-reciprocal plot of SIRT1 kinetics for linear4 aptamer is generated by plotting $1/V_0$ as a function $1/[S]$. The slope is the K_m/V_{max} , the intercept on the vertical axis is $1/V_{max}$, and the intercept on the horizontal axis is $-1/K_m$.

Table 0.5: V_{max} and K_m for L4 aptamer \pm standard error.

	5min		15min		30min		45min	
	V_{max}	K_m	V_{max}	K_m	V_{max}	K_m	V_{max}	K_m
Linear 4 at 0.0001, 0.0005, 0.001 and 0.002 mM	0.226 μ M \pm 0.0094	0.0000586 μ M \pm 0.0000099	0.125 μ M \pm 0.00186	0.000047 μ M \pm 0.0000052	0.103 μ M \pm 0.006	0.000033 μ M \pm 0.000018	0.074 μ M \pm 0.0015	0.0000277 μ M \pm 0.0000059
Resveratrol at 0.2 mM	0.25 μ M \pm 0.15	0.002 μ M \pm 0.0014	0.13 μ M \pm 0.09	0.002 μ M \pm 0.0014	0.069 μ M \pm 0.104	0.002 μ M \pm 0.0014	0.056 μ M \pm 0.043	0.002 μ M \pm 0.0014

The activity of SIRT1 enzyme at different concentration of L4 aptamer was similar the activity of SIRT1 enzyme at 1 and 2 μ M C3, C4 and L3 aptamers as compared with 200 μ M resveratrol ($p < 0.05$), while the activity of SIRT1 enzyme with 200 μ M resveratrol is higher than the activity of SIRT1 enzyme at low concentrations (0.1 and 0.5 μ M) as shown in figure 4.27.

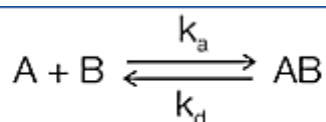
**Figure 0.27:** The amount of product formed at different concentrations (linear4 aptamers at 0.1, 0.5, 1 and 2 μ M and 200 μ M resveratrol) are plotted as a function of time, $p < 0.05$.

In summary, the results in tables 4.2-4.5 showed the low values of V_{max} in lower concentrations at 0.0001, 0.0005, 0.001 and 0.002 mM of C3, C4, L3 and L4 aptamers

respectively as compared with the lower V_{\max} value of high concentration of 0.2 mM resveratrol, the low values of kinetic results for V_{\max} and K_m of aptamers demonstrated that C3, C4, L3 and L4 aptamers are a good binding with SIRT1 enzyme.

4.3.3 Determination of Equilibrium Binding Characterisation of Circular3, Circular4, Linear3 and Linear4 Aptamers for SIRT1 using Surface Plasmon Resonance SPR

To determine the dissociation constants (KD) of C3, C4, L3 and L4 aptamers and SIRT1 enzyme binding, we performed a SPR kinetic analysis using a ProteOn™ XPR36 system. The sensorgram must be fitted to a kinetic model using a mathematical algorithm. In ProteOn software, the most commonly used binding model for SPR biosensors is the Langmuir model. It describes a 1:1 interaction in which one aptamer molecule interacts with one SIRT1 enzyme molecule. In theory, the formation of the ligand aptamer-SIRT1 complex follows second-order kinetics. However, because the majority of SPR biosensors are fluidics-based and capable of maintaining a constant aptamers concentration in a continuous liquid flow, complex formation actually follows pseudo-first-order kinetics. In addition, this model assumes that the binding reactions are equivalent and independent at all binding sites. It also assumes that the reaction rate is not limited by mass transport. Many interactions adhere to this model, in which the interaction is described by the simple equation shown below, where B represents the ligand (aptamer) and A is the analyte (SIRT1 enzyme). The rate of complex formation is represented by the association constant (K_a , in the unit of $M^{-1}s^{-1}$) and the rate of complex decay is represented by the dissociation constant (K_d , in the unit of s^{-1}), as given as:



In a kinetic analysis, the equilibrium constant (KD, in the unit of nM) is calculated from the two kinetic constants through the defining relation $KD = K_d/K_a$. Relating the interaction state to the SPR sensorgram is accomplished by applying specific equations relevant to the different sensorgram phases, as schematised in figure 4.28.

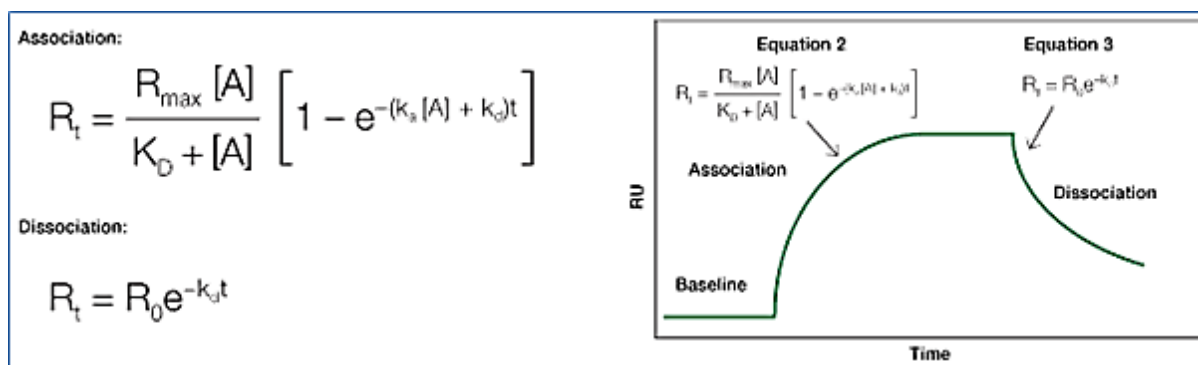


Figure 4.28: An idealised sensorgram showing the baseline, association, and dissociation phases.

For these experiments, highly purified SIRT1 enzyme was prepared as described in section (2.3.1) chapter 2. When various concentrations of SIRT1 were applied to 1 μ M of C3, C4, L3 and L4 aptamers immobilised on a sensor chip, a specific real-time binding between the SIRT1 enzyme and aptamers was observed and quantified (figure 4.29-4.32). Binding curves were globally fitted to various binding models, provided by the ProteOn™ XPR36 evaluation software. The molecular weight of the SIRT1 enzyme was considered in all calculations. Apparent rate constants obtained from the Langmuir model were demonstrated in table 4.7.

The results in figures 4.29-4.32 were showed the curve to determination the affinities of C3, C4, L3 and L4 aptamers for SIRT1 respectively using surface plasmon resonance. The KD values of all aptamers were in nM range and a good result for binding affinity but the KD value of C3 aptamers (KD = 27.07 nM) is the best one because is the lowest value from the rest aptamers and indicates that is at high affinity with the SIRT1 enzyme. The KD value in this method of SPR is the better than the KD value of all aptamer in the previous method because it is more sensitive to determined the KD value between aptamers and SIRT1 enzyme.

In summary, table 4.7 demonstrates the KD values of C3, C4, L3 and L4 aptamers with SIRT1 and showed the C3 aptamers is the best aptamer for binding with the SIRT1 enzyme.

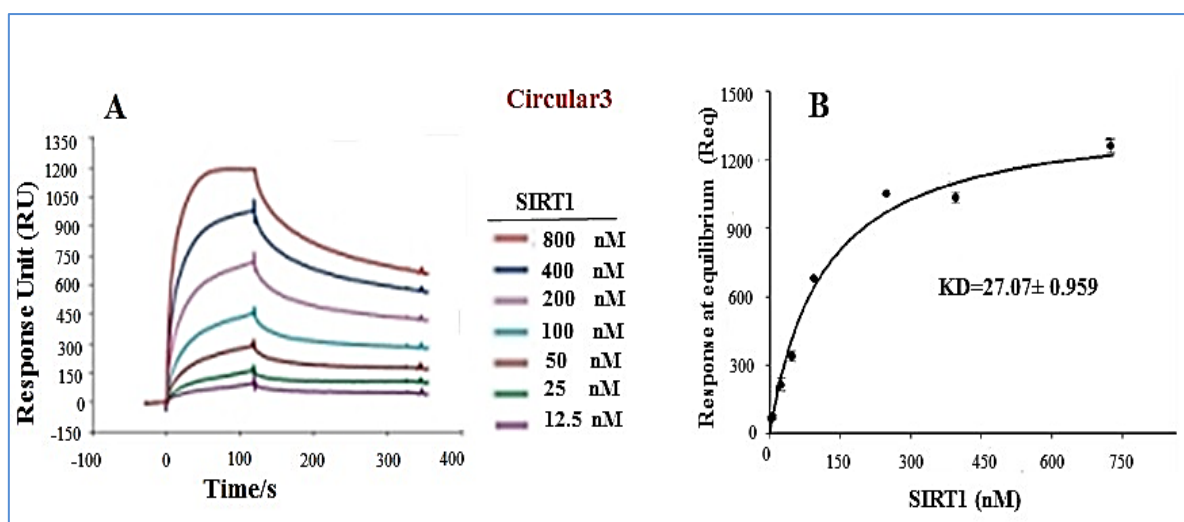


Figure 4.29: Determination of the affinities of aptamers for SIRT1 using surface plasmon resonance. (A) Sensorgrams of the binding response to C3 aptamer measured for concentrations of 12.5, 25, 50, 100, 200, 400 and 800 nM SIRT1. The $KD = 27.07$ nM as determined from a global fit of the kinetic simultaneous k_a/k_d model, assuming Langmuir (1:1) binding, and $\chi^2 = 0.959$, (B) Plot of the steady-state affinity for 'A' using the Req values derived from sensorgrams in (A) fitted locally.

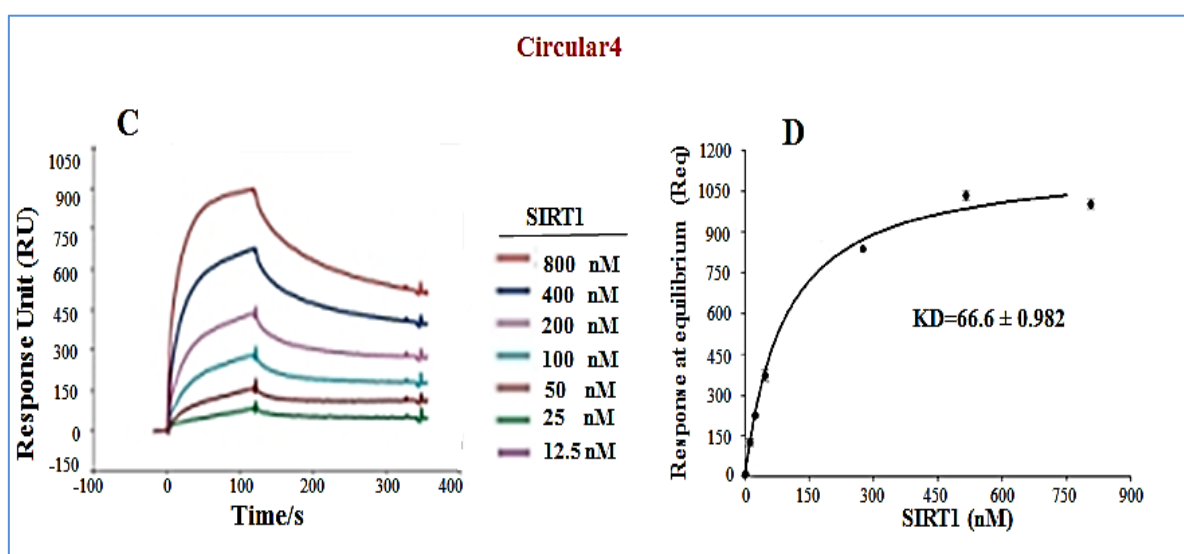


Figure 4.30: Determination of the affinities of aptamers for SIRT1 using surface plasmon resonance. (C) Sensorgrams of the binding response to C4 aptamer measured for concentrations of 12.5, 25, 50, 100, 200, 400 and 800 nM SIRT1. The $KD = 66.6$ nM as determined from a global fit of the kinetic simultaneous k_a/k_d model, assuming Langmuir (1:1) binding, and $\chi^2 = 0.982$, (D) Plot of the steady-state affinity for 'C' using the Req values derived from sensorgrams in (C) fitted locally.

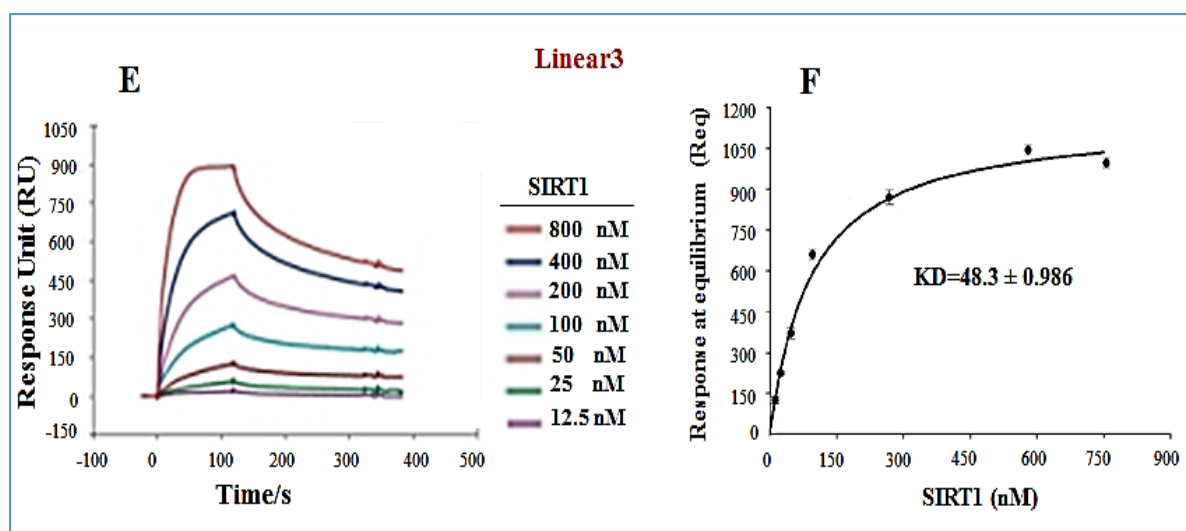


Figure 0.31: Determination of the affinities of aptamers for SIRT1 using surface plasmon resonance. (E) Sensorgrams of the binding response to L3 aptamer measured for concentrations of 12.5, 25, 50, 100, 200, 400 and 800 nM SIRT1. The $KD = 48.3$ nM as determined from a global fit of the kinetic simultaneous k_a/k_d model, assuming Langmuir (1:1) binding, and $\chi^2= 0.986$, (F) Plot of the steady-state affinity for 'E' using the Req values derived from sensorgrams in (E) fitted locally.

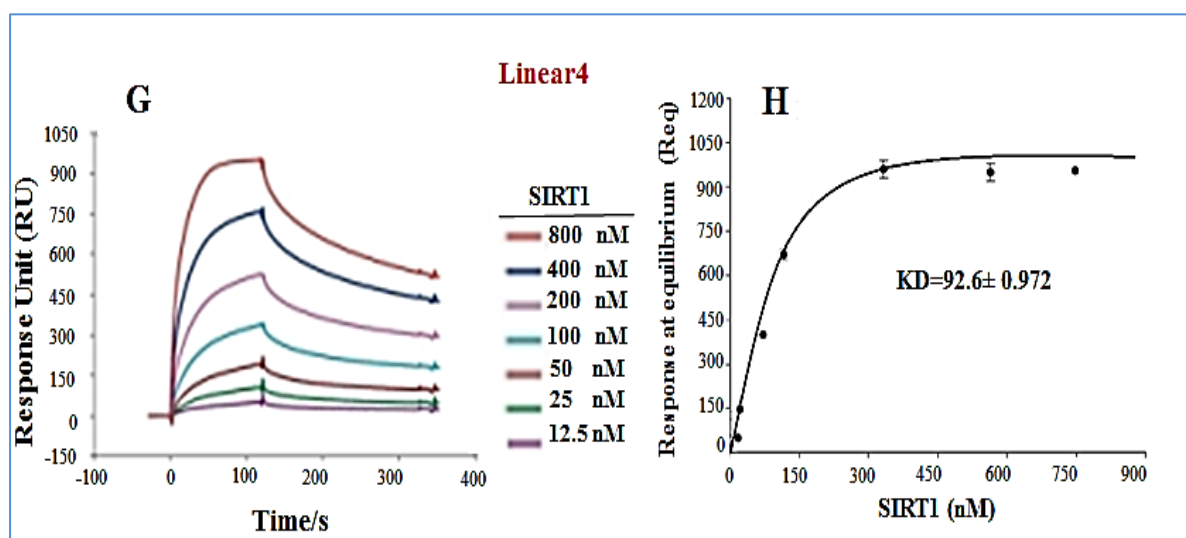


Figure 0.32: Determination of the affinities of aptamers for SIRT1 using surface plasmon resonance. (G) Sensorgrams of the binding response to L4 aptamer measured for concentrations of 12.5, 25, 50, 100, 200, 400 and 800 nM SIRT1. The $KD = 92.6$ nM as determined from a global fit of the kinetic simultaneous k_a/k_d model, assuming Langmuir (1:1) binding, and $\chi^2= 0.972$, (H) Plot of the steady-state affinity for 'G' using the Req values derived from sensorgrams in (G) fitted locally.

Table 0.6: Association binding parameters resulting from the analysis of the surface plasmon resonance data for the interaction between the selected aptamers and the SIRT1 enzyme.

Aptamers	K_a ($M^{-1} s^{-1}$)	K_a (s^{-1})	KD (nM) $\pm \chi^2$
Circular3	1.480×10^7	0.00401	27.07 ± 0.959
Circular4	0.237×10^7	0.00158	66.6 ± 0.982
Linear 3	0.480×10^7	0.00232	48.3 ± 0.986
Linear 4	0.340×10^7	0.0035	92.6 ± 0.972

4.3.4 Plasma Stability Assay of C3 Aptamer by Urea PAGE and HPLC

To test the stability of C3 aptamer in human plasma, stability assays were carried out by incubating the 1 μ M of C3 aptamer in human plasma for up to 24h by HPLC and urea PAGE methods in parallel. The incubation of C3 aptamer in human plasma by gel method only partial degradation was observed after four hours as shown in figure 4.33. Even after 24h of incubation, the aptamer could still be detected on the gel. However, HPLC method showed less degradation after 24h of incubation as showed in figure 4.34.

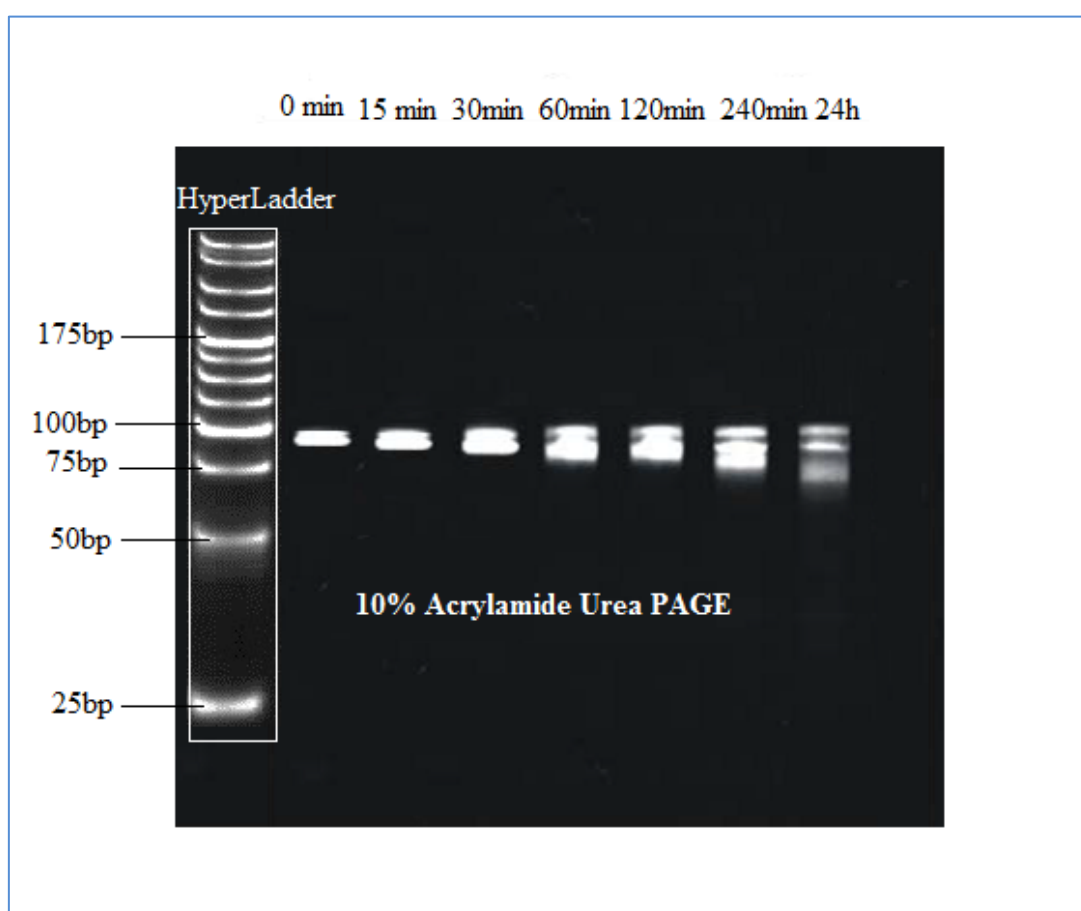


Figure 4.33: Stability of the circular3 aptamer in human plasma by 10% urea PAGE method. Aliquots were taken at the indicated times (0, 15, 30, 60, 120, 240 min and 24h). Lane1, HyperLadder 25bp; Lane2, the C3 aptamer band at 0 time; Lane3, the C3 aptamer band at 15 min; Lane4, the C3 aptamer band at 30 min; Lane5, the C3 aptamer band at 60 min; Lane6, the C3 aptamer band at 120 min; Lane7, the C3 aptamer band at 240 min; Lane8, the C3 aptamer band at 24h.

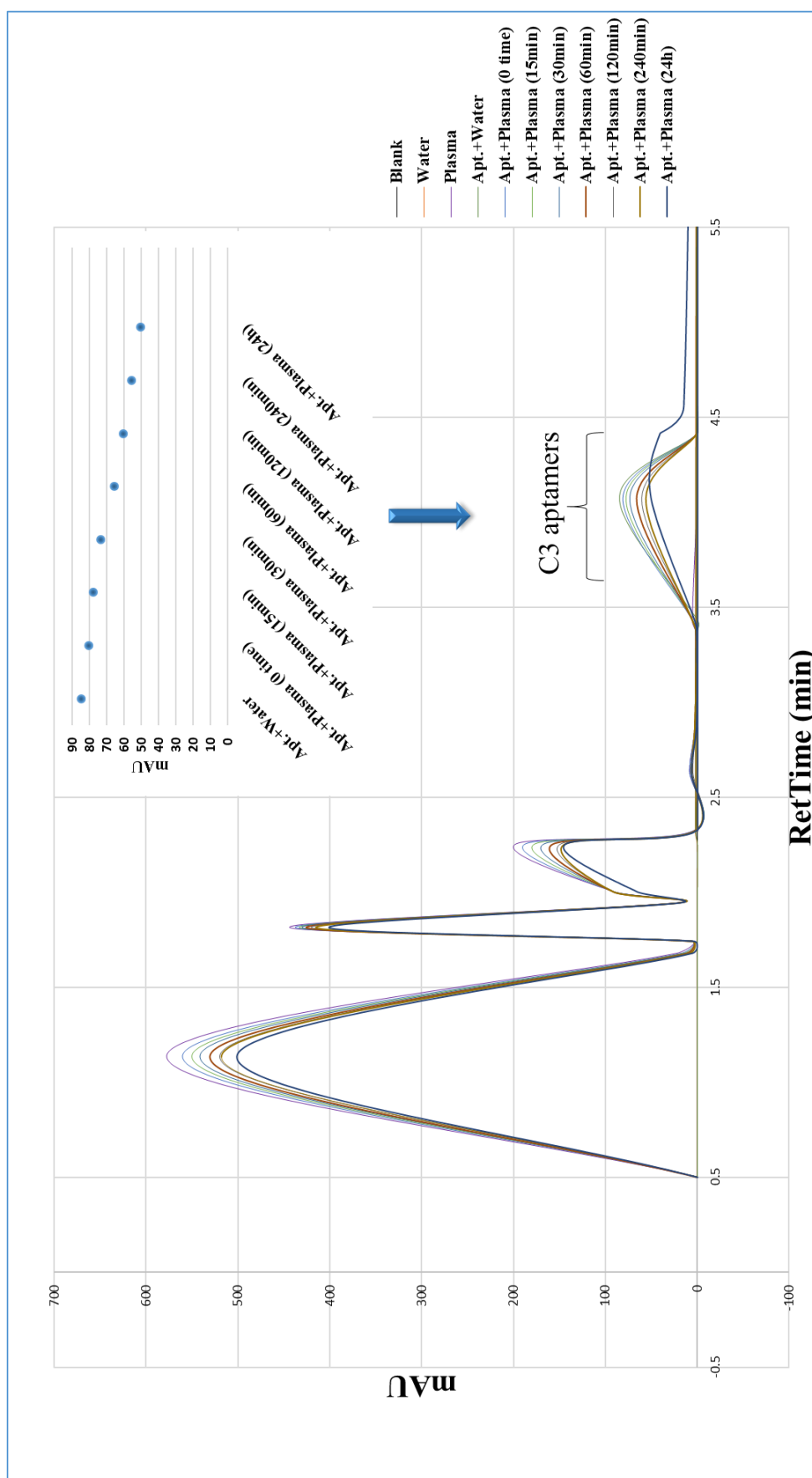


Figure 0.34: Stability of the circular3 aptamer in human plasma by HPLC-UV method. Aliquots were taken at the indicated times (0, 15, 30, 60, 120, 240 min and 24h) and compared with control (aptamer+water). The area from 0.5- 2.5 RT is plasma and the area from 3.5-4.5 RT is C3 aptamers.

The stability of the C3 aptamer when it was digested with endonuclease was much higher than of C3 aptamer without digestion in human plasma, which degrades after 24h in human plasma as shown in figure 4.35 and 4.36 in both methods.

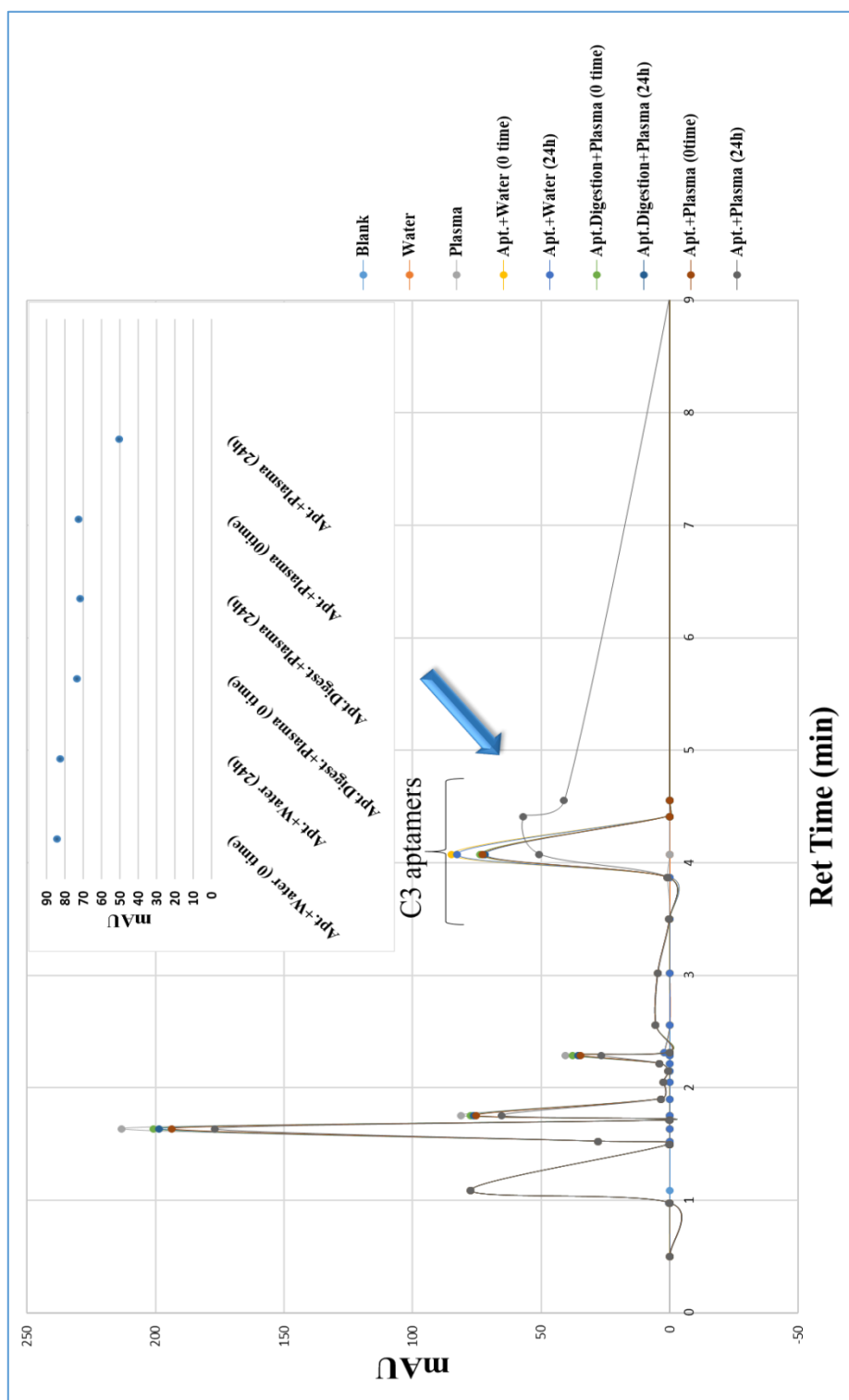


Figure 4.35: Stability of the circular3 aptamer (digested with endonuclease and without digestion) in human plasma by HPLC method. Aliquots were taken at the indicated times (0 and 24h) and compared with control (aptamer+water). The area from 0.5- 3.0 RT is plasma and the area from 3.5-4.5 RT is C3 aptamers.

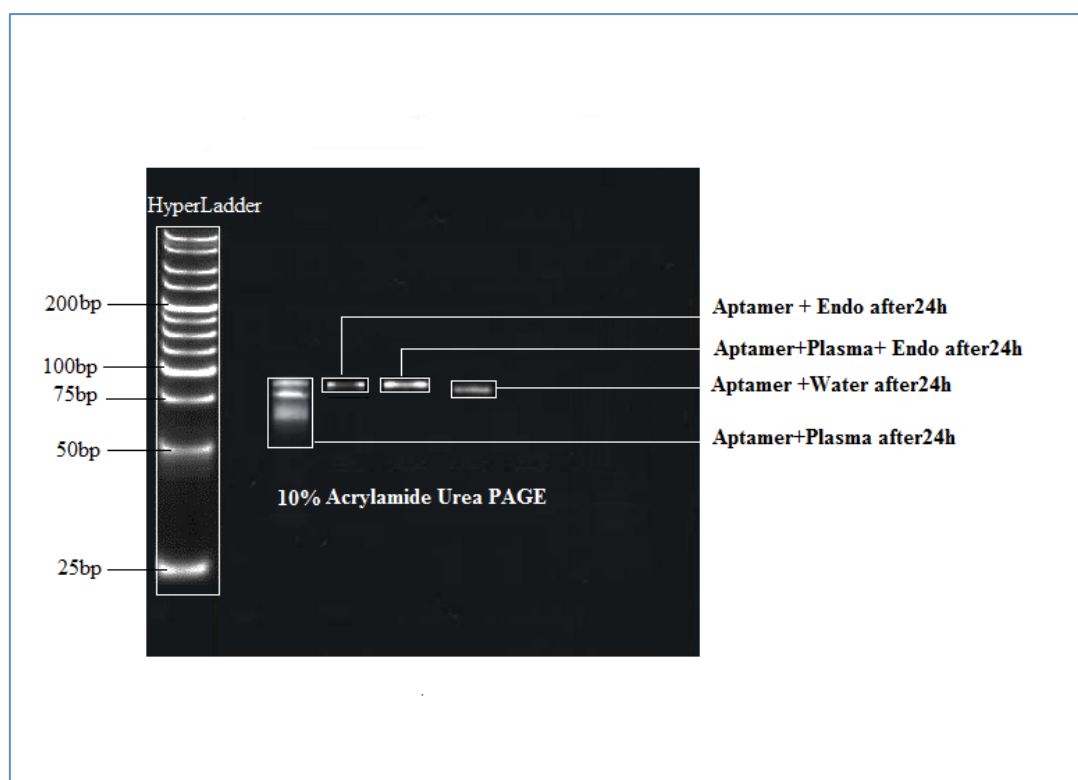


Figure 0.36: Stability of the circular C3 aptamer (digested with endonuclease and without digestion) in human plasma by 10% urea PAGE method. Aliquots were taken after 24h. Lane1, HyperLadder 25bp; Lane2, the C3 aptamer band with plasma after 24h; Lane3, the C3 aptamer band with Endo after 24h; Lane4, the C3 aptamer band at with plasma and Endo after 24h; Lane5, the C3 aptamer band with water after 24h (control).

To sum up, in this experiment to study the stability of C3 aptamer in plasma, two methods were used. The first one by urea-PAGE and the second one by HPLC, the results as demonstrates in figures 4.33-4.36 were showed that HPLC method is the best method and when the C3 aptamer was digested by the endonuclease, the degradation of aptamer was the less than the degradation without digestion.

4.4 Discussion

As the best-studied member of the Sirtuins family, SIRT1 is a 747-amino acid 83kDa (isoform a) class III (NAD⁺-dependent) (HDAC), a member of the Silent information regulator 2 (Sir2) protein family, SIRT1 influence a myriad of biological processes including inflammation, aging, metabolism, and oncogenesis (Zhao *et al.*, 2013). It is rising as an important therapeutic target for a number of age-associated diseases and possibly aging. While much attention has been focused on the identification of cellular targets of this Sirtuin, the network that regulates SIRT1 expression and activity has just begun to emerge (Kwon and Ott, 2008; Zschoering and Mahlknecht, 2008; Haigis *et al.*, 2010). Others recently shown that SIRT1 can be activated by small molecules like resveratrol which was discovered around 1999 (Howitz *et al.*, 2003). Resveratrol (trans-3, 5, 4'-trihydroxystilbene) is a polyphenolic compound that is synthesised in grapes, berries, peanuts and plants to respond to ecological strain and pathogenic infection (Gescher and Steward, 2003; Das *et al.*, 2008). This natural compound has been of great interest to many because of its cardiovascular benefits due to its presence in red wine. In addition, numerous cell culture studies have revealed its potential health benefits such as: anti-aging, anti-oxidative, anti-diabetic, anti-inflammatory, anti-obesity, neuroprotective and cardio-protective activities (Gescher and Steward, 2003; He *et al.*, 2006; Das *et al.*, 2008). Previous studies have shown resveratrol to also have pharmacological activities as a chemopreventive agent (Gescher and Steward, 2003; He *et al.*, 2006; Das *et al.*, 2008). It has been demonstrated several cellular mechanisms to prevent tumour initiation, promotion and development in the process of carcinogenesis (Delmas *et al.*, 2006). Although this dietary compound seems promising, studies revealed the pharmacokinetic parameters do not show the same advantages as its pharmacological activities (Das *et al.*, 2008). Previous studies suggest that high dose of resveratrol is not sufficient for systemic levels of chemoprevention suggesting that resveratrol undergoes significant biotransformation via conjugation pathways (Boocock *et al.*, 2007). However, other mechanisms such as rapid degradation in plasma, high binding to tissues or low binding to the plasma could occur. Therefore, it is still unclear of the degradation kinetics of resveratrol in biological medium (Robinson *et al.*, 2015), they observed that resveratrol is unstable in human and rat plasma samples at 37 °C up to 96h. Because of the results of these previous studies which did not reach to stable activating SIRT1 compounds, this study was focused on aptamers, which are nucleic acid ligands that can bind with SIRT1 enzyme. DNA aptamers are easily and inexpensively synthesised and modified. Several cases in which aptamers were applied instead of antibodies

have already been reported (Ikebukuro *et al.*, 2005; Murphy *et al.*, 2003), and it has been demonstrated that aptamers can be used as molecular recognition elements. Moreover, aptamers are single-strand DNAs or RNAs, and therefore, it is easy to design the way their structure changes; signal-generating molecules, which acquire their properties because of such changes, work like molecular beacons (Tyagi and Kramer, 1996). Recently, some designed aptamers that generate signals as a result of structural changes caused by their binding to their target molecules have been reported (Nutiu and Li, 2003; Stojanovic and Kolpashchikov, 2004). Such structural changes have also been applied to allosteric ribozymes (Piganeau *et al.*, 2001) and allosteric DNA enzymes (Liu and Lu, 2004).

In our studies, the activity of SIRT1 as assessed with our developed aptamers. Assays for enzymatic activities are based on the detection of consumption of substrates or formation of products. In the case of SIRT1, many assays have been developed by directly or indirectly tracking the consumption of acylated peptides, the formation of deacylated peptides, the release of nicotinamide. They are divided into two categories: one is called “label-free” approaches, which use detection of substrate and product peptides; the other is called “labeled” approaches, which involve a coupled two-step enzymatic assays to detect the formation of products. There are several methods to measure the activity of SIRT1 *in vitro*. These include fluorescence (Bitterman *et al.*, 2002; Marcotte *et al.*, 2004; Wegener *et al.*, 2003; Feng *et al.*, 2009), time-resolved fluorescence, chemiluminescence (Liu *et al.*, 2008), microfluidic mobility shift (Liu *et al.*, 2008), fluorescence polarisation (Milne *et al.*, 2007), mass spectrometry (Milne *et al.*, 2007; Pye *et al.*, 2011), capillary electrophoresis (Fan *et al.*, 2011), high-performance liquid chromatography (HPLC) (Jackson *et al.*, 2002) and radioactive formats (Grozinger *et al.*, 2001; Bedalov *et al.*, 2001; Borra and Denu, 2004). In terms of a high-throughput format, among the reported assay, the fluorescence-based assays should be the best one, which is easily miniaturised and automated (Borra and Denu, 2004; Li *et al.*, 2015). Fluor de lys fluorescent assay is one of the fluorescence-based assay which uses a small lysine-acetylated peptide, corresponding to K382 of human p53, as a substrate. The first SIRT1 activators identified with this assay were polyphenolic plant-derived compounds: resveratrol, butein, quercetin, piceatannol, and myricetin (Howitz *et al.*, 2003 and de Boer *et al.*, 2006).

Subsequently, more potent SIRT1's activators were reported as potential therapeutics for the treatment of diabetes (e.g. SRIT1720, SRT2183, and SRIT1460) (Milne *et al.*, 2007; Venkatasubramanian *et al.*, 2016), using a fluorescently labelled substrate in a fluorescence polarisation assay. It was realised quickly that SIRT1 biochemical activation by resveratrol

could only be demonstrated when the substrate was fluorescently tagged (Borra *et al.*, 2005; Kaerberlein *et al.*, 2005 and Pacholec *et al.*, 2010). Using a variety of nonfluorometric assay formats, it was found that these four compounds (resveratrol, SRIT1720, SRIT2183, and SRIT1460) did not directly activate SIRT1 when using native peptide or protein substrates (Pacholec *et al.*, 2010 and Huber *et al.*, 2010). Furthermore, SRIT1720 and SRIT2183 decreased acetylated p53 levels in SIRT1-deficient (siRNA) and null (SIRT^{-/-} MEFs) cells', again suggesting SIRT1 was not the direct target. One unconfirmed report claimed that SRT1720 and SRT2183, but not resveratrol, were p300 HAT inhibitors, accounting for their cellular effect on p53 acetylation in the absence of enzymatic modulation (Huber *et al.*, 2010). The selectivity of piceatannol for SIRT1 is also questionable as it inhibits tyrosine kinases such as Lck154 and mitochondrial ATP synthase (as do other polyphenols) (Dadi *et al.*, 2009). It is evident that more highly selective SIRT1 activators, which show correlative activity in both enzymatic and cellular SIRT1-dependent assays, are still needed to understand SIRT1 biology and therapeutic potential.

As mentioned above, the mechanism of SIRT1 activation was examined using selected circular and linear aptamers (linear1, linear2, linear3, linear4, circular1, circular2, circular3, circular4, circular5 and circular6) by using the commercially available Fluor de Lys-SIRT1 assay and compared the activity of SIRT1 enzyme-aptamers with the activators and inhibitors controls of SIRT1 enzyme (resveratrol, suramin and nicotinamide). Comparison of the rate of fluorescence increase in the presence 800 nM C3 aptamer showed that C3 aptamers activated SIRT1 enzyme more than the activated of SIRT1 by 200000 nM resveratrol and the activity of SIRT1 enzyme with 800 nM L3, 800 nM L4 and 300 nM C4 aptamers are increased nearly the level of SIRT1enzyme with resveratrol at a concentration 200000 nM as shown in figure 4.4. From the competition study, it is evident that C3, C4, L3 and L4 aptamers were significantly increased the activity of SIRT1 enzyme compared with the activators controls of SIRT1 enzyme with the low K_d constant (22.6 ± 4.9 , 7.1 ± 1.9 , 20.9 ± 3.7 and 3.5 ± 1.11 nM respectively) as shown in table 4.2 and figures 4.8, 4.9, 4.14 and 4.15. This study revealed that activation of SIRT1 by aptamers is strongly dependent on structural features of the aptamers. Rather, the data suggest that these four novel aptamers interact directly with SIRT1 enzyme and activate SIRT1-catalysed deacetylation through an allosteric mechanism. Furthermore, enzyme kinetic studies of SIRT1 with aptamers were examined through the values of K_m and V_{max} compared to kinetic of SIRT1 enzyme with resveratrol. Consequently, this new design of aptamers by immobilising ssDNA and SIRT1 enzyme showed great selectivity ligands against

SIRT1. The enzyme kinetics constants for SIRT1 enzyme with C3, C4, L3 and L4 are shown in tables 4.3-4.6 compared to those with resveratrol indicated that higher enzyme kinetic efficiency of SIRT1 with aptamers than resveratrol, for example, the K_m of SIRT1 enzyme with C3 at 5, 15, 30 and 45min are 0.000486, 0.000437, 0.00041 and 0.000267 nM respectively compared to the K_m of SIRT1 enzyme with resveratrol (0.002 nM) exhibited an 8-fold higher affinity to resveratrol. The decrease in the K_m values of immobilised SIRT1 enzymes is due to electrostatic attraction of hydrophobic adsorption of the aptamers to the solid it might lead to the presence of areas of increased aptamers concentration around the particle. The obtained maximum velocity V_{max} of the reaction catalysed by SIRT1 with C3 at 5, 15, 30 and 45min were 0.54, 0.24, 0.15 and 0.1 nM respectively, which is 3% in comparison to resveratrol catalysis (0.25 nM). From a reaction rate point of view, the maximal velocity of substrate change was calculated as a remaining amount of aptamer from SIRT1 digestion per minute. The high rate of enzyme reaction and catalytic efficiency of SIRT1 enzyme could be due to enough diffusion of aptamers molecules to the surface of the particles and to the active sites of the immobilised enzyme.

The Surface plasmon resonance (SPR) assay proved to be suitable for aptamer characterisation. Utilising this method, four acceptable aptamers C3, C4, L3 and L4 were examined, the sensor surface was build up by immobilisation of aptamers, for example (C3, C4, L3 or L4) on the sensor chip, and a concentration series of SIRT1 in the range of 12.5, 25, 50, 100, 200, 400 and 800nM was injected. An aptamer level of 1000–1200 RU on the sensor surface was adjusted in this experiment over the injection time during the immobilisation of the aptamer. The sensorgrams in figures 4.29A, 4.30C, 4.31E and 4.32G reveal a very tightly and stable binding behaviour of SIRT1 enzyme to the immobilised aptamers C3, C4, L3 and L4 respectively. Figures 4.29B, 4.30D, 4.31F and 4.32H show the corresponding saturation curves derived from the binding data at the end of the binding phases. Based on this, dissociation constants in the low nanomolar range were calculated: C3 aptamer was the best binder with an apparent $KD = 27.07 \pm 0.959$ nM. C4, L3 and L4 were following C3 with 66.6 ± 0.982 nM, 48.3 ± 0.986 nM and 92.6 ± 0.972 nM of KD respectively. The SPR data have confirmed the high affinity of the aptamers for the SIRT1 enzyme, with KD values in the nanomolar range. This is in good agreement with KD values obtained for aptamers against other targets. Such examples include the DNA aptamers to thrombin with $KD= 25\text{--}200$ nmol/l (Bock *et al.*, 1992; Griffin *et al.*; 1993), RNA aptamer to PSMA with $KD=2$ nmol/l (Lupold *et*

al., 2002), RNA aptamer to tenascin C with $KD=5$ nmol/l (Hicke *et al.*, 2001) and RNA aptamer to *Trypanosoma cruzi* cell surface receptor with $KD=172$ nmol/l (Ulrich *et al.*, 2002). After equilibrium binding characterisation study of both Linear and Circular aptamers by SPR, it has been found that circular³ and linear³ aptamers are a good binder to SIRT1 enzyme, with the ability to bind selectively and with high affinity to SIRT1 target. Because circular aptamers are more stable than linear, C3 aptamer was characterised for nuclease degradation by blood and was found to be stable, with less indication of degradation for 24h, as deemed by HPLC and gel electrophoresis as shown in figures 4.33-4.36. Previous studies already showed the stability of the modified aptamers in serum up to 12h (Borbas *et al.*, 2007). This significant human plasma stability of the C3 aptamer can be attributed to circularisation structure, which made the aptamer less susceptible to nuclease degradation in human plasma. Circularisation of aptamers is an attractive alternative to chemical modification for improving aptamer stability. With the majority of nucleic acid degradation activity arising from plasma exonucleases (Shaw *et al.*, 1995), modification of exposed termini often achieves a sufficient improvement in stability for use *in vivo* (Kurreck, 2003), and circular constructs eliminate this primary source of degradation entirely. Moreover, circularisation permits the use of natural nucleotides, which should avoid potential toxicity associated with chemical modification.

Overall, it was concluded that the four novel aptamers generated by SELEX procedure (C3, C4, L3 and L4) have high affinity and selectivity ligands against SIRT1 enzyme, based on the observed results of these aptamers in characterisation and kinetic study. These results suggest that C3 aptamer may well be an appropriate candidate for the development of biotherapy because it is achieved a higher affinity binding with SIRT1 enzyme ($KD = 27.07 \pm 0.959$ nM) and more stable than linear.

5 APTAMERS AS THERAPEUTICS

5.1 Introduction

Cancer is the second leading cause of age-related mortality in humans, therefore the ability to suppress carcinogenesis has attracted the widespread attention of cancer prevention and treatment researchers. Traditional cancer treatment approaches, such as chemotherapy, radiotherapy, photodynamic therapy, and photothermic therapy can cause serious side effects in patients due to their associated nonspecific toxicity. To counter or reduce the adverse side effects of anti-cancer drugs used in chemotherapy, much attention has been devoted to the development of targeted drug therapy in recent years. Targeted drug therapy is achieved through drug with inherent targeting properties or modification of the drug molecule with a ligand that can selectively recognise its target. Some problems frequently encountered in targeted drug therapy include stability of the targeting ligand, decrease in targeting efficacy of the ligand, and decrease in drug efficacy in cell killing or growth retardation after ligand modification. Recent clinical approaches for targeted cancer therapy employs antibody-predicated drugs. Although antibody-mediated therapy is highly selective, potential immunogenicity and high costs may limit its clinical applications. Oligonucleotide aptamer-predicated targeted therapeutics and categorical drug delivery systems have recently been explored, for example of cancer treatment AS1411 aptamer as discussed in section 1.9.4 chapter one.

In the present study, high-affinity circular and linear ssDNA aptamers binding to SIRT1 enzyme have been successfully selected as described in chapter 3. The high-affinity SIRT1-aptamers identified in this study may be used in the future to the cancer treatment as SIRT1 enzyme is a novel target and comes with the challenge of discovering molecules that are activators rather than inhibitors and would be developed as first-in-class cancer therapeutics.

The SIRT1 deacetylase activity towards p53 has been associated to a specific function in tumour promotion in the involved proteins, studies have been conducted on different aspects such as (i) expression studies in tumours, (ii) manipulation of SIRT1 levels in animals, and (iii) pharmacological approaches, have challenged this hypothesis, leading to the opposite view that SIRT1 may function as a tumour suppressor. The mechanism of activated SIRT1 triggering cell death, is explained by the researchers by demonstrating that SIRT1 negatively regulates expression of Survivin, which is responsible for encoding an anti-apoptotic protein, by

deacetylating H3K9 within the promoter of Survivin (Wang *et al.*, 2008). Conclusively, it can be established that SIRT1 mediates BRCA1 signalling and inhibits tumour growth by the suppression of transcription of oncogenes or activity of oncoproteins (figure 5.1).

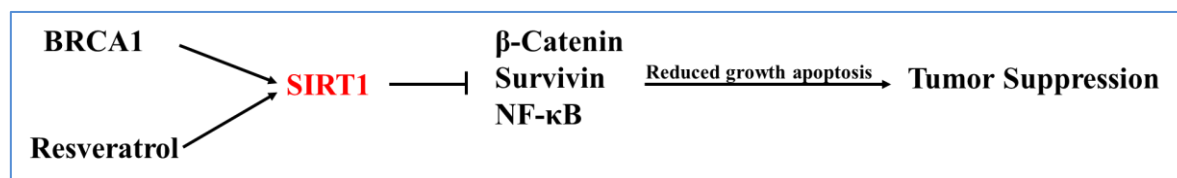


Figure 0.1: Models illustrating possible functions of SIRT1 in tumour suppression. BRCA1 and Resveratrol can positively regulate SIRT1 transcription and activity, respectively. Increased SIRT1, in turn, inhibits expression and/or activity of several oncogenes, leading to reduced cell proliferation, increased apoptosis, and tumour suppression (Adapted from Deng, 2009).

Considering previously conducted studies, the effect of small molecular compounds increases the activity of SIRT1, which could be a potential molecular therapy target for cancer cells. As longterm treatment with resveratrol or selective SIRT1 activators have not been associated with the incidence of tumours in animals. Resveratrol is used for treatment of multiple indications and is known to have multiple pharmacological effects of resveratrol in different model systems. However, the concentrations, needed for attaining pharmacological effects, are very high and this has urged the researchers to look for more potent SIRT1 activating compounds. The high throughput screening of oligonucleotide targeted therapeutics has helped identify four novel aptamers which can activate the SIRT1 enzyme, circular3, circular4, linear3 and linear4, these aptamers, however, are structurally unrelated to resveratrol on the basis that they are ssDNA and have a higher potency for activation of the SIRT1 enzyme. In this study, the impact of different on aptamers given for aiding SIRT1 on the growth of several cancer cell lines and normal cell lines have been carried out by using the colorimetric assay tetrazolium salt thiazolyl blue, also known as MTT.

A panel of cell lines were used in this study: colorectal adenocarcinoma (Caco-2), human adenocarcinoma of alveolar basal epithelial cells (A549), breast cancer cell lines oestrogen positive and model for majority of breast cancers (MCF-7), breast cancer oestrogen negative (MDA-MB-468), children liver hepatocellular carcinoma (HepG2), children human bone osteosarcoma (U2OS), adult human keratinocyte (HaCaT) and normal human bronchial epithelial cells (Beas-2b). The selection of these types of cell lines have been based on the expression data of SIRT1 in cells that comes from the Genomics Institute of the Novartis

Research Institute (<https://proteomescout.wustl.edu/proteins/74160/expression>) which also proved by other studies.

5.1.1 Background to the Cell Lines and Expression of SIRT1

In human colorectal cancer (CRC) and in CRC cell lines the SIRT1 expression was observed to be heterogeneous (Pazienza *et al.*, 2012). The mean SIRT1 expression levels were decreased in patients with CRC. The levels of SIRT1 appeared to be lower in Caco-2 cells (a type of colorectal cancer cells) (Pazienza *et al.* 2012). This type of cells has been employed as a model of down-expression of SIRT1 enzyme in CRC cancer cell line. Caco-2 cells are a human intestinal cell line present in human colon adenocarcinoma and are extensively used as an *in vitro* model to study the permeability of intestinal epithelium particularly for carrying out the analysis of intestinal absorption and metabolism of drugs under different conditions. Additionally, it is also useful in carrying out experiments of regulation and expression of intestinal genes. The *in vitro* culture of Caco-2 cells, produce a merging monolayer then immediately differentiate in different layers, and further changes in their morphology over time. Differentiated cells appear similar to the phenotype of epithelial cells in the small intestine and columnar and polarised cellular layers are formed. Additionally, these cells produce microvilli on the apical membrane and tight junctions between cells and expression of tissue-specific genes, digestive enzymes, and nutrient transport are their chief characteristic which makes them a popular choice among *in vitro* model (Lea, 2015).

According to the overexpression of SIRT1, Grbesa *et al.*, (2015) evaluated the expression of SIRT1 in human non-small cell lung cancer cell lines (A549) and they found that SIRT1 protein levels were clearly higher in these cancer cell lines than in immortalised epithelial cells. Therefore, it has been using this type of cells as a model of overexpression of SIRT1 enzyme in cancer cell line. Adenocarcinomic human alveolar basal epithelial cells are also known as A549. D. J. Giard *et al.*, (1973) was the one to develop the A549 cell line, he did so by removing and culturing cancerous lung tissue in the explanted tumour of a 58-year-old Caucasian male (Giard *et al.*, 1973; Jiang *et al.*, 2010). A549 cells are squamous cells which carry out the diffusion of some substances such as water and electrolytes across the alveoli of lungs. In *in vitro* cultures, the A549 cells grow as monolayer cells, adherent or attached to the culture flask (Giard *et al.*, 1973). Under specific conditions large number of cells can be obtained and controlled (Ramage, 2003). They are easy to grow, the cell counts become twice as much within

48 hours of cultivation (Giard *et al.*, 1973). A549 cells are not only used as a model in the research of lung epithelial structure and the occurrence, development and treatment of lung cancer, Jiang *et al.*, (2010), reports them to be a useful in studying promoter activity, apoptosis, and alveolar epithelial cell DNA damage (Kasai *et al.*, 2005). These cells can synthesise lecithin and are rich in unsaturated fatty acids, which are essential for the membrane phospholipids in cells. Another use of A549 cell lines is as an *in vitro* model for a type II pulmonary epithelial cell model for drug metabolism and as a host for transfection.

Zhang *et al.*, (2009) and Kuzmichev *et al.*, (2015) carried out studies which showed increased expression of SIRT1 in breast cancer. Literature supporting different arguments about the role of activation SIRT1 in breast cancer is available such as some researchers believe that it acts as an oncogene while there are others who believe it is a tumour suppressing agent. These contraindications are mostly considering the regulation of steroid hormone receptor signalling. Zhang *et al.*, (2016) reported in their study that overexpression of BRCA1 inhibits the expression of Androgen Receptor (AR) by activating the SIRT1 by resveratrol in breast cancer cells such as MCF-7 cell line and it is also deduced that BRCA1 weakens the AR-stimulated proliferation of breast cancer cells through the SIRT1 mediated pathway. For studying the effect of activation SIRT1 by aptamers for proliferation of breast cancer cell line, for this study (MCF-7) breast cancer cell line oestrogen positive were studied. MCF-7 was isolated in 1970 from the breast tissue of a 69-year old Caucasian woman for the first time (Soule *et al.*, 1973). MCF-7 cells retain many characteristics to the mammary epithelium and hence are useful for *in vitro* breast cancer studies. These mammary characters include the ability for MCF-7 cells to process estrogen, in the form of estradiol, via oestrogen receptors present in the cell cytoplasm. This means the MCF-7 cell line can be used as a positive control of oestrogen receptor (ER) (Huguet *et al.*, 1994). Additionally, MCF-7 cells show sensitivity towards cytokeratin. They do not respond to desmin, endothelin, GAP, and vimentin. In *in vitro* cultures, the cell line can form domes and their epithelial cells grow in form of monolayers. The tumour necrosis factor alpha (TNF alpha) can be used to inhibit the growth, and treatment of MCF-7 cancer cells with anti-oestrogen agents can imitate insulin-like growth factor binding protein's, which consequently cause the mitigation of cell growth (Lacroix *et al.*, 2006).

MDA-MB-468 cells are also used as model for breast cancer cells but these are oestrogen negative (Kim *et al.*, 2009). The expression of SIRT1 is higher in comparison to any other breast cancer cells. The pleural effusion of mammary gland/breast tissue was used for

extraction of this type of breast cancer cell line and is employed as a model of breast cancer cell line oestrogen negative.

In a study by Portmann *et al.*, (2013) a panel of hepatocellular cancer (HCC) cancer cell lines (Hep3B, HepG2, HuH7, HLE, HLF, HepKK1, skHep1) were screened to assess the expression of the SIRT1, the results were consistently overexpressed SIRT1 in comparison to other normal hepatocytes. Hao *et al.*, (2014) conducted another study to investigate the SIRT1 expression in hepatocellular carcinoma (HCC) and they found the SIRT1 were substantially overexpressed in the tumour tissues and HCC cell lines (HepG2, Huh7, Hep3B, and SMMC-7721). Additionally, the effect of resveratrol (50 μ mol/L) was measured on the basis of cell viability and apoptosis of HCC cells (HepG2 and SMMC-7721). The results showed that resveratrol is slightly effective in inhibiting the cell viability and enhancing apoptosis. Therefore, the authors selected HepG2 cell line for evaluating the effect of SIRT1 aptamers. HepG2 is a human liver cancer cell line. Morphologically they are cells and have modal chromosome number of 55, and do not cause tumours in nude mice. HepG2 cells can be used as *in vitro* model system for the study of polarised human hepatocytes (Ihrke *et al.*, 1993). Under specific culture conditions, HepG2 cells display robust morphological and functional differentiation and a manageable formation of apical and basolateral cell surface domains (van IJzendoorn *et al.*, 1997) which is similar to the bile canalicular (BC) and sinusoidal domains in appearance *in vivo*. HepG2 cells can be used as a model to study the intracellular trafficking and dynamics of bile canalicular and sinusoidal membrane proteins and lipids in human hepatocytes *in vitro* owing to their high degree of morphological and functional differentiation *in vitro*. This can prove significant in studying human liver diseases that are caused by improper subcellular distribution of cell surface proteins, e.g., hepatocanalicular transport defects for example Dubin-Johnson Syndrome and progressive familial intrahepatic cholestasis (PFIC), and familial hypercholesterolemia. HepG2 cells and their derivatives have been found useful for studying the liver metabolism and toxicity of xenobiotics, the detection of environmental and dietary cytotoxic and genotoxic (including cryoprotective, anti-genotoxic, and cogenotoxic) agents (Mersch-Sundermann *et al.*, 2004), they can be used in understanding hepatocarcinogenetic, and in drug targeting studies. HepG2 cells are also used in trials with bio-artificial liver devices.

U2OS cell line can also be used as an example of the cells that cause SIRT1 overexpression. Human osteosarcoma (U2OS) cell line is a primary malignant tumour of the skeletal cells and bone prevalent in children and young adults of ages 15-29 years and in geriatrics 60 years of

age and above. It is the 6th most prevalent cancer among children and the occurrence is reported during pre-teen and teen years of life in the adolescent growth period, with a high incidence in adolescent boys who are experiencing puberty (Niforou *et al.*, 2008). The cause of osteosarcoma is still a mystery; however, irradiation, genetic influences and rapid bone growth are considered to be contributing factors. The U2OS cell line is a popular research model in biomedical research such as biochemistry, molecular biology, bone formation, arthritis (Bartkova *et al.*, 2006; Furuya *et al.*, 2007). The human osteosarcoma U2OS cell line was first isolated in 1964 from a relatively differentiated sarcoma of the tibia of a 15-year-old girl. It was among the first generated cell lines and is still used commonly. Chromosomal instability, structural rearrangements and alterations and high incidence of aneuploidy was observed in spectral karyotyping analysis and cytogenetic analysis (Bayani *et al.*, 2003). Near-triploidy state of U2OS cells appeared on the spectral analysis, which is caused by both tetraploidisation and chromosomal losses. The SIRT1 expression in U2OS cell line was analysed and the results showed that there is extensive SIRT1 overexpression in this type of cells (Oberdoerffer *et al.* 2008). Because the characterisation of this cell is crucial to the study of biochemistry, it is used as a model for cells in this study where SIRT1 is overexpression.

Park and Lee, (2007) explained how resveratrol (activator SIRT1) may be used as a potential photochemoprotective agent against UVB-induced skin damage by used HaCaT cells. HaCaT is an aneuploid immortal keratinocyte cell line, which becomes transformed on its own from adult human skin (Boukamp *et al.*, 1988), and had wide application in scientific research (Schoop *et al.*, 1999). The high capacity of HaCaT cells to differentiate and proliferate *in vitro* has made them a popular research model (Schurer *et al.*, 1993). The human keratinocyte can be characterised by the use of this model because it is reproducible and does not limitise the research with problems such as short culture lifespan and variations between cell lines, which are a common issue in other models. Many processes (like Vitamin D3 metabolism in the skin) can be characterised using this cell line as a model (Lehmann *et al.*, 1997). The effects of SIRT1 aptamers on tissue organisation and keratinisation *in vitro* can be studied efficiently using the HaCaT cells.

In this study, Beas-2b cells are employed for the investigation of the effects of SIRT1 aptamers on normal cell line. Beas-2b cells are human bronchial epithelium normal cells, which were developed by using normal human bronchial epithelial cells obtained from autopsy of non-cancerous individuals, AD12-SV40 virus was employed for this extraction (Reddel *et al.*, 1988; Stewart *et al.*, 2012). Squamous differentiates upon exposure to the serum. This trait can

be employed in screening of chemical and biological agents inducing or affecting tumourigenesis and/or differentiation. The cell line has also been used to investigate the pneumococcal infection mechanisms.

In summary, the aim of this chapter was to establish the therapeutic effect of the activator SIRT1 aptamers as a pharmacological model for cancer treatment with the objectives of: [i] evaluating the effect of activators SIRT1 (aptamers) on the growth of a series of human cancer cell lines (Caco-2, A549, HepG2, MCF-7, MDA-MB-468, U2OS, HaCaT and Beas-2b); [ii] investigating the activity of SIRT1 in these cancer cells; [iii] measuring the Reactive Oxygen Species (ROS) production in these cancer cell lines after treated with aptamers; [iv] determining the IC₅₀ for C3 aptamer of these cells and [v] detecting the location and pathway of C3 aptamer by using fluorescence microscopy.

5.2 Methods

All methods were described in chapter 2, the measurement of cell viability in section 2.2.6.3, ROS production in section 2.2.6.4, SIRT1 activity in section 2.2.6.5, IC₅₀ in section 2.2.6.6 and imaging of C3 aptamer by immunofluorescence microscopy in section 2.2.6.7 in eight cell lines (A549, HepG2, MCF-7, MDA-MB-468, U2OS, Caco-2, HaCaT, and Beas-2b).

5.3 Results

The results of all the experiments in this study are representing the results of three independent experiments. The concentration of aptamers in cell viability experiments and ROS assay are 2.5 μ M because this concentration is the best one after doing the optimisation experiments to choose the best concentration between 1-4 μ M of C3, C4, L3 and L4 aptamers.

5.3.1 Effect of Linear3, Linear4, Circular3 and Circular4 Aptamers on 8 Cells Viability by MTT Assay

5.3.1.1 Human Adenocarcinoma of Alveolar Basal Epithelial Cells (A549)

A549 cells were pre-treated with L3, L4, C3 and C4 aptamers at concentrations 2.5 μM for 24, 48 and 72h to determine the effect of aptamers on A549 cell viability. L3, L4, C3 and C4 aptamers were decreased significantly the cell viability at 2.5 μM , $p < 0.005$, 0.001 and 0.00005 at 24, 48 and 72h respectively as shown in figure 5.2. To compare between aptamers group (L3, L4, C3 and C4), the results were established that C3 aptamer is significantly reduced A549 cells viability than L3, L4 and C4 aptamers ($p < 0.0001$).

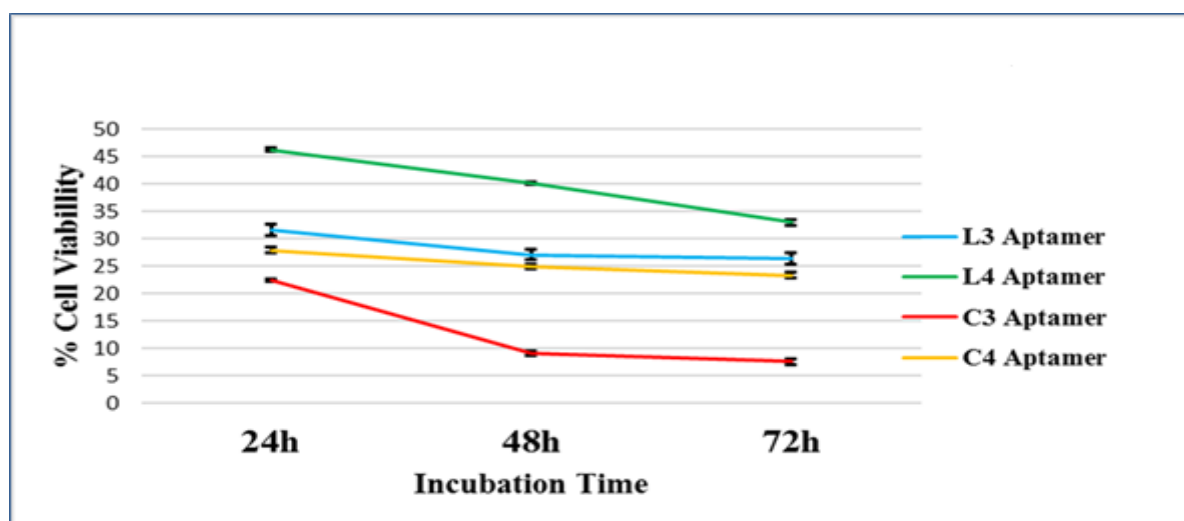


Figure 0.2: *In vitro* cell viability of the human adenocarcinoma of alveolar basal epithelial (A549) cells was detected by MTT assay. The results of A549 cells post 24, 48 and 72h treatment of 2.5 μM (L3, L4, C3 and C4) aptamers. The absorbance was measured at 540 nm (reference wavelength 650 nm) using a microplate reader. The results represent the mean \pm SEM of 3 independent experiments. Aptamers have a strong inhibition ability for A549 cells. $p < 0.005$, 0.001 and 0.00005 at 24, 48 and 72h respectively vs. control.

To investigate the protection upon challenging with 50 μM TBHP (Tert-Butyl Hydrogen Peroxide: it is the oxidative processes), cells were treated with 50 μM TBHP and showed a reduction of 19% in cell viability after 24h compared to untreated cells (control); however, the difference was not statistically significant. The reduction in cell viability became more pronounced after treated with 2.5 μM aptamers and 50 μM TBHP compared with the cells which pre-treated with 2.5 μM aptamer only (figures 5.3-5.6).

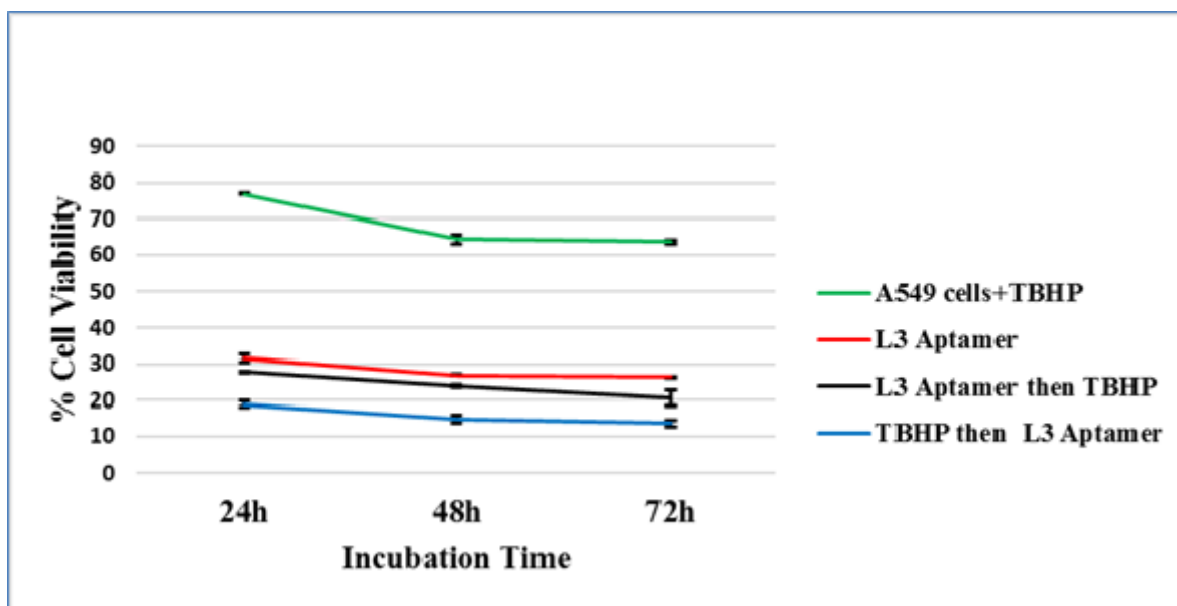


Figure 5.3: *In vitro* cell viability of the human adenocarcinoma of alveolar basal epithelial (A549) cells was detected by MTT assay. The results of A549 cells post 24, 48 and 72h treatment with 2.5 μM L3 aptamer also exposure to 50 μM TBHP. The absorbance was measured at 540 nm (reference wavelength 650 nm) using a microplate reader. The results represent the mean \pm SEM of 3 independent experiments. $p < 0.001$ vs. control.

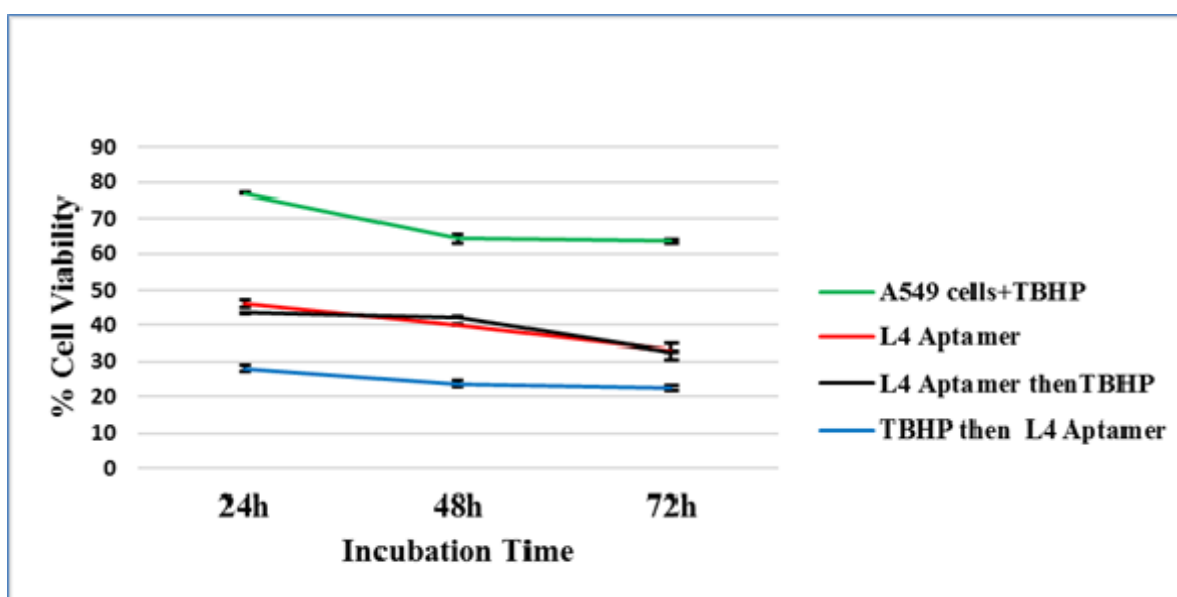


Figure 5.4: *In vitro* cell viability of the human adenocarcinoma of alveolar basal epithelial (A549) cells was detected by MTT assay. The results of A549 cells post 24, 48 and 72h treatment with 2.5 μM L4 aptamer also exposure to 50 μM TBHP. The absorbance was measured at 540 nm (reference wavelength 650 nm) using a microplate reader. The results represent the mean \pm SEM of 3 independent experiments. $p < 0.05$ vs. control.

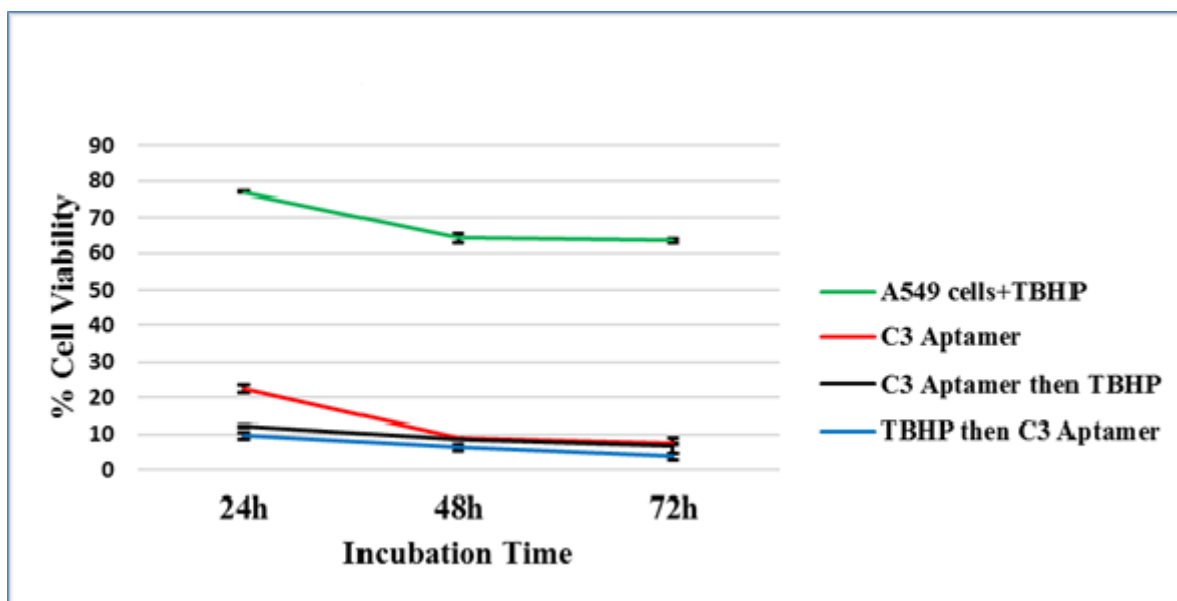


Figure 5.5: *In vitro* cell viability of the human adenocarcinoma of alveolar basal epithelial (A549) cells was detected by MTT assay. The results of A549 cells post 24, 48 and 72h treatment with 2.5 μ M C3 aptamer also exposure to 50 μ M TBHP. The absorbance was measured at 540 nm (reference wavelength 650 nm) using a microplate reader. The results represent the mean \pm SEM of 3 independent experiments. C3 aptamer with TBHP have a strong inhibition ability for A549 cells. $p < 0.00005$ vs. control.

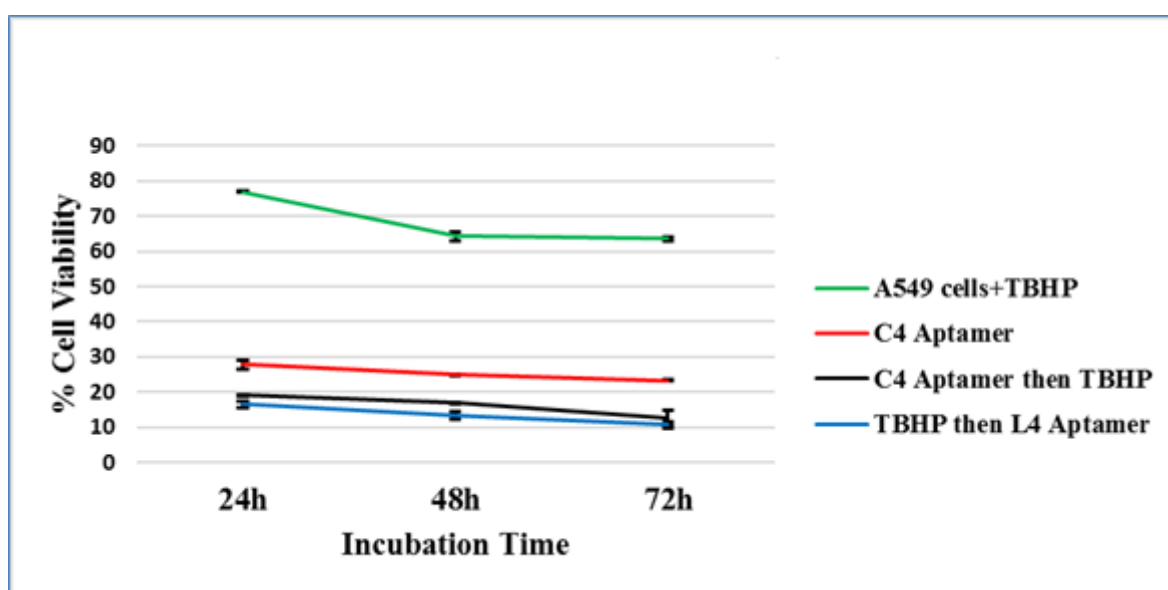


Figure 5.6: *In vitro* cell viability of the human adenocarcinoma of alveolar basal epithelial (A549) cells was detected by MTT assay. The results of A549 cells post 24, 48 and 72h treatment with 2.5 μ M C4 aptamer also exposure to 50 μ M TBHP. The absorbance was measured at 540 nm (reference wavelength 650 nm) using a microplate reader. The results represent the mean \pm SEM of 3 independent experiments. $p < 0.005$ vs. control.

Figure 5.7 illustrated the percentage of A549 cell death at 24, 48 and 72h after treatment with 2.5 μ M L3, L4, C3 and C4 aptamers, the results presented a statistically significant increase of cell death when compared to untreated cells ($p < 0.0005$). Based on the results presented in this figure, 2.5 μ M aptamers and 50 μ M TBHP treatment of A549 cells after 72h caused a cell death increase of 86.4%, 77.6%, 96.2% and 89.2% for L3, L4, C3 and C4

respectively. Between the groups of an aptamer, C3 aptamer was showed significantly higher percentage of cell death than L3, L4 and C4 aptamers ($p < 0.005$).

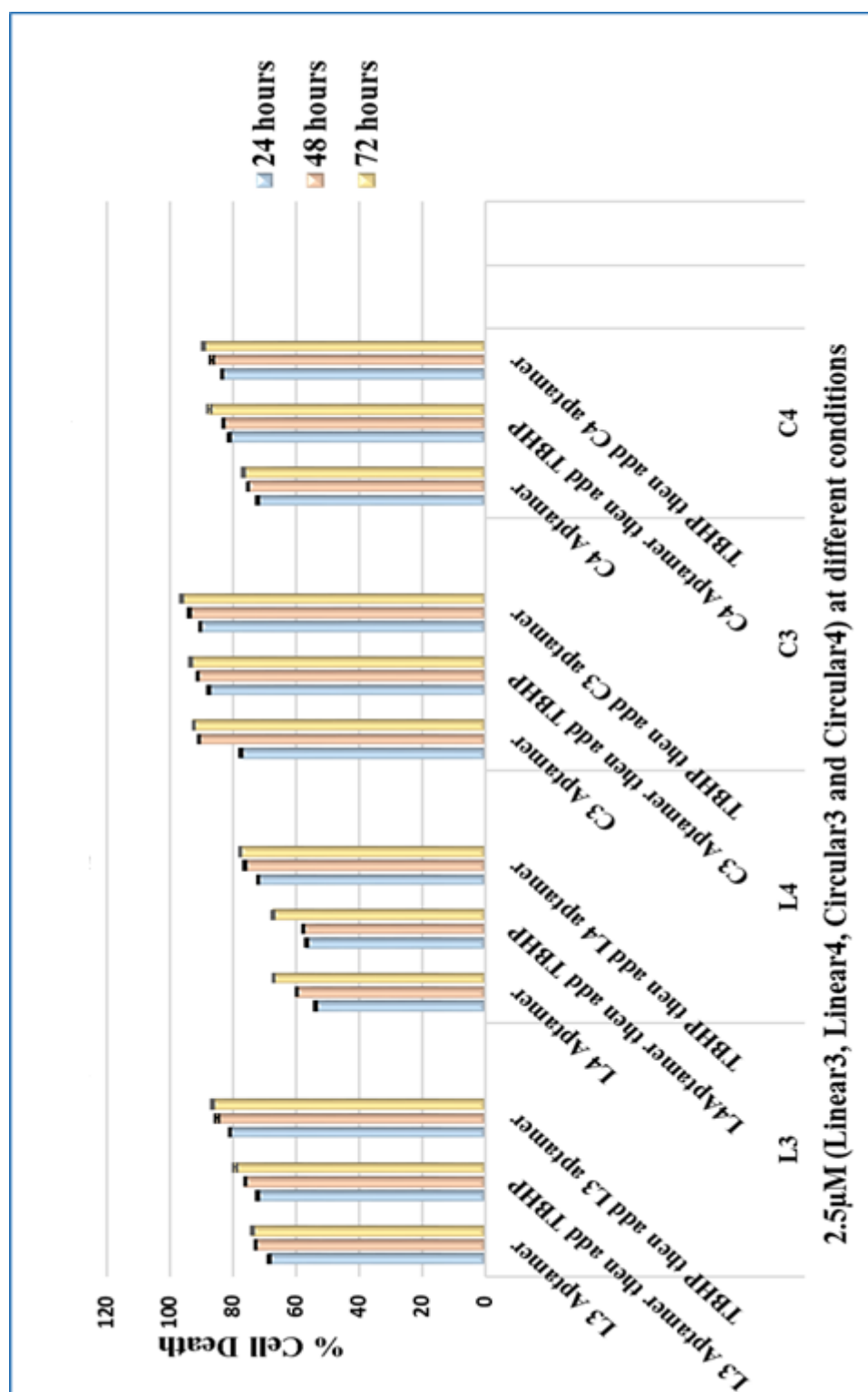


Figure 0.7: *In vitro* cell death percentage of the human adenocarcinoma of alveolar basal epithelial (A549) cells was estimated by MTT assay in 96-well plates following 24, 48 and 72h exposure to 2.5 μ M (L3, L4, C3 and C4) aptamers and 50 μ M TBHP. Data is shown as % mean \pm SEM of cell death for of 3 separate experiments. Treatment significantly different from the untreated controls $p < 0.005$.

5.3.1.2 Children Liver Hepatocellular Carcinoma Cells (HepG2)

To estimate the effect of aptamers on HepG2 cells viability, HepG2 cells were treated with 2.5 μM of L3, L4, C3 and C4 aptamers at 24, 48 and 72h. L3, L4, C3 and C4 aptamers significantly decreased the cell viability of HepG2 at 2.5 μM , $p < 0.0005$, at 24, 48 and 72h respectively as shown in figures 5.8.

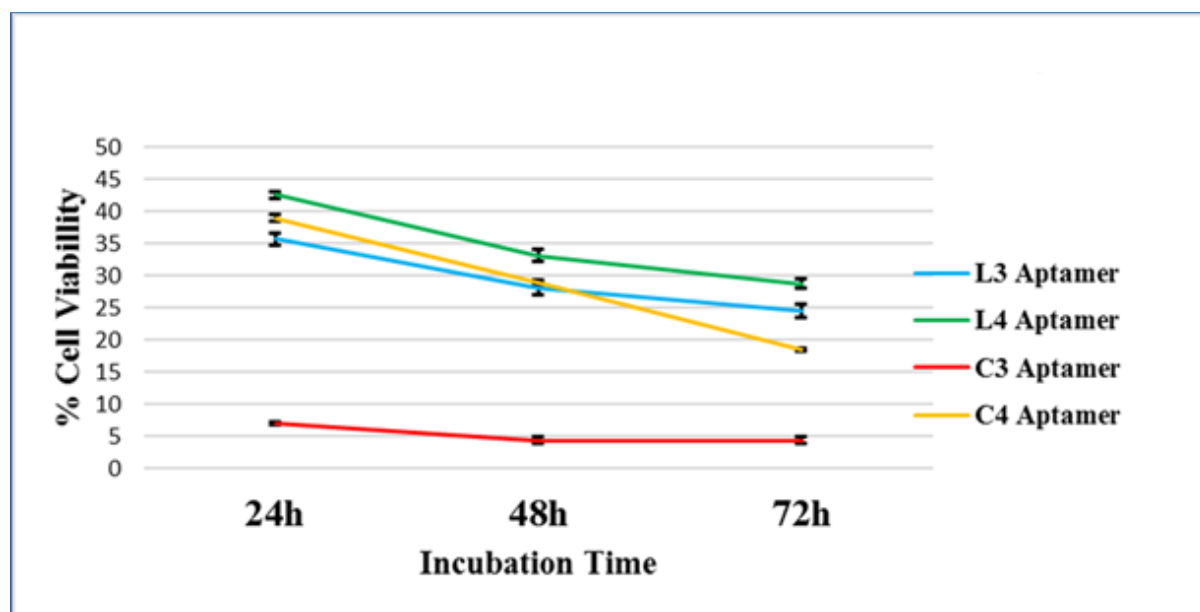


Figure 0.8: *In vitro* cell viability of the human hepatocellular carcinoma (HepG2) cells was detected by MTT assay. The results of HepG2 cells post 24, 48 and 72h treatment of 2.5 μM (L3, L4, C3 and C4) aptamers. The absorbance was measured at 540 nm (reference wavelength 650 nm) using a microplate reader. The results represent the mean \pm SEM of 3 independent experiments. Aptamers have a strong inhibition ability for HepG2 cells. $p < 0.0005$ at 24, 48 and 72h respectively vs. control.

HepG2 cells were treated with 50 μM TBHP and showed slightly decreased by 30% in cell viability after 24h compared to untreated cells (control), while the cell viability of HepG2 cells were a markedly decreased when treated with 2.5 μM L3, L4, C3 and C4 aptamers and 50 μM TBHP, $p < 0.00005$ (figures 5.9-5.12). According to the results presented in figure 5.13, 2.5 μM aptamers and 50 μM TBHP treatment of HepG2 cells after 72h caused a cell death increase of 90.8%, 86.5%, 98.3% and 88.8% for L3, L4, C3 and C4 respectively. Between the groups of aptamers, C3 aptamer was showed significantly higher percentage of cell death than L3, L4 and C4 aptamers ($p < 0.000001$).

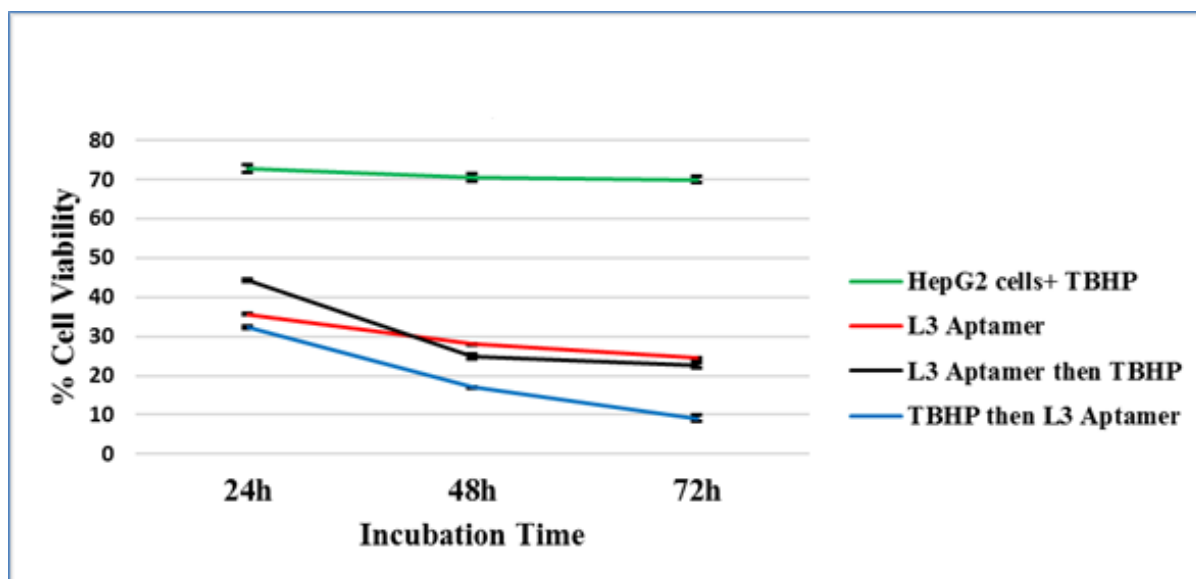


Figure 0.9: *In vitro* cell viability of the human hepatocellular carcinoma (HepG2) cells was detected by MTT assay. The results of HepG2 cells post 24, 48 and 72h treatment with 2.5 μ M L3 aptamer also exposure to 50 μ M TBHP. The absorbance was measured at 540 nm (reference wavelength 650 nm) using a microplate reader. The results represent the mean \pm SEM of 3 independent experiments. L3 aptamer with TBHP have a strong inhibition ability for HepG2 cells at 72h. $p < 0.00005$ vs. control.

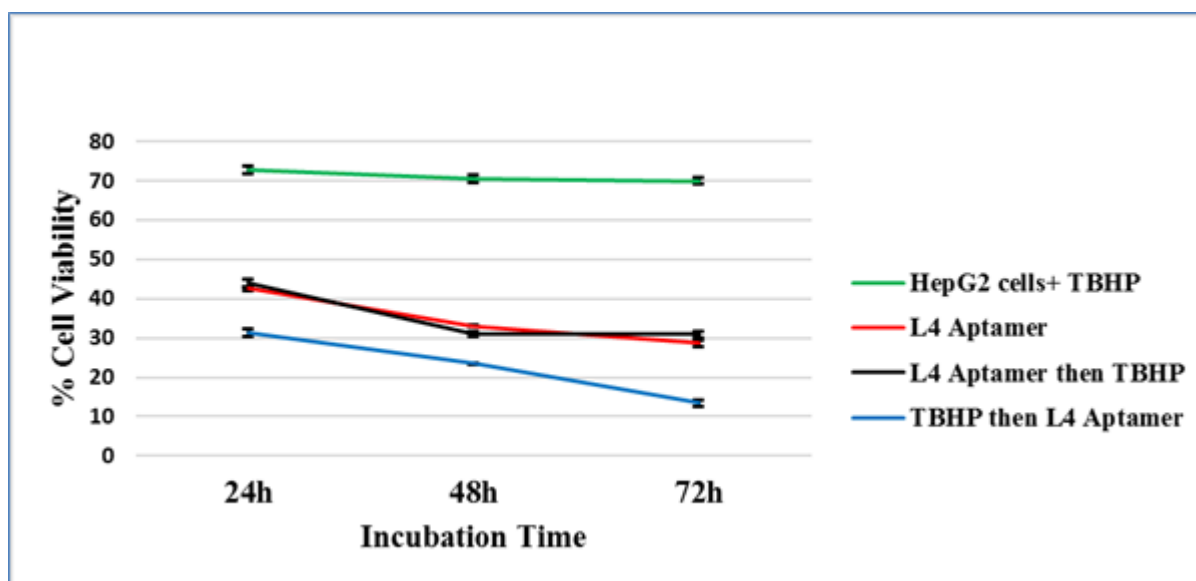


Figure 0.10: *In vitro* cell viability of the human hepatocellular carcinoma (HepG2) cells was detected by MTT assay. The results of HepG2 cells post 24, 48 and 72h treatment with 2.5 μ M L4 aptamer also exposure to 50 μ M TBHP. The absorbance was measured at 540 nm (reference wavelength 650 nm) using a microplate reader. The results represent the mean \pm SEM of 3 independent experiments. L4 aptamer with TBHP have a strong inhibition ability for HepG2 cells at 72h. $p < 0.00005$ vs. control.

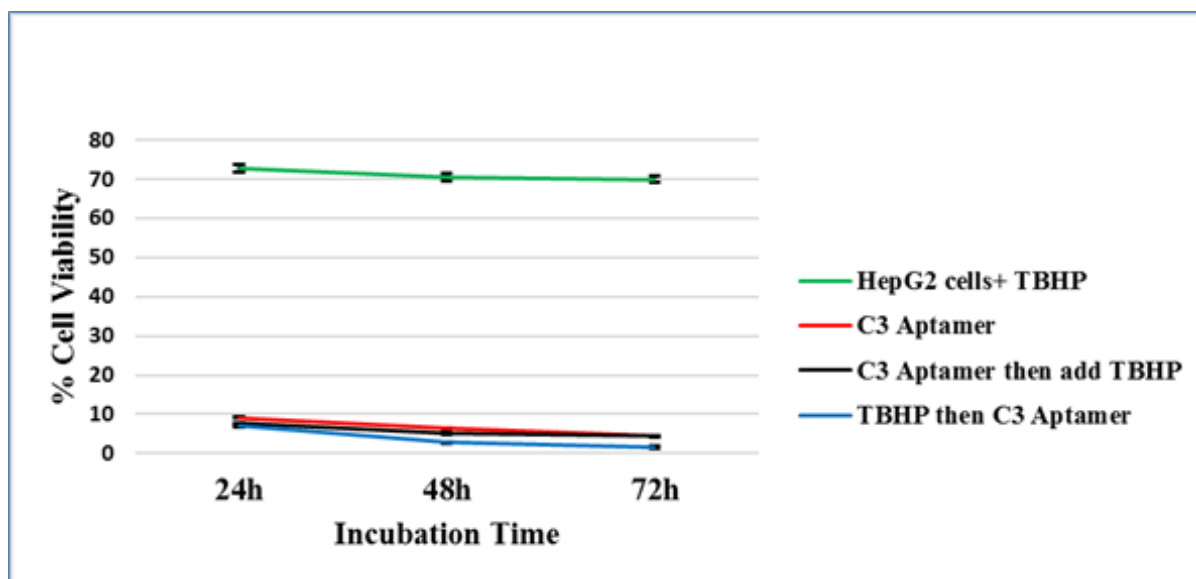


Figure 0.11: *In vitro* cell viability of the human hepatocellular carcinoma (HepG2) cells was detected by MTT assay. The results of HepG2 cells post 24, 48 and 72h treatment with 2.5 μM C3 aptamer also exposure to 50 μM TBHP. The absorbance was measured at 540 nm (reference wavelength 650 nm) using a microplate reader. The results represent the mean \pm SEM of 3 independent experiments. C3 aptamer with TBHP have a strong inhibition ability for HepG2 cells at 24, 48 and 72h. $p < 0.00005$ vs. control.

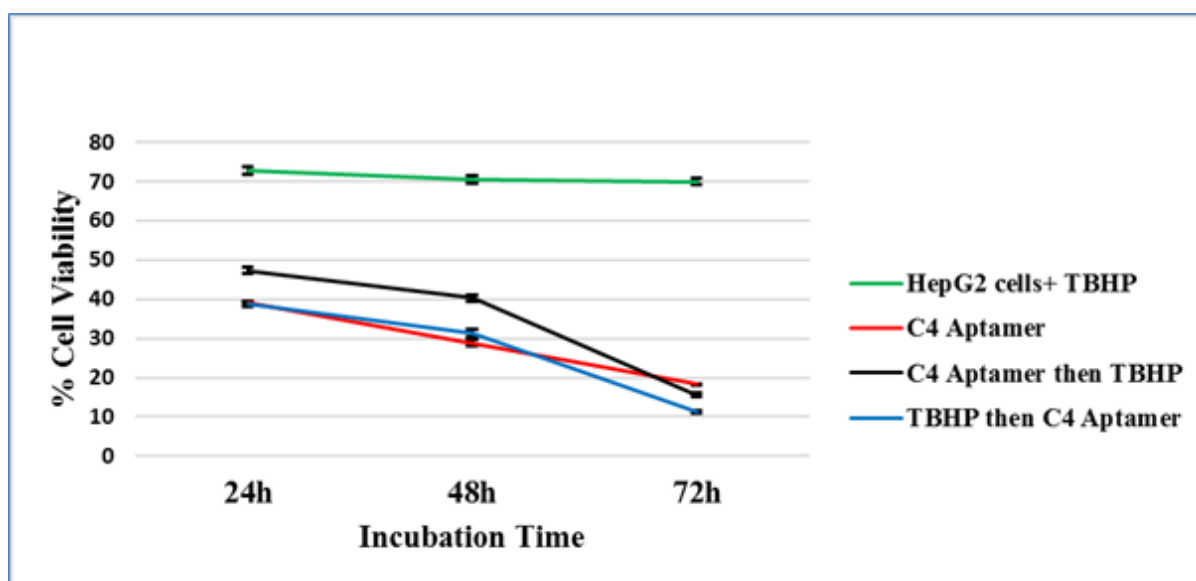


Figure 0.12: *In vitro* cell viability of the human hepatocellular carcinoma (HepG2) cells was detected by MTT assay. The results of HepG2 cells post 24, 48 and 72h treatment with 2.5 μM C4 aptamer also exposure to 50 μM TBHP. The absorbance was measured at 540 nm (reference wavelength 650 nm) using a microplate reader. The results represent the mean \pm SEM of 3 independent experiments. C4 aptamer with TBHP have a strong inhibition ability for HepG2 cells at 72h. $p < 0.00005$ vs. control.

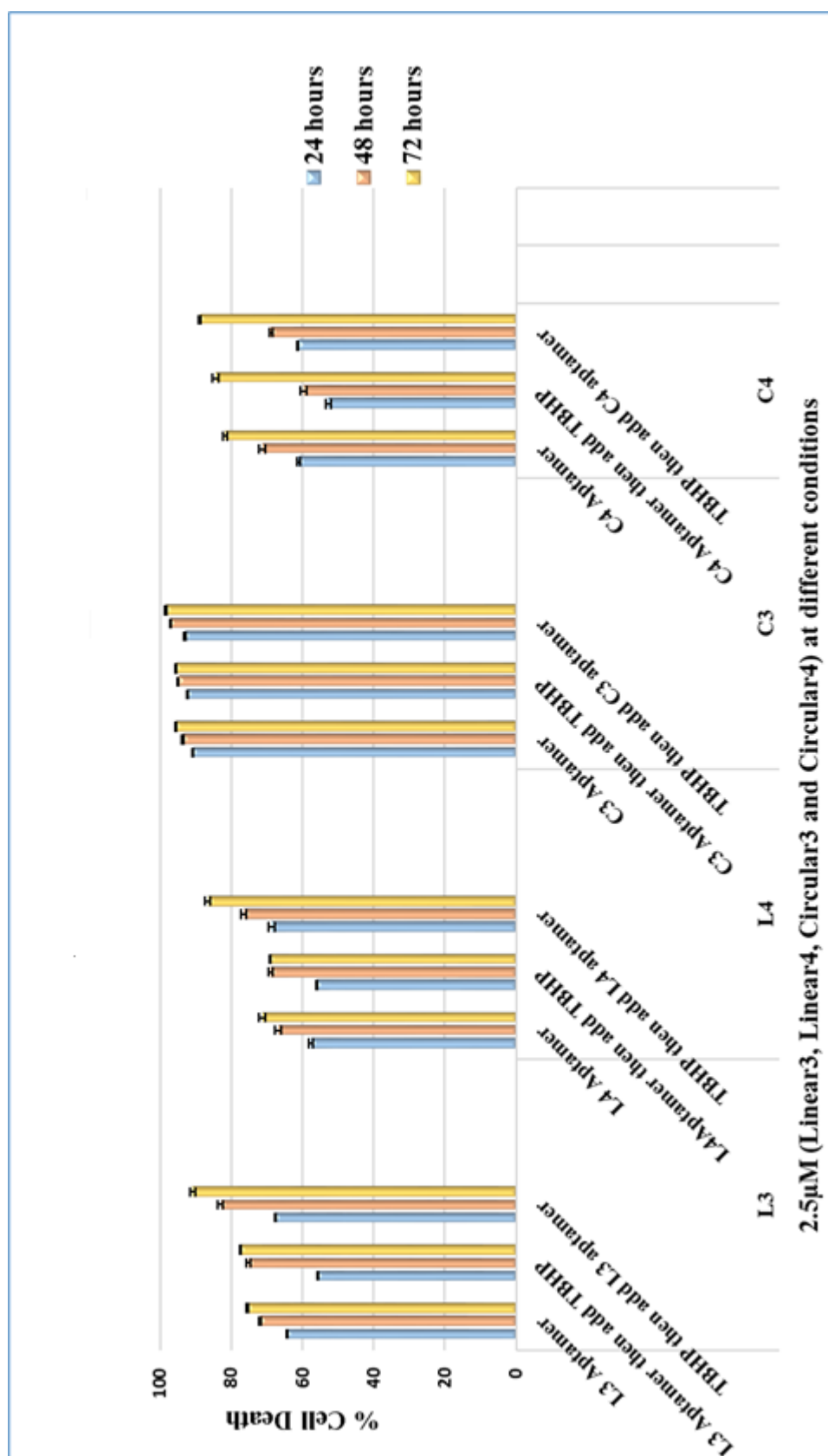


Figure 0.13: *In vitro* cell death percentage of the human hepatocellular carcinoma (HepG2) cells was estimated by MTT assay in 96-well plates following 24, 48 and 72h exposure to 2.5 μ M (L3, L4, C3 and C4) aptamers and 50 μ M TBHP. Data is shown as % mean \pm SEM of cell death for of 3 separate experiments. Treatment significantly different from the untreated controls $p < 0.000001$.

5.3.1.3 Breast Cancer (MCF7) Cells (oestrogen positive)

To determine aptamers effect on MCF-7 cells viability, MTT assay was conducted. The results of the MTT assay showed that L3, L4, C3 and C4 aptamers were clearly capable of reducing cell viability after 72h, $p < 0.0001$. The C3 aptamer was decreased significantly the cell viability of MCF-7 after 24h to 38% -18% at 72h, $p < 0.0005$ compared with L3, L4 and C4 aptamers (figure 5.14).

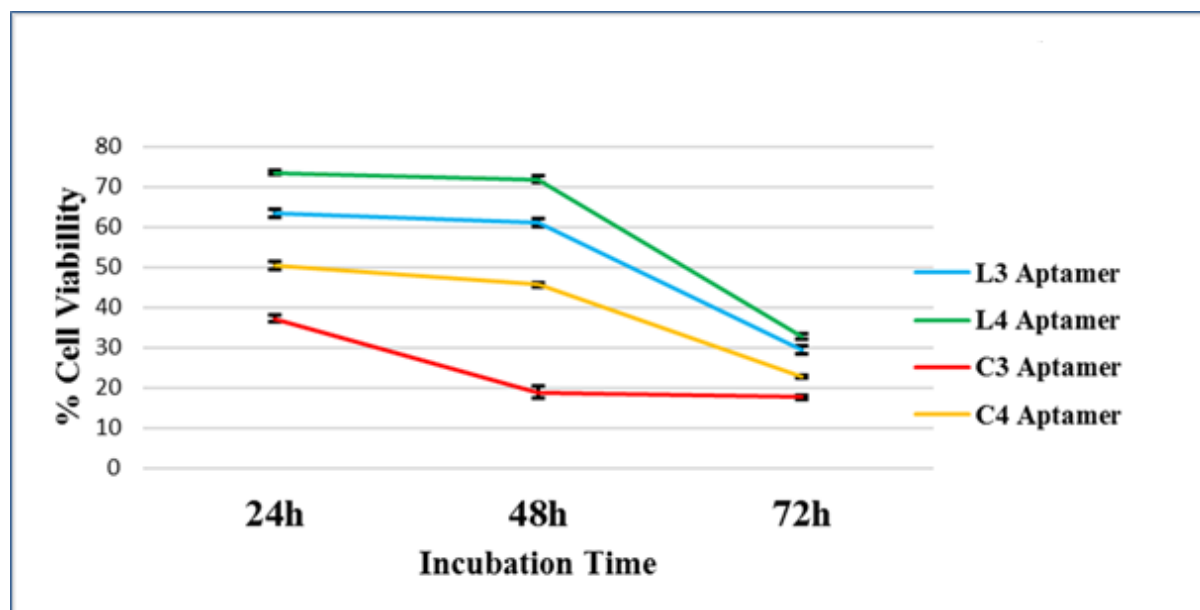


Figure 5.14: *In vitro* cell viability of the human breast cancer (MCF-7) cells was detected by MTT assay. The results of MCF-7 cells post 24, 48 and 72h treatment of 2.5 μ M (L3, L4, C3 and C4) aptamers. The absorbance was measured at 540 nm (reference wavelength 650 nm) using a microplate reader. The results represent the mean \pm SEM of 3 independent experiments. Aptamers have a strong inhibition ability for MCF-7 cells. $p < 0.0001$ at 72h vs. control.

Both 2.5 μ M L3, L4, C3 and C4 aptamers and 50 μ M TBHP treatments of cells caused a statistical significant reduction in cell viability compared to viability of untreated cells (2.5 μ M L3, L4 and C4: $p < 0.005$, 2.5 μ M C3: $p < 0.0005$; 50 μ M TBHP: $p \leq 0.05$) at 24, 48 and 72h respectively as shown in figures 5.15-5.18. C3 aptamer showed the highest increase of cell death by 82% when the cells were treated with C3 aptamer, 78.8% when the cells were treated with 2.5 μ M C3 aptamer then adding 50 μ M TBHP and 85.9% when the cells were treated with 50 μ M TBHP then adding 2.5 μ M C3 aptamer after 72h compared with the percentage of MCF-7 cell death which treated with the same condition from L3, L4 and C4 aptamers ($p < 0.0005$) as shown in figure 5.19.

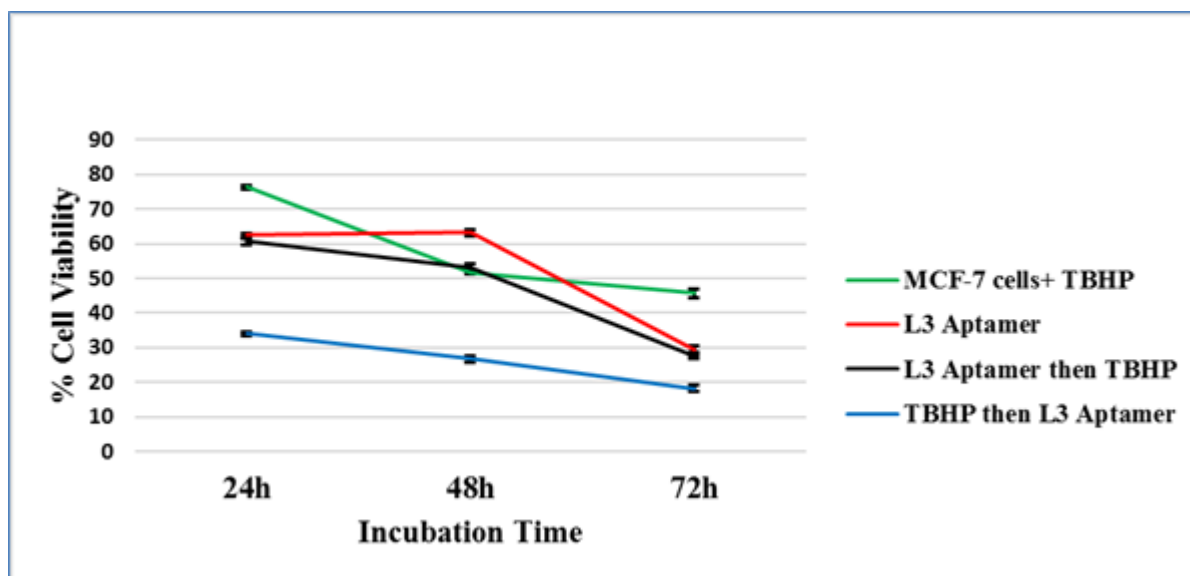


Figure 0.15: *In vitro* cell viability of the human breast cancer (MCF-7) cells was detected by MTT assay. The results of MCF-7 cells post 24, 48 and 72h treatment with 2.5 μM L3 aptamer also exposure to 50 μM TBHP. The absorbance was measured at 540 nm (reference wavelength 650 nm) using a microplate reader. The results represent the mean \pm SEM of 3 independent experiments. L3 aptamer with TBHP have a strong inhibition ability for MCF-7 cells at 24, 48 and 72h. $p < 0.005$ vs. control.

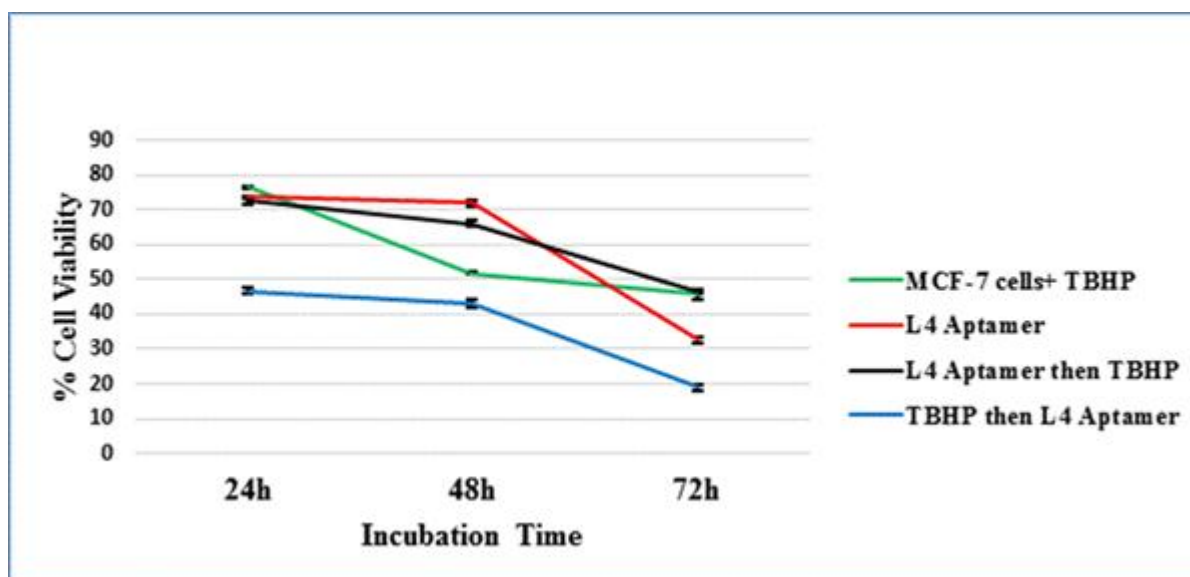


Figure 5.16: *In vitro* cell viability of the human breast cancer (MCF-7) cells was detected by MTT assay. The results of MCF-7 cells post 24, 48 and 72h treatment with 2.5 μM L4 aptamer also exposure to 50 μM TBHP. The absorbance was measured at 540 nm (reference wavelength 650 nm) using a microplate reader. The results represent the mean \pm SEM of 3 independent experiments. L4 aptamer with TBHP have a strong inhibition ability for MCF-7 cells at 72h. $p < 0.005$ vs. control.

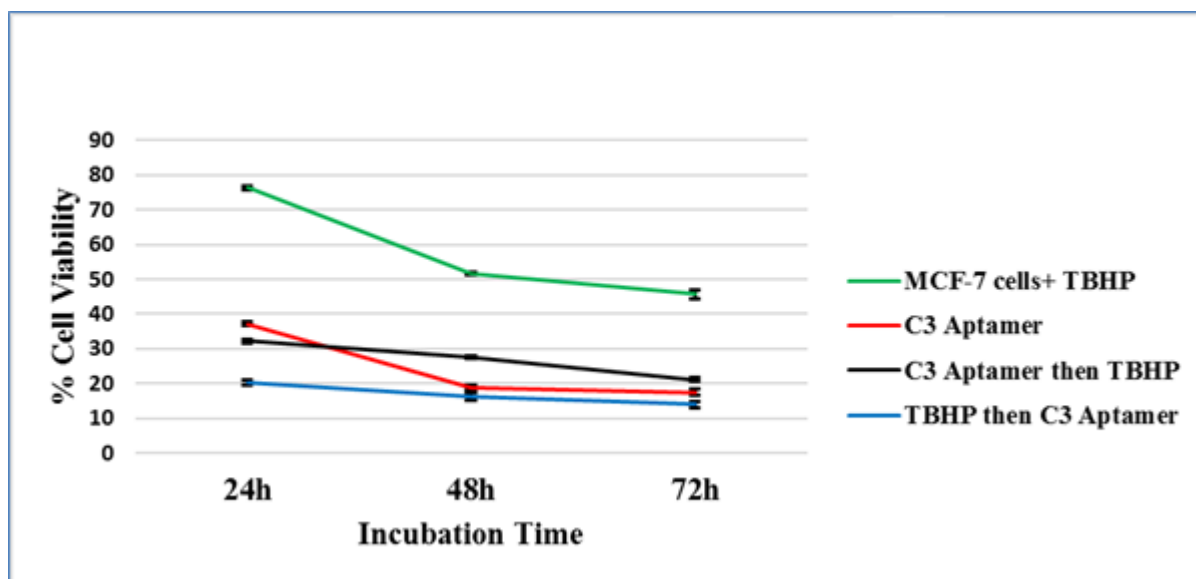


Figure 0.17: *In vitro* cell viability of the human breast cancer (MCF-7) cells was detected by MTT assay. The results of MCF-7 cells post 24, 48 and 72h treatment with 2.5 μM C3 aptamer also exposure to 50 μM TBHP. The absorbance was measured at 540 nm (reference wavelength 650 nm) using a microplate reader. The results represent the mean \pm SEM of 3 independent experiments. C3 aptamer with TBHP have a strong inhibition ability for MCF-7 cells at 72h. $p < 0.0005$ vs. control.

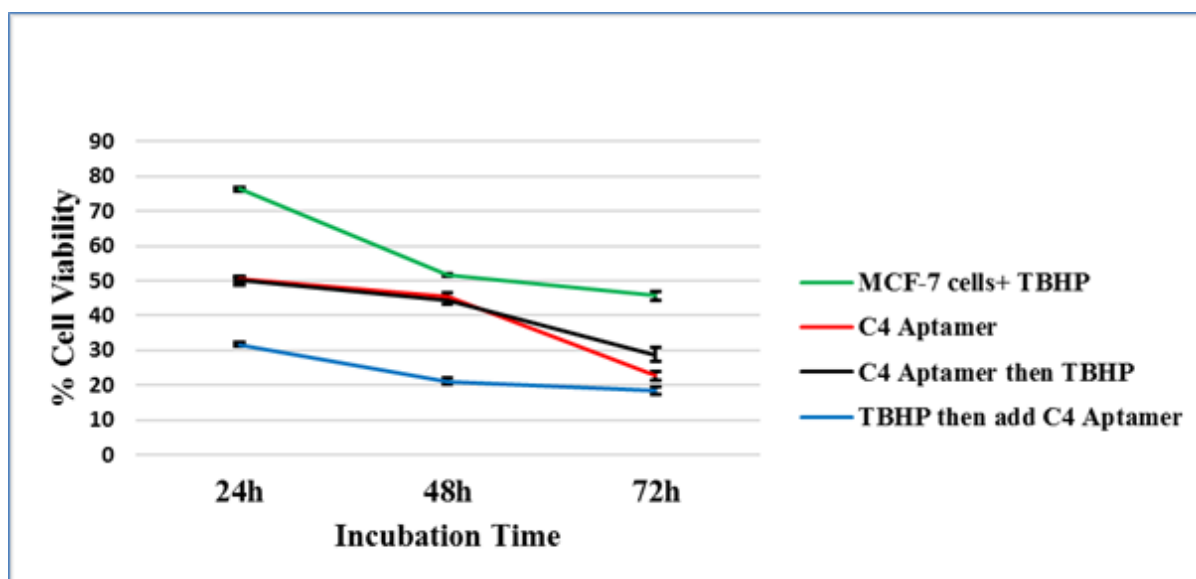


Figure 5.18: *In vitro* cell viability of the human breast cancer (MCF-7) cells was detected by MTT assay. The results of MCF-7 cells post 24, 48 and 72h treatment with 2.5 μM C4 aptamer also exposure to 50 μM TBHP. The absorbance was measured at 540 nm (reference wavelength 650 nm) using a microplate reader. The results represent the mean \pm SEM of 3 independent experiments. C4 aptamer with TBHP have a strong inhibition ability for MCF-7 cells at 72h. $p < 0.005$ vs. control.

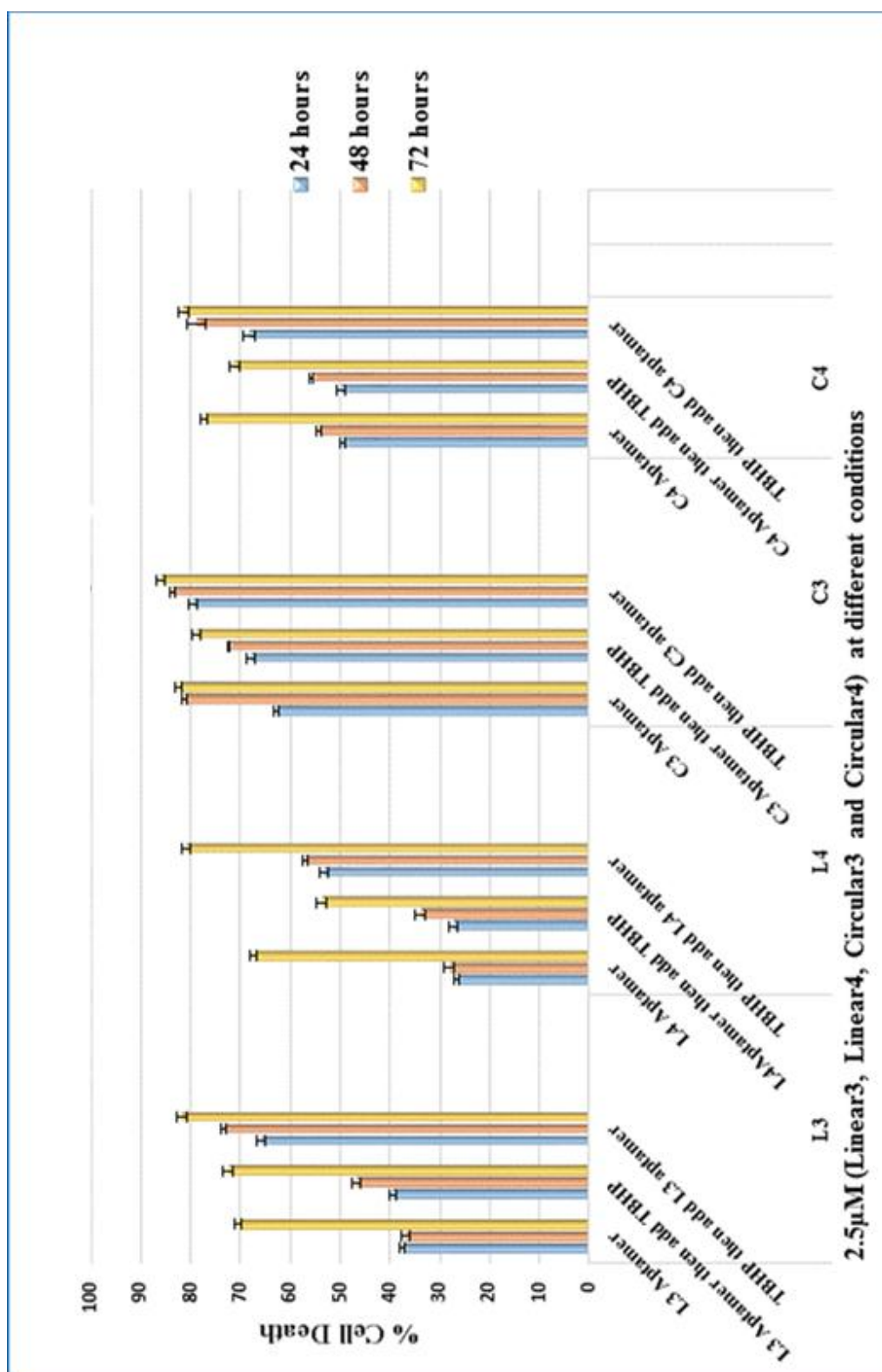


Figure 5.019: *In vitro* cell death percentage of the human breast cancer (MCF-7) cells was estimated by MTT assay in 96-well plates following 24, 48 and 72h exposure to 2.5 μ M (L3, L4, C3 and C4) aptamers and 50 μ M TBHP. Data is shown as % mean \pm SEM of cell death for of 3 separate experiments. Treatment significantly different from the untreated controls $p < 0.0005$.

5.3.1.4 Breast Cancer (MDA-MB-468) Cells (oestrogen negative)

MDA-MB-468 cells were exposed to 2.5 μM of L3, L4, C3 and C4 aptamers at 24, 48 and 72h to estimate the effect of aptamers on cell viability. After 72h, cells exposed to 2.5 μM L3, C3 and C4 aptamers presented a statistically significant decrease in cell viability compared to untreated cells ($p < 0.005$), while L4 aptamer was not effected on MDA-MB-468 cells viability compared to control ($p > 0.05$) as shown in figure 5.20.

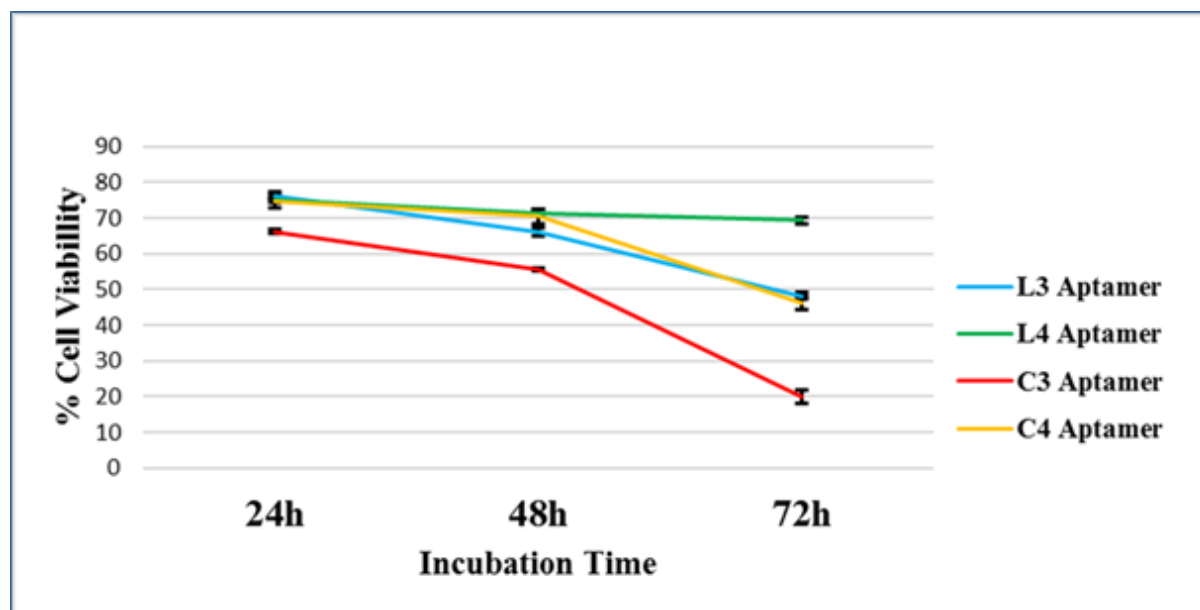


Figure 5.20: *In vitro* cell viability of the human breast cancer (MDA-MB-468) cells was detected by MTT assay. The results of MDA-MB-468 cells post 24, 48 and 72h treatment of 2.5 μM (L3, L4, C3 and C4) aptamers. The absorbance was measured at 540 nm (reference wavelength 650 nm) using a microplate reader. The results represent the mean \pm SEM of 3 independent experiments. C3 aptamer have a strong inhibition ability for MDA-MB-468 cells. $p < 0.005$ at 72h vs. control.

MDA-MB-468 cells treated with 50 μM TBHP also showed a reduction of 23% in cell viability after 24 and 48h compared to untreated cells (control); however, the difference was not statistically significant, while after 72h the cells which treated with 50 μM TBHP showed slightly decreased in cell viability as compared with untreated cells ($p < 0.05$). The reduction in cell viability became more pronounced after treated with aptamers and TBHP. At 24h, L3, L4 and C4 aptamers and 50 μM TBHP were not effecting on MDA-MB-468 cells viability ($p > 0.05$), while 2.5 μM C3 aptamer and 50 μM TBHP were significantly reduced the MDA-MB-468 cells viability at 24h ($p < 0.005$) as shown in figure 5.21-5.24. A similar observation has been detected after 48h (figure 5.21-5.24), whereas after 72h, L3, C3, and C4 aptamers were showed decreased on the cell viability of MDA-MB-468 cells which treated with 50 μM

TBHP then added 2.5 μM aptamers. The results of C4 aptamer was showed not effect on cell viability when the cells were treated with 2.5 μM C4 aptamer only and 2.5 μM L4 aptamer then added 50 μM TBHP. Whereas, MDA-MB-468 cells which treated with 50 μM TBHP then added 2.5 μM C4 aptamer was decreased significantly the cell viability at 72h, $p < 0.005$ (figure 5.24).

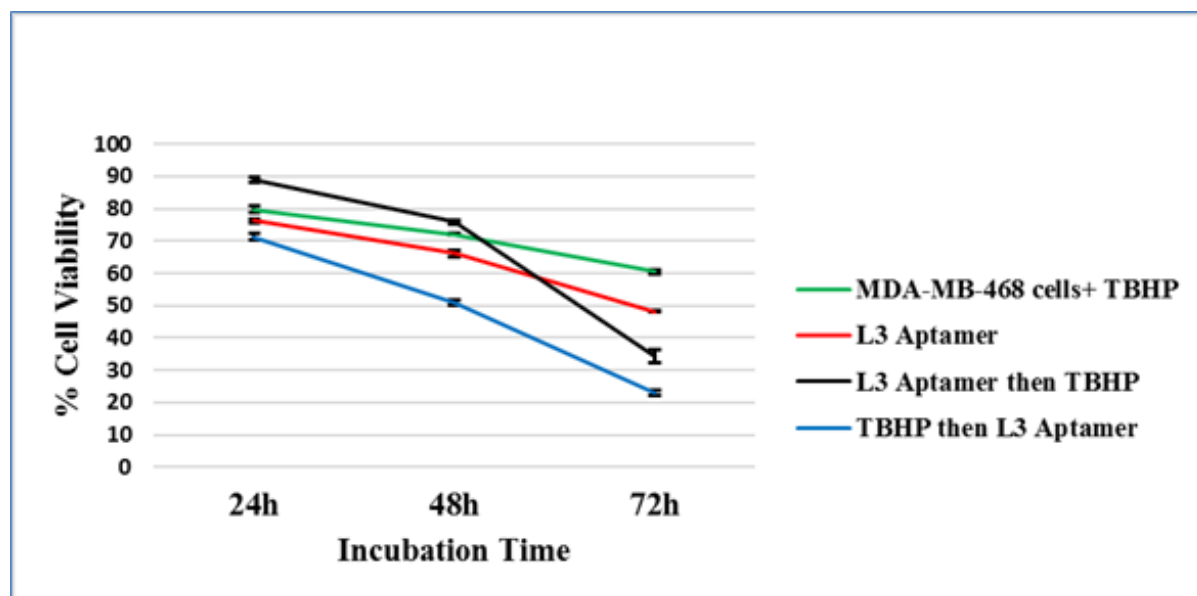


Figure 5.21: *In vitro* cell viability of the human breast cancer (MDA-MB-468) cells was detected by MTT assay. The results of MDA-MB-468 cells post 24, 48 and 72h treatment with 2.5 μM L3 aptamer also exposure to 50 μM TBHP. The absorbance was measured at 540 nm (reference wavelength 650 nm) using a microplate reader. The results represent the mean \pm SEM of 3 independent experiments. $p < 0.005$ vs. control.

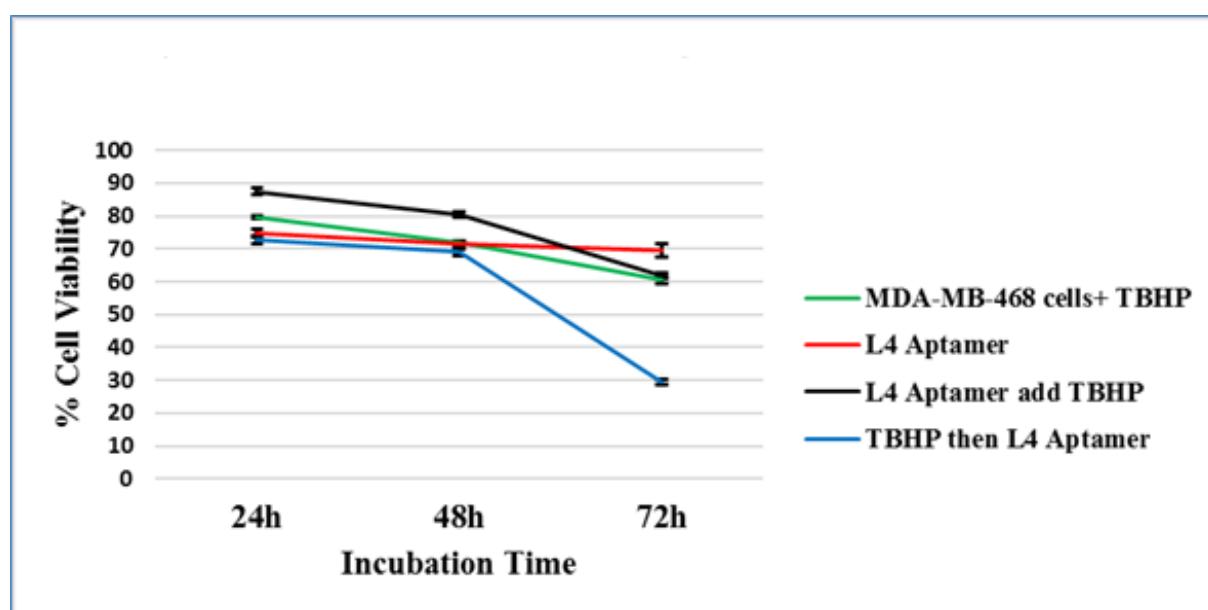


Figure 5.22: *In vitro* cell viability of the human breast cancer (MDA-MB-468) cells was detected by MTT assay. The results of MDA-MB-468 cells post 24, 48 and 72h treatment with 2.5 μM L4 aptamer also exposure to 50 μM TBHP. The absorbance was measured at 540 nm (reference wavelength 650 nm) using a microplate reader. The results represent the mean \pm SEM of 3 independent experiments. $p < 0.005$ vs. control.

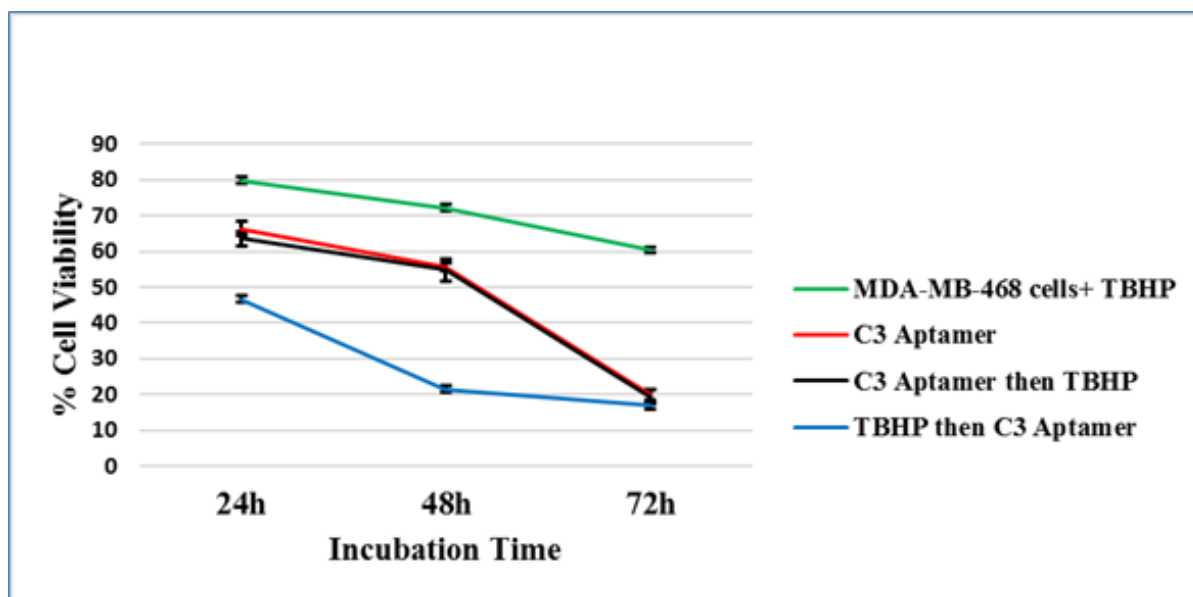


Figure 0.23: *In vitro* cell viability of the human breast cancer (MDA-MB-468) cells was detected by MTT assay. The results of MDA-MB-468 cells post 24, 48 and 72h treatment with 2.5 μ M C3 aptamer also exposure to 50 μ M TBHP. The absorbance was measured at 540 nm (reference wavelength 650 nm) using a microplate reader. The results represent the mean \pm SEM of 3 independent experiments. C3 aptamer with TBHP have a strong inhibition ability for MDA-MB-468 cells at 72h. $p < 0.005$ vs. control.

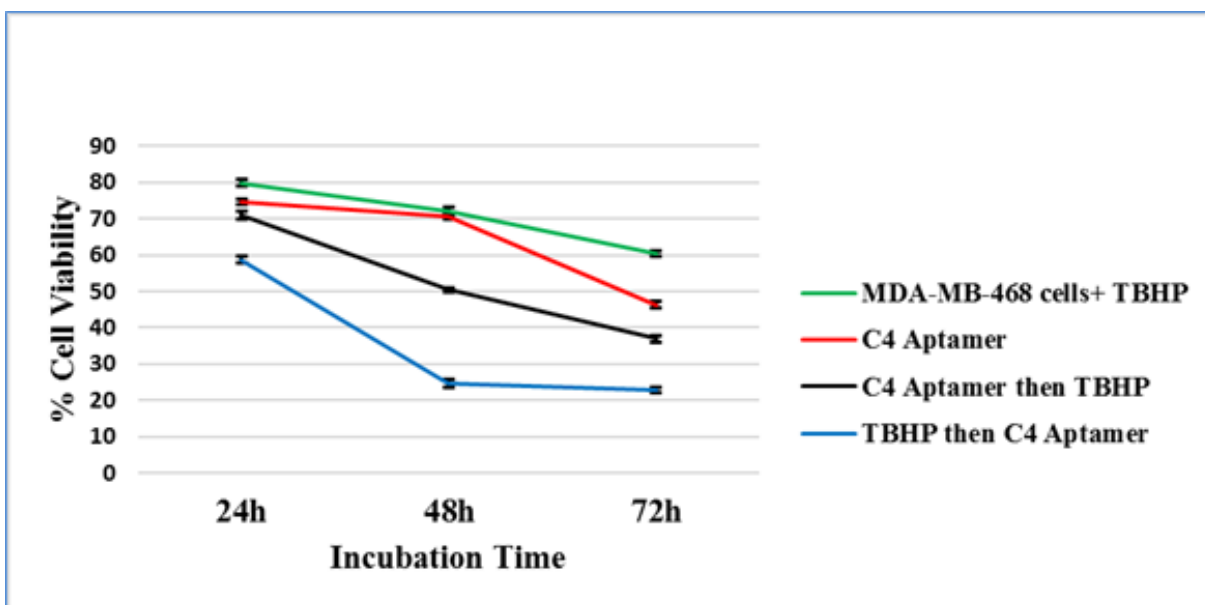


Figure 0.24: *In vitro* cell viability of the human breast cancer (MDA-MB-468) cells was detected by MTT assay. The results of MDA-MB-468 cells post 24, 48 and 72h treatment with 2.5 μ M C4 aptamer also exposure to 50 μ M TBHP. The absorbance was measured at 540 nm (reference wavelength 650 nm) using a microplate reader. The results represent the mean \pm SEM of 3 independent experiments. $p < 0.005$ vs. control.

Based on the results presented in figure 5.25, 2.5 μ M L3, L4, C3 and C4 aptamers and 50 μ M TBHP treatment to MDA-MB-468 cells after 72h caused a cell death increase of 77%, 70%, 83% and 77% respectively. Between the groups of aptamers, C3 aptamer was showed significantly higher percentage of cell death than L3, L4 and C4 aptamers ($p < 0.005$).

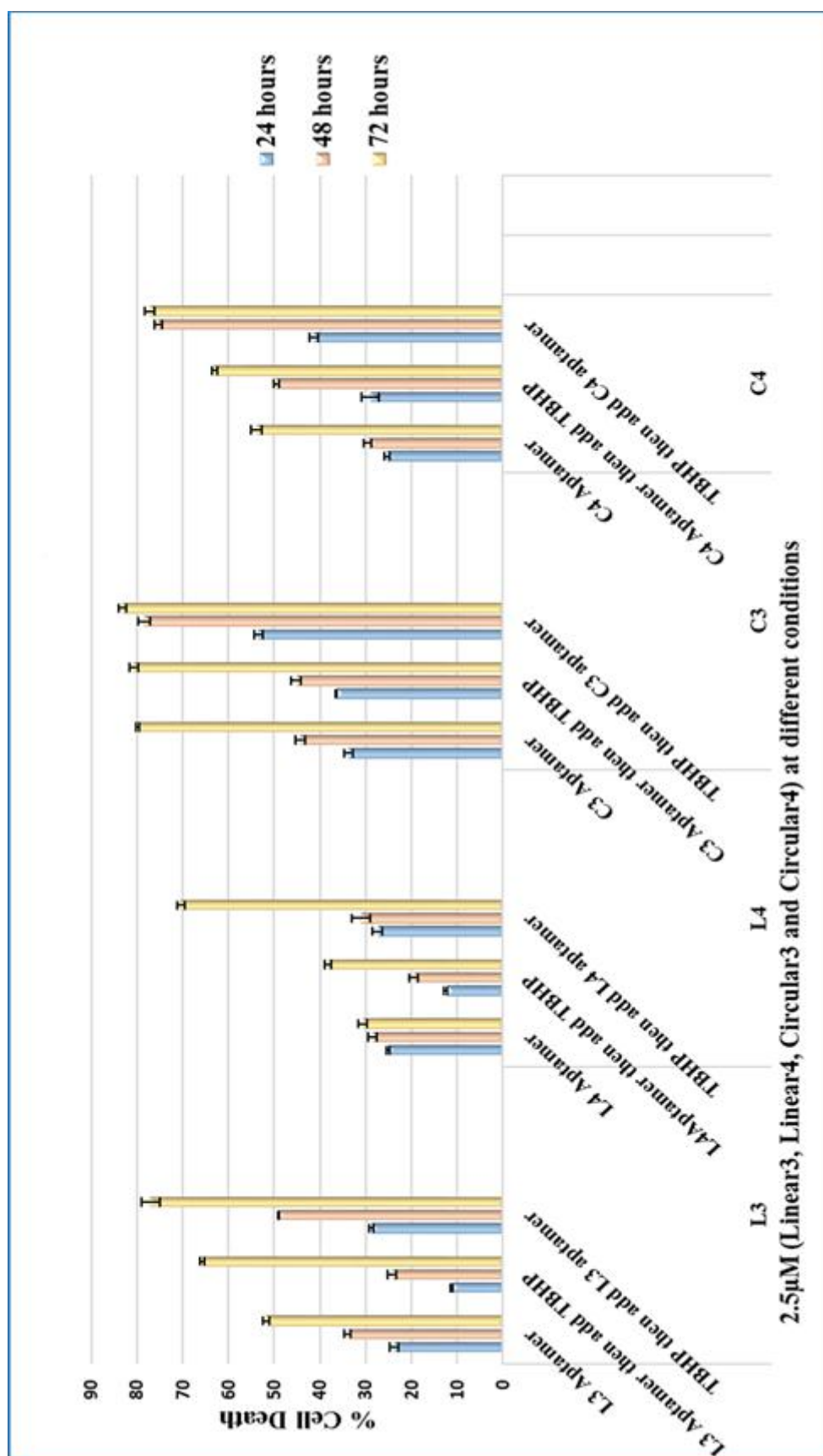


Figure 5.25: In vitro cell death percentage of the human breast cancer (MDA-MB-468) cells was estimated by MTT assay in 96-well plates following 24, 48 and 72 exposure to 2.5 μ M (L3, L4, C3 and C4) aptamers and 50 μ M TBHP. Data is shown as % mean \pm SEM of cell death for of 3 separate experiments. Treatment significantly different from the untreated controls $p < 0.005$.

5.3.1.5 Children Human Bone Osteosarcoma cells (U2OS)

To establish the effect of aptamers on cell viability of U2OS cells, L3, L4, C3 and C4 aptamers at concentrations 2.5 μM were pretreated to U2OS cells at 24, 48 and 72h. L3, L4, C3 and C4 aptamers were significantly decreased the cell viability of U2OS cells at 2.5 μM , $p < 0.0005$, at 72h as shown in figures 5.26. C3 aptamer showed the highly significant to reduce U2OS cells viability after 24, 48 and 72h when compared to untreated cells ($p < 0.000005$) and L3, L4 and C4 aptamers ($p < 0.005$).

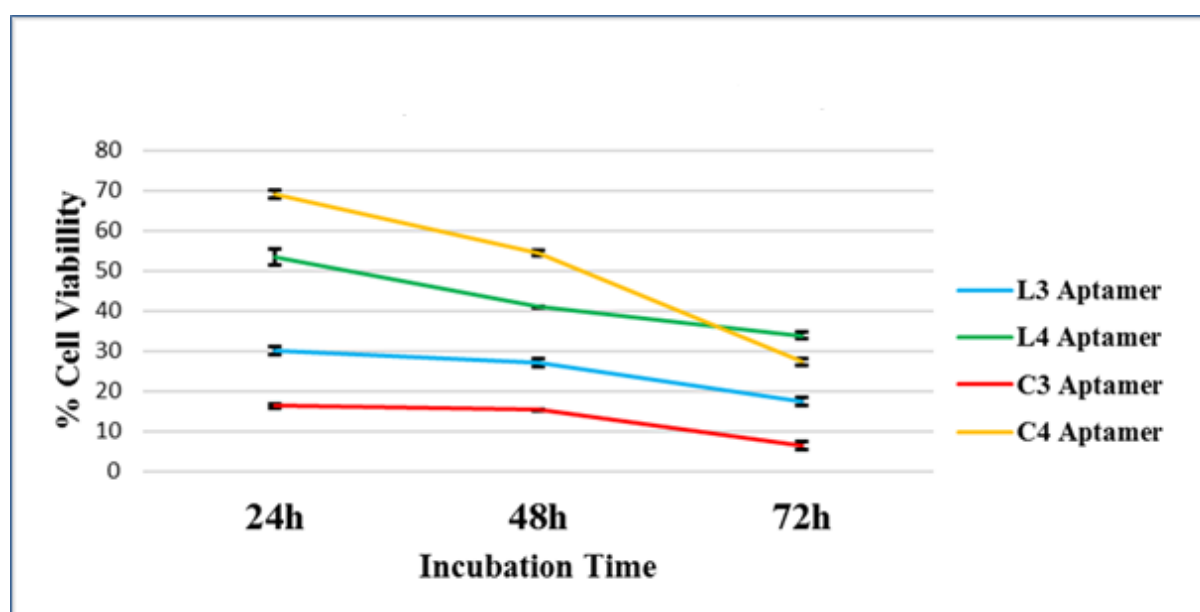


Figure 5.26: *In vitro* cell viability of the human bone osteosarcoma (U2OS) cells was detected by MTT assay. The results of U2OS cells post 24, 48 and 72h treatment of 2.5 μM (L3, L4, C3 and C4) aptamers. The absorbance was measured at 540 nm (reference wavelength 650 nm) using a microplate reader. The results represent the mean \pm SEM of 3 independent experiments. C3 aptamers have a strong inhibition ability for U2OS cells. $p < 0.0005$ at 72h vs. control.

To investigate the challenging of cells with TBHP, U2OS cells were treated with 50 μM TBHP and showed a reduction by 40% at 24 and 48h and 47% at 72h in cell viability compared to untreated cells (control). U2OS cells were illustrated significantly decrease on cell viability after treatment with 2.5 μM L3, L4 and C3 aptamers and 50 μM TBHP at 24, 48 and 72h, $p < 0.0001$ (figure 5.27-5.29), while C4 aptamer was reduced the U2OS cells viability after 72h, ($p < 0.005$) as described in figure 5.30.

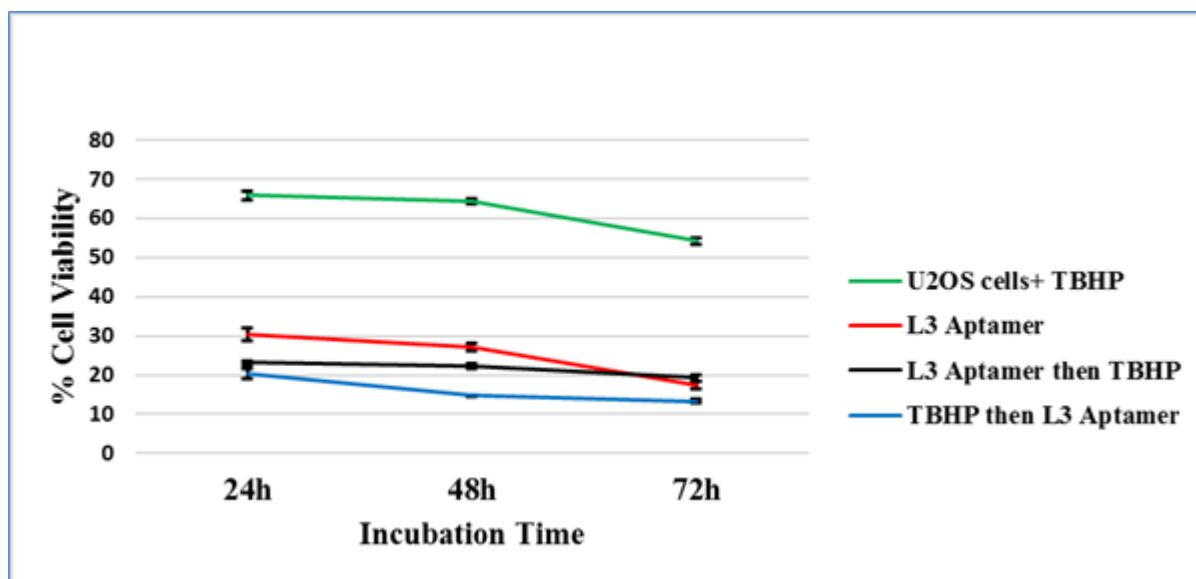


Figure 5.27: *In vitro* cell viability of the human bone osteosarcoma (U2OS) cells was detected by MTT assay. The results of U2OS cells post 24, 48 and 72h treatment with 2.5 μM L3 aptamer also exposure to 50 μM TBHP. The absorbance was measured at 540 nm (reference wavelength 650 nm) using a microplate reader. The results represent the mean \pm SEM of 3 independent experiments. L3 aptamer with TBHP have a strong inhibition ability for U2OS cells at 72h. $p < 0.0001$ vs. control.

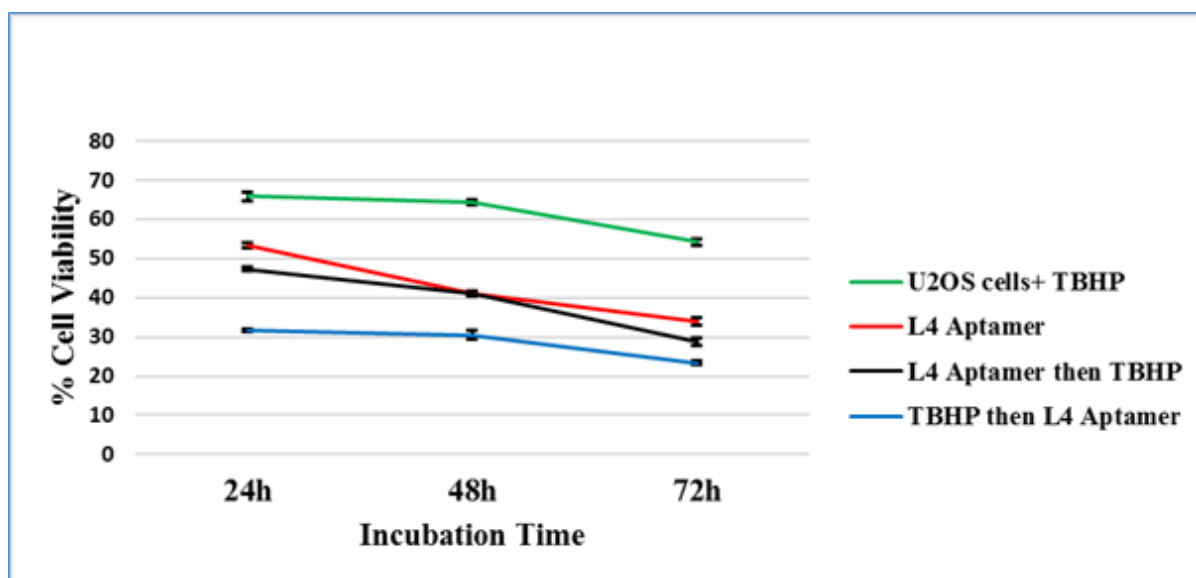


Figure 5.28: *In vitro* cell viability of the human bone osteosarcoma (U2OS) cells was detected by MTT assay. The results of U2OS cells post 24, 48 and 72h treatment with 2.5 μM L4 aptamer also exposure to 50 μM TBHP. The absorbance was measured at 540 nm (reference wavelength 650 nm) using a microplate reader. The results represent the mean \pm SEM of 3 independent experiments. L4 aptamer with TBHP have a strong inhibition ability for U2OS cells at 72h. $p < 0.0001$ vs. control.

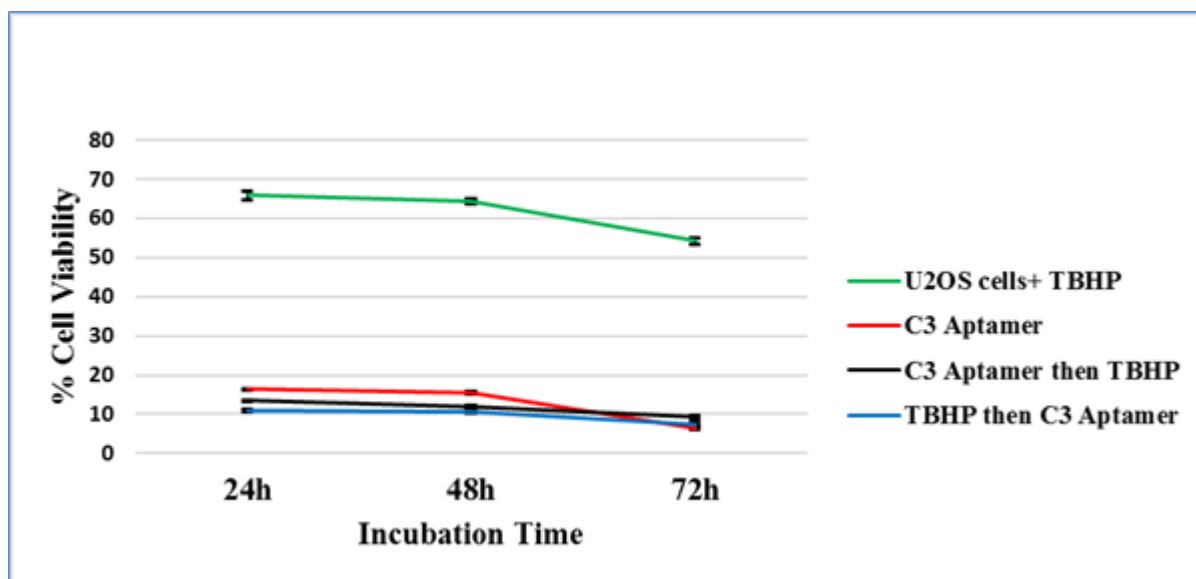


Figure 5.29: *In vitro* cell viability of the human bone osteosarcoma (U2OS) cells was detected by MTT assay. The results of U2OS cells post 24, 48 and 72h treatment with 2.5 μM C3 aptamer also exposure to 50 μM TBHP. The absorbance was measured at 540 nm (reference wavelength 650 nm) using a microplate reader. The results represent the mean \pm SEM of 3 independent experiments. C3 aptamer with TBHP have a strong inhibition ability for U2OS cells at 72h. $p < 0.0001$ vs. control.

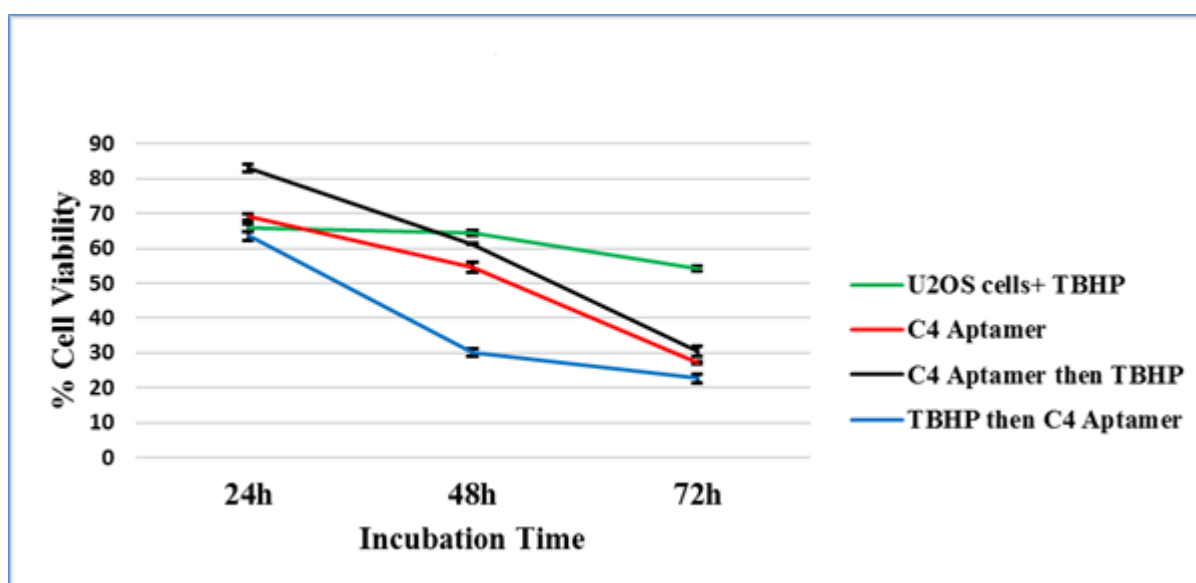


Figure 5.30: *In vitro* cell viability of the human bone osteosarcoma (U2OS) cells was detected by MTT assay. The results of U2OS cells post 24, 48 and 72h treatment with 2.5 μM C4 aptamer also exposure to 50 μM TBHP. The absorbance was measured at 540 nm (reference wavelength 650 nm) using a microplate reader. The results represent the mean \pm SEM of 3 independent experiments. $p < 0.005$ vs. control.

Based on the results presented in figure 5.31, 2.5 μM aptamers and 50 μM TBHP treatment after 72h caused a cell death increase of 86.6%, and 92.6% for L3 and C3 aptamers respectively. Between the groups of aptamers, C3 aptamer was showed significantly higher percentage of cell death than L3, L4 and C4 aptamers ($p < 0.00001$).

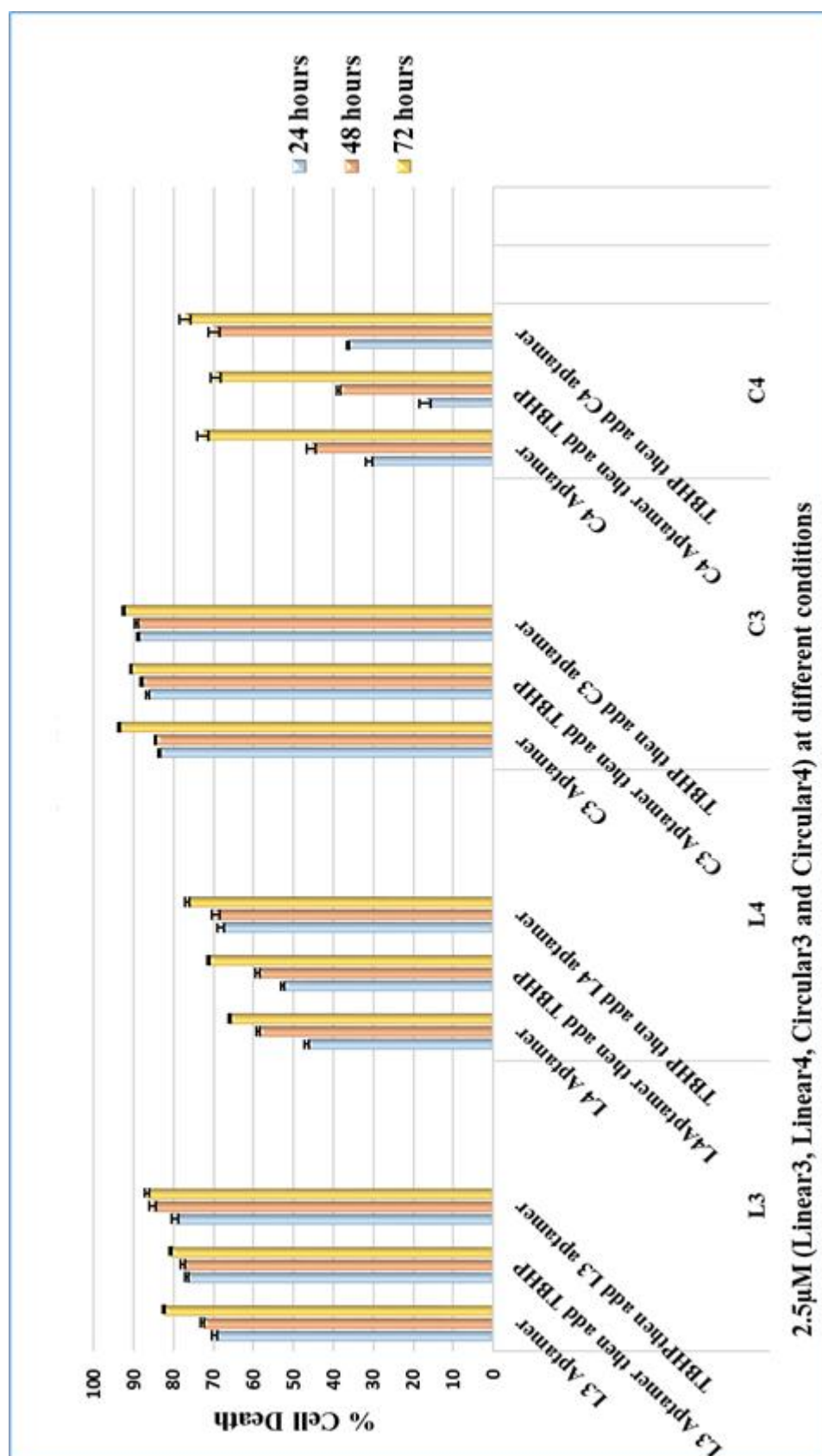


Figure 5.31: *In vitro* cell death percentage of the human bone osteosarcoma (U2OS) cells was estimated by MTT assay in 96-well plates following 24, 48 and 72 exposure to 2.5 μ M (L3, L4, C3 and C4) aptamers and 50 μ M TBHP. Data is shown as % mean \pm SEM of cell death for of 3 separate experiments. Treatment significantly different from the untreated controls $p < 0.00001$.

5.3.1.6 Colorectal Adenocarcinoma cells (Caco-2)

Caco-2 cells were exposed to 2.5 μM L3, L4, C3 and C4 aptamers at 24, 48 and 72h to estimate the effect of aptamers on Caco-2 cell viability. L3, C3 and C4 aptamers significantly reduced cell viability at 2.5 μM , $p < 0.05$, 0.005 and 0.001 at 24, 48 and 72h respectively as shown in figures 5.32, while L4 aptamer was not effected on Caco-2 cell viability at the same concentration ($p > 0.05$).

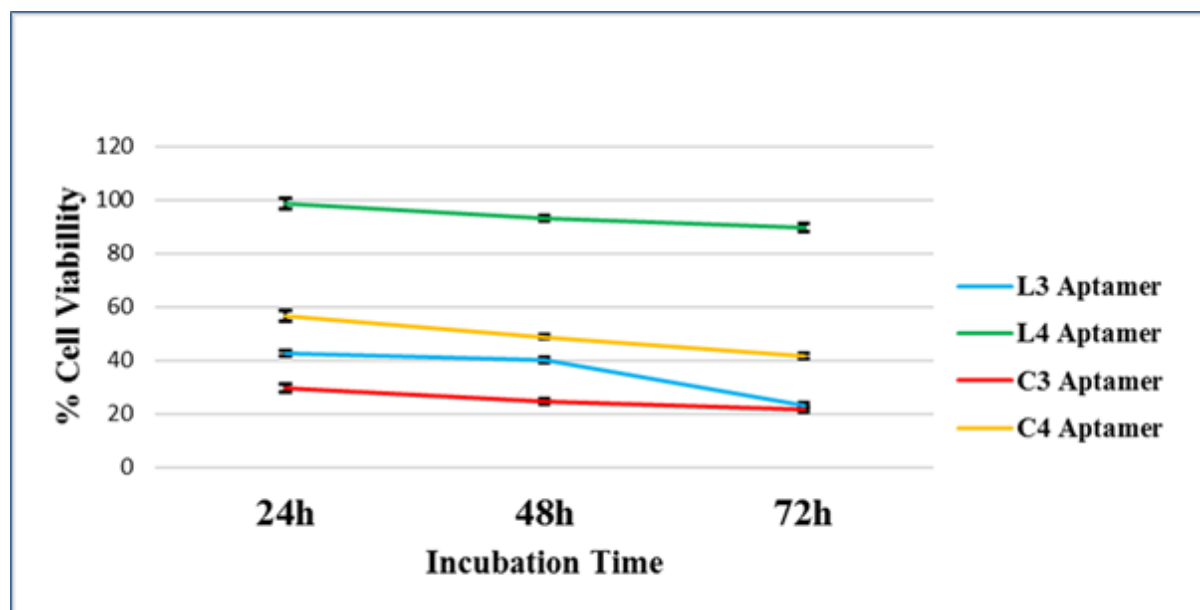


Figure 5.32: *In vitro* cell viability of the human colorectal adenocarcinoma (Caco-2) cells was detected by MTT assay. The results of Caco-2 cells post 24, 48 and 72h treatment of 2.5 μM (L3, L4, C3 and C4) aptamers. The absorbance was measured at 540 nm (reference wavelength 650 nm) using a microplate reader. The results represent the mean \pm SEM of 3 independent experiments. C3 aptamers have a strong inhibition ability for Caco-2 cells. $p < 0.05$, 0.005 and 0.001 at 24, 48 and 72h respectively vs. control.

Caco-2 cells which were treated with 50 μM TBHP also showed a reduction of 25% in cell viability after 24h compared to untreated cells; however, the difference was not statistically significant. The reduction in cell viability became more pronounced after treated with 2.5 μM L3, C3 and C4 aptamers and 50 μM TBHP, $p < 0.005$ (figures 5.33, 5.35 and 5.36). In addition, L4 aptamer was not effected to Caco-2 cells viability after treated with 50 μM TBHP, $p > 0.05$ (figure 5.34).

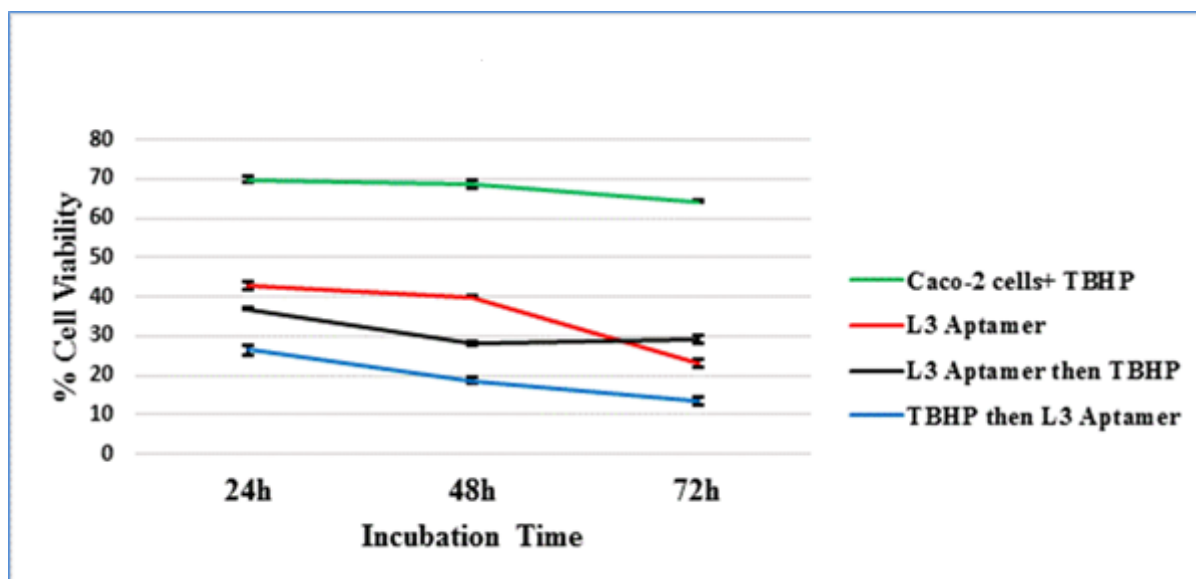


Figure 5.33: *In vitro* cell viability of the human colorectal adenocarcinoma (Caco-2) cells was detected by MTT assay. The results of Caco-2 cells post 24, 48 and 72h treatment with 2.5 μ M L3 aptamer also exposure to 50 μ M TBHP. The absorbance was measured at 540 nm (reference wavelength 650 nm) using a microplate reader. The results represent the mean \pm SEM of 3 independent experiments. $p < 0.005$ vs. control.

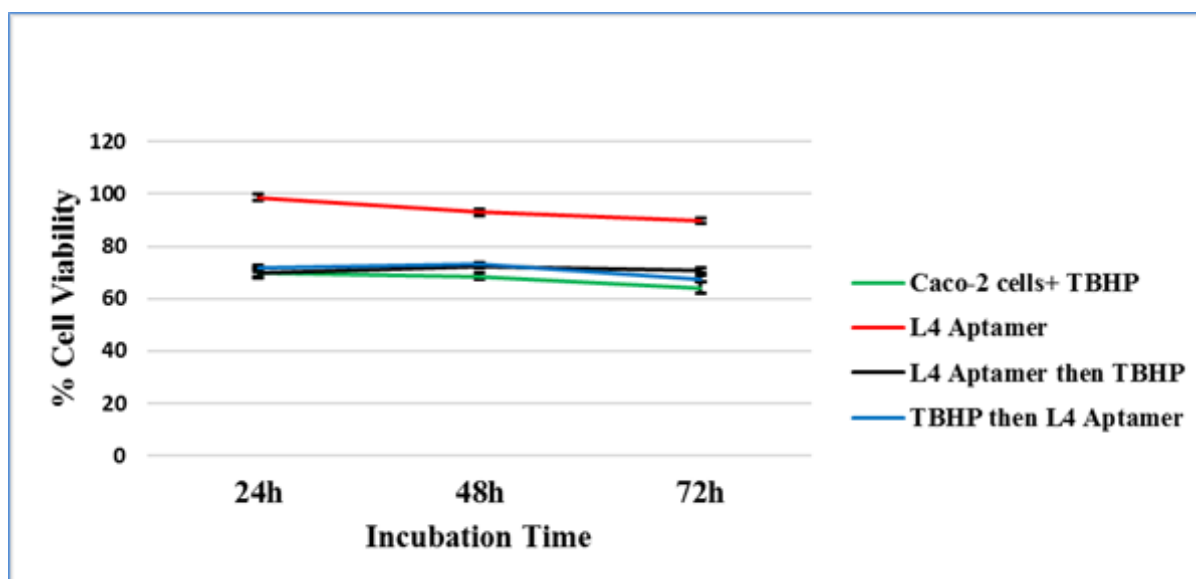


Figure 0.34: *In vitro* cell viability of the human colorectal adenocarcinoma (Caco-2) cells was detected by MTT assay. The results of Caco-2 cells post 24, 48 and 72h treatment with 2.5 μ M L4 aptamer also exposure to 50 μ M TBHP. The absorbance was measured at 540 nm (reference wavelength 650 nm) using a microplate reader. The results represent the mean \pm SEM of 3 independent experiments. $p > 0.05$ vs. control.

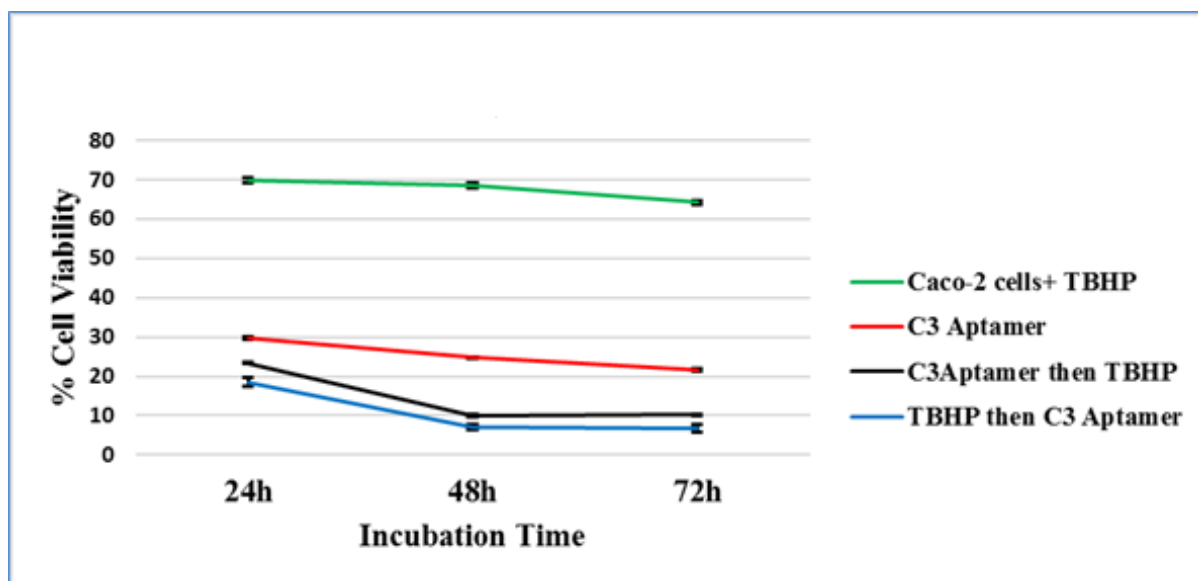


Figure 0.35: *In vitro* cell viability of the human colorectal adenocarcinoma (Caco-2) cells was detected by MTT assay. The results of Caco-2 cells post 24, 48 and 72h treatment with 2.5 μM C3 aptamer also exposure to 50 μM TBHP. The absorbance was measured at 540 nm (reference wavelength 650 nm) using a microplate reader. The results represent the mean \pm SEM of 3 independent experiments. $p < 0.005$ vs. control.

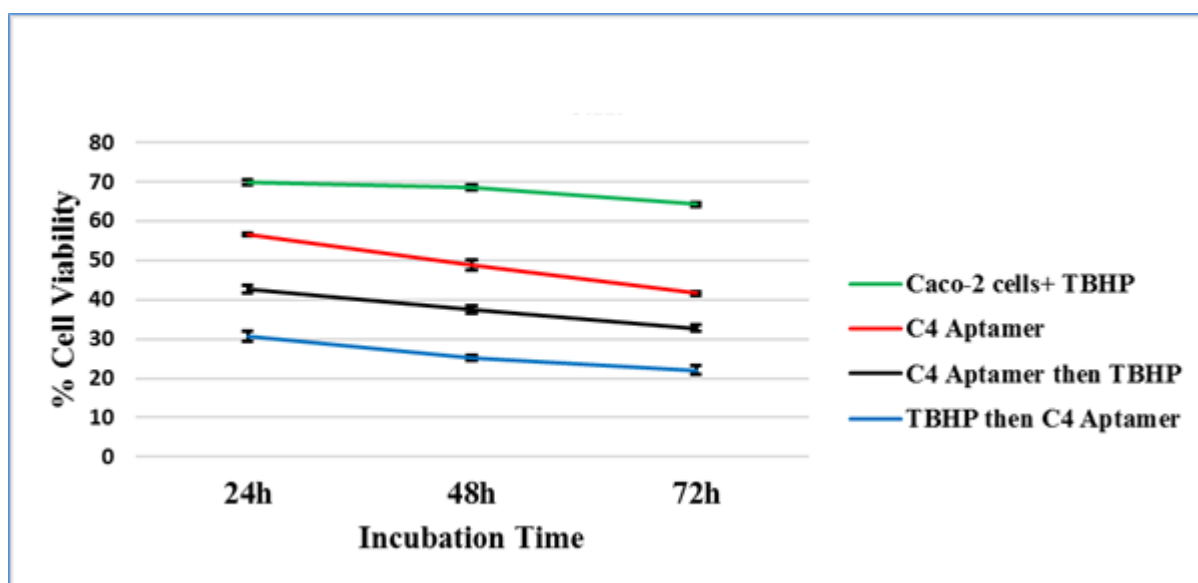


Figure 5.36: *In vitro* cell viability of the human colorectal adenocarcinoma (Caco-2) cells was detected by MTT assay. The results of Caco-2 cells post 24, 48 and 72h treatment with 2.5 μM C4 aptamer also exposure to 50 μM TBHP. The absorbance was measured at 540 nm (reference wavelength 650 nm) using a microplate reader. The results represent the mean \pm SEM of 3 independent experiments. $p < 0.005$ vs. control.

Based on the results presented in figure 5.37, cells exposed to 2.5 μM L3, C3 and C4 aptamers after 24h were presented a statistically significant increase of cell death when compared to untreated cells ($p < 0.005$). 2.5 μM aptamers and 50 μM TBHP treatment after 72h caused a cell death increase of 86.4%, 93.1% and 77.9% for L3, C3, and C4 respectively. Between the groups of aptamers, C3 aptamer was showed significantly higher percentage of cell death than L3, L4 and C4 aptamers ($p < 0.005$).

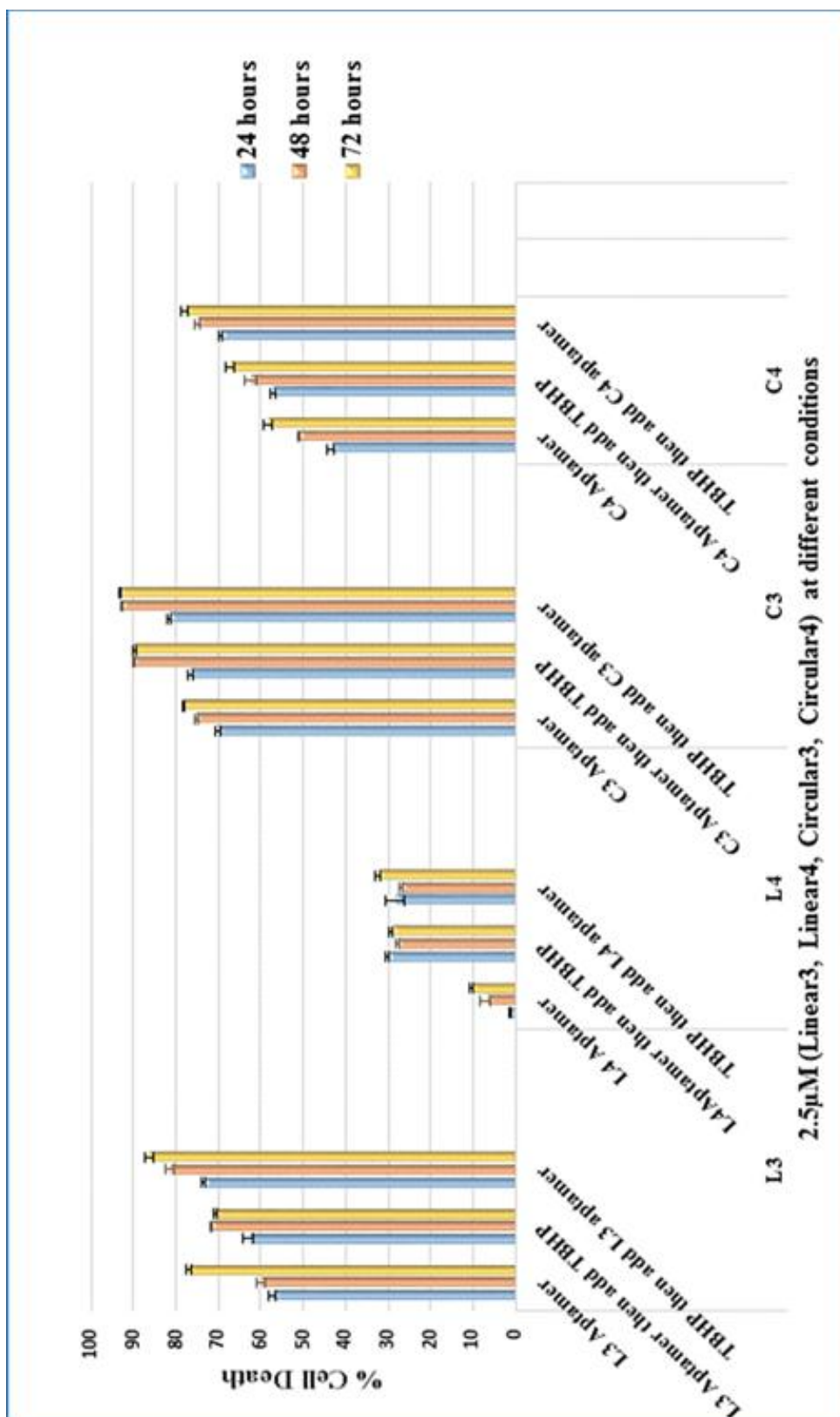


Figure 5.37: *In vitro* cell death percentage of the colorectal adenocarcinoma (Caco-2) cells was estimated by MTT assay in 96-well plates following 24, 48 and 72h exposure to 2.5 μ M (L3, L4, C3 and C4) aptamers and 50 μ M TBHP. Data is shown as % mean \pm SEM of cell death for 3 separate experiments. Treatment significantly different from the untreated controls $p < 0.005$.

5.3.1.7 Aneuploid Immortal Keratinocyte (HaCaT) Cells

Figure 5.38 illustrates the ability of L3, L4, C3 and C4 aptamers to inhibit the HaCaT cells viability. The C3 aptamer was significantly reduced the HaCaT cells viability after 24h compared with untreated cells ($p < 0.005$), while L3, L4, and C4 aptamers showed reduced the cell viability after 72h ($p < 0.05$).

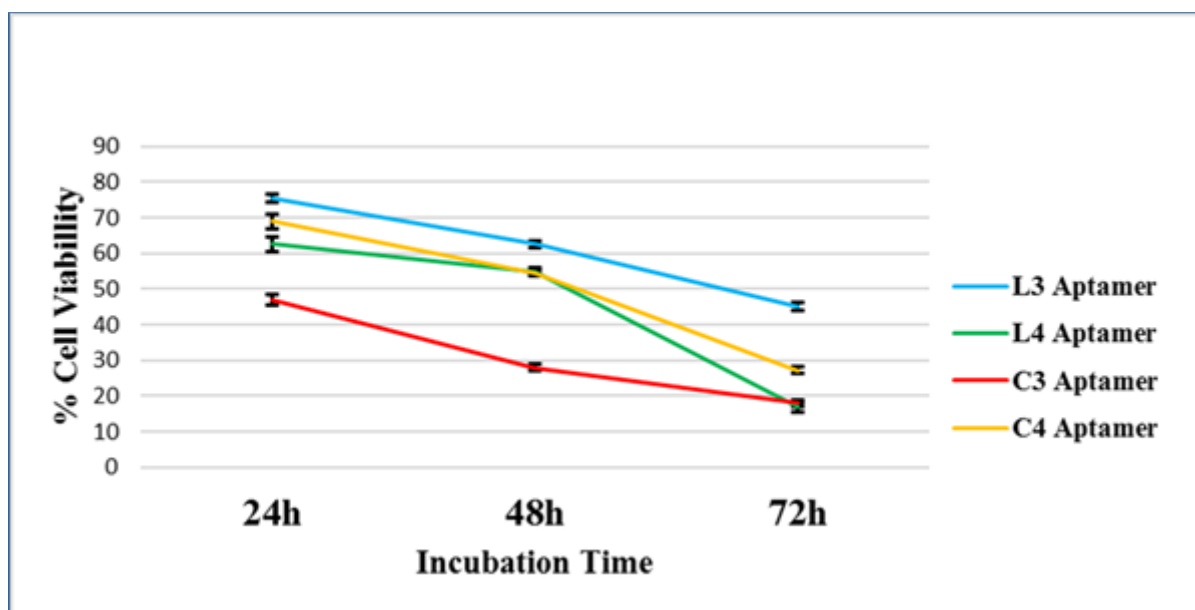


Figure 0.38: *In vitro* cell viability of the human aneuploid immortal keratinocyte (HaCaT) cells was detected by MTT assay. The results of HaCaT cells post 24, 48 and 72h treatment of 2.5 μ M (L3, L4, C3 and C4) aptamers. The absorbance was measured at 540 nm (reference wavelength 650 nm) using a microplate reader. The results represent the mean \pm SEM of 3 independent experiments. C3 aptamers have a strong inhibition ability for HaCaT cells. $p < 0.005$ vs. control.

Both 2.5 μ M C3 aptamer and 50 μ M TBHP treatments of HaCaT cells caused a statistical significant reduction in cell viability compared to viability of untreated cells ($p < 0.0001$) after 24h as shown in figures 5.41, while L3, L4, and C4 aptamers were showed reduce in cell viability after 48h when pre-treated with 50 μ M TBHP before added 2.5 μ M aptamers ($p < 0.05$) as described in figures 5.39, 5.40 and 5.42.

C3 aptamer showed the highest increase of HaCaT cell death by 82% when the cells were treated with 2.5 μ M C3 aptamer, 86.6% when the cells were treated with 2.5 μ M C3 aptamer then 50 μ M TBHP and 89% when the cells were treated with 50 μ M TBHP then 2.5 μ M C3 aptamer after 72h compared to L3, L4 and C4 aptamers ($p < 0.0005$) as shown in figure 5.43.

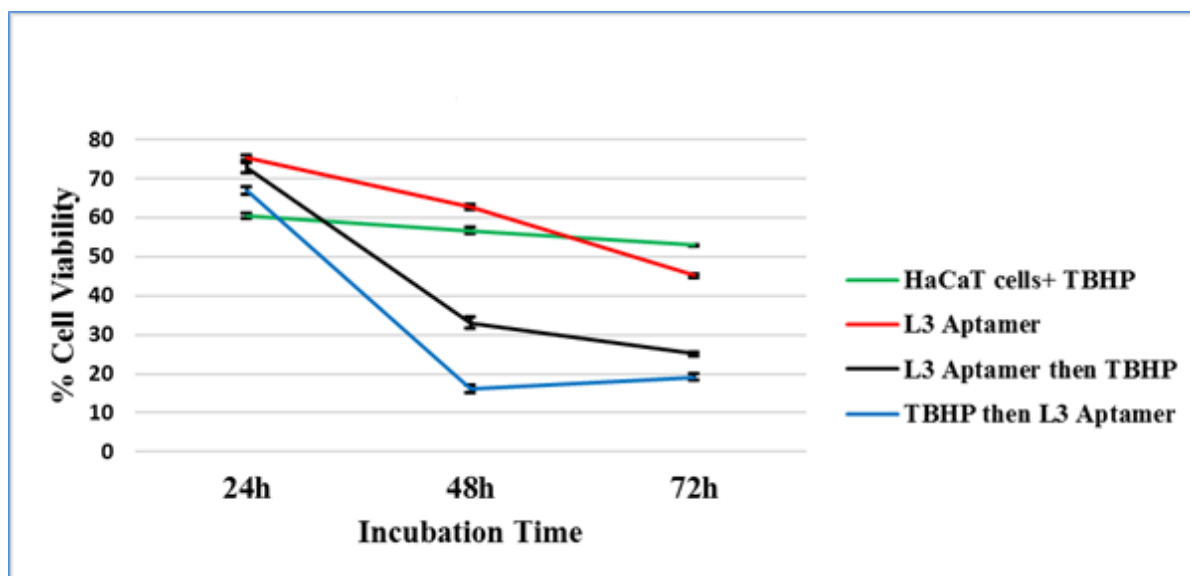


Figure 5.39: *In vitro* cell viability of the human aneuploid immortal keratinocyte (HaCaT) cells was detected by MTT assay. The results of HaCaT cells post 24, 48 and 72h treatment with 2.5 μ M L3 aptamer also exposure to 50 μ M TBHP. The absorbance was measured at 540 nm (reference wavelength 650 nm) using a microplate reader. The results represent the mean \pm SEM of 3 independent experiments. $p < 0.05$ vs. control.

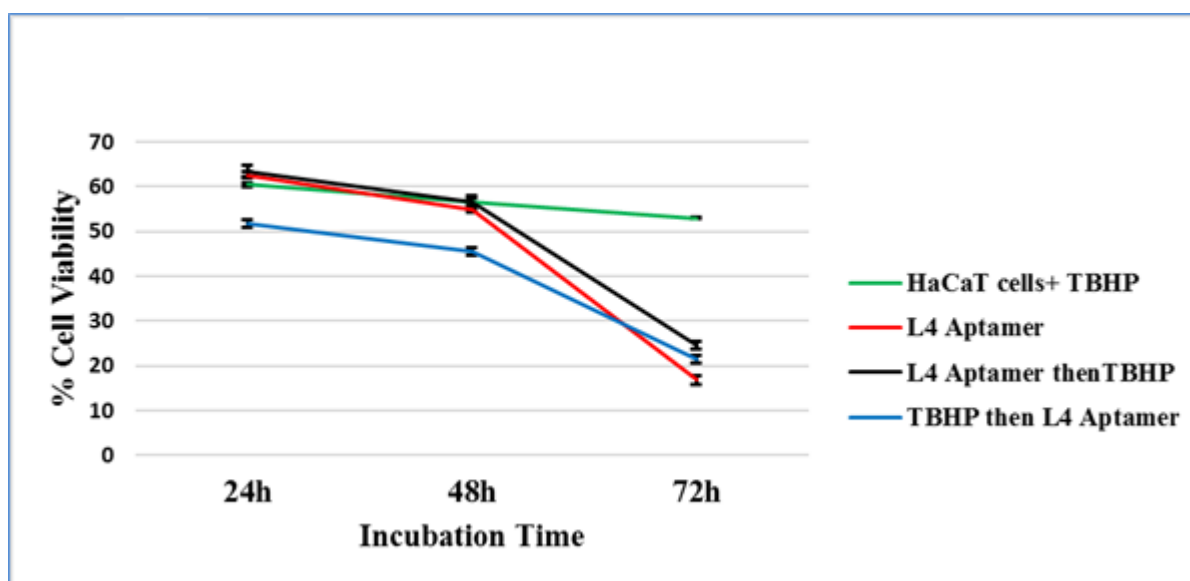


Figure 0.40: *In vitro* cell viability of the human aneuploid immortal keratinocyte (HaCaT) cells was detected by MTT assay. The results of HaCaT cells post 24, 48 and 72h treatment with 2.5 μ M L4 aptamer also exposure to 50 μ M TBHP. The absorbance was measured at 540 nm (reference wavelength 650 nm) using a microplate reader. The results represent the mean \pm SEM of 3 independent experiments. $p < 0.05$ vs. control.

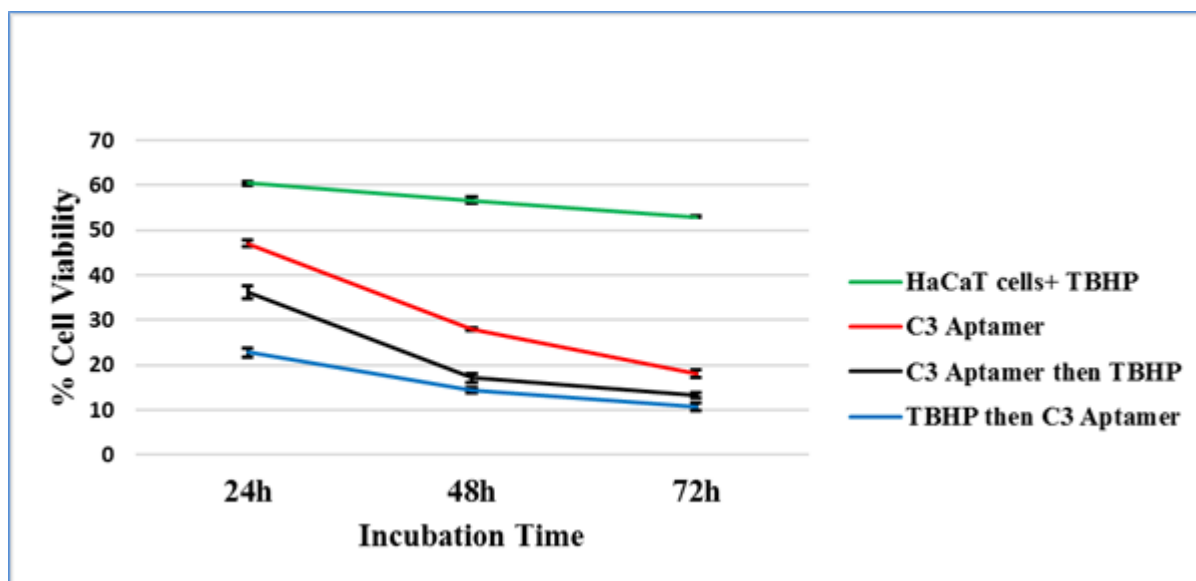


Figure 5.41: *In vitro* cell viability of the human aneuploid immortal keratinocyte (HaCaT) cells was detected by MTT assay. The results of haCaT cells post 24, 48 and 72h treatment with 2.5 μ M C3 aptamer also exposure to 50 μ M TBHP. The absorbance was measured at 540 nm (reference wavelength 650 nm) using a microplate reader. The results represent the mean \pm SEM of 3 independent experiments. C3 aptamer with TBHP have a strong inhibition ability for HaCaT cells at 24, 48 and 72h. $p < 0.0001$ vs. control.

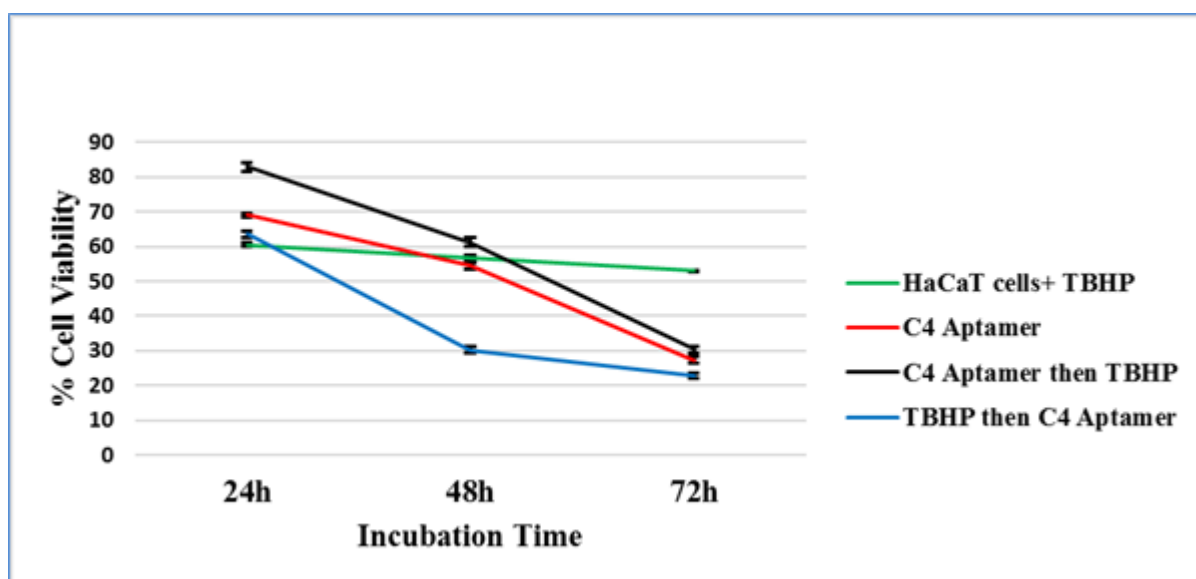


Figure 0.42: *In vitro* cell viability of the human aneuploid immortal keratinocyte (HaCaT) cells was detected by MTT assay. The results of HaCaT cells post 24, 48 and 72h treatment with 2.5 μ M C4 aptamers also exposure to 50 μ M TBHP. The absorbance was measured at 540 nm (reference wavelength 650 nm) using a microplate reader. The results represent the mean \pm SEM of 3 independent experiments. $p < 0.05$ vs. control.

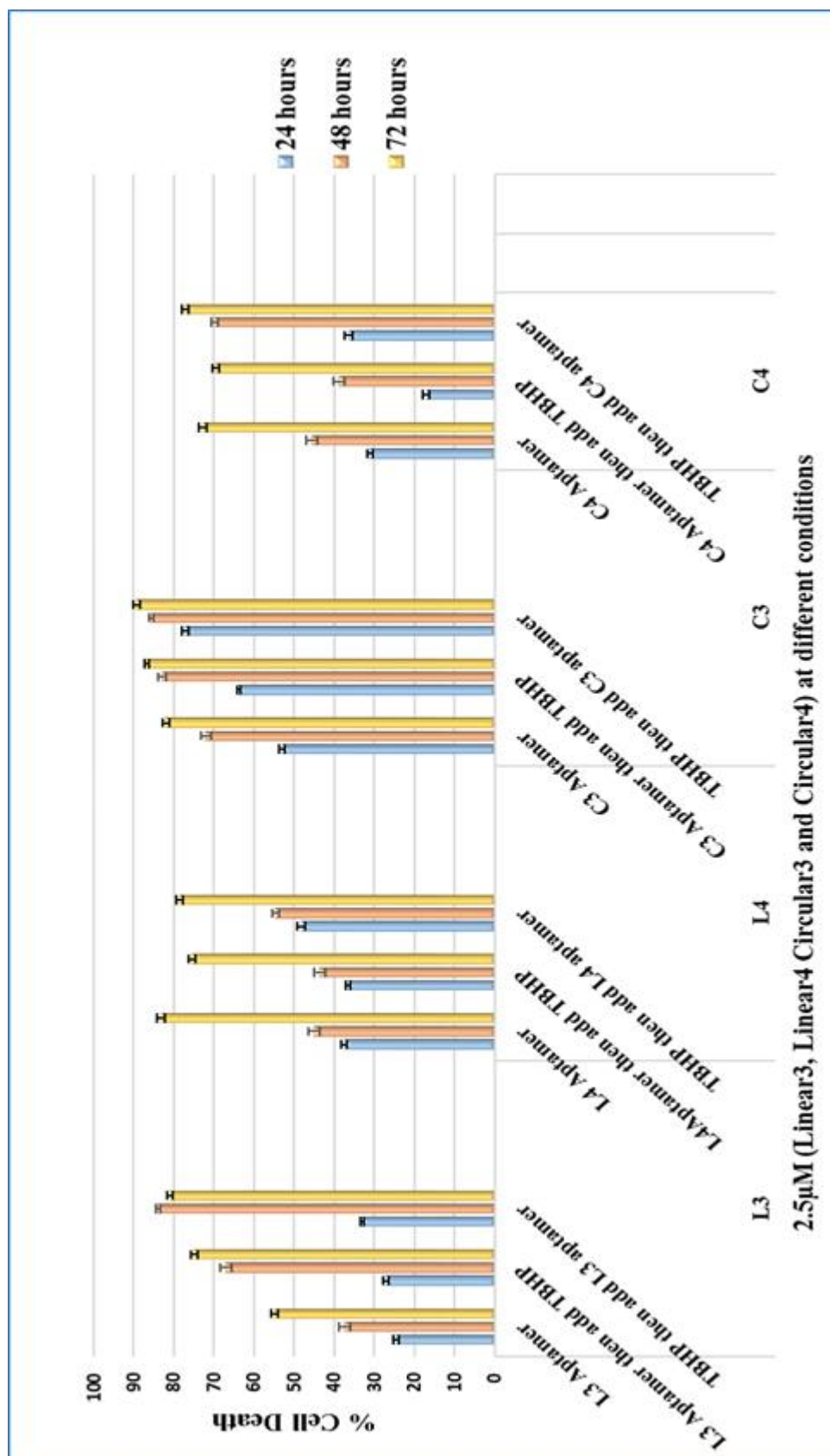


Figure 5.43: *In vitro* cell death percentage of the human aneuploid immortal keratinocyte (HaCaT) cells was estimated by MTT assay in 96-well plates following 24, 48 and 72 exposure to 2.5 μ M (L3, L4, C3 and C4) aptamers and 50 μ M TBHP. Data is shown as % mean \pm SEM of cell death for of 3 separate experiments. Treatment significantly different from the untreated controls $p < 0.0005$.

5.3.1.8 Normal Human Bronchial Epithelial Cells (Beas-2b)

Beas-2b cell line was used in this study to compare the effect of aptamers on cancer cell line with the normal cell line. Figure 5.44 demonstrates the cell viability of Beas-2b after treatment with 2.5 μM L3, L4, C3 and C4 aptamers at 24, 48 and 72h. Results were showed that all aptamers had not affected on Beas-2b cells viability.

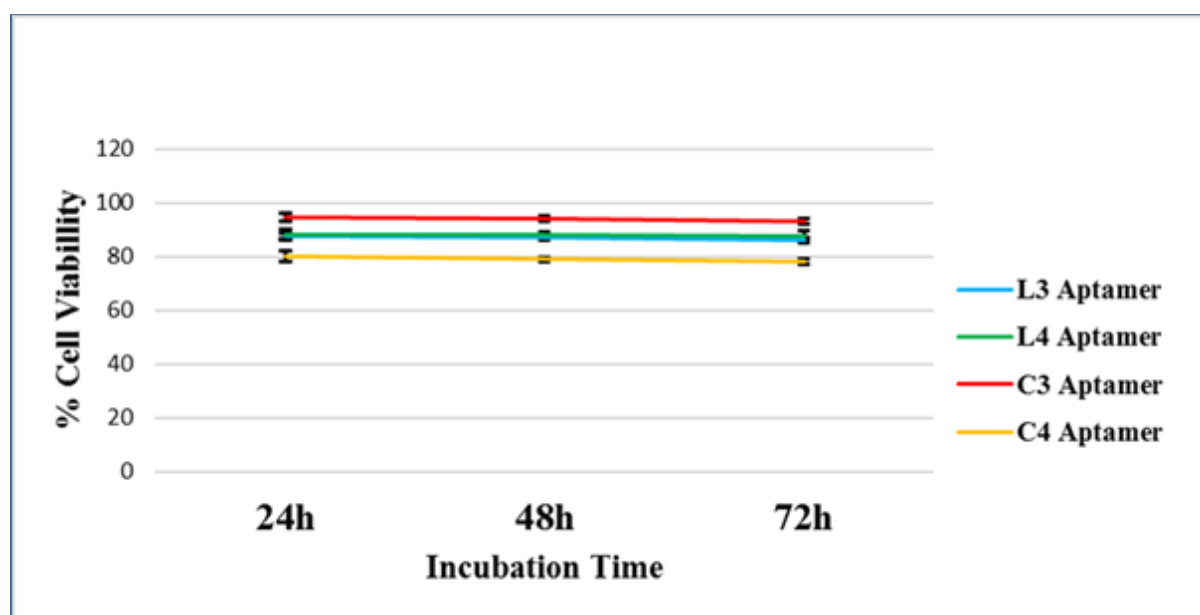


Figure 5.44: *In vitro* cell viability of normal human bronchial epithelial cells (Beas-2b) cells was detected by MTT assay. The results of Beas-2b cells post 24, 48 and 72h treatment of 2.5 μM (L3, L4, C3 and C4) aptamers. The absorbance was measured at 540 nm (reference wavelength 650 nm) using a microplate reader. The results represent the mean \pm SEM of 3 independent experiments. $p > 0.05$ vs. control.

Interestingly, pre-treated Beas-2b cells with 2.5 μM L3, L4, C3 and C4 aptamers and 50 μM TBHP were showed not affected on Beas-2b cells viability as described in figures 5.45-5.48. Figure 5.46 was illustrated the percentage of Beas-2b cell death after treatment with 2.5 μM aptamers and 50 μM TBHP.

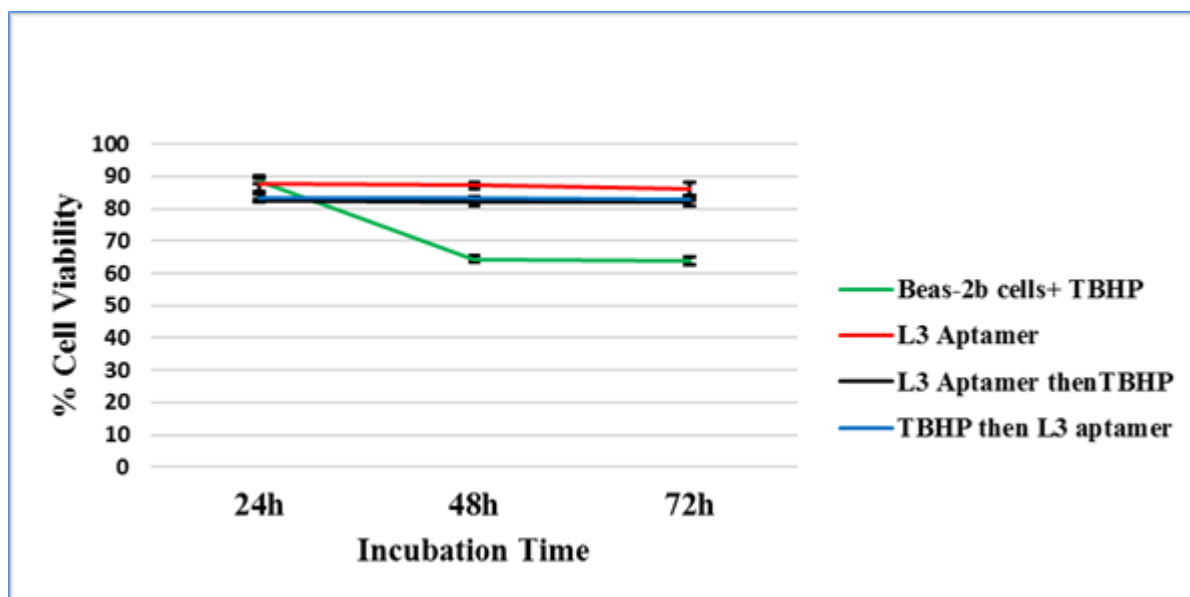


Figure 0.45: *In vitro* cell viability of normal human bronchial epithelial cells (Beas-2b) cells was detected by MTT assay. The results of Beas-2b cells post 24, 48 and 72h treatment with 2.5 μM L3 aptamer also exposure to 50 μM TBHP. The absorbance was measured at 540 nm (reference wavelength 650 nm) using a microplate reader. The results represent the mean \pm SEM of 3 independent experiments. $p > 0.05$ vs. control.

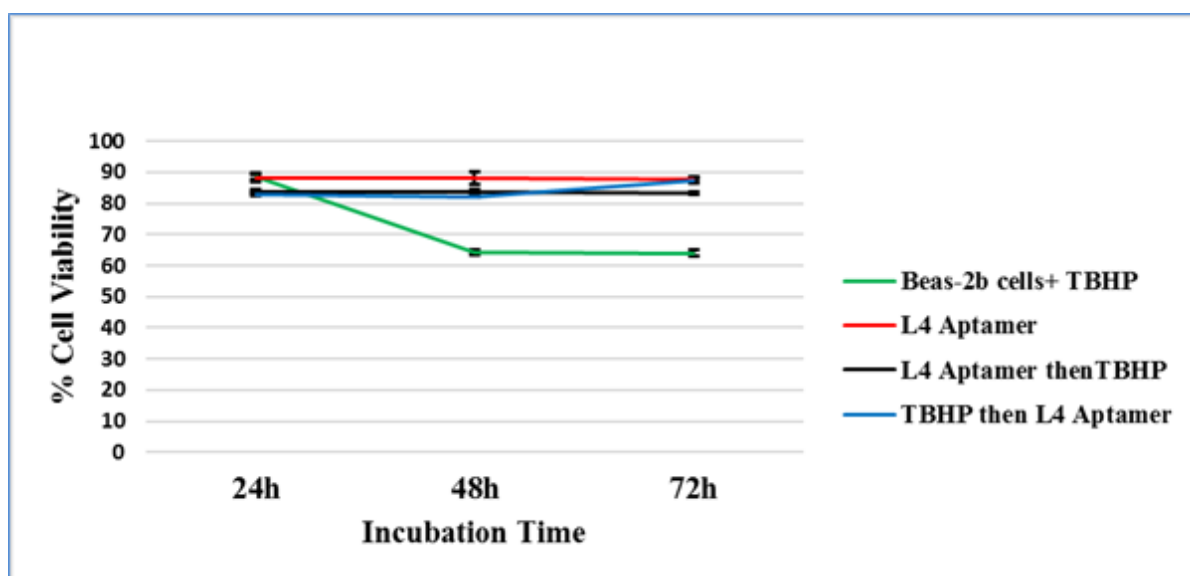


Figure 0.46: *In vitro* cell viability of normal human bronchial epithelial cells (Beas-2b) cells was detected by MTT assay. The results of Beas-2b cells post 24, 48 and 72h treatment with 2.5 μM L4 aptamer also exposure to 50 μM TBHP. The absorbance was measured at 540 nm (reference wavelength 650 nm) using a microplate reader. The results represent the mean \pm SEM of 3 independent experiments. $p > 0.05$ vs. control.

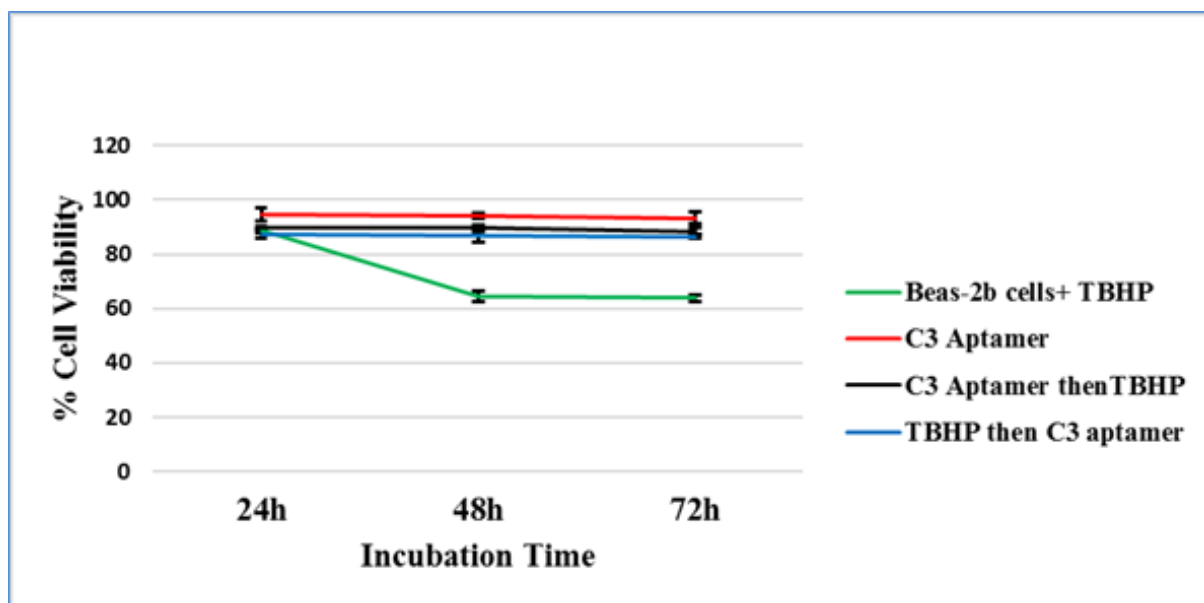


Figure 5.47: *In vitro* cell viability of normal human bronchial epithelial cells (Beas-2b) cells was detected by MTT assay. The results of Beas-2b cells post 24, 48 and 72h treatment with 2.5 μM C3 aptamer also exposure to 50 μM TBHP. The absorbance was measured at 540 nm (reference wavelength 650 nm) using a microplate reader. The results represent the mean \pm SEM of 3 independent experiments. $p > 0.05$ vs. control.

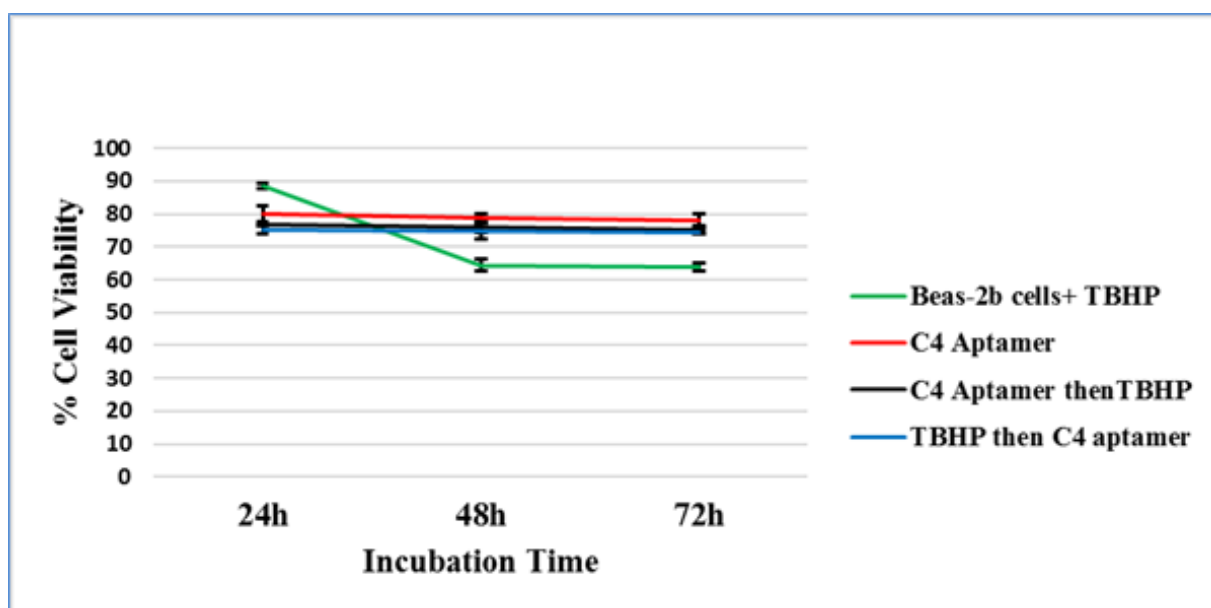


Figure 5.48: *In vitro* cell viability of normal human bronchial epithelial cells (Beas-2b) cells was detected by MTT assay. The results of Beas-2b cells post 24, 48 and 72h treatment with 2.5 μM C4 aptamer also exposure to 50 μM TBHP. The absorbance was measured at 540 nm (reference wavelength 650 nm) using a microplate reader. The results represent the mean \pm SEM of 3 independent experiments. $p > 0.05$ vs. control.

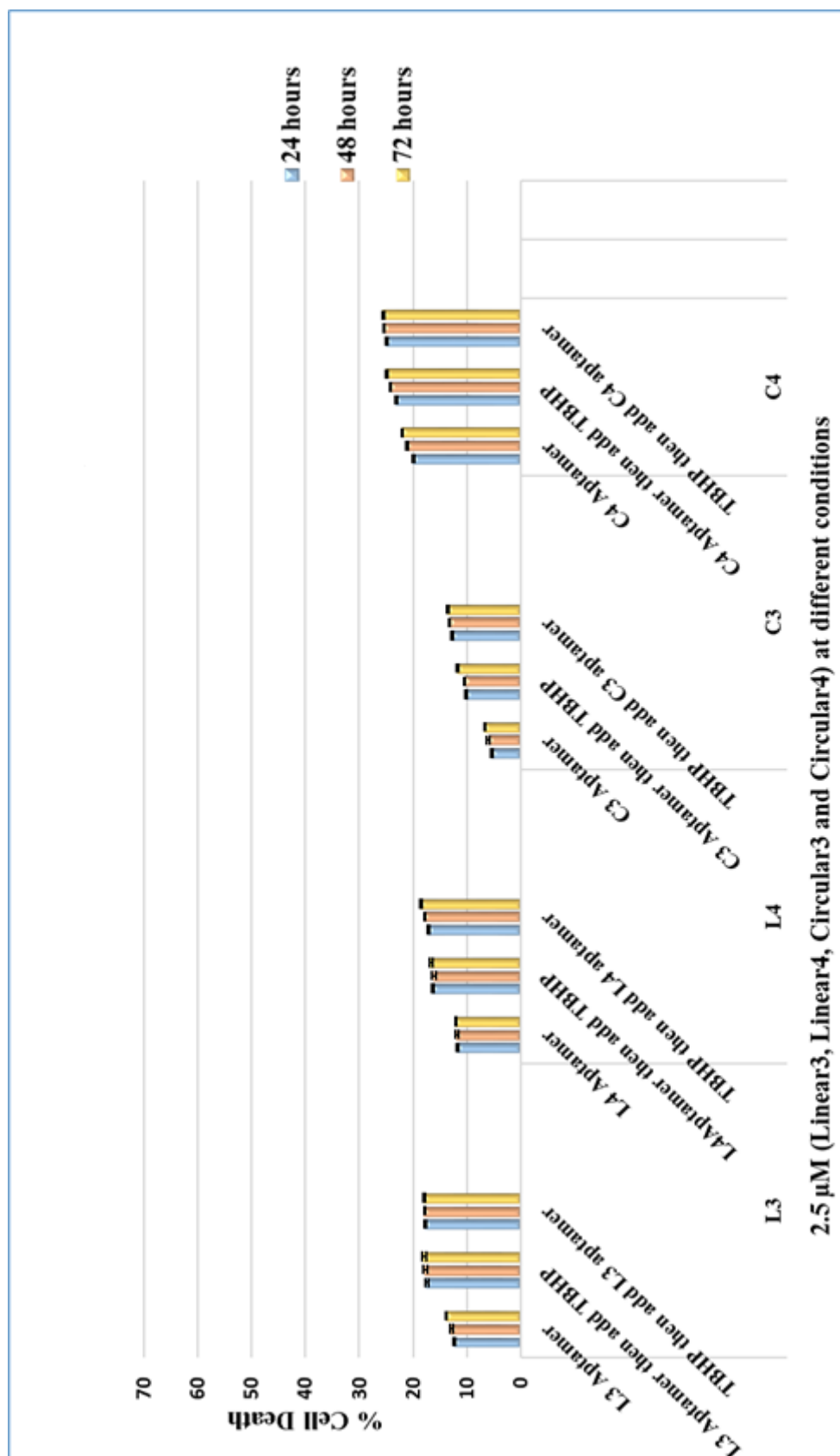


Figure 0.49: *In vitro* cell viability of normal human bronchial epithelial cells (Beas-2b) was detected by MTT assay. The results of Beas-2b cells post 24h treatment of 2.5 μM (L3, L4, C3 and C4) aptamers also exposure to 50 μM TBHP at 24h. The absorbance was measured at 540 nm (reference wavelength 650 nm) using a microplate reader. The results represent the mean absorbance ± SEM of 3 independent experiments. Aptamers have not affected on Beas-2b cells viability. $p > 0.05$ vs. control.

In summary, the percentage of cell death for all cancer cells A549, HepG2, MCF-7, MDA-MB-468, U2OS, Caco-2 that they were treated with C3 aptamer was significantly higher than the percentage of cell death when the cells were pre-treated with other aptamers (C4, L3 and L4). In conclusion, we will recommend that C3 aptamer is the best-selected aptamer to use as therapeutic for cancer between all aptamers, where it was achieved the highest affinity and selectivity with SIRT1 and the highest percentage of cancer cell death.

5.3.2 Effect of Linear3, Linear4, Circular3 and Circular4 aptamers on Intracellular ROS Production in 8 Cell Lines

To investigate the antioxidative effect of L3, L4, C3, and C4 aptamers, the ability to prevent the production of ROS in 8 cell lines (A549, HepG2, MCF-7, MDA-MB-468, U2OS, Caco-2, HaCaT, and Beas-2b) was evaluated. As shown in figure 5.50-5.54 for A549, MCF-7, MDA-MB-468, U2OS and Caco-2 cell lines, incubation of these cells with 2.5 μM L3, L4, C3 and C4 aptamers at 6h were slightly decreased the levels of endogenous ROS as assessed using the fluorescent probe DCF. When cells were exposed to 50 μM TBHP (tert-Butyl hydroperoxide (tBuOOH) is an organic peroxide widely used in a variety of oxidation processes), a marked increase was observed in the intracellular ROS level ($p < 0.005$). In fact, when cells were pre-incubated with 2.5 μM L3, L4, C3 and C4 aptamers for 4h before being exposed to 50 μM TBHP, the levels of ROS observed after 45 min were slightly increased than the same cells which were pre-treated with 2.5 μM L3, L4, C3 and C4 aptamers only ($p < 0.05$). When the same cells were exposed to 50 μM TBHP before adding 2.5 μM L3, L4, C3 and C4 aptamers, the levels of ROS observed after 45 min were increased significantly than cells of control and cells were pre-treated with aptamers firstly ($p < 0.005$). The C3 aptamer was significantly decreased the ROS level on A549, MCF-7, MDA-MB-468, U2OS and Caco-2 cell lines compared with L3, L4 and C4 aptamers, $p < 0.005$.

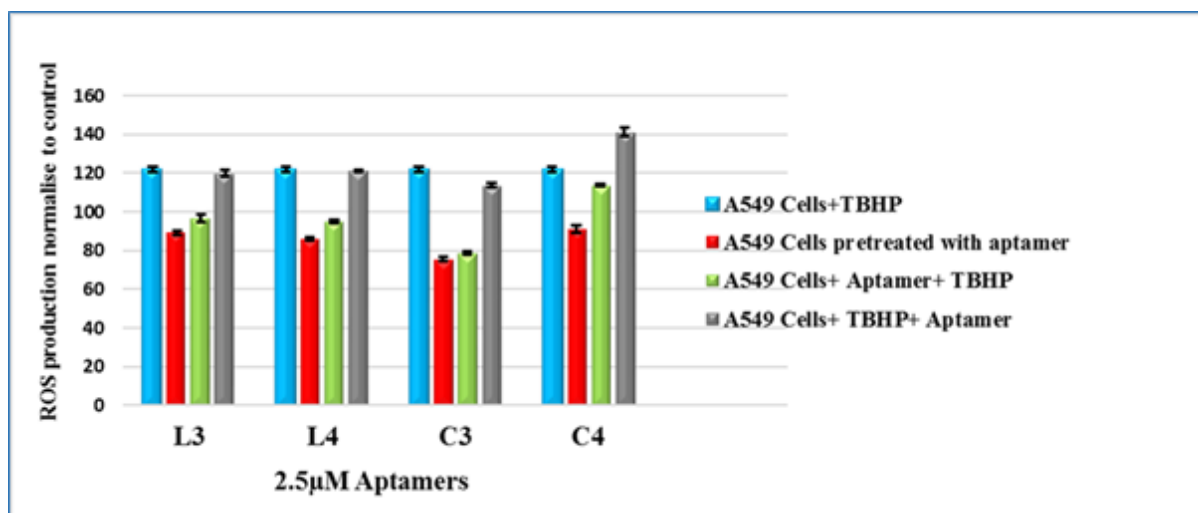


Figure 0.50: Effects of L3, L4, C3 and C4 aptamers on intracellular ROS production in A549 cells, using DCF as fluorescent probe. Cells were pre-incubated with the 2.5 μ M of L3, L4, C3 and C4 aptamers, then cells were exposed to 50 μ M TBHP (Tert-Butyl Hydrogen Peroxide) before and after 4h from adding the aptamers. After a recovery period 6h, the culture was incubated with the DCFDA solution for about 45min at 37° C. DCF fluorescence was measured at an excitation wavelength of 485 nm and an emission wavelength of 535 nm. The results represent the mean \pm SEM of three different experiments performed in triplicate. $p < 0.005$.

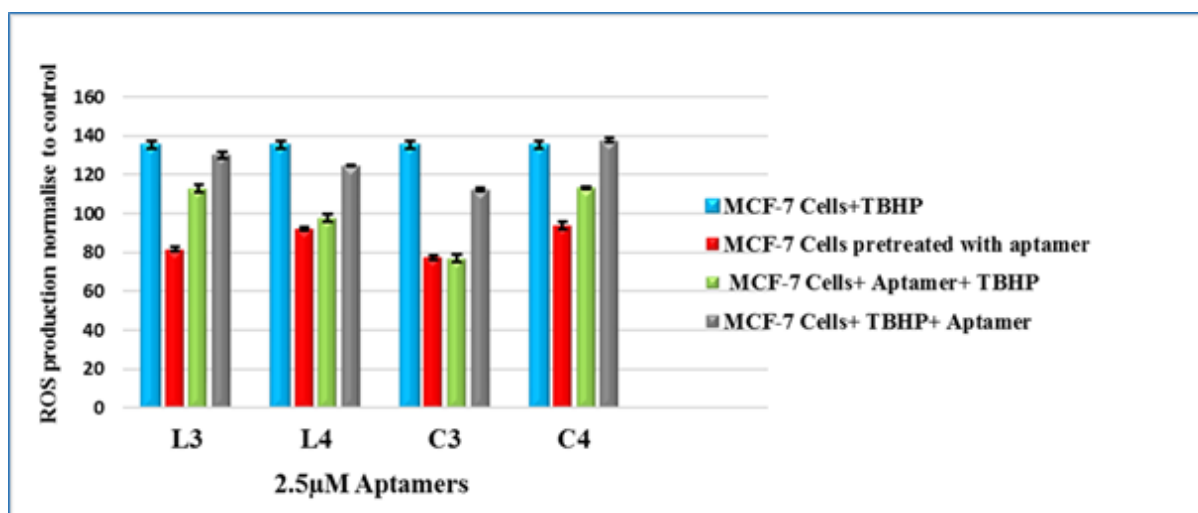


Figure 0.51: Effects of L3, L4, C3 and C4 aptamers on intracellular ROS production in MCF-7 cells, using DCF as fluorescent probe. Cells were pre-incubated with the 2.5 μ M of L3, L4, C3 and C4 aptamers, then cells were exposed to 50 μ M TBHP (Tert-Butyl Hydrogen Peroxide) before and after 4h from adding the aptamers. After a recovery period 6h, the culture was incubated with the DCFDA solution for about 45min at 37° C. DCF fluorescence was measured at an excitation wavelength of 485 nm and an emission wavelength of 535 nm. The results represent the mean \pm SEM of three different experiments performed in triplicate. $p < 0.005$.

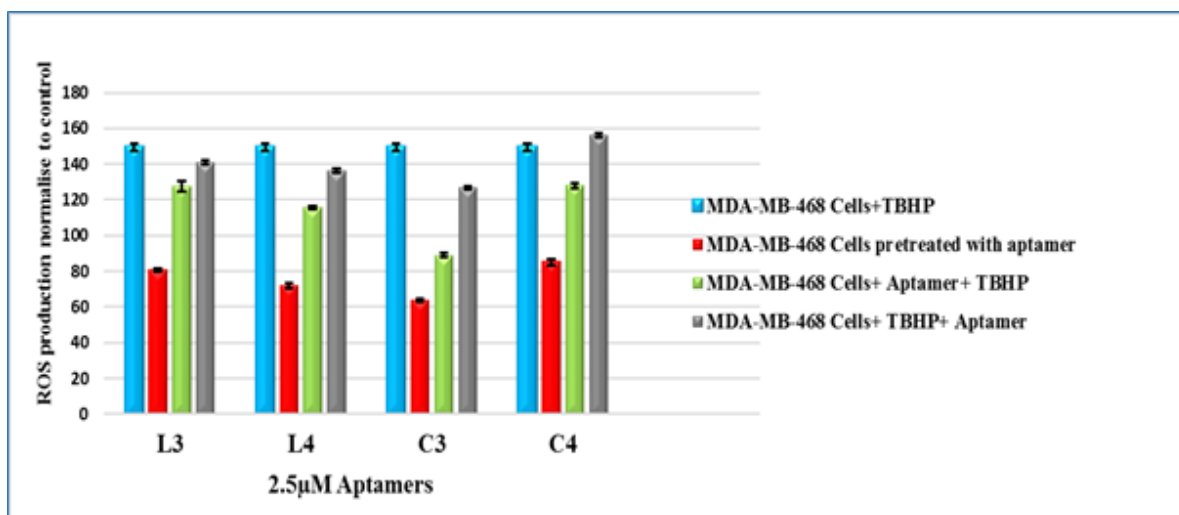


Figure 0.52: Effects of L3, L4, C3 and C4 aptamers on intracellular ROS production in MDA-MB-468 cells, using DCF as fluorescent probe. Cells were pre-incubated with the 2.5 µM of L3, L4, C3 and C4 aptamers, then cells were exposed to 50 µM TBHP (Tert-Butyl Hydrogen Peroxide) before and after 4h from adding the aptamers. After a recovery period 6h, the culture was incubated with the DCFDA solution for about 45min at 37° C. DCF fluorescence was measured at an excitation wavelength of 485 nm and an emission wavelength of 535 nm. The results represent the mean ± SEM of three different experiments performed in triplicate. $P < 0.005$.

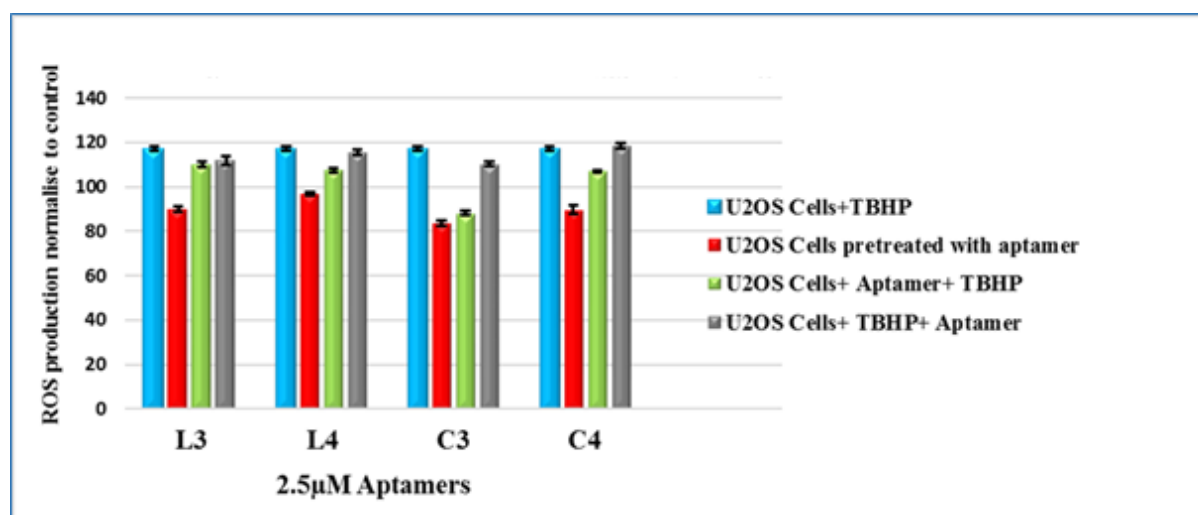


Figure 0.53: Effects of L3, L4, C3 and C4 aptamers on intracellular ROS production in U2OS cells, using DCF as fluorescent probe. Cells were pre-incubated with the 2.5 µM of L3, L4, C3 and C4 aptamers, then cells were exposed to 50 µM TBHP (Tert-Butyl Hydrogen Peroxide) before and after 4h from adding the aptamers. After a recovery period 6h, the culture was incubated with the DCFDA solution for about 45min at 37° C. DCF fluorescence was measured at an excitation wavelength of 485 nm and an emission wavelength of 535 nm. The results represent the mean ± SEM of three different experiments performed in triplicate. $p < 0.005$.

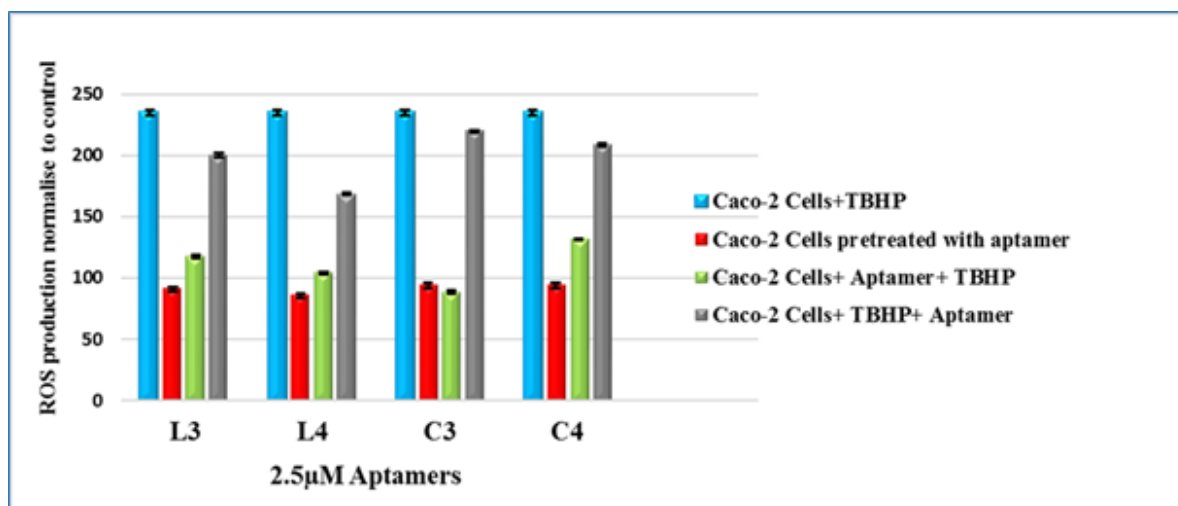


Figure 0.54: Effects of L3, L4, C3 and C4 aptamers on intracellular ROS production in Caco-2 cells, using DCF as fluorescent probe. Cells were pre-incubated with the 2.5 μM of L3, L4, C3 and C4 aptamers, then cells were exposed to 50 μM TBHP (Tert-Butyl Hydrogen Peroxide) before and after 4h from adding the aptamers. After a recovery period 6h, the culture was incubated with the DCFDA solution for about 45min at 37° C. DCF fluorescence was measured at an excitation wavelength of 485 nm and an emission wavelength of 535 nm. The results represent the mean ± SEM of three different experiments performed in triplicate. $p < 0.005$.

According to the effect of L3, L4, C3 and C4 aptamers on intracellular ROS production in HepG2 cells, the results showed that ROS level were decreased in cells pre-treated with aptamers and more decreased when cells treated with aptamers and exposed to 50 μM TBHP except C4 aptamer was showed increased the ROS level after adding 50 μM TBHP. However, the ROS level was increased again when cells exposed to 50 μM TBHP before adding the aptamers (figure 5.55). The C3 aptamer was significantly decreased the ROS level on HepGe2 cell lines compared with L3, L4 and C4 aptamers, $p < 0.005$.

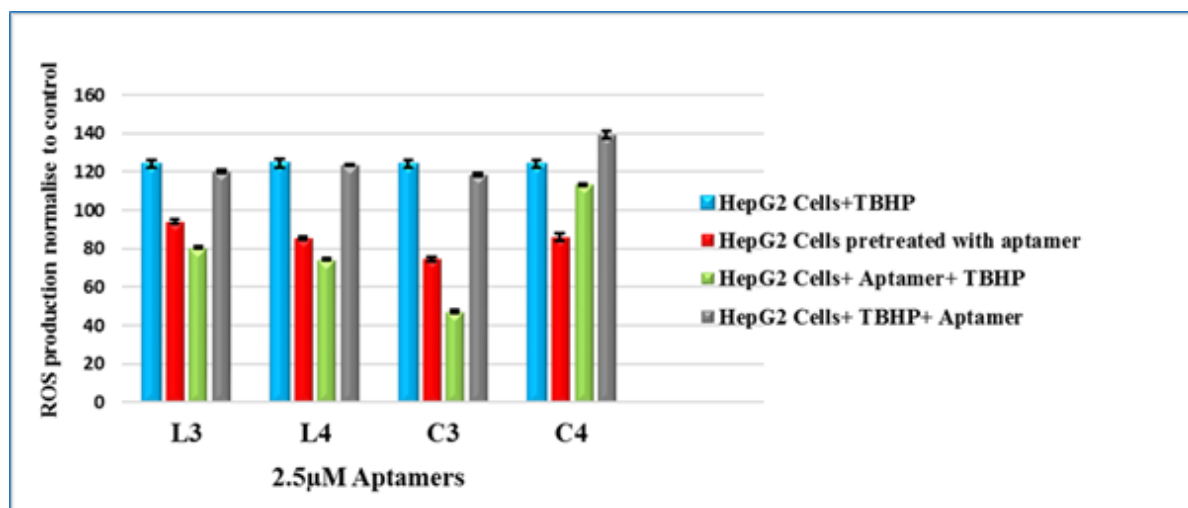


Figure 5.55: Effects of L3, L4, C3 and C4 aptamers on intracellular ROS production in HepG2 cells, using DCF as fluorescent probe. Cells were pre-incubated with the 2.5 µM of L3, L4, C3 and C4 aptamers, then cells were exposed to 50 µM TBHP (Tert-Butyl Hydrogen Peroxide) before and after 4h from adding the aptamers. After a recovery period 6h, the culture was incubated with the DCFDA solution for about 45min at 37° C. DCF fluorescence was measured at an excitation wavelength of 485 nm and an emission wavelength of 535 nm. The results represent the mean ± SEM of three different experiments performed in triplicate. $p < 0.005$.

In contrast, L3, L4, C3 and C4 aptamers were increased the intracellular ROS production in HaCaT cells as shown in figure 5.56 ($p < 0.001$).

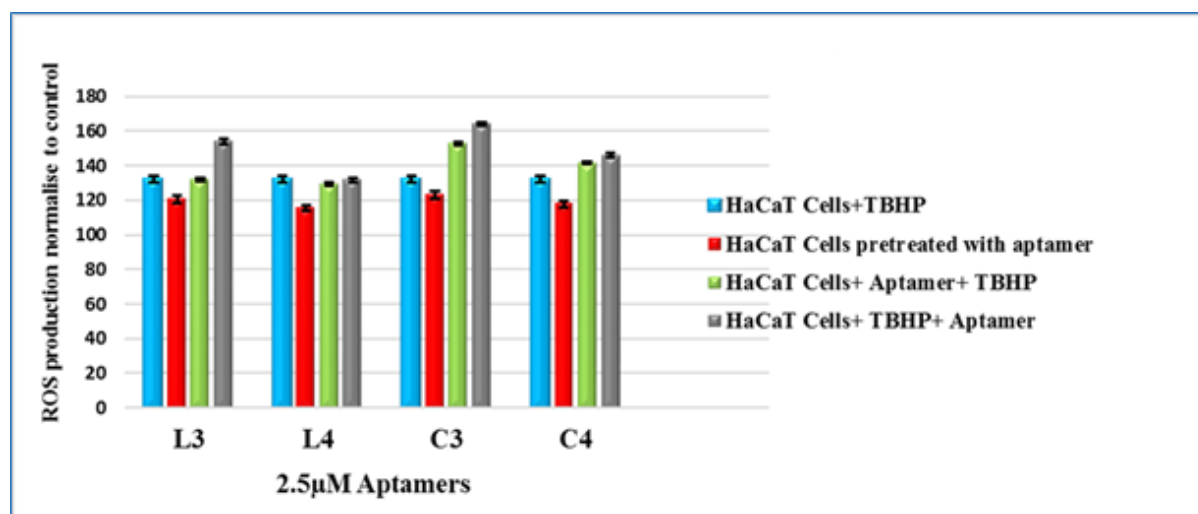


Figure 0.56: Effects of L3, L4, C3 and C4 aptamers on intracellular ROS production in HaCaT cells, using DCF as fluorescent probe. Cells were pre-incubated with the 2.5 µM of L3, L4, C3 and C4 aptamers, then cells were exposed to 50 µM TBHP (Tert-Butyl Hydrogen Peroxide) before and after 4h from adding the aptamers. After a recovery period 6h, the culture was incubated with the DCFDA solution for about 45min at 37° C. DCF fluorescence was measured at an excitation wavelength of 485 nm and an emission wavelength of 535 nm. The results represent the mean ± SEM of three different experiments performed in triplicate. $p < 0.005$.

According to the results of Beas-2b cells, it was observed that all aptamers have not effect on intracellular ROS production ($p > 0.05$) as shown in figure 5.57.

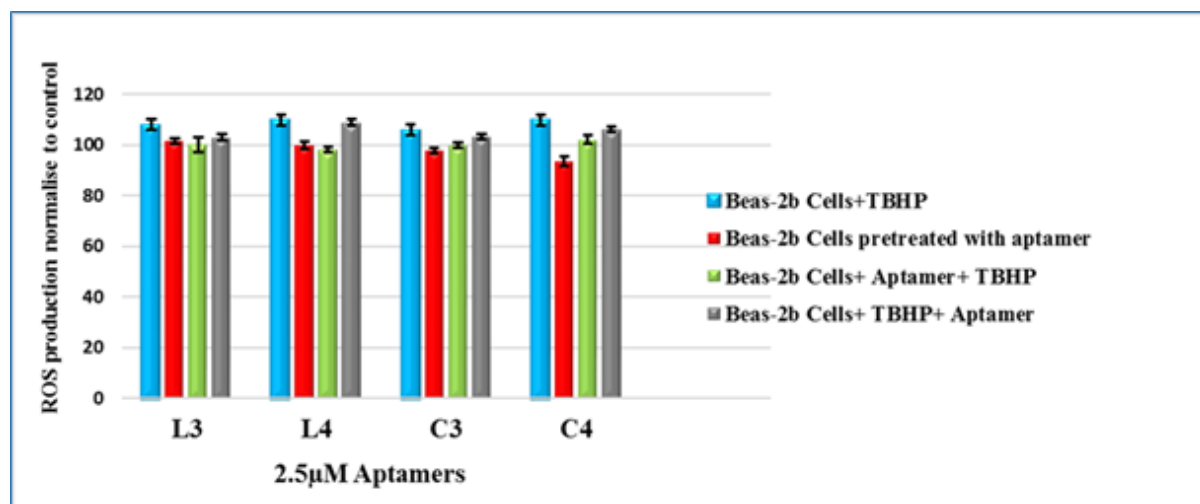


Figure 0.57: Effects of L3, L4, C3 and C4 aptamers on intracellular ROS production in Beas-2b cells, using DCF as fluorescent probe. Cells were pre-incubated with the 2.5 μ M of L3, L4, C3 and C4 aptamers, then cells were exposed to 50 μ M TBHP (Tert-Butyl Hydrogen Peroxide) before and after 4h from adding the aptamers. After a recovery period 6h, the culture was incubated with the DCFDA solution for about 45min at 37° C. DCF fluorescence was measured at an excitation wavelength of 485 nm and an emission wavelength of 535 nm. The results represent the mean \pm SEM of three different experiments performed in triplicate. $p > 0.05$.

In summary, the results in figures 5.50-5.55 were illustrates that ROS level were decreased in cancer cells which treated with aptamers since it increases the activity of SIRT1 enzyme, therefore the increased activity of SIRT1 enzyme can control and inhibited the level of ROS when the cells treated with aptamers before added the TBHP if they compared with the increased level of ROS in cancer cells when these cells were treated with TBHP before added aptamers whereas this increase in the level of ROS can be inhibited the activity of SIRT1.

5.3.3 *In vitro* Study the Activity of SIRT1 Enzyme by C3 in Cells by Fluor de Lys Deacetylase Assay

After the obtained results from the performed studies of mechanisms and stability on the L3, L4, C3 and C4 aptamers in current work, and studying their effect on the growth of the 6 cancer cells and 2 normal cells, it has been found that C3 is the best aptamer among them because it has several factors that helped it to be the best aptamer among them like the KD value and the highest percentage of cancer cell death. Therefore, a study of aptamers mechanism on growth inhibition of cancer cells was limited to C3 aptamer at different lower concentrations. In this experiment, SIRT1 activity, cell viability and intracellular ROS production was estimated on A549, HepG2, MCF-7, MDA-MB-468, U2OS, Caco-2, HaCaT, and Beas-2b cell lines in parallel under the same conditions to investigate the mechanism of

C3 aptamer in cells (Data for the effect of C3 aptamer on % cell death and intracellular ROS production in section 5.3.4).

The activity of SIRT1 on A549 cells which are pretreated with C3 aptamer at concentrations 0.5 and 1 μM were markedly increased compared with control (the level of SIRT1 in A549 cells) and 100 μM resveratrol (SIRT1 activators) ($p < 0.0005$) as shown in figure 5.58.

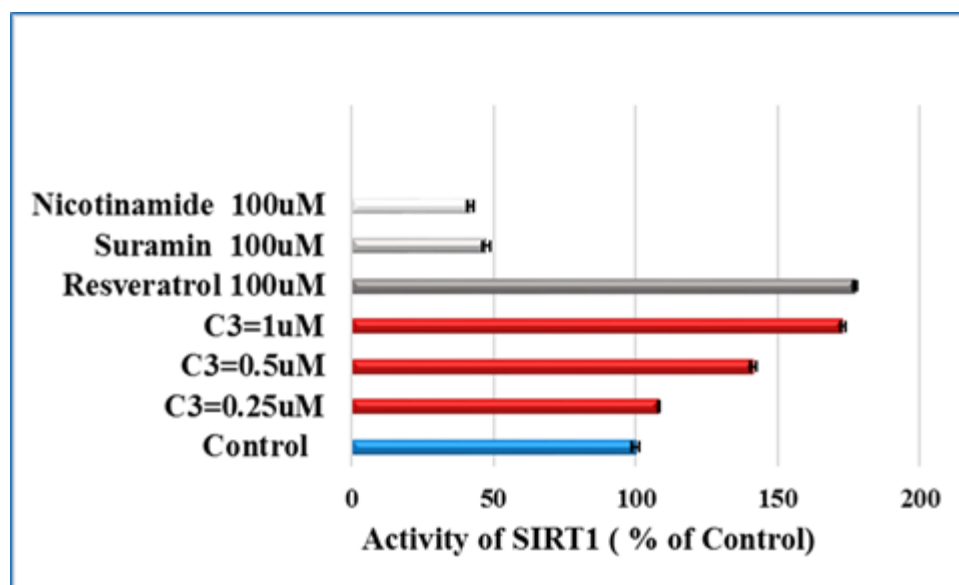


Figure 0.58: SIRT1 activity in A549 cells line at 0.25, 0.5 and 1 μM C3 aptamer, 100 μM resveratrol (SIRT1 activator control), 100 μM suramin and nicotinamide (SIRT1 inhibitor control). The results represent the mean \pm SEM of three different experiments performed in triplicate. $p < 0.0005$.

As it can be seen in figure 5.59, the 1 μM of C3 aptamer can activate the SIRT1 more than twice its value compared with control (the level of SIRT1 in HepG2 cells) ($p < 0.0001$). However, 0.25, 0.5 μM of C3 aptamer was slightly increased the activity of SIRT1 compared with control, $p < 0.005$.

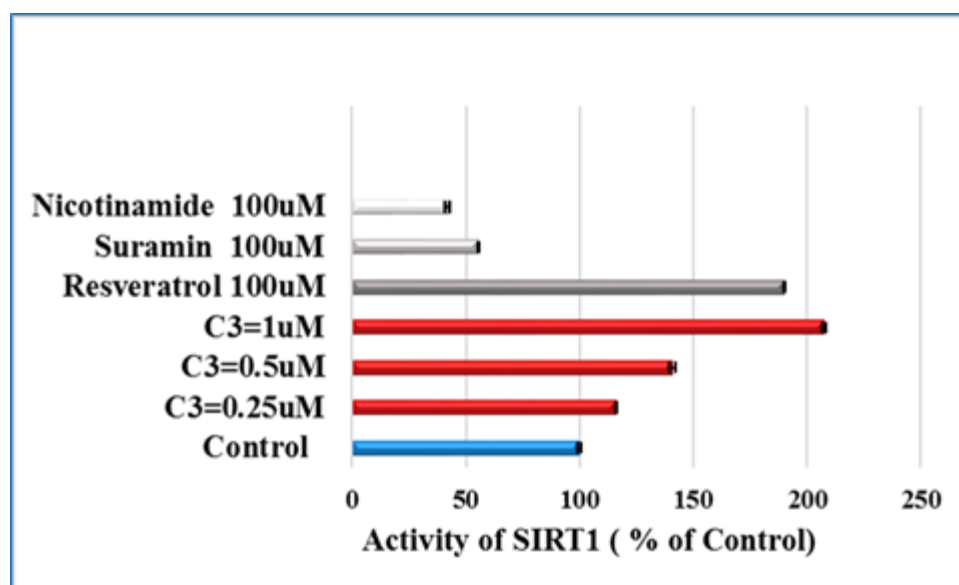


Figure 5.59: SIRT1 activity in HepG2 cells line at 0.25, 0.5 and 1 μ M C3 aptamer, 100 μ M resveratrol (SIRT1 activator control), 100 μ M suramin and nicotinamide (SIRT1 inhibitor control). The results represent the mean \pm SEM of three different experiments performed in triplicate. $p < 0.0001$.

The results of activator SIRT1 by C3 aptamer in MCF-7, MDA-MB-468, and U2OS cells were described in figures (5.60-5.62). C3 aptamers were markedly increased the activity of SIRT1 at concentration 0.25, 0.5 and 1 μ M compared to control (the level of SIRT1 in MCF-7, MDA-MB-468 and U2OS cells) ($p < 0.001$, 0.0005, 0.00005 at 0.25, 0.5 and 1 μ M respectively). The increased level of SIRT1 activity by 1 μ M C3 aptamer led to increasing the percentage of cell death in MCF-7, MDA-MB-468 and U2OS cells to 46%, 61%, and 42% respectively.

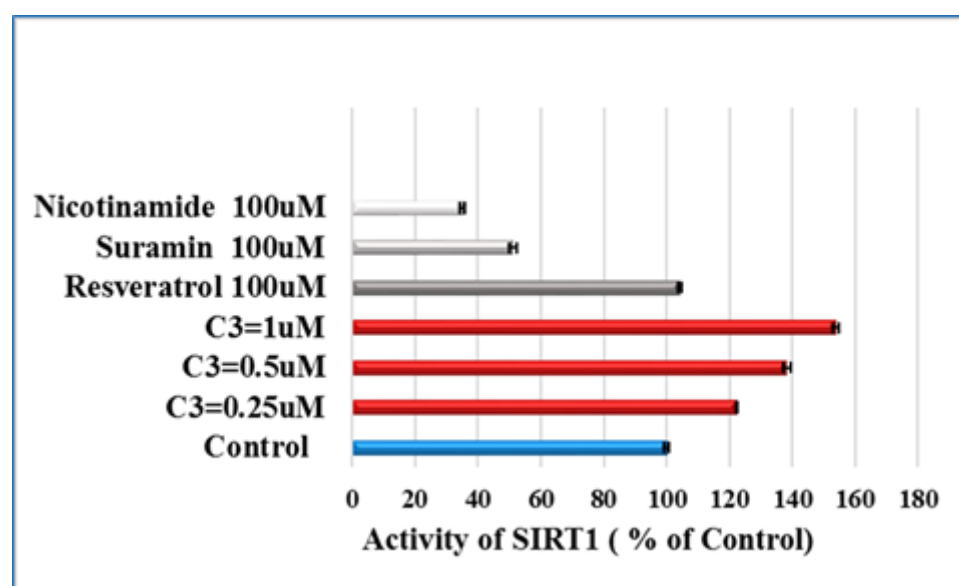


Figure 0.60: SIRT1 activity in MCF-7 cells line at 0.25, 0.5 and 1 μ M C3 aptamer, 100 μ M resveratrol (SIRT1 activator control), 100 μ M suramin and nicotinamide (SIRT1 inhibitor control). The results represent the mean \pm SEM of three different experiments performed in triplicate. $p < 0.001$, 0.0005, 0.00005 at 0.25, 0.5 and 1 μ M respectively.

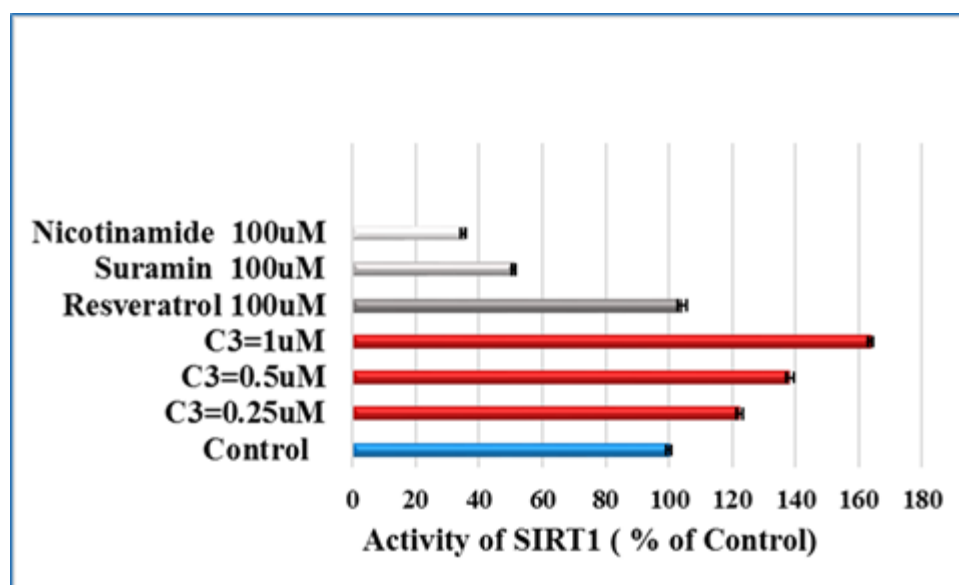


Figure 0.61: SIRT1 activity in MDA-MB-468 cells line at 0.25, 0.5 and 1 μM C3 aptamer, 100 μM resveratrol (SIRT1 activator control), 100 μM suramin and nicotinamide (SIRT1 inhibitor control). The results represent the mean \pm SEM of three different experiments performed in triplicate. $p < 0.001, 0.0005, 0.00005$ at 0.25, 0.5 and 1 μM respectively.

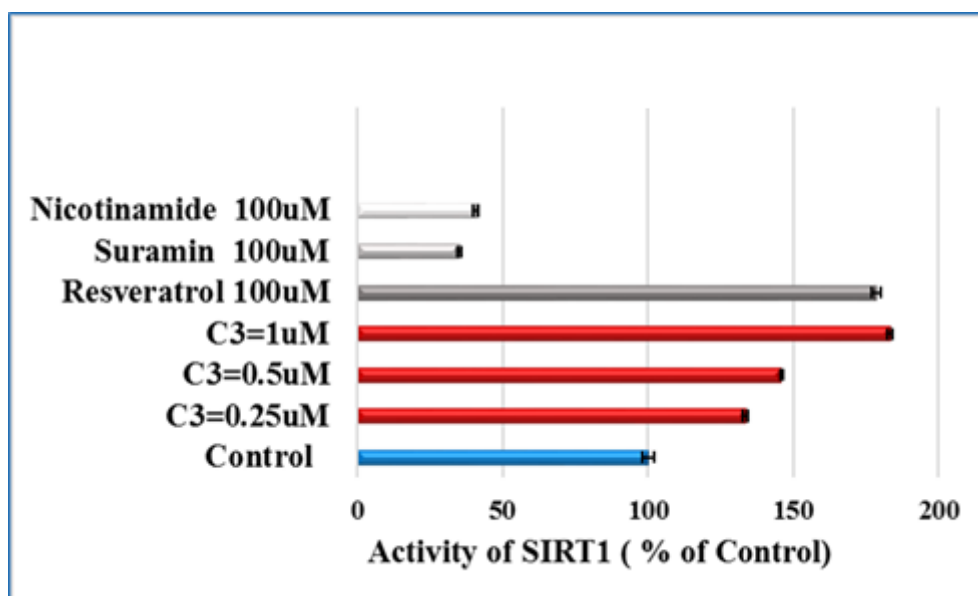


Figure 0.62: SIRT1 activity in U2OS cells line at 0.25, 0.5 and 1 μM C3 aptamer, 100 μM resveratrol (SIRT1 activator control), 100 μM suramin and nicotinamide (SIRT1 inhibitor control). The results represent the mean \pm SEM of three different experiments performed in triplicate. $p < 0.001, 0.0005, 0.00005$ at 0.25, 0.5 and 1 μM respectively.

As it has been shown in figure 5.63, the activity of SIRT1 on Caco-2 cells which pretreated with C3 aptamer at concentrations 0.25, 0.5 μM were slightly increased compared with control (the level of SIRT1 in Caco-2 cells) and 100 μM resveratrol (SIRT1 activators) ($p < 0.01$). However, the activity of SIRT1 on Caco-2 cells which pretreated with C3 aptamer at concentration 1 μM was increased significantly compared with control (the level of SIRT1 in Caco-2 cells) and 100 μM Resveratrol (SIRT1 activators) ($p < 0.00001$).

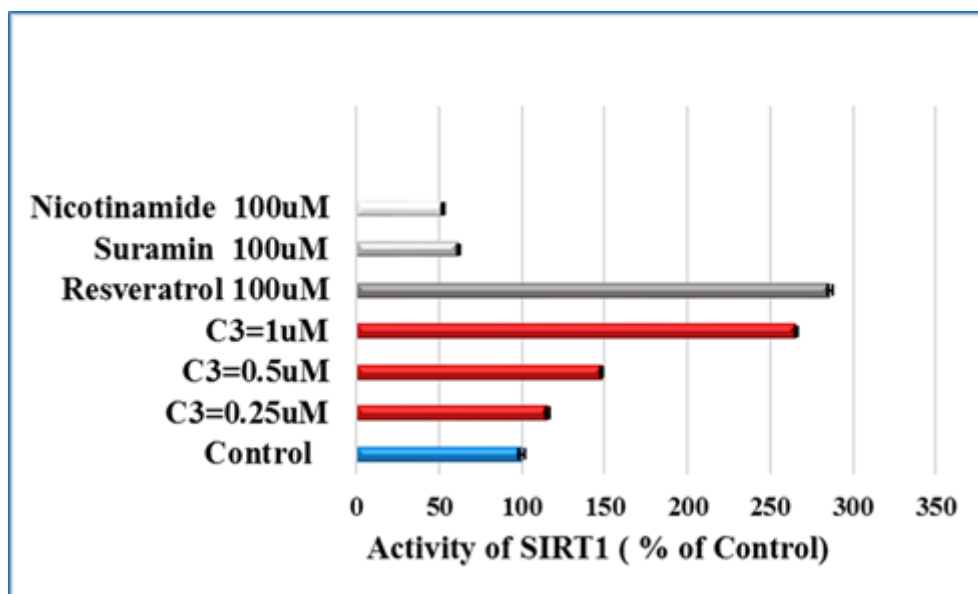


Figure 0.63: SIRT1 activity in Caco-2 cells line at 0.25, 0.5 and 1 μ M C3 aptamer, 100 μ M resveratrol (SIRT1 activator control), 100 μ M suramin and nicotinamide (SIRT1 inhibitor control). The results represent the mean \pm SEM of three different experiments performed in triplicate. $p < 0.00001$.

HaCaT cells were used as a non-cancer cell line to study the effect of C3 aptamer in these cells. The results of these cells as shown in figure 5.64 are suggesting that 1 μ M of the C3 aptamer is activating SIRT1 in these cells compared with control (the level of SIRT1 in HaCaT cells) ($p < 0.001$).

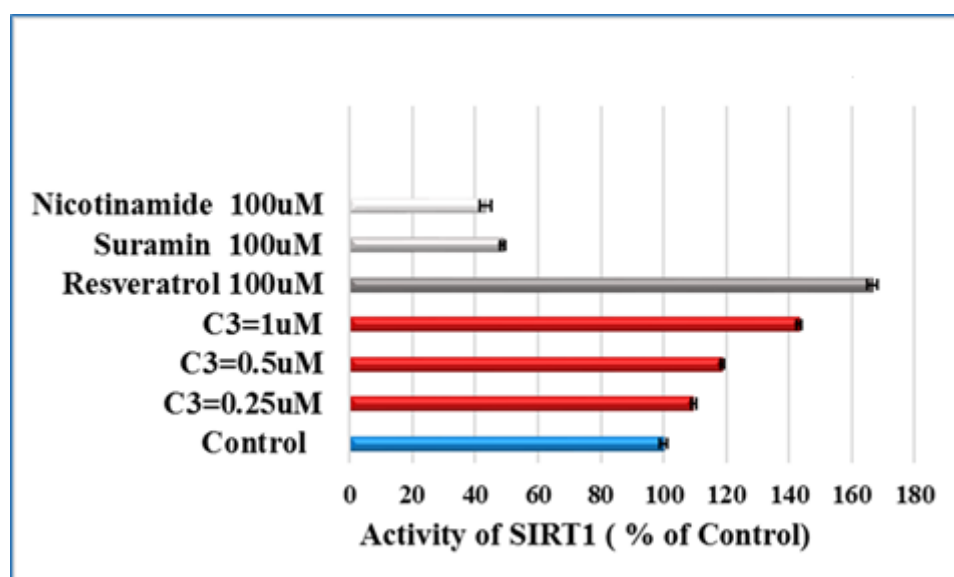


Figure 0.64: SIRT1 activity in HaCaT cells line at 0.25, 0.5 and 1 μ M C3 aptamer, 100 μ M resveratrol (SIRT1 activator control), 100 μ M suramin and nicotinamide (SIRT1 inhibitor control). The results represent the mean \pm SEM of three different experiments performed in triplicate. $p < 0.001$.

Regarding Beas-2b cells, data analysis as shown in figures 5.65 have disclosed that C3 aptamer, not effects on the activity of SIRT1 in Beas-2b cells. Therefore, C3 aptamer does not inhibit the growth of cells.

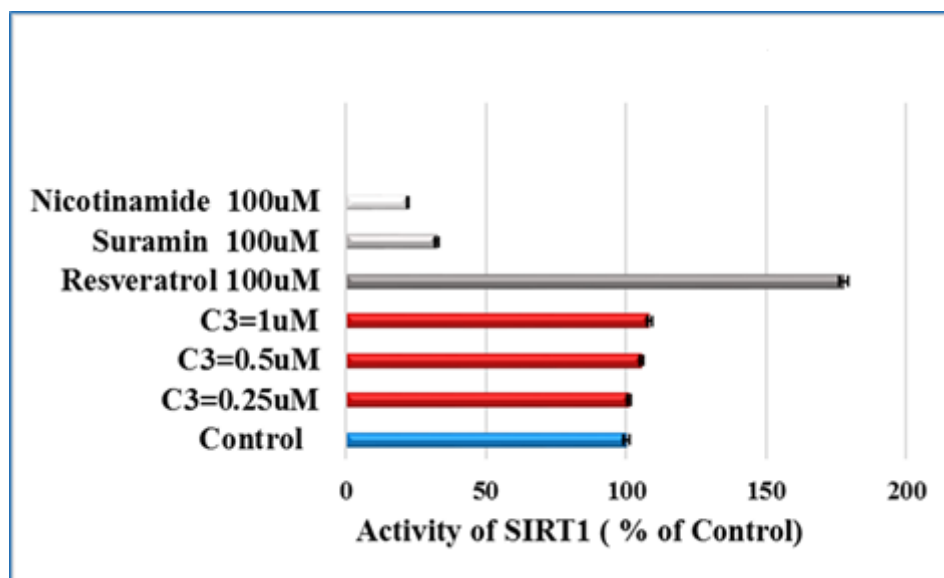


Figure 5.65: SIRT1 activity in Beas-2b cells line at 0.25, 0.5 and 1 μM C3 aptamer, 100 μM resveratrol (SIRT1 activator control), 100 μM suramin and nicotinamide (SIRT1 inhibitor control). The results represent the mean \pm SEM of three different experiments performed in triplicate. $p > 0.05$.

In summary, the results in figures 5.58-5.65 were indicated that A549, HepG2, MCF-7, MDA-MB-468, U2OS, Caco-2, HaCaT cells which were treated with C3 aptamer had a markedly increased the activity of SIRT1 and this increase of SIRT1 activity led to decreased the cell viability of cancer cell lines as well as HaCaT cell line. In contrast, the C3 aptamer was not effecting on the activity of SIRT1 in Beas-2b cells.

5.3.4 Effect of C3 Aptamer on Ratio of Intracellular ROS Production and Cell Viability

To investigate the causes of increased cell death in cancer cell lines and HaCaT cell line by C3 aptamer, cell viability and intracellular ROS production was estimated on A549, HepG2, MCF-7, MDA-MB-468, U2OS, Caco-2, and HaCaT cell lines in parallel under the same conditions by treatment with 0.25, 0.5, 1 μM C3 aptamer and then exposed these cells to the same concentration of C3 aptamer with 50 μM TBHP.

Table 5.1-5.7 demonstrates the data of percentage ROS normalised to control, cell viability of A549, HepG2, MCF-7, U2OS, MDA-MB-468, Caco-2, and HaCaT as well as the ratio of ROS/Cell viability. The results were showed that C3 aptamer at 0.25, 0.5, 1 μM reduced the ROS level, while the cells which exposed to 50 μM TBHP (positive control) were increased the ROS level, these results indicate that C3 was a protective effect, though resveratrol at 100 μM does the same effect. According to MTT, results were showed the same inhibition of cell viability. Because of C3 aptamer and resveratrol kill the cells, the ratio of ROS and cell viability should be calculated. Anything close to 1 means that protection is happening so the cells are reducing the ROS in comparison to a number of cells there. So, with the ratio, at 1 is control, C3 aptamer at lower concentrations has a closer to 1 ratio but also because the cells are dying. At 1 μM , 50% of the cell with 50% of the ROS so there is less ROS but also fewer cells. When 50 μM TBHP was added, the level of ROS is normalised, considering the cells are dying too, so even though C3 aptamer was anticancer activity, it also helps as an added mechanism to survive the damage from ROS. The data suggests that C3 aptamer might produce the anticancer activity through another mechanism rather than ROS. However, the data of HaCaT cells were showed increased the ratio of ROS/Cell viability of 0.25, 0.5, 1 μM C3 aptamer by 1.7, 1.8 and 2.5 respectively. These data indicate that 1 μM C3 aptamer was killed the HaCaT cells because of increased the level of ROS.

Table 0.1: The percentage of ROS normalised to control, cell viability and ratio of ROS/Cell viability of A549 cell line with 0.25, 0.5, 1 μM C3 aptamer and 100 μM resveratrol with and without 50 μM TBHP.

A549	% ROS to control normalise	STD	% cell viability	STD	Ratio ROS/cell viability
C3 at 0.25 μM	63.2	0.45	81.0	0.026	0.8
C3 at 0.5 μM	47.3	1.92	55.1	0.002	0.9
C3 at 1 μM	27.5	1.83	47.4	0.030	0.6
A549 cells +TBHP (positive control)	143.0	1.25	34.3	0.016	4.2
C3 at 0.25 μM+TBHP	93.7	4.23	85.0	0.003	1.1
C3 at 0.5 μM+TBHP	73.2	1.77	61.4	0.002	1.2
C3 at 1 μM+TBHP	63.2	0.77	56.8	0.010	1.1
Resveratrol at 100 μM	31.0	1.52	59.0	0.002	0.5
Resveratrol at 100 μM+TBHP	47.1	2.46	67.5	0.010	0.7

Table 5.2: The percentage of ROS normalised to control, cell viability and ratio of ROS/Cell viability of HepG2 cell line with 0.25, 0.5, 1 μM C3 aptamer and 100 μM resveratrol with and without 50 μM TBHP.

HepG2	% ROS to control normalise	STD	% cell viability	STD	Ratio ROS/cell viability
C3 at 0.25 μM	49.5	1.36	83.0	0.004	0.6
C3 at 0.5 μM	43.3	2.26	59.7	0.003	0.7
C3 at 1 μM	28.0	2.09	47.6	0.001	0.6
HepG2 cells +TBHP (positive control)	129.8	0.554	41.4	0.026	3.1
C3 at 0.25 μM+TBHP	84.7	1.432	88.1	0.014	1.0
C3 at 0.5 μM+TBHP	77.4	1.213	58.9	0.001	1.3
C3 at 1 μM+TBHP	53.8	0.919	53.4	0.001	1.0
Resveratrol at 100 μM	38.9	0.952	53.8	0.003	0.7
Resveratrol at 100 μM+TBHP	49.6	2.004	60.0	0.001	0.8

Table 0.3: The percentage of ROS normalised to control, cell viability and ratio of ROS/Cell viability of MCF-7 cell line with 0.25, 0.5, 1 μM C3 aptamer and 100 μM resveratrol with and without 50 μM TBHP.

MCF-7	% ROS to control normalise	STD	% cell viability	STD	Ratio ROS/cell viability
C3 at 0.25 μM	57.6	1.89	81.4	0.021	0.7
C3 at 0.5 μM	52.0	3.203	69.9	0.011	0.7
C3 at 1 μM	36.8	2.54	43.9	0.008	0.8
MCF-7 cells +TBHP (positive control)	127.1	0.786	39.7	0.042	3.2
C3 at 0.25 μM+TBHP	92.6	1.53	99.1	0.055	0.9
C3 at 0.5 μM+TBHP	81.4	0.981	70.8	0.009	1.1
C3 at 1 μM+TBHP	74.7	3.24	62.3	0.026	1.2
Resveratrol at 100 μM	47.2	1.42	56.9	0.006	0.8
Resveratrol at 100 μM+TBHP	53.5	2.09	59.9	0.017	0.9

Table 5.4: The percentage of ROS normalised to control, cell viability and ratio of ROS/Cell viability of U2OS cell line with 0.25, 0.5, 1 μM C3 aptamer and 100 μM resveratrol with and without 50 μM TBHP.

U2OS	% ROS to control normalise	STD	% cell viability	STD	Ratio ROS/cell viability
C3 at 0.25 μM	59.3	1.76	82.6	0.006	0.7
C3 at 0.5 μM	54.4	1.59	76.3	0.011	0.7
C3 at 1 μM	38.9	1.09	41.6	0.003	0.9
U2OS cells +TBHP (positive control)	113.2	0.782	39.8	0.020	2.8
C3 at 0.25 μM+TBHP	87.0	0.987	96.6	0.031	0.9
C3 at 0.5 μM+TBHP	70.2	1.013	65.7	0.001	1.1
C3 at 1 μM+TBHP	58.1	0.999	57.7	0.008	1.0
Resveratrol at 100 μM	35.8	2.32	57.4	0.003	0.6
Resveratrol at 100 μM+TBHP	54.3	1.75	61.9	0.006	0.9

Table 0.5: The percentage of ROS normalised to control, cell viability and ratio of ROS/Cell viability of MDA-MB-468 cell line with 0.25, 0.5, 1 μM C3 aptamer and 100 μM resveratrol with and without 50 μM TBHP.

MDA-MB-468	% ROS to control normalise	STD	% cell viability	STD	Ratio ROS/cell viability
C3 at 0.25 μM	61.2	1.019	92.9	0.011	0.7
C3 at 0.5 μM	53.9	0.932	55.1	0.003	1.0
C3 at 1 μM	30.8	0.765	39.1	0.001	0.8
MDA-MB-468 cells +TBHP (positive control)	141.1	2.94	47.3	0.020	3.0
C3 at 0.25 μM+TBHP	91.1	2.342	86.8	0.025	1.0
C3 at 0.5 μM+TBHP	80.0	1.25	65.5	0.015	1.2
C3 at 1 μM+TBHP	51.9	0.98	41.2	0.003	1.3
Resveratrol at 100 μM	29.0	0.932	50.6	0.008	0.6
Resveratrol at 100 μM+TBHP	46.0	1.763	60.0	0.055	0.8

Table 0.6: The percentage of ROS normalised to control, cell viability and ratio of ROS/Cell viability of Caco-2 cell line with 0.25, 0.5, 1 μM C3 aptamer and 100 μM resveratrol with and without 50 μM TBHP.

Caco-2	% ROS to control normalise	STD	% cell viability	STD	Ratio ROS/cell viability
C3 at 0.25 μM	68.9	2.34	79.8	0.004	0.9
C3 at 0.5 μM	54.5	1.065	68.5	0.004	0.8
C3 at 1 μM	46.7	0.987	46.4	0.004	1.0
Caco-2 cells +TBHP (positive control)	144.6	0.65	34.2	0.010	4.2
C3 at 0.25 μM+TBHP	84.3	0.774	72.1	0.015	1.2
C3 at 0.5 μM+TBHP	81.6	0.896	67.7	0.010	1.2
C3 at 1 μM+TBHP	68.5	1.03	56.4	0.003	1.2
Resveratrol at 100 μM	29.5	0.33	53.8	0.002	0.5
Resveratrol at 100 μM+TBHP	39.5	0.63	59.1	0.010	0.7

Table 5.7: The percentage of ROS normalised to control, cell viability and ratio of ROS/Cell viability of HaCaT cell line with 0.25, 0.5, 1 μM C3 aptamer and 100 μM resveratrol with and without 50 μM TBHP.

HaCaT	% ROS to control normalise	STD	% cell viability	STD	Ratio ROS/ cell viability
C3 at 0.25 μM	127.8	1.01	75.4	0.012	1.7
C3 at 0.5 μM	127.3	0.23	71.9	0.001	1.8
C3 at 1 μM	119.3		48.5	0.001	2.5
HaCaT cells +TBHP (positive control)	137.4	0.399	27.3	0.015	5.0
C3 at 0.25 μM+TBHP	140.5	0.543	83.2	0.005	1.7
C3 at 0.5 μM+TBHP	136.5	0.89	81.3	0.034	1.7
C3 at 1 μM+TBHP	162.7	1.09	75.3	0.001	2.2
Resveratrol at 100 μM	45.3	1.29	88.8	0.010	0.5
Resveratrol at 100 μM+TBHP	59.2	0.99	86.0	0.006	0.7

5.3.5 Determination the Half Maximal Inhibitory Concentration (IC_{50})

Value

The dose-response curve generated by Origin 9.1 using nonlinear regression analysis for C3 aptamer in A549, HepG2, MCF-7, MDA-MB-468, U2OS, Caco-2 and HaCaT cells are shown in figures 5.66-5.72 respectively. The IC_{50} values were obtained to a range of concentrations of C3 aptamer from 0.0078 – 1 μM) by MTT assay. The results of IC_{50} for C3 aptamer were (0.32, 0.2, 0.144, 0.13, 0.1, 0.3 and 0.23 μM) in A549, HepG2, MCF-7, MDA-MB-468, U2OS, Caco-2 and HaCaT cells respectively as shown in figures 5.66-5.72.

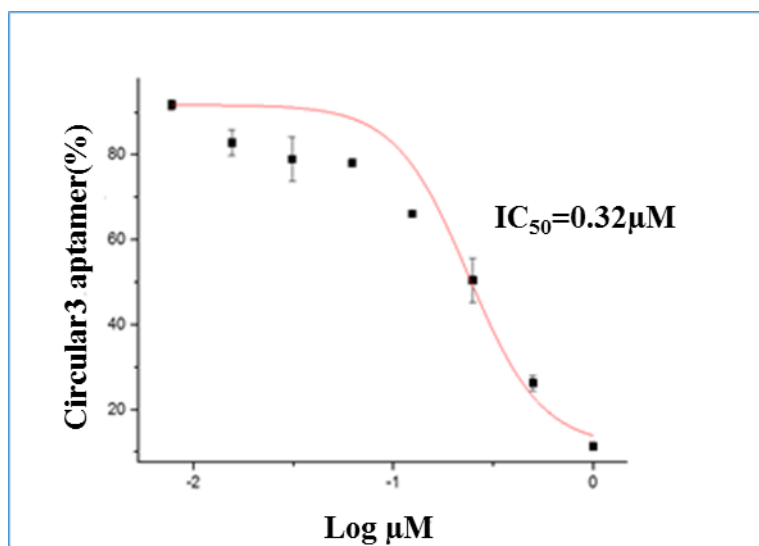


Figure 5.66: Dose-response curves of IC₅₀ for C3 aptamer. A549 cells were treated for 72h with 0.0078, 0.0156, 0.0312, 0.625, 0.125, 0.25, 0.5 and 1 μM dose ranges of C3 aptamer. The normalised dose response for C3 aptamer was plotted over log transformed aptamer concentrations. IC₅₀ values were determined using nonlinear regression analysis (Origin 9.1). Error bars represent the standard error of the mean (SEM) for triplicate data.

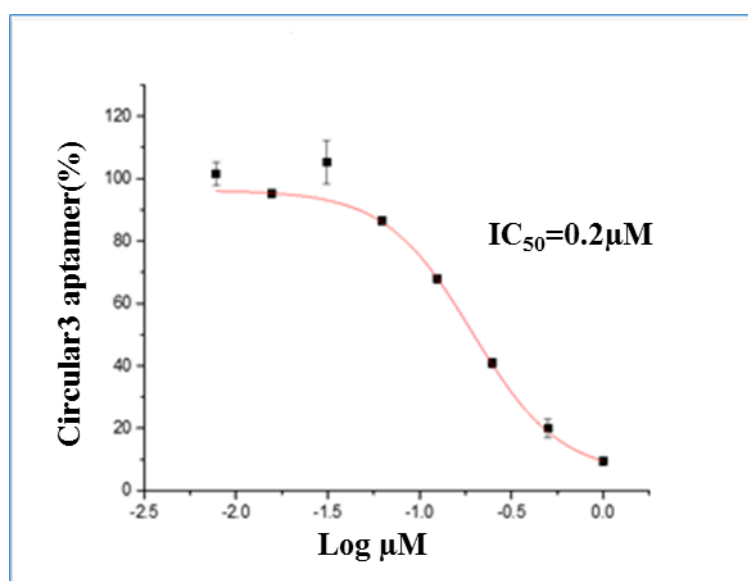


Figure 0.67: Dose-response curves of IC₅₀ for C3 aptamer. HepG2 cells were treated for 72h with 0.0078, 0.0156, 0.0312, 0.625, 0.125, 0.25, 0.5 and 1 μM dose ranges of C3 aptamer. The normalised dose response for C3 aptamer was plotted over log transformed aptamer concentrations. IC₅₀ values were determined using nonlinear regression analysis (Origin 9.1). Error bars represent the standard error of the mean (SEM) for triplicate data.

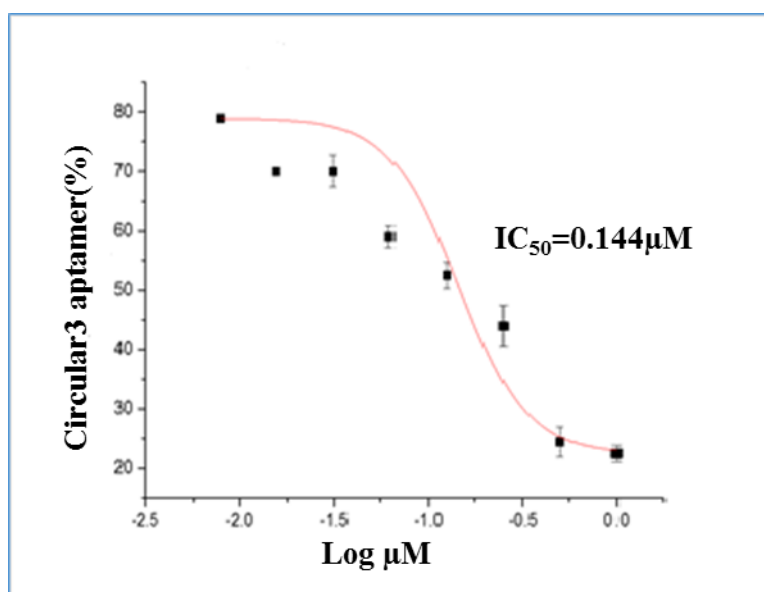


Figure 0.68: Dose-response curves of IC₅₀ for C3 aptamer. MCF-7 cells were treated for 72h with 0.0078, 0.0156, 0.0312, 0.625, 0.125, 0.25, 0.5 and 1 μM dose ranges of C3 aptamer. The normalised dose response for C3 aptamer was plotted over log transformed aptamer concentrations. IC₅₀ values were determined using nonlinear regression analysis (Origin 9.1). Error bars represent the standard error of the mean (SEM) for triplicate data.

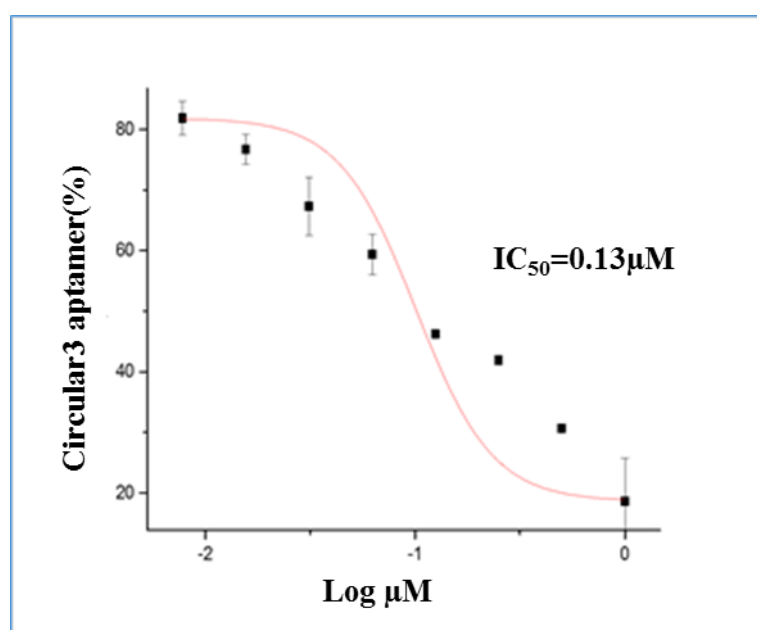


Figure 5.69: Dose-response curves of IC₅₀ for C3 aptamer. MDA-MB-468 cells were treated for 72h with 0.0078, 0.0156, 0.0312, 0.625, 0.125, 0.25, 0.5 and 1 μM dose ranges of C3 aptamer. The normalised dose response for C3 aptamer was plotted over log transformed aptamer concentrations. IC₅₀ values were determined using nonlinear regression analysis (Origin 9.1). Error bars represent the standard error of the mean (SEM) for triplicate data.

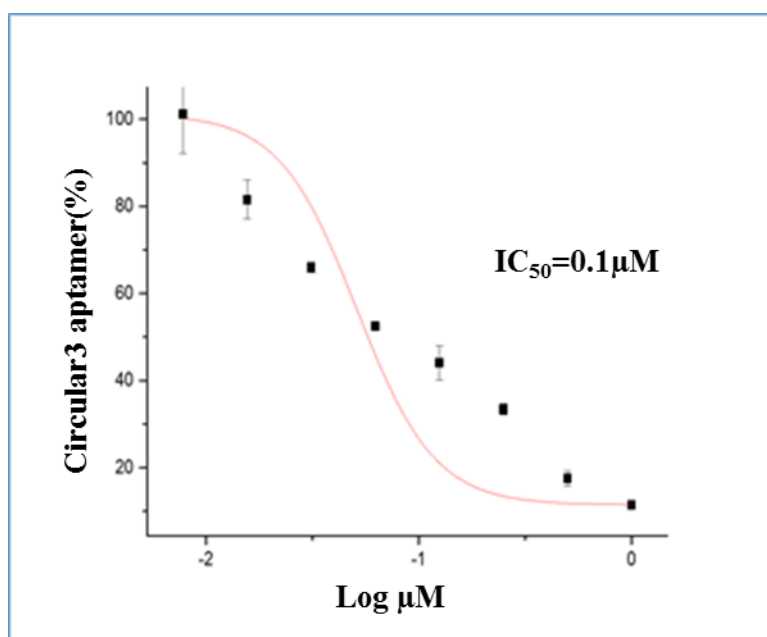


Figure 5.70: Dose-response curves of IC₅₀ for C3 aptamer. U2OS cells were treated for 72h with 0.0078, 0.0156, 0.0312, 0.625, 0.125, 0.25, 0.5 and 1 μM dose ranges of C3 aptamer. The normalised dose response for C3 aptamer was plotted over log transformed aptamer concentrations. IC₅₀ values were determined using nonlinear regression analysis (Origin 9.1). Error bars represent the standard error of the mean (SEM) for triplicate data.

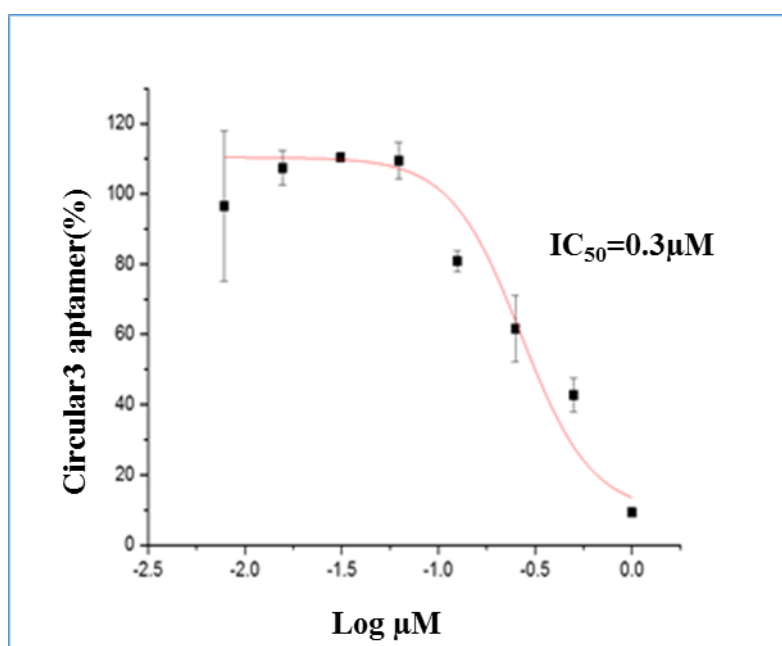


Figure 0.71: Dose-response curves of IC₅₀ for C3 aptamer. Caco-2 cells were treated for 72h with 0.0078, 0.0156, 0.0312, 0.625, 0.125, 0.25, 0.5 and 1 μM dose ranges of C3 aptamer. The normalised dose response for C3 aptamer was plotted over log transformed aptamer concentrations. IC₅₀ values were determined using nonlinear regression analysis (Origin 9.1). Error bars represent the standard error of the mean (SEM) for triplicate data.

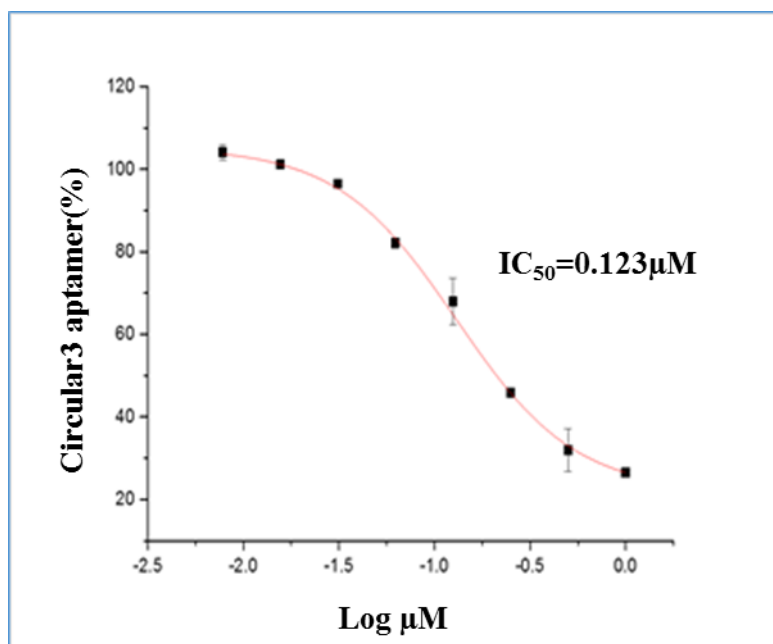


Figure 5.72: Dose-response curves of IC_{50} for C3 aptamer. HaCaT cells were treated for 72h with 0.0078, 0.0156, 0.0312, 0.625, 0.125, 0.25, 0.5 and 1 μM dose ranges of C3 aptamer. The normalised dose response for C3 aptamer was plotted over log transformed aptamer concentrations. IC_{50} values were determined using nonlinear regression analysis (Origin 9.1). Error bars represent the standard error of the mean (SEM) for triplicate data.

In conclude, the results were indicated that these values of IC_{50} of C3 aptamers in all cells are very good value because a very low concentration of C3 aptamer can inhibit the half number of cancer cell viability as compared with the IC_{50} of resveratrol (70–150 μM) in MCF7, SW480, HCE7, Seg-1, Bic-1, and HL60 cell lines according to Joe *et al.*, (2002).

5.3.6 Determine the Location of C3 Aptamer by Fluorescence Microscopy

To determine the location of the C3 aptamer, fluorescence microscopy was used in this experiment. The C3 aptamer was labelled with green fluorescent protein (GFP), DAPI (4', 6-Diamidino-2-Phenylindole, Dihydrochloride) was used to locate the nuclei and a Texas Red (sulfonyl chloride) antibody for SIRT1. The cells were challenged with the C3 aptamer at a lower concentration (0.1 μM to U2OS, MDA-MB-468 and HaCaT, 0.2 μM to MCF-7 and HepG2, 0.3 μM to A549 and Caco-2, and 1 μM to Beas-2b) at 72h. Thus, figures 5.73-5.80 showed that fluorescence microscopy is very useful tool for studying the location of C3 aptamer in cancer and non-cancer cell lines. Cells treated with C3 aptamers were brightly fluorescent and overexpression of SIRT1 as showed in figures 5.73-5.79B, while fluorescence of SIRT1 was weakly when cells were untreated with C3 aptamer (figures 5.73-5.79A), confirming the binding specificity of the selected C3 aptamer. In contrast, there was no

observable fluorescence signal from control Beas-2b cells treated with the C3 aptamer or untreated aptamer (figure 5.80).

Figure 5.73, 5.74 and 5.75 shown the localisation of SIRT1 in A549, HepG2, Caco-2 cells and demonstrates that SIRT1 was localised in the cytoplasm of these cells, while in MDA-MB-468, U2OS, HaCaT and Beas-2b cells, the SIRT1 was localised in the nucleus as shown in figures 5.77-5.80.

These results strongly suggested that this aptamer is highly affinity and selectivity binding with SIRT1 as the results of fluorescent imaging shown that when the aptamer present in this cancer cells it could be activated and increased the expression of the SIRT1 enzyme.

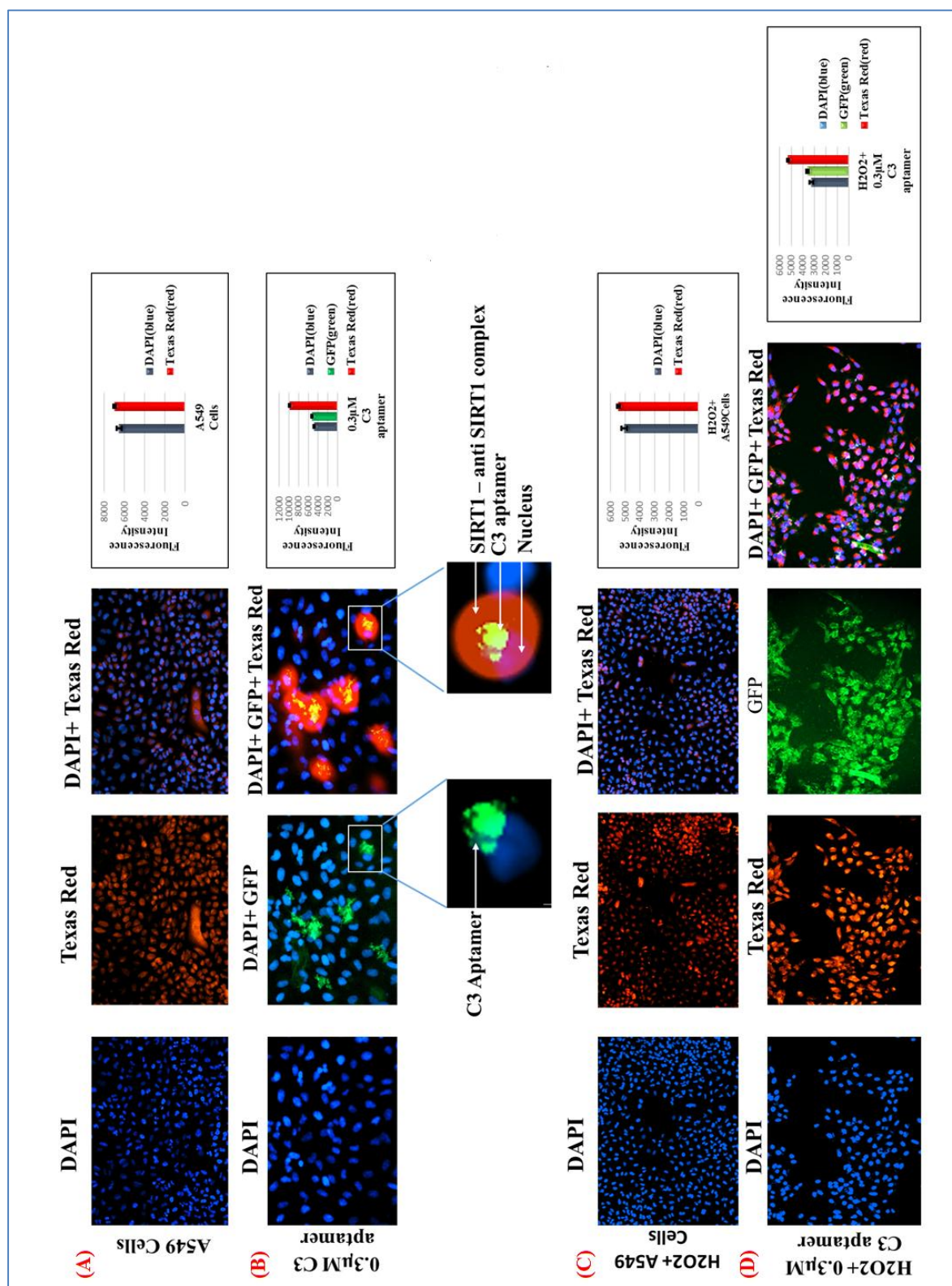


Figure 0.73: Fluorescence microscopy analysis of C3 aptamer binding to SIRT1 enzyme in A549 cell line. (A) A549 cell line (control), (B) A549 cells pretreated with 0.3 μM C3 aptamer at 72h, (C) A549 cell line pretreated with 50 μM H₂O₂, (D) A549 cells pretreated with 0.3 μM C3 aptamer and 50 μM H₂O₂ at 72h. C3 aptamer was labelled with green fluorescent protein (GFP), nuclei were stained with DAPI (Blue) and a Texas Red antibody for SIRT1 (Red). Fluorescence intensity were measured by Luminometer Microplate Readers, fluorescence measurement system with an excitation wavelength of 395, 359 and 596 nm and an emission wavelength of 509, 461 and 615 nm of GFP, DAPI and Texas Red respectively. The results represent the mean ± SEM of two different experiments performed in twice. Images were taken at a magnification of 100X.

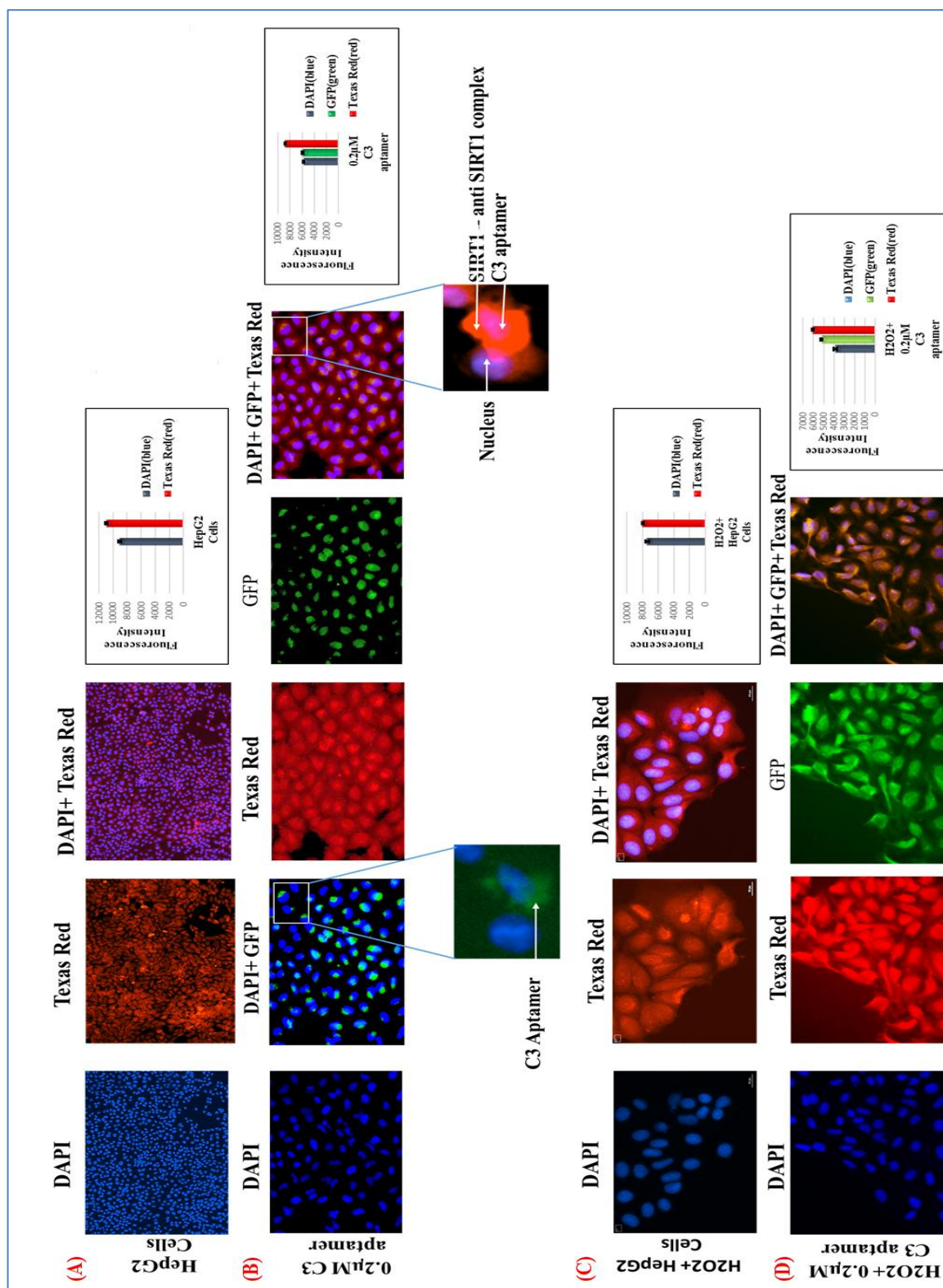


Figure 0.74: Fluorescence microscopy analysis of C3 aptamer binding to SIRT1 enzyme in HepG2 cell line. (A) HepG2 cell line (control), (B) HepG2 cells pretreated with 0.2 μM C3 aptamer at 72h, (C) HepG2 cell line pretreated with 50 μM H₂O₂, (D) HepG2 cells pretreated with 0.2 μM C3 aptamer and 50 μM H₂O₂ at 72h. C3 aptamer was labelled with green fluorescent protein (GFP), nuclei were stained with DAPI (Blue) and a Texas Red antibody for SIRT1 (Red). Fluorescence intensity were measured by Luminometer Microplate Readers, fluorescence measurement system with an excitation wavelength of 395, 359 and 596 nm and an emission wavelength of 509, 461 and 615 nm of GFP, DAPI and Texas Red respectively. The results represent the mean ± SEM of two different experiments performed in twice. Images were taken at a magnification of 100X and 200X.

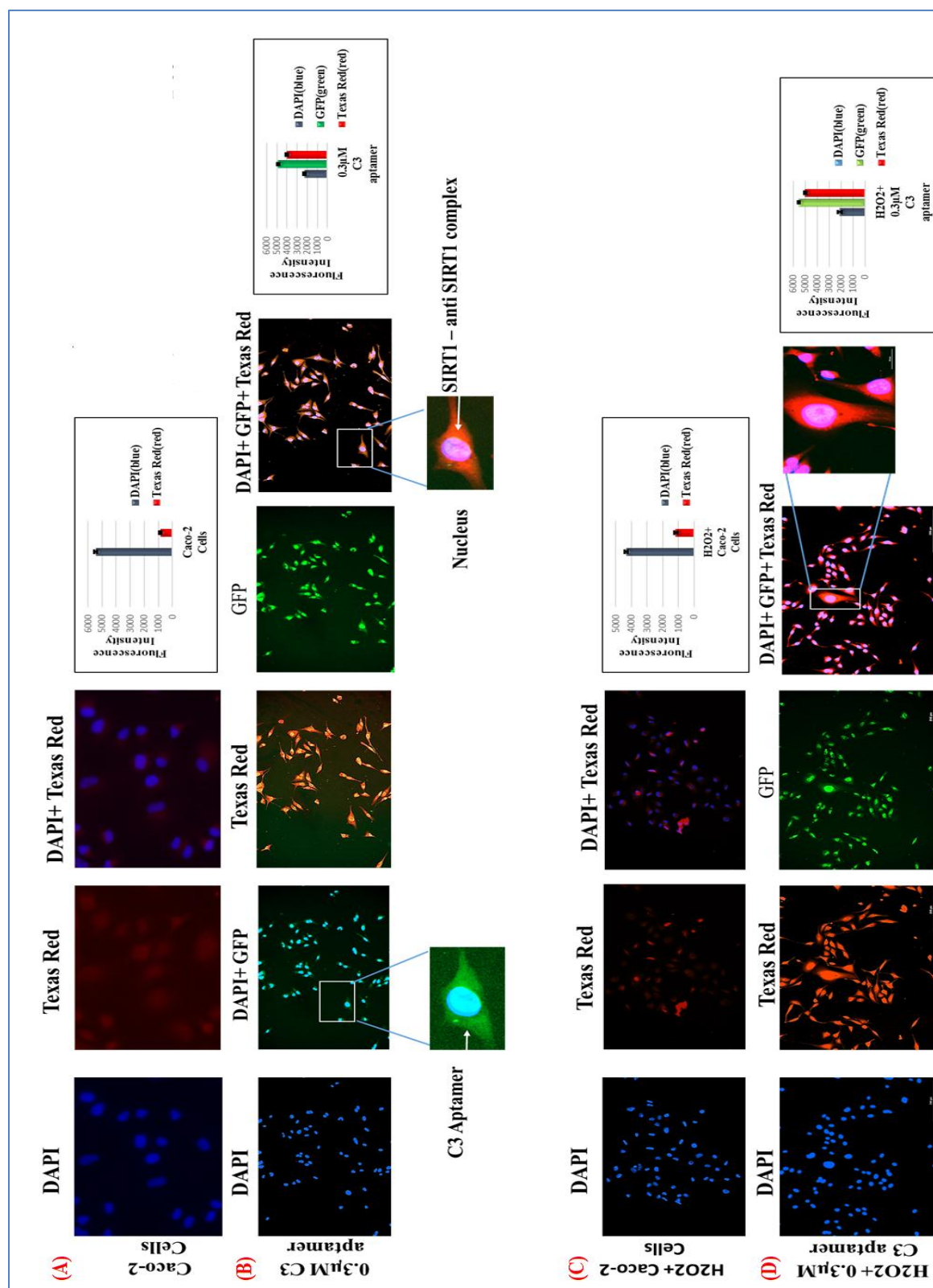


Figure 0.75: Fluorescence microscopy analysis of C3 aptamer binding to SIRT1 enzyme in Caco-2 cell line. (A) Caco-2 cell line (control), (B) Caco-2 cells pretreated with 0.3 μM C3 aptamer at 72h, (C) Caco-2 cell line pretreated with 50 μM H_2O_2 , (D) Caco-2 cells pretreated with 0.3 μM C3 aptamer and 50 μM H_2O_2 at 72h. C3 aptamer was labelled with green fluorescent protein (GFP), nuclei were stained with DAPI (Blue) and a Texas Red antibody for SIRT1 (Red). Fluorescence intensity were measured by Luminometer Microplate Readers, fluorescence measurement system with an excitation wavelength of 395, 359 and 596 nm and an emission wavelength of 509, 461 and 615 nm of GFP, DAPI and Texas Red respectively. The results represent the mean \pm SEM of two different experiments performed in twice. Images were taken at a magnification of 100X.

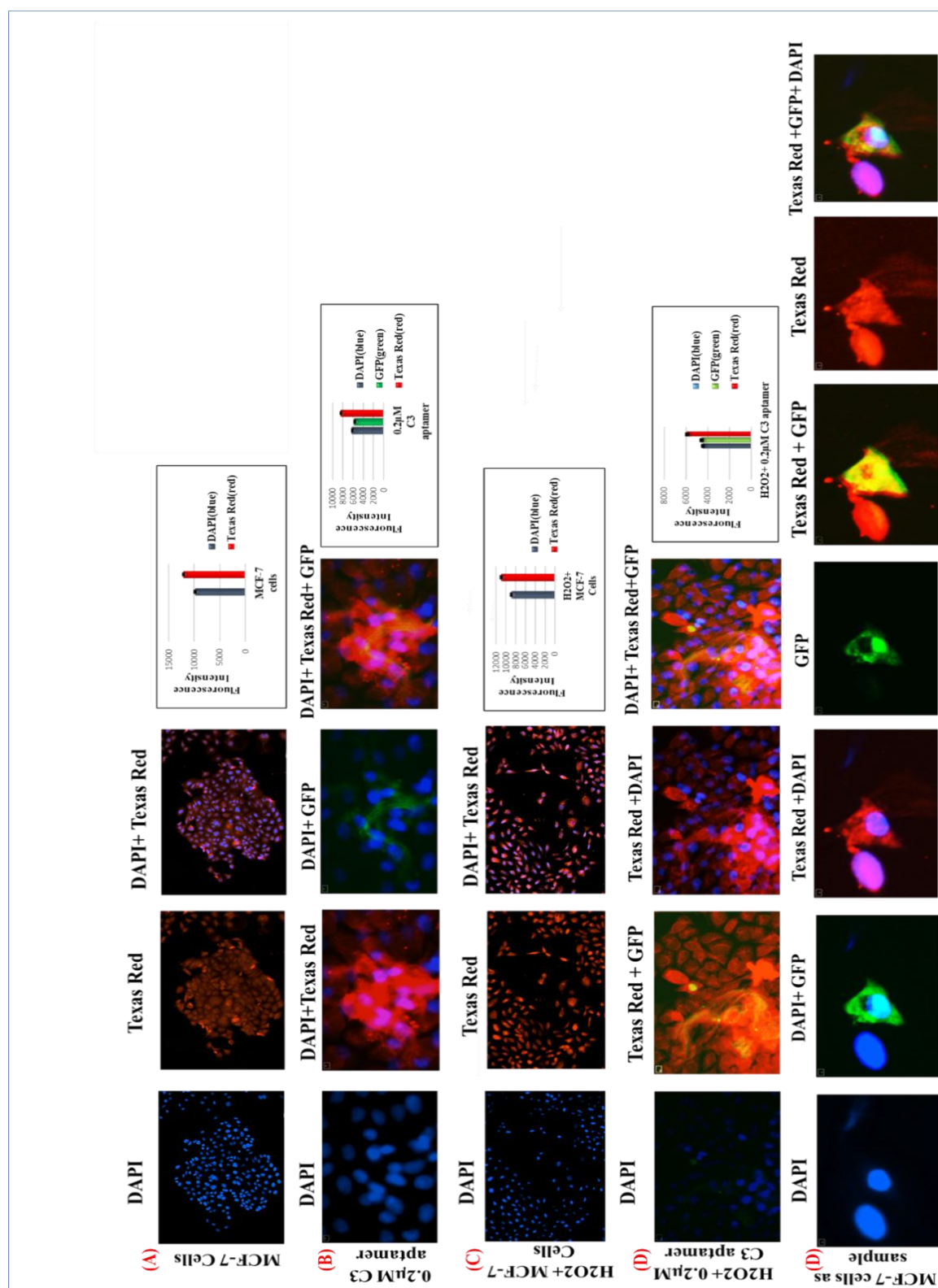


Figure 0.76: Fluorescence microscopy analysis of C3 aptamer binding to SIRT1 enzyme in MCF-7 cell line. (A) MCF-7 cell line (control), (B) MCF-7 cells pretreated with 0.2 μM C3 aptamer at 72h, (C) MCF-7 cell line pretreated with 50 μM H_2O_2 , (D) MCF-7 cells pretreated with 0.2 μM C3 aptamer and 50 μM H_2O_2 at 72h. C3 aptamer was labelled with green fluorescent protein (GFP), nuclei were stained with DAPI (Blue) and a Texas Red antibody for SIRT1 (Red). Fluorescence intensity were measured by Luminometer Microplate Readers, fluorescence measurement system with an excitation wavelength of 395, 359 and 596 nm and an emission wavelength of 509, 461 and 615 nm of GFP, DAPI and Texas Red respectively. The results represent the mean \pm SEM of two different experiments performed in twice. Images were taken at a magnification of 100X and 200X.

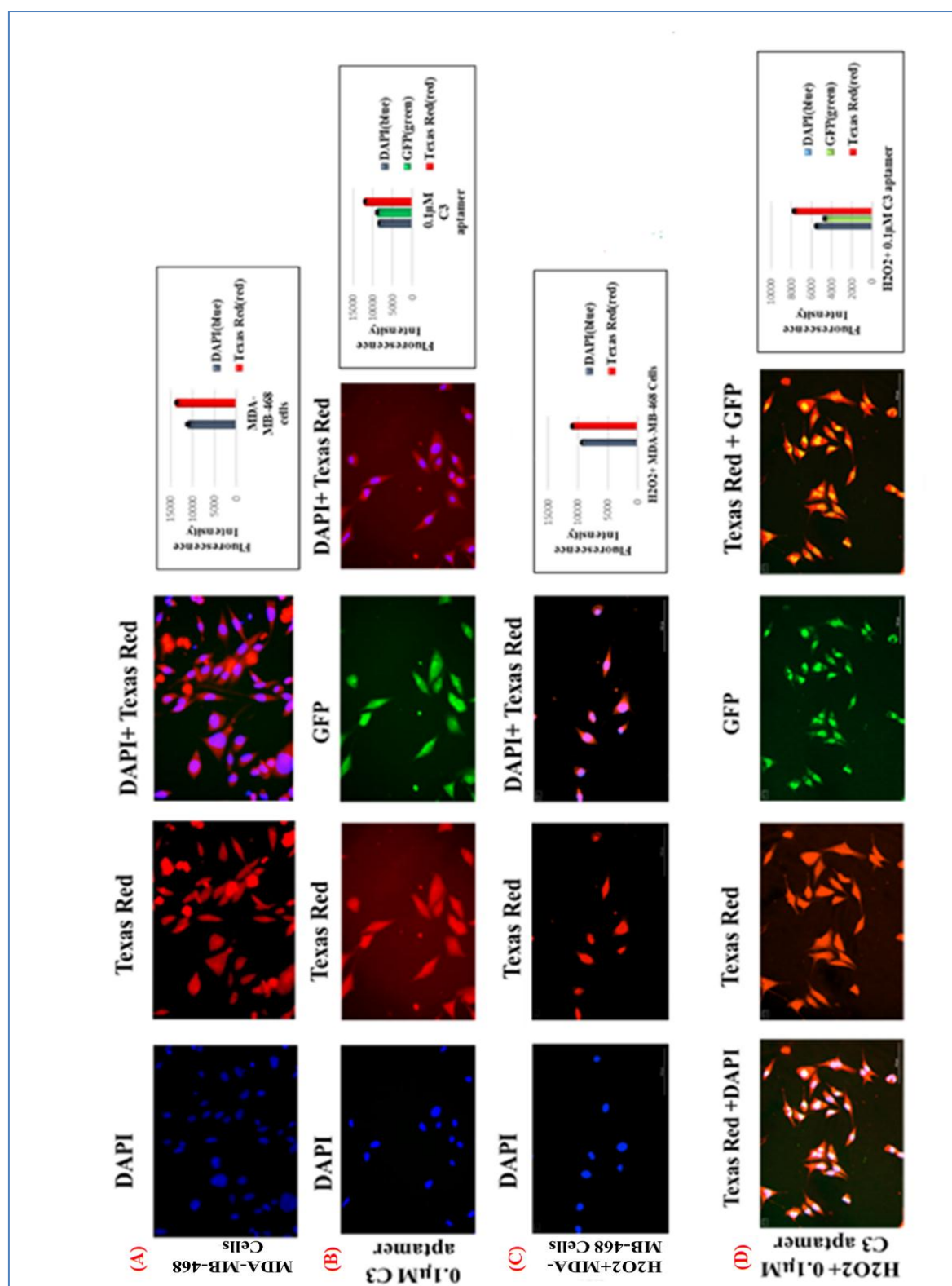


Figure 5.77: Fluorescence microscopy analysis of C3 aptamer binding to SIRT1 enzyme in MDA-MB-468 cell line. (A) MDA-MB-468 cell line (control), (B) MDA-MB-468 cells pretreated with 0.1 μM C3 aptamer at 72h, (C) MDA-MB-468 cell line pretreated with 50 μM H₂O₂, (D) MDA-MB-468 cells pretreated with 0.1 μM C3 aptamer and 50 μM H₂O₂ at 72h. C3 aptamer was labelled with green fluorescent protein (GFP), nuclei were stained with DAPI (Blue) and a Texas Red antibody for SIRT1 (Red). Fluorescence intensity were measured by Luminometer Microplate Readers, fluorescence measurement system with an excitation wavelength of 395, 359 and 596 nm and an emission wavelength of 509, 461 and 615 nm of GFP, DAPI and Texas Red respectively. The results represent the mean \pm SEM of two different experiments performed in twice. Images were taken at a magnification of 200X.

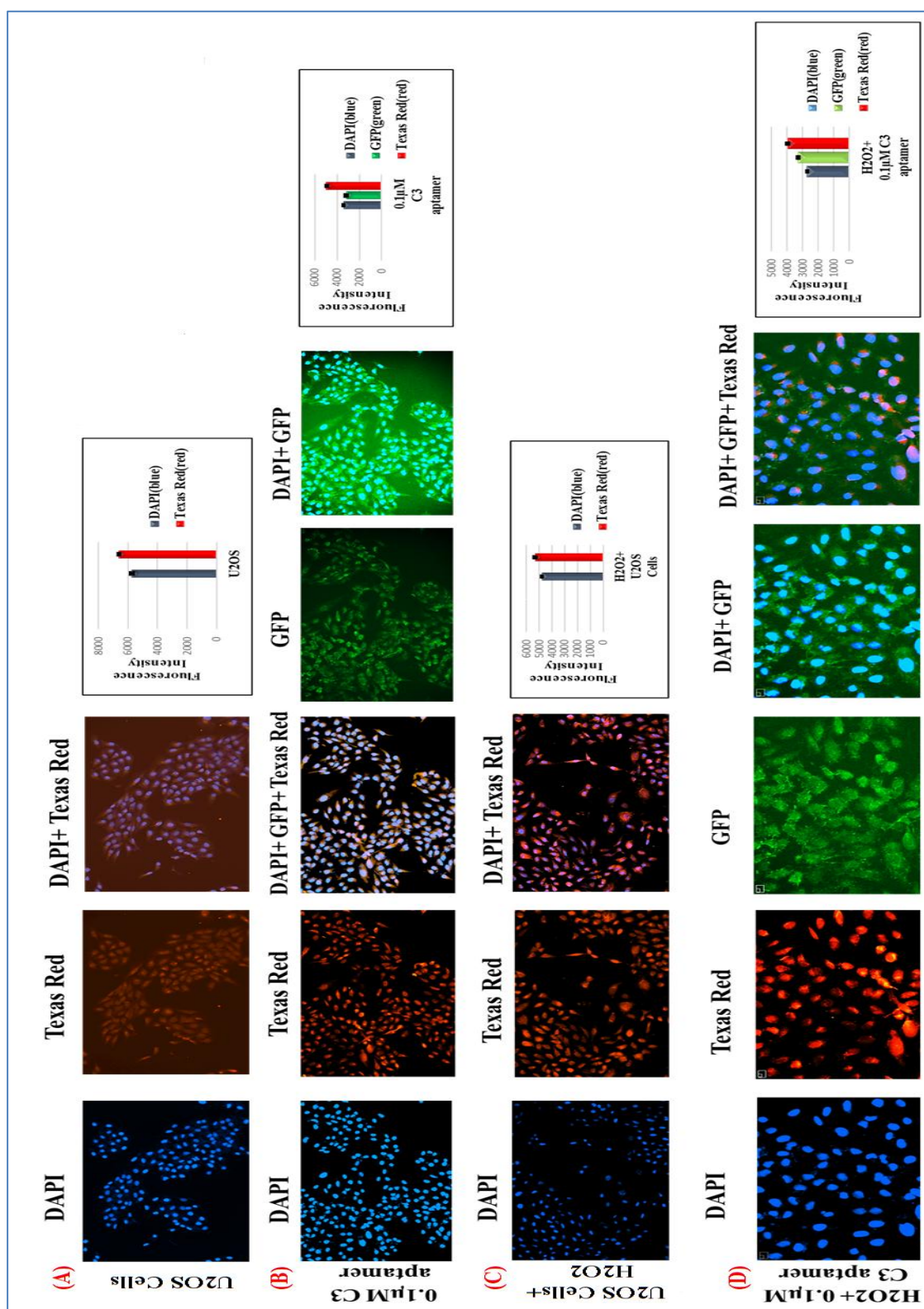


Figure 5.78: Fluorescence microscopy analysis of C3 aptamer binding to SIRT1 enzyme in U2OS cell line. (A) U2OS cell line (control), (B) U2OS cells pretreated with 0.1 μM C3 aptamer at 72h, (C) U2OS cell line pretreated with 50 μM H_2O_2 , (D) U2OS cells pretreated with 0.1 μM C3 aptamer and 50 μM H_2O_2 at 72h. C3 aptamer was labelled with green fluorescent protein (GFP), nuclei were stained with DAPI (Blue) and a Texas Red antibody for SIRT1 (Red). Fluorescence intensity were measured by Luminometer Microplate Readers, fluorescence measurement system with an excitation wavelength of 395, 359 and 596 nm and an emission wavelength of 509, 461 and 615 nm of GFP, DAPI and Texas Red respectively. The results represent the mean \pm SEM of two different experiments performed in twice. Images were taken at a magnification of 100X and 200X.

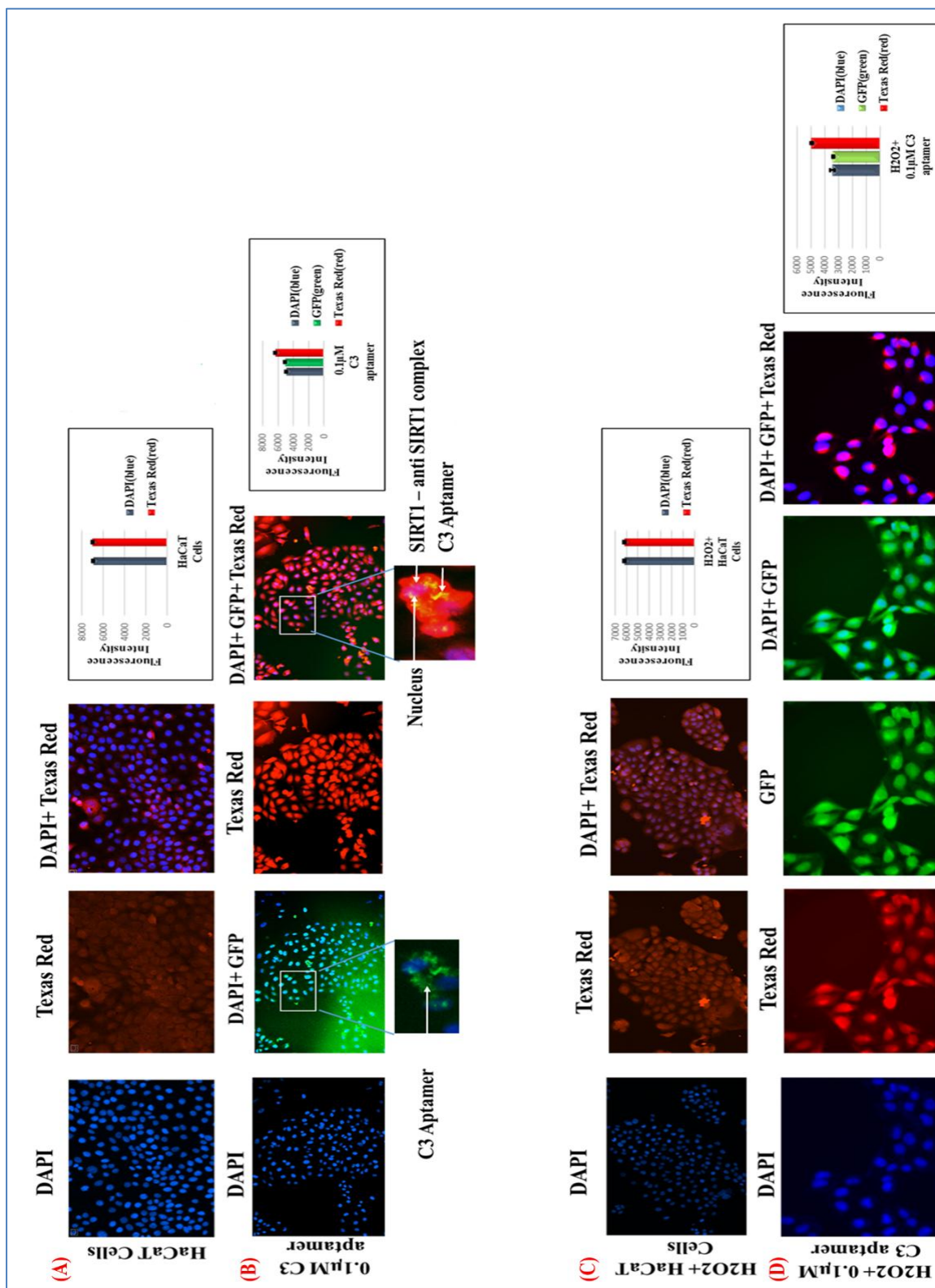


Figure 5.79: Fluorescence microscopy analysis of C3 aptamer binding to SIRT1 enzyme in HaCaT cell line. (A) HaCaT cell line (control), (B) HaCaT cells pretreated with 0.1 μ M C3 aptamer at 72h, (C) HaCaT cell line pretreated with 50 μ M H₂O₂, (D) HaCaT cells pretreated with 0.1 μ M C3 aptamer and 50 μ M H₂O₂ at 72h. C3 aptamer was labelled with green fluorescent protein (GFP), nuclei were stained with DAPI (Blue) and a Texas Red antibody for SIRT1 (Red). Fluorescence intensity were measured by Luminometer Microplate Readers, fluorescence measurement system with an excitation wavelength of 395, 359 and 596 nm and an emission wavelength of 509, 461 and 615 nm of GFP, DAPI and Texas Red respectively. The results represent the mean \pm SEM of two different experiments performed in twice. Images were taken at a magnification of 100X and 200X.

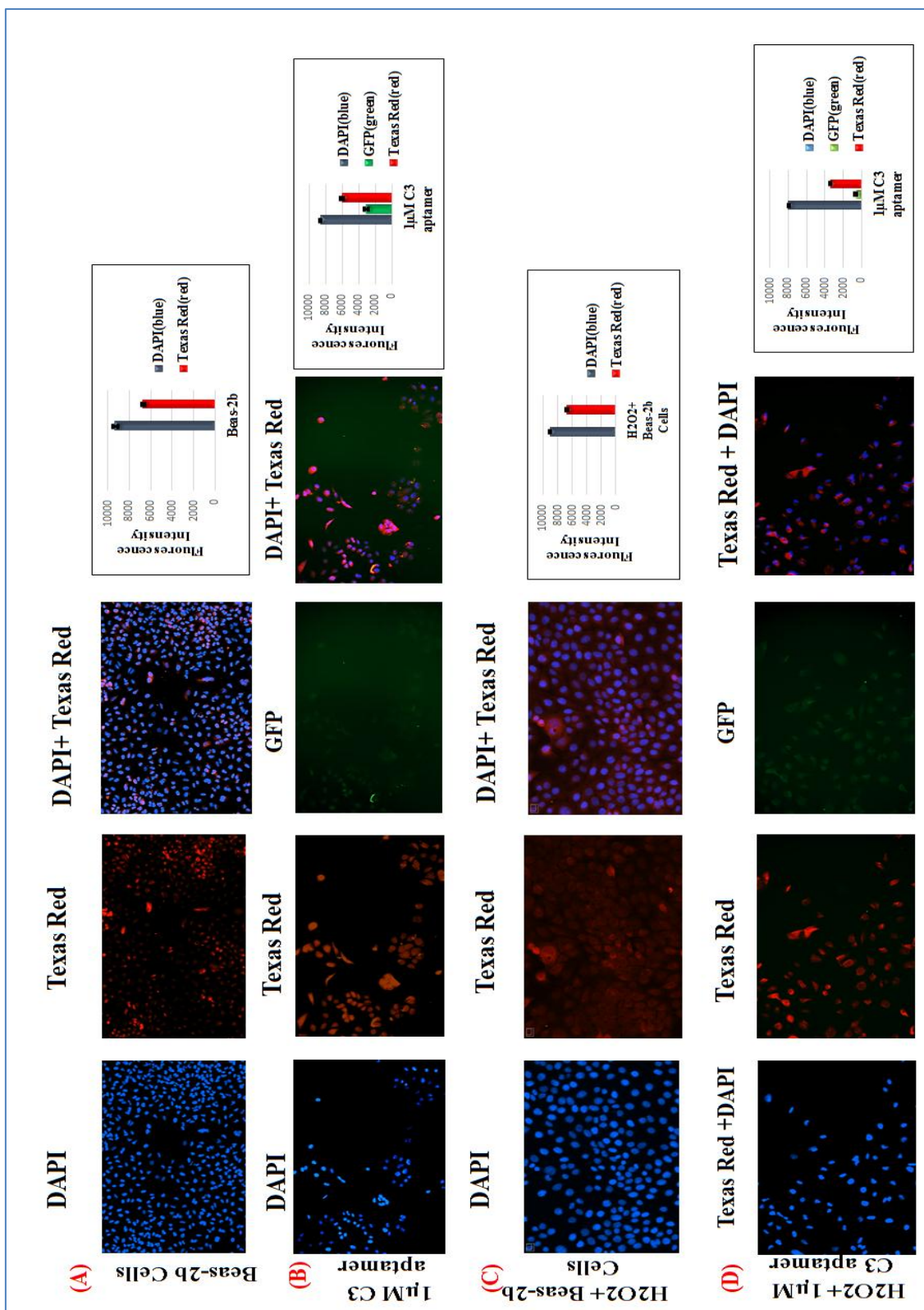


Figure 0.80: Fluorescence microscopy analysis of C3 aptamer binding to SIRT1 enzyme in Beas-2b cell line. (A) Beas-2b cell line (control), (B) Beas-2b cells pretreated with 1 μ M C3 aptamer at 72h, (C) Beas-2b cell line pretreated with 50 μ M H₂O₂, (D) Beas-2b cells pretreated with 1 μ M C3 aptamer and 50 μ M H₂O₂ at 72h. C3 aptamer was labelled with green fluorescent protein (GFP), nuclei were stained with DAPI (Blue) and a Texas Red antibody for SIRT1 (Red). Fluorescence intensity were measured by Luminometer Microplate Readers, fluorescence measurement system with an excitation wavelength of 395, 359 and 596 nm and an emission wavelength of 509, 461 and 615 nm of GFP, DAPI and Texas Red respectively. The results represent the mean \pm SEM of two different experiments performed in twice. Images were taken at a magnification of 100X.

5.4 Discussion

This study has investigated oligonucleotide aptamer as can use for anticancer drug discovery. In doing so, the work in this chapter has provided information in greater detail regarding the use of MTT assay to investigate the inhibitory effect of SIRT1-aptamers on viability of cancer cells (A549, HepG2, MCF-7, MDA-MB-468, U2OS and Caco-2) and non-cancer cells (HaCaT and Beas-2b) and study the activity of SIRT1 in these cells. SIRT1 is implicated in cell proliferation (Brow, 2015). Most studies have established that SIRT1 was involved in cancer cells. For instance, Li *et al.*, (2012) were established that downregulation of SIRT1 inhibits proliferation of breast cancer cells (BT-474, MDA-MB-231, MDA-MB-435, SK-BR-3), and inhibition of SIRT1 blocks proliferation of chronic lymphocytic leukemia cells. In contrary to this, increased expression of SIRT1 after resveratrol treatment inhibits proliferation of osteosarcoma cells (HOS, Saos-2, U2OS and MG-63) (Li *et al.*, 2009), breast cancer cells (MCF-7, MDA-MB-231) (Lin *et al.*, 2010) and human colon cancer cells (Caco-2) (Jensen, 2013).

In the current study, our experiments using cultured cancer cell lines (A549, HepG2, MCF-7, MDA-MB-468, U2OS, and Caco-2) demonstrates that SIRT1 activated by L3, L4, C3 and C4 aptamers has properties of a growth suppressor. Kaba, (2010) was found that knockdown of SIRT1 increases the rate of tumour growth by enhancing cell proliferation, whereas overexpression of SIRT1 reduces tumour initiation and growth in nude mice, this results is agreement with our suggestion that the pharmacological activation of SIRT1 by aptamers decreases the rate of cell viability in cancer cell lines (A549, HepG2, MCF-7, MDA-MB-468, U2OS and Caco-2) as shown in figures (5.2, 5.8, 5.14, 5.20, 5.26 and 5.32) respectively. Together, these results suggest that SIRT1 functions as a context-dependent tumour suppressor where activation of SIRT1 suppress tumour initiation and promote cell death. SIRT1 has a well-established anti-apoptotic function which has led to the presumption that it acts as an oncogene. However, a study showed that transgenic mice overexpressing SIRT1 reduced the development of neoplasia in the intestine caused by *Apc^{Min}* mutation suggesting a tumour suppressive role of SIRT1 (Firestein *et al.*, 2008). Wang *et al.*, (2008) demonstrated that *Sirt1*^{+/-} mice showed increased tumour incidence when crossed to a *p53*^{+/-} background. These genetic models strongly suggest that SIRT1 has properties of a tumour suppressor and our results lend further support to this function of SIRT1. It is noticeable that our results regarding the anti-proliferative properties of SIRT1 contradict many published studies that show an anti-

apoptotic function of SIRT1. According to these published studies, tumour cells undergo apoptosis or growth arrest after transient knockdown of SIRT1 or treatment with SIRT1 inhibitors such as sirtinol, splitomicin and cambinol (Ford *et al.*, 2005; Heltweg *et al.*, 2006; Ota *et al.*, 2006). Based on our results, aptamers have increased the activity of SIRT1 in cancer cell lines thereby sensitising these cells to DNA damage-induced apoptosis and promotes cell death. A possible explanation for the discrepancies between the studies might be that, in the studies published by other research groups tumour cells treated with SIRT1 shRNA (small hairpin RNA, is an artificial RNA molecule with a tight hairpin turn that can be used to silence target gene expression via RNA interference) may be sensitised to apoptosis due to additional transfection associated stress. Furthermore, the off-target toxicity of the first-generation small molecule SIRT1 inhibitors could be responsible for the cell death or growth arrest responses that they observed (Kabra, 2010). In fact, the recent development of the nanomolar SIRT1 inhibitor EX-527 demonstrated that specific inhibition of SIRT1 alone does not cause apoptosis in tumour cell lines (Solomon *et al.*, 2006; Kabra, 2010).

Several studies have suggested that SIRT1 may act as an oncogene based on the correlation of higher than normal expression levels of SIRT1 in certain tumours compared to normal tissue (Hida *et al.*, 2007; Huffman *et al.*, 2007; Stunkel *et al.*, 2007). In contrast, Kabra, (2010) established that SIRT1 levels are variable in different stages of colon cancer tumours, such a staining pattern can be interpreted as SIRT1 having both oncogenic and tumour-suppressive properties which are consistent with the pleiotropic effects of SIRT1, *i.e.* anti-apoptotic and growth suppressive depending on cellular context and a subset of tumours downregulate SIRT1 to obtain a proliferation advantage, whereas some could increase SIRT1 expression to benefit from its anti-apoptotic function. Although the mechanism by which SIRT1 inhibits cell proliferation remains to be further investigated, previous studies suggested that inhibition of E2F1 is partly responsible for this observed effect as shown in (figure 1.6, chapter 1, page 12). SIRT1 interacts with E2F1, inhibits E2F1 acetylation, and is recruited by E2F1 to target promoters (Wang *et al.*, 2006). When expressed at high levels, SIRT1 is a potent inducer of G1 arrest (Kabra, 2010). Indeed, our results confirmed these previous suggestions that activators of SIRT1 by aptamers could have therapeutic potential as an anti-cancer target. Another scenario is that activators of SIRT1 may impart cancer preventative effects by enhancing the growth-inhibitory effect of SIRT1 in cancer cell line and revealed the decrease level of intracellular ROS production. As mentioned earlier, SIRT1 inactivates the p65 subunit of NF- κ B through direct deacetylation. NF- κ B inhibition suppresses the iNOS (inducible nitric oxide

synthase are a family of enzymes catalysing the production of nitric oxide (NO) from L-arginine) and nitrous oxide production and thus may lower the cellular ROS load (Lee *et al.*, 2009; Merksamer *et al.*, 2013). To further our investigation on the function of SIRT1, C3 aptamer was used to study the activity of SIRT1 in (A549, HepG2, MCF-7, MDA-MB-468, U2OS, and Caco-2) cells. Moreover, our results clearly show that treatment of these cells with lower concentration of C3 aptamer significantly increases the SIRT1 activity in these cells compared with control and resveratrol (figures 5.58, -5.65 respectively), this elevation of SIRT1 activity led to decelerated ROS production but this decreasing in ROS level was not the cause of decreased cell viability of these cancer cells. Based on table 5.1-5.7, when 50 μM TBHP is added, the level of ROS is normalised, considering the cells are dying, so even though C3 aptamer kills cancer cells, it also helps as an added mechanism to survive the damage from ROS, this is suggesting that C3 aptamer might produce the anticancer activity in a different way and not through ROS.

The mechanism underlying the expression control of SIRT1 is poorly understood. To the best of our knowledge, we demonstrate here for the first time that aptamers induce the expression of SIRT1. The results observed in this study are consistent with several research groups have reported that resveratrol which activator SIRT1 was inhibited much more cancer cells proliferation such as Caco-2 (Jensen, 2013), MCF-7, A549 (Lin *et al.*, 2010), U2OS ((Li *et al.*, 2009), MDA-MB-468 (Serrero and Lu, 2001) and HepG2 (Massimi *et al.*, 2012; Hao *et al.*, 2014). To investigate the protective effects of aptamers on skin cells, HaCaT cell line, a well-known model of keratinocytes *in vitro*, was used in this study. Our data clearly show that aptamers were inhibited cell viability through the increased production of ROS. These results suggesting that L3, L4, C3, C4 aptamers which activated SIRT1 could not be used as a protective agent because aptamers should have the ability to increase cell viability and decreased the ROS production as observed in resveratrol effect on this cell line by (Park and lee, 2007; Park and Lee, 2008), but it might be possible to use aptamers in skin cancer as a preventing agent and try to study the effects of C3 aptamer on skin cancer cells. In regard to aptamers effect on normal cells, Bease-2b cell line has been used as a model system of normal cells to compare the result of aptamers on these cells with the observed results in cancer cells (A549, HepG2, MCF-7, MDA-MB-468, U2OS, and Caco-2). Interestingly, it has been demonstrated that there is not effect to used SIRT1-aptamers on Bease-2b cells viability, which indicating that aptamers have actively killing cancer cells without affecting normal cells. The IC_{50} of C3 aptamer was very low concentration (0.32, 0.2, 0.144, 0.13, 0.1, 0.3 and 0.23 μM)

in A549, HepG2, MCF-7, MDA-MB-468, U2OS, Caco-2 and HaCaT cells respectively as shown in figures 5.66-5.72. This low concentration of IC₅₀ is very good results because the low dose of C3 aptamer can inhibit the growth of cancer cells. To study the localisation of SIRT1 in these cells, fluorescence microscopy was used and the results were showed the different location of SIRT1 between cytoplasm and nuclei depending on the type of cells. In A549, HepG2, Caco-2 cells our results were shown that SIRT1 was localised in the cytoplasm (figure 5.73, 5.74 and 5.75 respectively), while in MDA-MB-468, U2OS, HaCaT and Beas-2b cells, the SIRT1 was localised in the nucleus (figures 5.77-5.80).

In summary, our study provides important information regarding SIRT1 aptamers effect on cancer cells. The results presented here suggest that C3 aptamer might be useful in the treatment of these types of cancer because its properties of a growth suppressor for specific killing of the tumour cells only avoiding unpleasant side effects from damage to the rest of the body. More studies are needed, for example, the cellular mechanism of action of SIRT1 in aptamer-mediated apoptosis demands further investigation and, furthermore, the C3 aptamer-induced apoptosis of these cells needs to be investigated in appropriate *in vivo* models.

6 GENERAL DISCUSSION AND FUTURE PERSPECTIVES

6.1 Discussion

Aptamers have been proven to be highly versatile reagents for biological, diagnostic and therapeutic applications ever since the concept was developed in 1990. A multitude of cancer therapeutic usages of aptamers has been reported. In the present study, novel aptamers were developed by used SELEX technology to produce the first known circular³ aptamer capable of binding to the SIRT1 enzyme.

The systemic evolution of ligands by exponential enrichment technique is a powerful and effective aptamer-selection procedure. However, modifications to the process can dramatically improve selection efficiency and aptamer performance. Therefore, the conditions of an individual *in vitro* selection need to be optimised according to the target properties and the requirements of selected aptamers. The most important point of success during aptamer selection is highly dependent on the design of the library. There are some rules to design a suitable library and primers for SELEX. A library cannot be too stable as it must be easily denaturated at 95°C for PCR. Our library; 5'-TTCGGAAGAGATGGCGAC-N40-CGAGCTGATCCTGATGGAA -3' had a mean melting temperature of 72°C. Primers should not have the guanine at 5' or 3' ends. Guanine can quench the fluorescent molecules if it is close enough. Fluorescence quenching by an adjacent guanosine nucleotide is an under-appreciated phenomenon that can significantly affect quantum yield. Depending upon the fluorophore, this effect can be as much as 40%. The mechanism of fluorophore quenching has been explained by electron sharing/donor properties of the adjacent base (Nazarenko *et al.*, 2002). Quenching of 2- aminopurine fluorescence in DNA is dominated by distance-dependent electron transfer from 2-aminopurine to guanosine (Kelly and Barton, 1999). Seidel *et al.* (1996) found that photo-induced electron transfer plays an important role in this type of quenching. The order of quenching efficiency is G<A<C<T if the nucleobase is reduced but it is the reverse, G>A>C>T if the nucleobase is oxidised (Seidel *et al.*, 1996). Nazarenko *et al.*, (2002) also report that quenching by adjacent nucleobases is dependent upon the location of the fluorophore within the oligonucleotide. The primers must be 18 to 20 base pairs, must have GC content of 50% or more and anneal to a library around 55°C to 60°C. Our primers 5'-TTCGGAAGAGATGGCGAC-3' and 5'-CGAGCTGATCCTGATGGAA-3' had a GC content of 52.5 %. They had a melting temperature of 60°C, respectively. Also, each primer

must have a ΔG lower than 5kcal/mol. Our primers had ΔG of -7.04kcal/mol and -8kcal/mol, respectively. The library was synthesised by TriLink BioTechnology and the successfully synthesised DNA library was separated and purified by reversed-phase ion pairing HPLC. SELEX methodology was successfully used to select specific aptamers for the SIRT1 enzyme. In our SELEX strategy, we did not use any negative selection round because the aim of this study is select aptamers broadly recognising the SIRT1 enzyme, the smooth and uninterrupted selection is very important for successive SELEX. In negative selection, disrupting the SELEX exponential enrichment chain can easily be broken and some enriched sequences can be lost. Therefore, only purified SIRT1 enzyme was used and increased the stringency of SELEX by decreasing the time of incubation, increasing the washing, and adding high concentration salt from 150mM-1500mM NaCl+5mM MgCl₂ for later rounds of SELEX without negative selection. After first incubation of library with SIRT1 enzyme target, each round was followed by a preparative PCR of eluted binders. This step is one of the most important steps in the SELEX. In the current study, circular and linear aptamers against SIRT1 enzyme were selected. For circular aptamer, circularisation library was carried out before starting each round of SELEX.

After the 8th round SELEX of circular aptamers (figure 3.13) and 12th round SELEX of linear aptamers (figure 3.15), a total of 144 clones (72 circular and 72 linear) were sent for sequencing resulting in 100 (50 for Circular and 50 for Linear) complete sequences used in analysis sequencing. The 100 sequences were sorted into 8 classes as shown in table 3.1 (linear1, linear2, linear3, linear4, circular1, circular2, circular3, and circular4) with sizes ranging from 6-19% frequency. After selecting candidate aptamers, the sequences were grouped according to frequency of sequences to (linear3, linear4, circular2, circular3 and circular4). Then 10 aptamers (table 3.2) were chosen to study the characterisation that are: {(linear3= L1 and L2), (linear4= L3 and L4), (circular2= C1 and C2), (circular3= C3 and C4) and (circular4= C5 and C6)}, 5 aptamers with primer to find out if primer is important for the effectiveness of aptamer or not (L2, L4, C2, C4 and C6) and 5 aptamers the primer regions were removed (L1, L3, C1, C3 and C5). A representative set of 10 abundant sequences was chosen for testing their binding abilities and activity to the SIRT1 enzyme. (L1, L2, L3, L4, C1, C2, C3, C4, C5, and C6) aptamers were initially checked for SIRT1 activity and binding affinities using Fluor de Lys-SIRT1 assay, the best activities and binders from these aptamers were further selected for studies characterisation. From the competition study for these 10 aptamers, it is evident that C3, C4, L3 and L4 aptamers were significantly increased the activity

of SIRT1 enzyme compared with the activators controls of the SIRT1 enzyme (figure 4.4) with the low K_d constant (22.6 ± 4.9 , 7.1 ± 1.9 , 20.9 ± 3.7 and 3.5 ± 1.11 nM respectively). This study revealed that activation of SIRT1 by aptamers is strongly dependent on structural features of the aptamers. The structures formed within and between single-stranded nucleic acid of C3, C4, L3 and L4 aptamers are mainly a result of the interactions between their nitrogenous bases and these bases. These bases are decorated with a number of complementary hydrogen bond acceptors and donors. The common mechanism of association between two complementary sequences is by Watson-Crick base-pairing, in which purine nitrogenous bases (guanine and adenine) form hydrogen bonds with the pyrimidine nitrogenous bases (cytosine and thymine). The sequences of C3 and C4 aptamers as shown in table 3.2 (CGAGTGGGTTACATCGAAACTGGATCTCAACAGCGGTAAC and TTCGGAAGAGATGGCGACCGAGTGGGTTACATCGAAACTGGATCTCAACAGCGTAACCGAGCTGATCCTGATGGAA respectively) were demonstrated that contents more guanines, these guanines interact with cytosines through 3 hydrogen bonds, while adenines only form 2 hydrogen bonds with thymines, also these circular aptamers contents G:C base pairings and they are more stable than A:T interactions. In addition to the Watson-Crick interactions, base-pairing between nucleotides can occur through other mechanisms, such as Hoogsteen base-pairing, which involves the formation of hydrogen bonds between atoms at the Hoogsteen interface of the nitrogenous bases rather than at the Watson-Crick interface (Bloomfield *et al.*, 2000). Since the nitrogenous bases are non-polar structures, they may also associate by stacking on each other through hydrogen bonding, hydrophobic interactions, electrostatic forces and van der Waals forces in order to reduce the area exposed to polar solvents. Moreover, the bases can also interact by a combination of hydrogen bonding and base stacking to produce more complex structures. For example, in L3 and L4 aptamers sequences as shown in table 3.2 chapter 3 (CACTTTTCGGGGAAATGTGCGCGGAACCCCTATTTGTTTA and TTCGGAAGAGATGGCGACCACTTTTCGGGGAAATGTGCGCGGAACCCCTATTTGTTTA CGAGCTGATCCTGATGGAA respectively) demonstrated that within guanine-rich regions of a nucleic acid sequence, four guanine residues can assemble into a square coplanar array known as a guanine quartet through 8 hydrogen bonds. The guanines of these quartets can further be stacked, thus resulting in the formation of a stable quadruplex structure consisting of 4 strands (Parkinson, 2006). These interactions are the principle instigators of the activity of functional aptamers. Not only are they the driving force behind the folding of single-stranded sequences into specific catalytic structures, they grant these

sequences the ability to selectively bind their target substrates and ligands (SIRT1 enzyme). Additionally, the data suggest that these four novel aptamers interact directly with SIRT1 enzyme and activate SIRT1-catalysed deacetylation through an allosteric mechanism. Furthermore, enzyme kinetic studies of SIRT1 with aptamers were examined through the values of K_m and V_{max} compared to kinetic of the SIRT1 enzyme with resveratrol (tables 4.2-4.5). Consequently, this new design of aptamers by immobilising ssDNA and SIRT1 enzyme showed great selectivity ligands against SIRT1. The enzyme kinetics constants for the SIRT1 enzyme with C3, C4, L3 and L4 compared to those with resveratrol indicated that higher enzyme kinetic efficiency of SIRT1 with aptamers than resveratrol. The decrease in the K_m and V_{max} values of immobilised SIRT1 enzymes is due to electrostatic attraction of hydrophobic adsorption of the aptamers to the solid it might lead to the presence of areas of increased aptamers concentration around the particle. From a reaction rate point of view, the maximal velocity of substrate change was calculated as a remaining amount of aptamer from SIRT1 digestion per minute. The high rate of enzyme reaction and catalytic efficiency of the SIRT1 enzyme could be due to enough diffusion of aptamer molecules to the surface of the particles and to the active sites of the immobilised enzyme. The surface plasmon resonance SPR data have confirmed the high affinity of the aptamers for the SIRT1 enzyme, with the low KD values in the nanomolar range where the C3 aptamer was the best binder with an apparent $KD = 27.07 \pm 0.959$ nM as shown in figure 4.29. The C3 aptamer was characterised for nuclease degradation by blood and was found to be stable, with no indication of degradation for 24 h, as deemed by HPLC and gel electrophoresis (figures 4.33-4.36). This significant human plasma stability of the C3 aptamer can be attributed to circularisation structure, which made the aptamer less susceptible to nuclease degradation in human plasma. Circularisation of aptamers is an attractive alternative to chemical modification for improving aptamer stability. Moreover, circularisation permits the use of natural nucleotides, which should avoid potential toxicity associated with chemical modification. These results suggest that C3 aptamer may well be an appropriate candidate for the development of biotherapy.

The high-affinity SIRT1- aptamers identified in this study may be used in the future to the cancer treatment because the SIRT1 enzyme is a novel target and comes with the challenge of discovering molecules that are activators rather than inhibitors and would be developed as first-in-class cancer therapeutics. Our data in this study using cultured cancer cell lines (A549, HepG2, MCF-7, MDA-MB-468, U2OS, and Caco-2) demonstrates that SIRT1 activated by aptamers has anticancer properties. According to the previous studies, it can be suggesting the

small molecular compounds lead to increase the activity of SIRT1 could be a potential molecular therapy target for cancer cells since there is no recorded data indicating that longer term treatment with resveratrol or selective SIRT1 activators causes tumours in animals.

Several studies reports have provided evidence for a tumour suppressive function of SIRT1 (Firestein *et al.*, 2008; Wang *et al.*, 2008). Stunkel *et al.*, (2007) compared the levels of SIRT1 in cancer cell lines with normal cells and found that SIRT1 was overexpressed in almost all the cancer cell lines that were tested. When stained with the anti-SIRT1 antibody, HeLa and SW620 cell lines exhibited cytoplasmic localisation of SIRT1. Staining of a colon tumour microarray (TMA) also revealed cytoplasmic localisation of SIRT1 in the tumour as well as normal colon tissues. This result was unexpected since the nuclear localisation of SIRT1 is a well-established fact and further investigation of this expression pattern will reveal its significance. Another research group identified two nuclear import and two export sequences on the SIRT1 enzyme and found that SIRT1 could shuttle between the nucleus and cytoplasm in C2C12 myoblast cells (Tanno *et al.*, 2007). SIRT1 was nuclear in undifferentiated C2C12 and localised to the cytoplasm upon differentiation. Nuclear SIRT1 was found to protect the cells against oxidative damage induced cell death but the function of cytoplasmic SIRT1 is yet to be determined. It was hypothesised that the cytoplasmic localisation of SIRT1 is a mode of regulation such that removal of SIRT1 from the nucleus allows for acetylation and activation of certain nuclear substrates of SIRT1. In the current study, the localisation of SIRT1 was determined by fluorescence microscopy and the results were showed the different location of SIRT1 between cytoplasm and nuclei depending on the type of cells. For example, in A549, HepG2, Caco-2 cells our results were shown that SIRT1 was localised in the cytoplasm (figure 5.73, 5.74 and 5.75), while in MDA-MB-468, U2OS, HaCaT and Beas-2b cells, the SIRT1 was localised in the nucleus (figures 5.77-5.80).

To study the role of SIRT1 in cancer, Huffman, *et al.*, (2007) developed a prostate cancer mouse model called TRAMP (Transgenic adenocarcinoma of mouse prostate). SIRT1 levels were found to be elevated in prostate adenocarcinomas in these mice. Simultaneously, HIC1 levels were downregulated leading the authors to suggest that lower levels of HIC1 (Hypermethylated in cancer 1 protein) expression were responsible for the observed increase in SIRT1. Levels of acetylated lys9 on histone H3 were also reduced in these cancers. Upon staining prostate tumour biopsies, it was found that SIRT1 expression was high in the cancer cells as compared to the normal surrounding cells. Based on the association of elevated SIRT1 levels with advanced prostate cancer, the authors summarised that SIRT1 functions as an

oncogene and may serve as a potential target for prostate cancer therapy. However, this model does not provide conclusive evidence for SIRT1 as a cause of prostate cancer. It merely shows an association between high SIRT1 expression and prostate cancer. Another research group generated an SIRT1 null mouse model to determine the role of SIRT1 in tumorigenesis (Wang *et al.*, 2008). They discovered that cells obtained from *Sirt1*^{-/-} embryos exhibited incomplete chromosome condensation and chromosome instability. These cells also demonstrated cell cycle abnormalities and impaired DNA damage repair as compared to *Sirt1*^{+/+} cells. Furthermore, it was discovered that *Sirt1*^{+/-}; *p53*^{+/-} mice were more prone to development of spontaneous tumours as compared to *Sirt1*^{+/-} or *p53*^{+/-} mice. These observations led the authors to suggest that SIRT1 may function as a tumour suppressor. They then analysed a set of clinical tissues to study the levels of SIRT1 expression in tumours and found that SIRT1 levels were lower than normal in glioblastoma, bladder carcinoma, prostate carcinoma and certain ovarian cancers. This expression pattern in the different tumours along with observations from the SIRT1 null mice led the authors to suggest that SIRT1 has a tumour suppressive function.

To study the effect of SIRT1 on tumour formation and growth in colon, the *Apc*^{Min} colon cancer mouse model was bred to an SIRT1 transgenic mouse to obtain progenies that overexpress SIRT1. Polyp formation in SIRT1 overexpressing mice was compared to control *Apc*^{Min} mice. As observed by Firestein, *et al.*, (2008) SIRT1 overexpression was associated with fewer adenomas in the colon of *Apc*^{Min} mice suggesting a tumour suppressive role for SIRT1. It was shown that SIRT1 inhibited colon tumorigenesis by deacetylating and negatively regulating the oncogene, β -catenin. Indeed, in a colon TMA (tissue microarray technology), the nuclear localisation of SIRT1 was associated with a cytoplasmic localisation of β -catenin suggesting that SIRT1 inhibits β -catenin by nuclear exclusion besides deacetylating and inhibiting its transcriptional function (Firestein *et al.*, 2008). McBurney *et al.*, (2003) generated a transgenic mouse model for SIRT1 null genotype. Most of these transgenic mice grew to adulthood probably due to their outbred background and were used to test whether SIRT1 inhibits or promotes the development of cancer (Boily *et al.*, 2009). To study the effect of SIRT1 on skin carcinogenesis, DMBA (7,12-Dimethylbenz[a]anthracene is an immunosuppressor and a powerful organ-specific laboratory carcinogen) was applied to the skin to initiate cancer and TPA (Tissue plasminogen activator, is a protein involved in the breakdown of blood clots) to promote the cancer in wild type and SIRT1 null mice. No difference in tumour formation was observed between the two genotypes but interestingly,

treatment with resveratrol could reduce the tumours in both groups although to a lower extent in SIRT1 null genotypes suggesting an SIRT1-dependent as well as the independent antitumourigenic role of resveratrol. Upon crossing SIRT1 transgenic mice with *Apc^{Min}* mice to study the effect of SIRT1 in colon cancer, it was found that the number of polyps that developed in the *Apc^{Min}; Sirt1^{+/+}* and *Apc^{Min}; Sirt1^{-/-}* mice were almost the same but the *Apc^{Min}; Sirt1^{-/-}* mice had smaller sized polyps. We conclude from this research that SIRT1, at its endogenous expression level, does not modulate susceptibility to tumour formation but is essential for resveratrol-mediated chemoprotection and that the SIRT1 gene expression may have to be induced to a certain level for it to function as a tumour suppressor. The above observations concerning the role of SIRT1 in cancer are conflicting at best.

Based on the early mentioned research above and strong discussions about the role of SIRT1 in cancer, there is a strong evidence to suggest that increasing the activity of SIRT1 leads to inhibition of growth of cancer cells as demonstrated in our results. The data in the current study were established that C3 aptamer at a lower concentration 1 μ M was significantly decreased the cell cancer viability to 47.4, 47.6, 43.9, 41.6, 39.1, and 46.4 in A549, HepG2, MCF-7, U2OS, MDA-MB-468, and Caco-2 cells respectively. Since C3 aptamer show high SIRT1 activity in (A549, HepG2, MCF-7, MDA-MB-468, U2OS, and Caco-2) cancer cell lines, similar to the resveratrol, we investigated if the SIRT1 activator (C3 aptamer) could suppress the ROS level in these cancer cell lines, as it might be SIRT1 activator (C3 aptamer) block the growth of cancer cells by reduction the ROS production. Our result showed that SIRT1 activator (C3 aptamer) could suppress ROS production in cancer cells and increased the percentage of cell death of these cancer cells but this decreasing in ROS level was not the cause of decreased the cell viability of these cancer cells, because C3 aptamer at lower concentrations 0.025 μ M has a closer to 1 ratio (%ROS/ Cell viability) in cancer cells as described in tables 5.1-5.6 chapter 5. The data suggesting that C3 aptamer is killing the cells in different mechanisms and not through ROS.

Furthermore, activation and increased the level of SIRT1 in HaCaT cells was inhibited the growth cells. In contrast to cancer cell line which has been used in this study, the data of HaCaT cells were showed increased the ratio of ROS/Cell viability of 0.25, 0.5, 1 μ M C3 aptamer by 1.7, 1.8 and 2.5 respectively (table 5.7 chapter 5). These data indicate that C3 aptamer was killed the HaCaT cells because of increased the level of ROS. Therefore, the increased activity of SIRT1 in HaCaT cells was not further enhanced to protective these cells but it was helped to inhibition their growth, indicating that SIRT1 potentially used as anti-cancer skin drug.

Regarding the non-cancerous Beas-2b cells, the data analysis has shown that C3 aptamer has no effects on the activity of SIRT1 and does not inhibit the growth of cells. While 100 μM of resveratrol were increased the percentage of Beas-2b cell death to 91%. In addition, the ROS level of Beas-2b cells after treated with C3 aptamer was stayed on its normal value compared with control.

The results above were showed that SIRT1 enzyme's level was increased after adding the C3 aptamer to these cells. It is predicted that this elevation in enzyme's level lead to inhibited the NF- κ B by decreased the nuclear p65 protein the subunit of NF- κ B and decreased the DNA binding through direct deacetylation, according to the earlier studies which have been reported that increasing activity of SIRT1 enzyme leads to inhibiting NF- κ B by SIRT1 which can be blocked cytokine-induced NF- κ B and led to downstream gene iNOS. This, in turn, led to decrease ROS level as was found in the results obtained in this study. According to the results of mechanisms and stability of C3 aptamer and its ability to inhibited the cancer cell line, it can be suggested that C3 aptamer can be used in the future to the cancer treatment.

To summarise, current cancer therapies are varied depending on the type and stage of cancer. In the case of osteosarcoma, therapies involve small drugs and surgery, something practically impossible when it is in a late stage. Colon cancer is a very difficult to treat cancer with bad prognosis if discovered at a later stage. Lung cancers have been in the eye of the storm for many decades, different therapies have been made available, and nevertheless outcome is poor when found at a later stage. Breast cancer has seen different waves, with oestrogen positive being more successful in treatment and oestrogen negative experiencing less success. In the area of biologics, different antibodies have been used to treat some form of cancers, some being used as drug delivery, some for imaging, and some to stimulate the immune system and some targeting cytokines and factors. As any antibody-based therapy, the main side effects are related to interference with the immune system, either shutting it down or overloading, with different outcomes such as mild infections to shock syndrome and over-expression cytokines. Unlike antibodies, aptamers are not immune response inducers, they have the capability of targeting selectively the desired protein, without exerting an immune response. They are also more stable and most important of all, circular aptamers like C3 can enter the cells and reach the target, something antibodies are not capable of performing. This novel C3 aptamer can enter the cells to activate SIRT1 and destroy the cells from within.

In conclusion, using SELEX methodology we have produced an aptamer which is i) selective for SIRT1, ii) enters the cells and iii) interacts only with SIRT1, iv) is stable upon enzymatic attack, v) active on cancer cells, vi) the mode of action is through activation of SIRT1 and vii) is safe on non-cancer cells.

6.2 Future perspectives

As the Circular3 aptamer against SIRT1 enzyme was successfully selected, further efforts will be done to identify its function as a cancer therapy. Oligonucleotide C3 aptamer has become an attractive and promising tool for targeted cancer therapy after obtained our results for inhibited viability of cancer cells. Therefore, we suggest further investigation of clinical data about the cellular mechanism of action for the SIRT1-aptamer in cancer cells by:

- 1) Test the aptamer in an extensive panel of cancer cell lines including difficult to treat cancers such as pancreatic cancer, this will provide us with more information about which other cancers can be affected by activation of SIRT1.
- 2) Test the aptamer in more normal human cells to compare selective toxicity for cancer cells and establish the safety profile.
- 3) Test extensive pharmacokinetics parameters *in vitro* using different enzymes and cell-based assays to work dosage.
- 4) Test the proof of concept *in vivo* models to assess the anticancer activity *in vivo* as well as its pharmacokinetics and pharmacodynamics.

REFERENCES

7 REFERENCES

Albani, D., Polito, L., Forloni, G., (2010). Sirtuins as novel targets for Alzheimer's disease and other neurodegenerative disorders: experimental and genetic evidence. *Journal Alzheimer's Disease*, 19(1), 11–26.

Alzoubi, S., (2013). Histone Acetylation and Chemoresistance in Colorectal Cancer: An Opportunity for Effective Personalized Treatment (Doctoral dissertation, Imperial College London).

Anastasiou, D., and Krek, W., (2006). SIRT1: linking adaptive cellular responses to aging-associated changes in organismal physiology. *Physiology (Bethesda)*, 21, 404-410.

Andreola, M.L., Pileur, F., Calmels, C., Ventura, M., Tarrago-Litvak, L., Toulme, J.J., Litvak, S., (2001). DNA aptamers selected against the HIV-1 RNase H display *in vitro* antiviral activity. *Biochemistry*, 40, 10087–10094.

Anekonda, T.S., (2006). Resveratrol--a boon for treating Alzheimer's disease? *Brain Res Rev.*, 52(2): 316-326.

AntiSoma. Press Release 16/12/2009. AS1411 shows activity in kidney cancer but AML remains priority. Antisoma website [online], <http://www.antisoma.com/asm/media/press/pr2009/2009-12-16/> (2009).

Aparicio, O. M., Billington, B. L., and Gottschling, D. E., (1991). Modifiers of position effect are shared between telomeric and silent mating-type loci in *S. cerevisiae*. *Cell*, 66, 1279-1287.

Ashburner, B. P., Westerheide, S. D., and Baldwin, A. S., Jr., (2001). The p65 (RelA) subunit of NF-kappaB interacts with the histone deacetylase (HDAC) corepressors HDAC1 and HDAC2 to negatively regulate gene expression. *Mol Cell Biol.*, 21, 7065-7077.

Ashraf, N., Zino, S., Macintyre, A., Kingsmor, D., Payne, A.P., George, W.D. *et al.*, (2006). Altered sirtuin expression is associated with node-positive breast cancer. *Br J Cancer*, 9, 1056–1061.

Athar, M., Back, J.H., Tang, X., Kim, K.H., Kopelovich, L., Bickers, D.R. and Kim, A.L., 2007. Resveratrol: a review of preclinical studies for human cancer prevention. *Toxicology and applied pharmacology*, 224(3), pp.274-283.

REFERENCES

- Autiero, I., Costantini, S., Colonna, G., (2009). Human Sirt-1: molecular modeling and structure-function relationships of an unordered protein. *PLoS One*, 4, 7350.
- Ávalos, Y., Canales, J., Bravo-Sagua, R., Criollo, A., Lavandero, S. and Quest, A.F., 2014. Tumour suppression and promotion by autophagy. *BioMed research international*, 2014.
- Avogaro, A., De Kreutzenberg, S.V., Fadini, G.P., (2010). Insulin signaling and life span. *Pflugers Archive European Journal of Physiology*, 459(2), 301–314.
- Aziz, M.H., Afaq, F., Ahmad, N., (2005). Prevention of ultraviolet-B radiation damage by resveratrol in mouse skin is mediated via modulation in survivin. *Photochem Photobiol.*, 81:25-31
- Bae, N. S., Swanson, M. J., Vassilev, A., and Howard, B. H., (2004). Human histone deacetylase SIRT2 interacts with the homeobox transcription factor HOXA10. *J Biochem.*, 135, 695-700.
- Barneda-Zahonero, B., Parra, M., (2012). Histone deacetylases and cancer. *Molecular Oncology*. 6 (6): 579–89.
- Barrett, M. T., Sanchez, C. A., Prevo, L. J., Wong, D. J., Galipeau, P. C., Paulson, T. G., Rabinovitch, P. S., and Reid, B. J., (1999). Evolution of neoplastic cell lineages in Barrett oesophagus. *Nat Genet*, 22, 106-109.
- Bartkova, J., Rezaei, N., Liontos, M., Karakaidos, P., Kletsas, D., Issaeva, N., Vassiliou, L.V.F., Kolettas, E., Niforou, K., Zoumpourlis, V.C., Takaoka, M., Nakagawa, H., Tort, F., Fugger, K., Johansson, F., Sehested, M., Andersen, C. L., Dyrskjot, L., Ørntoft, T., Lukas, J., Kittas, C., Helleday, T., Halazonetis, T.D., Bartek, J. Gorgoulis, V.G., (2006). Oncogene-induced senescence is part of the tumorigenesis barrier imposed by DNA-damage checkpoints. *Nature*, 444(7119): 633-637.
- Bates, P. J. *et al.*, (1999). Antiproliferative activity of G-rich oligonucleotides correlates with protein binding. *J. Biol. Chem*, 274, 26369–26377.
- Bates, P.J., Laber, D.A., Miller, D.M., (2009). Discovery and development of the G-rich oligonucleotide AS1411 as a novel treatment for cancer. *Exp. Mol. Pathol*, 86: 151–164.
- Baur, J.A. and Sinclair, D.A., (2006). Therapeutic potential of resveratrol: the in vivo evidence. *Nat Rev Drug Discov*, 5(6): 493-506.

REFERENCES

- Baur, J.A., Pearson, K.J., Price, N.L., Jamieson, H.A., Lerin, C., Kalra, A., Prabhu, V.V., Allard, J.S., Lopez-Lluch, G., Lewis, K. and Pistell, P.J., 2006. Resveratrol improves health and survival of mice on a high-calorie diet. *Nature*, 444(7117), pp.337-342.
- Bayani, J., Zielenska, M., Pandita, A., Al-Romaih, K., Karaskova, J., Harrison, K., Bridge, J.A., Sorensen, P., Thorner, P., Squire, J.A., (2003). Spectral karyotyping identifies recurrent complex rearrangement of chromosomes 8, 17, 20 in osteosarcomas. *Genes Chromosomes Cancer* 36: 7-16.
- Bayrac, A.T., Sefah, K., Parekh, P., Bayrac, C., Gulbakan, B., Oktem, H.A., Tan, W., (2011). In Vitro Selection of DNA Aptamers to Glioblastoma Multiforme. *ACS Chemical Neuroscience*, 2: 175-181.
- Bedalov, A., Gatabont, T., Irvine, W. P., Gottschling, D. E., Simon, J. A., (2001). Identification of a Small Molecule Inhibitor of Sir2. *Proc. Natl. Acad. Sci. U. S. A.*, 98(26), 15113–15118.
- Beinoraviciute-Kellner, R., Lipps, G., Krauss, G., (2005). *In vitro* selection of DNA binding sites for ABF1 protein from *Saccharomyces cerevisiae*. *FEBS letters*, 579, 4535-40.
- Bellizzi, D., Rose, G., Cavalcante, P., Covello, G., Dato, S., De Rango, F., Greco, V., Maggiolini, M., Feraco, E., Mari, V., et al., (2005). A novel VNTR enhancer within the SIRT3 gene, a human homologue of SIR2, is associated with survival at oldest ages. *Genomics.*, 85, 258-263.
- Berezhnoy, A., Stewart, C. A., Mcnamara, J. O., (2012). Isolation and optimization of murine IL-10 receptor blocking oligonucleotide aptamers using high-throughput sequencing. *Molecular Therapy*.20(6):1242–1250.
- Berg, J.M., Tymoczko, J.L. and Stryer, L., 2002. The Michaelis-Menten model accounts for the kinetic properties of many enzymes. *Biochemistry*, pp.319-330.
- Bertos, N. R., Gilquin, B., Chan, G. K., Yen, T. J., Khochbin, S., and Yang, X. J., (2004). Role of the tetradecapeptide repeat domain of human histone deacetylase 6 in cytoplasmic retention. *J Biol Chem*, 279, 48246-48254.
- Bhat, K. P., and Pizzuto, J. M., (2002). Cancer chemopreventive activity of resveratrol. *Ann N Y Acad Sci.*, 957, 210-229.

REFERENCES

- Bhat, K. P., Kosmeder, J. W., Pezzuto, J. M., (2001). Biological effects of resveratrol. *Antioxid Redox Signal*, 3, 1041-1064.
- Bianchini, M., Radrizzani, M., Brocardo, M.G., Reyes, G.B., Gonzalez, S.C., Santa-Coloma, T.A., (2001). Specific oligobodies against ERK-2 that recognize both the native and the denatured state of the protein. *Journal of Immunological Methods*, 252, 191-197.
- Bitterman, K. J., Anderson, R. M., Cohen, H. Y., Latorre-Esteves, M., Sinclair, D. A., (2002). Inhibition of Silencing and Accelerated Aging by Nicotinamide, a Putative Negative Regulator of Yeast sir2 and Human SIRT1. *J. Biol. Chem.*, 277(47), 45099–45107.
- Blander, G., and Guarente, L., (2004). The Sir2 family of protein deacetylases. *Annu Rev biochem*, 73, 417-35.
- Blank, M., Weinschenk, T., Priemer, M., Schluesener, H., (2001). Systematic evolution of a DNA aptamer binding to rat brain tumour microvessels—selective targeting of endothelial regulatory protein pigpen. *J. Biol. Chem*, 276, 16464–16468.
- Bloomfield, V.A., Crothers, D.M. and Tinoco, I., (2000). *Nucleic acids: structures, properties, and functions*. Sterling Publishing Company.
- Bock, L.C., Griffin, L.C., Latham, J.A., Vermaas, E.H., Toole, J.J., (1992). Selection of single-stranded DNA molecules that bind and inhibit human thrombin. *Nature*, 355, 564– 566.
- Boily, G., He, X. H., Pearce, B., Jardine, K., and McBurney, M. W., (2009). SirT1-null mice develop tumours at normal rates but are poorly protected by resveratrol. *Oncogene*, 28, 2882-2893.
- Boiziau, C., Dausse, E., Yurchenko, L., and Toulme, J. J., (1999). DNA aptamers selected against the HIV-1trans-activation-responsive RNA element form RNA-DNA kissing complexes. *J. Biol. Chem*, 274, 12730–12737.
- Boocock, D.J., Faust, G.E., Patel, K.R., (2007). Phase I dose escalation pharmacokinetic study in healthy volunteers of resveratrol, a potential cancer chemopreventive agent. *Cancer Epidemiol Biomarkers Prev.*, 16:1246–1252.
- Borbas, K., Ferreira, C., Perkins, A., Bruce, A., Missailidis, S., (2007). Design and Synthesis of Mono- and Multimeric Targeted Radiopharmaceuticals Based on novel cyclin ligands

REFERENCES

coupled to anti-MUC1 aptamers for the diagnostic imaging and targeted radiotherapy of cancer. *Bioconjugate Chem.*, 18 (4), 1205–1212.

Bordone, L., Motta, M.C., Picard, F., Robinson, A., Jhala, U.S., Apfeld, J., McDonagh, T., Lemieux, M., McBurney, M., Szilvasi, A., Easlou, E.J., Lin, S.J., and Guarente, L., (2006). Sirt1 regulates insulin secretion by repressing UCP2 in pancreatic beta cells. *PLoS Biol*, 4(2): 31.

Borra, M. T., Denu, J. M., (2004). Quantitative assays for characterisation of the Sir2 family of NAD⁺-dependent deacetylases. *Methods Enzymol.*, 376, 171–187.

Borra, M. T., Smith, B. C., Denu, J. M., (2005). Mechanism of human SIRT1 activation by resveratrol. *J. Biol. Chem.* 280(17), 17187–17195.

Bosch-Presegué, L., and Vaquero, A., (2011). The Dual Role of Sirtuins in Cancer. *Genes & Cancer*, 2(6), 648–662.

Boukamp, P., Petrussevska, R.T., Breitkreutz, D., Hornung, J., Markham, A., Fusenig, N.E., (1988). Normal keratinization in a spontaneously immortalised aneuploid human keratinocyte cell line. *The Journal of Cell Biology*. 106 (3): 761–771.

Bouras, T., Fu, M., Sauve, A.A., Wang, F., Quong, A.A., Perkins, N.D., Hay, R.T., Gu, W., and Pestell, R.G., (2005). SIRT1 deacetylation and repression of p300 involves lysine residues 1020/1024 within the cell cycle regulatory domain 1. *J Biol Chem*, 280(11): 10264-10276.

Bowser, M.T., (2005). SELEX: just another separation? *The Analyst*, 130: 128-130.

Boyault, C., Gilquin, B., Zhang, Y., Rybin, V., Garman, E., Meyer-Klaucke, W., Matthias, P., Muller, C. W., and Khochbin, S., (2006). HDAC6-p97/VCP controlled polyubiquitin chain turnover. *EMBO J.*, 25, 3357-3366.

Bradbury, C.A., Khanim, F.L., Hayden, R., Bunce, C.M., White, D.A., Drayson, M.T., Craddock, C., (2005). Turner BM. Histone deacetylases in acute myeloid leukaemia show a distinctive pattern of expression that changes selectively in response to deacetylase inhibitors. *Leukemia*, 19, 1751–1759.

Brooks, C. L. and Gu, W. (2008) p53 Activation: a case against Sir. *Cancer Cell*, 13, 377-378.

REFERENCES

- Brow, S., (2015). Investigating the Potential Role of SIRT1 in Glioblastoma Multiforme: A Comparison Between Glioma and Normal Astrocyte Cells in Culture.
- Brown, N. S., and Bicknell, R., (2001). Hypoxia and oxidative stress in breast cancer. Oxidative stress: its effects on the growth, metastatic potential and response to therapy of breast cancer. *Breast Cancer Res.*, 3, 323-327.
- Brunet, A., Sweeney, L.B., Sturgill, J.F., Chua, K.F., Greer, P.L., Lin, Y., Tran, H., Ross, S.E., Mostoslavsky, R., Cohen, H.Y., Hu, L.S., Cheng, H.L., Jedrychowski, M.P., Gygi, S.P., Sinclair, D.A., Alt, F.W., and Greenberg, M.E., (2004). Stress-dependent regulation of FOXO transcription factors by the SIRT1 deacetylase. *Science*, 303(5666): 2011-2015.
- Bunka, D.H., Platonova, O., Stockley, P.G., (2010). Development of aptamer therapeutics. *Curr Opin Pharmacol.* 10, 557–562.
- Bunka, D.H., Stockley, P.G., (2006). Aptamers come of age - at last. *Nat Rev Microbiol*, 4,588-96.
- Burke, D.H., Scates, L., Andrews, K., Gold, L., (1996). Bent pseudoknots and novel RNA inhibitors of type 1 human immunodeficiency virus (HIV-1) reverse transcriptase. *J. Mol. Biol.* 264, 650–666.
- Burmeister, P.E., Lewis, S.D., Silva, R.F., (2005). Direct in vitro selection of a 2'-O-methyl aptamer to VEGF. *Chemistry and Biology*, 12, 25-33.
- Cai, B., Yang, X., Sun, L., Fan, S., Li, L., Jin, H., Wu, Y., Guan, Z., Zhang, L., Zhanga, L., Yang, Z., (2014). Stability and bioactivity of thrombin binding aptamers modified with D-/L-isothymidine in the loop regions. *Org. Biomol. Chem.*,12, 8866-8876.
- Canto', C. and Auwerx, J., (2012). Targeting Sirtuin 1 to Improve Metabolism: All You Need Is NAD? *Pharmacol Rev*, 64, 166–187.
- Carafa, V., Rotili, D., Forgione, M., Cuomo, F., Serretiello, E., Hailu, G. S., Altucci, L. (2016). Sirtuin functions and modulation: from chemistry to the clinic. *Clinical Epigenetics*, 8, 61.
- Chaloin, L., Lehmann, M.J., Sczakiel, G., Restle, T., (2002). Endogenous expression of a high-affinity pseudoknot RNA aptamer suppresses replication of HIV-1. *Nucleic Acids Res*, 30, 4001–4008.

REFERENCES

Chen, J., Zhou, Y., Mueller-Steiner, S., Chen, L.F., Kwon, H., Yi, S., Mucke, L., and Gan, L., (2005). SIRT1 protects against microglia-dependent amyloid-beta toxicity through inhibiting NF-kappaB signaling. *J Biol Chem*, 280(48): 40364-40374.

Chen, W. Y., Wang, D. W., Yen, R. C., Luo, J., Gu, W. and Baylin, S. B., (2005). Tumour suppressor HIC1 directly regulates SIRT1 to modulate p53-dependent DNA-damage responses. *Cell*, 123, 437-448.

Cheng, H. L., Mostoslavsky, R., Saito, S., Manis, J. P., Gu, Y., Patel, P., Bronson, R., Appella, E., Alt, F. W., and Chua, K. F., (2003). Developmental defects and p53 hyperacetylation in Sir2 homolog (SIRT1)-deficient mice. *Proc Natl Acad Sci U S A.*, 100, 10794-10799.

Choi, E. W., Nayak, L. V., and Bates, P. J., (2010). Cancer-selective antiproliferative activity is a general property of some G-rich oligodeoxynucleotides. *Nucleic Acids Res.*, 38(5), 1623-1635.

Chu, F., Chou, P.M., Zheng, X., Mirkin, B.L., Rebbaa, A., (2005). Control of multidrug resistance gene *mdr1* and cancer resistance to chemotherapy by the longevity gene *sirt1*. *Cancer Res.*, 65:10183-7.

Chua, K.F., Mostoslavsky, R., Lombard, D.B., Pang, W.W., Saito, S., Franco, S., Kaushal, D., Cheng, H.L., Fischer, M.R., Stokes, N., Murphy, M.M., Appella, E., and Alt, F.W., (2005). Mammalian SIRT1 limits replicative life span in response to chronic genotoxic stress. *Cell Metab*, 2(1): 67-76.

Chuprina, V. P., U Heinemann, A. A., Nurislamov, P., Zielenkiewicz, R. E., Dickerson, and WSAenger., (1991): Molecular dynamics simulation of the hydration shell of a B-DNA decamer reveals two main types of minor-groove hydration depending on groove width. *Proc Natl Acad Sci.*, 88, (2) 593-597.

Ciesiolka, J., Gorski, J., Yarus, M., (1995). Selection of an RNA domain that binds Zn^{2+} . *RNA*, 1, 538-550.

Clawson, G. A., (2016). Histone deacetylase inhibitors as cancer therapeutics. *Annals of Translational Medicine*, 4(15), 287.

REFERENCES

Cohen, H. Y., Lavu, S., Bitterman, K. J., Hekking, B., Imahiyerobo, T. A., Miller, C., Frye, R., Ploegh, H., Kessler, B. M., and Sinclair, D. A., (2004). Acetylation of the C terminus of Ku70 by CBP and PCAF controls Bax-mediated apoptosis. *Mol Cell*, 13, 627-638.

Comings, D. E., (1973). A general theory of carcinogenesis. *Proc Natl Acad Sci U S A*, 70, 3324-3328.

Conklin, K.A., (2004). Chemotherapy-associated oxidative stress: impact on chemotherapeutic effectiveness. *Integr Cancer Her*, 3: 294-300. 91.

Conrad, R., Keranen, L.M., Ellington, A.D., Newton, A.C., (1994). Isozyme- specific inhibition of protein kinase C by RNA aptamers. *Journal of Biological Chemistry*, 269, 32051-32054.

Conrad, R.C., Baskerville, S., Ellington, A.D., (1995). *In vitro* selection methodologies to probe RNA function and structure. *Mol. Div*,1, 69–78.

Cox, J.C., and Ellington, A.D., (2001). Automated selection of anti-protein aptamers. *Bioorganic and Medicinal Chemistry*, 9, 2525-2531.

Dadi, P. K., Ahmad, M., Ahmad, Z., (2009). Inhibition of ATPase Activity of Escherichia coli ATP Synthase by Polyphenols. *Int. J. Biol. Macromol.* 45(1), 72–79.

Dai, J.M., Wang, Z.Y., Sun, D.C., Lin, R.X., and Wang, S.Q., (2007). SIRT1 interacts with p73 and suppresses p73-dependent transcriptional activity. *J Cell Physiol*, 210(1): 161-166.

Dali-Youcef, N., Lagouge, M., Froelich, S., Koehl, C., Schoonjans, K., Auwerx, J., (2007). Sirtuins: the 'magnificent seven', function, metabolism and longevity. *Annals of Medicine*, 39(5),335–345.

Daniel, A., Di, G., Sarah, M., Knox, D., Yuching, L., Gregory, D.T., May, T.A., and Garry, C.K., (2006). Multitasking by Multivalent Circular DNA Aptamers. *ChemBioChem*,7 (3), 535–544.

Dapic, V., Bates, P. J., Trent, J. O., Rodger, A., Thomas, S. D., and Miller, D. M., (2002). Antiproliferative activity of G-quartet-forming oligonucleotides with backbone modifications. *Biochemistry*, 41, 3676-3685.

REFERENCES

- Das, S., Lin, H.S., Ho, P.C., Ng, K.Y., (2008). The impact of aqueous solubility and dose on the pharmacokinetic profiles of resveratrol. *Pharm Res.*, 25:2594–2600.
- Dasgupta, B. and Milbrandt, J., (2007). Resveratrol stimulates AMP kinase activity in neurons. *Proc Natl Acad Sci U S A*, 104(17): 7217-7222.
- David, G., Neptune, M. A., and DePinho, R. A., (2002). SUMO-1 modification of histone deacetylase 1 (HDAC1) modulates its biological activities. *J Biol Chem*, 277, 23658-23663.
- David, J., (2013). A Reversible Cause of Aging. *Tsunster Innovations*, 27.
- Davis, K.A., Abrams, B., Lin, Y., Jayasena, S.D., (1996). Use of a high affinity DNA ligand in flow cytometry. *Nucleic Acids Research*, 24, 702-706.
- de Boer, V. C., de Goffau, M. C., Arts, I. C., Hollman, P. C., Keijer, J., (2006). SIRT1 Stimulation by Polyphenols Is Affected by Their Stability and Metabolism. *Mech. Ageing Dev.* 127(7), 618–627.
- De Nigris, F., Cerutti, J., Morelli, C., Califano, D., Chiariotti, L., Viglietto, G. *et al.*, (2002). Isolation of a SIR-like gene, SIR-T8, that is overexpressed in thyroid carcinoma cell lines and tissues. *Br J Cancer*, 87, 1479.
- de Ruijter, A. J., van Gennip, A. H., Caron, H. N., Kemp, S., and van Kuilenburg, A. B., (2003). Histone deacetylases (HDACs): characterization of the classical HDAC family. *Biochem J*, 370, 737-749.
- Delmas, D., Lançon, A., Colin, D., Jannin, B. and Latruffe, N., (2006). Resveratrol as a chemopreventive agent: a promising molecule for fighting cancer. *Current drug targets*, 7(4), pp.423-442.
- Deng, C.X., (2009). SIRT1, Is it a tumour promoter or tumour suppressor? *Int J Biol Sci*, 5, 147–152.
- Di Primo, C., Dausse, E., Toulmé, J.J., (2011). Surface plasmon resonance investigation of RNA aptamer–RNA ligand interactions. in: J. Goodchild, (Ed.), *Therapeutic oligonucleotides*, humana Press., pp. 279-300.
- Dimitrios, A., and Wilhelm, K., (2006). SIRT1: Linking Adaptive Cellular Responses to Aging-Associated Changes in Organismal Physiology. *Physiology*, 21(6) 404-410.

REFERENCES

- Dobbelstein, M., and Shenk, T., (1995). *In vitro* selection of RNA ligands for the ribosomal L22 protein associated with Epstein-Barr virus-expressed RNA by using randomized and cDNA-derived RNA libraries. *Journal of Virology*, 69, 8027-8034.
- Dokmanovic, M., Clarke, C., Marks, P. A., (2007). Histone deacetylase inhibitors: Overview and Perspectives. *Mol Cancer Res.*,5(10).
- Dong, M., Liu, B., Zhu, R., (2016). Targeting ROS for cancer therapy. *Chemo Open Access*, 5:2.
- Donmez, G., and Outeiro, T. F., (2013). SIRT1 and SIRT2: emerging targets in neurodegeneration. *EMBO Mol. Med.*, 5, 344–352
- Dryden, S. C., Nahhas, F. A., Nowak, J. E., Goustin, A. S., and Tainsky, M. A., (2003). Role for human SIRT2 NAD-dependent deacetylase activity in control of mitotic exit in the cell cycle. *Mol Cell Biol.*, 23, 3173-3185.
- Duconge, F., Toulme, J.J., (1999). *In vitro* selection identifies key determinants for loop-loop interactions: RNA aptamers selective for the TAR RNA element of HIV-1. *RNA-A*, 5, 1605–1614.
- Ellington, A.D., Conrad, R., (1995). Aptamers as potential nucleic acid pharmaceuticals. *Biotechnology Annual Review*, 1: 185-214.
- Ellington, A.D., Szostak, J.W., (1990). *In vitro* selection of RNA molecules that bind specific ligands. *Nature* 346, 818–822.
- Ellington, A.D., Szostak, J.W., (1992). Selection *in vitro* of single-stranded DNA molecules that fold into specific ligand-binding structures. *Nature*, 355, 850– 852.
- Esteves, A.R., Lu, J., Rodova, M., *et al.*, (2010). Mitochondrial respiration and respiration-associated proteins in cell lines created through Parkinson's subject mitochondrial transfer. *Journal of Neurochemistry*, 113(3), 674–682.
- Eulberg, D., and Klussmann, S., (2003). Spiegelmers: biostable aptamers. *ChemBiochem*.4, 979-83.

REFERENCES

- Eyetechnology Study Group., (2003). Antivascular endothelial growth factor therapy for subfoveal choroidal neovascularization secondary to age-related macular degeneration, phase II study results. *Ophthalmology*, 110, 979–86.
- Famulok, M., (1999). Oligonucleotide aptamers that recognize small molecules. *Curr. Opin. Struct. Biol*, 9, 324–329.
- Famulok, M., (2009). Exploring chemical space with aptamers. *J Med Chem*, 52, 6951-7.
- Fan, W., Luo, J., (2010). SIRT1 regulates UV-induced DNA repair through deacetylating XPA. *Mol Cell*, 39:247-58.
- Fan, Y., Hense, M., Ludewig, R., Weisgerber, C., Scriba, G. K., (2011). Capillary Electrophoresis-Based Sirtuin Assay Using Non-Peptide Substrates. *J. Pharm. Biomed. Anal.*, 54(4), 772–778.
- Feinberg, A. P., and Tycko, B., (2004). The history of cancer epigenetics. *Nat Rev Cancer*, 4, 143-153.
- Feinberg, A. P., Cui, H., and Ohlsson, R., (2002). DNA methylation and genomic imprinting: insights from cancer into epigenetic mechanisms. *Semin Cancer Biol.*, 12, 389-398.
- Feng, H., Beck, J., Nassal, M., and Hu, K., (2011). A SELEX-screened aptamer of human hepatitis B Virus RNA encapsidation signal suppresses viral replication. *PLoS ONE*, 6, 27862.
- Feng, Y., Wu, J., Chen, L., Luo, C., Shen, X., Chen, K., Jiang, H., Liu, D., (2009). A fluorometric assay of SIRT1 deacetylation activity through quantification of nicotinamide adenine dinucleotide. *Anal. Biochem.*, 395(2), 205–210.
- Ferreira, C.S., Cheung, M.C., Missailidis, S., Bisland, S. and Gariépy, J., (2009). Phototoxic aptamers selectively enter and kill epithelial cancer cells. *Nucleic acids research*, 37(3), pp.866-876.
- Findeisen, H. M., Gizard, F., Zhao, Y., Qing, H., Heywood, E. B., Jones, K. L., Bruemmer, D. (2011). Epigenetic Regulation of Vascular Smooth Muscle Cell Proliferation and Neointima Formation by Histone Deacetylase Inhibition. *Arteriosclerosis, Thrombosis, and Vascular Biology*, 31(4), 851–860.

REFERENCES

- Firestein, R., Blander, G., Michan, S., Oberdoerffer, P., Ogino, S., Campbell, J., Bhimavarapu, A., Luikenhuis, S., de Cabo, R., Fuchs, C., Hahn, W.C., Guarente, L.P., Sinclair, D.A., (2008). The SIRT1 deacetylase suppresses intestinal tumorigenesis and colon cancer growth. *PLoS ONE*, 3, 2020.
- Fischer, D. D., Cai, R., Bhatia, U., Asselbergs, F. A., Song, C., Terry, R., Trogani, N., Widmer, R., Atadja, P., and Cohen, D. (2002). Isolation and characterization of a novel class II histone deacetylase, HDAC10. *J Biol Chem*, 277, 6656-6666.
- Fischle, W., Dequiedt, F., Fillion, M., Hendzel, M. J., Voelter, W., and Verdin, E. (2001). Human HDAC7 histone deacetylase activity is associated with HDAC3 in vivo. *J Biol Chem*, 276, 35826-35835.
- Ford, E., Voit, R., Liszt, G., Magin, C., Grummt, I., and Guarente, L., (2006). Mammalian Sir2 homolog SIRT7 is an activator of RNA polymerase I transcription. *Genes Dev*, 20(9): 1075-1080.
- Ford, J., Jiang, M. and Milner, J., (2005) Cancer-specific functions of SIRT1 enable human epithelial cancer cell growth and survival. *Cancer Res*, 65, 10457-10463.
- Fraga, M.F., Ballestar, E., Villar-Garea, A., Boix-Chornet, M., Espada, J., Schotta, G., Bonaldi, T., Haydon, C., Ropero, S., Petrie, K., Iyer, N.G., Perez-Rosado, A., Calvo, E., Lopez, J.A., Cano, A., Calasanz, M.J., Colomer, D., Piris, M.A., Ahn, N., Imhof, A., Caldas, C., Jenuwein, T., and Esteller, M., (2005). Loss of acetylation at Lys16 and trimethylation at Lys20 of histone H4 is a common hallmark of human cancer. *Nat Genet*, 37(4): 391-400.
- Frescas, D., Valenti, L., and Accili, D., (2005). Nuclear trapping of the forkhead transcription factor FoxO1 via Sirt-dependent deacetylation promotes expression of glucogenetic genes. *J Biol Chem*, 280(21): 20589-20595.
- Fritze, C. E., Verschueren, K., Strich, R., and Easton Esposito, R., (1997). Direct evidence for SIR2 modulation of chromatin structure in yeast rDNA. *EMBO J*, 16, 6495-6509.
- Fruehauf, J.P., Meyskens, F.L., (2007). Reactive oxygen species: a breath of life or death? *Clin Cancer Res.*, 13:789–794.

REFERENCES

- Frye, R.A., (1999). Characterization of five human cDNAs with homology to the yeast SIR2 gene: Sir2-like proteins (sirtuins) metabolize NAD and may have protein ADP-ribosyltransferase activity. *Biochem. Biophys. Res. Commun.*, 260 (1), 273–9.
- Frye, R.A., (2000). Phylogenetic classification of prokaryotic and eukaryotic Sir2-like proteins. *Biochemical and Biophysical Research Communications*, 273(2):793–798.
- Fu, M., Liu, M., Sauve, A. A., Jiao, X., Zhang, X., Powell, M., Yang, T., Gu, W., Avantaggiati, M. L., Pattabiraman, N., Pestell, T. G., Wang, F., Quong, A., Wang, C. and Pestell R. G., (2006) Hormonal control of androgen receptor function through SIRT1. *Mol. Cell. Biol*, 26, 8122-8135.
- Fulco, M., Schiltz, R.L., Iezzi, S., King, M.T., Zhao, P., Kashiwaya, Y., Hoffman, E., Veech, R.L., and Sartorelli, V., (2003). Sir2 regulates skeletal muscle differentiation as a potential sensor of the redox state. *Mol Cell*, 12(1): 51-62.
- Furuya, K., Ozaki, T., Hanamoto, T., Hosoda, M., Hayashi, S., Barker, P.A., Takano, K., Matsumoto, M., Nakagawara, A., (2007). Stabilisation of p73 by nuclear I{kappa}B kinase- α mediates cisplatin-induced apoptosis. *J Biol Chem.*, 282(25): 18365-18378.
- Gao, F., Cheng, J., Shi, T., and Yeh, E.T., (2006). Neddylated of a breast cancer-associated protein recruits a class III histone deacetylase that represses NFkappaB-dependent transcription. *Nat Cell Biol.*, 8(10): 1171-1177.
- Gao, J., Siddoway, B., Huang, Q., and Xia, H., (2009). Inactivation of CREB mediated gene transcription by HDAC8 bound protein phosphatase. *Biochem Biophys Res Commun*, 379, 1-5.
- Gao, L., Cueto, M. A., Asselbergs, F., and Atadja, P., (2002). Cloning and functional characterization of HDAC11, a novel member of the human histone deacetylase family. *J Biol Chem.*, 277, 25748-25755.
- Geiger, A., Burgstaller, P., von der Eltz, H., Roeder, A., and Famulok, M., (1996). RNA aptamers that bind L-arginine with sub-micromolar dissociation constants and high enantioselectivity. *Nucleic acids research*, 24, 1029-1036.

REFERENCES

- Gerhart-Hines, Z., Rodgers, J.T., Bare, O., Lerin, C., Kim, S.H., Mostoslavsky, R., Alt, F.W., Wu, Z., Puigserver, P., (2007). Metabolic control of muscle mitochondrial function and fatty acid oxidation through SIRT1/PGC-1 α . *EMBO J*, 26, 1913–1923.
- Gescher, A.J., Steward, W.P., (2003). Relationship between mechanisms, bioavailability, and preclinical chemopreventive efficacy of resveratrol: a conundrum. *Cancer Epidemiol Biomarkers Prev.*, 12:953–957.
- Ghosh, S., George, S., Roy, U., Ramachandran, D., Kolthur-Seetharam, U., (2010). NAD: a master regulator of transcription. *Biochimica et Biophysica Acta*, 1799(10-12), 681– 693.
- Giard, D. J., Aaronson, S.A., Todaro, G. J., Arnstein, P., Kersey, J. H., Dosik, H. and Parks, W. P. (1973). In vitro cultivation of human tumours: Establishment of cell lines derived from a series of solid tumours. *J of the National Cancer Institute.*, 51 (5): pp. 1417-1423.
- Gilboa, E., Berezhnoy, A., Schrand, B., (2015). Reducing toxicity of immune therapy using aptamer-targeted drug delivery. *Cancer Immunology Research*, 3(11):1195–1200.
- Gilboa, E., McNamara, J., Pastor, F., (2013). Use of oligonucleotide aptamer ligands to modulate the function of immune receptors. *Clinical Cancer Research*, 19(5):1054–1062.
- Giono, L. E., and Manfredi, J. J., (2006). The p53 tumour suppressor participates in multiple cell cycle checkpoints. *J Cell Physiol*, 209, 13-20.
- Glozak, M. A., and Seto, E., (2007). Histone deacetylases and cancer. *Oncogene*, 26, 5420-5432.
- Gold, L., Brody, E., Heilig, J., Singer, B., (2002). One, two, infinity: genomes filled with aptamers. *Chem.Biol*, 9(12), 1259-64.
- Gopinath, S.C., Sakamaki, Y., Kawasaki, K. and Kumar, P.K., 2006. An efficient RNA aptamer against human influenza B virus hemagglutinin. *Journal of biochemistry*, 139(5), pp.837-846.
- Gopinath, S.C.B., Kawasaki, K., and Kumar, P.K.R., (2005). *Nucleic Acids Sympser*, 49, 85.
- Gopinath, S.C.B., Misono, T.S., Kawasaki, K., Mizuno, T., Imai, M., Odagiri, T., and Kumar, P.K.R., (2006). An RNA aptamer that distinguishes between closely related human influenza viruses and inhibits haemagglutinin-mediated membrane fusion. *Journal of General Virology*, 87, 479-487.

REFERENCES

- Grbesa, I., Pajares, M. J., Martínez-Terroba, E., Agorreta, J., Mikecin, A.-M., Larráyo, M., ... Montuenga, L. M., (2015). Expression of Sirtuin 1 and 2 Is Associated with Poor Prognosis in Non-Small Cell Lung Cancer Patients. *PLoS ONE*, 10(4), e0124670.
- Green, L.S., Jellinek, D., Jenison, R., Ostman, A., Heldin, C.H., Janjic, N., (1996). Inhibitory DNA ligands to platelet-derived growth factor B-chain. *Biochemistry*, 35, 14413–14424.
- Gregoret, I. V., Lee, Y. M., and Goodson, H. V., (2004). Molecular evolution of the histone deacetylase family: functional implications of phylogenetic analysis. *J Mol Biol*, 338, 17-31.
- Griffin, L. C., Toole, J. J., Leung, L. L. K., (1993), The discovery and characterisation of a novel nucleotide-based thrombin inhibitor. *Gene*, 137, 25-31.
- Grozing, C. M., and Schreiber, S. L., (2000). Regulation of histone deacetylase 4 and 5 and transcriptional activity by 14-3-3-dependent cellular localization. *Proc Natl Acad Sci U S A*, 97, 7835-7840.
- Grozing, C. M., Chao, E. D., Blackwell, H. E., Moazed, D., Schreiber, S. L., (2001). Identification of a class of small molecule inhibitors of the Sirtuin family of NAD-dependent deacetylases by phenotypic screening. *J. Biol. Chem.*, 276(42), 38837–38843
- Grozing, C. M., Hassig, C. A., and Schreiber, S. L., (1999). Three proteins define a class of human histone deacetylases related to yeast Hda1p. *Proc Natl Acad Sci U S A*, 96, 4868- 4873.
- Gu, J., (2011). Selection of cell- internalizing circular DNA aptamers, (Doctoral dissertation).
- Gu, W., and Roeder, R. G., (1997). Activation of p53 sequence-specific DNA binding by acetylation of the p53 C-terminal domain. *Cell*, 90, 595-606.
- Guardiola, A. R., and Yao, T. P., (2002). Molecular cloning and characterization of a novel histone deacetylase HDAC10. *J Biol Chem*, 277, 3350-3356.
- Gupta, S. C., Hevia, D., Patchva, S., Park, B., Koh, W., & Aggarwal, B. B. (2012). Upsides and downsides of reactive oxygen species for cancer: The roles of reactive oxygen species in tumorigenesis, prevention, and therapy. *Antioxidants & Redox Signaling*, 16(11), 1295–1322.
- Göringer, H.U., Homann, M., Lorger, M., (2003). *In vitro* selection of highaffinity nucleic acid ligands to parasite target molecules. *Int. J. Parasitol.* 33,1309–1317.

REFERENCES

- Haberland, M., Arnold, M. A., McAnally, J., Phan, D., Kim, Y., and Olson, E. N., (2007). Regulation of HDAC9 gene expression by MEF2 establishes a negative-feedback loop in the transcriptional circuitry of muscle differentiation. *Mol Cell Biol*, 27, 518-525.
- Haigis, M. C., & Sinclair, D. A. (2010). Mammalian Sirtuins: Biological Insights and Disease Relevance. *Annual Review of Pathology*, 5, 253–295.
- Haigis, M. C., Mostoslavsky, R., Haigis, K. M., Fahie, K., Christodoulou, D. C., Murphy, A. J., Valenzuela, D. M., Yancopoulos, G. D., Karow, M., Blander, G., et al., (2006). SIRT4 inhibits glutamate dehydrogenase and opposes the effects of calorie restriction in pancreatic beta cells. *Cell*, 126, 941-954.
- Halkidou, K., Gaughan, L., Cook, S., Leung, H. Y., Neal, D. E., and Robson, C. N., (2004). Upregulation and nuclear recruitment of HDAC1 in hormone refractory prostate cancer. *Prostate*, 59, 177-189.
- Hall, B., Arshad, S., Seo, K., Bowman, C., Corley, M., Jhaveri, S.D. and Ellington, A.D., (2010). In vitro selection of RNA aptamers to a protein target by filter immobilization. *Current protocols in nucleic acid chemistry*, pp.9-3.
- Hallows, W.C., Lee, S., and Denu, J.M., (2006). Sirtuins deacetylate and activate mammalian acetyl-CoA synthetases. *Proc Natl Acad Sci U S A*, 103(27): 10230-10235.
- Hamilton, B., Dong, Y., Shindo, M., *et al.*, (2005). A systematic RNAi screen for longevity genes in *C. elegans*. *Genes and Development*, 19(13), 1544–1555.
- Hanahan, D., and Weinberg, R. A., (2000). The hallmarks of cancer, *Cell* 100, 57-70.
- Hansen, M., Taubert, S., Crawford, D., Libina, N., Lee, S.J., Kenyon, C., (2007). Lifespan extension by conditions that inhibit translation in *Caenorhabditis elegans*. *Aging Cell*, 6(1), 95–110.
- Hao, C., Zhu, P., Yang, X., Han, Z., Jiang, J., Zong, C., (2014). Overexpression of SIRT1 promotes metastasis through epithelial-mesenchymal transition in hepatocellular carcinoma. *BMC Cancer*, 14:978.
- Hardin, C. C., Perry, A. G., and White, K., (2000). Thermodynamic and Kinetic Characterisation of the Dissociation and Assembly of Quadruplex Nucleic Acids. *Biopolymers: Nucleic Acid Sciences*, 56, 147-194.

REFERENCES

- Harper, C.E., Patel, B.B., Wang, J., Arabshahi, A., Eltoum, I.A., Lamartiniere, C.A., (2007) Resveratrol suppresses prostate cancer progression in transgenic mice. *Carcinogenesis*, 28:1946-53.
- Haworth, R. S., and Avkiran, M., (2001). Inhibition of protein kinase D by resveratrol. *Biochem Pharmacol.*, 62, 1647-1651.
- He, H., Chen, X., Wang, G., (2006). High-performance liquid chromatography spectrometric analysis of trans-resveratrol in rat plasma. *J Chromatogr B Analyt Technol Biomed Life Sci.* 832:177–180.
- Heltweg, B., Gatbonton, T., Schule, A.D., Posakony, J., Li, H., Goehle, S., (2006). Antitumour activity of a small-molecule inhibitor of human silent information regulator 2 enzymes. *Cancer Res*, 66, 4368–4377.
- Hermann, T., Patel, D.J., (2000). Adaptive recognition by nucleic acid aptamers. *Science*, 287, 820–825.
- Herranz, D., Munoz-Martin, M., Canamero, M., (2010). Sirt1 improves healthy ageing and protects from metabolic syndrome-associated cancer. *Nat Commun.*, 1:1-8.
- Hicke, B.J., Marion, C., Chang, Y.F., Gould, T., Lynott, C.K., Parma, D., Schmidt, P.G., Warren, S., (2001). Tenascin-C aptamers are generated using tumour cells and purified protein. *J Biol Chem.*, 28;276(52):48644-54.
- Hida, Y., Kubo, Y., Murao, K., (2007). Arase S. Strong expression of a longevity-related protein, SIRT1, in Bowen's disease. *Arch Dermatol Res.*, 299:103-6.
- Hofmann, H.P., Limmer, S., Hornung, V., Sprinzl, M., (1997). Ni²⁺-binding RNA motifs with an asymmetric purine-rich internal loop and a G-A base pair. *RNA*, 3,1289–1300.
- Homann, M., Göringer, H.U., (1999). Combinatorial selection of high affinity RNA ligands to live African trypanosomes. *Nucleic Acids Research*, 27, 2006-2014.
- Horn, W.T., Convery, M.A., Stonehouse, N.J., Adams, C.J., Liljas, L., Phillips, S.E.V., Stockley, P.G., (2004). The crystal structure of a high affinity RNA stem-loop complexed with the bacteriophage MS2 capsid: further challenges in the modeling of ligand-RNA interactions. *RNA-A*, 10, 1776–1782.

REFERENCES

- Howitz, K.T., Bitterman, K.J., Cohen, H.Y., Lamming, D.W., Lavu, S., Wood, J.G., Zipkin, R.E., Chung, P., Kisielewski, A., Zhang, L.L., Scherer, B., and Sinclair, D.A., (2003). Small molecule activators of sirtuins extend *Saccharomyces cerevisiae* lifespan. *Nature*, 425(6954): 191-196.
- Hu, E., Chen, Z., Fredrickson, T., Zhu, Y., Kirkpatrick, R., Zhang, G. F., Johanson, K., Sung, C. M., Liu, R., and Winkler, J., (2000). Cloning and characterisation of a novel human class I histone deacetylase that functions as a transcription repressor. *J Biol Chem*, 275, 15254-15264.
- Huang, B. H., Laban, M., Leung, C. H., Lee, L., Lee, C. K., Salto-Tellez, M., Raju, G. C., and Hooi, S. C., (2005). Inhibition of histone deacetylase 2 increases apoptosis and p21^{Cip1}/WAF1 expression, independent of histone deacetylase 1. *Cell Death Differ*, 12, 395-404.
- Huang, J.Y., Hirsche, M.D., Shimazu, T., Ho, L., Verdin, E., (2010). Mitochondrial sirtuins. *Biochimica et Biophysica Acta*, 1804(8), 1645–1651.
- Hubbert, C., Guardiola, A., Shao, R., Kawaguchi, Y., Ito, A., Nixon, A., Yoshida, M., Wang, X. F., and Yao, T. P., (2002). HDAC6 is a microtubule-associated deacetylase. *Nature*, 417, 455- 458.
- Huber, J. L., McBurney, M. W., Distefano, P. S., McDonagh, T., (2010). SIRT1-Independent Mechanisms of the Putative Sirtuin Enzyme Activators SRT1720 and SRT2183. *Future Med. Chem.* 2(12), 1751–1759.
- Huffman, D.M., Grizzle, W.E., Bamman, M.M., (2007). SIRT1 is significantly elevated in mouse and human prostate cancer. *Cancer Res.*, 67:6612-8.
- Huguet, E.L., (1994). Differential expression of human Wnt genes 2, 3, 4, and 7B in human breast cell lines and normal and disease states of human breast tissue. *Cancer Res.*, 54: 2615-2621.
- Ihrke, G., Neufeld, E.B., Meads, T., (1993). WIF-B cells: an in vitro model for studies of hepatocyte polarity. *Journal of Cell Biology*, 123 (6): 1761–1775.
- Ikebukuro, K., Okumura, Y., Sumikura, K., Karube, I., (2005). A novel method of screening thrombin-inhibiting DNA aptamers using an evolution-mimicking algorithm. *Nucleic Acids Res.*, 33, e108.

REFERENCES

- Imai, S., Armstrong, C.M., Kaeberlein, M., and Guarente, L., (2000). Transcriptional silencing and longevity protein Sir2 is an NAD-dependent histone deacetylase. *Nature*, 403(6771): 795-800.
- Inoue, T., Hiratsuka, M., Osaki, M., and Oshimura, M., (2007). The molecular biology of mammalian SIRT proteins: SIRT2 in cell cycle regulation. *Cell Cycle.*, 6, 1011-1018.
- Jackson, M. D., Denu, J. M. (2002). Structural identification of 2'- and 3'-O-Acetyl-ADP-Ribose as novel metabolites derived from the Sir2 family of β -NAD⁺-dependent Histone/Protein Deacetylases. *J. Biol. Chem.*, 277(21), 18535–18544.
- Jagasia, R., Steib, K., Englberger, E., Herold, S., Faus-Kessler, T., Saxe, M., Lie, D. C. (2009). GABA-CREB signalling regulates maturation and survival of newly generated neurons in the adult hippocampus. *The Journal of Neuroscience: The Official Journal of the Society for Neuroscience*, 29(25), 7966–7977.
- James, W., (2000). Aptamers. In: Meyers, R.A. (Ed.), *Encyclopedia of analytical chemistry*. John Wiley & Sons Ltd., Chichester, pp. 4848–4871.
- Jayasena, S.D., (1999). Aptamers: an emerging class of molecules that rival antibodies in diagnostics. *Clin Chem*, 45,1628-50.
- Jellinek, D., Green, L.S., Bell, C., Janjic, N., (1994). Inhibition of receptor binding by high-affinity RNA ligands to vascular endothelial growth factor. *Biochemistry*, 33, 10450–10456.
- Jensen, C.H., (2013). The effect of resveratrol on the human colon cancer cell line Caco-2. (MSc. Dissertation).
- Jensen, K.B., Atkinson, B.L., Willis, M.C., Koch, T.H. and Gold, L., (1995). Using in vitro selection to direct the covalent attachment of human immunodeficiency virus type 1 Rev protein to high-affinity RNA ligands. *Proceedings of the National Academy of Sciences*, 92(26), pp.12220-12224.
- Jenuwein, T., and Allis, C. D., (2001). Translating the histone code. *Science*, 293, 1074-1080.
- Jeong, J., Juhn, K., Lee, H., Kim, S.H., Min, B.H., Lee, K.M., Cho, M.H., Park, G.H., and Lee, K.H., (2007). SIRT1 promotes DNA repair activity and deacetylation of Ku70. *Exp Mol Med*, 39(1): 8-13.

REFERENCES

- Jiang, L., Suri, A.K., Fiala, R., Patel, D.J., (1997). Saccharide-RNA recognition in an aminoglycoside antibiotic-RNA aptamer complex. *Chem. Biol*, 4, 35–50.
- Jiang, R., Shen, H. and Piao, Y. (2010). The morphometrical analysis on the ultrastructure of A549 cells. *Romanian Journal of Morphology and Embryology*. 51(4): pp. 663–667.
- Jiehua, Z., Maggie, L.B., John, C.B., and John J. R., (2012). Current progress of RNA aptamer. *Based Therapeutics*, 3, 234.
- Joe, A.K., Liu, H., Suzui, M., Vural, M.E., Xiao, D. and Weinstein, I.B., 2002. Resveratrol induces growth inhibition, S-phase arrest, apoptosis, and changes in biomarker expression in several human cancer cell lines. *Clinical Cancer Research*, 8(3), pp.893-903.
- Jones, P. A. and Baylin, S. B., (2002). The fundamental role of epigenetic events in cancer. *Nat. Rev. Genet.*, 3, 415-428.
- Jones, P.A., Baylin, S.B., (2007). The epigenomics of cancer. *Cell*, 128, 683–692.
- Joseph, J., SIDERIS, M.L., Polly, M.A.K., LORIMER, D.D., MCINTOSH, B. and CLARK, J.M., 2000. Cloning and characterization of a novel human histone deacetylase, HDAC8. *Biochemical Journal*, 350(1), pp.199-205.
- Joyce, G.F., (1989). Amplification, mutation and selection of catalytic RNA. *Gene*, 82: 83-87.
- Kabra, N., 2010. A potential tumour suppressive role of SIRT1 in cancer.
- Kaeberlein, M., McDonagh, T., Heltweg, B., Hixon, J., Westman, E. A., Caldwell, S. D.; Napper, A., Curtis, R., DiStefano, P. S., Fields, S., (2005). Substrate-Specific Activation of Sirtuins by Resveratrol. *J. Biol. Chem.* 280(17), 17038–17045.
- Kaeberlein, M., McVey, M., Guarente, L., (1999). The SIR2/3/4 complex and SIR2 alone promote longevity in *Saccharomyces cerevisiae* by two different mechanisms. *Genes and Development*, 13(19), 2570–2580.
- Kamel, C., Abrol, M., Jardine, K., He, X., and McBurney, M. W., (2006). SirT1 fails to affect p53-mediated biological functions. *Aging Cell*, 5, 81-88.

REFERENCES

- Kanfi, Y., Shalman, R., Peshti, V., Pilosof, S. N., Gozlan, Y. M., Pearson, K. J., Lerrer, B., Moazed, D., Marine, J. C., de Cabo, R., and Cohen, H. Y., (2008). Regulation of SIRT6 protein levels by nutrient availability. *FEBS Lett.*, 582, 543-548.
- Kao, H. Y., Lee, C. H., Komarov, A., Han, C. C., and Evans, R. M., (2002). Isolation and characterization of mammalian HDAC10, a novel histone deacetylase. *J Biol Chem*, 277, 187-193.
- Kawahara, T. L., Michishita, E., Adler, A. S., Damian, M., Berber, E., Lin, M., McCord, R. A., Ongaigui, K. C., Boxer, L. D., Chang, H. Y., and Chua, K. F., (2009). SIRT6 links histone H3 lysine 9 deacetylations to NF-kappaB-dependent gene expression and organismal life span. *Cell.*, 136, 62-74.
- Keefe, A. D., Pai, S., Ellington, A., (2010). Aptamers as therapeutics. *Nature Reviews Drug Discovery*. 9(7):537–550.
- Keefe, A.D., Cload, S.T., (2008). SELEX with modified nucleotides. *Curr Opin Chem Biol*, 12,448-56.
- Keener, J., Sneyd, J., (2008). *Mathematical Physiology: I: Cellular Physiology* (2^{ed}). Springer. ISBN 978-0-387-75846-6.
- Kelley, S.O., and Barton, J.K., (1999). Electron transfer between bases in double helical DNA. *Science*, 283:375-381.
- Kiernan, R., Bres, V., Ng, R.W., (2003). Post-activation turn-off of NF-kappa B-dependent transcription is regulated by acetylation of p65. *J Biol Chem*. 278:2758-66.
- Kikuchi, K., Umehara, T., Fukuda, K., Hwang, J., Kuno, A., Hasegawa, T., Nishikawa Satoshi., (2003). RNA aptamers targeted to domain II of hepatitis C virus IRES that bind to its apical loop region. *Journal of Biochemistry*,133, 263-270.
- Kim, E. J., Kho, J. H., Kang, M. R. and Um, S. J., (2007). Active regulator of SIRT1 cooperates with SIRT1 and facilitates suppression of p53 activity. *Mol. Cell*, 28, 277-290.
- Westphal, C. H., Dipp, M. A. and Guarente, L., (2007). A therapeutic role for sirtuins in diseases of aging? *Trends Biochem. Sci*, 32, 555-560.

REFERENCES

- Kim, J. E., Chen, J and Lou, Z., (2008). DBC1 is a negative regulator of SIRT1. *Nature*, 451, 583-586.
- Kim, J., Lou, Z., Chen, J., (2009). Interactions between DBC1 and SIRT1 are deregulated in breast cancer cells. *Cell Cycle*, 8:22, 3784-3785.
- Kim, M., Um, H.J., Bang, S., Lee, S.H., Oh, S.J., Han, J.H., Kim, K.W., Min, J., and Kim, Y. H., (2009). Arsenic removal from vietnamese groundwater using the arsenic-binding DNA aptamer. *Environmental Science & Technology*, 43, 9335-9340.
- Kim, S.J., Kim, M.Y., Lee, J.H., You, J.C., and Jeong, S., (2002). *Biochem. Biophys. Res. Commun*, 291, 925-931.
- Kitamura, Y.I., Kitamura, T., Kruse, J.P., Raum, J.C., Stein, R., Gu, W., and Accili, D., (2005). FoxO1 protects against pancreatic beta cell failure through NeuroD and MafA induction. *Cell Metab*, 2(3): 153-163.
- Kloting, N., and Bluher, M., (2005). Extended longevity and insulin signaling in adipose tissue. *Exp Gerontol*, 40, 878-883.
- Klug, S.J., Huttenhofer, A., Famulok, M., (1999). In vitro selection of RNA aptamers that bind special elongation factor SelB, a protein with multiple RNA-binding sites, reveals one major interaction domain at the carboxyl terminus. *RNA*, 5, 1180–1190.
- Klussmann, S., (2006). *The Aptamer Handbook. Functional Oligonucleotides and Their Applications*. WILEY-VCH Verlag GmbH & Co., KGaA, Weinheim.
- Klussmann, S., Nolte, A., Bald, R., Erdmann, V.A., Fürste, J.P., (1996). Mirror–image RNA that binds D–adenosine. *Nat. Biotechnol.*14, 1112–1115.
- Knudson, A. G., (1971). Mutation and Cancer: Statistical Study of Retinoblastoma. *Proceedings of the National Academy of Sciences of the United States of America*, 68(4), 820–823.
- Kobayashi, T., Horiuchi, T., Tongaonkar, P., Vu, L., Nomura, M., (2004). SIR2 Regulates Recombination between Different rDNA Repeats, but Not Recombination within Individual rRNA Genes in Yeast. *Cell*, 117, 441–453.

REFERENCES

- Kobayashi, Y., Furukawa-Hibi, Y., Chen, C., Horio, Y., Isobe, K., Ikeda, K., and Motoyama, N., (2005). SIRT1 is critical regulator of FOXO-mediated transcription in response to oxidative stress. *Int J Mol Med.*, 16(2): 237-243.
- Kotamraju, S., Chitambar, C.R., Kalivendi S.V., Joseph. J., Kalyanaraman, B., (2002). Transferrin receptor-dependent iron uptake is responsible for doxorubicin-mediated apoptosis in endothelial cells: role of oxidant-induced iron signaling in apoptosis. *J Biol Chem.*, 277: 17179-17187.
- Kovacs, J. J., Murphy, P. J., Gaillard, S., Zhao, X., Wu, J. T., Nicchitta, C. V., Yoshida, M., Toft, D. O., Pratt, W. B., and Yao, T. P., (2005). HDAC6 regulates Hsp90 acetylation and chaperone-dependent activation of glucocorticoid receptor. *Mol Cell*, 18, 601-607.
- Kruszewski, M., and Szumiel, I., (2005). Sirtuins (histone deacetylases III) in the cellular response to DNA damage--facts and hypotheses. *DNA Repair (Amst)*, 4, 1306-1313.
- Kuhn, H., Frank-Kamenetskii, M.D., (2005), Template-independent ligation of single-stranded DNA by T4 DNA ligase. *FEBS J.*, 272(23):5991-6000.
- Kuningas, M., Putters, M., Westendorp, R.G.J., Slagboom, P.E., Van Heemst, D., (2007). SIRT1 gene, age-related diseases, and mortality: the Leiden 85-plus study. *Journals of Gerontology Series A*, 62(9), 960–965.
- Kurosaki, T., Higuchi, N., Kawakami, S., *et al.*, (2012). Self-assemble gene delivery system for molecular targeting using nucleic acid aptamer. *Gene*, 491:205–209.
- Kurreck, J., (2003). Antisense technologies (Improvement through novel chemical modifications). *Eur. J. Biochem.*, 270, 1628–1644.
- Kuzmichev, A., Margueron, R., Vaquero, A., Preissner, T.S., Scher, M., Kirmizis, A., Ouyang, X., Brockdorff, N., Abate-Shen, C., Farnham, P., and Reinberg, D., (2005). Composition and histone substrates of polycomb repressive group complexes change during cellular differentiation. *Proc Natl Acad Sci U S A.*, 102(6): 1859-1864.
- Kwon, H.S. and Ott, M., (2008). The ups and downs of SIRT1. *Trends in biochemical sciences*, 33(11), pp.517-525.

REFERENCES

- Labinskyy, N., Csiszar, A., Veress, G., Stef, G., Pacher, P., Oroszi, G., Wu, J., and Ungvari, Z., (2006). Vascular dysfunction in aging: potential effects of resveratrol, an anti-inflammatory phytoestrogen. *Curr Med Chem.*, 13(9): 989-996.
- Lacroix, M., Toillon, R., Leclercq, G., (2006). p53 and breast cancer, an update *Endocrine-Related Cancer*, 13 293–325.
- Lagger, G., O'Carroll, D., Rembold, M., Khier, H., Tischler, J., Weitzer, G., Schuettengruber, B., Hauser, C., Brunmeir, R., Jenuwein, T., and Seiser, C., (2002). Essential function of histone deacetylase 1 in proliferation control and CDK inhibitor repression. *EMBO J.*, 21, 2672-2681.
- Lagouge, M., Argmann, C., Gerhart-Hines, Z., Meziane, H., Lerin, C., Daussin, F., Messadeq, N., Milne, J., Lambert, P., Elliott, P., Geny, B., Laakso, M., Puigserver, P., and Auwerx, J., (2006). Resveratrol improves mitochondrial function and protects against metabolic disease by activating SIRT1 and PGC-1alpha. *Cell*, 127(6): 1109-1122.
- Lai, A., Lee, J. M., Yang, W. M., DeCaprio, J. A., Kaelin, W. G., Jr., Seto, E., and Branton, P. E., (1999). RBP1 recruits both histone deacetylase-dependent and -independent repression activities to retinoblastoma family proteins. *Mol Cell Biol.*, 19, 6632-6641.
- Lain, S., Hollick, J. J., Campbell, J., Staples, O. D., Higgins, M., Aoubala, M., McCarthy, A., Appleyard, V., Murray, K. E., Baker, L., Thompson, A., Mathers, J., Holland, S. J., Stark, M. J., Pass, G., Woods, J., Lane, D. P. and Westwood, N. J., (2008). Discovery, in vivo activity, and mechanism of action of a small-molecule p53 activator. *Cancer Cell*, 13, 454-463.
- Lakshminarasimhan, M., (2012). Biochemical and structural characterization of Sirtuins from mammals and *Thermotoga maritima* (Doctoral dissertation).
- Lane, D. P., (1992). Cancer. p53, guardian of the genome. *Nature*, 358, 15-16.
- Lane, D. P., and Crawford, L. V., (1979). T antigen is bound to a host protein in SV40 transformed cells. *Nature*, 278, 261-263.
- Langley, E., Pearson, M., Faretta, M., Bauer, U. M., Frye, R. A., Minucci, S., Pelicci, P. G., and Kouzarides, T., (2002). Human SIR2 deacetylates p53 and antagonizes PML/p53-induced cellular senescence. *EMBO J.*, 21, 2383-2396.
- Lea, T., (2010). Caco-2 Cell Line. *The Impact of Food Bioactives on Health*, Springer International Publishing AG Switzerland, chapter10, p111-113.

REFERENCES

- Lee, H., Rezai-Zadeh, N., and Seto, E., (2004). Negative regulation of histone deacetylase 8 activity by cyclic AMP-dependent protein kinase A. *Mol Cell Biol.*, 24, 765-773.
- Lee, J.H., Song, M.Y., Song, E.K., Kim, E.K., Moon, W.S., Han, M.K., Park, J.W., Kwon, K.B., Park, B.H., (2009). Overexpression of SIRT1 protects pancreatic beta-cells against cytokine toxicity by suppressing the nuclear factor-kappaB signaling pathway. *Diabetes*, 58:344–351.
- Lee, S.K., Park, M.W., Yang, E.G., Yu, J.H., Jeong, S.J., (2005). An RNA aptamer that binds to the beta-catenin interaction domain of TCF-1 protein. *Biochem. Biophys. Res. Commun.*, 327, 294–299.
- Legiewicz, M., Lozupone, C., Knight, R. and Yarus, M., (2005). Size, constant sequences, and optimal selection. *RNA*, 11, 1701–1709.
- Lehmann, B., (1997). HaCaT cell line as a model system for vitamin D3 metabolism in human skin." *Journal of Investigative Dermatology*. 108 (1): 78–82.
- Lemercier, C., Verdel, A., Galloo, B., Curtet, S., Brocard, M. P., and Khochbin, S., (2000). mHDA1/HDAC5 histone deacetylase interacts with and represses MEF2A transcriptional activity. *J Biol Chem*, 275, 15594-15599.
- Levin, A. A., (1999). A review of issues in the pharmacokinetics and toxicology of phosphorothioate antisense oligonucleotides. *BBA-Gene Str. Expr.*, 1489, 69–84.
- Li, L., Yuan, L., Luo, J., Gao, J., Guo, J., Xie, X., (2013). MiR-34a inhibits proliferation and migration of breast cancer through down-regulation of Bcl-2 and SIRT1. *Clin Exp Med.*, 13(2):109-17.
- Li, X., Song, S., Liu, Y., Ko, S. H., and Kao, H. Y., (2004). Phosphorylation of the histone deacetylase 7 modulates its stability and association with 14-3-3 proteins. *J Biol Chem.*, 279, 34201-34208.
- Li, Y., Backesjo, C.M., Haldosen, L.A., Lindgren, U., (2009). Resveratrol inhibits proliferation and promotes apoptosis of osteosarcoma cells. *Eur J Pharmacol.*, 609: 13-8.
- Libert, S., Pointer, K., Bell, Eric L., Das, A., Cohen, Dena E., Asara, John M., Kapur, K., Bergmann, S., Preisig, M., Otowa, T., *et al.*, (2011). SIRT1 Activates MAO-A in the Brain to Mediate Anxiety and Exploratory Drive, *Cell*, 147, 1459–1472.

REFERENCES

- Lim, C.S., (2006). SIRT1: Tumour promoter or tumour suppressor? *Med Hypotheses*, 67, 341–344.
- Lin, J.N., Lin, V.C., Rau, K.M., Shieh, P.C., Kuo, D.H., (2010). Resveratrol modulates tumour cell proliferation and protein translation via SIRT1-dependent AMPK activation. *J Agric Food Chem.*, 58: 1584-92
- Lin, S. J., Defossez, P. A., and Guarente, L., (2000). Requirement of NAD and SIR2 for lifespan extension by calorie restriction in *Saccharomyces cerevisiae*. *Science*, 289, 2126-2128.
- Lin, S. J., Kaeberlein, M., Andalis, A. A., Sturtz, L. A., Defossez, P. A., Culotta, V. C., Fink, G. R., and Guarente, L., (2002). Calorie restriction extends *Saccharomyces cerevisiae* lifespan by increasing respiration. *Nature*, 418, 344-348.
- Liu, J., Lu, Y., (2004). Adenosine-dependent assembly of aptazymefunctionalized gold nanoparticles and its application as a colorimetric biosensor. *Anal Chem.* 76, 1627-1632.
- Liu, J., Stormo, G.D., (2005). Combining SELEX with quantitative assays to rapidly obtain accurate models of protein–DNA interactions. *Nucleic Acids Research*, 33: 141.
- Liu, Y., Gerber, R., Wu, J., Tsuruda, T., McCarter, J. D., (2008). High-Throughput Assays for Sirtuin Enzymes: A Microfluidic Mobility Shift Assay and a Bioluminescence Assay. *Anal. Biochem.*, 378(1), 53–59.
- Lodish, H., Berk, A., Zipursky, S.L., (2000). *Molecular Cell Biology Section 24.2*. 4th edition: Proto-Oncogenes and Tumour-Suppressor Genes. W. H. Freeman and Company, New York.
- Loftus, R. M., and Finlay, D. K., (2017). Cellular metabolism of myeloid cells in sepsis. *J. Leukoc. Biol.*, 101: 151.
- Low, S.Y., Hill, J.E., and Peccia, J., (2009). A DNA aptamer recognizes the Asp f1 allergen of *Aspergillus fumigatus*. *Biochemical and Biophysical Research Communications*, 386, 544-548.
- Lu, S., Jang, H., Nussinov, R., Zhang, J., (2016). The Structural Basis of Oncogenic Mutations G12, G13 and Q61 in Small GTPase K-Ras4B. *Scientific Reports*. 6:21949: 1038.

REFERENCES

- Luca, M., Irene, P., Jesus, M. B., Antonio. B., Marco, M., (2013). The significance of genetics for cholangiocarcinoma development. *Ann Transl Med.*,1(3):28.
- Luo, J., Nikolaev, A.Y., Imai, S., Chen, D., Su, F., Shiloh, A., Guarente, L., Gu, W., (2001). Negative control of p53 by Sir2alpha promotes cell survival under stress. *Cell*, 107, 137– 148.
- Luo, R. X., Postigo, A. A., and Dean, D. C., (1998). Rb interacts with histone deacetylase to repress transcription. *Cell*, 92, 463-473.
- Lupold, S.E., Hicke, B. J., Lin, Y., Coffey, D.S., (2002). Identification and characterization of nuclease-stabilized RNA molecules that bind human prostate cancer cells via the prostate-specific membrane antigen. *Cancer Research*, 62, 4029- 4033.
- Macaya, R.F., Schultze, P., Smith, F.W., Roe, J.A., Feigon, J., (1993). Thrombinbinding DNA aptamer forms a unimolecular quadruplex structure in solution. *Proc. Natl. Acad. Sci. U. S. A.*,90, 3745–3749.
- Maniatis, T., Fritsch, E.F. and Sambrook, J., (1982). *Molecular cloning: a laboratory manual* (Vol. 545). Cold Spring Harbor, NY: Cold Spring harbor laboratory.
- Mann, D., Reinemann, C., Stoltenburg, R., Strehlitz, B., (2005). *In vitro* selection of DNA aptamers binding ethanolamine. *Biochem. Biophys. Res. Commun*, 338, 1928–1934.
- Manna, S. K., Mukhopadhyay, A., Aggarwal, B. B., (2000). Resveratrol suppresses TNF-induced activation of nuclear transcription factors NF-kappa B, activator protein-1, and apoptosis: potential role of reactive oxygen intermediates and lipid peroxidation. *J Immunol.*, 164, 6509-6519.
- Marcotte, P. A., Richardson, P. L., Guo, J., Barrett, L. W., Xu, N., Gunasekera, A., Glaser, K. B., (2004). Fluorescence Assay of SIRT Protein Deacetylases Using an Acetylated Peptide Substrate and a Secondary Trypsin Reaction. *Anal. Biochem.*, 332(1), 90–99.
- Markus, M. A., & Morris, B. J. (2008). Resveratrol in prevention and treatment of common clinical conditions of aging. *Clinical Interventions in Aging*, 3(2), 331–339.
- Marmorstein. R., (2001). Structure of Histone Deacetylases: ReviewInsights into Substrate Recognition and Catalysis. *Structure*. 9, 1127–1133.

REFERENCES

- Maroni, L., Pierantonelli, I., Banales, J. M., Benedetti, A., & Marzioni, M. (2013). The significance of genetics for cholangiocarcinoma development. *Annals of Translational Medicine*, 1(3), 28.
- Marshall, K.A., Ellington, A.D., (2000). *In vitro* selection of RNA aptamers. *Methods Enzymol*, 318, 193–214.
- Massimi, M., Tomassini, A., Sciubba, F., Sobolev, A.P., Conti Devirgiliis, L., Miccheli, A., (2012). Effects of resveratrol on HepG2 cells as revealed by ¹H-NMR based metabolic profiling. *Biochimica et Biophysica Acta (BBA) - General Subjects*, 1820, 1–8.
- Matlashewski, G., Lamb, P., Pim, D., Peacock, J., Crawford, L., and Benchimol, S., (1984). Isolation and characterisation of a human p53 cDNA clone: expression of the human p53 gene. *EMBO J*, 3, 3257-3262.
- Matsuyama, A., Shimazu, T., Sumida, Y., Saito, A., Yoshimatsu, Y., Seigneurin-Berny, D., Osada, H., Komatsu, Y., Nishino, N., Khochbin, S., *et al.*, (2002). *In vivo* destabilisation of dynamic microtubules by HDAC6-mediated deacetylation. *EMBO J.*, 21, 6820-6831.
- Mau, T., and Yung, R. (2014). Potential of epigenetic therapies in non-cancerous conditions. *Frontiers in Genetics*, 5, 438.
- McBurney, M. W., Yang, X., Jardine, K., Hixon, M., Boekelheide, K., Webb, J. R., Lansdorp, P. M., and Lemieux, M., (2003). The mammalian SIR2alpha protein has a role in embryogenesis and gametogenesis. *Mol Cell Biol.*, 23, 38-54.
- McGuinness, D., McGuinness, D.H., McCaul, J.A. and Shiels, P.G., (2011). Sirtuins, bioageing, and cancer. *Journal of aging research*, 2011.
- Meijsing, H. S., and Ehrenhofer-Murray, A. E., (2001). The silencing complex SAS-I links histone acetylation to the assembly of repressed chromatin by CAF-I and Asf1 in *Saccharomyces cerevisiae*. *Genes Dev.*, 1; 15(23): 3169–3182.
- Mendonsa, S. D., Bowser, M. T., (2004). *In vitro* selection of high-affinity DNA ligands for human IgE using capillary electrophoresis. *Analytical Chemistry*, 76, 5387-92.
- Merksamer, P.I., Liu, Y., He, W., Hirschey, M.D., Chen, D., Verdin, E., (2013). The sirtuins, oxidative stress and aging: an emerging link. *Aging*, 5: 144-50.

REFERENCES

- Mersch-Sundermann, V., Knasmüller, S., Wu, X. J., Darroudi, F., Kassie, F., (2004). Use of a human-derived liver cell line for the detection of cytoprotective, antigenotoxic and cogenotoxic agents. *Toxicology*, 198 (1–3): 329–340.
- Michan S., Sinclair D., (2007). Sirtuins in mammals: insights into their biological function. *Biochem J.*, 15, 404(1), 1-13.
- Michishita, E., McCord, R. A., Berber, E., Kioi, M., Padilla-Nash, H., Damian, M., Cheung, P., Kusumoto, R., Kawahara, T. L., Barrett, J. C., et al. (2008). SIRT6 is a histone H3 lysine 9 deacetylase that modulates telomeric chromatin. *Nature*, 452, 492-496.
- Michishita, E., Park, J. Y., Burneskis, J. M., Barrett, J. C., and Horikawa, I. (2005). Evolutionarily conserved and nonconserved cellular localizations and functions of human SIRT proteins. *Mol Biol Cell*, 16, 4623-4635.
- Milburn, M. V., Tong, L., deVos, A. M., Brunger, A., Yamaizumi, Z., Nishimura, S., and Kim, S. H., (1990). Molecular switch for signal transduction: structural differences between active and inactive forms of protooncogenic ras proteins. *Science*, 247, 939-945.
- Millevoi, S., Moine, H., Vagner, S., (2012). G-quadruplexes in RNA biology. *WIREs RNA*, 3(4):495-507.
- Milne, J. C., Lambert, P. D., Schenk, S., Carney, D. P., Smith, J. J., Gagne, D. J., Jin, L., Boss, O., Perni, R. B., Vu, C. B. Bemis, J. E., Xie, R., Disch, J. S., Ng, P. Y., Nunes, J. J., Lynch, A. V., Yang, H., Galonek, H., Israelian, K., Choy, W., Iffland, A., Lavu, S., Medvedik, O., Sinclair, D. A., Olefsky, J. M., Jirousek, M. R., Elliott, P. J. and Westphal, C. H., (2007). Small molecule activators of SIRT1 as therapeutics for the treatment of type 2 diabetes. *Nature*, 450, 712-716.
- Miska, E. A., Karlsson, C., Langley, E., Nielsen, S. J., Pines, J., and Kouzarides, T., (1999). HDAC4 deacetylase associates with and represses the MEF2 transcription factor. *EMBO J.*, 18, 5099-5107.
- Misono, T.S., and Kumar, P., (2005). Selection of RNA aptamers against human influenza virus hemagglutinin using surface plasmon resonance. *Analytical Biochemistry*, 342, 312-7.

REFERENCES

- Morris, K.N., Jensen, K.B., Julin, C.M., Weil, M., and Gold, L., (1998). High affinity ligands from in vitro selection: Complex targets. *Proceedings of the National Academy of Sciences of the United States of America*, 95, 2902-2907.
- Mosing, R.K., Mendonsa, S. D., Bowser, M., T., (2005). Capillary electrophoresis-SELEX selection of aptamers with affinity for HIV-1 reverse transcriptase. *Analytical Chemistry*, 77, 6107-6112.
- Mostoslavsky, R., Chua, K.F., Lombard, D.B., Pang, W.W., Fischer, M.R., Gellon, L., Liu, P., Mostoslavsky, G., Franco, S., Murphy, M.M., Mills, K.D., Patel, P., Hsu, J.T., Hong, A.L., Ford, E., Cheng, H.L., Kennedy, C., Nunez, N., Bronson, R., Frendewey, D., Auerbach, W., Valenzuela, D., Karow, M., Hottiger, M.O., Hursting, S., Barrett, J.C., Guarente, L., Mulligan, R., Demple, B., Yancopoulos, G.D., and Alt, F.W., (2006). Genomic instability and aging-like phenotype in the absence of mammalian SIRT6. *Cell*, 124(2): 315-329.
- Motta, M. C., Divecha, N., Lemieux, M., Kamel, C., Chen, D., Gu, W., Bultsma, Y., McBurney, M., and Guarente, L., (2004). Mammalian SIRT1 represses forkhead transcription factors. *Cell*, 116, 551-563.
- Mueller, I., Zimmermann, M., Becker, D., Floemer, M., (1980). Calendar life span versus budding life span of *Saccharomyces cerevisiae*. *Mechanisms of Ageing and Development*, 12(1), 47-52.
- Murphy, M. B., Fuller, S. T., Richardson, P. M., & Doyle, S. A. (2003). An improved method for the in vitro evolution of aptamers and applications in protein detection and purification. *Nucleic Acids Research*, 31(18), e110.
- Murry, A., (2004). Recycling the Cell Cycle Cyclins Revisited. *Cell*, 116, 221-234.
- Muth, V., Nadaud, S., Grummt, I., and Voit, R., (2001). Acetylation of TAF(I) 68, a subunit of TIF-IB/SL1, activates RNA polymerase I transcription. *Embo J.*, 20(6), 1353-1362.
- Nahoum, S.R., (2006). Why Cancer and Inflammation? *Yale Journal of Biology and Medicine*, 79 (3-4): 123-130.
- Nakae, J., Cao, Y., Daitoku, H., Fukamizu, A., Ogawa, W., Yano, Y., and Hayashi, Y., (2006). The LXXLL motif of murine forkhead transcription factor FoxO1 mediates Sirt1-dependent transcriptional activity. *J Clin Invest*, 116(9): 2473-2483.

REFERENCES

- Nakagawa, T., Lomb, D. J., Haigis, M. C., and Guarente, L. (2009). SIRT5 Deacetylates carbamoyl phosphate synthetase 1 and regulates the urea cycle. *Cell*, 137, 560-570.
- Napper, A.D., Hixon, J., McDonagh, T., Keavey, K., Pons, J.F., Barker, J., Yau, W.T., Amouzegh, P., Flegg, A., Hamelin, E., Thomas, R.J., Kates, M., Jones, S., Navia, M.A., Saunders, J.O., DiStefano, P.S., and Curtis, R., (2005). Discovery of indoles as potent and selective inhibitors of the deacetylase SIRT1. *J Med Chem*, 48(25): 8045-8054.
- Nazarenko, I., Pires, R., Lowe, B., Obaidy, M., and Rashtchian, A., (2002). Effect of primary and secondary structure of oligodeoxyribonucleotides on the fluorescent properties of conjugated dyes. *Nuc. Acids. Res.* 30:2089-2195.
- Neganova, I., and Lako, M., (2008). G1 to S phase cell cycle transition in somatic and embryonic stem cells. *J Anat.*, Jul; 213(1): 30–44.
- Nemoto, S., Fergusson, M. M., and Finkel, T., (2005). SIRT1 functionally interacts with the metabolic regulator and transcriptional coactivator PGC-1{alpha}. *J Biol Chem.*, 280, 16456-16460.
- Nemoto, S., Fergusson, M.M, Finkel, T., (2004). Nutrient availability regulates SIRT1 through a forkhead-dependent pathway. *Science*, 306, 2105–2108.
- Nguyen, H. H., Park, J., Kang, S., & Kim, M. (2015). Surface Plasmon Resonance: A Versatile Technique for Biosensor Applications. *Sensors (Basel, Switzerland)*, 15(5), 10481–10510.
- Niforou, K.M., Anagnostopoulos, A.K., Vougas, K., Kittas, C., Gorgoulis., V.G., Tsangaris, G.T., (2008). The proteome profile of the human osteosarcoma U2OS cell line. *Cancer Genomics Proteomics*, 5(1):63-78.
- Nimjee, S.M., Rusconi, C.P. and Sullenger, B.A., (2005). Aptamers, an emerging class of therapeutics. *Annu. Rev. Med.*, 56, 555–583.
- Nishikawa, F., Funaji, K., Fukuda, K., Nishikawa, S., (2004). In vitro selection of RNA aptamers against the HCVNS3 helicase domain. *Oligonucleotides*, 14, 114–129.
- Nix, J., Sussman, D., Wilson, C., (2000). The 1.3 angstrom crystal structure of a biotin-binding pseudoknot and the basis for RNA molecular recognition. *J. Mol. Biol.*, 296, 1235–1244.

REFERENCES

- Norman, K. E., Cotter, M. J., Stewart, J. B., Abbitt, K. B., Ali, M., Wagner, B. E., Wallace, W. A. H., Forlow, S. B., and Hellewell, P. G., (2003). Combined anticoagulant and antiselectin treatments prevent lethal intravascular coagulation. *Blood*, 101, 921–928.
- North, B. J., Marshall, B. L., Borra, M. T., Denu, J. M., and Verdin, E., (2003). The human Sir2 ortholog, SIRT2, is an NAD⁺-dependent tubulin deacetylase. *Mol Cell.*, 11, 437-444.
- North, B.J., Verdin, E., (2007). Interphase nucleo-cytoplasmic shuttling and localization of SIRT2 during mitosis. *PLoS One*, 2(8), 784.
- Nowell, P. C., (1976). The clonal evolution of tumour cell populations. *Science*, 194, 23-28.
- Nutiu, R., and Li, Y., (2005). Aptamers with fluorescence-signaling prooerties. *Methods*, 37,16-25.
- Oberdoerffer, P., Michan, S., McVay, M., Mostoslavsky, R., Vann, J., Park, S.-K., Sinclair, D. A. (2008). DNA damage-induced alterations in chromatin contribute to genomic integrity and age-related changes in gene expression. *Cell*, 135(5), 907–918.
- Ogasawara, D., Hasegawa, H., Kaneko, K., Sode, K., and Ikebukuro K., (2007). Screening of DNA aptamer against mouse prion protein by competitive selection. *Prion*, 1, 248-254.
- Ohsawa, S. and Miura, M., (2006). Caspase-mediated changes in Sir2alpha during apoptosis. *FEBS Lett*, 580(25): 5875-5879.
- Oney, S., Lam, R.T., Bompiani, K.M., Blake, C.M., Quick, G., *et al.*, (2009). Development of universal antidotes to control aptamer activity. *Nat Med.*, 15,1224-8.
- Onyango, P., Celic, I., McCaffery, J. M., Boeke, J. D., and Feinberg, A. P. (2002). SIRT3, a human SIR2 homologue, is an NAD-dependent deacetylase localized to mitochondria. *Proc Natl Acad Sci U S A.*, 99, 13653-13658.
- Opalinska, J. B.; Gewirtz, A. M., (2002). Nucleic-acid therapeutics: basic principles and recent applications. *Nat. Rev. Drug Discovery*, 1 (7), 503–514.
- Ota, H., Akishita, M., Eto, M., Iijima, K., Kaneki, M., and Ouchi, Y., (2007). Sirt1 modulates premature senescence-like phenotype in human endothelial cells. *J Mol Cell Cardiol.*, 43(5):571-9.

REFERENCES

- Ota, H., Eto, M., Ogawa, S., Iijima, K., Akishita, M., Ouchi, Y., (2010). Sirt1/eNOS axis as a potential target against vascular senescence, dysfunction and atherosclerosis. *Journal of Atherosclerosis and Thrombosis*, 17(5), 431–435.
- Pacholec, M., Bleasdale, J. E., Chrnyk, B., Cunningham, D., Flynn, D., Griffith, D. A., Griffor, M., Loulakis, P., Pabst, B., Qiu, X., (2010). SRT1720, SRT2183, SRT1460, and Resveratrol Are Not Direct Activators of SIRT1. *J. Biol. Chem.* 285(11), 8340–8351.
- Pagans, S., Pedal, A., North, B.J., Kaehlcke, K., Marshall, B.L., Dorr, A., Hetzer-Egger, C., Henklein, P., Frye, R., McBurney, M.W., Hruby, H., Jung, M., Verdin, E., and Ott, M., (2005). SIRT1 regulates HIV transcription via Tat deacetylation. *PLoS Biol.*, 3(2): 41.
- Pardo, P.S., Boriek, A.M., (2012). An autoregulatory loop reverts the mechanosensitive Sirt1 induction by EGR1 in skeletal muscle cells. *Aging (Albany NY)*, 4:456–461.
- Pardo, P.S., Mohamed, J.S., Lopez, M.A., Boriek, A.M., (2011). Induction of Sirt1 by mechanical stretch of skeletal muscle through the early response factor EGR1 triggers an antioxidative response. *J Biol Chem.*, 286:2559–2566.
- Park L.K., and Lee, J., (2008). Protective effects of resveratrol on UVB-irradiated HaCaT cells through attenuation of the caspase pathway. *Oncology Reports*, 19: 413-417.
- Parker, J.A., Arango, M., Abderrahmane, S., Lambert, E., Tourette, C., Catoire, H., and Neri, C., (2005). Resveratrol rescues mutant polyglutamine cytotoxicity in nematode and mammalian neurons. *Nat Genet.*, 37(4): 349-350.
- Parkinson, G.N., (2006). Fundamentals of Quadruplex Structures. In *Quadruplex nucleic acids*; Neidle, S., Balasubramanian, S., Eds.; The Royal Society of Chemistry: Cambridge, UK; pp. 1–27.
- Pastor, F., Soldevilla, M. M., Villanueva, H., (2013). CD28 aptamers as powerful immune response modulators. *Molecular Therapy—Nucleic Acids*. 2, article e98.
- Patching, S.G., (2014). Surface plasmon resonance spectroscopy for characterisation of membrane protein–ligand interactions and its potential for drug discovery. *Biochim. Biophys. Acta Biomembr.* 1838:43–55.
- Patel, D.J., Suri, A.K., Jiang, F., Jiang, L.C., Fan, P., Kumar, R.A., Nonin, S., (1997). Structure, recognition and adaptive binding in RNA aptamer complexes. *J. Mol. Biol.*, 272, 645–664.

REFERENCES

- Pazienza, V., Piepoli, A., Panza, A., (2012). SIRT1 and the Clock Gene Machinery in Colorectal Cancer. *Journal Cancer Investigation*, 30, 2.
- Perrod, S., Cockell, M. M., Laroche, T., Renaud, H., Ducrest, A. L., Bonnard, C., and Gasser, S. M. (2001). A cytosolic NAD-dependent deacetylase, Hst2p, can modulate nucleolar and telomeric silencing in yeast. *EMBO J.*, 20, 197-209.
- Picard, F., Kurtev, M., Chung, N., Topark-Ngarm, A., Senawong, T., Machado De Oliveira, R., Leid, M., McBurney, M. W., and Guarente, L., (2004). Sirt1 promotes fat mobilization in white adipocytes by repressing PPAR-gamma. *Nature*, 429, 771-776.
- Piganeau, N., Thuillier, V., and Famulok, M. 2001. In vitro selection of allosteric ribozymes: Theory and experimental validation. *J. Mol. Biol.* 312: 1177–1190.
- Poole, A. M., Kobayashi, T., & Ganley, A. R. D. (2012). A positive role for yeast extrachromosomal rDNA circles? *Bioessays*, 34(9), 725–729.
- Portmann, S., Fahrner, R., Lechleiter, A., Keogh, A., Overney, A., Laemmle, A., (2013). Antitumour effect of SIRT1 inhibition in human HCC tumour models *in vitro* and *in vivo*. *Cancer Therapeutics Insights*, 10,1535-7163.
- Potente, M., Ghaeni, L., Baldessari, D., Mostoslavsky, R., Rossig, L., Dequiedt, F., Haendeler, J., Mione, M., Dejana, E., Alt, F.W., Zeiher, A.M., Dimmeler, S., (2007). SIRT1 controls endothelial angiogenic functions during vascular growth. *Genes Dev.*, 21, 2644–2658.
- Prior, I. A., Lewis, P. D., & Mattos, C., (2012). A comprehensive survey of Ras mutations in cancer. *Cancer Research*, 72(10), 2457–2467.
- Pruitt, K., Zinn, R.L., Ohm1, J.E., McGarvey, K.M., Kang1, S.L., Watkins, D.N., Herman, J.G., Baylin, S.B., (2006). Inhibition of SIRT1 reactivates silenced cancer genes without loss of promoter DNA hypermethylation. *PLoS Genet*, 2, 40.
- Puiu, M., & Bala, C. (2016). SPR and SPR Imaging: Recent Trends in Developing Nanodevices for Detection and Real-Time Monitoring of Biomolecular Events. *Sensors (Basel, Switzerland)*, 16(6), 870.
- Qiao, L. and Shao, J., (2006). SIRT1 regulates adiponectin gene expression through Foxo1-C/enhancer-binding protein alpha transcriptional complex. *J Biol Chem*, 281(52): 39915-39924.

REFERENCES

- Qiu, X., Brown, K.V., Moran, Y., Chen, D., (2010). Sirtuin regulation in calorie restriction. *Biochimica et Biophysica Acta*, 1804(8), 1576–1583.
- Rabindra, K. J., Sandeep, S. K, Trupti, R. S., (2012). Cancer Stem Cell – Essence of Tumourigenesis. *J Carcinogen Mutagen*, S1:006.
- Rahman, S. and Islam, R., (2011). Mammalian Sirt1insights on its biological functions. *Cell Communication and Signaling*, 9 (1), 11.
- Ramsey, J.J., Colman, R.J., Binkley, N.C., *et al.*, (2000). Dietary restriction and aging in rhesus monkeys: the University of Wisconsin study. *Experimental Gerontology*, 35(9-10), 1131–1149.
- Reddel, R.R., Ke, Y., Gerwin, B.I., McMenamin, M.G., Lechner, J.F., Su, R.T., Brash, D.E., Park, J.B., Rhim, J.S. and Harris, C.C., (1988). Transformation of human bronchial epithelial cells by infection with SV40 or adenovirus-12 SV40 hybrid virus, or transfection via strontium phosphate coprecipitation with a plasmid containing SV40 early region genes. *Cancer research*, 48(7), pp.1904-1909.
- Reed, N. A., Cai, D., Blasius, T. L., Jih, G. T., Meyhofer, E., Gaertig, J., and Verhey, K. J., (2006). Microtubule acetylation promotes kinesin-1 binding and transport. *Curr Biol*, 16, 2166-2172.
- Rhie, A., Kirby, L., Sayer, N., Wellesley, R., Disterer, P., Sylvester, I., Gill, A., Hope, J., James, W., Tahiri-Alaoui, A., (2003). Characterisation of 2'- fluoro-RNA aptamers that bind preferentially to disease-associated conformations of prion protein and inhibit conversion. *The Journal of Biological Chemistry*, 278, 39697- 39705.
- Riesen, M., and Morgan, A., (2009). Calorie restriction reduces rDNA recombination independently of rDNA silencing. *Aging Cell*, 8, 624-632.
- Rimmele, M., (2003). Nucleic acid aptamers as tools and drugs: recent developments. *Chembiochemistry*, 4, 963–971.
- Rine, J., Strathern, J.N., Hicks, J.B., Herskowitz, I., (1979). A suppressor of mating-type locus mutations in *Saccharomyces cerevisiae*: evidence for and identification of cryptic mating-type loci. *Genetics*, 93(4), 877–901.

REFERENCES

- Robertson, K. D., Ait-Si-Ali, S., Yokochi, T., Wade, P. A., Jones, P. L., and Wolffe, A. P., (2000). DNMT1 forms a complex with Rb, E2F1 and HDAC1 and represses transcription from E2F-responsive promoters. *Nat Genet*, 25, 338-342.
- Robinson, K., Mock, C., & Liang, D. (2015). Pre-formulation studies of resveratrol. *Drug Development and Industrial Pharmacy*, 41(9), 1464–1469.
- Rodgers, J.T., Lerin, C., Haas, W., Gygi, S.P., Spiegelman, B.M., and Puigserver, P., (2005). Nutrient control of glucose homeostasis through a complex of PGC-1alpha and SIRT1. *Nature*, 434(7029): 113-118.
- Rogina, B., and Helfand, S. L., (2004). Sir2 mediates longevity in the fly through a pathway related to calorie restriction. *Proc Natl Acad Sci U S A*, 101, 15998-16003.
- Róisín, M. L., and David, K. F., (2016). Immunometabolism: Cellular Metabolism Turns Immune Regulator. *The Journal of Biological Chemistry*. 291(1), 1–10.
- Rong, T., Linda, Y., Timothy, M., Fan, J., (2010). The formulation of aptamer- coated paclitaxel– polylactide nanoconjugates and their targeting to cancer cells. *Cheng Biomaterials*, 31, 3043–3053.
- Rose, G., Dato, S., Altomare, K., *et al.*, (2003). Variability of the SIRT3 gene, human silen information regulator Sir2 homologue, and survivorship in the elderly. *Experimental Gerontology*, 38(10), 1065–1070.
- Rountree, M. R., Bachman, K. E., and Baylin, S. B., (2000). DNMT1 binds HDAC2 and a new co-repressor, DMAP1, to form a complex at replication foci. *Nat Genet*, 25, 269-277.
- Rusconi, C. P., Scardino, E., Layzer, J., Pitoc, G. A., Ortel, T. L., Monroe, D., and Sullenger, B. A. (2002). RNA aptamers as reversible antagonists of coagulation factor IXa. *Nature*, 419, 90–94.
- Rusconi, C.P., Roberts, J.D., Pitoc, G.A., Nimjee, S.M., White, R.R., Quick, G., Jr., Scardino, E., Fay, W.P., and Sullenger, B.A., (2004). Antidote-mediated control of an anticoagulant aptamer in vivo. *Nat Biotechnol*, 22, 1423-1428.
- Rye, P. T., Frick, L. E., Ozbal, C. C., LaMarr, W. A., (2011). Advances in label-free screening approaches for studying histone acetyltransferases. *J. Biomol. Screen.*, 16(10), 1186–1195.

REFERENCES

Sack, M. N., and Finkel, T. (2012). Mitochondrial Metabolism, Sirtuins, and Aging. *Cold Spring Harbor Perspectives in Biology*, 4(12).

Sakamoto, J., Miura, T., Shimamoto, K., and Horio, Y., (2004). Predominant expression of Sir2alpha, an NAD-dependent histone deacetylase, in the embryonic mouse heart and brain. *FEBS Lett*, 556(1-3): 281-286.

Sampson, T., (2003). Aptamers and SELEX: the technology. *World Patent Inf*, 25, 123–129.

Santulli-Marotto, S., Nair, S. K., Rusconi, C., Sullenger, B., Gilboa, E., (2003). Multivalent RNA aptamers that inhibit CTLA-4 and enhance tumour immunity. *Cancer Research*. 63(21):7483–7489.

Sasaki, T., Maier, B., Bartke, A., and Scrable, H., (2006). Progressive loss of SIRT1 with cell cycle withdrawal. *Aging Cell*, 5(5): 413-422.

Saunders, L.R., Verdin, E., (2007). Sirtuins: critical regulators at the crossroads between cancer and aging. *Oncogene.*, 26:5489-504.

Sauve, A.A., Wolberger, C., Schramm, V.L., Boeke, J.D., (2006). The biochemistry of sirtuins. *Annual Review of Biochemistry*, 75, 435–465.

Savla R., Taratula, O., Garbuzenko, O., & Minko, T., (2011). Tumour targeted quantum dot-mucin 1 aptamer-doxorubicin conjugate for imaging and treatment of cancer. *J Control Release*, 153(1):16-22.

Schena, M. and Shalon, D., (1995). Quantitative monitoring of gene expression patterns with a complementary DNA microarray. *Science*, 270, 467-470.

Scher, M. B., Vaquero, A., and Reinberg, D. (2007). SirT3 is a nuclear NAD⁺-dependent histone deacetylase that translocates to the mitochondria upon cellular stress. *Genes Dev.*, 21, 920-928.

Schlicker, C., Gertz, M., Papatheodorou, P., Kachholz, B., Becker, C. F., and Steegborn, C., (2008). Substrates and regulation mechanisms for the human mitochondrial sirtuins Sirt3 and Sirt5. *J Mol Biol.*, 382, 790-801.

Schneider, D., Gold, L., Platt, T., (1993). Selective enrichment of RNA species for tight binding to Escherichia coli rho factor. *FASEB J.*, 7, 201-207.

REFERENCES

- Schoop, V.M., Mirancea, N., Fusenig, N. E., (1999). Epidermal Organization and Differentiation of HaCaT Keratinocytes in Organotypic Coculture with Human Dermal Fibroblasts. *Journal of Investigative Dermatology*, 112 (3): 343–353.
- Schumacker, P.T., (2006). Reactive oxygen species in cancer cells: live by the sword, die by the sword. *Cancer Cell*,10:175–176.
- Schumacker, P.T., (2010). A tumour suppressor SIRTainty. *Cancer Cell*, 17(1), 5–6.
- Schürer, N., Köhne, A., Schliep, V., Barlag, K., Goerz, G., (1993). Lipid composition and synthesis of HaCaT cells, an immortalized human keratinocyte line, in comparison with normal human adult keratinocytes. *Experimental Dermatology*, 2 (4): 179–85.
- Schwer, B., Bunkenborg, J., Verdin, R.O., Andersen, J.S., and Verdin, E., (2006). Reversible lysine acetylation controls the activity of the mitochondrial enzyme acetyl-CoA synthetase 2. *Proc Natl Acad Sci U S A*, 103(27): 10224-10229.
- Sefah, K., Meng, L., Lopez-Colon, D., Jimenez, E., Liu, C., Tan, W., (2010). DNA aptamers as molecular probes for colorectal cancer study. *PLoS One*, 10, 5(12): 14269.
- Seidel, C.A.M., Schulz, A., Sauer, M.H.M., (1996). Nucleobase-specific quenching of fluorescent dyes. 1. Nucleobase one-electron redox potentials and their correlation with static and dynamic quenching efficiencies. *J. Phys. Chem.*, 100:5541-5553.
- Seigneurin-Berny, D., Verdel, A., Curtet, S., Lemercier, C., Garin, J., Rousseaux, S., and Khochbin, S., (2001). Identification of components of the murine histone deacetylase 6 complex: link between acetylation and ubiquitination signaling pathways. *Mol Cell Biol*, 21, 8035-8044.
- Senawong, T., Peterson, V.J., Avram, D., Shepherd, D.M., Frye, R.A., Minucci, S., and Leid, M., (2003). Involvement of the histone deacetylase SIRT1 in chicken ovalbumin upstream promoter transcription factor (COUP-TF)-interacting protein 2-mediated transcriptional repression. *J Biol Chem.*, 278(44): 43041-43050.
- Serrero, G., and Lu, R., (2001). Effect of resveratrol on the expression of autocrine growth modulators in human breast cancer cells. *Antioxidants & Redox Signaling*, 3(6): 969-979.
- Seto, E., and Yoshida, M., (2014). Erasers of histone acetylation: The histone deacetylase enzymes. *Cold Spring Harb Perspect Biol*, 6(4): a018713.

REFERENCES

- Shauna, A. H., and Frederick, A. D., (2012). The retinoblastoma family of proteins and their regulatory functions in the mammalian cell division cycle. *Cell Division*, 7:10.
- Shaw, J. P., Kent, K., Bird, J., Fishback, J., and Froehler, B., (1991). Modified deoxyoligonucleotides stable to exonuclease degradation in serum. *Nucleic Acids Res*, 19, 747–750.
- Shaw, J., Fishback, J.A., Cundy, K.C., William, A.L., (1995). Anovel oligodeoxynucleotide inhibitor of thrombin, *I.in vitro* metabolic stability in plasma and serum. *Pharmaceutical Research*,12:12, 1937-1941.
- Sheehan, J.P. and Lan, H.C., (1998). Phosphorothioate Oligonucleotides Inhibit the Intrinsic Tenase Complex. *Blood*, 92:1617-1625.
- Sherr, C. J., (2004). Principles of tumour suppression. *Cell*, 116, 235-246.
- Shi, H., Fan, X., Ni, Z., Lis John, T., (2002). Evolutionary dynamics and population control during in vitro selection and amplification with multiple targets. *Rna New York Ny.*, 8, 1461-1470.
- Shi, H., Hoffman, B.E., Lis, J.T., (1999). RNA aptamers as effective protein antagonists in a multicellular organism. *Proceedings of the National Academy of Sciences of the United States of America*, 96: 10033-10038.
- Shi, T., Wang, F., Stieren, E., and Tong, Q., (2005). SIRT3, a mitochondrial sirtuin deacetylase, regulates mitochondrial function and thermogenesis in brown adipocytes. *J Biol Chem.*, 280(14): 13560-13567.
- Shiratawa, K., Chaver, L., Hakre, S., Clavanese, V., and Verdin, E., (2013). Reactivation of latent HIV by histon deacetylase inhibitors. *21, 6, 277-285.*
- Siddiqui, I.A., Sanna, V., Ahmad, N., Sechi, M., Mukhtar, H., (2015). Resveratrol nanoformulation for cancer prevention and therapy. *Ann N Y Acad Sci.*, 1348(1):20-31.
- Sinclair, D. A., and Guarente, L., (1997). Extrachromosomal rDNA circles--a cause of aging in yeast. *Cell*, 91, 1033-1042.

REFERENCES

- Soldevilla, M. M., Villanueva, H., Bendandi, M., Inoges, S., López-Díaz de Cerio, A., Pastor, F., (2015). 2-fluoro-RNA oligonucleotide CD40 targeted aptamers for the control of B lymphoma and bone-marrow aplasia. *Biomaterials*, 67:274–285.
- Soldevilla, M. M., Villanueva, H., Pastor, F., (2016). Aptamers: A feasible technology in cancer immunotherapy. *J Immunol Res.*, 2016; 2016: 1083738.
- Solomon, J. M., Pasupuleti, R., Xu, L., McDonagh, T., Curtis, R., DiStefano, P. S., and Huber, L. J., (2006). Inhibition of SIRT1 catalytic activity increases p53 acetylation but does not alter cell survival following DNA damage. *Mol Cell Biol.*, 26, 28-38.
- Soule, H. D., Vazquez, J., Long, A., Albert, S., Brennan, M., (1973). A Human cell line from a pleural effusion derived from a breast carcinoma. *J Natl Cancer Inst.*, 51 (5): 1409-1416.
- Stewart, C.E., Torr, E., Mohd Jamili, N., Bosquillon, C., Sayers, I., (2012). Evaluation of differentiated human bronchial epithelial cell culture systems for asthma research. *Journal of Allergy*, 943982, 11.
- Stewart, J. R., and O'Brian, C. A., (2004). Resveratrol Antagonizes EGFR-Dependent Erk1/2 Activation in Human Androgen-Independent Prostate Cancer Cells with Associated Isozyme-Selective PKC α Inhibition. *Invest New Drugs*, 22, 107-117.
- Stewart, J. R., Christman, K. L., O'Brian, C. A., (2000). Effects of resveratrol on the autophosphorylation of phorbol ester-responsive protein kinases: inhibition of protein kinase D but not protein kinase C isozyme autophosphorylation. *Biochem Pharmacol.*, 60, 1355- 1359.
- Stivala, L. A., Savio, M., Carafoli, F., Perucca, P., Bianchi, L., Maga, G., Forti, L., Pagnoni, U. M., Albini, A., Prosperi, E., Vannini, V., (2001). Specific structural determinants are responsible for the antioxidant activity and the cell cycle effects of resveratrol. *J Biol Chem.*, 276, 22586-22594.
- Stojanovic, M.N., and Kolpashchikov, D.M., (2004). Modular aptameric sensors. *J Am Chem Soc.*, 126, 9266-9270.
- Stoltenburg, R., Reinemann, C., and Strehlitz, B., (2005). FluMag-SELEX as an Advantageous method for DNA aptamer selection. *Analytical and Bioanalytical Chemistry*, 383, 83-91.

REFERENCES

- Stoltenburg, R., Reinemann, C., Strehlitz, B., (2007). SELEX—a (r) evolutionary method to generate high-affinity nucleic acid ligands. *Biomolecular engineering*, 24: 381-403.
- Storz, p., (2005). Reactive oxygen species in tumour progression. *Frontiers in Bioscience*, 10, 1881-1896.
- Storz, P., H., Doppler and Toker, A., (2004). Activation loop phosphorylation controls protein kinase D dependent activation of nuclear factor kappaB. *Mol Pharmacol.*, 66, 870-879.
- St-Pierre, J., Drori, S., Uldry, M., Silvaggi, J.M., Rhee, J., Jager, S., Handschin, C., Zheng, K., Lin, J., Yang, W., Simon, D.K., Bachoo, R., Spiegelman, B.M., (2006). Suppression of reactive oxygen species and neurodegeneration by the PGC-1 transcriptional coactivators. *Cell*, 127:397–408.
- Strahl, B. D., and Allis, C. D., (2000). The language of covalent histone modifications. *Nature*, 403, 41-45.
- Stümel, W., and Campbe, R., (2011). Sirtuin 1 (SIRT1): The Misunderstood HDAC. *Journal of Biomolecular Screening*, 16(10).
- Stunkel, W., Peh, B.K., Tan, Y.C., Nayagam, V.M., Wang, X., Salto-Tellez, M., Ni, B., Entzeroth, M., Wood, J., (2007). Function of the SIRT1 protein deacetylase in cancer. *Biotechnol J*, 2, 1360–1368.
- Subbaramaiah, K., Chung, W. J., Michaluart, P., Telang, N., Tanabe, T., Inoue, H., Jang, M., Pezzuto, J. M., Dannenberg, A. J., (1998). Resveratrol inhibits cyclooxygenase-2 transcription and activity in phorbol ester-treated human mammary epithelial cells. *J Biol Chem.*, 273, 21875-21882.
- Summer, H., Grämer, R., Dröge, P., (2009). Denaturing urea polyacrylamide gel electrophoresis (Urea PAGE). *J. Vis. Exp.*, 32, 1485.
- Sun, C., Zhang, F., Ge, X., Yan, T., Chen, X., Shi, X., and Zhai, Q., (2007). SIRT1 improves insulin sensitivity under insulin-resistant conditions by repressing PTP1B. *Cell Metab.*, 6, 307-319.
- Takagaki, Y., and Manley, J.L., (1997). RNA recognition by the human polyadenylation factor CstF. *Molecular and Cellular Biology*, 17, 3907-3914.

REFERENCES

- Takami, Y., and Nakayama, T. (2000). N-terminal region, C-terminal region, nuclear export signal, and deacetylation activity of histone deacetylase-3 are essential for the viability of the DT40 chicken B cell line. *J Biol Chem.*, 275, 16191-16201.
- Takata, T. and Ishikawa, F., (2003). Human Sir2-related protein SIRT1 associates with the bHLH repressors HES1 and HEY2 and is involved in HES1- and HEY2-mediated transcriptional repression. *Biochem Biophys Res Commun*, 301(1): 250-257.
- Tang, J., Xie, J., Shao, N., Yan, Y., (2006). The DNA aptamers that specifically recognize ricin toxin are selected by two in vitro selection methods. *Electrophoresis*, 27, 1303-1311.
- Tanner, K. G., Landry, J., Sternglanz, R., and Denu, J. M., (2000). Silent information regulator 2 family of NAD- dependent histone/protein deacetylases generates a unique product, 1-Oacetyl-ADP-ribose. *Proc Natl Acad Sci U S A.*, 97, 14178-14182.
- Tanno, M., Sakamoto, J., Miura, T., Shimamoto, K., Horio, Y., (2007). Nucleocytoplasmic shuttling of the NAD⁺-dependent histone deacetylase SIRT1. *Journal of Biological Chemistry*, 282(9), 6823–6832.
- Teng, Y., Girvan, A. C., Casson, L. K., Pierce, W. M., Jr, Qian, M., Thomas, S. D., and Bates, P. J., (2007). AS1411 Alters the Localization of a Complex Containing Protein Arginine Methyltransferase 5 and Nucleolin. *Cancer Res.*, 67, 10491-10500.
- Thiel, K., (2004). Oligo oligarchy—the surprisingly small world of aptamers. *Nat. Biotechnol.*, 22, 649–651.
- Tissenbaum, H. A., and Guarente, L., (2001). Increased dosage of a sir-2 gene extends lifespan in *Caenorhabditis elegans*. *Nature*, 410, 227-230.
- Tombelli, S., Minunni, M., Luzi, E., Mascini, M., (2005). Aptamer-based biosensors for the detection of HIV-1 Tat protein. *Bioelectrochemistry Amsterdam Netherlands*, 67: 135-141.
- Toulme, J.J., Darfeuille, F., Kolb, G.L., Chabas, S., Staedel, C., (2003). Modulating viral gene expression by aptamers to RNA structures. *Biol. Cell*, 95, 2.
- Trachootham, D., Alexandre, J., Huang, P., (2009). Targeting cancer cells by ROS-mediated mechanisms: a radical therapeutic approach? *Nat Rev Drug Discov.*, 8:579–591.

REFERENCES

- Tsai, R.Y., Reed, R.R., (1998). Identification of DNA recognition sequences and protein interaction domains of the multiple-Zn-finger protein Roaz. *Molecular and Cellular Biology*, 18, 6447-6456.
- Tsang, A. W., and Escalante-Semerena, J. C., (1998). CobB, a new member of the SIR2 family of eucaryotic regulatory proteins, is required to compensate for the lack of nicotinate mononucleotide:5,6-dimethylbenzimidazole phosphoribosyltransferase activity in cobT mutants during cobalamin biosynthesis in *Salmonella typhimurium* LT2. *J Biol Chem.*, 273, 31788-31794.
- Tsujii, S., Tanaka, T., Hirabayashi, N., Kato, S., Akitomi, J., Egashira, H., Waga, I., Ohtsu, T., (2009). RNA aptamer binding to polyhistidine-tag. *Biochemical and Biophysical Research Communications*. 386: 227-231.
- Tuerk, C., Gold, L., (1990). Systematic evolution of ligands by exponential enrichment: RNA ligands to bacteriophage T4 DNA polymerase. *Science*, 249, 505–510.
- Tuerk, C., MacDougall, S., Gold, L., (1992). RNA pseudoknots that inhibit human immunodeficiency virus type 1 reverse transcriptase. *Proc Natl Acad Sci U S A*, 89,6988-92.
- Tyagi, S., and Kramer, F.R., (1996). Molecular beacons: Probes that uoresce upon hybridization. *Nature Biotechnol.*, 14, 303±308.
- Ulrich, H., Magdesian, M. H., Alves, M. J. M., Colli, W., (2002), In vitro selection of RNA aptamers that bind to cell adhesion receptors of *Trypanosoma cruzi* and inhibit cell invasion. *J. Biol. Chem.*, 277, 20756- 20762.
- Ulrich, H., Trujillo, C.A., Nery, A.A., Alves, J.M., Majumder, P., Resende, R.R., Martins, A.H., (2006). DNA and RNA aptamers: from tools for basic research towards therapeutic applications. *Comb. Chem. High Throughput Screen*. 9, 619–632.
- Vachharajani, T. V., Liu, T., Wang, X., Hoth, J. J., Yoza, B. K., McCall, C.E., (2016). Sirtuins link inflammation and metabolism. *Journal of Immunology Research*. 8167273, 10.
- Van den Wyngaert, I., de Vries, W., Kremer, A., Neefs, J., Verhasselt, P., Luyten, W. H., and Kass, S. U., (2000). Cloning and characterisation of human histone deacetylase 8. *FEBS Lett*, 478, 77-83.

REFERENCES

- van der Horst, A., Tertoolen, L.G., de Vries-Smits, L.M., Frye, R.A., Medema, R.H., Burgering, B.M., (2004). FOXO4 is acetylated upon peroxide stress and deacetylated by the longevity protein hSir2(SIRT1). *J Biol Chem.*, 279:28873–28879.
- van IJzendoorn, S.C.D., Zegers, M.M.P., Kok, J.W., Hoekstra, D., (1997). Segregation of glucosylceramide and sphingomyelin occurs in the apical to basolateral transcytotic route in HepG2 cells. *J Cell Biol.*,137:347–357.
- Vannini, A., Volpari, C., Filocamo, G., Casavola, E. C., Brunetti, M., Renzoni, D., Chakravarty, P., Paolini, C., De Francesco, R., Gallinari, P., *et al.*, (2004). Crystal structure of a eukaryotic zinc-dependent histone deacetylase, human HDAC8, complexed with a hydroxamic acid inhibitor. *Proc Natl Acad Sci U S A.*, 101, 15064-15069.
- Vaquero, A., Scher, M. B., Lee, D. H., Sutton, A., Cheng, H. L., Alt, F. W., Serrano, L., Sternglanz, R., and Reinberg, D., (2006). SirT2 is a histone deacetylase with preference for histone H4 Lys 16 during mitosis. *Genes Dev.*, 20, 1256-1261.
- Vaquero, A., Scher, M., Lee, D., Erdjument-Bromage, H., Tempst, P., and Reinberg, D., (2004). Human SirT1 interacts with histone H1 and promotes formation of facultative heterochromatin. *Mol Cell*, 16, 93-105.
- Vater, A., and Klussmann, S., (2003). Toward third-generation aptamers: Spiegelmers and their therapeutic prospects. *Curr Opin Drug Discov Devel.*, 6, 253-61.
- Vaziri, H., Dessain, S.K., Ng Eaton, E., Imai, S.I., Frye, R.A., Pandita, T.K., Guarente, L., and Weinberg, R.A., (2001). hSIR2(SIRT1) functions as an NAD-dependent p53 deacetylase. *Cell*, 107(2): 149-159.
- Veedu, R. N., and Wengel, J., (2009). Locked nucleic acid as a novel class of therapeutic agents. *RNA Biol.*, 6, 321-323.
- Venkatasubramanian, S., Noh, R., Daga, S., Langrish, J., Mills, N., Waterhouse, B., Hoffmann, E., Jacobson, E., (2016). Effects of the small molecule SIRT1 activator, SRT2104 on arterial stiffness in otherwise healthy cigarette smokers and subjects with type 2 diabetes mellitus. *Open Heart*. 3: e000402.

REFERENCES

- Verdel, A., and Khochbin, S., (1999). Identification of a new family of higher eukaryotic histone deacetylases. Coordinate expression of differentiation-dependent chromatin modifiers. *J Biol Chem.*, 274, 2440-2445.
- Verdel, A., Curtet, S., Brocard, M. P., Rousseaux, S., Lemercier, C., Yoshida, M., and Khochbin, S., (2000). Active maintenance of mHDA2/mHDAC6 histone-deacetylase in the cytoplasm. *Curr Biol.*, 10, 747-749.
- Villagra, A., Cheng, F., Wang, H. W., Suarez, I., Glozak, M., Maurin, M., Nguyen, D., Wright, K. L., Atadja, P. W., Bhalla, K., et al., (2009). The histone deacetylase HDAC11 regulates the expression of interleukin 10 and immune tolerance. *Nat Immunol.*, 10, 92-100.
- Vineis, P., Schatzkin, A., Potter, J. D. (2010). Models of carcinogenesis: an overview. *Carcinogenesis*, 31(10), 1703–1709.
- Wałtroba, M., Szukiewicz, D., (2016). The role of sirtuins in aging and age-related diseases. *Advances in Medical Sciences*, 61:52–62.
- Wang, A. H., and Yang, X. J., (2001). Histone deacetylase 4 possesses intrinsic nuclear import and export signals. *Mol Cell Biol.*, 21, 5992-6005.
- Wang, A. H., Kruhlak, M. J., Wu, J., Bertos, N. R., Vezmar, M., Posner, B. I., Bazett-Jones, D. P., and Yang, X. J. (2000). Regulation of histone deacetylase 4 by binding of 14-3-3 proteins. *Mol Cell Biol.*, 20, 6904-6912.
- Wang, C., Chen, L., Hou, X., Li, Z., Kabra, N., Ma, Y., Nemoto, S., Finkel, T., Gu, W., Cress, W. D., and Chen, J., (2006). Interactions between E2F1 and SirT1 regulate apoptotic response to DNA damage. *Nat Cell Biol.*, 8, 1025-1031.
- Wang, C., Zhang, M., Yang, G., Zhang, D., Ding, H., Wang, H., Fan, M., Shen, B., Shao, N., (2003). Single-stranded DNA aptamers that bind differentiated but not parental cells: subtractive systematic evolution of ligands by exponential enrichment. *J. Biotechnol.*, 102, 15–22.
- Wang, F., Nguyen, M., Qin, F. X., and Tong, Q., (2007). SIRT2 deacetylates FOXO3a in response to oxidative stress and caloric restriction. *Aging Cell*, 6, 505-514.
- Wang, J., Yi, J., (2008). Cancer cell killing via ROS: to increase or decrease, that is the question. *Cancer Biol Ther.*, 7:1875–1884.

REFERENCES

- Wang, R.H., Sengupta, K., Li, C., Kim, H.S., Cao, L., Xiao, C., Kim, S., Xu, X., Zheng, Y., Chilton, B., Jia, R., Zheng, Z.M., Appella, E., Wang, X.W., Ried, T., Deng, C.X., (2008). Impaired DNA damage response, genome instability, and tumorigenesis in SIRT1 mutant mice. *Cancer Cell*, 14, 312–323.
- Wapenaar, H., & Dekker, F. J. (2016). Histone acetyltransferases: challenges in targeting bi-substrate enzymes. *Clinical Epigenetics*, 8, 59.
- Waybrant, B., Pearce, T.R., Wang, P., Sreevatsan, S., and Kokkoli, E., (2012). Development and characterization of an aptamer binding ligand of fractalkine using domain targeted SELEX. *Chemical Communications*, 48, 10043-10045.
- Wegener, D., Hildmann, C., Riester, D., Schwienhorst, A., (2003). Improved fluorogenic histone deacetylase assay for high-throughput-screening applications. *Anal. Biochem.*, 321(2), 202–208.
- Weiss, S., Proske, D., Neumann, M., Groschup, M.H., Kretzschmar, H.A., Famulok, M., and Winnacker, E.L., (1997). RNA aptamers specifically interact with the prion protein PrP. *Journal of Virology*, 71, 8790-8797.
- Wen, H., Craig, P.S., (1994). Immunoglobulin G subclass responses in human cystic and alveolar echinococcosis. *Am. J. Trop. Med. Hyg.*, 51(6), 741-748.
- Wen, Y. D., Perissi, V., Staszewski, L. M., Yang, W. M., Krones, A., Glass, C. K., Rosenfeld, M. G., and Seto, E., (2000). The histone deacetylase-3 complex contains nuclear receptor corepressors. *Proc Natl Acad Sci U S A.*, 97, 7202-7207.
- Westendorf, J. J., Zaidi, S. K., Cascino, J. E., Kahler, R., van Wijnen, A. J., Lian, J. B., Yoshida, M., Stein, G. S., and Li, X., (2002). Runx2 (Cbfa1, AML-3) interacts with histone deacetylase 6 and represses the p21(CIP1/WAF1) promoter. *Mol Cell Biol*, 22, 7982-7992.
- Whitsett, T., Carpentier, M., Lamartiniere, C.A., (2006). Resveratrol, but not EGCG, in the diet suppresses DMBA-induced mammary cancer in rats. *J Carcinog.*, 5:15.
- Widmaier, E. P.; Hershel, R., Kevin., T. S., (2008). *Vander's human physiology*, 11th Ed. McGraw-Hill. pp. 108–12.

REFERENCES

Wiegand, T.W, Williams, P.B., Dreskin, S.C., Jouvin, M.H., Kinet, J.P., and Tasset, D., (1996). High-affinity oligonucleotide ligands to human IgE inhibit binding to Fcε receptor I. *Journal of Immunology*, 157, 221-230.

Wilson, C., Szostak, J., (1995). *In vitro* evolution of a self-alkylating ribozyme. *Nature*, 374, 777–782.

Wlotzka, B., Leva, S., Eschgfäller, B., Burmeister, J., Kleinjung, F., *et al.*, (2002). *In vivo* properties of an anti-GnRH Spiegelmer: an example of an oligonucleotide-based therapeutic substance class. *Proc Natl Acad Sci U S A*, 99,8898-902.

Wood, J. G., Rogina, B., Lavu, S., Howitz, K., Helfand, S. L., Tatar, M., Sinclair, D., (2004). Sirtuin activators mimic caloric restriction and delay ageing in metazoans. *Nature*, 430, 686-689.

Wood, J.G., Rogina, B., Lavu, S., Howitz, K., Helfand, S.L., Tatar, M., and Sinclair, D., (2004). Sirtuin activators mimic caloric restriction and delay ageing in metazoans. *Nature*, 430(7000): 686-689.

Wu, V.C.H., Chen, S.-H., and Lin, C.-S., (2007). Real-time detection of *Escherichia coli* O157:H7 sequences using a circulating-flow system of quartz crystal microbalance. *Biosensors and Bioelectronics*, 22, 2967-2975.

Xu, S., Gao, Y., Zhang, Q., Wei, S., Chen, Z., Zeng, Z., Zhao, K., (2016). SIRT1/3 activation by resveratrol attenuates acute kidney injury in a septic rat model. *Oxidative Medicine and Cellular Longevity*. 7296092, 12.

Yang S.h., (2011). Nanoparticle-based cellular machinery for the degradation of specific RNA and protein. Thesis.

Yang, C., Wang, Y., Marty, J. L., Yang, X. R., (2011). Aptamer-based colorimetric biosensing of Ochratoxin A using unmodified gold nanoparticles indicator, *Biosensors & Bioelectronics*, 26, 2724-2727.

Yang, S.R., Wright, J., Bauter, M., Seweryniak, K., Kode, A., and Rahman, I., (2007). Sirtuin regulates cigarette smoke-induced proinflammatory mediator release via RelA/p65 NF-kappaB in macrophages *in vitro* and in rat lungs *in vivo*: implications for chronic inflammation and aging. *Am J Physiol Lung Cell Mol Physiol*, 292(2): L567-576.

REFERENCES

- Yang, W. M., Inouye, C., Zeng, Y., Bearss, D., and Seto, E., (1996). Transcriptional repression by YY1 is mediated by interaction with a mammalian homolog of the yeast global regulator RPD3. *Proc Natl Acad Sci U S A.*, 93, 12845-12850.
- Yang, W. M., Tsai, S. C., Wen, Y. D., Fejer, G., and Seto, E., (2002). Functional domains of histone deacetylase-3. *J Biol Chem.*, 277, 9447-9454.
- Yang, W. M., Yao, Y. L., Sun, J. M., Davie, J. R., and Seto, E., (1997). Isolation and characterisation of cDNAs corresponding to an additional member of the human histone deacetylase gene family. *J Biol Chem.*, 272, 28001-28007.
- Yang, X. J., and Gregoire, S., (2005). Class II histone deacetylases: from sequence to function, regulation, and clinical implication. *Mol Cell Biol.*, 25, 2873-2884.
- Yang, X. J., and Seto, E. (2008). The Rpd3/Hda1 family of lysine deacetylases: from bacteria and yeast to mice and men. *Nat Rev Mol Cell Biol.*, 9, 206-218.
- Yang, X., Li, X., Prow, T.W., Reece, L.M., Bassett, S.E., Luxon, B.A., Herzog, N.K., Aronson, J., Shope, R.E., Leary, J.F., Gorenstein, D.G., (2003). Immunofluorescence assay and flow-cytometry selection of bead-bound aptamers *Nucleic Acids Res.*, 31(10),54.
- Yeung, F., Hoberg, J. E., Ramsey, C. S., Keller, M. D., Jones, D. R., Frye, R. A., and Mayo, M. W., (2004). Modulation of NF-kappaB-dependent transcription and cell survival by the SIRT1 deacetylase. *EMBO J.*, 23, 2369-2380.
- Yokomizo, A. M., Ono, H., Nanri, Y., Makino, T., Ohga, M., Wada, T., Okamoto, J., Yodoi, M., Kuwano, K., (1995). Cellular levels of thioredoxin associated with drug sensitivity to cisplatin, mitomycin C, doxorubicin, and etoposide. *Cancer Res.*, 55, 4293-4296.
- Yuan, J., Minter-Dykhouse, K., Lou, Z.A., (2009). c-Myc-SIRT1 feedback loop regulates cell growth and transformation. *J Cell Biol.*, 185,203–211.
- Yuan, Z., and Seto, E., (2007). A functional link between SIRT1 deacetylase and NBS1 in DNA damage response. *Cell Cycle*, 6, 2869-2871.
- Yuan, Z., Zhan, X., Sengupta, N., Lane, W.S., Seto, E., (2007). SIRT1 regulates the function of the Nijmegen breakage syndrome protein. *Mol Cell*, 27:149-62.

REFERENCES

- Zacharski, L. R., (2002). Anticoagulants in cancer treatment: malignancy as a solid phase coagulopathy. *Cancer Lett.*, 186, 1–9.
- Zeugin, J.A., Hartley, J.L., (1985). Ethanol Precipitation of DNA. *Focus* 7 (4): 1–2. Zhao, W., Kruse, J.P., Tang, Y., Jung, S.Y., Qin, J., Gu, W., (2008). Negative regulation of the deacetylase SIRT1 by DBC1. *Nature*, 451, 587–590.
- Zhang, C. L., McKinsey, T. A., Lu, J. R., and Olson, E. N., (2001). Association of COOH terminal-binding protein (CtBP) and MEF2-interacting transcription repressor (MITR) contributes to transcriptional repression of the MEF2 transcription factor. *J Biol Chem.*, 276, 35-39.
- Zhang, J., (2006). Resveratrol inhibits insulin responses in a SirT1-independent pathway. *Biochem J*, 397(3): 519-527.
- Zhang, W., Luo, J., Yang, F., Wang, y., Yin, Y., Strom, A., Gustafsson, A., Guan, X., (2016). BRCA1 inhibits AR-mediated proliferation of breast cancer cells through the activation of SIRT1. *Scientific Reports*, 6:22034.
- Zhang, Y., Zhang, M., Dong, H., (2009). Deacetylation of cortactin by SIRT1 promotes cell migration. *Oncogene*. 28:445–460.
- Zhao, W., Kruse, J. P., Tang, Y., Jung, S. Y., Qin, J. and Gu, W., (2008). Negative regulation of the deacetylase SIRT1 by DBC1. *Nature*, 451, 587-590.
- Zhao, X., Allison, D., Condon, B., Zhang, F., Gheyi, T., Zhang, A., Ashok, S., Russell, M., MacEwan, I., Qian, Y., Jamison, J. A., Luz, J. G., 2013. The 2.5 Å crystal structure of the SIRT1 catalytic domain bound to nicotinamide adenine dinucleotide (NAD⁺) and an indole (EX527analogue) reveals a novel mechanism of histone deacetylase inhibition. *J Med Chem.*, 56, 963-969.
- Zhao, X., Sternsdorf, T., Bolger, T.A., Evans, R.M., and Yao, T.P., (2005). Regulation of MEF2 by histone deacetylase 4- and SIRT1 deacetylase-mediated lysine modifications. *Mol Cell Biol.*, 25(19): 8456-8464.
- Zhou, X., Marks, P. A., Rifkind, R. A., and Richon, V. M., (2001). Cloning and characterization of a histone deacetylase, HDAC9. *Proc Natl Acad Sci U S A.*, 98, 10572-10577.

REFERENCES

Zhou, X., Richon, V. M., Rifkind, R. A., and Marks, P. A., (2000). Identification of a transcriptional repressor related to the noncatalytic domain of histone deacetylases 4 and 5. *Proc Natl Acad Sci U S A.*, 97, 1056-1061.

Zhou, X., Richon, V. M., Wang, A. H., Yang, X. J., Rifkind, R. A., and Marks, P. A., (2000). Histone deacetylase 4 associates with extracellular signal-regulated kinases 1 and 2, and its cellular localisation is regulated by oncogenic Ras. *Proc Natl Acad Sci U S A.*, 97, 14329-14333.

Zhu, P., Martin, E., Mengwasser, J., Schlag, P., Janssen, K. P., and Gottlicher, M., (2004). Induction of HDAC2 expression upon loss of APC in colorectal tumourigenesis. *Cancer Cell*, 5, 455-463.

Zschoernig, B., and Mahlknecht, U., (2008). SIRTUIN 1: Regulating the regulator. *Biochemical and Biophysical Research Communications*. 376, 2(14), 251–255.

Zuker, M., (2003). M fold web server for nucleic acid folding and hybridisation prediction. *Nucleic Acids Res.*, 31, 3406–3415.